frontiers | Research Topics

Redox-signaling in neurodegenerative diseases: Biomarkers, targets, and therapies

Edited by
Andreia Neves Carvalho, Luciano Saso, Jack Van Horssen and Vasco Branco

Published in
Frontiers in Cellular Neuroscience

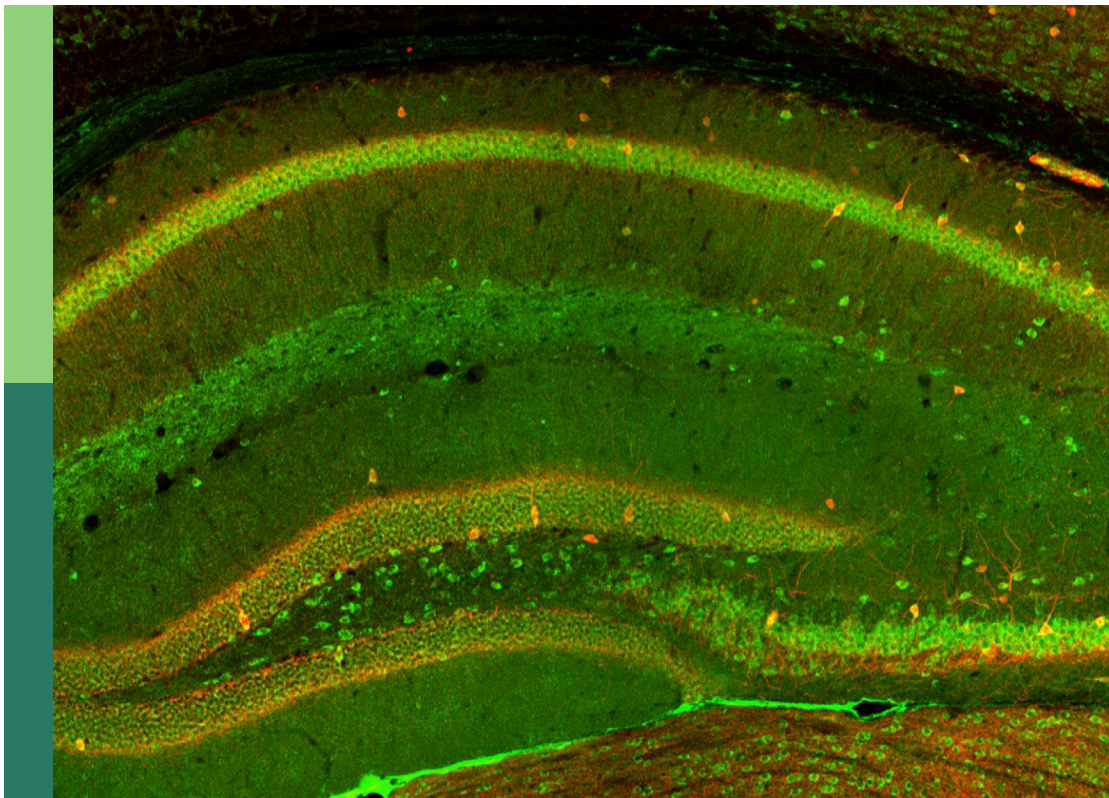

ISSN 1664-8714
ISBN 978-2-8325-2353-7
DOI 10.3389/978-2-8325-2353-7

About Frontiers

Frontiers is more than just an open access publisher of scholarly articles: it is a pioneering approach to the world of academia, radically improving the way scholarly research is managed. The grand vision of Frontiers is a world where all people have an equal opportunity to seek, share and generate knowledge. Frontiers provides immediate and permanent online open access to all its publications, but this alone is not enough to realize our grand goals.

Frontiers journal series

The Frontiers journal series is a multi-tier and interdisciplinary set of open-access, online journals, promising a paradigm shift from the current review, selection and dissemination processes in academic publishing. All Frontiers journals are driven by researchers for researchers; therefore, they constitute a service to the scholarly community. At the same time, the *Frontiers journal series* operates on a revolutionary invention, the tiered publishing system, initially addressing specific communities of scholars, and gradually climbing up to broader public understanding, thus serving the interests of the lay society, too.

Dedication to quality

Each Frontiers article is a landmark of the highest quality, thanks to genuinely collaborative interactions between authors and review editors, who include some of the world's best academicians. Research must be certified by peers before entering a stream of knowledge that may eventually reach the public - and shape society; therefore, Frontiers only applies the most rigorous and unbiased reviews. Frontiers revolutionizes research publishing by freely delivering the most outstanding research, evaluated with no bias from both the academic and social point of view. By applying the most advanced information technologies, Frontiers is catapulting scholarly publishing into a new generation.

What are Frontiers Research Topics?

Frontiers Research Topics are very popular trademarks of the *Frontiers journals series*: they are collections of at least ten articles, all centered on a particular subject. With their unique mix of varied contributions from Original Research to Review Articles, Frontiers Research Topics unify the most influential researchers, the latest key findings and historical advances in a hot research area.

Find out more on how to host your own Frontiers Research Topic or contribute to one as an author by contacting the Frontiers editorial office: frontiersin.org/about/contact

Redox-signaling in neurodegenerative diseases: Biomarkers, targets, and therapies

Topic editors

Andreia Neves Carvalho — University of Lisbon, Portugal
Luciano Saso — Sapienza University of Rome, Italy
Jack Van Horssen — VU Medical Center, Netherlands
Vasco Branco — University of Lisbon, Portugal

Citation

Carvalho, A. N., Saso, L., Van Horssen, J., Branco, V., eds. (2023). *Redox-signaling in neurodegenerative diseases: Biomarkers, targets, and therapies*. Lausanne: Frontiers Media SA. doi: 10.3389/978-2-8325-2353-7

Table of contents

frontiers | Frontiers in Cellular Neuroscience

TYPE Editorial
PUBLISHED 20 April 2023
DOI 10.3389/fncel.2023.1198669

OPEN ACCESS

EDITED AND REVIEWED BY
Dirk M. Hermann,
University of Duisburg-Essen, Germany

*CORRESPONDENCE
Andreia N. Carvalho
✉ amcarvalho@ff.ulisboa.pt

RECEIVED 01 April 2023
ACCEPTED 03 April 2023
PUBLISHED 20 April 2023

CITATION
Carvalho AN, Branco V, van Horssen J and Saso L (2023) Editorial: Redox-signaling in neurodegenerative diseases: biomarkers, targets, and therapies.
Front. Cell. Neurosci. 17:1198669.
doi: 10.3389/fncel.2023.1198669

Editorial: Redox-signaling in neurodegenerative diseases: biomarkers, targets, and therapies

Andreia N. Carvalho[1]*, Vasco Branco[1,2], Jack van Horssen[3] and Luciano Saso[4]

[1]Research Institute for Medicines (iMed.ULisboa), Faculty of Pharmacy, Universidade de Lisboa, Lisbon, Portugal, [2]Centro de Investigação Interdisciplinar Egas Moniz, Instituto Universitário Egas Moniz, Caparica, Portugal, [3]Department of Molecular Cell Biology and Immunology, MS Center Amsterdam, Vrije Universiteit Amsterdam, Amsterdam Neurosciences, Amsterdam UMC Location VUmc, Amsterdam, Netherlands, [4]Department of Physiology and Pharmacology, Faculty of Pharmacy and Medicine, Sapienza University of Rome, Rome, Italy

KEYWORDS

neurodegenerative diseases, post-translational modifications (PTMs), redox-signaling, Nrf2, oxidative stress, antioxidants

Editorial on the Research Topic
Redox-signaling in neurodegenerative diseases: biomarkers, targets, and therapies

Neurodegenerative diseases share common pathological hallmarks such as mitochondrial dysfunction and oxidative stress, which leads to neuronal loss. Redox regulation of key cellular functions is an important signaling mechanism and post-translational modifications (PTMs) are relevant in redox signal transduction and might be instrumental in uncovering pathophysiological mechanisms and identify novel therapeutic targets in neurodegenerative diseases. Promising novel redox-based therapeutics include strategies aimed at enhancing the endogenous antioxidant machinery through activation of the antioxidant master regulator nuclear factor erythroid 2-related factor 2 (Nrf2) or modulation of reactive oxygen species (ROS) production by nicotinamide adenine dinucleotide phosphate (NADPH) oxidases (NOXs) inhibitors (Carvalho et al., 2017).

This Research Topic focuses on redox signaling, particularly Nrf2-driven mechanisms, and aims to provide novel insights into redox regulation involving PTMs in the pathophysiology of neurodegenerative diseases.

Seminotti et al. review the current knowledge on the dysregulation of the Nrf2 pathway in the pathophysiology of inherited metabolic disorders (IMDs), rare genetic conditions affecting predominantly the central nervous system (CNS). The authors revise the critical role of Nrf2 signaling in IMDs and discuss the beneficial effects of Nrf2 activators as potential therapeutic options. Nrf2 pathway dysfunction has been associated with complex metabolic disorders, such as diabetes. This highlights the importance of adequate Nrf2 function in preventing the onset of diabetes and impaired Nrf2 function as a critical mediator of diabetes progression (Dodson et al., 2022). In type II diabetes chronic hyperglycaemia is associated to increased pro-inflammatory signaling, mitochondrial dysfunction, and impaired autophagy, contributing to neurodegeneration. In this issue Dedert et al. investigated the role of progranulin in preserving the autophagic flux and mitochondrial function in neurons under hyperglycaemic conditions. Progranulin treatment upon high-glucose stress conditions, led to the activation of glycogen synthase kinase 3β (GSK3β). GSK3β is a known endogenous

negative regulator of Nrf2 activity (Rada et al., 2011), which suggests that modulation of Nrf2 might constitute an alternative mechanism for neuronal autophagic flux regulation under high-glucose stress conditions.

Hyperglycaemia is a risk factor for several neurodegenerative diseases, such as Alzheimer's and Parkinson's disease (Madhusudhanan et al., 2020). Saha et al. reviewed the potential role of Nrf2 as a key target for therapeutic intervention in these neurodegenerative conditions due to its dual anti-inflammatory and antioxidant functions. They suggest that Nrf2 activation could be a novel therapeutic approach since it serves as an integration hub for inflammatory and oxidative signals.

In fact, the protective role of Nrf2 in the CNS extends beyond neurodegenerative conditions. In an original research article Yang et al. demonstrated that Nrf2 protects sensory hair cells from gentamicin-induced damage and ototoxicity and eventual hearing loss, *via* induction of its downstream target heme oxygenase 1. This protective effect was absent in the presence of Nrf2 or heme oxygenase inhibitors.

Additional articles in this topic issue focus on the role of ROS in stroke, a devastating medical condition classified as both cardiovascular and neurological disorder. Liu X. et al. reported that serum levels of 4-hydroxynonenal, a product of lipid peroxidation frequently used as a biomarker of oxidative stress (Carvalho et al., 2017), are related with increased risk of recurrence of patients with primary cerebral infarction, establishing serum 4-hydroxynonenal levels as an independent risk factor that may become a new target for prevention of stroke recurrence. Lõhelaid et al. discuss potential strategies to boost endogenous protective pathways to improve stroke outcomes. One such strategy might be promoting the unfolded protein response, an evolutionary conserved adaptive stress response. The authors focus on mesencephalic astrocyte-derived neurotrophic factor (MANF) due to its putative pro-survival effects in several disease models such as diabetes, neurodegeneration and stroke, and perform a systematic comparative analysis of MANF and X-box binding protein 1, another important effector of the unfolded protein response.

In the CNS, ROS are important regulatory signals for synaptic plasticity. Sobrido-Cameán et al. reported that activity regulated growth of motoneurons at the neuromuscular junction is mediated by ROS sources, namely NOXs. The authors found fundamental differences between pre- and post-synaptic responses and showed that specific aquaporins are mediators of NOXs-dependent changes in pre-synaptic motoneuron growth.

Another regulatory layer of post-synaptic signaling that is redox-mediated is the modulation of chloride ions concentration by nitric oxide, that was investigated by Rodriguez et al. in their paper and that determines the inhibitory or excitatory nature of GABAergic and glycinergic synapses. The authors suggested that reduced expression of TMEM16A, a calcium activated chloride channel that is also expressed in neurons, impairs the nitric oxide-dependent chloride release in retinal amacrine cells.

PTMs might be a critical phenomenon in redox mediated signaling. In this Topic issue, Liu D. et al. reviewed N6-methyladenosine (m6A) modification as a potential regulatory mechanism in spinal cord injury, a traumatic injury that severely affects the CNS. Changes in m6A levels are associated with alterations in the spinal cord microenvironment upon injury, such as ischemia, inflammation and apoptosis. The latest progresses made in the regulation of m6A modification and its relationship with pathological mechanisms involved in spinal cord injury are discussed.

Coenzyme A (CoA), a key metabolite in cellular bioenergetics and neurotransmitter biosynthesis, has recently been attributed a new antioxidant function involving covalent protein modification, CoAlation, which was reported to modulate protein activity and protects cysteine residues from overoxidation (Tsuchiya et al., 2017). Here, Lashley et al. reported extensive anti-CoA immunostaining in brain tissue of various neurodegenerative diseases. The authors show that Tau is covalently modified by CoAlation, with the modification mapped by mass spectrometry to a conserved cysteine residue in the microtubule binding region, suggesting that this PTM might play an important role in protecting redox-sensitive tau cysteine from irreversible overoxidation. CoAlation was additionally shown to consistently co-localize with tau-positive neurofibrillary tangles in AD brains, highlighting the relevance of this PTM in AD.

Overall, the present collection of articles contributes to the identification of mechanisms of redox regulation in neurophysiology and neuropathology and deepen our understanding on the role of reactive species in neurodegenerative diseases, with particular emphasis on Nrf2-driven mechanisms and redox-regulation involving post-translational modifications.

Author contributions

This editorial was led by AC who wrote the draft of the manuscript. AC, VB, JH, and LS critically revised the manuscript for important intellectual content. All authors provided approval for publication of the content.

Funding

This work was supported in part by national funds from Fundação para a Ciência e Tecnologia (FCT), Portugal through Norma Transitória – DL57/2016 and grant EXPL/BIA-BQM/0793/2021 (to AC) and Norma Transitória – DL57/2016/CP1376/CT002 (to VB).

Conflict of interest

The authors declare that the research was conducted in the absence of any commercial or financial relationships that could be construed as a potential conflict of interest.

Publisher's note

All claims expressed in this article are solely those of the authors and do not necessarily represent those of their affiliated

organizations, or those of the publisher, the editors and the reviewers. Any product that may be evaluated in this article, or claim that may be made by its manufacturer, is not guaranteed or endorsed by the publisher.

References

Carvalho, A. N., Firuzi, O., Gama, M. J., Horssen, J., and Saso, L. (2017). Oxidative stress and antioxidants in neurological diseases: Is there still hope? *Curr. Drug Targets.* 18, 705–718. doi: 10.2174/1389450117666160401120514

Dodson, M., Shakya, A., Anandhan, A., Chen, J., Garcia, J. G. N., and Zhang, D. D. (2022). NRF2 and diabetes: The good, the bad, and the complex. *Diabetes* 71, 2463–2476. doi: 10.2337/db22-0623

Madhusudhanan, J., Suresh, G., and Devanathan, V. (2020). Neurodegeneration in type 2 diabetes: Alzheimer's as a case study. *Brain Behav.* 10, e01577. doi: 10.1002/brb3.1577

Rada, P., Rojo, A. I., Chowdhry, S., McMahon, M., Hayes, J. D., and Cuadrado, A. (2011). SCF/ß-TrCP promotes glycogen synthase kinase 3-dependent degradation of the Nrf2 transcription factor in a Keap1-independent manner. *Mol. Cell. Biol.* 31, 1121–1133. doi: 10.1128/MCB.01204-10

Tsuchiya, Y., Peak-Chew, S. Y., Newell, C., Miller-Aidoo, S., Mangal, S., Zhyvoloup, A., et al. (2017). Protein CoAlation: a redox-regulated protein modification by coenzyme A in mammalian cells. *Biochem. J.* 474, 2489–2508. doi: 10.1042/BCJ20170129

frontiers in Cellular Neuroscience

ORIGINAL RESEARCH
published: 15 October 2021
doi: 10.3389/fncel.2021.739425

Extensive Anti-CoA Immunostaining in Alzheimer's Disease and Covalent Modification of Tau by a Key Cellular Metabolite Coenzyme A

Tammaryn Lashley[1,2†], Maria-Armineh Tossounian[3], Neve Costello Heaven[2,3], Samantha Wallworth[3], Sew Peak-Chew[4], Aaron Bradshaw[5], J. Mark Cooper[5], Rohan de Silva[6], Surjit Kaila Srai[3], Oksana Malanchuk[7], Valeriy Filonenko[7], Margreet B. Koopman[8,9], Stefan G. D. Rüdiger[8,9], Mark Skehel[4] and Ivan Gout[3,7*†]*

[1] Queen Square Brain Bank, UCL Queen Square Institute of Neurology, London, United Kingdom, [2] Department of Neurodegenerative Disease, UCL Queen Square Institute of Neurology, London, United Kingdom, [3] Department of Structural and Molecular Biology, University College London, London, United Kingdom, [4] MRC Laboratory of Molecular Biology, Cambridge Biomedical Campus, Cambridge, United Kingdom, [5] Department of Molecular Neuroscience, Faculty of Brain Sciences, Royal Free Campus, London, United Kingdom, [6] Reta Lila Weston Institute of Neurological Studies, University College London, London, United Kingdom, [7] Department of Cell Signaling, Institute of Molecular Biology and Genetics, Kyiv, Ukraine, [8] Cellular Protein Chemistry, Bijvoet Center for Biomolecular Research, Utrecht University, Utrecht, Netherlands, [9] Science for Life, Utrecht University, Utrecht, Netherlands

OPEN ACCESS

Edited by:
Andreia Neves Carvalho, University of Lisbon, Portugal

Reviewed by:
Jack Harry Brelstaff, University of Cambridge, United Kingdom
Liviu-Gabriel Bodea, University of Queensland, Australia

***Correspondence:**
Tammaryn Lashley
t.lashley@ucl.ac.uk
Ivan Gout
i.gout@ucl.ac.uk

† These authors share senior authorship

Specialty section:
This article was submitted to Cellular Neuropathology, a section of the journal Frontiers in Cellular Neuroscience

Received: *10 July 2021*
Accepted: *17 September 2021*
Published: *15 October 2021*

Citation:
Lashley T, Tossounian M-A, Costello Heaven N, Wallworth S, Peak-Chew S, Bradshaw A, Cooper JM, de Silva R, Srai SK, Malanchuk O, Filonenko V, Koopman MB, Rüdiger SGD, Skehel M and Gout I (2021) Extensive Anti-CoA Immunostaining in Alzheimer's Disease and Covalent Modification of Tau by a Key Cellular Metabolite Coenzyme A. Front. Cell. Neurosci. 15:739425. doi: 10.3389/fncel.2021.739425

Alzheimer's disease (AD) is a neurodegenerative disorder, accounting for at least two-thirds of dementia cases. A combination of genetic, epigenetic and environmental triggers is widely accepted to be responsible for the onset and development of AD. Accumulating evidence shows that oxidative stress and dysregulation of energy metabolism play an important role in AD pathogenesis, leading to neuronal dysfunction and death. Redox-induced protein modifications have been reported in the brain of AD patients, indicating excessive oxidative damage. Coenzyme A (CoA) is essential for diverse metabolic pathways, regulation of gene expression and biosynthesis of neurotransmitters. Dysregulation of CoA biosynthesis in animal models and inborn mutations in human genes involved in the CoA biosynthetic pathway have been associated with neurodegeneration. Recent studies have uncovered the antioxidant function of CoA, involving covalent protein modification by this cofactor (CoAlation) in cellular response to oxidative or metabolic stress. Protein CoAlation has been shown to both modulate the activity of modified proteins and protect cysteine residues from irreversible overoxidation. In this study, immunohistochemistry analysis with highly specific anti-CoA monoclonal antibody was used to reveal protein CoAlation across numerous neurodegenerative diseases, which appeared particularly frequent in AD. Furthermore, protein CoAlation consistently co-localized with tau-positive neurofibrillary tangles, underpinning one of the key pathological hallmarks of AD. Double immunihistochemical staining with tau and CoA antibodies in AD brain tissue revealed co-localization of the two immunoreactive signals. Further, recombinant 2N3R and 2N4R tau isoforms were found to be CoAlated *in vitro* and the site of CoAlation mapped by mass spectrometry to conserved cysteine 322, located in the microtubule binding

region. We also report the reversible H_2O_2-induced dimerization of recombinant 2N3R, which is inhibited by CoAlation. Moreover, CoAlation of transiently expressed 2N4R tau was observed in diamide-treated HEK293/Pank1β cells. Taken together, this study demonstrates for the first time extensive anti-CoA immunoreactivity in AD brain samples, which occurs in structures resembling neurofibrillary tangles and neuropil threads. Covalent modification of recombinant tau at cysteine 322 suggests that CoAlation may play an important role in protecting redox-sensitive tau cysteine from irreversible overoxidation and may modulate its acetyltransferase activity and functional interactions.

Keywords: Coenzyme A, protein CoAlation, neurodegeneration, Alzheimer's disease, oxidative stress, tau

INTRODUCTION

Presenting as the most common form of dementia, Alzheimer's disease (AD) is a progressive disease affecting millions of people worldwide (Alzheimer, 1906; Selkoe et al., 1999; Przedborski et al., 2003). AD is characterized by cognitive deterioration, changes in behavior and psychiatric disturbances (Burns and Iliffe, 2009). The multifactorial nature of AD with various genetic, biochemical and molecular abnormalities provides a challenge for disease prevention, early onset diagnostics and the development of effective therapies. The majority of AD cases (∼95%) occur sporadically, with no obvious related risk factors (Castellano et al., 2012), whereas a small percentage of hereditary/familial AD (∼5%) are caused by mutations in genes encoding amyloid precursor protein (*APP*), presenilin-1 (*PS1*) and presenilin-2 (*PS2*). Pathological build-up of the β-amyloid peptide (Aβ) in extracellular plaques and intracellular neurofibrillary tangles (NFT) composed of hyperphosphorylated tau are hallmarks of both familial and sporadic AD (Lee et al., 2001). Other pathological features of AD include altered synaptic transmission, impaired calcium and lipid homeostasis, inflammation, mitochondrial dysfunction, and oxidative stress (Hoover et al., 2010; Huang et al., 2016; Magi et al., 2016; Kinney et al., 2018; Chew et al., 2020; Wang et al., 2020).

Mitochondrial homeostasis and function are central to maintaining healthy neurons (Mandal and Drerup, 2019). Healthy and functional mitochondria are vital in neuronal ATP production, intracellular calcium signaling, establishing membrane potential, and efficient neurotransmission. The hippocampal and cortical brain regions are especially vulnerable to mitochondrial disruption and oxidative stress, due to their high oxygen consumption and reliance on mitochondrial energy generation, in combination with inherently low levels of antioxidants and low neuronal cell repair capacity (Cenini and Voos, 2019; Lee et al., 2020). Build-up of damaged mitochondria and autophagic vacuoles is also a prominent feature in neurons of several neurodegenerative diseases, including AD (Nixon and Yang, 2012). Various factors have been found to induce mitochondrial damage, such as abnormal protein aggregates (Aβ, tau), reduced glucose metabolism, and exposure to toxic drugs, and prolonged production of reactive oxygen species (ROS) (Hashimoto et al., 2003; Guo et al., 2013; Stoker et al., 2019). At low levels, ROS may induce subtle changes in intracellular redox signaling. Increased and sustained production of mitochondrial ROS leads to irreversible damage of major cellular biomolecules such as proteins, lipids, and DNA through pathological redox reactions. An imbalance between ROS and antioxidant species triggers oxidative stress. Consequently, increased ROS-induced protein modifications, such as protein cysteine oxidation, carbonylation, *S*-glutathionylation and nitrosylation, have been reported in post-mortem AD brain tissue and AD animal models, indicating excessive oxidative stress-related damage (Sultana et al., 2009). The activity of several key metabolic and signaling enzymes as well as antioxidant proteins has been found modulated by oxidative stress and implicated in the progression of AD.

Tau is the main microtubule-associated protein in neurons. Under physiological conditions, tau promotes the assembly of tubulin heterodimers into microtubules, and stabilizes microtubule networks, which comprise the neuronal cytoskeleton (Grundke-Iqbal et al., 1986). In the brain, the level of tau expression is two times higher in gray matter than white matter (Binder et al., 1985). Alternative splicing of the tau gene *MAPT* generates six distinct molecular isoforms in adult human brain, ranging from 352 to 441 amino acids. At the N-terminus, tau isoforms differ by the presence of one or two N-terminal inserts encoded by exon 2, or exons 2, and 3 (1N and 2N, respectively). Exon 3 is present only in accompaniment of exon 2, therefore exclusion of both sequences generates tau isoforms lacking N-terminal inserts (0N). At the C-terminus, alternative splicing of exon 10 produces isoforms featuring three or four microtubule-binding repeats (MTBR) containing one or two naturally occurring cysteine residues, thus distinguishing between 3-repeat (3R) and 4-repeat (4R) tau, respectively (Goedert et al., 1989; Liu and Gong, 2008). The MTBRs are highly positively charged which facilitates their binding to negatively charged tubulin in microtubules. All six tau isoforms have been found in neurofibrillary tangles of AD (Goedert et al., 1992).

Tau is regarded as an intrinsically disordered protein (IDP) and forms random-coil conformations with some transient secondary structures, including α-helices, β-strands, and polyproline II helices (Battisti et al., 2012). It exists in monomeric, dimeric, oligomeric, and fibrillar forms which are implicated in physiological functions and in pathology (Meraz-Rios et al., 2010). Tau monomers are thought to form dimers in antiparallel fashion, involving hydrophobic interactions and/or covalent cysteine-mediated disulfide bonds. Tau dimers were

found to assemble into oligomeric structures, which have the propensity to form paired helical filaments (PHFs) or straight filaments (SFs). Both PHFs and SFs can then assemble further into neurotoxic NFTs.

Recent analysis of neurofibrillary tangles from AD brain by cryo-electron microscopy revealed the ordered pairs of protofilaments comprising residues 306–378 and disordered amino- and carboxy-termini which form the fuzzy coat by projecting away from the core (Fitzpatrick et al., 2017). Generated atomic models of PHFs and SFs reveal inter-protofilament packing and how 3R and 4R tau isoforms can be assembled into the growing filament. Hydrophobic and polar interactions facilitate the anti-parallel β-sheet packing where hexapeptide ^{306}VQIVYK^{311} is essential for the assembly of tau filaments. Residues ^{321}KCGS^{324} of the first and ^{313}VELSK^{317} of the second protofilament mediate the interaction between the two protofilaments. In contrast, the NMR structure of tau bound to microtubules reveals a hairpin conformation of residues 269–284 and 300–312 and the disordered structure of the N- and C-termini (Kadavath et al., 2015).

Post-translational modifications (PTMs) of tau have been extensively studied and found to modulate its microtubule-binding ability and aggregation. Tau is highly phosphorylated in normal brain and hyperphosphorylated in pathologies. In healthy brain, approximately 10 serine, threonine, and tyrosine phosphorylated sites on tau are commonly detected, in contrast to approximately 45 phosphorylation sites in AD brain (Wang et al., 2013; Iqbal et al., 2016). These sites of phosphorylation are predominantly located within the proline rich region and flanking the MTBRs. Abnormal hyperphosphorylation of tau in AD renders it unable to support microtubule function and promotes its dissociation from microtubules. Consequently, cytosolic tau favors the formation of tau aggregates (Lindwall and Cole, 1984; Ramkumar et al., 2018).

Tau is reversibly oxidized by ROS and reactive nitrogen species (RNS), which promote redox-mediated oxidative PTMs, including cysteine oxidation, S-glutathionylation, and nitrosylation. The MTBRs contain redox-sensitive cysteine residues, which have been implicated in contributing to microtubule binding (Martinho et al., 2018). Tau oxidation was shown to be associated with very slow MT polymerization, whereas glutathionylation of oxidized cysteines reversed this inhibitory effect (Landino et al., 2004). Tau is also known to possess intrinsic acetyltransferase activity, which requires Cys291 and Cys322 to function as intermediates in the transfer acetyl from acetyl-CoA to lysine residues during self-acetylation (Cohen et al., 2013). Moreover, lysine acetylation was shown to decrease microtubule binding and thereby promoting tau aggregation and NFT formation.

Coenzyme A is an essential cofactor in all living cells with diverse cellular functions (Lipmann and Kaplan, 1946; Leonardi et al., 2005; Davaapil et al., 2014; Srinivasan and Sibon, 2014; Theodoulou et al., 2014). The biosynthesis of CoA in prokaryotic and eukaryotic cells occurs via a conserved pathway involving enzymatic conjugation of ATP, pantothenate (vitamin B5) and cysteine (Leonardi et al., 2005). The presence of a highly reactive thiol group allows CoA to be involved in numerous biochemical reactions and to generate diverse metabolically active thioesters, such as Acetyl-CoA, Malonyl-CoA, HMG-CoA, and others (Tsuchiya et al., 2017). CoA and its thioesters are involved in critical anabolic and catabolic pathways, the regulation of gene expression via protein acetylation and the biosynthesis of neurotransmitters. In mammalian cells, CoA/CoA derivatives are predominantly sequestered in mitochondria (2–5 mM) and peroxisomes (0.5–1 mM), while cytosolic/nuclear levels are significantly lower (20–140 μM) (Leonardi et al., 2005). The intracellular levels of CoA/CoA derivatives fluctuate in cellular response to nutrients, hormones, metabolites, and stress (Theodoulou et al., 2014). Abnormal biosynthesis and homeostasis of CoA and its derivatives are associated with various human pathologies, including diabetes, cancer, cardiac hypertrophy, and vitamin B12 deficiency (Reibel et al., 1981; McAllister et al., 1988; Brass et al., 1990). Inborn mutations in the human genes encoding two rate-limiting enzymes of the CoA biosynthetic pathway (*PANK2* and *COASY*) have been implicated in neurodegeneration with brain iron accumulation (NBIA) demonstrating the importance of CoA/CoA derivatives in the maintenance of central nervous system function (Zhou et al., 2001; Dusi et al., 2014).

A novel function of CoA in the antioxidant defense mechanisms has been recently revealed in our laboratory. Using cell-based and animal models, we demonstrated covalent modification of cellular proteins by CoA in cellular response to oxidative or metabolic stress (Tsuchiya et al., 2017, 2018). To discover and study this novel PTM termed "protein CoAlation," we have developed novel reagents and methodologies: (a) anti-CoA monoclonal antibodies, which specifically recognize free CoA and CoA bound to proteins via a disulfide bond in ELISA, Western blotting, immunoprecipitation, immunohistochemistry; (b) a reliable mass spectrometry-based methodology for the identification of CoAlated proteins; and (c) efficient *in vitro* CoAlation and deCoAlation assays (Malanchuk et al., 2015; Tsuchiya et al., 2017, 2018). To date, over 2200 CoAlated proteins have been identified in prokaryotic and eukaryotic cells exposed to oxidative or metabolic stress. Protein CoAlation has been shown to regulate the activity and subcellular localization of modified proteins, protect oxidized cysteine residues from irreversible overoxidation, and to induce conformational changes (Gout, 2018, 2019; Bakovic et al., 2019; Tossounian et al., 2020; Tsuchiya et al., 2020; Yu et al., 2021). The antioxidant function of CoA and protein CoAlation in pathologies associated with oxidative stress, such as neurodegeneration, cancer, and diabetes, remains to be investigated.

Here, immunohistochemistry analysis with anti-CoA mAb was used to examine the extent of protein CoAlation in post-mortem human brain tissues from NBIA, AD, Corticobasal Degeneration (CBD), Progressive Supranuclear Palsy (PSP), Multiple System Atrophy (MSA), Parkinson's Disease (PD), and matched controls. This analysis revealed positive immunoreactivity with anti-CoA in different structures within the brain tissue of NBIA, CDB, PD, and AD, when compared to matched controls. No anti-CoA immunoreactive signal was observed in PSP or MSA. Extensive anti-CoA immunoreactivity was detected in all brain regions apart from the basal ganglia

in 70% of AD samples. Notably, the anti-CoA immunoreactive signal is readily observed in structures resembling NFTs. Double immunohistochemistry with anti-tau and anti-CoA antibodies showed co-localization of both antibodies within NFTs. This data encouraged us to demonstrate CoAlation of recombinant 2N4R and 2N3R tau isoforms, which was subsequently confirmed by mass spectrometry to occur at the conserved cysteine residue (Cys322 of 2N4R and Cys291 of 2N3R tau isoforms). Furthermore, reversible H_2O_2-induced dimerization of recombinant 2N3R, but not 2N4R isoform was reproducibly observed and shown to be completely inhibited by *in vitro* CoAlation. We have also found that transiently overexpressed tau is CoAlated in HEK2093/Pank1β cells treated with the thiol-oxidizing agent diamide. Considering the importance of cysteines in tau acetyl-transferase activity, we speculate that CoAlation of Cys322 would inhibit this function. Further, since the conserved cysteine residue is located within the microtubule binding region, tau CoAlation may potentially modulate its binding to microtubules and/or form a new binding site for regulatory interactions in redox signaling. Overall, CoAlation of tau may protect redox-sensitive cysteine 322 from irreversible overoxidation, modulate its acetyl-transferase activity and regulatory interactions.

MATERIALS AND METHODS

Materials

All chemicals were purchased from Sigma–Aldrich unless otherwise noted here. Anti-CoA monoclonal antibody was produced via hybridoma cell line 1F10 (Malanchuk et al., 2015) and used in following dilutions (1:200 for IHC and 1:6,000 in WB). Biotinylated anti-mouse or anti-rabbit, respectively (both 1:200; Invitrogen). Monoclonal anti-tau (1:200 for IHC) was purchased from Thermo Fisher Scientific. All cell lines were purchased from American Tissue Culture Collection (ATCC, Manassas, VA, United States). Alexa Fluor 555- and 647-conjugated secondary antibodies (1:10,000 for WB) were purchased from Invitrogen.

Brains were donated to the Queen Square Brain Bank (QSBB) for neurological disorders (UCL Queen Square Institute of Neurology). All tissue samples were donated with the full, informed consent. Accompanying clinical and demographic data of all cases used in this study were stored electronically in compliance with the 1998 data protection act and are summarized in **Table 1**. Ethical approval for the study was obtained from the NHS research ethics committee (NEC) and in accordance with the human tissue authority's (HTA's) code of practice and standards under license number 12198.

All cases were diagnosed pathologically according to current consensus criteria (Montine et al., 2012; Kovacs, 2015). The cohort included pathologically diagnosed cases of AD (n = 15), CBD (n = 5), PSP (n = 5), MSA (n = 5), PD (n = 5), and neurologically normal controls (n = 5). The control cases used in this study had no clinical symptoms of a neurodegenerative disease reports, however, they all had a certain degree of Aβ and tau deposition (**Supplementary Table 1**).

Methods

Immunohistochemistry

A total of 8 μm paraffin-embedded formalin-preserved tissue sections were cut from the hippocampus and temporal cortex. Routine IHC was performed on sequential sections using anti-tau and anti-CoA, an in-house developed monoclonal antibody. In brief, tissue sections were de-waxed in xylene and rehydrated through various alcohol concentrations, then pre-blocked using methanol and hydrogen peroxide to prohibit endogenous peroxidase activity. Antigen retrieval was carried out by pressure cooking slides in pH 6.0 citrate buffer. A solution of 10% milk/TBS-T was used to prevent non-specific antigen/antibody binding. Tissue sections underwent incubation with primary antibody anti-CoA (1:200; inhouse) or anti-tau (1:200; Invitrogen) for 1 h at room temperature, followed by biotinylated anti-mouse secondary antibody (1:200; DAKO) and finally avidin-biotin complex (ABC), both for 30-min incubations. Di-aminobenzidine (DAB) was used as the chromogen. Sections were counterstained in Mayer's hematoxylin, dehydrated, cleared, and mounted.

Double Staining Immunohistochemistry

After identical initial pre-treatments to routine IHC, tissue samples were similarly incubated with anti-CoA (1:200; inhouse), biotinylated anti-mouse (1:200; DAKO), and ABC. This was followed by 20 min incubation with Tyramide Signal Amplification (TSA) Red. Samples were then incubated with anti-tau polyclonal antibody (1:200; Invitrogen) and Alexa Fluor 488 Anti-Rabbit (1:1000; Invitrogen) for one and 2 h respectively at room temperature. 4′-6-diamidino-2-phenylindol (DAPI) was used to counterstain nuclei (1:1000; Vector) before slides were viewed under Leica confocal fluorescent microscope.

Quantitation of Neurofibrillary Tangles

The number of CoA and Tau positive NFTs were quantitated in the second frontal gyrus gray matter from the AD cases. IHC sequentially stained slides were scanned using an Olympus Slide Scanner at x20 magnification. Regions of interest were extracted from the digital images and the number of NFTs counted. The numbers of NFTs were then corrected for area (number of NFTs per mm^2). The percentage of CoA positive NFTs were then calculated against the number of tau positive NFTS.

Purification of Recombinant 2N3R and 2N4R Tau Isoforms

Recombinant 2N4R and 2N3R tau isoforms were purified as described in Ferrari and Rüdiger (2018). Briefly, Rosetta (DE3) cells containing pSUMO-Flag 2N4R or 2N3R tau plasmid were grown in YT medium supplemented with 10 mg/L of kanamycin (Sigma-Aldrich) and 33 mg/L of chloramphenicol (Sigma-Aldrich), until OD_{600} reached 0.8. Subsequently, 2N4R and 2N3R tau expression was induced with 0.15 mM IPTG followed by incubation at 18°C for 16 h. Cells were then harvested, and the pellets were resuspended in lysis buffer (50 mM HEPES pH 8.5, 50 mM KCl, half a tablet of EDTA-free protease inhibitor (Roche), 5 mM β-mercaptoethanol). The cells were lysed and centrifuged, to remove cell debris. The

TABLE 1 | Summarized case demographic data for the post-mortem cases used in the study.

Case ID	AAO (years)	AAD (years)	DD (years)	Sex	Path diagnosis	PM delay (hours)	Brain weight (g)	Braak Tau	Thal	CERAD	ABC score
1	59	74	15	F	AD	102:55:00	1265	6	4	3	A3B3C3
2	59	76	17	F	AD	60:25:00	1191	6	5	3	A3B3C3
3	60	71	11	M	AD	52:39:00	1327	6	3	3	A2B3C3
4	74	79	5	F	AD	60:40:00	1200	6	5	3	A3B3C3
5	52	68	16	M	AD	73:45:00	1234	6	5	3	A3B3C3
6	55	67	12	M	AD	28:35:00	1015	6	5	3	A3B3C3
7	72	88	16	M	AD	58:10:00	1084	6	5	2	A3B3C2
8	63	73	10	M	AD	31:10:00	1269	6	5	3	A3B3C3
9	49	62	13	F	AD	76:40:00	996	6	5	3	A3B3C3
10	63	74	11	M	AD	33:26:00	1022	6	5	3	A3B3C3
11	48	61	13	M	AD	40:40:00	1650	6	5	3	A3B3C3
12	58	72	14	F	AD	81:26:00	820	6	5	3	A3B3C3
13	48	63	15	M	AD	31:42:00	1042	6	5	3	A3B3C3
14	51	69	18	F	AD	81:00:00	1056	6	5	3	A3B3C3
15	54	65	11	M	AD	34:25:00	1089	6	5	3	A3B3C3
16	na	103	na	F	Control	26:35:00	975	4	5	1	A3B2C1
17	na	88	na	M	Control	27:30:00	1330	4	3	2	A2B2C2
18	na	83	na	M	Control	105:28:00	1244	4	3	2	A2B2C2
19	na	92	na	M	Control	46:15:00	1213	4	3	2	A2B2C2
20	na	91	na	F	Control	69:20:00	1311	4	4	2	A3B2C2
21	60	68	8	F	PSP	36:50:00	1177	1	1	0	A1B1C0
22	75	84	9	F	PSP	70:00:00	1095	0	3	1	A2B0C1
23	76	84	8	M	PSP	50:00:00	1370	0	4	1	A3B0C1
24	57	62	5	M	PSP	72:20:00	1369	5	5	2	A3B3C2
25	66	79	13	F	PSP	73:55:00	1141	0	3	1	A2B0C1
26	58	65	7	M	CBD	48:04:00	1232	0	0	0	A0B0C0
27	54	61	7	M	CBD	102:30:00	1389	0	0	0	A0B0C0
28	58	69	11	F	CBD	103:15:00	917	0	0	0	A0B0C0
29	57	64	7	M	CBD	41:25:00	1456	0	0	0	A0B0C0
30	63	69	6	M	CBD	81:36:00	1291	0	2	1	A1B0C1
31	60	84	24	M	PD	71:05:00	1484	2	1	0	A1B1C0
32	80	89	9	M	PD	26:45:00	1493	4	4	2	A3B2C2
33	69	78	9	M	PD	95:15:00	1600	2	5	2	A3B1C2
34	77	83	6	M	PD	96:25:00	1644	1	3	1	A2B1C1
35	65	78	13	F	PD	84:50:00	1203	1	1	0	A1B1C0
36	67	75	8	M	MSA	54:00:00	1359	1	1	0	A1B1C0
37	46	52	6	F	MSA	79:00:00	1354	1	0	0	A0B1C0
38	33	42	9	M	MSA	30:10:00	1380	0	0	0	A0B0C0
39	63	72	9	M	MSA	82:00:00	1450	1	0	0	A0B1C0
40	57	63	6	M	MSA	102:55:00	1234	0	2	0	A1B0C0

Detailing the number of cases used for each neurodegenerative disease; Alzheimer's disease (AD), Progressive supranuclear palsy (PSP), coricobasal degeneration (CBD), Parkinson's disease (PD), and Multiple system atrophy (MSA). Detailing the mean age at disease onset (AAO), mean age at death (AAD), disease duration (DD), mean hours to post-mortem (PM), and the brain weight.

lysates were loaded onto a POROS 20MC affinity purification column, with a column, and the proteins were eluted with a 0–100% gradient of 0.5 M imidazole. Fractions of interest were loaded onto a POROS 20HQ anion exchange column. The proteins were then eluted using a 0–100% linear gradient of 1 M KCl, which was then repeated using a POROS 20HS column for cation exchange of fractions of interest. The final fractions were concentrated (Vivaspin, cut-off 5 kDa), and stored at −20°C with DTT.

In vitro CoAlation of Recombinant 2N3R and 2N4R Tau Isoforms

Prior to the *in vitro* CoAlation assay of the 2N3R and 2N4R tau isoforms, the proteins were incubated for 30 min at room temperature with DTT (10 mM). Micro Biospin 6 columns (BioRad), equilibrated with 1X PBS, were used to remove excess of DTT. 2N3R and 2N4R tau isoforms (8 μM) were incubated (40 min, 25°C) with H_2O_2 (200 μM) in the presence or absence of CoA (70 μM). To stop the reaction, 5 mM N-ethyl maleimide

(NEM) was added, and the samples were incubated for 10 min at 25°C. NEM is a thiol alkylating agent.

To study the reversibility of tau CoAlation or dimerization, two additional samples were prepared. Following oxidation and/or CoAlated of the 2N3R and 2N4R tau isoforms, 5 mM DTT (reducing agent) was added to each sample. The samples were then incubated for 10 min at 25°C. The reaction was stopped by the addition of NEM. Following alkylation with NEM, the samples were boiled in 1X non-reducing loading buffer and separated by SDS-PAGE.

Anti-CoA Western Blot Analysis of CoAlated 2N3R and 2N4R Tau Isoforms

Resolved proteins were transferred to low-fluorescence polyvinylidene fluoride (PVDF) membranes (BioRad) according to manufacturer's instruction. Membranes were blocked in LiCor blocking buffer for 30 min at room temperature (RT), then washed three-times for 3 min in 1X Tris-buffered saline with 0.05% tween-20 (TBS-T). The membranes were then incubated overnight at 4°C with mouse anti-CoA monoclonal antibodies (mAbs) (1:6,000). The membranes were then washed three-times for 3 min with 1X TBS-T, and incubated for 30 min at RT with goat anti-mouse AlexaFluor680 antibodies (1:10,000). Washing was repeated three-times for 3 min in 1X TBS-T then again in 1X TBS. Fluorescence signal at 702 nm was measured using LiCor Odyssey-CLx.

Liquid Chromatography-Tandem Mass Spectrometry Analysis of CoAlated 2N3R and 2N4R Tau Isoforms

Reduced 2N3R and 2N4R tau isoforms (10 μM) were incubated for 30 min at 25°C with H_2O_2 (100 μM) in the presence of CoA (100 μM). To stop the reaction, 5 mM N-ethyl maleimide (NEM) was added, and the samples were further incubated for 10 min at 25°C. Excess CoA, H_2O_2 and NEM were removed by desalting using the MicroBiospin6 columns. The samples were then analyzed by MS.

The LC-MS/MS analysis of CoAlated peptides was carried out as described previously (Brass et al., 1990; Dusi et al., 2014). Briefly, the samples predicted to contain CoAlated tau were tryptic digested, and the peptides were analyzed by nano-scale capillary liquid chromatography-tandem mass spectrometry (LC-MS/MS) using an Ultimate 3000 RSLC System (Thermo Fisher Scientific) integrated with a 100 μm × 2 cm PepMap100 C_{18} nano-trap column and an EASY-Spray PepMap RSLC C_{18} 2 μm, 25 cm × 75 μm analytical column (Thermo Fisher Scientific). Nano-flow electrospray ionization was used to directly spray peptides eluted by an acetonitrile gradient into the Q Exactive Orbitrap mass spectrometer (Thermo Fisher Scientific). Operated in data-dependent mode, the mass spectrometer utilized an Orbitrap analyzer with a resolution of 35,000 at mass-to-charge ratio (m/z) of 200. Subsequently, MS/MS of the 10 most intense ions were acquired. Maximum accumulation time for MS full scan and MS2 were set at 50 and 100 ms, respectively. Internal calibration of Orbitrap measurements involved the lock mass of polydimethylcyclosiloxane at m/z 445.120025. MaxQuant v1.6.6.0 was used to process LC-MS/MS raw data files (Cox and Mann, 2008). Processed data were searched against Human (2019) UniProt protein databases[1]. Carbamidomethyl cysteine, Acetyl N-terminal, N-ethylmaleimide cysteine, oxidation of methionines, and CoAlation of cysteine with delta mass 356 and 765, were set as variable modifications. All data sets used default MaxQuant parameters with the second peptide ID remaining unselected.

Generation of the pEGFP-N1/His-2N4R Plasmid

6xHis-tag sequence was introduced at the N-terminus of WT 2N4R *tau* (pEGFP-N1 plasmid) to generate the His-2N4R tau-pEGFP-N1 plasmid. Using phosphorylated Fw (5′-ATGGGCAGCCAT CATCATCATCATCACAGCGGCATGGCTGAGCCCCGCCA G-3′) and Rv (5′-GGTGGCAGA TCTGAGTCCGGTAGC-3′) primers, the plasmid was amplified and an overhang with the His-tag sequence was introduced. T4 DNA ligase (Thermo Fisher Scientific) was used to circularize the plasmid, which was then electroporated in *E. coli* Top10 cells. The plasmid was then amplified and purified. The integration of the 6xHis-tag at the N-terminus of the 2N4R *tau* within the pEGFP-N1 plasmid was confirmed by DNA sequencing. The presence of a stop codon at the C-terminus of 2N4R *tau* prevents the expression of downstream GFP sequence in the pEGFP-N1 plasmid.

Mammalian Cell Culturing, Transfection, and Treatment With Diamide

In this study, we used HEK293 cells with stable overexpression of Pank1β. Overexpression of this rate-limiting enzyme in CoA biosynthesis increases the level of CoA to that observed in primary cell lines (rat primary cardiomyocytes) and rat tissues (liver, heart, or kidney) (Tsuchiya et al., 2017). The increase in CoA level in HEK293/Pank1β cells results in significant increase of protein CoAlation in response to oxidative or metabolic stress (Tsuchiya et al., 2017, 2020; Bakovic et al., 2019; Yu et al., 2021). HEK293/Pank1β cells were maintained in DMEM (Dulbecco's Modified Eagle Medium) supplemented with fetal bovine serum (10% – FBS, Gibco), penicillin (50 U/mL) and streptomycin (0.25 μg/mL – Lonza) at 37°C and 5% CO_2. Around 0.6 million cells were seeded onto 60 mm plates, and at ∼60% confluency, the cells were transiently transfected with pEGFP-N1/His-2N4R *tau* plasmid using XtremeGene HP transfection reagent (Roche), according to the manufacturer's protocol. After 24 h, cells were primed for oxidative stress by changing the medium to pyruvate and glucose-free DMEM (10% FBS) supplemented with 5 mM glucose. After 18 h of culturing, cells were treated with diamide (500 μM) for 30 min at 37°C. After harvesting, cells were lysed on ice for 20 min in lysis buffer [50 mM Tris pH 7.5, 150 mM NaCl, 5 mM EDTA, 50 mM NaF, and 5 mM sodium pyrophosphate, 1% triton X-100, 1X PIC (cOmplete mini protease inhibitor cocktail), and 25 mM NEM]. Following centrifugation, 30 μg of lysate was mixed/boiled with SDS-PAGE loading dye, and the rest of the lysate was incubated overnight at 4°C with nickel-NTA beads equilibrated in wash buffer (lysis buffer without PIC and NEM). The beads were then washed 3 times with lysis buffer and mixed/boiled with SDS-PAGE loading dye. Immunoblotting

[1]https://www.uniprot.org/uniprot/

with mouse anti-CoA (1:6,000) and mouse anti-tau12 (Merck) (1:5,000) was performed as described earlier.

RESULTS

Optimization of Anti-CoA Immunohistochemistry

Recent discovery of the antioxidant function of CoA and the development of anti-CoA monoclonal antibody 1F10, which works efficiently in various immunological approaches (Malanchuk et al., 2015), prompted us to investigate its suitability for immunohistochemical (IHC) analysis of post-mortem human tissues. In previous studies, we showed that 1F10 antibody specifically recognizes in Western blotting CoA covalently bound to proteins via a disulfide bond in mammalian cells and tissues, exposed to oxidative or metabolic stress (Tsuchiya et al., 2017, 2018). Moreover, this antibody is also efficient in immunoprecipitating CoAlated peptides, when employed for the identification of CoA-modified proteins by mass spectrometry (Malanchuk et al., 2015).

In this study, our efforts were focused on examining the suitability of 1F10 antibody for IHC analysis of protein CoAlation in pathologies associated with oxidative stress. Initial optimization studies of 1F10 antibody were carried out in post-mortem NBIA brain samples and age-matched controls with no cognitive impairment. Several pre-treatments were tested (no pre-treatment, pressure cooking in citrate buffer pH6.0, proteinase K and formic acid) to determine the best pre-treatment and this was paired with titrating the antibodies concentration for optimum staining. We determined that pre-treating the section in a pressure cooker and using the antibody at 1:200 ratio, gave the optimum staining intensity compared to background staining in formalin fixed paraffin embedded tissue.

Using optimized IHC conditions (**Figure 1**), we observed readily detectable anti-CoA immunoreactive signal in NBIA brain samples located predominantly in the neuronal and glial nuclei, as well as cytoplasmic staining in the larger neurons in the gray matter (**Figure 1A** and insert). In contrast, anti-CoA immunoreactivity of age-matched controls demonstrated very little nuclear staining (**Figure 1B**).

Anti-CoA Immunohistochemistry of Post-mortem Brain Tissues of Patients With Various Neurodegenerative Pathologies

Following the optimization studies and the positive IHC staining found in the NBIA brain samples, we investigated the profile of anti-CoA immunoreactivity in brain tissues from several neurodegenerative diseases and age-matched controls. These included AD, Corticobasal Degeneration (CBD), Progressive Supranuclear Palsy (PSP), Multiple System Atrophy (MSA), and Parkinson's disease (PD). Brain regions where the majority of pathology is exhibited in each disease were analyzed, including frontal cortex, temporal cortex, hippocampus, basal ganglia, upper midbrain, and anterior cingulate.

The IHC analysis showed that other neurodegenerative diseases exhibited varying degrees of positive immunoreactivity with anti-CoA, which was typically seen in different pathological structures within the brain tissue. In a small subset of PD samples (15%), positive anti-CoA staining of structures resembling Lewy body (**Figure 1C** and insert) were present in the anterior cingulate and upper midbrain. No anti-CoA immunoreactivity was observed in either gray or white matter in MSA (**Figure 1D**) or in any of the PSP cases. In 20% of CBD samples, anti-CoA immunoreactive staining was primarily observed in the neuronal axons in the white matter of basal ganglia samples (**Figure 1E**).

Anti-CoA immunoreactive signal was observed in AD brain samples (frontal cortex) in structures resembling neuropil threads and NFT's (**Figures 1G–I**, arrows).

Analysis of Anti-CoA Immunoreactivity in Alzheimer's Disease Brain Samples

The anti-CoA immunoreactivity was detected in all brain regions, apart from the basal ganglia, in AD brain samples. When compared to control samples (**Figure 1B**), anti-CoA immunoreactivity in AD brain samples was detected consistently in assemblies resembling NFT's and neuropil threads, both of which are characteristic pathophysiological markers of AD (**Figure 1F**). The immunoreactive signal was observed in frontal cortex (**Figure 1G**), temporal cortex (**Figure 1H**), and hippocampus (**Figure 1I**) but not in the basal ganglia. Taking into account that the structures stained with anti-CoA antibody resembled tau-positive NFT's, the same cases and brain regions were analyzed using anti-tau antibody (**Figure 1F**) and showed strong immunoreactivity, including in structures similar to NFT.

To investigate whether anti-CoA and anti-tau immunoreactive signals co-localize in NFTs, double staining IHC of AD brain samples with tau and CoA antibodies was carried out. Immunoreactivity with anti-CoA (**Figures 1K,N**) and anti-tau (**Figures 1J,M**) was clearly observed and immunofluorescent co-localization of the two antibodies within NFT structures was revealed, demonstrated by the yellow immunofluorescent signals (**Figures 1L,O**). Notably, antibody co-localization was not seen with the same intensity at every instance where anti-tau had bound to NFT proteins (**Figures 1M–O**, asterisks), suggesting CoAlation of NFTs is not uniform or an inevitable PTM in these structures. Quantitative analysis was undertaken to assess the number of CoA positive NFTs compared to the number of tau positive NFTs (**Figures 2A,B**). NFTs were counted in the frontal gray matter. In all AD cases a large proportion of NFTs were found to be CoA positive. The average number of CoA positive NFTs per mm^2 was 10 and the average number of Tau positive NFTs was 22 per mm^2, equating on average to around 50% of tau positive NFTs were also CoA positive.

2N3R and 2N4R Tau Isoforms Are CoAlated *in vitro*

In this study, we used 2N3R and 2N4R tau isoforms, which are distinguished only by the configuration of their microtubule-binding repeat domains. Within the second and third microtubule-binding repeat domains (R2 and R3,

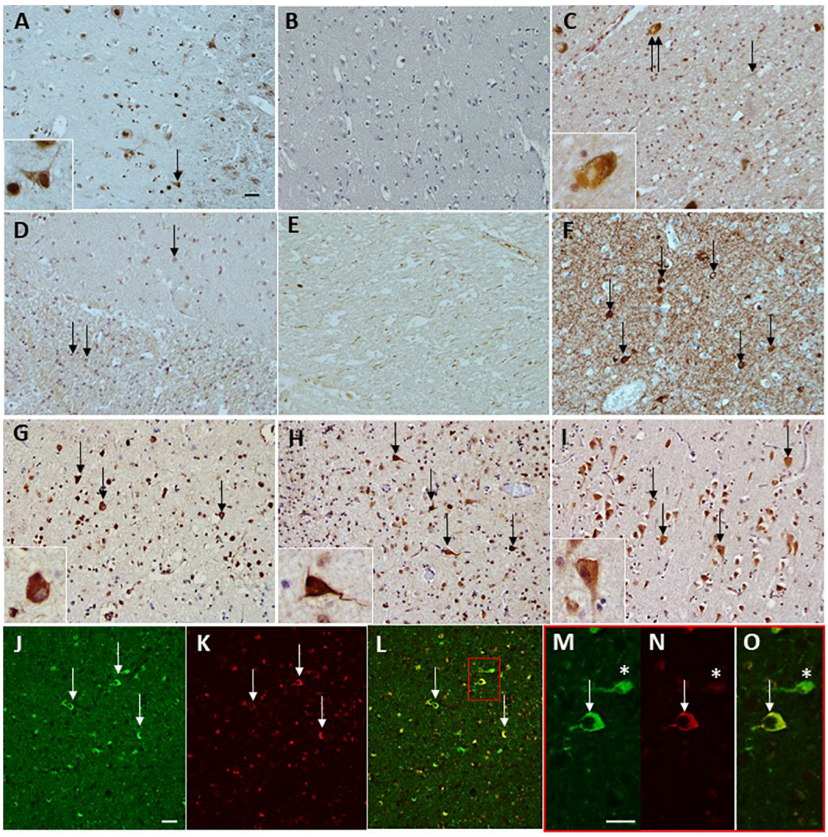

FIGURE 1 | Immunohistochemical staining of anti-CoA and tau antibodies in neurodegenerative diseases. CoA deposition is found in a case with NBIA **(A)** used as a positive control for the immunohistochemical preparations. No CoA immunoreactivity was observed in a neurologically normal control without the presence of tau pathology **(B)**. CoA immunoreactivity was observed in PD, in the occasional Lewy body (**C**, double arrow and insert), as well as the occasional Lewy neurite (**C**, arrow). No CoA immunoreactivity was observed in either MSA white matter (WM) or gray matter (GM). Both PSP and CBS were negative for CoA in the frontal and temporal cortices. However, axonal CoA staining was observed in the basal ganglia in CBD **(E)**. Tau immunohistochemistry demonstrating the level of tau pathology in the form of neurofibrillary tangles (**F**, arrows) surrounded by neuropil threads in an AD case. CoA immunohistochemistry in AD also shows positivity in the neurofibrillary tangles in the frontal cortex (**G**, arrows and insert), temporal cortex (**H**, arrows and insert), and CA1 subregion of the hippocampus (**I**, arrows and insert). Double immunohistochemical staining with CoA (red; **K,N**) and tau (green; **J,M**) shows co-localization of the two proteins (arrows, **L**) and at higher magnification **(O)**, but also reveals neurofibrillary tangles that are negative for CoA (asterisks, **M–O**). Bar in a represents 50 μm in panels **(A–L)**, inserts 20 μm. Bar in panels **(J,M)** represents 50 μm. PD, Parkinson's disease; MSA, multiple system atrophy; AD, Alzheimer's disease; PSP, progressive supranucelar palsy; CBD, corticobasal degeneration.

respectively) are one or two naturally occurring cysteine residues (according to nomenclature of the longest tau isoform, Cys291 and Cys322, respectively) (**Figure 3A**). 2N3R tau does not possess the second repeat domain (R2) and therefore only contains the cysteine within R3, which is at position 291. 2N3R Cys291 and 2N4R Cys322 are therefore structurally equivalent and highly conserved (**Figure 3A**).

We expressed and purified 2N3R and 2N4R tau proteins, which were used in the *in vitro* CoAlation assays. The *in vitro* tau CoAlation reaction was carried out in the presence of H_2O_2 and CoA, and the samples were then separated by SDS-PAGE under non-reducing conditions and immunoblotted with anti-CoA 1F10 antibody. Both 2N3R and 2N4R tau proteins were found to be efficiently CoAlated *in vitro* (**Figure 3B**). Both isoforms were predominantly CoAlated in the monomeric state, but low level of CoA-modified 2N4R dimer was also detected. Mass spectrometry analysis of CoAlated samples revealed one CoA-modified peptide (C*GSLGNIHHKPGGGQVEVK) in both 2N3R and 2N4R isoforms (**Figure 3C**). Cys322 was CoAlated in 2N4R isoform, and Cys291 in the 2N3R isoform. Multiple sequence analysis of 2N3R and 2N4R tau isoforms (data not shown) revealed this CoAlated cysteine residue to be the ubiquitously conserved cysteine across all isoforms of tau, and present within R2 and R3 of 2N3R and 2N4R tau, respectively.

Diamide-Induced Oxidative Stress Causes CoAlation of His-2N4R Tau in HEK293/Pank1β Cells

To explore the role of tau CoAlation *in vivo*, HEK293/Pank1β cells transiently over-expressing His-2N4R tau were incubated with or without diamide as described in M&M. His-2N4R tau was pulled-down from lysed cells using Nickel-NTA beads. The pulled-down protein was then mixed/boiled with SDS-PAGE

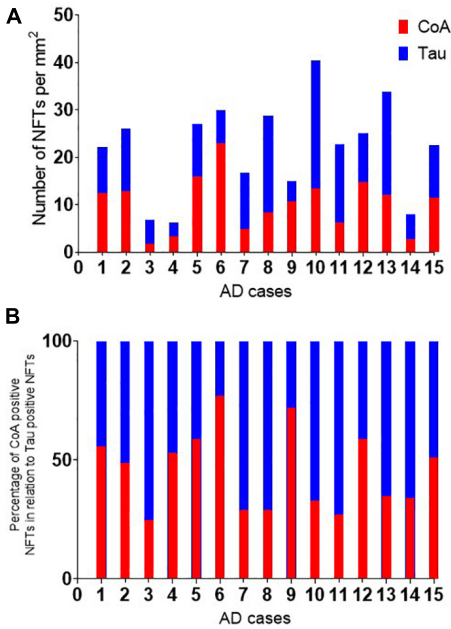

FIGURE 2 | Quantitative analysis of Tau and CoA positive neurofibrillary tangles. The number of neurofibrillary tangles (NFTs) positive with tau and CoA immunohistochemistry were quantitated in the frontal cortex of Alzheimer's disease cases. The number of NFTs were counted in a region of interest in the frontal gray matter and corrected per mm^2. **(A)** The percentage of CoA NFTs relative to the number of tau positive NFTs are shown in panel **(B)**.

loading dye, and separated on SDS-PAGE gel under non-reducing conditions. Anti-tau12 and anti-CoA Western blots were performed to visualize the expression and pull-down efficiency of His-2N4R tau, and the pattern of CoAlation in analyzed samples. As shown in **Figure 3D**, His-2N4R tau is efficiently expressed in HEK293/Pank1β cells and pulled-down on Nickel-NTA beads. We have reproducibly observed CoAlation of His-2N4R tau in samples prepared from diamide-treated HEK293/Pank1β cells. Interestingly, a significant increase in tau oligomerization was detected in cells exposed to diamide, when compared to non-treated controls.

Reversible *in vitro* CoAlation of 2N3R Prevents H_2O_2-Induced Tau Dimerization

To further understand the role of CoA and tau CoAlation in the presence of H_2O_2, which is a strong oxidant, we analyzed the oligomerization and CoAlation states of the H_2O_2-treated 2N3R and 2N4R tau isoforms in the presence and absence of CoA (**Figures 4A,B**). H_2O_2-induced dimerization of the 2N3R tau isoform is reproducibly observed and mediated via the formation of an intermolecular disulfide bond (**Figure 4A** – Sample 2). On the other hand, 2N4R tau isoform, showed a weaker dimerization band (**Figure 4B** – Sample 2), as it may be more likely to engage in intramolecular disulfide bond formation due to the proximity of the two cysteine residues (Cys291 and Cys322) within the MTBR.

To determine whether CoAlation of the 2N3R tau isoform interferes with its dimerization, the protein was incubated with H_2O_2 in the presence of CoA. Interestingly, H_2O_2-induced 2N3R dimerization is nearly completely inhibited in the presence of CoA (**Figure 4A** – Sample 3). With anti-CoA WB, we show that the latter monomeric band of 2N3R tau is strongly CoAlated (**Figure 4A** – Samples 3 and 3′). This may indicate that CoAlation protects 2N3R tau from disulfide bond-mediated dimerization. For the 2N4R tau isoform, both the monomeric (major form) and dimeric (minor form) bands showed CoAlation in the presence of H_2O_2 and CoA (**Figure 4B** – Sample 3′). As the dimeric 2N4R tau contains free thiols, CoAlation could occur on these residues. Overall, we showed that both 2N3R and 2N4R tau isoforms are CoAlated in the presence of H_2O_2, but 2N3R tau dimerizes more readily compared to 2N4R isoform. These findings suggest that CoA may have a protective role against H_2O_2-induced overoxidation of cysteine residues in tau.

To determine whether CoAlation of 2N3R and 2N4R tau isoforms in the presence of H_2O_2 is a reversible modification, CoAlated proteins were treated with excess of DTT, which is a reducing agent. For the case of the H_2O_2-treated 2N3R tau isoform, the dimerization band was completely shifted to its monomeric form (**Figure 4A** – Sample 4). DeCoAlation of 2N3R and 2N4R isoforms was also observed in the presence of DTT (**Figures 4A,B** – Samples 5 and 5′). Overall, these results suggest that CoAlation has a potential to protect the cysteine residues of tau from oxidative damage and the formation of intermolecular disulfide bond-mediated dimerization.

DISCUSSION

The antioxidant function of CoA and protein CoAlation have recently emerged as a novel mechanism of redox regulation in health and disease. The development of highly specific anti-CoA mAb and a reliable MS-based methodology allowed the identification of over 1400 CoAlated proteins in mammalian cells and tissues exposed to oxidative or metabolic stress. In this study, we report that anti-CoA immunoreactivity is readily observed by IHC in several neurodegenerative diseases, including NBIA and Parkinson's disease, but with a substantial prevalence in AD. Utilizing anti-CoA mAb for the first time on post-mortem formalin fixed tissue, extensive protein CoAlation was detected in tau positive pathological structures in several brain regions in AD in contrast to control brain samples. Double immunohistochemical staining with tau and CoA antibodies in AD brain tissue revealed co-localization of the two immunoreactive signals in a proportion of NFTs, suggesting that protein CoAlation takes place during the maturation of the NFTs. We have also shown that recombinant 2N3R and 2N4R tau isoforms are CoAlated *in vitro* and the site of CoAlation mapped by mass spectrometry to the conserved cysteine residue among the tau isoforms. Furthermore, H_2O_2-induced oxidation can cause the dimerization of 2N3R, which was inhibited in the presence of both H_2O_2 and CoA. This could suggest a protective role of CoA against H_2O_2-induced oxidation and dimerization of tau. Therefore, we propose that covalent tau modification by CoA has a potential to protect tau cysteine residues from irreversible overoxidation.

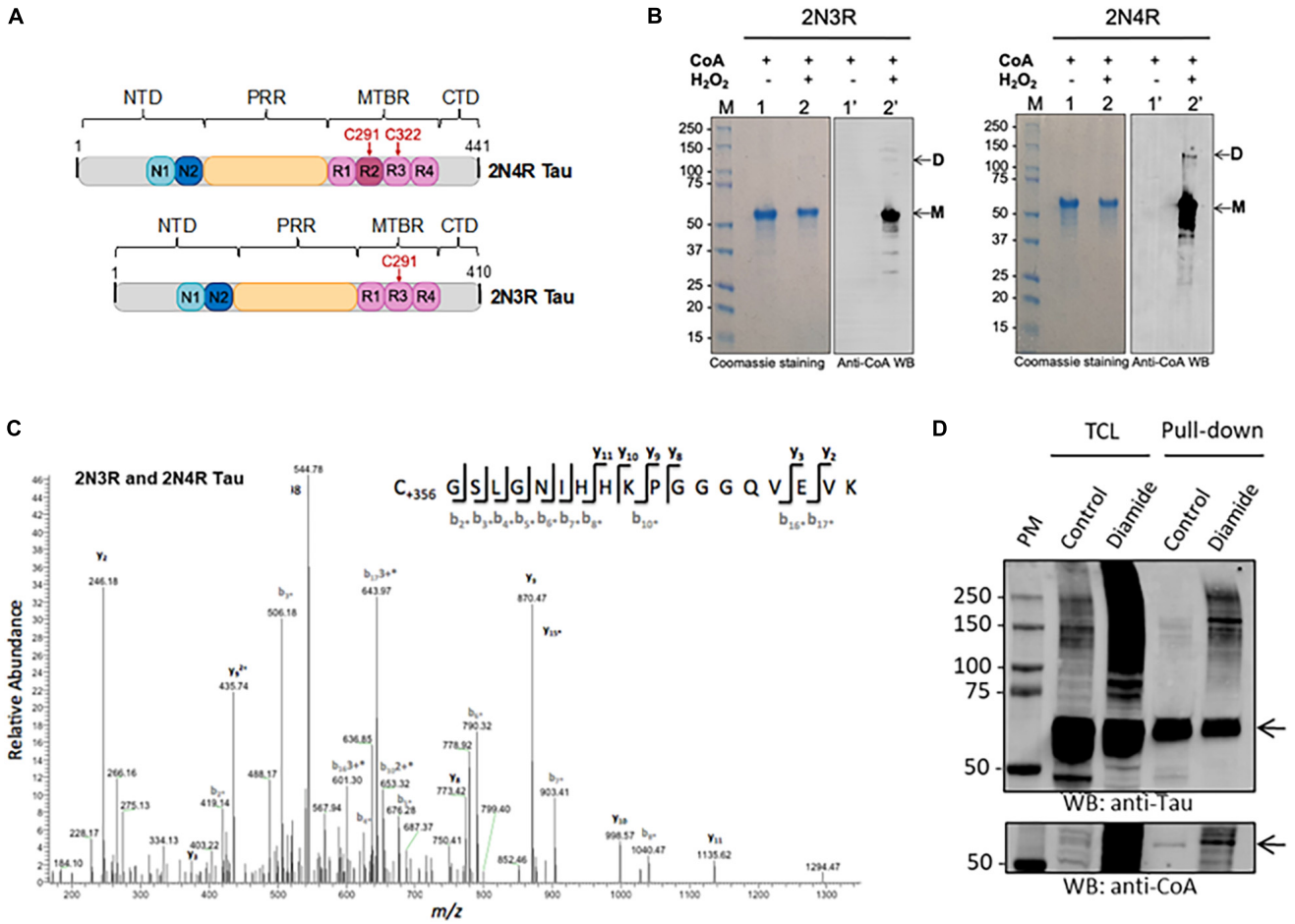

FIGURE 3 | Analysis of tau CoAlation *in vitro* and *in vivo*. **(A)** Schematic diagram of human 2N4R and 2N3R tau isoforms (441 and 410 amino acids in length, respectively). N-terminal inserts, proline rich region (PRR), and microtubule-binding region (MTBR) are shown in blue, yellow, and pink, respectively. Conserved cysteine residues within MTBR are indicated in red. 2N3R tau lacks the second MTBR and thus only features the conserved cysteine residue (in this case, Cys291). N- and C-terminal domains (NTD and CTD, respectively) are shown in gray. **(B)** *In vitro* CoAlation of recombinant 2N4R and 2N3R tau isoforms occurs following exposure to hydrogen peroxide. Lane L indicates protein molecular weight marker. Lanes 1 and 1′ contain reduced tau in the presence of CoA. Lanes 2 and 2′ contain H_2O_2- and CoA-treated tau. CoAlated tau remains largely monomeric (M) yet CoAlated dimers are also present for 2N4R **(D)**. **(C)** Mass spectrometry analysis of the CoAlated peptide (C*GSLGNIHHKPGGGQVEVK) indicates covalent modification of cysteine (C_{+356}) by CoA at the conserved cysteine residue (Cys322 and Cys291 in 4R and 3R tau, respectively). **(D)** Transiently overexpressed His-2N4R tau is CoAlated in HEK293/Pank1β cells exposed to diamide-induced oxidative stress. Total cell lysates and Ni-NTA pulled-down proteins were separated by SDS-PAGE under non-reducing conditions and immunoblotted with anti-CoA and anti-tau12 antibodies. The position of His-2N4R tau in total lysates and pulled-down samples is shown with the arrow. Oligomerization of His-2N4R tau in total lysates and pulled-down samples readily detected with anti-Tau antibodies. TLC, total cell lysate; Pull-down, the use of Ni-NTA affinity beads to pull-down His-tag fusion proteins from cell lysates.

The identification of CoAlation in NFTs raises more questions for extensive further studies. One key aspect to be addressed is that the double IHC staining revealed that CoA did not co-localize with every NFT. Speculation for the consequences of tau CoAlation can be drawn from what is known about existing PTMs that target and regulate this protein. Tau undergoes a plethora of modifications that are critical to its regulation and localization in AD brains, including – but not limited to – polyubiquitination, O-glycosylation, glycation, oxidation and phosphorylation, the latter of which has been most extensively reported (Gong et al., 2005). Indeed, in AD hyperphosphorylation of tau confers profound biological consequences. Tau contains an abundance of potential phosphorylation sites, including 80 serines/threonines and 5 tyrosines (Vasili et al., 2019). The addition of phosphoryl groups at these sites contributes to the loss of physiological tau function and its gain in toxicity as it self- assembles into PHFs mixed with straight filaments, aggregating into NFTs (Iqbal et al., 2010; Miao et al., 2019). It has been shown *in vitro* that prolong oxidative stress can increase tau phosphorylation (Martin et al., 2011). Therefore, it seems logical to postulate that during oxidative stress, the level of tau CoAlation would simultaneously increase. Existing research on tau oxidation is limited, but the assembly of PHFs *in vitro* and *in vivo* was found to be promoted by the oxidation of tau. In the largest human tau isoform (2N4R) oxidation has been reported at cysteine 322, which is localized

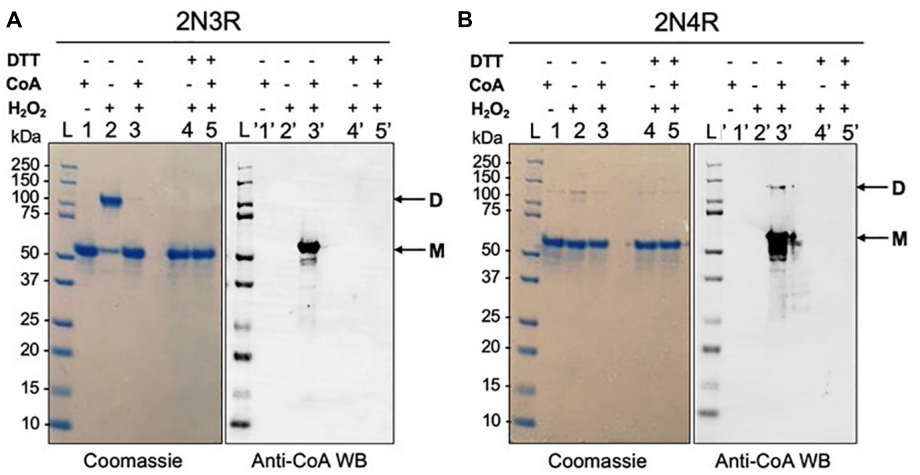

FIGURE 4 | H_2O_2-induced dimerization of 2N3R tau isoform is inhibited by CoAlation. **(A)** H_2O_2-treatment of 2N3R tau causes its dimerization (Lane 2 – D). In the presence of CoA and H_2O_2, 2N3R becomes *in vitro* CoAlated (Lane 3′), and its dimerization is inhibited (Lane 3 – M). In the presence of DTT, both dimerization and CoAlation of 2N3R tau are inhibited (Lanes 4, 4′, 5 and 5′ – M). **(B)** H_2O_2-treatment of 2N4R tau shows only a minor dimerization band (Lane 2and 2′ – M and D), probably due to the formation of intramolecular disulfide bond formation, rather than an intermolecular disulfide formation. H_2O_2 and CoA-treated 2N4R tau shows CoAlation (Lane 3′ – M and D). In the presence of DTT, CoAlation is absent (Lane 5′). Lane L represents the molecular weight marker, and lane 1 represents the reduced form of 2N3R and 2N4R tau isoforms in the presence of CoA, where CoAlation is not observed (Lane 1′).

in the R3 repeat domain of the microtubule binding domain region (Martin et al., 2011). Given the location of the cysteine residue in the microtubule binding domain, it could be plausible that the covalent attachment of CoA causes disruption to the association of tau to microtubules, diminishing its stabilizing effects and contributing to AD etiopathogenesis (as is seen in tau phosphorylation). CoA is a 767 Da molecule with a bulky 3′, 5′-ADP and pantetheine moieties, which may sterically hinder the interaction of CoA-modified tau with microtubules and promote regulatory interactions with proteins possessing the nucleotide binding fold. Targeted biochemical studies will be necessary to examine the consequences of CoAlation on binding properties and physiological functions of tau.

A hallmark occurrence of multiple incurable neurodegenerative diseases is abnormal protein aggregation and accumulation, including several clinicopathological entities in which tau aggregates are implicated, known as tauopathies including AD. Leading to cellular dysfunction, synaptic damage and neuronal death, aberrant protein aggregation in the brain is one of the main events in brain disease pathology (Soto, 2003; Ross and Poirier, 2004; Goedert, 2015). Tau is an IDP subject to highly sophisticated regulation by a diverse set of PTMs. Evidently, this has presented difficulties in the precise elucidation of the role of tau in AD and its position along the chain of events leading to neurodegeneration. Given the extensive pathological role of tau in numerous neurodegenerative diseases, the acceleration in the number of AD cases accompanying a continual expansion in life expectancy has created an indispensable requirement for AD therapeutic interventions. Despite substantial efforts, only symptomatic treatments exist for AD, and disease-modifying treatment strategies are still under extensive research (Yiannopoulou and Papageorgiou, 2020). To inhibit the progression of AD, treatments must interfere with pathogenic advancements responsible for clinical AD symptoms, including NFT formation and oxidative damage. Two types of tau filaments have been identified to be involved in the pathogenesis of AD. Together, PHFs and SFs comprise intraneuronal NFTs, a pivotal hallmark lesion of AD. Importantly, compelling evidence has shown that oxidation of tau cysteine in R3 is critical in NFT formation *in vitro* through the formation of intermolecular disulfide bridges formed by Cys322 (Schweers et al., 1995). This highlights the potential importance of oxidative stress tau aggregation, where the link between oxidation and AD is increasingly recognized. While the source of oxidative stress in AD is somewhat unclear, our data indicates that dimerization of tau induced by oxidizing agents could be a key step in tau aggregation. Certainly, this requires further investigation into the precise role of oxidative stress mechanisms in AD pathogenesis, and could lead to the development of novel clinical interventions acting to prevent tau dimerization via cysteines.

It is now well established that the brain is particularly vulnerable to oxidative stress due to high oxidative metabolic activity and lower level of antioxidants when compared to other tissues. The emerging antioxidant function of CoA mediated by protein CoAlation provides an additional mechanism for protecting surface exposed cysteines in neuronal proteins from overoxidation, including Cys322 in tau. Taking into account the involvement of tau cysteine residues in facilitating intrinsic acetyl-transferase activity, CoAlation of Cys322 under oxidative stress may mediate reversible inhibition and downstream effect of tau auto-acetylation.

Protein CoAlation has been shown to regulate the activity of modified proteins, in a manner similar to the regulatory changes induced by other covalent PTMs, including protein *S*-glutathionylation, phosphorylation, or acetylation. For instance, *S*-glutathionylated tau has been detected through

mass spectrometry, and its function has been shown to alter the polymerization of 3-repeat tau (Landino et al., 2004). *S*-Glutathionylated 3-repeat tau was demonstrated to be capable of polymerization, which suggests that disulfide-linked tau dimerization is not an essential step in tau filament assembly leading to NFT formation. Further, recent studies have demonstrated double-cysteine tau mutants to be aggregation-competent. However, aggregation has been found to be dependent on cysteines for rapid initiation (Chidambaram and Chinnathambi, 2020). This suggests a significant role for disulfide bond formation in the early stages of tau aggregation, which may subsequently proceed via cysteine-independent mechanisms including hexapeptide motifs. Therefore, we hypothesize that the CoA antioxidant function could prevent intermolecular disulfide bond formation prompting accelerated tau aggregation during oxidizing conditions.

While our results primarily suggest a role of CoA in protecting tau from dimerization, which may lead its pathological accumulation, alternate mechanisms for tau aggregation exist. For instance, two hexapeptide motifs within the MTBR of tau are reported to be critical in driving tau fibril formation via the adoption of β-sheet structures (Von Bergen et al., 2000). Under physiological conditions tau protein is involved in the regulation of assembly, dynamic behavior, and the spatial organization of microtubules. Further, a model of tau-tubulin interaction suggests the formation of disulfide linkages between tau and tubulin cysteines: specifically, Cys291 of tau R2 first binds Cys347 of α-tubulin at "Site 1," which allows Cys322 of tau R3 to subsequently bind C131 of β-tubulin at "Site 2" (Martinho et al., 2018). Therefore, we propose CoAlation at the conserved cysteine residue (Cys322 in 2N4R tau) could modulate disulfide bond mediated tau dimerization alongside the binding to tubulin. As the residues responsible for binding are located within the MTBR, this suggests that tau CoAlation may be involved in regulating microtubule-binding in response to fluctuations in the redox state of the cell. For instance, the presence of a bulky CoA group within the MTBR could sterically hinder access to the microtubule and inhibit the tau-tubulin functional interaction. As such, CoAlated tau would remain unable to bind microtubules for the duration of increased oxidative stress levels. When cells recover, deCoAlation of tau would allow microtubule stabilization to resume, thus proving an additional layer of regulation of cytoskeletal dynamics in response to cellular redox shifts.

Finally, it will also be interesting to consider the effect of tau CoAlation on other PTMs of tau. Importantly, tau is subject to regulation by a wealth of PTMs. Phosphorylation presents one of the most extensively studied PTMs of tau. Tau possesses over 80 potential sites for phosphorylation (Goedert et al., 1989). In AD, at least 40 phosphorylation sites have been identified in pathological tau through comprehensive MS analysis (Morishima-Kawashima et al., 1995; Hanger et al., 2007). However, a recent study (Wesseling et al., 2020) compiling an extensive catalog of PTMs including (but not limited to) ubiquitination, acetylation, and methylation across the full length of tau has highlighted the heterogeneity of these modifications. By nature, PTMs are incredibly complex as they occur in multitudes and may be combined in several ways. Tau PTMs are also prone to crosstalk and competition. For instance, acetylation of tau can also inhibit the phosphorylation of nearby residues. Acetylation of Lys321, Lys259, and Lys353 inhibits phosphorylation of Ser324, Ser262, and Ser356 respectively. This crosstalk generates complexity since acetylation is directly impairing but also indirectly activating tau functionality. A potential opposition in which the addition of certain chemical groups can block the addition of another on a given residue further suggests multifaceted regulation of tau biology (Liu et al., 2004, 2009; Yang and Seto, 2008; Bourré et al., 2018). As such, the recent explosion of knowledge on tau PTMs provides the opportunity to better understand these modifications in the context of tau homeostasis, and their perturbation in aging and disease. Oxidative stress was shown to induce the formation of the CoA biosynthetic complex and CoA production, a local increase in CoA occurs during protein acetylation, as acetyl-CoA provides the acetyl group for histone acetyl-transferases. The availability of reduced CoA in close vicinity may Therefore, it will be interesting to consider the effect of CoAlation on PTM of sites in tau in particular, phosphorylation and/or acetylation.

Overall, the involvement of the altered mitochondrial function and oxidative stress in neurodegenerative diseases including AD, combined with findings which link CoA dysregulation to neurodegeneration in NBIA raises the questions as to whether protein CoAlation could occur in neurodegenerative disorders and whether it has a protective role against oxidative damage and aggregation. In this study, we examined the pattern and distribution of CoAlation among different brain regions. We further explored tau CoAlation using *in vitro* studies, where we identified the site of tau CoAlation using MS, and determined that CoAlation can protect 2N3R tau from dimerization in the presence of H_2O_2.

DATA AVAILABILITY STATEMENT

The data presented in the study are stored electronically at the main UCL server in suitable file formats and will be available if requested by other researchers. The summary of case demographic data for the post-mortem cases used in the study is presented in **Table 1**.

ETHICS STATEMENT

The studies involving human participants were reviewed and approved by the NHS Research Ethics Committee (NEC) and in accordance with the Human Tissue Authority's (HTA's) code of practice and standards under license number 12198. The patients/participants provided their written informed consent to participate in this study.

AUTHOR CONTRIBUTIONS

IG conceived the present study. TL, M-AT, and IG designed the experiments. TL and NC performed the IHC studies. M-AT performed the *in vitro* studies. M-AT, JC, AB, and SW

performed the *in vivo* experiments. SP-C and MS performed the MS analysis. OM and VF developed and produced the anti-CoA monoclonal antibody. MK and SR purified the tau isoforms for the *in vitro* studies. TL, M-AT, NC, SW, AB, JC, RS, SS, MK, SR, and IG analyzed and discussed generated results. TL, M-AT, SW, and IG wrote the manuscript with the assistance and approval of all other authors. All authors contributed to the article and approved the submitted version.

FUNDING

This work was funded by grants to IG (UCLB 13-014 and 11-018; Rosetrees Trust CM239-F2; and BBSRC BB/L010410/1 and BB/S009027/1). TL was funded by an Alzheimer's Research United Kingdom senior fellowship. AB and JC were supported by a project grant from 'CurePSP'. SR was supported by Campaign Team Huntington, Alzheimer's Nederland and a ZonMW TOP grant ("Chaperoning axonal transport in neurodegenerative disease"; No. 91215084).

SUPPLEMENTARY MATERIAL

The Supplementary Material for this article can be found online at: https://www.frontiersin.org/articles/10.3389/fncel.2021.739425/full#supplementary-material

REFERENCES

Alzheimer, A. (1906). Über einen eigenartigen schweren Erkrankungsprozeβ der Hirnrincle. *Neurol. Cent.* 25:1134.

Bakovic, J., Yu, B. Y. K., Silva, D., Chew, S. P., Kim, S., Ahn, S. H., et al. (2019). A key metabolic integrator, coenzyme A, modulates the activity of peroxiredoxin 5 via covalent modification. *Mol. Cell. Biochem.* 461, 91–102. doi: 10.1007/s11010-019-03593-w

Battisti, A., Ciasca, G., Grottesi, A., Bianconi, A., and Tenenbaum, A. (2012). Temporary secondary structures in tau, an intrinsically disordered protein. *Mol. Simul.* 38, 525–533. doi: 10.1080/08927022.2011.633347

Binder, L. I., Frankfurter, A., and Rebhun, L. I. (1985). The distribution of tau in the mammalian central nervous system. *J. Cell Biol.* 101, 1371–1378. doi: 10.1083/jcb.101.4.1371

Bourré, G., Cantrelle, F. X., Kamah, A., Chambraud, B., Landrieu, I., and Smet-Nocca, C. (2018). Direct crosstalk between O-GlcNAcylation and phosphorylation of tau protein investigated by NMR spectroscopy. *Front. Endocrinol.* 9:595. doi: 10.3389/fendo.2018.00595

Brass, E. P., Tahiliani, A. G., Allen, R. H., and Stabler, S. P. (1990). Coenzyme A metabolism in vitamin B-12 deficient rats. *J. Nutr.* 120, 290–297. doi: 10.1093/jn/120.3.290

Burns, A., and Iliffe, S. (2009). Alzheimer's disease. *BMJ* 338, 467–471.

Castellano, J. M., Deane, R., Gottesdiener, A. J., Verghese, P. B., Stewart, F. R., West, T., et al. (2012). Low-density lipoprotein receptor overexpression enhances the rate of brain-to-blood Aβ clearance in a mouse model of β-amyloidosis. *Proc. Natl. Acad. Sci. U. S. A.* 109, 15502–15507. doi: 10.1073/pnas.1206446109

Cenini, G., and Voos, W. (2019). Mitochondria as potential targets in Alzheimer disease therapy: an update. *Front. Pharmacol.* 10:902. doi: 10.3389/fphar.2019.00902

Chew, H., Solomon, V. A., and Fonteh, A. N. (2020). Involvement of Lipids in Alzheimer's Disease Pathology and Potential Therapies. *Front. Physiol.* 11:598. doi: 10.3389/fphys.2020.00598

Chidambaram, H., and Chinnathambi, S. (2020). Role of cysteines in accelerating tau filament formation. *J. Biomol. Struct. Dyn.* 15, 1–10. doi: 10.1080/07391102.2020.1856720

Cohen, T. J., Friedmann, D., Hwang, A. W., Marmorstein, R., and Lee, V. M. (2013). The microtubule-associated tau protein has intrinsic acetyltransferase activity. *Nat. Struct. Mol. Biol.* 20, 756–762. doi: 10.1038/nsmb.2555

Cox, J., and Mann, M. (2008). MaxQuant enables high peptide identification rates, individualized p.p.b.-range mass accuracies and proteome-wide protein quantification. *Nat. Biotechnol.* 26, 1367–1372. doi: 10.1038/nbt.1511

Davaapil, H., Tsuchiya, Y., and Gout, I. (2014). Signalling functions of coenzyme A and its derivatives in mammalian cells. *Biochem. Soc. Trans.* 42, 1056–1062.

Dusi, S., Valletta, L., Haack, T. B., Tsuchiya, Y., Venco, P., Pasqualato, S., et al. (2014). Exome sequence reveals mutations in CoA synthase as a cause of neurodegeneration with brain iron accumulation. *Am. J. Hum. Genet.* 94, 11–22. doi: 10.1016/j.ajhg.2013.11.008

Ferrari, L., and Rüdiger, S. G. D. (2018). Recombinant production and purification of the human protein tau. *Protein Eng. Des. Sel.* 31, 447–455. doi: 10.1093/protein/gzz010

Fitzpatrick, A. W. P., Falcon, B., He, S., Murzin, A. G., Murshudov, G., Garringer, H. J., et al. (2017). Cryo-EM structures of tau filaments from Alzheimer's disease. *Nature* 547, 185–190.

Goedert, M. (2015). Neurodegeneration. Alzheimer's and Parkinson's diseases: the prion concept in relation to assembled Aβ, tau, and α-synuclein. *Science* 349:1255555. doi: 10.1126/science.1255555

Goedert, M., Spillantini, M. G., Cairns, N. J., and Crowther, R. A. (1992). Tau proteins of Alzheimer paired helical filaments: abnormal phosphorylation of all six brain isoforms. *Neuron* 1, 159–168. doi: 10.1016/0896-6273(92)90117-v

Goedert, M., Spillantini, M. G., Jakes, R., Rutherford, D., and Crowther, R. A. (1989). Multiple isoforms of human microtubule-associated protein tau: sequences and localization in neurofibrillary tangles of Alzheimer's disease. *Neuron* 3, 519–526. doi: 10.1016/0896-6273(89)90210-9

Gong, C. X., Liu, F., Grundke-Iqbal, I., and Iqbal, K. (2005). Post-translational modifications of tau protein in Alzheimer's disease. *J. Neural Transm.* 112, 813–838.

Gout, I. (2018). Coenzyme A, protein CoAlation and redox regulation in mammalian cells. *Biochem. Soc. Trans.* 46, 721–728. doi: 10.1042/bst20170506

Gout, I. (2019). Coenzyme A: a protective thiol in bacterial antioxidant defence. *Biochem. Soc. Trans.* 47, 469–476. doi: 10.1042/bst20180415

Grundke-Iqbal, I., Iqbal, K., Tung, Y. C., Quinlan, M., Wisniewski, H. M., and Binder, L. I. (1986). Abnormal phosphorylation of the microtubule-associated protein tau (tau) in Alzheimer cytoskeletal pathology. *Proc. Natl. Acad. Sci. U. S. A.* 83, 4913–4917. doi: 10.1073/pnas.83.13.4913

Guo, C., Sun, L., Chen, X., and Zhang, D. (2013). Oxidative stress, mitochondrial damage and neurodegenerative diseases. *Neural Regen. Res.* 8, 2003–2014.

Hanger, D. P., Byers, H. L., Wray, S., Leung, K. Y., Saxton, M. J., Seereeram, A., et al. (2007). Novel phosphorylation sites in tau from Alzheimer brain support a role for casein kinase 1 in disease pathogenesis. *J. Biol. Chem.* 282, 23645–23654. doi: 10.1074/jbc.m703269200

Hashimoto, M., Rockenstein, E., Crews, L., and Masliah, E. (2003). Role of protein aggregation in mitochondrial dysfunction and neurodegeneration in Alzheimer's and Parkinson's diseases. *Neuromolecular. Med.* 4, 21–36. doi: 10.1385/nmm:4:1-2:21

Hoover, B. R., Reed, M. N., Su, J., Penrod, R. D., Kotilinek, L. A., Grant, M. K., et al. (2010). tau mislocalization to dendritic spines mediates synaptic dysfunction independently of neurodegeneration. *Neuron* 68, 1067–1081. doi: 10.1016/j.neuron.2010.11.030

Huang, W. J., Zhang, X., and Chen, W. W. (2016). Role of oxidative stress in Alzheimer's disease. *Biomed. Rep.* 4, 519–522.

Iqbal, K., Liu, F., and Gong, C. X. (2016). Tau and neurodegenerative disease: the story so far. *Nat. Rev. Neurol.* 12, 15–27. doi: 10.1038/nrneurol.2015.225

Iqbal, K., Liu, F., Gong, C.-X., and Grundke-Iqbal, I. (2010). tau in Alzheimer Disease and Related tauopathies. *Curr. Alzheimer Res.* 7, 656–664. doi: 10.2174/156720510793611592

Kadavath, H., Jaremko, M., Jaremko, L., Biernat, J., Mandelkow, E., and Zweckstetter, M. (2015). Folding of the tau protein on microtubules. *Angew. Chem. Int. Ed. Engl.* 54, 10347–10351. doi: 10.1002/anie.201501714

Kinney, J. W., Bemiller, S. M., Murtishaw, A. S., Leisgang, A. M., Salazar, A. M., and Lamb, B. T. (2018). Inflammation as a central mechanism in Alzheimer's disease. *Alzheimers Dement.* 4, 575–590.

Kovacs, G. G. (2015). Invited review: neuropathology of tauopathies: principles and practice. *Neuropathol. Appl. Neurobiol.* 41, 3–23.

Landino, L. M., Robinson, S. H., Skreslet, T. E., and Cabral, D. M. (2004). Redox modulation of tau and microtubule-associated protein-2 by the glutathione/glutaredoxin reductase system. *Biochem. Biophys. Res. Commun.* 323, 112–117. doi: 10.1016/j.bbrc.2004.08.065

Lee, K. H., Cha, M., and Lee, B. H. (2020). Neuroprotective effect of antioxidants in the brain. *Int. J. Mol. Sci.* 21:7152. doi: 10.3390/ijms21197152

Lee, V. M., Goedert, M., and Trojanowski, J. Q. (2001). Neurodegenerative tauopathies. *Annu. Rev. Neurosci.* 24, 1121–1159.

Leonardi, R., Zhang, Y. M., Rock, C. O., and Jackowski, S. (2005). Coenzyme A: back in action. *Prog. Lipid Res.* 44, 125–153.

Lindwall, G., and Cole, R. D. (1984). Phosphorylation affects the ability of tau protein to promote microtubule assembly. *J. Biol. Chem.* 259, 5301–5305. doi: 10.1016/s0021-9258(17)42989-9

Lipmann, F., and Kaplan, N. O. (1946). A common factor in the enzymatic acetylation of sulfanilamide and of choline. *J. Biol. Chem*. 162, 743–744. doi: 10.1016/s0021-9258(17)41419-0

Liu, F., and Gong, C. X. (2008). tau exon 10 alternative splicing and tauopathies. *Mol. Neurodegener*. 3:8. doi: 10.1186/1750-1326-3-8

Liu, F., Iqbal, K., Grundke-Iqbal, I., Hart, G. W., and Gong, C.-X. (2004). O-GlcNAcylation regulates phosphorylation of tau: a mechanism involved in Alzheimer's disease. *Proc. Natl. Acad. Sci. U. S. A*. 101, 10804–10809. doi: 10.1073/pnas.0400348101

Liu, F., Shi, J., Tanimukai, H., Gu, J., Grundke-Iqbal, I., Iqbal, K., et al. (2009). Reduced O-GlcNAcylation links lower brain glucose metabolism and tau pathology in Alzheimer's disease. *Brain J. Neurol.* 132, 1820–1832. doi: 10.1093/brain/awp099

Magi, S., Castaldo, P., Macrì, M., Maiolino, M., Matteucci, A., Bastioli, G., et al. (2016). Intracellular Calcium Dysregulation: implications for Alzheimer's Disease. *Biomed. Res. Int.* 2016, 1–14.

Malanchuk, O. M., Panasyuk, G. G., Serbyn, N. M., Gout, I. T., and Filonenko, V. V. (2015). Generation and characterization of monoclonal antibodies specific to Coenzyme A. *Biopolym. Cell* 31, 187–192. doi: 10.7124/bc.0008df

Mandal, A., and Drerup, C. M. (2019). Axonal transport and mitochondrial function in neurons. *Front. Cell. Neurosci*. 13:373. doi: 10.3389/fncel.2019.00373

Martin, L., Latypova, X., and Terro, F. (2011). Post-translational modifications of tau protein: implications for Alzheimer's disease. *Neurochem. Int.* 58, 458–471. doi: 10.1016/j.neuint.2010.12.023

Martinho, M., Allegro, D., Huvent, I., Chabaud, C., Eteinnel, E., Kovacic, H., et al. (2018). Two tau binding sites on tubulin revealed by thiol-disulfde exchanges. *Sci. Rep*. 8:13846.

McAllister, R. A., Fixter, L. M., and Campbell, E. H. G. (1988). The effect of tumour growth on liver pantothenate, CoA, and fatty acid synthetase activity in the mouse. *Br. J. Cancer* 57, 83–86. doi: 10.1038/bjc.1988.14

Meraz-Rios, M. A., Lira-De Leon, L., Campos-Pena, V., De Anda-Hernandez, M., and Mena-Lopez, R. (2010). Tau oligomers and aggregation in alzheimer's disease. *J. Neurochem.* 112, 1353–1367.

Miao, J., Shi, R., Li, L., Chen, F., Zhou, Y., Tung, Y. C., et al. (2019). Pathological tau from alzheimer's brain induces site-specific hyperphosphorylation and SDS- and reducing agent-resistant aggregation of tau in vivo. *Front. Aging Neurosci.* 11:34. doi: 10.3389/fnagi.2019.00034

Montine, T. J., Phelps, C. H., Beach, T. G., Bigio, E. H., Cairns, N. J., Dickson, D. W., et al. (2012). National Institute on Aging-Alzheimer's Association guidelines for the neuropathologic assessment of Alzheimer's disease: a practical approach. *Acta Neuropathol*. 123, 1–11.

Morishima-Kawashima, M., Hasegawa, M., Takio, K., Suzuki, M., Yoshida, H., Titani, K., et al. (1995). Proline-directed and non-proline-directed phosphorylation of PHF-tau. *J. Biol. Chem*. 270, 823–829. doi: 10.1074/jbc.270.2.823

Nixon, R. A., and Yang, D. S. (2012). Autophagy and neuronal cell death in neurological disorders. *Cold Spring Harb. Perspect. Biol.* 4:a008839. doi: 10.1101/cshperspect.a008839

Przedborski, S., Vila, M., and Jackson-Lewis, V. (2003). Neurodegeneration: what is it and where are we? *J. Clin. Invest*. 111, 3–10.

Ramkumar, A., Jong, B. Y., and Ori-McKenney, K. M. (2018). ReMAPping the microtubule landscape: how phosphorylation dictates the activities of microtubule-associated proteins. *Dev. Dyn.* 247, 138–155. doi: 10.1002/dvdy.24599

Reibel, D. K., Wyse, B. W., Berkich, D. A., and Neely, J. R. (1981). Regulation of coenzyme A synthesis in heart muscle: effects of diabetes and fasting. *Am. J. Physiol.* 240, H606–H611.

Ross, C. A., and Poirier, M. A. (2004). Protein aggregation and neurodegenerative disease. *Nat. Med.* 10, S10–S17.

Schweers, O., Mandelkow, E. M., Biernat, J., and Mandelkow, E. (1995). Oxidation of cysteine-322 in the repeat domain of microtubule-associated protein tau controls the *in vitro* assembly of paired helical filaments. *Proc. Natl. Acad. Sci. U. S. A.* 92, 8463–8467. doi: 10.1073/pnas.92.18.8463

Selkoe, D. J., and Lansbury, P. J. Jr. (1999). *Alzheimer's Disease is The Most Common Neurodegenerative Disorder (Basic Neurochemistry: Molecular, Cellular and Medical Aspects)*. Philadelphia, PA: Lippincott-Raven.

Soto, C. (2003). Unfolding the role of protein misfolding in neurodegenerative diseases. *Nat. Rev. Neurosci.* 4, 49–60. doi: 10.1038/nrn1007

Srinivasan, B., and Sibon, O. C. M. (2014). Coenzyme A, more than 'just' a metabolic cofactor. *Biochem. Soc. Trans.* 42, 1075–1079. doi: 10.1042/bst20140125

Stoker, M. L., Newport, E., Hulit, J. C., West, A. P., and Morten, K. J. (2019). Impact of pharmacological agents on mitochondrial function: a growing opportunity? *Biochem. Soc. Trans.* 47, 1757–1772. doi: 10.1042/bst20190280

Sultana, R., Perluigi, M., and Butterfield, D. A. (2009). Oxidatively modified proteins in Alzheimer's disease (AD), mild cognitive impairment and animal models of AD: role of Abeta in pathogenesis. *Acta Neuropathol.* 118, 131–150. doi: 10.1007/s00401-009-0517-0

Theodoulou, F. L., Sibon, O. C. M., Jackowski, S., and Gout, I. (2014). Coenzyme A and its derivatives: renaissance of a textbook classic. *Biochem. Soc. Trans*. 42, 1025–1032. doi: 10.1042/bst20140176

Tossounian, M. A., Zhang, B., and Gout, I. (2020). The writers, readers, and erasers in redox regulation of GAPDH. *Antioxidants* 9:1288. doi: 10.3390/antiox9121288

Tsuchiya, Y., Byrne, D. P., Burgess, S. G., Bormann, J., Bakovic, J., Huang, Y., et al. (2020). Covalent Aurora A regulation by the metabolic integrator coenzyme A. *Redox Biol.* 28:101318. doi: 10.1016/j.redox.2019.101318

Tsuchiya, Y., Peak-Chew, S. Y., Newell, C., Miller-Aidoo, S., Mangal, S., Zhyvoloup, A., et al. (2017). Protein CoAlation: a redox-regulated protein modification by coenzyme A in mammalian cells. *J. Biochem.* 474, 2489–2508. doi: 10.1042/bcj20170129

Tsuchiya, Y., Zhyvoloup, A., Bakovicì, J., Thomas, N., Yu, B., Das, S., et al. (2018). Protein CoAlation and antioxidant function of coenzyme A in prokaryotic cells. *J. Biochem.* 475, 1909–1937. doi: 10.1042/bcj20180043

Vasili, E., Dominguez-Meijide, A., and Fleming-Outeiro, T. (2019). Spreading of α-Synuclein and tau: a systematic comparison of the mechanisms involved. *Front. Mol. Neurosci.* 12:107. doi: 10.3389/fnmol.2019.00107

Von Bergen, M., Friedhoff, P., Biernat, J., Heberle, J., Mandelkow, E.-M., and Mandelkow, E. (2000). Assembly of tau protein into Alzheimer paired helical filaments depends on a local sequence motif ((306)VQIVYK(311)) forming beta structure. *Proc. Natl. Acad. Sci. U. S. A*. 97, 5129–5134. doi: 10.1073/pnas.97.10.5129

Wang, J. Z., Xia, Y. Y., Grundke-Iqbal, I., and Iqbal, K. (2013). Abnormal hyperphosphorylation of tau: sites, regulation, and molecular mechanism of neurofibrillary degeneration. *J. Alzheimers Dis.* 33, S123–S139.

Wang, W., Zhao, F., Ma, X., Perry, G., and Zhu, X. (2020). Mitochondria dysfunction in the pathogenesis of Alzheimer's disease: recent advances. *Mol. Neurodegener*. 15:30.

Wesseling, H., Mair, W., Kumar, M., Schlaffner, C. N., Tang, S., Beerepoot, P., et al. (2020). tau PTM profiles identify patient heterogeneity and stages of Alzheimer's disease. *Cell* 183, 1699–1713. doi: 10.1016/j.cell.2020.10.029

Yang, X. J., and Seto, E. (2008). Lysine acetylation: codified crosstalk with other posttranslational modifications. *Mol. Cell* 31, 449–461. doi: 10.1016/j.molcel.2008.07.002

Yiannopoulou, K. G., and Papageorgiou, S. G. (2020). Current and Future Treatments in Alzheimer Disease: an Update. *J. Cent. Nerv. Syst. Dis.* 12:1179573520907397.

Yu, B. Y. K., Tossounian, M. A., Hristov, S. D., Lawrence, R., Arora, P., Tsuchiya, Y., et al. (2021). Regulation of metastasis suppressor NME1 by a key metabolic cofactor coenzyme A. *Redox Biol.* 44:101978. doi: 10.1016/j.redox.2021.101978

Zhou, B., Westaway, S. K., Levinson, B., Johnson, M. A., Gitschier, J., and Hayflick, S. J. (2001). A novel pantothenate kinase gene (PANK2) is defective in Hallervorden-Spatz syndrome. *Nat. Genet.* 28, 345–349. doi: 10.1038/ng572

Conflict of Interest: The authors declare that the research was conducted in the absence of any commercial or financial relationships that could be construed as a potential conflict of interest.

Publisher's Note: All claims expressed in this article are solely those of the authors and do not necessarily represent those of their affiliated organizations, or those of the publisher, the editors and the reviewers. Any product that may be evaluated in this article, or claim that may be made by its manufacturer, is not guaranteed or endorsed by the publisher.

frontiers in Cellular Neuroscience

REVIEW
published: 26 November 2021
doi: 10.3389/fncel.2021.785057

Nuclear Factor Erythroid-2-Related Factor 2 Signaling in the Neuropathophysiology of Inherited Metabolic Disorders

Bianca Seminotti[1†], Mateus Grings[1†], Paolo Tucci[2†], Guilhian Leipnitz[1,3,4†] and Luciano Saso[5*†]*

[1] Postgraduate Program in Biological Sciences: Biochemistry, Department of Biochemistry, Institute of Basic Health Sciences, Universidade Federal do Rio Grande do Sul, Porto Alegre, Brazil, [2] Department of Clinical and Experimental Medicine, University of Foggia, Foggia, Italy, [3] Department of Biochemistry, Institute of Basic Health Sciences, Federal University of Rio Grande do Sul, Porto Alegre, Brazil, [4] Postgraduate Program in Biological Sciences: Physiology, Institute of Basic Health Sciences, Universidade Federal do Rio Grande do Sul, Porto Alegre, Brazil, [5] Department of Physiology and Pharmacology "Vittorio Erspamer", Sapienza University of Rome, Rome, Italy

Inherited metabolic disorders (IMDs) are rare genetic conditions that affect multiple organs, predominantly the central nervous system. Since treatment for a large number of IMDs is limited, there is an urgent need to find novel therapeutical targets. Nuclear factor erythroid-2-related factor 2 (Nrf2) is a transcription factor that has a key role in controlling the intracellular redox environment by regulating the expression of antioxidant enzymes and several important genes related to redox homeostasis. Considering that oxidative stress along with antioxidant system alterations is a mechanism involved in the neuropathophysiology of many IMDs, this review focuses on the current knowledge about Nrf2 signaling dysregulation observed in this group of disorders characterized by neurological dysfunction. We review here Nrf2 signaling alterations observed in X-linked adrenoleukodystrophy, glutaric acidemia type I, hyperhomocysteinemia, and Friedreich's ataxia. Additionally, beneficial effects of different Nrf2 activators are shown, identifying a promising target for treatment of patients with these disorders. We expect that this article stimulates research into the investigation of Nrf2 pathway involvement in IMDs and the use of potential pharmacological modulators of this transcription factor to counteract oxidative stress and exert neuroprotection.

Keywords: Nrf2 signaling, antioxidant defenses, inherited metabolic disorders, neurometabolism, neurodegeneration

OPEN ACCESS

Edited by:
Sharon DeMorrow,
The University of Texas at Austin,
United States

Reviewed by:
Shinji Saiki,
Juntendo University, Japan
Ilaria Meloni,
University of Siena, Italy

***Correspondence:**
Bianca Seminotti
bianca.seminotti@ufrgs.br
Luciano Saso
luciano.saso@uniroma1.it

†ORCID:
Bianca Seminotti
orcid.org/0000-0002-9803-7746
Mateus Grings
orcid.org/0000-0002-2439-3350
Paolo Tucci
orcid.org/0000-0001-7314-445X
Guilhian Leipnitz
orcid.org/0000-0001-7964-8923
Luciano Saso
orcid.org/0000-0003-4530-8706

Specialty section:
This article was submitted to Cellular Neuropathology, a section of the journal Frontiers in Cellular Neuroscience

Received: *28 September 2021*
Accepted: *05 November 2021*
Published: *26 November 2021*

Citation:
Seminotti B, Grings M, Tucci P, Leipnitz G and Saso L (2021) Nuclear Factor Erythroid-2-Related Factor 2 Signaling in the Neuropathophysiology of Inherited Metabolic Disorders. Front. Cell. Neurosci. 15:785057. doi: 10.3389/fncel.2021.785057

INHERITED METABOLIC DISORDERS AND NEUROLOGICAL DYSFUNCTION

The central nervous system (CNS) is a complex structure formed by distinct cell types organized in interacting substructures, whose development is dependent on the interactions between several single genes and non-genetic factors. Thus, CNS is highly susceptible to disturbances caused by genetic mutations that may be associated to external damaging factors (e.g., infection or

vaccination), resulting in a broad range of disorders, including the so-called inherited metabolic disorders (IMDs) (Rose et al., 2020; Schiller et al., 2020).

Inherited metabolic disorders are a heterogeneous group of disorders caused by mutations that may affect thousands of molecules and proteins of human metabolism, mostly enzymes, cofactors, receptors and transporters, disrupting metabolic networks that underlie development and homeostasis. More than 1,100 different IMDs have been identified so far (Ferreira et al., 2019, 2021) and most of them involve the nervous system (Mankad et al., 2018). IMDs can lead to disruption of enzyme activity, cellular transport, or energy production, altering the metabolism of small or complex molecules and therefore causing their accumulation in tissues and biological fluids (Saudubray and Garcia-Cazorla, 2018b). The accumulation of these molecules, the reduced ability to synthesize intermediates or the defects in energy supply can severely interfere with the complex and finely tuned process of early brain development (Schiller et al., 2020). Thus, many IMDs are prevalent as diseases of the nervous system, being called neurometabolic diseases (García-Cazorla and Saudubray, 2018; Karimzadeh et al., 2020).

A simplified classification for IMDs affecting neurodevelopment has been proposed, based on the diagnostic approach, pathophysiology and size of accumulating molecules (small and simple or large and complex) in each disorder (Saudubray and Garcia-Cazorla, 2018a). Three large categories have been determined: disorders of small molecules, energy-related defects and complex molecule defects. It should be noted that the accumulating metabolites, independent of their size, may behave in the brain as signaling molecules, structural components and fuels so that alterations in their levels may severely damage neural cells (García-Cazorla and Saudubray, 2018).

The onset of symptoms in neurometabolic diseases can occur from neonatal period to adult life. A number of them may be present even after a period of normal growth and development. The estimated general prevalence is 1 in 1,000 live births (Karimzadeh et al., 2020). Clinical manifestations are diverse and may include seizures, global developmental delay, neuropathy, hypomyelination, microcephaly, and motor alterations (Mankad et al., 2018; Saudubray and Garcia-Cazorla, 2018a; Karimzadeh et al., 2020). Metabolic acidosis, hyperammonemia and lactic acidemia are common laboratory findings. The latter is mainly observed in disorders of small molecules and energy-related defects (García-Cazorla and Saudubray, 2018).

Many neurometabolic diseases have limited treatment so that early diagnosis is crucial to prevent devastating and long-term complications (Karimzadeh et al., 2020). In this scenario, several studies have aimed to characterize changes at molecular and structural levels, as well as alterations in redox homeostasis and energy metabolism in these diseases as an effort to discover novel therapeutical targets for these disorders (Swerdlow, 2016; García-Cazorla and Saudubray, 2018).

OXIDATIVE STRESS IN THE NEUROPATHOPHYSIOLOGY OF INHERITED METABOLIC DISORDERS

A great amount of evidence shows that oxidative stress contributes to the pathogenesis of the neurological dysfunction in various IMDs (Mc Guire et al., 2009; Ribas et al., 2014; Wajner et al., 2020). Biomarkers of lipid, protein and DNA oxidative damage and altered antioxidant defenses, have been demonstrated in *in vitro* and *in vivo* disease models, as well as in cells of patients affected by these disorders (Mc Guire et al., 2009; Halliwell and Gutteridge, 2015; Faverzani et al., 2017; Parmeggiani and Vargas, 2018; Richard et al., 2018; Wajner et al., 2019, 2020).

As aforementioned, it is important to highlight that the brain has a high rate of oxidative metabolism coupled to reactive oxygen species (ROS) production, high amount of iron and greater peroxidation potential due to its elevated content of polyunsaturated fatty acids, and considerable low levels of antioxidant defenses, making this tissue highly vulnerable to oxidative stress (Halliwell, 2006; Halliwell and Gutteridge, 2015). In this scenario, it has been widely demonstrated that the metabolites accumulated in some inherited neurometabolic disorders, including amino acids, organic acids and acylcarnitines, act as neurotoxins and cause mitochondrial dysfunction leading to augmented generation of reactive species. Many of these neurotoxins disrupt mitochondrial homeostasis by causing disturbances in electron transport chain, which lead to increased electron leakage and a consequent overproduction of ROS (Wajner et al., 2004, 2019, 2020; Berger et al., 2014; Ribas et al., 2014; Leipnitz et al., 2015; Wyse et al., 2021). Therefore, the quantification of oxidative stress biomarkers may provide an approach for monitoring of redox status in individuals affected by IMDs and elucidation of a possible role of mitochondrial dysfunction in these disorders (Mc Guire et al., 2009; Leipnitz et al., 2015).

Treatment for many IMDs is limited and usually involves dietary restriction, supplementation of metabolic deficiencies and controlling of the main symptoms (Ribas et al., 2014; Saudubray and Garcia-Cazorla, 2018b; Kripps et al., 2021). Thus, in the last two decades, there has been intense research focusing on the development of new drugs aiming to target specific neural processes that have been shown to be disturbed in these disorders (Mazzola et al., 2013; Ribas et al., 2014; El-Hattab et al., 2017; Wajner, 2019). In this regard, antioxidant molecules were demonstrated to prevent not only oxidative stress, but also neurocognitive deficits observed in animal models of inherited neurometabolic diseases (Ribas et al., 2014; Leipnitz et al., 2015). Nevertheless, there is no consensus about the beneficial effects of antioxidants since this approach seems to be promising in preventing or dealing with a non-established process instead of reverting an installed damage.

Based on these observations, the modulation of nuclear factor erythroid-2-related factor 2 (Nrf2) signaling pathway has been studied as a therapeutical target for diseases related to oxidative stress and inflammation. Nrf2 modulators, mainly

activators, have been already demonstrated to elicit beneficial effects in models of different human pathologies, such as cancer, autoimmune diseases, liver, kidney, and lung diseases, as well as common neurodegenerative disorders (Adelusi et al., 2020; Panieri et al., 2020; Scuderi et al., 2020; Sharma et al., 2020; Kim, 2021; Kourakis et al., 2021; Sezgin-Bayindir et al., 2021; Telkoparan-Akillilar et al., 2021; Zhao et al., 2021). Of note, some Nrf2 modulators are being currently evaluated in clinical trials for different disorders, such as cancer, neurodegenerative disorders and autoimmune diseases (Chartoumpekis et al., 2020; Panieri et al., 2020; Scuderi et al., 2020). In the following topics we will discuss recent evidence showing that Nrf2 pathway is altered in inherited neurometabolic conditions and that its modulation may represent an interesting therapeutic strategy for these disorders.

Nrf2 SIGNALING PATHWAY OVERVIEW

The Nrf2, encoded by *NFE2L2*, is a basic leucine zipper transcription factor, member of the cap "n" collar proteins (Sykiotis and Bohmann, 2010) containing seven Nrf2-ECH homology (Neh) functional domains, Neh1-Neh7 (Canning et al., 2015). Nrf2 is located in the cytosol in an inactive form bound to Kelch-like ECH associated protein-1 (Keap1) through DLG and ETGE motifs present in the Neh2 domain. Keap1 also binds cullin 3 (CUL3), a member of cullin proteins that play a role in ubiquitination (Andérica-Romero et al., 2013; Ahmed et al., 2017). CUL3 activates the ubiquitination process and hence the proteasome degradation of Nrf2. This Keap1 activity explains the instability of Nrf2, which has a half-life of 15–40 min and low abundance under basal conditions (Cuadrado et al., 2019).

The Nrf2 dissociates from Keap1 due to the thiol modification of Keap1 cysteine residues following oxidative stress or exposure to activators (Yamamoto et al., 2018). Nrf2 then translocates into the nucleus, heterodimerizes with musculoaponeurotic fibrosarcoma (Maf) proteins through Neh1 domain and transactivates an antioxidant response element (ARE) (**Figure 1**). The Neh3, Neh4, and Neh5 domains are the transactivation domain and Neh5 is fundamental for the regulation and cellular localization of Nrf2 (Li et al., 2006). It is established that Nrf2-ARE interaction regulates the expression of about 250 genes, with emphasis to genes involved in oxidative stress responses (Cuadrado et al., 2019). For instance, Nrf2 regulates the expression of glucose 6-phosphate dehydrogenase, 6-phosphogluconate dehydrogenase, malic enzyme 1, and isocitrate dehydrogenase 1 genes, which are involved in the generation of NADPH, a crucial cofactor for many redox enzymes. It also regulates the expression of heme oxygenase-1 (HO-1) and enzymes involved in the synthesis and use of reduced glutathione (GSH), such as subunits of glutamate-cysteine ligase, glutathione reductase, glutathione peroxidase (GPx) and several glutathione S-transferases (Cuadrado et al., 2019). It is also noteworthy that Nrf2 further regulates the expression of some cytochrome P450 oxidoreductases (Cuadrado et al., 2019). In this scenario, mounting evidence has suggested that the activation of Nrf2-ARE signaling pathway plays a role in the improvement

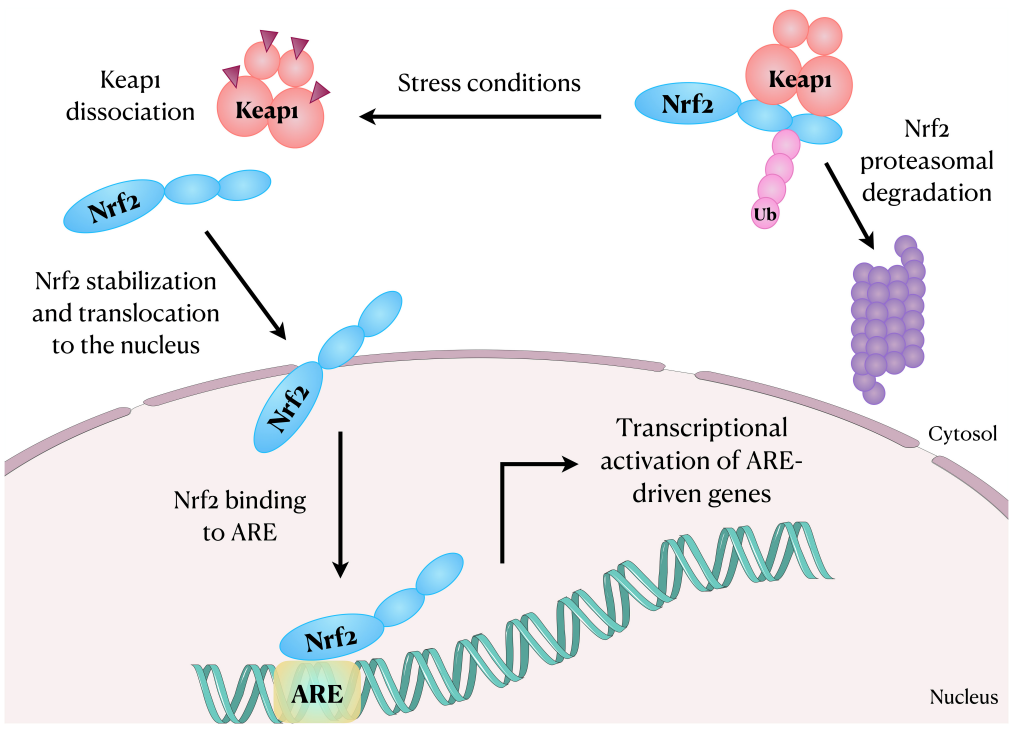

FIGURE 1 | Schematic representation showing Nrf2 translocation to the nucleus after dissociation from its inhibitory protein Keap1. In the nucleus, Nrf2 binds and activates ARE in the DNA, regulating the expression of several genes, including those involved in oxidative stress responses. ARE, antioxidant response element; Keap1, Kelch-like ECH associated protein-1; Nrf2, nuclear factor erythroid-2-related factor 2; Ub, Ubiquitin.

of chronic inflammation involved in several autoimmune, autoinflammatory, metabolic, infectious, neurodegenerative diseases, and in cancer (Hennig et al., 2018). Moreover, the Nrf2 and the NLRP3 inflammasome are inversely correlated in regulating inflammation.

Other mechanisms independent of Keap1 for Nrf2 regulation have been proposed. The Neh6 domain of Nrf2 binds β-transducin repeat-containing protein (β-TrCP) that marks Nrf2 for ubiquitination and proteasomal degradation. The glycogen synthase kinase-3 (GSK3) phosphorylates Nrf2 in the Neh6 domain to expedite the recognition of Nrf2 by β-TrCP (Rada et al., 2011; Chowdhry et al., 2013). In addition, an alternative pathway where the p62, an autophagosome cargo protein (Liu et al., 2016), induces autophagic degradation of Keap1 and the release of Nrf2 has been also shown (Komatsu et al., 2010; Lau et al., 2010).

BRAIN METABOLISM AND Nrf2 SIGNALING

The brain has a high metabolic rate and consumes about 20% of inhaled O_2 suggesting a high-energy-demanding tissue. Although a variety of carbon sources may be oxidized, glucose is the primary fuel in the adult brain, which constitutes only about 2% of the total body weight but takes up to 20% of the body's glucose disposal at rest (Bolaños, 2016; Belenguer et al., 2019). Neurotransmission is the process responsible for most of the neural energy expenditure, requiring a continuous control of ion gradients across the plasma membrane through primary active transporters (Bolaños, 2016; Belenguer et al., 2019). Thus, neurotransmission unavoidably increases reactive species generation in neurons due to enhanced oxidative phosphorylation (Bolaños, 2016). Furthermore, the brain is especially rich in redox transition metals, favoring the Fenton reaction and generating highly oxidant radicals, which easily react with polyunsaturated lipids, forming lipid radicals and other products. Of note, these products can react with amino acids residues, altering structural, catalytic and transport proteins. Since polyunsaturated fatty acids are abundant in the brain, their oxidation may cause damage to membranes and consequently affect neurotransmission, signal transduction, ion transport and electrical conduction (Díaz et al., 2021).

Although brain metabolism generates considerable levels of ROS, neuronal antioxidant defenses are not sufficient to cope with these species. For instance, concentrations of GSH are remarkably low in nerve cells and becomes even lower with aging (Díaz et al., 2021). Weak neuronal antioxidant defenses are also a result of the continuous protein destabilization of Nrf2, the master antioxidant transcriptional activator (Jimenez-Blasco et al., 2015). Nevertheless, Nrf2 is highly stable in astrocytes, conferring a more efficient antioxidant system to these cells compared to neurons (Bolaños, 2016). Accordingly, the levels of products from gene activation mediated by Nrf2 are higher in astrocytes than in neurons (Rosito et al., 2020). In this scenario, astrocytes play a key role in providing antioxidant support to nearby neurons by releasing GSH precursors, which are taken up by neurons and used to synthesize their own GSH *de novo* (Baxter and Hardingham, 2016; Rosito et al., 2020). Moreover, it has been proposed that endogenous and exogenous modulation of Nrf2 expression could increase the expression of specific genes resulting in neuroprotection and neurogenesis, since Nrf2 plays an important role in neural stem cells, maintaining the homeostasis of neural tissue and supporting neurogenesis in physiological and pathological conditions (Qiu et al., 2020; Kahroba et al., 2021).

Since Nrf2 signaling pathway plays an important role in the redox regulatory system between astrocytes and neurons and oxidative stress is commonly observed as a pathomechanism in many IMDs (Mc Guire et al., 2009; Ribas et al., 2014; Grings et al., 2020; Wajner et al., 2020; Ravi et al., 2021), it is conceivable that alterations in Nrf2 expression are involved in the pathophysiology of neurometabolic disorders, representing a promising target for the development of novel therapies that may improve the quality of life of patients.

Nrf2 SIGNALING DISRUPTION IN INHERITED METABOLIC DISORDERS

X-Linked Adrenoleukodystrophy

X-linked adrenoleukodystrophy (X-ALD) (OMIM 300100) is a complex molecule defect, caused by mutations in the ABCD1 (ATP-binding cassette, subfamily D, member 1) gene, which encodes the peroxisomal ABC half-transporter ALD protein. While it is estimated to affect approximately 1 in 42,000 males, it has been also reported that 1 in 28,000 females are estimated to be heterozygous for an ABCD1 mutation. The deficient ALD protein leads to abnormal breakdown of very long-chain fatty acids (VLCFA), a process that predominantly affects adrenal and nervous system tissues. Thus, X-ALD is biochemically characterized by elevated levels of VLCFA, especially C26:0, in tissues and plasma and constitute a pathognomonic biomarker for diagnosis (Engelen et al., 2012; Kemper et al., 2017).

X-linked adrenoleukodystrophy has a broad phenotype and there is no genotype-phenotype correlation, even within families (Wiesinger et al., 2015), suggesting the influence of modifier genes or environmental factors (Berger et al., 1994; Turk et al., 2017). Two main forms of the disease have been described (Engelen et al., 2012). The most severe form, childhood cerebral ALD, affects between 31 and 57% of hemizygous males and is mostly present in boys between 5 and 10 years (35–40% of the cases), who present a strong inflammatory demyelinating reaction in CNS white matter. Patients present with behavioral changes including memory impairment and emotional instability, followed by progressive deterioration of the vision, hearing, and motor function. Adrenal dysfunction or gonadal insufficiency may be also seen, besides the CNS symptoms (Engelen et al., 2012, 2014). The other form is called adrenomyeloneuropathy (AMN) and occurs in 60% of the cases, affecting adult men and heterozygous women over the age of 40 (Engelen et al., 2014). AMN is characterized by peripheral neuropathy and distal axonopathy involving the corticospinal tract of the spinal cord. In addition to

myeloneuropathy, around 80% of all male X-ALD patients develop adrenocortical insufficiency (Dubey et al., 2005). Symptomatology includes progressive stiffness and weakness of the legs, sphincter disturbances, sexual dysfunction, a baldness pattern and increased skin pigmentation, clinical signs that are usually progressive over decades (Li et al., 2019).

To our knowledge, so far only one study has verified alterations in Nrf2 pathway in X-ALD (Ranea-Robles et al., 2018). Reduced Nrf2 protein levels were shown in spinal cord of *Abcd1*$^{-}$ mice (AMN mice model) (Pujol et al., 2002), along with decreased mRNA levels of its target genes *Hmox1* (heme oxygenase-1, HO-1), *Nqo1* (NADH quinone oxidoreductase 1, NQO1) and *Gsta3* (glutathione S-transferase alpha-3) (Ranea-Robles et al., 2018). It was seen that these alterations were mediated by a dysregulation in AKT/GSK3β/Nrf2 axis with a defective AKT phosphorylation and a consequent activation of GSK3β. n addition, when patients' fibroblasts were exposed to both C26:0, the main VLCFA accumulated in patients, and oligomycin, an ATP synthase inhibitor that induces ROS generation, there was no activation of Nrf2-dependent responses due to abnormal GSK3β activation (Ranea-Robles et al., 2018). Importantly, it was demonstrated that the addition of dimethyl fumarate (DMF), a classical activator of Nrf2, to the deficient fibroblasts reactivated Nrf2 pathway (**Table 1**). Moreover, feeding *Abcd1*$^{-}$ mice with DMF-containing chow rescued Nrf2 pathway, improved antioxidant system, bioenergetics and mitochondrial biogenesis, and prevented inflammation in the spinal cord of these animals (Ranea-Robles et al., 2018). Further data on DMF beneficial effects were shown in *Abcd1*$^{-}$/*Abcd2*$^{-/-}$ mice, a model of X-ALD with development of a more severe and earlier onset axonopathy (Launay et al., 2015). When these mice were fed DMF, they presented a reversal of astrocytosis, microgliosis, and axonal and myelin degeneration in their spinal cord. Locomotor performance was also improved by DMF, indicating that this compound ameliorated the neuropathology of X-ALD (Ranea-Robles et al., 2018).

Hyperhomocysteinemia

Hyperhomocysteinemia (HHcy) is a condition characterized by high plasma levels of the amino acid homocysteine (Hcy) (greater than 15 μmol/L) (Kim et al., 2018), a non-protein sulfur amino acid originated from the essential amino acid methionine. HHcy is an independent risk factor for the development of various serious medical conditions, such as neurodegenerative, cardiovascular, cerebrovascular, and thromboembolic diseases (Son and Lewis, 2021).

Homocysteine is synthesized by the demethylation of methionine via formation of two intermediate compounds, S-adenosylmethionine (SAM) and S-adenosylhomocysteine (SAH). Methionine is first converted to SAM through the catalytic action of methionine adenosyltransferase. Different methyltransferases remove the methyl group from SAM generating SAH, which is then converted into Hcy and adenosine by SAH hydrolase The formation of Hcy from methionine is the only pathway of Hcy biosynthesis in humans (Barić et al., 2017; Cordaro et al., 2021).

In turn, Hcy may be converted to methionine and cysteine by the action of different enzymes and a combination of B vitamins (B12, B6, and folate). Specifically, Hcy is converted to methionine by a process known as remethylation, that can occur by a folate-dependent or -independent pathway. 5-Methyltetrahydrofolate (5-MTHF) is the active folate derivative and the main circulating form of folate in plasma. In the folate-dependent pathway, 5-MTHF supplies the methyl group used by the vitamin B12-dependent methionine synthase to remethylate Hcy and produce methionine and tetrahydrofolate (THF). THF is then converted to 5,10-methylenetetrahydrofolate (5,10-MeTHF) in the presence of serine and vitamin B6 by the enzyme serine hydroxymethyltransferase e. 5,10-MeTHF is reduced to 5-MTHF by 5,10-methylenetetrahydrofolate reductase (MTHFR) with flavin adenine dinucleotide as cofactor, being available for the remethylation of a second molecule of Hcy. The folate-dependent remethylation pathway is present in nearly all cells. Additionally, in liver and kidney, remethylation also occurs by the folate-independent pathway in which methyl groups are donated by betaine in a reaction catalyzed by the enzyme betaine-homocysteine methyltransferase (Barić et al., 2017; Cordaro et al., 2021).

On the other hand, Hcy may be irreversibly converted to cysteine through the transsulfuration pathway. In the first step, the enzyme cystathionine β-synthase (CBS) catalyzes the condensation of Hcy and serine to form cystathionine using pyridoxal phosphate (PLP or vitamin B6) as a cofactor. Cystathionine is further metabolized by cystathionine γ-lyase using PLP, to produce cysteine (Barić et al., 2017; Cordaro et al., 2021).

Elevations in Hcy levels may be caused by deficiency in any of the components of these reactions. Owing to the crucial role of vitamins in Hcy metabolism, any causes of vitamin B12, B6, and folate deficiency (i.e., alcohol use, proton pump inhibitors) can induce elevation of Hcy levels (Son and Lewis, 2021). Classic homocystinuria is an autosomal recessive disorder caused by mutations in *CBS* gene on chromosome 21q22.3 leading to deficient activity of CBS (OMIM 236200). It belongs to the category of the disorders of small molecules. The clinical features usually manifest in the first or second decade of life and include myopia, ectopia lentis, intellectual disability, skeletal anomalies and thromboembolic events. Biochemical features include increased urinary excretion of Hcy and methionine. There are two main phenotypes of the classic disorder: a milder pyridoxine (vitamin B6)-responsive form, and a more severe pyridoxine-non-responsive form (Reish et al., 1995; Testai and Gorelick, 2010). Another common cause of HHcy is the deficient enzyme activity of MTHFR caused by mutations in the gene *MTHFR*, on chromosome 1p36.22, a common inherited disorder of folate metabolism (OMIM 236250). The individuals diagnosed with this disorder present with a phenotypic spectrum that ranges from severe neurologic deterioration and early death to asymptomatic adults (Goyette et al., 1995; Strauss et al., 2007).

Data have shown the involvement of Nrf2 signaling pathway in HHcy. Alterations in this pathway as well as oxidative stress were verified in prefrontal cortex and amygdala of Wistar rats that received chronic Hcy administration (a model of mild

TABLE 1 | Summary of Nrf2 modulators evaluated in cellular and animal models, as well as in samples from patients affected by inherited metabolic disorders (IMD).

Compound	IMD	Effects	Active/completed clinical trials	References
Dimethyl fumarate (DMF)	X-linked Adrenoleukodystrophy (X-ALD)	Promotes Nrf2 nuclear translocation by interacting with Keap1 cysteine residues. Increases Nrf2 mRNA levels.	–	Ranea-Robles et al., 2018
	Friedreich's ataxia (FRDA)			Hayashi and Cortopassi, 2016; Jasoliya et al., 2019; Petrillo et al., 2019
Sulforaphane (SFN)	Friedreich's ataxia (FRDA)	Promotes Nrf2 nuclear translocation by interacting with Keap1 cysteine residues. Increases Nrf2 mRNA levels.	–	Abeti et al., 2015; Petrillo et al., 2017, 2019; La Rosa et al., 2019, 2021
TBE-31	Friedreich's ataxia (FRDA)	Promotes Nrf2 nuclear translocation by interacting with Keap1 cysteine residues. Increases Nrf2 mRNA levels.	–	Abeti et al., 2015
RTA 408 (Omaveloxolone; Omav)	Friedreich's ataxia (FRDA)	Promotes Nrf2 nuclear translocation by interacting with Keap1 cysteine residues. Increases Nrf2 mRNA levels.	Phase II clinical trial (ClinicalTrials.gov Identifier: NCT02255435; MOXIe)	Abeti et al., 2018; Lynch et al., 2018, 2021; Petrillo et al., 2019
N-acetylcysteine (NAC)	Friedreich's ataxia (FRDA)	Antioxidant that induces Nrf2 expression.	–	Petrillo et al., 2019
EPI-743	Friedreich's ataxia (FRDA)	Promotes Nrf2 nuclear translocation. Increase Nrf2 mRNA levels.	–	La Rosa et al., 2019, 2021; Petrillo et al., 2019
Idebenone	Friedreich's ataxia (FRDA)	CoQ10 analog that induces Nrf2 expression.	–	Petrillo et al., 2019
Dyclonine	Friedreich's ataxia (FRDA)	Activates the ARE/Nrf2 pathway, by enhanced binding of Nrf2 to ARE sites.	–	Sahdeo et al., 2014

HHcy) (Dos Santos et al., 2019). A marked increase of Nrf2 protein content was seen in nucleus of rat amygdala, whereas no alterations were observed in the cytosol of amygdala as well as in nucleus and cytosol of pre-frontal cortex (Dos Santos et al., 2019). Furthermore, the increased levels of Nrf2 in the amygdala were seen to occur concomitantly with augmented activities of superoxide dismutase (SOD), GPx, and catalase (CAT), suggesting that the translocation of this transcription factor to nucleus correlated with higher expression of antioxidant defenses. Increased nitrite levels and DNA damage, probably provoked by higher levels of reactive oxygen and nitrogen species, were also verified in amygdala (Dos Santos et al., 2019). In addition, chronic HHcy also compromised the mitochondrial respiratory chain with a consequent reduction of ATP levels in the amygdala, effects that may have also contributed to the induction of Nrf2 translocation (Dos Santos et al., 2019).

Another study investigated the effects of chronic Hcy administration, as well as the influence of hydrogen sulfide treatment in adult Sprague Dawley rats (Kumar and Sandhir, 2018). Of note, hydrogen sulfide is suggested to mediate S-sulfhydration of Keap1, thus leading to Nrf2 activation (Xie et al., 2016; Kumar and Sandhir, 2018). Marked alterations in oxidative stress parameters were induced by Hcy in rat cerebral cortex and hippocampus, including lipid peroxidation, increased levels of ROS, protein carbonyls and 4-hydroxynonenal-modified proteins, as well as decreased GSH/GSSG ratio and SOD, GPx, glutathione reductase, and glutathione-S-transferase activities (Kumar and Sandhir, 2018). All these effects were prevented by hydrogen sulfide (Kumar and Sandhir, 2018). The same study also evidenced a decrease of cytosolic protein levels and mRNA expression of Nrf2 in cerebral cortex of Hcy-treated animals, without changes in hippocampus. However, nuclear Nrf2 content was decreased in both cerebral cortex and hippocampus. Hydrogen sulfide supplementation significantly increased Nrf2 protein and mRNA levels in both brain structures. Overall, these findings indicate that disturbances in Nrf2 signaling pathway caused by Hcy possibly contribute to the alterations in redox homeostasis.

The studies aforementioned reported different results regarding the alterations on Nrf2 levels caused by Hcy, though the same dose of Hcy was used in both studies (0.03 μmol/g of body weight). While the first report showed that Hcy increased Nrf2 protein levels (Dos Santos et al., 2019), the second demonstrated that Hcy treatment decreased mRNA and protein levels of Nrf2 (Kumar and Sandhir, 2018). Nevertheless, these apparent controversial results may be explained by differences in the rat species used in both studies, as well as the age of the animals.

In addition, there is mounting evidence that Hcy also alters Nrf2 signaling in other rodent tissues. In this regard, a decrease of Nrf2 levels was observed in lens epithelial cells exposed to Hcy (experimental model to study cataracts) (Elanchezhian et al., 2012; Yang et al., 2015). On the other hand, another report showed increased ROS and Nrf2 levels in retina of hyperhomocysteinemic mice (Mohamed et al., 2017).

Glutaric Acidemia Type I

Glutaric acidemia type I (GA I) (OMIM 231670) is an autosomal recessive disorder caused by mutations in the gene *GCDH*, located on the short arm of the chromosome 19, leading to deficient activity of the mitochondrial enzyme glutaryl-CoA dehydrogenase (GCDH). This cerebral organic aciduria is

categorized as a disorder of small molecules The enzyme GCDH participates in the metabolic pathway of the amino acids lysine (Lys), tryptophan and hydroxylysine, converting glutaryl-CoA to crotonyl-CoA in a two-step reaction (Larson and Goodman, 2019). The biochemical profile of GA I patients includes the accumulation of the metabolites glutarylcarnitine, glutaric acid (GA), and 3-hydroxygluric acid (3HGA) in all tissues of the patients, but predominantly within the brain (Kölker et al., 2006). The predicted worldwide frequency of GA I ranges from 1:30,000 to 1:100,000 newborns, being one of the most prevalent organic acidurias (Wajner, 2019). Affected patients have encephalopathic crises manifested by convulsions during the first 3 years of life, which are normally provoked by catabolic events, such as fever, infection or prolonged fasting. These events usually cause irreversible striatum degeneration, resulting in dystonia, dyskinesia, muscle stiffness and general developmental deterioration (Strauss and Morton, 2003). Gliosis and neuronal loss especially in the basal ganglia are also commonly observed (Larson and Goodman, 2019; Wajner, 2019).

A knockout model of GA I ($Gcdh^{-/-}$) was developed in mice by replacing exons 1–7 of the *GCDH* gene with the *nlacF* and *NEO* genes (Koeller et al., 2002). Exposing $Gcdh^{-/-}$ animals to high protein or Lys intake resulted in elevated serum and brain GA and 3HGA accumulation, as well as neuronal loss, myelin disruption and gliosis mostly in the striatum and deep cortex (Zinnanti et al., 2006, 2007). Therefore, the $Gcdh^{-/-}$ mouse model exposed to Lys overload has been preferentially used as an appropriate GA I animal model to study the neuropathology of this disorder (Wajner et al., 2019). Different approaches were used to achieve high Lys levels in these animals, including Lys intraperitoneal or intracerebral injections, as well as chow supplemented with Lys (Zinnanti et al., 2006; Wajner et al., 2019).

Oxidative stress and neuroinflammation have been postulated to be involved in the pathogenesis of GA I, as observed by many studies using GA I animal models and cells from patients (Wajner, 2019; Wajner et al., 2019; Guerreiro et al., 2021), as well as of many other neurologic diseases (Freeman and Ting, 2016). As for the role of oxidative stress and Nrf2 pathway disruption in the pathophysiology of GA I, a study showed that the administration of quinolinic acid (QA), a metabolite synthesized by the kynurenine pathway during inflammatory process, induced oxidative stress in young $Gcdh^{-/-}$ mice fed a high Lys chow (Seminotti et al., 2016). In detail, QA induced lipid and protein oxidative damage, disturbed antioxidant defenses and increased reactive species production in striatum of $Gcdh^{-/-}$ mice fed a high Lys chow (Seminotti et al., 2016). All these changes occurred in parallel with increased levels of the transcription factors Nrf2 and NF-κB in the nucleus, as well as augmented Erk1/2 phosphorylation and Akt levels. Importantly, both ERK and Akt are kinases that participate in various signaling pathways, including Nrf2 translocation (Ishii and Warabi, 2019). Moreover, Keap1 and IκBα, the inhibitory proteins of Nrf2 and NF-κB, respectively, were seen to be decreased in the cytosol $Gcdh^{-/-}$ mice (Seminotti et al., 2016).

Another work showed that a single intrastriatal administration of Lys to young $Gcdh^{-/-}$ mice augmented Nrf2 protein expression in the nucleus of striatum (Amaral et al., 2019). It was also found that NF-κB expression was increased whereas HO-1 content was decreased in the striatum of these animals (Amaral et al., 2019).

Taken together, these findings demonstrated that Nrf2 signaling and redox homeostasis are altered in brain of $Gcdh^{-/-}$ mice submitted to Lys overload, effects that are induced at least partially by increased brain concentrations of GA and 3HGA derived from high Lys levels (Wajner, 2019).

Friedreich's Ataxia

Friedreich's ataxia (FRDA) (OMIM 229300) is the most common autosomal recessive inherited ataxia, with an estimated prevalence of 1:50,000 (Dürr et al., 1996). The first symptoms usually appear between 10 and 15 years of age due to progressive degeneration of large dorsal root ganglion (DRG) cells, dorsal spinocerebellar, and corticospinal tracts, as well as dentate nucleus of the cerebellum and other nuclei (Dürr et al., 1996; Koeppen and Mazurkiewicz, 2013; Patel et al., 2016). This results in neurological manifestations that include cerebellar and sensory ataxia, dysarthria, lack of deep tendon reflexes, pyramidal weakness of the legs, optic atrophy and visual and hearing impairment. Systemic presentations, such as hypertrophic cardiomyopathy, diabetes mellitus, kyphoscoliosis, and pes cavus, may be also observed (Kipps et al., 2009; Reetz et al., 2018; Hanson et al., 2019; Pandolfo, 2019). Patients usually lose the ability to ambulate around their mid-20 s (Campuzano et al., 1996; Lynch et al., 2021). Less frequent late onset (after 25 years) and very late-onset (after 40 years) FRDA variants commonly present with milder phenotypes and absence of systemic symptoms (Koeppen et al., 2011). Currently, there is no approved therapy for this disorder.

In most cases, FRDA occurs as a consequence of homozygous expanded guanosine-adenosine-adenosine (GAA) repeats in the first intron of the *FXN* gene, which usually contains up to 40 GAA triplets and may increase to over 1,700 in disease-associated alleles. The number of repeats is associated with earlier onset and disease severity (Campuzano et al., 1996; Dürr et al., 1996). As a result of the GAA expansion, the *FXN* gene is partially silenced and lower levels of the gene-encoded protein frataxin are expressed (Groh et al., 2014). The rare non-expansion mutations, on the other hand, may lead to the synthesis of partial or non-functional protein (Correia et al., 2008). Frataxin is a mitochondrial protein involved in cellular iron homeostasis and functions as a chaperone during iron-sulfur cluster and heme synthesis by incorporating iron to their precursors (Yoon and Cowan, 2004). The deficiency of frataxin has been associated with reduced activity of mitochondrial respiratory chain complexes, lower ATP production and decreased mitochondrial content, as well as iron accumulation and oxidative stress (Lodi et al., 1999; Bradley et al., 2000; Schulz et al., 2000; Jasoliya et al., 2017; Lin et al., 2017; Doni et al., 2021). Even though it was not previously classified (Saudubray and Garcia-Cazorla, 2018a),

since the deficient protein leads to mitochondrial iron overload and consequent defective energy supply (Yoon and Cowan, 2004), FRDA might be categorized either in the group of small molecule defects or energy-related disorders. However, it remains to be stablished.

Nuclear factor erythroid-2-related factor 2 signaling pathway has been shown to be disrupted in patients' cells and different FRDA models, rendering the cells more susceptible to oxidative damage due to decreased antioxidant dxsefenses (Wong et al., 1999; Chantrel-Groussard et al., 2001; Sturm et al., 2005; Al-Mahdawi et al., 2006). Initial evidence of decreased Nrf2 signaling in FRDA was demonstrated by Paupe et al. (2009). Upon treatment of FRDA fibroblasts with oligomycin and tert-butylhydroquinone (tBHQ) to induce oxidative stress, deficient cells did not present increased nuclear translocation of Nrf2, in contrast to normal cells (without deficiency). In addition, while tBHQ and oligomycin treatment increased mRNA levels of antioxidant enzymes regulated by Nrf2 in normal fibroblasts, FRDA fibroblasts failed to induce the expression of these proteins. Similar findings were observed in neuroblastoma-derived cell lines (SKNAS) challenged with tBHQ and oligomycin (Paupe et al., 2009). Furthermore, frataxin-deficient motor neuron-like cells (NSC34) exposed to GSSG also failed to induce nuclear translocation of Nrf2 (D'Oria et al., 2013).

Another study did not observe altered Nrf2 nuclear translocation in frataxin-deficient HeLa cells and DRG neurons (ND7/23), as well as in patient's lymphoblasts when treated with tBHQ. On the other hand, a reduction in Nrf2 content was seen in these cells, as well as in frataxin-deficient fibroblasts and Schwann cells (T265 cell line). In line with this, protein content and activity of thioredoxin reductase 1 (TxnRD1) were also decreased in some of these cells. Furthermore, transcripts and protein levels of Nrf2 were found reduced in DGR tissue and cerebellum of YG8R mice (FRDA model), which express expanded mutant alleles of human frataxin. This reduction was accompanied by lower GSH levels and protein content of HO-1, NQO1, and SOD2 in DRG. Moreover, in cerebellum and DRG Nrf2 expression was correlated with frataxin expression, which was further correlated with Nrf2-regulated genes in DRG (Shan et al., 2013). NSC34 neurons also presented a decrease in basal Nrf2 transcript and protein content along with reduced SOD and GST levels (D'Oria et al., 2013). Downregulation of Nrf2 pathway was further observed in peripheral blood cells of FRDA patients (Haugen et al., 2010).

The mechanisms underlying the impairment of Nrf2 signaling are not fully understood. Nevertheless, it was observed that under basal conditions the Nrf2 transcription factor is abnormally located in FRDA fibroblasts, which could be involved in the dysfunctional Nrf2 activation. In detail, while in normal fibroblasts Keap1 and Nrf2 were associated to actin stress fibers, in patient cells Keap1 and Nrf2 were not bound to these fibers, which were atypically distributed in the cell periphery (Paupe et al., 2009). This is in agreement with previous studies that showed disorganized actin structure, as well as increased actin glutathionylation in FRDA fibroblasts, an alteration that may disturb cytoskeleton stabilization (Pastore et al., 2003). Another study performed in a mouse conditional frataxin knockout model in heart and skeletal muscle showed that cardiac frataxin deficiency resulted in enhanced Keap1 expression and GSK3β-induced activation of a nuclear export machinery, leading to reduced cytosolic and nuclear Nrf2, respectively. Interestingly, although a decrease of mRNA levels of Nrf2 downstream antioxidant genes was observed, the correspondent proteins presented increased or unaltered content. No changes in Nrf2 signaling were found in the skeletal muscle of conditional knockout mice (Anzovino et al., 2017). Consistent with this study, the content of Keap1 was augmented, whereas DJ-1, a protein that stabilizes Nrf2 by preventing its association with Keap1, was reduced in FRDA fibroblasts (Petrillo et al., 2019).

Other studies explored Nrf2 signaling as a potential therapeutical target for FRDA by evaluating the effects Nrf2-activating compounds in FRDA models and patients. Among these compounds, sulforaphane (SFN), DMF, TBE-31 and RTA 408 (Omaveloxolone; Omav) are known to directly activate Nrf2 due to their interaction with Keap1 cysteine residues, which inhibits Nrf2 ubiquitination and degradation (Takaya et al., 2012; Kostov et al., 2015; Shekh-Ahmad et al., 2018). Other compounds, such as *N*-acetylcysteine (NAC), EPI-743, idebenone and dyclonine, also induced Nrf2 expression in different FRDA models (**Table 1**).

Additionally, it was observed that fibroblasts from the FRDA mice models YG8R and KIKO presented increased susceptibility to hydrogen peroxide and that treatment with SFN and TBE-31 prevented the hydrogen peroxide-induced decrease of cell viability. Of note, KIKO mouse model is characterized by knock-in-expanded GAA repeat on one allele (230 GAAs) and a knockout of FXN on the other allele, causing moderate overall deficiency of frataxin early in life. Lipid peroxidation and mitochondrial membrane depolarization were also ameliorated in these fibroblasts by both SFN and TBE-31 (Abeti et al., 2015). Moreover, treatment of FRDA patient's fibroblasts with SFN induced higher mRNA levels of Nrf2 and downstream genes (Petrillo et al., 2017). Similarly, in frataxin-deficient motor neurons, SFN and DMF augmented Nrf2 mRNA and protein levels, in addition to protein content of Nrf2 downstream genes. A decrease in GSSG/GSH ratio and axonal regrowth, with a reorganization and increased number of neurites, were also observed with SFN and DMF treatment (Petrillo et al., 2017). Noteworthy, La Rosa et al. (2019) found that such defects in the Nrf2 pathway may occur at early stages of neurogenesis, and treatment with SFN and EPI-743 showed beneficial effects in KIKO mouse embryonic cortex neural stem cells. Besides enhancing mRNA and protein levels of Nrf2 and its downstream target genes, SFN and EPI-743 decreased ROS overload and, importantly, reestablished the cellular differentiation program in these cortex neural stem cells, increasing the number and the length of neurites.

Sulforaphane and EPI-743 were further shown to rescue alterations associated with ferroptosis in FRDA fibroblasts by promoting Nrf2 nuclear translocation, decreasing lipid peroxides and glutathionylated proteins levels, and restoring the mitochondrial morphology from small and fragmented

organelles to tubular networks (La Rosa et al., 2021). Ferroptosis-related alterations, such as increased content of the lipid peroxidation marker 4-hydroxynonenal and reduced expression of Nrf2 and some of its target genes, were also ameliorated in leukocytes of FRDA patients treated with idebenone (La Rosa et al., 2021).

In contrast to SFN and DMF that possess effects on a wide range of proteins, cyanoenone triterpenoids, such as Omav, are more potent and target specifically Nrf2 activation (Satoh and Lipton, 2017; Shekh-Ahmad et al., 2018). In this regard, it was observed that treatment of cerebellar granule neurons from KIKO and YG8R mice with Omav restored the activity of respiratory chain complex I, which is highly dependent on iron-sulfur clusters. Similar findings were verified in FRDA patient's fibroblasts. Omav reverted increased lipid peroxidation and mitochondrial ROS levels, as well as decreased GSH content under basal conditions in FRDA fibroblasts. Upon challenge with hydrogen peroxide, Omav further protected fibroblasts from mitochondrial membrane potential dissipation and cell death (Abeti et al., 2018). Noteworthy, Omav is currently in Phase II clinical trial in FRDA patients (ClinicalTrials.gov Identifier: NCT02255435; MOXIe), showing improvement in the neurological dysfunction and general safety (Lynch et al., 2018, 2021).

Other investigations evaluated the effects of these Nrf2-activating compounds on the expression of frataxin, the primary defect in FRDA, in parallel to the alterations seen on Nrf2 pathway. In this regard, a study showed that dyclonine, an oral anesthetic that confers topical anesthesia to mucous membranes, induced frataxin expression in FRDA lymphoblasts and cerebellum of YG8R and KIKO mice, as well as in buccal cells of FRDA patients (Sahdeo et al., 2014). Dyclonine was found to activate the ARE/Nrf2 pathway in YG8R mouse cerebellum. Interestingly, it was verified that ARE sites are present in the *FXN* gene, and dyclonine-treated FRDA lymphoblasts had enhanced binding of Nrf2 to these sites in the *FXN* and *Hmox1* genes (Sahdeo et al., 2014).

Another work compared the effects of SFN, DMF, Omav, idebenone, EPI-743 and NAC (redox-active compound) on Nrf2 pathway activation and frataxin expression in FRDA fibroblasts (Petrillo et al., 2019). Although these compounds elicited differential effects on Nrf2 target genes and GSH levels, all of them augmented previously reduced Nrf2 transcripts in these cells. Moreover, SFN, DMF, NAC, and EPI-743 increased frataxin transcripts (Petrillo et al., 2019). Further data demonstrated increased levels of frataxin mRNA levels in FRDA lymphoblasts and fibroblasts, and elevated frataxin protein content in cerebellum of YG8R and KIKO mice treated with DMF (Hayashi and Cortopassi, 2016; Jasoliya et al., 2019). It was also found in FRDA lymphoblasts that DMF stimulated frataxin expression (Jasoliya et al., 2019).

Finally, a recent study analyzed the GSH system and Nrf2 signaling in the modulation of the phenotype of a family with a proband affected by late-onset FRDA and his asymptomatic mother and younger sister, that also presented decreased frataxin levels (Petrillo et al., 2021). Surprisingly, the affected proband presented high levels of GSH and low levels of GSSG, while the asymptomatic mother and sister had low GSH and increased GSSG in leukocytes. Similar findings were observed in fibroblasts. Additionally, the unaffected mother presented higher mRNA levels of GCL, which participates in GSH synthesis, and of GR in leukocytes and fibroblasts, probably as a compensatory mechanism. The affected proband and the unaffected sister only presented increased transcripts of GR. Interestingly, the mother and the younger sister presented augmented Nrf2 expression in leukocytes and fibroblasts, whereas induction of Nrf2 was not found in fibroblasts of the proband. However, Nrf2 levels were increased in leukocytes of the proband, which could be a consequence of idebenone treatment, as reported previously (Petrillo et al., 2019, 2021; La Rosa et al., 2021).

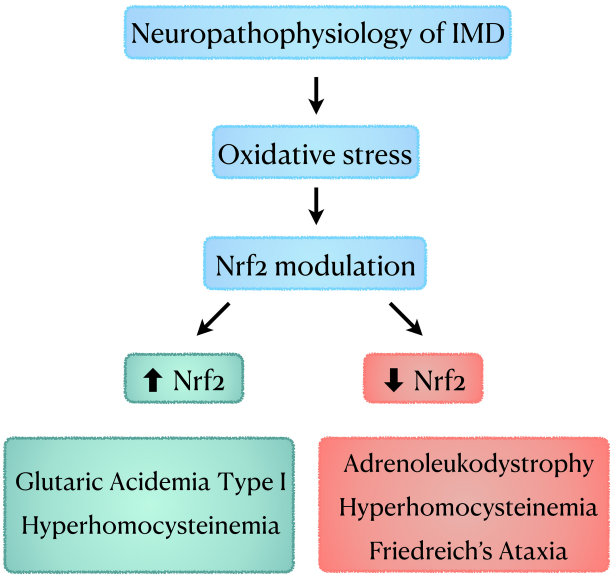

FIGURE 2 | Schematic diagram showing the role of oxidative stress and Nrf2 modulation in the neuropathophysiology of IMD. IMD, Inherited Metabolic Disorders; Nrf2, nuclear factor erythroid-2-related factor 2.

In summary, these data not only reinforce the involvement of Nrf2 signaling disruption in the neuropathophysiology of FRDA but also show that this signaling pathway could be a promising therapeutical target in this disorder. Additional investigations are also needed to better clarify the initial cause of dysfunctional Nrf2 signaling in different tissues affected in FRDA, especially in neuronal models.

CONCLUSION AND FUTURE DIRECTIONS

Inherited metabolic disorders are caused by abnormal functioning or reduced levels of specific proteins related to metabolic pathways. Disturbances in these metabolic pathways result in a spectrum of clinical findings affecting multiple

organs, predominantly the nervous system (Saudubray and Garcia-Cazorla, 2018a). Regarding the mechanisms involved in the pathophysiology of these disorders, mounting evidence has shown that oxidative stress often plays a key role in IMDs clinically characterized by neurological dysfunction (Ristoff and Larsson, 2002; Mc Guire et al., 2009; Leipnitz et al., 2015; Zubarioglu et al., 2017; Cansever et al., 2019; Wajner, 2019; Wyse et al., 2019, 2021; Grings et al., 2020; Ikawa et al., 2021). Therefore, it is not surprising that Nrf2 signaling disruption is also an important pathomechanism, although only few studies have investigated this transcription factor in IMDs.

We reviewed here data demonstrating that Nrf2 factor is differentially modulated not only among different IMDs (e.g., GA I × adrenoleukodystrophy) but also in different animal models of the same disease (HHcy), as well as in patient cells (FRDA) (**Figure 2**). When analyzing the data for HHcy, it seems that Nrf2 response was dependent on the rodent species used for each disease model and age of animals. Thus, if we extrapolate these data for the human condition, it may be speculated that the age of patients influences Nrf2 response. This is in line with data showing that Nrf2 response varies with age even in normal individuals (Schmidlin et al., 2019). Furthermore, in the studies focusing on the investigation of Nrf2 activators in FRDA models, it was seen that different compounds induced variable sets of Nrf2 downstream genes and had different effects on frataxin levels, which were dependent on the cell type (model) evaluated. This implies the existence of drug and cellular-specific transcriptional regulatory mechanisms for these genes. Another important factor that may influence Nrf2 alterations seen in IMDs is whether the patients have a residual activity of the deficient enzyme, or it is null. Noteworthy, the degree of enzymatic activity often correlates with the disease phenotype (e.g., higher enzyme activity usually causes milder phenotypes) (Gieselmann, 2005; Oliveira and Ferreira, 2019; Grünert et al., 2021; Zanfardino et al., 2021). As for FRDA, it should be highlighted that the content of frataxin may influence Nrf2 activation. Indeed, a correlation between frataxin and Nrf2 levels, as well as between frataxin levels and Nrf2 downstream genes has been verified in animal studies (Shan et al., 2013).

More studies with different models (cultured cells, patients' cells, biological fluids and animal models) are necessary in order to determine how Nrf2 response is modulated in IMDs, and whether it is dependent on different factors (age, mutation, phenotype, etc.). It is also expected that future studies may encourage the investigation of pharmacological therapies aiming at Nrf2 modulation and consequent amelioration of oxidative stress state in these disorders.

AUTHOR CONTRIBUTIONS

BS and MG searched for the literature material. BS designed the figures. BS, MG, PT, GL, and LS wrote and revised the manuscript. BS and GL designed the outline. LS provided the financial support. All authors approved the last version of the manuscript.

REFERENCES

Abeti, R., Baccaro, A., Esteras, N., and Giunti, P. (2018). Novel Nrf2-inducer prevents mitochondrial defects and oxidative stress in Friedreich's ataxia models. *Front. Cell Neurosci.* 12:188. doi: 10.3389/fncel.2018.00188

Abeti, R., Uzun, E., Renganathan, I., Honda, T., Pook, M. A., and Giunti, P. (2015). Targeting lipid peroxidation and mitochondrial imbalance in Friedreich's ataxia. *Pharmacol. Res.* 99, 344–350. doi: 10.1016/j.phrs.2015.05.015

Adelusi, T. I., Du, L., Hao, M., Zhou, X., Xuan, Q., Apu, C., et al. (2020). Keap1/Nrf2/ARE signaling unfolds therapeutic targets for redox imbalanced-mediated diseases and diabetic nephropathy. *Biomed. Pharmacother.* 123:109732. doi: 10.1016/j.biopha.2019.109732

Ahmed, S. M., Luo, L., Namani, A., Wang, X. J., and Tang, X. (2017). Nrf2 signaling pathway: Pivotal roles in inflammation. *Biochim. Biophys. Acta Mol. Basis Dis.* 1863, 585–597. doi: 10.1016/j.bbadis.2016.11.005

Al-Mahdawi, S., Pinto, R. M., Varshney, D., Lawrence, L., Lowrie, M. B., Hughes, S., et al. (2006). GAA repeat expansion mutation mouse models of Friedreich ataxia exhibit oxidative stress leading to progressive neuronal and cardiac pathology. *Genomics* 88, 580–590. doi: 10.1016/j.ygeno.2006.06.015

Amaral, A. U., Seminotti, B., da Silva, J. C., de Oliveira, F. H., Ribeiro, R. T., Leipnitz, G., et al. (2019). Acute lysine overload provokes marked striatum injury involving oxidative stress signaling pathways in glutaryl-CoA dehydrogenase deficient mice. *Neurochem. Int.* 129:104467. doi: 10.1016/j.neuint.2019.104467

Andérica-Romero, A. C., González-Herrera, I. G., Santamaría, A., and Pedraza-Chaverri, J. (2013). Cullin 3 as a novel target in diverse pathologies. *Redox Biol.* 1, 366–372. doi: 10.1016/j.redox.2013.07.003

Anzovino, A., Chiang, S., Brown, B. E., Hawkins, C. L., Richardson, D. R., and Huang, M. L. (2017). Molecular alterations in a mouse cardiac model of Friedreich ataxia: an impaired Nrf2 response mediated via upregulation of Keap1 and activation of the Gsk3β axis. *Am. J. Pathol.* 187, 2858–2875. doi: 10.1016/j.ajpath.2017.08.021

Barić, I., Staufner, C., Augoustides-Savvopoulou, P., Chien, Y. H., Dobbelaere, D., Grünert, S. C., et al. (2017). Consensus recommendations for the diagnosis, treatment and follow-up of inherited methylation disorders. *J. Inherit. Metab. Dis.* 40, 5–20. doi: 10.1007/s10545-016-9972-7

Baxter, P. S., and Hardingham, G. E. (2016). Adaptive regulation of the brain's antioxidant defences by neurons and astrocytes. *Free Radic. Biol. Med.* 100, 147–152. doi: 10.1016/j.freeradbiomed.2016.06.027

Belenguer, P., Duarte, J. M. N., Schuck, P. F., and Ferreira, G. C. (2019). Mitochondria and the brain: bioenergetics and beyond. *Neurotox. Res.* 36, 219–238. doi: 10.1007/s12640-019-00061-7

Berger, J., Forss-Petter, S., and Eichler, F. S. (2014). Pathophysiology of X-linked adrenoleukodystrophy. *Biochimie* 98, 135–142. doi: 10.1016/j.biochi.2013.11.023

Berger, J., Molzer, B., Faé, I., and Bernheimer, H. (1994). X-linked adrenoleukodystrophy (ALD): a novel mutation of the ALD gene in 6 members of a family presenting with 5 different phenotypes. *Biochem. Biophys. Res. Commun.* 205, 1638–1643. doi: 10.1006/bbrc.1994.2855

Bolaños, J. P. (2016). Bioenergetics and redox adaptations of astrocytes to neuronal activity. *J. Neurochem.* 139, 115–125. doi: 10.1111/jnc.13486

Bradley, J. L., Blake, J. C., Chamberlain, S., Thomas, P. K., Cooper, J. M., and Schapira, A. H. (2000). Clinical, biochemical and molecular genetic correlations in Friedreich's ataxia. *Hum. Mol. Genet.* 9, 275–282. doi: 10.1093/hmg/9.2.275

Campuzano, V., Montermini, L., Moltò, M. D., Pianese, L., Cossée, M., Cavalcanti, F., et al. (1996). Friedreich's ataxia: autosomal recessive disease caused by an intronic GAA triplet repeat expansion. *Science* 271, 1423–1427. doi: 10.1126/science.271.5254.1423

Canning, P., Sorrell, F. J., and Bullock, A. N. (2015). Structural basis of Keap1 interactions with Nrf2. *Free Radic. Biol. Med.* 88, 101–107. doi: 10.1016/j.freeradbiomed.2015.05.034

Cansever, M. S., Zubarioglu, T., Oruc, C., Kiykim, E., Gezdirici, A., Neselioglu, S., et al. (2019). Oxidative stress among L-2-hydroxyglutaric aciduria disease

patients: evaluation of dynamic thiol/disulfide homeostasis. *Metab. Brain Dis.* 34, 283–288. doi: 10.1007/s11011-018-0354-8

Chantrel-Groussard, K., Geromel, V., Puccio, H., Koenig, M., Munnich, A., Rötig, A., et al. (2001). Disabled early recruitment of antioxidant defenses in Friedreich's ataxia. *Hum. Mol. Genet.* 10, 2061–2067. doi: 10.1093/hmg/10.19.2061

Chartoumpekis, D. V., Fu, C. Y., Ziros, P. G., and Sykiotis, G. P. (2020). Patent review (2017-2020) of the Keap1/Nrf2 pathway using PatSeer Pro: Focus on autoimmune diseases. *Antioxidants* 9:1138. doi: 10.3390/antiox9111138

Chowdhry, S., Zhang, Y., McMahon, M., Sutherland, C., Cuadrado, A., and Hayes, J. D. (2013). Nrf2 is controlled by two distinct β-TrCP recognition motifs in its Neh6 domain, one of which can be modulated by GSK-3 activity. *Oncogene* 32, 3765–3781. doi: 10.1038/onc.2012.388

Cordaro, M., Siracusa, R., Fusco, R., Cuzzocrea, S., Di Paola, R., and Impellizzeri, D. (2021). Involvements of hyperhomocysteinemia in neurological disorders. *Metabolites* 11:37. doi: 10.3390/metabo11010037

Correia, A. R., Pastore, C., Adinolfi, S., Pastore, A., and Gomes, C. M. (2008). Dynamics, stability and iron-binding activity of frataxin clinical mutants. *FEBS J.* 275, 3680–3690. doi: 10.1111/j.1742-4658.2008.06512.x

Cuadrado, A., Rojo, A. I., Wells, G., Hayes, J. D., Cousin, S. P., Rumsey, W. L., et al. (2019). Therapeutic targeting of the NRF2 and KEAP1 partnership in chronic diseases. *Nat. Rev. Drug Discov.* 18, 295–317. doi: 10.1038/s41573-018-0008-x

D'Oria, V., Petrini, S., Travaglini, L., Priori, C., Piermarini, E., Petrillo, S., et al. (2013). Frataxin deficiency leads to reduced expression and impaired translocation of NF-E2-related factor (Nrf2) in cultured motor neurons. *Int. J. Mol. Sci.* 14, 7853–7865. doi: 10.3390/ijms14047853

Díaz, M., Mesa-Herrera, F., and Marín, R. (2021). DHA and its elaborated modulation of antioxidant defenses of the brain: implications in aging and AD neurodegeneration. *Antioxidants* 10:907. doi: 10.3390/antiox10060907

Doni, D., Rigoni, G., Palumbo, E., Baschiera, E., Peruzzo, R., De Rosa, E., et al. (2021). The displacement of frataxin from the mitochondrial cristae correlates with abnormal respiratory supercomplexes formation and bioenergetic defects in cells of Friedreich ataxia patients. *FASEB J.* 35:e21362. doi: 10.1096/fj.202000524RR

Dos Santos, T. M., Siebert, C., de Oliveira, M. F., Manfredini, V., and Wyse, A. T. S. (2019). Chronic mild Hyperhomocysteinemia impairs energy metabolism, promotes DNA damage and induces a Nrf2 response to oxidative stress in rats brain. *Cell Mol. Neurobiol.* 39, 687–700. doi: 10.1007/s10571-019-00674-8

Dubey, P., Raymond, G. V., Moser, A. B., Kharkar, S., Bezman, L., and Moser, H. W. (2005). Adrenal insufficiency in asymptomatic adrenoleukodystrophy patients identified by very long-chain fatty acid screening. *J. Pediatr.* 146, 528–532. doi: 10.1016/j.jpeds.2004.10.067

Dürr, A., Cossee, M., Agid, Y., Campuzano, V., Mignard, C., Penet, C., et al. (1996). Clinical and genetic abnormalities in patients with Friedreich's ataxia. *N. Engl. J. Med.* 335, 1169–1175. doi: 10.1056/NEJM199610173351601

Elanchezhian, R., Palsamy, P., Madson, C. J., Lynch, D. W., and Shinohara, T. (2012). Age-related cataracts: Homocysteine coupled endoplasmic reticulum stress and suppression of Nrf2-dependent antioxidant protection. *Chem. Biol. Interact.* 200, 1–10. doi: 10.1016/j.cbi.2012.08.017

El-Hattab, A. W., Zarante, A. M., Almannai, M., and Scaglia, F. (2017). Therapies for mitochondrial diseases and current clinical trials. *Mol. Genet. Metab.* 122, 1–9. doi: 10.1016/j.ymgme.2017.09.009

Engelen, M., Barbier, M., Dijkstra, I. M., Schür, R., de Bie, R. M., Verhamme, C., et al. (2014). X-linked adrenoleukodystrophy in women: a cross-sectional cohort study. *Brain* 137, 693–706. doi: 10.1093/brain/awt361

Engelen, M., Kemp, S., de Visser, M., van Geel, B. M., Wanders, R. J., Aubourg, P., et al. (2012). X-linked adrenoleukodystrophy (X-ALD): clinical presentation and guidelines for diagnosis, follow-up and management. *Orphanet. J. Rare Dis.* 7:51. doi: 10.1186/1750-1172-7-51

Faverzani, J. L., Hammerschmidt, T. G., Sitta, A., Deon, M., Wajner, M., and Vargas, C. R. (2017). Oxidative stress in homocystinuria due to cystathionine ß-synthase deficiency: findings in patients and in animal models. *Cell. Mol. Neurobiol.* 37, 1477–1485. doi: 10.1007/s10571-017-0478-0

Ferreira, C. R., Rahman, S., Keller, M., Zschocke, J., Icimd Advisory, and Group. (2021). An international classification of inherited metabolic disorders (ICIMD). *J. Inherit. Metab. Dis.* 44, 164–177. doi: 10.1002/jimd.12348

Ferreira, C. R., van Karnebeek, C. D. M., Vockley, J., and Blau, N. (2019). A proposed nosology of inborn errors of metabolism. *Genet. Med.* 21, 102–106. doi: 10.1038/s41436-018-0022-8

Freeman, L. C., and Ting, J. P. (2016). The pathogenic role of the inflammasome in neurodegenerative diseases. *J. Neurochem.* 136, 29–38. doi: 10.1111/jnc.13217

García-Cazorla, À, and Saudubray, J. M. (2018). Cellular neurometabolism: a tentative to connect cell biology and metabolism in neurology. *J. Inherit. Metab. Dis.* 41, 1043–1054. doi: 10.1007/s10545-018-0226-8

Gieselmann, V. (2005). What can cell biology tell us about heterogeneity in lysosomal storage diseases? *Acta Paediatr. Suppl.* 94, 80–86. doi: 10.1111/j.1651-2227.2005.tb02118.x

Goyette, P., Frosst, P., Rosenblatt, D. S., and Rozen, R. (1995). Seven novel mutations in the methylenetetrahydrofolate reductase gene and genotype/phenotype correlations in severe methylenetetrahydrofolate reductase deficiency. *Am. J. Hum. Genet.* 56, 1052–1059.

Grings, M., Wajner, M., and Leipnitz, G. (2020). Mitochondrial dysfunction and redox homeostasis impairment as pathomechanisms of brain damage in ethylmalonic encephalopathy: insights from animal and human studies. *Cell. Mol. Neurobiol.* 2020, 976–972. doi: 10.1007/s10571-020-00976-2

Groh, M., Lufino, M. M., Wade-Martins, R., and Gromak, N. (2014). R-loops associated with triplet repeat expansions promote gene silencing in Friedreich ataxia and fragile X syndrome. *PLoS Genet.* 10:e1004318. doi: 10.1371/journal.pgen.1004318

Grünert, S. C., Hannibal, L., and Spiekerkoetter, U. (2021). The phenotypic and genetic spectrum of glycogen storage disease type VI. *Genes* 12:1205. doi: 10.3390/genes12081205

Guerreiro, G., Faverzani, J., Moura, A. P., Volfart, V., Gome Dos, Reis, B., et al. (2021). Protective effects of L-carnitine on behavioral alterations and neuroinflammation in striatum of glutaryl-COA dehydrogenase deficient mice. *Arch. Biochem. Biophys.* 709:108970. doi: 10.1016/j.abb.2021.108970

Halliwell, B. (2006). Oxidative stress and neurodegeneration: where are we now? *J. Neurochem.* 97, 1634–1658. doi: 10.1111/j.1471-4159.2006.03907.x

Halliwell, B., and Gutteridge, J. M. C. (2015). "Cellular responses to oxidative stress: adaptation, damage, repair, senescence and death," in *Free radicals in biology and medicine*, eds B. Halliwell and J. M. C. Gutteridge (Oxford: Oxford University Press Inc), 199–283.

Hanson, E., Sheldon, M., Pacheco, B., Alkubeysi, M., and Raizada, V. (2019). Heart disease in Friedreich's ataxia. *World J. Cardiol.* 11, 1–12. doi: 10.4330/wjc.v11.i1.1

Haugen, A. C., Di Prospero, N. A., Parker, J. S., Fannin, R. D., Chou, J., Meyer, J. N., et al. (2010). Altered gene expression and DNA damage in peripheral blood cells from Friedreich's ataxia patients: cellular model of pathology. *PLoS Genet.* 6:e1000812. doi: 10.1371/journal.pgen.1000812

Hayashi, G., and Cortopassi, G. (2016). Lymphoblast oxidative stress genes as potential biomarkers of disease severity and drug effect in Friedreich's ataxia. *PLoS One* 11:e0153574. doi: 10.1371/journal.pone.0153574

Hennig, P., Garstkiewicz, M., Grossi, S., Di Filippo, M., French, L. E., and Beer, H. D. (2018). The crosstalk between Nrf2 and inflammasomes. *Int. J. Mol. Sci.* 19:562. doi: 10.3390/ijms19020562

Ikawa, M., Okazawa, H., and Yoneda, M. (2021). Molecular imaging for mitochondrial metabolism and oxidative stress in mitochondrial diseases and neurodegenerative disorders. *Biochim. Biophys. Acta Gen. Subj.* 1865:129832. doi: 10.1016/j.bbagen.2020.129832

Ishii, T., and Warabi, E. (2019). Mechanism of rapid nuclear factor-E2-related factor 2 (Nrf2) activation via membrane-associated estrogen receptors: roles of NADPH oxidase 1, neutral sphingomyelinase 2 and epidermal growth factor receptor (EGFR). *Antioxidants* 8:69. doi: 10.3390/antiox8030069

Jasoliya, M. J., McMackin, M. Z., Henderson, C. K., Perlman, S. L., and Cortopassi, G. A. (2017). Frataxin deficiency impairs mitochondrial biogenesis in cells, mice and humans. *Hum. Mol. Genet.* 26, 2627–2633. doi: 10.1093/hmg/ddx141

Jasoliya, M., Sacca, F., Sahdeo, S., Chedin, F., Pane, C., Brescia Morra, V., et al. (2019). Dimethyl fumarate dosing in humans increases frataxin expression: A potential therapy for Friedreich's Ataxia. *PLoS One* 14:e0217776. doi: 10.1371/journal.pone.0217776

Jimenez-Blasco, D., Santofimia-Castaño, P., Gonzalez, A., Almeida, A., and Bolaños, J. P. (2015). Astrocyte NMDA receptors' activity sustains neuronal survival through a Cdk5-Nrf2 pathway. *Cell Death Differ.* 22, 1877–1889. doi: 10.1038/cdd.2015.49

Kahroba, H., Ramezani, B., Maadi, H., Sadeghi, M. R., Jaberie, H., and Ramezani, F. (2021). The role of Nrf2 in neural stem/progenitors cells: From maintaining stemness and self-renewal to promoting differentiation capability and facilitating therapeutic application in neurodegenerative disease. *Ageing Res. Rev.* 65:101211. doi: 10.1016/j.arr.2020.101211

Karimzadeh, P., Ghofrani, M., and Nasiri, S. (2020). Approach to Pptients with neurometabolic diseases who show characteristic signs and symptoms. *Iran J. Child Neurol.* 14, 19–32.

Kemper, A. R., Brosco, J., Comeau, A. M., Green, N. S., Grosse, S. D., Jones, E., et al. (2017). Newborn screening for X-linked adrenoleukodystrophy: evidence summary and advisory committee recommendation. *Genet. Med.* 19, 121–126. doi: 10.1038/gim.2016.68

Kim, J. (2021). Pre-clinical neuroprotective evidences and plausible mechanisms of sulforaphane in Alzheimer's Disease. *Int. J. Mol. Sci.* 22:2929. doi: 10.3390/ijms22062929

Kim, J., Kim, H., Roh, H., and Kwon, Y. (2018). Causes of hyperhomocysteinemia and its pathological significance. *Arch. Pharm. Res.* 41, 372–383. doi: 10.1007/s12272-018-1016-4

Kipps, A., Alexander, M., Colan, S. D., Gauvreau, K., Smoot, L., Crawford, L., et al. (2009). The longitudinal course of cardiomyopathy in Friedreich's ataxia during childhood. *Pediatr. Cardiol.* 30, 306–310. doi: 10.1007/s00246-008-9305-1

Koeller, D. M., Woontner, M., Crnic, L. S., Kleinschmidt-DeMasters, B., Stephens, J., Hunt, E. L., et al. (2002). Biochemical, pathologic and behavioral analysis of a mouse model of glutaric acidemia type I. *Hum. Mol. Genet.* 11, 347–357. doi: 10.1093/hmg/11.4.347

Koeppen, A. H., and Mazurkiewicz, J. E. (2013). Friedreich ataxia: neuropathology revised. *J. Neuropathol. Exp. Neurol.* 72, 78–90. doi: 10.1097/NEN.0b013e31827e5762

Koeppen, A. H., Morral, J. A., McComb, R. D., and Feustel, P. J. (2011). The neuropathology of late-onset Friedreich's ataxia. *Cerebellum* 10, 96–103. doi: 10.1007/s12311-010-0235-0

Kölker, S., Sauer, S. W., Okun, J. G., Hoffmann, G. F., and Koeller, D. M. (2006). Lysine intake and neurotoxicity in glutaric aciduria type I: towards a rationale for therapy? *Brain* 129:e54. doi: 10.1093/brain/awl137

Komatsu, M., Kurokawa, H., Waguri, S., Taguchi, K., Kobayashi, A., Ichimura, Y., et al. (2010). The selective autophagy substrate p62 activates the stress responsive transcription factor Nrf2 through inactivation of Keap1. *Nat. Cell. Biol.* 12, 213–223. doi: 10.1038/ncb2021

Kostov, R. V., Knatko, E. V., McLaughlin, L. A., Henderson, C. J., Zheng, S., Huang, J. T., et al. (2015). Pharmacokinetics and pharmacodynamics of orally administered acetylenic tricyclic bis(cyanoenone), a highly potent Nrf2 activator with a reversible covalent mode of action. *Biochem. Biophys. Res. Commun.* 465, 402–407. doi: 10.1016/j.bbrc.2015.08.016

Kourakis, S., Timpani, C. A., de Haan, J. B., Gueven, N., Fischer, D., and Rybalka, E. (2021). Targeting Nrf2 for the treatment of Duchenne Muscular Dystrophy. *Redox Biol.* 38:101803. doi: 10.1016/j.redox.2020.101803

Kripps, K. A., Baker, P. R. II, Thomas, J. A., Skillman, H. E., Bernstein, L., Gaughan, S., et al. (2021). REVIEW: Practical strategies to maintain anabolism by intravenous nutritional management in children with inborn metabolic diseases. *Mol. Genet. Metab.* 133, 231–241. doi: 10.1016/j.ymgme.2021.04.007

Kumar, M., and Sandhir, R. (2018). Neuroprotective effect of hydrogen sulfide in hyperhomocysteinemia is mediated through antioxidant action involving Nrf2. *Neuromol. Med.* 20, 475–490. doi: 10.1007/s12017-018-8505-y

La Rosa, P., Petrillo, S., Turchi, R., Berardinelli, F., Schirinzi, T., Vasco, G., et al. (2021). The Nrf2 induction prevents ferroptosis in Friedreich's Ataxia. *Redox Biol.* 38:101791. doi: 10.1016/j.redox.2020.101791

La Rosa, P., Russo, M., D'Amico, J., Petrillo, S., Aquilano, K., Lettieri-Barbato, D., et al. (2019). Nrf2 induction re-establishes a proper neuronal differentiation program in Friedreich's Ataxia neural stem cells. *Front. Cell. Neurosci.* 13:356. doi: 10.3389/fncel.2019.00356

Larson, A., and Goodman, S. (2019). "Glutaric Acidemia Type 1 Summary Genetic counseling," in *GeneReviews$[Internet]*, eds M. P. Adam, H. H. Ardinger, R. A. Pagon, S. E. Wallace, L. J. H. Bean, K. Stephens, et al. (Seattle, WA: University of Washington), 1–27.

Lau, A., Wang, X. J., Zhao, F., Villeneuve, N. F., Wu, T., Jiang, T., et al. (2010). A noncanonical mechanism of Nrf2 activation by autophagy deficiency: direct interaction between Keap1 and p62. *Mol. Cell. Biol.* 30, 3275–3285. doi: 10.1128/MCB.00248-10

Launay, N., Aguado, C., Fourcade, S., Ruiz, M., Grau, L., Riera, J., et al. (2015). Autophagy induction halts axonal degeneration in a mouse model of X-adrenoleukodystrophy. *Acta Neuropathol.* 129, 399–415. doi: 10.1007/s00401-014-1378-8

Leipnitz, G., Vargas, C. R., and Wajner, M. (2015). Disturbance of redox homeostasis as a contributing underlying pathomechanism of brain and liver alterations in 3-hydroxy-3-methylglutaryl-CoA lyase deficiency. *J. Inherit. Metab. Dis.* 38, 1021–1028. doi: 10.1007/s10545-015-9863-3

Li, J., Wang, H., He, Z., Wang, X., Tang, J., and Huang, D. (2019). Clinical, neuroimaging, biochemical, and genetic features in six Chinese patients with Adrenomyeloneuropathy. *BMC Neurol.* 19:227. doi: 10.1186/s12883-019-1449-5

Li, W., Yu, S. W., and Kong, A. N. (2006). Nrf2 possesses a redox-sensitive nuclear exporting signal in the Neh5 transactivation domain. *J. Biol. Chem.* 281, 27251–27263. doi: 10.1074/jbc.M602746200

Lin, H., Magrane, J., Rattelle, A., Stepanova, A., Galkin, A., Clark, E. M., et al. (2017). Early cerebellar deficits in mitochondrial biogenesis and respiratory chain complexes in the KIKO mouse model of Friedreich ataxia. *Dis. Model. Mech.* 10, 1343–1352. doi: 10.1242/dmm.030502

Liu, W. J., Ye, L., Huang, W. F., Guo, L. J., Xu, Z. G., Wu, H. L., et al. (2016). p62 links the autophagy pathway and the ubiqutin-proteasome system upon ubiquitinated protein degradation. *Cell. Mol. Biol. Lett.* 21:29. doi: 10.1186/s11658-016-0031-z

Lodi, R., Cooper, J. M., Bradley, J. L., Manners, D., Styles, P., Taylor, D. J., et al. (1999). Deficit of in vivo mitochondrial ATP production in patients with Friedreich ataxia. *Proc. Natl. Acad. Sci. U S A.* 96, 11492–11495. doi: 10.1073/pnas.96.20.11492

Lynch, D. R., Chin, M. P., Delatycki, M. B., Subramony, S. H., Corti, M., Hoyle, J. C., et al. (2021). Safety and efficacy of Omaveloxolone in Friedreich ataxia (MOXIe Study). *Ann. Neurol.* 89, 212–225. doi: 10.1002/ana.25934

Lynch, D. R., Farmer, J., Hauser, L., Blair, I. A., Wang, Q. Q., Mesaros, C., et al. (2018). Safety, pharmacodynamics, and potential benefit of omaveloxolone in Friedreich ataxia. *Ann. Clin. Transl. Neurol.* 6, 15–26. doi: 10.1002/acn3.660

Mankad, K., Talenti, G., Tan, A. P., Gonçalves, F. G., Robles, C., Kan, E. Y. L., et al. (2018). Neurometabolic disorders of the newborn. *Top. Magn. Reson. Imaging* 27, 179–196. doi: 10.1097/RMR.0000000000000176

Mazzola, P. N., Karikas, G. A., Schulpis, K. H., and Dutra-Filho, C. S. (2013). Antioxidant treatment strategies for hyperphenylalaninemia. *Metab. Brain Dis.* 28, 541–550. doi: 10.1007/s11011-013-9414-2

Mc Guire, P. J., Parikh, A., and Diaz, G. A. (2009). Profiling of oxidative stress in patients with inborn errors of metabolism. *Mol. Genet. Metab.* 98, 173–180. doi: 10.1016/j.ymgme.2009.06.007

Mohamed, R., Sharma, I., Ibrahim, A. S., Saleh, H., Elsherbiny, N. M., Fulzele, S., et al. (2017). Hyperhomocysteinemia alters retinal endothelial cells barrier function and angiogenic potential via activation of oxidative stress. *Sci. Rep.* 7:11952. doi: 10.1038/s41598-017-09731-y

Oliveira, J. P., and Ferreira, S. (2019). Multiple phenotypic domains of Fabry disease and their relevance for establishing genotype- phenotype correlations. *Appl. Clin. Genet.* 12, 35–50. doi: 10.2147/TACG.S146022

Pandolfo, M. (2019). Friedreich ataxia: the clinical picture. *J. Neurol.* 256, 3–8. doi: 10.1007/s00415-009-1002-3

Panieri, E., Buha, A., Telkoparan-Akillilar, P., Cevik, D., Kouretas, D., Veskoukis, A., et al. (2020). Potential applications of NRF2 modulators in cancer therapy. *Antioxidants* 9:193. doi: 10.3390/antiox9030193

Parmeggiani, B., and Vargas, C. R. (2018). Oxidative stress in urea cycle disorders: Findings from clinical and basic research. *Clin. Chim. Acta* 477, 121–126. doi: 10.1016/j.cca.2017.11.041

Pastore, A., Tozzi, G., Gaeta, L. M., Bertini, E., Serafini, V., Di Cesare, S., et al. (2003). Actin glutathionylation increases in fibroblasts of patients with Friedreich's ataxia: a potential role in the pathogenesis of the disease. *J. Biol. Chem.* 278, 42588–42595. doi: 10.1074/jbc.M301872200

Patel, M., Isaacs, C. J., Seyer, L., Brigatti, K., Gelbard, S., Strawser, C., et al. (2016). Progression of Friedreich ataxia: quantitative characterization over 5 years. *Ann. Clin. Transl. Neurol.* 3, 684–694. doi: 10.1002/acn3.332

Paupe, V., Dassa, E. P., Goncalves, S., Auchère, F., Lönn, M., Holmgren, A., et al. (2009). Impaired nuclear Nrf2 translocation undermines the oxidative stress response in Friedreich ataxia. *PLoS One* 4:e4253. doi: 10.1371/journal.pone.0004253

Petrillo, S., D'Amico, J., La Rosa, P., Bertini, E. S., and Piemonte, F. (2019). Targeting NRF2 for the treatment of Friedreich's ataxia: A comparison among drugs. *Int. J. Mol. Sci.* 20:5211. doi: 10.3390/ijms20205211

Petrillo, S., Piermarini, E., Pastore, A., Vasco, G., Schirinzi, T., Carrozzo, R., et al. (2017). Nrf2-Inducers counteract neurodegeneration in frataxin-silenced motor neurons: Disclosing new therapeutic targets for Friedreich's ataxia. *Int. J. Mol. Sci.* 18:2173. doi: 10.3390/ijms18102173

Petrillo, S., Santoro, M., La Rosa, P., Perna, A., Gallo, M. G., Bertini, E. S., et al. (2021). Nuclear Factor Erythroid 2-Related Factor 2 activation might mitigate clinical symptoms in Friedreich's ataxia: Clues of an "Out-Brain Origin" of the disease from a family study. *Front. Neurosci.* 15:638810. doi: 10.3389/fnins.2021.638810

Pujol, A., Hindelang, C., Callizot, N., Bartsch, U., Schachner, M., and Mandel, J. L. (2002). Late onset neurological phenotype of the X-ALD gene inactivation in mice: a mouse model for adrenomyeloneuropathy. *Hum. Mol. Genet.* 11, 499–505. doi: 10.1093/hmg/11.5.499

Qiu, J., Dando, O., Febery, J. A., Fowler, J. H., Chandran, S., and Hardingham, G. E. (2020). Neuronal activity and its role in controlling antioxidant genes. *Int. J. Mol. Sci.* 21:1933. doi: 10.3390/ijms21061933

Rada, P., Rojo, A. I., Chowdhry, S., McMahon, M., Hayes, J. D., and Cuadrado, A. (2011). SCF/{beta}-TrCP promotes glycogen synthase kinase 3-dependent degradation of the Nrf2 transcription factor in a Keap1-independent manner. *Mol. Cell. Biol.* 31, 1121–1133. doi: 10.1128/MCB.01204-10

Ranea-Robles, P., Launay, N., Ruiz, M., Calingasan, N. Y., Dumont, M., Naudí, A., et al. (2018). Aberrant regulation of the GSK-3β/NRF2 axis unveils a novel therapy for adrenoleukodystrophy. *EMBO Mol. Med.* 10:e8604. doi: 10.15252/emmm.201708604

Ravi, K., Paidas, M. J., Saad, A., and Jayakumar, A. R. (2021). Astrocytes in rare neurological conditions: Morphological and functional considerations. *J. Comp. Neurol.* 529, 2676–2705. doi: 10.1002/cne.25118

Reetz, K., Dogan, I., Hohenfeld, C., Didszun, C., Giunti, P., Mariotti, C., et al. (2018). EFACTS Study Group. Nonataxia symptoms in Friedreich Ataxia: Report from the Registry of the European Friedreich's Ataxia Consortium for Translational Studies (EFACTS). *Neurology* 91, e917–e930. doi: 10.1212/WNL.0000000000006121

Reish, O., Townsend, D., Berry, S. A., Tsai, M. Y., and King, R. A. (1995). Tyrosinase inhibition due to interaction of homocyst(e)ine with copper: the mechanism for reversible hypopigmentation in homocystinuria due to cystathionine beta-synthase deficiency. *Am. J. Hum. Genet.* 57, 127–132.

Ribas, G. S., Vargas, C. R., and Wajner, M. (2014). L-carnitine supplementation as a potential antioxidant therapy for inherited neurometabolic disorders. *Gene* 533, 469–476. doi: 10.1016/j.gene.2013.10.017

Richard, E., Gallego-Villar, L., Rivera-Barahona, A., Oyarzábal, A., Pérez, B., Rodríguez-Pombo, P., et al. (2018). Altered redox homeostasis in branched-chain amino acid disorders, organic acidurias, and homocystinuria. *Oxid. Med. Cell. Longev.* 2018:1246069. doi: 10.1155/2018/1246069

Ristoff, E., and Larsson, A. (2002). Oxidative stress in inborn errors of metabolism: lessons from glutathione deficiency. *J. Inherit. Metab. Dis.* 25, 223–226. doi: 10.1023/a:1015634032042

Rose, J., Brian, C., Pappa, A., Panayiotidis, M. I., and Franco, R. (2020). Mitochondrial metabolism in astrocytes regulates brain bioenergetics, neurotransmission and redox balance. *Front. Neurosci.* 14:536682.

Rosito, M., Testi, C., Parisi, G., Cortese, B., Baiocco, P., and Di Angelantonio, S. (2020). Exploring the use of Dimethyl Fumarate as microglia modulator for neurodegenerative diseases treatment. *Antioxidants* 9:700. doi: 10.3390/antiox9080700

Sahdeo, S., Scott, B. D., McMackin, M. Z., Jasoliya, M., Brown, B., Wulff, H., et al. (2014). Dyclonine rescues frataxin deficiency in animal models and buccal cells of patients with Friedreich's ataxia. *Hum. Mol. Genet.* 23, 6848–6862. doi: 10.1093/hmg/ddu408

Satoh, T., and Lipton, S. (2017). Recent advances in understanding NRF2 as a druggable target: development of pro-electrophilic and non-covalent NRF2 activators to overcome systemic side effects of electrophilic drugs like dimethyl fumarate. *F1000Res* 6:2138. doi: 10.12688/f1000research.12111.1

Saudubray, J. M., and Garcia-Cazorla, À (2018b). Inborn errors of metabolism overview: Pathophysiology, manifestations, evaluation, and management. *Pediatr. Clin. North Am.* 65, 179–208. doi: 10.1016/j.pcl.2017.11.002

Saudubray, J. M., and Garcia-Cazorla, A. (2018a). An overview of inborn errors of metabolism affecting the brain: from neurodevelopment to neurodegenerative disorders. *Dialogues Clin. Neurosci.* 20, 301–325. doi: 10.31887/DCNS.2018.20.4/jmsaudubray

Schiller, S., Rosewich, H., Grünewald, S., and Gärtner, J. (2020). Inborn errors of metabolism leading to neuronal migration defects. *J. Inherit. Metab. Dis.* 43, 145–155. doi: 10.1002/jimd.12194

Schmidlin, C. J., Dodson, M. B., Madhavan, L., and Zhang, D. D. (2019). Redox regulation by NRF2 in aging and disease. *Free Radic. Biol. Med.* 134, 702–707. doi: 10.1016/j.freeradbiomed.2019.01.016

Schulz, J. B., Dehmer, T., Schöls, L., Mende, H., Hardt, C., Vorgerd, M., et al. (2000). Oxidative stress in patients with Friedreich ataxia. *Neurology* 55, 1719–1721. doi: 10.1212/wnl.55.11.1719

Scuderi, S. A., Ardizzone, A., Paterniti, I., Esposito, E., and Campolo, M. (2020). Antioxidant and anti-inflammatory effect of Nrf2 inducer Dimethyl Fumarate in neurodegenerative diseases. *Antioxidants* 9:630. doi: 10.3390/antiox9070630

Seminotti, B., Amaral, A. U., Ribeiro, R. T., Rodrigues, M. D. N., Colín-González, A. L., Leipnitz, G., et al. (2016). Oxidative stress, disrupted energy metabolism, and altered signaling pathways in glutaryl-CoA dehydrogenase knockout mice: potential implications of quinolinic acid toxicity in the neuropathology of glutaric acidemia type I. *Mol. Neurobiol.* 53, 6459–6475. doi: 10.1007/s12035-015-9548-9

Sezgin-Bayindir, Z., Losada-Barreiro, S., Bravo-Díaz, C., Sova, M., Kristl, J., and Saso, L. (2021). Nanotechnology-based drug delivery to improve the therapeutic benefits of NRF2 modulators in cancer therapy. *Antioxidants* 10:685. doi: 10.3390/antiox10050685

Shan, Y., Schoenfeld, R. A., Hayashi, G., Napoli, E., Akiyama, T., Iodi Carstens, M., et al. (2013). Frataxin deficiency leads to defects in expression of antioxidants and Nrf2 expression in dorsal root ganglia of the Friedreich's ataxia YG8R mouse model. *Antioxid. Redox Signal.* 19, 1481–1493. doi: 10.1089/ars.2012.4537

Sharma, V., Kaur, A., and Singh, T. G. (2020). Counteracting role of nuclear factor erythroid 2-related factor 2 pathway in Alzheimer's disease. *Biomed. Pharmacother.* 129:110373. doi: 10.1016/j.biopha.2020.110373

Shekh-Ahmad, T., Eckel, R., Dayalan Naidu, S., Higgins, M., Yamamoto, M., Dinkova-Kostova, A. T., et al. (2018). KEAP1 inhibition is neuroprotective and suppresses the development of epilepsy. *Brain* 141, 1390–1403. doi: 10.1093/brain/awy071

Son, P., and Lewis, L. (2021). *"Hyperhomocysteinemia" in StatPearls [Internet]*. Treasure Island, FL: StatPearls Publishing.

Strauss, K. A., and Morton, D. H. (2003). Type I glutaric aciduria, part 2: a model of acute striatal necrosis. *Am. J. Med. Genet. C. Semin. Med. Genet.* 121C, 53–70. doi: 10.1002/ajmg.c.20008

Strauss, K. A., Morton, D. H., Puffenberger, E. G., Hendrickson, C., Robinson, D. L., Wagner, C., et al. (2007). Prevention of brain disease from severe 5,10-methylenetetrahydrofolate reductase deficiency. *Mol. Genet. Metab.* 91, 165–175. doi: 10.1016/j.ymgme.2007.02.012

Sturm, B., Bistrich, U., Schranzhofer, M., Sarsero, J. P., Rauen, U., Scheiber-Mojdehkar, B., et al. (2005). Friedreich's ataxia, no changes in mitochondrial labile iron in human lymphoblasts and fibroblasts: a decrease in antioxidative capacity? *J. Biol. Chem.* 280, 6701–6708. doi: 10.1074/jbc.M408717200

Swerdlow, R. H. (2016). Bioenergetics and metabolism: a bench to bedside perspective. *J. .Neurochem.* 139, 126–135. doi: 10.1111/jnc.13509

Sykiotis, G. P., and Bohmann, D. (2010). Stress-activated cap'n'collar transcription factors in aging and human disease. *Sci. Signal.* 3:re3. doi: 10.1126/scisignal.3112re3

Takaya, K., Suzuki, T., Motohashi, H., Onodera, K., Satomi, S., Kensler, T. W., et al. (2012). Validation of the multiple sensor mechanism of the Keap1-Nrf2 system. *Free Radic. Biol. Med.* 53, 817–827. doi: 10.1016/j.freeradbiomed.2012.06.023

Telkoparan-Akillilar, P., Panieri, E., Cevik, D., Suzen, S., and Saso, L. (2021). Therapeutic targeting of the NRF2 signaling pathway in cancer. *Molecules* 26:1417. doi: 10.3390/molecules26051417

Testai, F. D., and Gorelick, P. B. (2010). Inherited metabolic disorders and stroke part 2: homocystinuria, organic acidurias, and urea cycle disorders. *Arch. Neurol.* 67, 148–153. doi: 10.1001/archneurol.2009.333

Turk, B. R., Theisen, B. E., Nemeth, C. L., Marx, J. S., Shi, X., Rosen, M., et al. (2017). Antioxidant capacity and superoxide dismutase activity in

adrenoleukodystrophy. *JAMA Neurol.* 74, 519–524. doi: 10.1001/jamaneurol.2016.5715

Wajner, M. (2019). Neurological manifestations of organic acidurias. *Nat. Rev. Neurol.* 15, 253–271. doi: 10.1038/s41582-019-0161-9

Wajner, M., Amaral, A. U., Leipnitz, G., and Seminotti, B. (2019). Pathogenesis of brain damage in glutaric acidemia type I: Lessons from the genetic mice model. *Int. J. Dev. Neurosci.* 78, 215–221. doi: 10.1016/j.ijdevneu.2019.05.005

Wajner, M., Latini, A., Wyse, A. T., and Dutra-Filho, C. S. (2004). The role of oxidative damage in the neuropathology of organic acidurias: insights from animal studies. *J. Inherit. Metab. Dis.* 27, 427–448. doi: 10.1023/B:BOLI.0000037353.13085.e2

Wajner, M., Vargas, C. R., and Amaral, A. U. (2020). Disruption of mitochondrial functions and oxidative stress contribute to neurologic dysfunction in organic acidurias. *Arch. Biochem. Biophys.* 696:108646. doi: 10.1016/j.abb.2020.108646

Wiesinger, C., Eichler, F. S., and Berger, J. (2015). The genetic landscape of X-linked adrenoleukodystrophy: inheritance, mutations, modifier genes, and diagnosis. *Appl. Clin. Genet.* 8, 109–121. doi: 10.2147/TACG.S49590

Wong, A., Yang, J., Cavadini, P., Gellera, C., Lonnerdal, B., Taroni, F., et al. (1999). The Friedreich's ataxia mutation confers cellular sensitivity to oxidant stress which is rescued by chelators of iron and calcium and inhibitors of apoptosis. *Hum. Mol. Genet.* 8, 425–430. doi: 10.1093/hmg/8.3.425

Wyse, A. T. S., Dos Santos, T. M., Seminotti, B., and Leipnitz, G. (2021). Insights from animal models on the pathophysiology of hyperphenylalaninemia: role of mitochondrial dysfunction, oxidative stress and inflammation. *Mol. Neurobiol.* 58, 2897–2909. doi: 10.1007/s12035-021-02304-1

Wyse, A. T. S., Grings, M., Wajner, M., and Leipnitz, G. (2019). The role of oxidative stress and bioenergetic dysfunction in sulfite oxidase deficiency: insights from animal models. *Neurotox. Res.* 35, 484–494. doi: 10.1007/s12640-018-9986-z

Xie, L., Gu, Y., Wen, M., Zhao, S., Wang, W., Ma, Y., et al. (2016). Hydrogen sulfide induces Keap1 S-sulfhydration and suppresses diabetes-accelerated atherosclerosis via Nrf2 activation. *Diabetes* 65, 3171–3184. doi: 10.2337/db16-0020

Yamamoto, M., Kensler, T. W., and Motohashi, H. (2018). The KEAP1-NRF2 system: a thiol-based sensor-effector apparatus for maintaining redox homeostasis. *Physiol. Rev.* 98, 1169–1203. doi: 10.1152/physrev.00023.2017

Yang, S. P., Yang, X. Z., and Cao, G. P. (2015). Acetyl-l-carnitine prevents homocysteine-induced suppression of Nrf2/Keap1 mediated antioxidation in human lens epithelial cells. *Mol. Med. Rep.* 12, 1145–1150. doi: 10.3892/mmr.2015.3490

Yoon, T., and Cowan, J. A. (2004). Frataxin-mediated iron delivery to ferrochelatase in the final step of heme biosynthesis. *J. Biol. Chem.* 279, 25943–25946. doi: 10.1074/jbc.C400107200

Zanfardino, P., Doccini, S., Santorelli, F. M., and Petruzzella, V. (2021). Tackling dysfunction of mitochondrial bioenergetics in the brain. *Int. J. Mol. Sci.* 22:8325. doi: 10.3390/ijms22158325

Zhao, F., Ci, X., Man, X., Li, J., Wei, Z., and Zhang, S. (2021). Food-derived pharmacological modulators of the Nrf2/ARE pathway: their role in the treatment of diseases. *Molecules* 26:1016. doi: 10.3390/molecules26041016

Zinnanti, W. J., Lazovic, J., Housman, C., LaNoue, K., O'Callaghan, J. P., Simpson, I., et al. (2007). Mechanism of age-dependent susceptibility and novel treatment strategy in glutaric acidemia type I. *J. Clin. Invest.* 117, 3258–3270. doi: 10.1172/JCI31617

Zinnanti, W. J., Lazovic, J., Wolpert, E. B., Antonetti, D. A., Smith, M. B., Connor, J. R., et al. (2006). A diet-induced mouse model for glutaric aciduria type I. *Brain* 129, 899–910. doi: 10.1093/brain/awl009

Zubarioglu, T., Kiykim, E., Cansever, M. S., Neselioglu, S., Aktuglu-Zeybek, C., and Erel, O. (2017). Evaluation of dynamic thiol/disulphide homeostasis as a novel indicator of oxidative stress in maple syrup urine disease patients under treatment. *Metab. Brain Dis.* 32, 179–184. doi: 10.1007/s11011-016-9898-7

Conflict of Interest: The authors declare that the research was conducted in the absence of any commercial or financial relationships that could be construed as a potential conflict of interest.

Publisher's Note: All claims expressed in this article are solely those of the authors and do not necessarily represent those of their affiliated organizations, or those of the publisher, the editors and the reviewers. Any product that may be evaluated in this article, or claim that may be made by its manufacturer, is not guaranteed or endorsed by the publisher.

frontiers in Cellular Neuroscience

REVIEW
published: 21 January 2022
doi: 10.3389/fncel.2021.787258

A Perspective on Nrf2 Signaling Pathway for Neuroinflammation: A Potential Therapeutic Target in Alzheimer's and Parkinson's Diseases

Sarmistha Saha[1]*, *Brigitta Buttari*[1], *Elisabetta Profumo*[1], *Paolo Tucci*[2] and *Luciano Saso*[3]

[1] Department of Cardiovascular, Endocrine-Metabolic Diseases and Aging, Italian National Institute of Health, Rome, Italy, [2] Department of Clinical and Experimental Medicine, University of Foggia, Foggia, Italy, [3] Department of Physiology and Pharmacology "Vittorio Erspamer", Sapienza University of Rome, Rome, Italy

OPEN ACCESS

Edited by:
Ulises Gomez-Pinedo,
Instituto de Investigación Sanitaria del Hospital Clínico San Carlos, Spain

Reviewed by:
Aaron Del Pozo Sanz,
University of Washington, United States
Leyre Sanchez Sanchez De Rojas,
Agencia Española de Medicamentos y Productos Sanitarios, Spain
Mª Salomé Sirerol Piquer,
Center for Biomedical Research on Neurodegenerative Diseases (CIBERNED), Spain

***Correspondence:**
Sarmistha Saha
sarmistha_pharmacol@yahoo.com

Specialty section:
This article was submitted to Cellular Neuropathology, a section of the journal Frontiers in Cellular Neuroscience

Received: 30 September 2021
Accepted: 13 December 2021
Published: 21 January 2022

Citation:
Saha S, Buttari B, Profumo E, Tucci P and Saso L (2022) A Perspective on Nrf2 Signaling Pathway for Neuroinflammation: A Potential Therapeutic Target in Alzheimer's and Parkinson's Diseases. Front. Cell. Neurosci. 15:787258. doi: 10.3389/fncel.2021.787258

Neuroinflammation plays a pivotal role in Alzheimer's disease (AD) and Parkinson's disease (PD), the leading causes of dementia. These neurological disorders are characterized by the accumulation of misfolded proteins such as amyloid-ß (Aß), tau protein and α-synuclein, contributing to mitochondrial fragmentation, oxidative stress, and neuroinflammation. Misfolded proteins activate microglia, which induces neuroinflammation, expression of pro-inflammatory cytokines and subsequently facilitates synaptic damage and neuronal loss. So far, all the proposed drugs were based on the inhibition of protein aggregation and were failed in clinical trials. Therefore, the treatment options of dementia are still a challenging issue. Thus, it is worthwhile to study alternative therapeutic strategies. In this context, there is increasing data on the pivotal role of transcription factor NF- E2 p45-related factor 2 (Nrf2) on the redox homeostasis and anti-inflammatory functions in neurodegenerative disorders. Interestingly, Nrf2 signaling pathway has shown upregulation of antioxidant genes, inhibition of microglia-mediated inflammation, and improved mitochondrial function in neurodegenerative diseases, suggesting Nrf2 activation could be a novel therapeutic approach to target pathogenesis. The present review will examine the correlation between Nrf2 signaling with neuroinflammation in AD and PD.

Keywords: Alzheimer's disease, Parkinson's disease, Nrf2 signaling pathway, neuroinflammation, oxidative stress, Keap1

INTRODUCTION

Neuroinflammation is a crucial hallmark in the progression of neurodegenerative conditions such as Alzheimer's disease (AD), Parkinson's disease (PD), Huntington's disease, multiple sclerosis, Friedrich's ataxia, and stroke (Stephenson et al., 2018). Alzheimer's disease (AD), the most common neurological disorder is an irreversible progressive neurodegenerative disease characterized by abnormal aggregation of amyloid β-peptide (Aβ), and hyperphosphorylated tau protein (p-tau) accumulation leading to the neuroinflammation, oxidative stress and a gradual loss in cholinergic, synaptic and cognitive functions (Li and Götz, 2017). Parkinson's disease (PD), the second

most common neurological disorder, is characterized by progressive degeneration and death of dopaminergic neurons and the characteristic feature is the formation of fibrillar aggregates into intraneuronal inclusions, called Lewy bodies (LBs) which constitute more than 70% of a-synuclein (Mahul-Mellier et al., 2020). Protein misfolding, mitochondrial damages, oxidative stress and inflammation are the primary risk factors in AD and PD.

A common feature of all neurodegenerative diseases is immense oxidative stress leading to the dysfunction of neuronal cells. Oxidative stress is a biological condition driven by the imbalance between reactive oxygen species (ROS) production and cellular antioxidant defense response. Oxidative stress cause membrane lipid oxidation, ROS attack cellular membranes leading to functional and/or structural impairment of the membranes and to the formation of toxic lipid products as 4-hydroxy-2,3-nonenal (HNE), malondialdehyde, acrolein, and F2-isoprostanes. In respect of their oxidative-induced damage properties, these compounds are considered as disease mediators and due to their more stable forms their measure render quantifiable the magnitude of oxidative stress in biological samples (Erejuwa et al., 2013; Sultana et al., 2013). Indeed, the brain tissue in AD and PD and the cerebrospinal fluid (CSF) of ALS patients showed high levels of HNE (Dexter et al., 1989; Pedersen et al., 1998; Selley et al., 2002). Similarly, thiobarbituric acid-reactive substances (TBARs), acrolein, and F2-isoprostanes are all found to be elevated in AD (Arlt et al., 2002) and PD brains (Dexter et al., 1989), whereas elevated TBARs have been observed in the plasma of amyotrophic lateral sclerosis (ALS) patients (Sayre et al., 2001). As an endogenous defense mechanism, the activity of the antioxidant proteins such as catalase, superoxide dismutase (SOD), glutathione peroxidase and glutathione reductase are significantly up-regulated in the hippocampus and amygdala of AD brains (Pappolla et al., 1992). Furthermore, Aβ42 binds copper (I) ions forming Aβ42-Cu^{+} complex which could reduce oxygen to generate H_2O_2 and free radicals (Jiang et al., 2007).

It is well established that the development and progression of PD involved oxidative stress, mitochondrial dysfunction, and also neuroinflammation (Di Filippo et al., 2010). *In vivo* and *in vitro* studies have shown disruption of mitochondrial function in the dopamine neurons in the substantia nigra in early stages of PD (Hattingen et al., 2009), and decreased enzymes activity in the electron transport chain has been observed throughout the course of the disease (Schapira et al., 1989, 1990; Trimmer et al., 2000; Tysnes and Storstein, 2017). Moreover, increased mutations in mitochondrial DNA (mtDNA) with impaired Complex I and consequently increased oxidative stress was observed in later stages of PD patients, (Schapira, 2008; Moon and Paek, 2015).

In PD, α-synuclein has a mitochondrial targeted amino-terminal sequence which is responsible for the interactions with the inner mitochondrial membrane and disruption of complex I function, thereby triggers oxidative stress (Chinta et al., 2010). Moreover, the parkin protein, which is constitutively expressed in normal mitochondria, reportedly found to be inhibited with impaired complex I activity in oxidative stress conditions (Muftuoglu et al., 2004). In addition, DJ-1, a protein with antioxidant properties, is a well-known oxidative stress sensor as excess oxidation of DJ-1, renders this protein inactive. The oxidized form of DJ-1 protein has been observed in patients with sporadic PD and AD, suggesting the role of DJ-1 in the onset and pathogenesis of sporadic PD as well as familial PD (Cookson, 2010). In response to oxidative stress, nuclear factor (erythroid-derived 2)-like2 (Nrf2) plays a crucial role by inducing expression of a wide range of cytoprotective genes. Overexpression of DJ-1 has been reported to increase the Nrf2 protein levels and enhances its antioxidant role to improve the phase II response (Im et al., 2012).

Nrf2 plays a crucial role in regulation of cellular redox homeostasis and neuroinflammation. Accumulating evidences indicated the expression of Nrf2 in neurons, astrocytes, and glial cells (Cuadrado et al., 2019). Interestingly, Nrf2 expression is found to be higher in astrocytes than in neurons and activation of Nrf2 triggers Nrf2 target genes in astrocytes (Lee et al., 2003). Furthermore, astrocytes overexpressing Nrf2 protects neurons from oxidative stress (Johnson et al., 2008).

NRF2-KEAP1 SIGNALING PATHWAY

Nrf2 (NF-E2-related factor 2), is a member of the Cap'n'collar (CNC) transcription factor family and involved in redox signaling, xenobiotic metabolism (Lin et al., 2015), metabolism of carbohydrates (Heiss et al., 2013), lipids and iron (Chambel et al., 2015), antioxidant responses, and anti-inflammatory responses. Nrf2 protein consists of 605 amino acids and is divided into seven highly conserved functional domains, namely Neh1-Neh7 (**Figure 1A**). The Neh1 domain has a cap "n" collar basic-region leucine zipper (bZIP) domain, which is responsible for DNA-binding (Sun et al., 2009) and a nuclear localization signal (NLS) that regulates nuclear translocation of Nrf2 (Theodore et al., 2008). The Neh3, Neh4, and Neh5 are transactivation domains which regulates the binding of Nrf2 with other coactivators (Nioi et al., 2005). The Neh6 domain acts as a negative regulatory domain and binds with a β-transducin repeat-containing protein (β-TrCP) for Nrf2 ubiquitination (Rada et al., 2012). The Neh7 domain is involved in the direct binding to the retinoic X receptor α (RXRα), a repressor of NRF2, thus contributing to the inhibition of Nrf2-ARE signaling pathway (Wang et al., 2013). On the other hand, the Neh2 domain constitutes an N-terminal regulatory domain and regulates the stability of Nrf2 by influencing binding with different proteins. Neh2 domain consists of seven lysine residues which are responsible for ubiquitin conjugation. In addition, it also consists of two peptide-binding motifs (DLG and ETGE), which interact with Keap1 and is responsible for Nrf2 ubiquitination and its proteasomal degradation under normal physiological conditions (Lin et al., 2015).

Keap1, the main intracellular regulator of Nrf2, is a cysteine-rich protein, which is divided into five domains (**Figure 1B**), an N-terminal region (NTR), a Tramtrack-Bric-a-Brac (BTB) domain, a central intervening region (IVR) with a nuclear export signal (NES) regulating the cytoplasmic localization of Keap1,

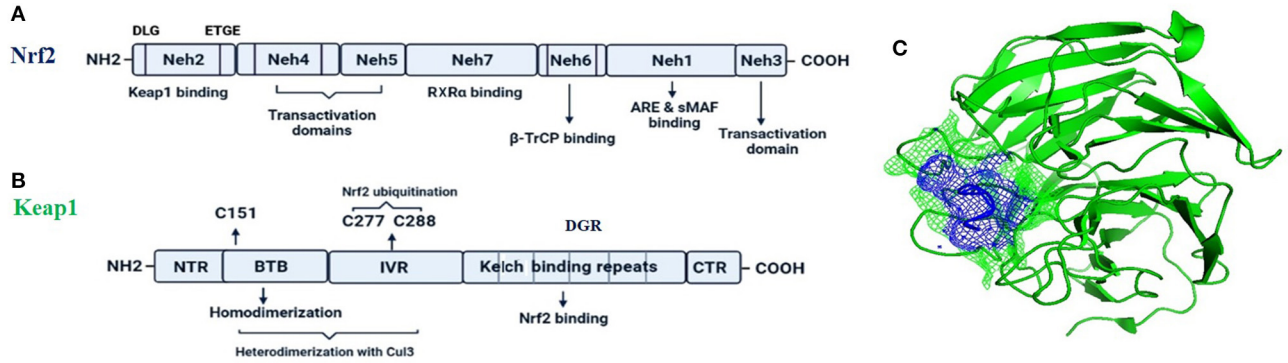

FIGURE 1 | The fundamental structures of Nrf2 **(A)** and Keap1 **(B)**. In **(C)** is reported a surface presentation of the N-terminal region of the Nrf2 (purple color in mesh) in complexed with the Keap1 protein (green color in carton) from crystal structures: 2DYH.

six Kelch repeats, and a C-terminal domain (CTR) (Ogura et al., 2010).

Under normal conditions, Nrf2 is sequestered by cytoplasmic Keap1 and targeted to proteasomal degradation (Wakabayashi et al., 2003). During homeostasis, the BTB domain regulates Keap1 homodimerization and its binding to the cullin-based (Cul3) E3 ligase, forming Keap1-Cul3-RBX1 (Ring box protein-1) (**Figure 1C**) E3 ligase complex (Zipper and Mulcahy, 2002), whereas Kelch repeats are reportedly regulate the binding of Keap1 to Nrf2 and p62 (Hayes and McMahon, 2009; Komatsu et al., 2010).

During oxidative stress conditions, the DLG motif dissociates from Keap1 protein leading to a disruption in the alignment of Nrf2 lysine residues that prevents its ubiquitination and consequently, Nrf2 is released from Keap1-Cul3-RBX1 complex, translocate into the nucleus and heterodimerizes with one of the sMaf (musculoaponeurotic fibrosarcoma oncogene homolog) proteins (Suzuki and Yamamoto, 2015) and up-regulates electrophile response element (EpRE)-mediated transcription (Itoh et al., 1999). This activates the transcription of a cascade of genes containing an antioxidant response element (ARE) within their promoter region (Hayes et al., 2010). However, the binding of DGR domain to Nrf2 is competitively inhibited by proteins with specific motifs, such as p62 and localizer of BRCA2 (Keum and Choi, 2014; Canning et al., 2015; Lu et al., 2016), thus responsible for sensing of cellular stress (Rachakonda et al., 2008). A non-canonical pathway for activation of Nrf2 involves competitive inhibition of the Keap1-Nrf2 interaction *via* p62/Sqstm1 (Komatsu et al., 2010; **Figure 2**). In case of p62-Keap1-Nrf2 axis, p62 acts as a modulator of Nrf2 activation. The Keap1-interacting region (KIR) of p62 interacts with Keap1, preventing Keap1 from trapping Nrf2, which leads to the Nrf2 stabilization following its activation (Komatsu et al., 2010). The KIR region of p62 consists of serine 349, which is phosphorylated during oxidative stress conditions. The phosphorylated p62 in turn has a higher affinity for Keap1 (Ichimura et al., 2013), and is responsible for the interference of Keap1-mediated Nrf2 ubiquitination.

Another model, Nrf2-EpRE pathway regulation *via* nicotinic receptors postulates that in oxidative stress conditions, after receptor activation, post-translational modifications occurs in Nrf2 which stimulates nuclear translocation and binding of Nrf2 with the EpRE sequences (Parada et al., 2014). Interestingly, this model represents a correlation between anti-inflammatory pathway and the Nrf2-dependent phase II antioxidant regulation (Martelli et al., 2014). The phosphorylation of Nrf2 by different kinases has been reported to affect the Nrf2 translocation. Phosphorylation of Ser40 residue of Nrf2 by atypical PKC iota (aPKCι) releases Nrf2 from Keap1 (Bloom and Jaiswal, 2003), allowing Nrf2 transport to the nucleus (Bloom and Jaiswal, 2003; Numazawa et al., 2003). Similarly, other kinases such as casein kinase-2 (CK2) (Pi et al., 2007), c-Jun N-terminal kinase (JNK) and extracellular regulated kinase (ERK) (Keum et al., 2006), and phosphatidylinositide-3-kinases (PI3K) (Nakaso et al., 2003) are also involved in the activation of Nrf2 translocation to the nucleus.

Several kinases are constitutively activated or over-expressed in chronic inflammation or oxidative stress conditions. Glycogen synthase kinase 3-beta (GSK3β) can phosphorylate Nrf2 leading to the recognition of Nrf2 by an E3 ligase receptor and the F-box protein β-TrCP followed by its degradation in a Keap1-independent manner (Chowdhry et al., 2013). It has been shown that the Neh6 domain of Nrf2 consists of two motifs, the activity of one of which, DSGIS, is significantly up-regulated by GSK3β activity (Chowdhry et al., 2013). On the other hand, accumulating evidences also indicated that, GSK3β activation could phosphorylate Fyn, which in turn regulates Nrf2 *via* phosphorylation, nuclear export and proteasomal degradation during pathological conditions (Jain and Jaiswal, 2007). Another kinase, MAPK p38 reportedly stabilizes the interaction between Keap1 and Nrf2 thereby induces the Nrf2 breakdown (Keum et al., 2006).

ROLE OF NRF2 IN ALZHEIMER'S DISEASE

AD affects more than 50 million people, and medical management is still a challenge as its pathogenesis still needs to be explored (Zhang et al., 2021). The pathogenesis in AD is related to the aggregation of Aß plaques and hyperphosphorylation of the microtubule-associated protein, tau resulting in neurofibrillary

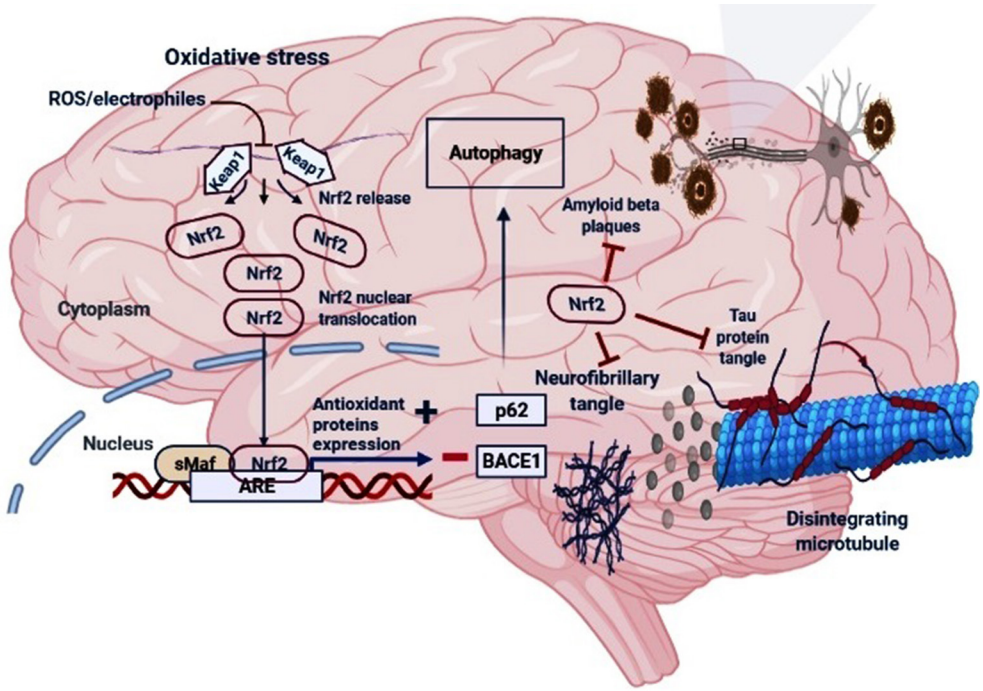

FIGURE 2 | The regulatory mechanism of Nrf2 in AD. Under oxidative stress (electrophiles or ROS conditions) Nrf2 is released from Keap1-Cul3-RBX1 complex for translocation into the nucleus followed by its heterodimerization with sMaf which leads to its binding with the antioxidant response elements (AREs), and transcription of ARE-driven genes. Nrf2 activation may increase the levels of p62 which is responsible for the autophagic process and inhibit the BACE1 that generate amyloid-β peptides in the neurons. Moreover, Nrf2 counteracts neurofibrillary, tau proteins tangle and amyloid-β plaques.

tangles (NFTs). The AßPP processing by proteases leads to the generation of Aß, which is then transferred from the brain to the cerebrospinal fluid (CSF) and is engulfed by microglia by phagocytosis (Heneka et al., 2015). On the other hand, hyperphosphorylated tau protein forms oligomeric paired helical fragments (PHFs), leading to intracellular NFTs, forming abnormal aggregates.

The level of Nrf2 is reportedly decrease as a function of age (Zhang et al., 2015) and observed to be reduced in AD patients (Ramsey et al., 2007). Accumulating evidences also suggested a significant negative correlation between Nrf2 deficits and AD (Zhang et al., 2015; Rojo et al., 2017), which might be due to the fact that the transcription factor, Nrf2 is responsible for the amelioration of oxidative stress and inflammation. Also, Nrf2 directly and indirectly influences changes in autophagy *in vivo* and *in vitro* (Riley et al., 2014; Joshi et al., 2015). Some other reports have shown the cognitive deficits in AD animal models and aggravates AD-like pathology *via* Nrf2 ablation (Joshi et al., 2015; Rojo et al., 2017). Furthermore, activation of Nrf2 by genetic and pharmaceutical inteventions leads to a neuroprotective role in AD patients (Bahn and Jo, 2019).

Nrf2 target genes such as NADPH quinone oxidoreductase I (NQO1), Heme oxygenase-1 (HO-1), and glutamate-cysteine ligase catalytic subunit (GCLC) expressions were observed in AD brains (Silva-Palacios et al., 2018). Nrf2-regulated target genes, NQO1 and NQO2, are two cytosolic flavoproteins responsible for the catalysis of two-electron mediated reduction of quinones to hydroquinones (Ross and Siegel, 2017). NQO1 maintains the reduced form of CoQ9 and CoQ10 inside the lipid vesicles and thus protects the plasma membrane from membrane lipid peroxidation and free radicals. A number of evidence suggest a NQO1 role in development and progression of AD (Chhetri et al., 2018). In this respect, it was reported that NQO1 enzyme activity is up-regulated in the brain areas involved in AD pathology such as frontal cortex (SantaCruz et al., 2004). Another recent study showed the elevation in NQO1 expression in 3xTg-AD mice preceded any intraneuronal Aβ immunoreactivity suggesting that up-regulation of NQO1 in AD pathology (Bahn et al., 2019). In contrast, in another study performed in AD human and mouse models, it has been demonstrated that Nrf2 activation was not able to regulate some of its target genes thus determining repressed expression of antioxidant defenses (Mota et al., 2015). This discordance could depend on the stage of disease. In fact, during the initial phases of AD, Nrf2-dependent gene expression is up-regulated due to the initial defensive cellular mechanism against ROS, however in the latter stages, as oxidative stress increases, Nrf2-dependent gene expression was shown to either reduced or remains stationary (Ansari and Scheff, 2010). The protective role of Nrf2 in AD is supported by results derived from Nrf2-deficient mice. In fact, $Nrf2^{-/-}$ mice crossed with mutant APP/PS1 mice leads to the increase in Aβ and AβPP intracellular levels compared to mutant AβPP/PS1 mice (Joshi et al., 2015). A

significant increase was also observed in the insoluble p-tau and Aβ levels in Nrf2-deficient mice was observed (Rojo et al., 2017). It was shown that the lack of Nrf2 significantly worsens cognitive deficits in the APP/PS1 mouse model of AD (Branca et al., 2017).

Impaired proteostasis is a crucial hallmark of neurodegenerative diseases (Hara et al., 2006; Inoue et al., 2012). Macroautophagy is one of the main mechanisms that ensure timely degradation of misfolded, oxidized or altered proteins that otherwise develop proteinopathy (Ciechanover and Kwon, 2015). A functional connection between Nrf2 and macroautophagy gene expression was shown in a mouse model of AD that reproduces impaired APP (amyloid β precursor protein) and human (Hs)MAPT/Tau processing, clearance and aggregation (Pajares et al., 2016). Nrf2-regulated autophagy marker SQSTM1/p62 was observed to be reduced in the absence of Nrf2 (Pajares et al., 2016). Other reports stated that Nrf2 has an impact on chaperone-mediated autophagy (Pajares et al., 2018). Nrf2 binding sequences were identified in the LAMP2 (lysosomal associated membrane protein 2A) gene in several human and mouse cell types and Nrf2 deficiency and overexpression was found to be correlated with reduced and increased LAMP2A levels, respectively (Pajares et al., 2018).

Nrf2 deletion in APP/PS1 mice reportedly enhanced inflammatory response and increase in intracellular APP, Aβ42 and Aβ40 levels. Mechanistically, neurons from Nrf2-deficient APP/PS1 mice shows enhanced accumulation of endosomes, lysosomes, and multivesicular bodies (Joshi et al., 2015). These findings indicated Nrf2-dependent processing and accumulation of APP/Aβ, and autophagic dysfunction. In agreement with these findings, *in vivo* Nrf2 activation in response to the AD-initiating Aβ42 peptide, was shown to prevent neuronal toxicity (Kerr et al., 2017). Another study in the AD animal model reported the reduction in Aβ42 level and p-tau after treatment with Nrf2 activator, isoastilbin (Yu et al., 2019). Accordingly, further analysis revealed that Nrf2 inhibits the beta-site amyloid precursor protein cleaving enzyme 1 (BACE1) expression by binding to the AREs in the promoter of BACE1 in AD animal models. This further inhibits Aβ production, and ameliorates cognitive deficits, however, Nrf2-dependent regulation of BACE1 is independent of ROS repression (Bahn et al., 2019). BACE1 is a beta secretase that generate amyloid-β peptides in the neurons.

Importantly, Nrf2 could reduce the levels of p-tau in AD by inducing nuclear dot protein 52 (NDP52) by binding to the AREs in the promoter of NDP52 (Jo et al., 2014). NDP52, is an autophagy-associated protein which facilitates autophagy-mediated degradation of p-tau (Jo et al., 2014). Consistent with this, another study reported the Nrf2-dependent modulation of selective autophagy processes which facilitates the clearance of tau species (Tang et al., 2018). The down-regulation in the expression of BAG3, NBR1, NDP52, and p62 genes were observed in aged $Nrf2^{-/-}$ animals compared to those in young $Nrf2^{-/-}$ animals, suggesting the role of Nrf2 in gene expressions during aging (Tang et al., 2018). In the hippocampus of mice expressing human TAUP301L protein and AD patients with tauopathy, the TAU-injured neurons release the chemokine fractalkine CX3CL1 and an increase in the Nrf2 and HO-1 proteins levels (Lastres-Becker et al., 2014), suggesting an attempt of the diseased brain to limit microgliosis. The plasma and CSF levels of soluble CX3CL1 was reportedly found to be elevated in cognitive impairment and AD (Kim et al., 2008; Shi et al., 2011). The interconnection between CX3CL1 and NRF2 in the modulation of neuroinflammation was elucidated by Lastres-Becker et al. (2014) using the murine microglia (BV-2 microglial cell lines). The authors showed that CX3CL1 stimulation increases the NRF2-ARE gene expression by activating AKT (phospho-AKTSer473), leading to the inhibition of GSK3B by phosphorylation of Ser9 (phospho-GSK-3βSer9). On the contrary, by using primary microglia from mouse strains that lack either NRF2 ($Nrf2^{-/-}$) or CX3CR1 ($Cx3cr1^{-/-}$) *in vitro* stimulation with CX3CL1 failed to induce the HO-1 expression. Of note, both knockout mice showed microgliosis and astrogliosis in case of neuronal TAUP301L expression, suggesting the CXCL1/NRF2/HO-1-dependent mitigation of the pro-inflammatory phenotype. Moreover, inhibition of GSK3β correlated with a stability in the Nrf2 levels, indicating that inhibition of GSK3β prevents Nrf2 degradation bypassing the KEAP1. Indeed, GSK3β activity in the Neh6 domain of NRF2 creates a degradation domain that is then recognized by β-TrCP (Rada et al., 2011, 2012). Therefore, the lack of CX3CR1/PI3K/AKT signaling results in the non-phosphorylated active conformation of GSK3β which in turn leads to the Nrf2 downregulation *via* GSK3β/β-TrCP pathway. A summary of the regulatory mechanism of Nrf2 in AD is reported in **Figure 2**.

ROLE OF NRF2 IN PARKINSON'S DISEASE

Parkinson's Disease (PD) is another common neurodegenerative disorder affecting 1-4% of people above 65 (Miller and O'Callaghan, 2015). The pathological feature of PD includes the loss of dopaminergic neurons in the substantia nigra pars compacta and intraneuronal accumulations of a-synuclein into Lewy body inclusions (**Figure 3**). PD patients show resting tremor, postural instability, gait imbalance, bradykinesia, and dementia in some cases as the most characteristic symptoms (Vranová et al., 2014). Microglia, a cell type of the monocyte-macrophage linage, is mainly responsible for inflammation in the brain. PD is observed to be associated with the up-regulation of the free radical generating enzymes and the accumulation of CA-MO microglia (Pajares et al., 2020). The Nrf2 activity was found to be significantly reduced in the 1-methyl-4-phenyl-1,2,3,6-tetrahydropyridine (MPTP) model of PD, and loss of Nrf2 further exacerbated the phenotype (Chen et al., 2009). Mice and monkeys when treated with MPTP showed astroglial HO-1 expression in striatum and elevated iron deposition (Youdim et al., 2004). In support of these, several studies have demonstrated increased markers of oxidative damage along with decreased levels of antioxidants in the blood and CSF of PD patients, which was found to be linked with Nrf2 pathway (Dias et al., 2013; Wei et al., 2018).

Expression of Nrf2 was strongly nuclear in PD nigral neurons, whereas it is cytoplasmic in normal conditions (Ramsey et al., 2007). Furthermore, Nrf2 signature, represented by NQO1 and HO-1 expressions are up-regulated, suggesting

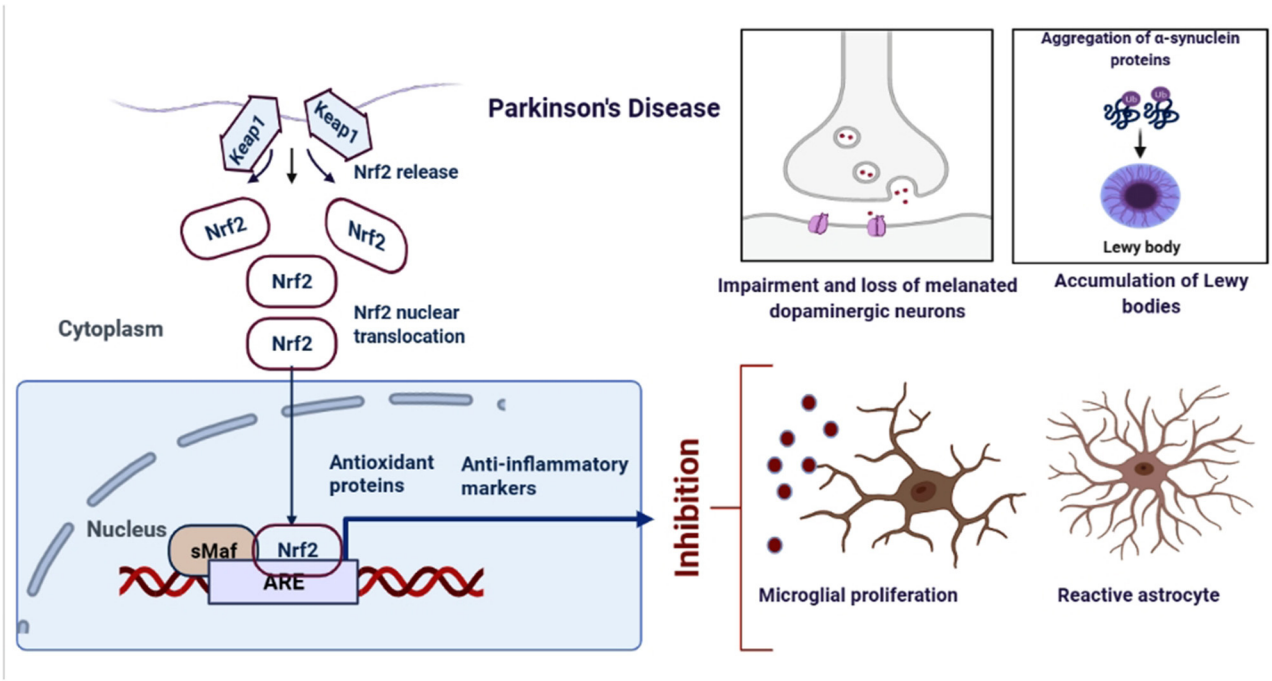

FIGURE 3 | Schematic representation of the role of Nrf2 in PD. An upregulation in the dopamine release could result into the oxidative stress, increased ROS production and neuroinflammation. However, when astrocytes and microglia produces Nrf2, it activates the antioxidant and anti-inflammatory gene expressions.

Nrf2-dependent brain protection (van Muiswinkel et al., 2004; Cuadrado et al., 2009; Yoo et al., 2013). Another report showed the sequestering of NQO1 and p62 protein expressions in Lewy bodies in postmortem samples of PD patients, suggesting Nrf2-dependent neuroprotection (Lastres-Becker et al., 2016). Similarly, in a PD *Drosophila* model, Nrf2 overexpression and Keap1 knockdown attenuated the reduced locomotor activity and dopaminergic neuron degeneration (Nakabeppu et al., 2007; Barone et al., 2011).

Activated microglia play a key role in neuroinflammation by release of cytokines. Microglia are resident innate immune cells of the brain that act as macrophages, which ranges from pro-inflammatory M1 phenotype to immunosuppressive M2 phenotype. Activated microglia encompasses multiple functions: clearance of accumulated or deteriorated neuronal and tissue elements, dynamic interaction with neurons whilst regulating the synaptic pruning process, and maintaining overall brain homeostasis as well as maintenance of chronic inflammation (Moehle and West, 2015). A significant increase was observed in proinflammatory cytokines in the experimental models and cerebrospinal fluid of PD patients (Mogi et al., 1994, 1999; Blum-Degen et al., 1995; Starhof et al., 2018). *In vivo* findings confirmed that widespread microglial activation is associated with the pathological process in PD thus supporting the hypothesis that inflammation is a significant component of progressive dopaminergic degeneration *via* cytokine release (Cicchetti et al., 2002).

Evidence for a role of NRF2 in the modulation of microglial dynamics between pro-inflammatory M1 and anti-inflammatory M2 phenotypes was reported by Cuadrado's group (Rojo et al., 2010). In Nrf2-knockout mice with MPTP treatment, basal ganglia show a more severe dopaminergic dysfunction than wild type. Nrf2-deficient mice exhibited intense astrogliosis and microgliosis indicated by an increase in expressions of GFAP and F4/80, respectively. These changes were also associated with an increase in the levels of COX-2, iNOS, IL-6, and TNF-α with a significant decrease in anti-inflammatory markers such as FIZZ-1, YM-1, Arginase-1, and IL-4. These results were further confirmed in microglial cultures stimulated with apoptotic conditioned medium from MPP1-treated dopaminergic cells. These findings indicated a role of Nrf2 in tuning microglial activation in PD progression (Rojo et al., 2010).

Multiple studies investigated expression profiles at cellular levels and reports showed selective expression of Nrf2 in astrocytes as compared with neurons (Shih et al., 2003). Additionally, it has also been shown that astrocyte specific Nrf2 pathway activation confers protection to vulnerable neurons (Kraft et al., 2004).

Using a cell model derived from biopsies of the olfactory mucosa termed, human olfactory neurosphere-derived cells (hONS), it has been observed that a significant alteration of "Nrf2-dependent antioxidant response pathway" was associated to reduced levels of glutathione and salt, a measure of cellular metabolic activity based on reduction by NAD(P)H-dependent dehydrogenase enzymes in PD patient-derived hONS cell lines when compared with control-donor derived cells (Matigian

et al., 2010). Another study, reported that knocking down Nrf2 with siRNA in control-donor derived hONS cells leads to the cellular phenotypes seen in PD cell lines (Cook et al., 2011). In this hONS model, Nrf2 pathway activation by treatment with L-Sulforaphane, restored disease-specific deficits in cellular functions (glutathione content and MTS metabolism) (Cook et al., 2011).

Reports showed the up-regulation in Nrf2 expression in the hippocampal cells of AD brain tissue (Lastres-Becker et al., 2014; Joshi et al., 2015; Liddell, 2017). DJ-1 (gene; PARK7) a recessively inherited Parkinson's gene, prevents oxidative stress in a Nrf2-dependent manner by preventing Keap1-mediated ubiquitination (Clements et al., 2006). In addition to this, a short, cell penetrating, peptide derivative of DJ-1 prevents H_2O_2, 6-OHDA, and DA-induced oxidative stress in Nrf2-dependent pathway in neuroblastoma cell lines (Lev et al., 2015). Furthermore, mutant isoforms, knockdown, and knockout models of DJ-1 have shown to prevent the expression of the Nrf2-mediated redox signaling molecules, thioredoxin 1 (Im et al., 2012) and glutathione (Zhou and Freed, 2005). Therefore, a strong relationship between Nrf2 and PD is well established till date and it has been proposed that intervening oxidative stress through the Nrf2-dependent pathway could be useful in the treatment of PD.

Another line of evidence revealed the key role of phosphatidylinositol 3-kinase (PI3K) and Akt kinases in the activation of the Nrf2-mediated antioxidant response (Martin et al., 2004; Salazar et al., 2006; Lim et al., 2008; Rojo et al., 2008). The regulation of neuroprotection in PD involving PI3K/Akt/GSK3β signaling axis is supported by the fact that Akt activity declines with age, which is the main risk factor for sporadic PD (Ikeyama et al., 2002). Additionally, an association between PD and single nucleotide polymorphism has been reported in the GSK3B gene leading to the elevation of GSK3β expression and activity (Kwok et al., 2005). Furthermore, inhibition of GSK3β enhanced Nrf2 activity and increased expression of Phase II antioxidant genes, thereby protecting against oxidants such as H_2O_2, 6-hydroxydopamine (6-OHDA) and MPP^+ (Salazar et al., 2006; Jain and Jaiswal, 2007; Rojo et al., 2008). A summary of the regulatory mechanism of Nrf2 in PD is reported in **Figure 3**.

CROSS-TALK BETWEEN NRF2 AND NEUROINFLAMMATION IN AD AND PD

It is assumed that Nrf2 and nuclear factor kappa-light-chain-enhancer of activated B cells (NF-κB) signaling pathways cooperate for the maintenance of the physiological tissue homeostasis and for the regulation of the cellular response to stress and inflammation. Several pro-inflammatory cytokines regulated by NF-κB, such as TNF-α, IL-1β, IL-6 and matrix metallopeptidase 9 (MMP9), have been shown to be enhanced in Nrf2-deficient mice in neuroinflammation as compared with wild-type mice, indicating that Nrf2 silencing promotes NF-κB -mediated inflammation (Mao et al., 2010).

Since a bidirectional connection occurs between the brain and the peripheral immune system, therefore, Nrf2 plays a crucial role in neuroinflammation (Jarrott and Williams, 2016). In neurodegenerative disorders, microglial cells become activated, leading to the release of pro-inflammatory cytokines and the production of ROS and reactive nitrogen species (RNS) (Hoenen et al., 2016). To circumvent the damaging effect of oxidative stress and inflammation, cells have developed several defense mechanisms. Nrf2/ARE signaling influences anti-inflammatory changes in many kinds of brain injuries, such as subarachnoid hemorrhage, traumatic brain injury, ischemia and neurodegenerative disease (Yan et al., 2008; Zhang et al., 2010; Wu et al., 2014). The Nrf2 activation pathway promotes the expression of antioxidative response elements, whereas nuclear factor kappa B (NF-κB), a protein complex which influences cytokine production and cell survival, also promotes cellular responses to neuronal injury and synaptic plasticity (Shih et al., 2015). Aging *per se* is associated with Nrf2 dysfunction and continuous, low-grade inflammation. These processes further contribute to neurodegeneration. So far, results have shown that neuroinflammation has a vital role in the progression and development of AD and PD and the imbalance between Nrf2 and Nuclear factor kappa B (NF-κB) could contribute to their pathogenesis of neuroinflammation.

Considerable evidence has revealed oxidative stress as well as chronic inflammation and autophagy in the brain correlated with the slow deterioration of AD (Prasad, 2017). In addition, experimental data so far suggest that all these changes are associated with impaired Nrf2 activity (Pajares et al., 2016; Zhang et al., 2019). The impaired spatial learning and memory abilities of mice and the accumulation of Aβ and p-tauS404 in the hippocampus were observed to be aggravated in a mouse model of AD (APP/PS1 transgenic (AT) mice with genetic removal of Nrf2 (Ren et al., 2020). Furthermore, astroglial and microglial activation was exacerbated along with upregulation of the proinflammatory cytokines IL-1β, IL-6, and TNF-α (Ren et al., 2020).

Since, inflammation is implicated as the key mechanism that actively contributes to neurodegeneration, by influencing the responses of microglia and astrocytes. Nrf2 is the key regulator for the two important cytoprotective pathways, anti-inflammation and anti-oxidation. Nrf2, which is essential for protection against oxidative/xenobiotic stresses, has been shown to block transcriptional upregulation of the proinflammatory cytokines IL-6 and IL-1β in myeloid cells by binding to the proximity of proinflammatory genes that guide the macrophage activation toward the M1 proinflammatory phenotype (Kobayashi et al., 2016). Treatment of neural stem/progenitor cells with Aβ induced reduction of neuronal differentiation which was prevented by Nrf2 over-expression, while Nrf2 deficiency enhanced impairment of neuronal differentiation (Kärkkäinen et al., 2014). In the same study, the Aβ40 treatment had no direct effect on neurosphere proliferation, however, when associated with Nrf2 overexpression it led to an enhanced proliferation of neurospheres and Nrf2 deficiency reduced neurospheres proliferation. Knockout of Nrf2 in mice crossed with AT or mutant HsAPPV717I/HsMAPTP301L mice

showed exacerbated astrocyte and microglial activation (Lastres-Becker et al., 2014; Joshi et al., 2015). However, treatment with the kavalactone methysticin, an Nrf2 activator, significantly reduced microglial infiltration, astrogliosis, and the secretion of the proinflammatory cytokines TNF-α and IL-17A in APP/Psen1 mice (Rojo et al., 2010). Furthermore, Nrf2 deletion exacerbated the inflammatory response in AT mice as shown by increased proinflammatory factors and hippocampal astrogliosis and activation of microglia surrounding the Aβ plaque, and NFTs (neurofibrillary tangles) in AD animal models or human patients (Griffin et al., 1989; Simard and Rivest, 2006; Lok et al., 2013; Licht-Murava et al., 2016). Indeed, hyperphosphorylated tau protein and fibrillar Aβ lead to inflammatory processes and the release of IL-1β *in vivo* and *in vitro* (Halle et al., 2008; Sarlus and Heneka, 2017). Other reports showed that Aβ accumulation induced progressive impairment in microglial cells in their ability to phagocytize Aβ (Shi and Holtzman, 2018). However, Nrf2 absence induced more aggressive activation of astroglia and inflammation in AT mice, which might be through activation of the NF-κB pathway (Fragoulis et al., 2012; Buendia et al., 2016).

Microglia-mediated neuroinflammation is also a crucial pathological process and the key factor is glial activation, especially microglial activation. It has already been reported that chronic Nrf2 deficient microglia leads to neuroinflammation and AD, and loss of Nrf2 primed microglia toward inflammatory phenotype with an increase in Clec7a and CD68 markers (Yu et al., 2019). Nrf2 knockout in aged mice leads to increased reactive microglia, proinflammatory cytokines, and infiltrating immune cells in the brain with AD-like impairment. Nrf2 knockout microglia showed increased NF-κB p65 and CD86 suggesting inflammatory phenotypes. Moreover, loss of Nrf2 leads to the reduction in microglial expressions of P2ry12, Tmem119, Gpr34, Tgfbr1, and Mafb, suggesting the Nrf2-dependent regulation of microglial homeostasis.

On the other hand, astrocytes are also well-known for active involvement in AD disease progression by influencing accumulation of amyloid plaques, neuroinflammation, and oxidative stress. It has been shown that Presenilin 1 mutated (PSEN1ΔE9) AD patient astrocytes have altered cytokine secretion upon inflammatory stimulation and exploits higher oxidative metabolism, thereby leading to the high production of ROS than healthy control astrocytes (Oksanen et al., 2017). The same study shows that inflammation activates the metabolism of human astrocytes. In a consecutive study, it has been shown that Nrf2 activation reduces amyloid secretion, cytokine release, with a subsequent increase in GSH secretion in AD astrocytes (Oksanen et al., 2020). Activation of Nrf2 also enhances the metabolism of astrocytes and increases the utilization of glycolysis.

It is well established that inflammation is a complex interplay of different pathways. In this context, heme oxygenase-1 (HO-1, HMOX1, EC 1.14.99.3), is an inducible 32 kDa protein which is responsible for the catalysis of the rate-limiting step of oxidative heme degradation which converts heme into three bioactive products namely free iron, carbon monoxide (CO) and biliverdin. Biliverdin is further rapidly converted into bilirubin and plays crucial roles in inflammation, apoptosis and oxidative stress (Wunder and Potter, 2003). Nrf2 directly regulates the expression of the HMOX1 gene responsible for the activity of HO-1 enzyme. Several *in vitro* and *in vivo* experiments have shown the role of Nrf2-dependent HO-1 expression for the anti-inflammatory activity. In presence of AD, HO-1 is observed to be increased in the temporal cortex and hippocampus in human brains (SantaCruz et al., 2004). Hippocampal expression of mutated tau induces increase in HO-1 and GCLC transcripts in wild type mice but not in Nrf2 knockout mice, indicating the crucial role of Nrf2 in the reduction of oxidative stress and inflammation (SantaCruz et al., 2004).

Apart from this, NF-κB p65 subunit downregulated the Nrf2-ARE pathway at transcriptional level by competitive interaction with the CH1-KIX domain of CREB-binding protein (CBP), which results in Nrf2 inactivation, or by the recruitment of the corepressor histone deacetylase 3 to ARE, thus promoting local histone hypoacetylation (Liu et al., 2008). Accordingly, silencing of p65 by knockdown promotes Nrf2 complex formation with CBP (Liu et al., 2008).

A study in primary cultured astrocytes from Nrf2 wild type or knockout mice exposed with oxyhemoglobin (OxyHb) has shown activation of NF-κB and an up-regulation of downstream pro-inflammatory cytokines in astrocytes. Moreover, this up-regulation was much greater in knockout astrocytes than in wild type astrocytes (Pan et al., 2011). Recently a study was conducted in a transgenic mouse that combines amyloidopathy and tauopathy with either wild type (AT-Nrf2-WT) or Nrf2-deficiency (AT-Nrf2-KO) (Rojo et al., 2017, Rojo et al., 2018). The results showed that AT-Nrf2-WT mice died prematurely, at around 14 months of age, due to motor deficits and a terminal spinal deformity, whereas AT-Nrf2-KO mice died roughly 2 months earlier. Nrf2-deficiency mice showed exacerbated astrogliosis and microgliosis, with a significant increase in GFAP, IBA1 and CD11b levels. However, treatment with Nrf2 activator, dimethyl fumarate (DMF) showed a reduction in pro-inflammatory mediators COX2 and NOS2, as well as the gliosis markers GFAP, IBA1 and MHCII with a significant increase in the expression of Nrf2, Nqo1, Osgin1, and Gstm1 in the brain, thereby preventing cognition and motor complications (Rojo et al., 2017, 2018). With aging, the cerebral blood vessels of Nrf2-deficient mice showed enhanced senescence markers, aging-induced vascular inflammation and blood-brain barrier leakage (Fulop et al., 2018; Tarantini et al., 2018) along with white matter leukoencephalopathy (Hubbs et al., 2007).

Astrocytes provide trophic support for neurons, promote formation and function of synapses, and prune synapses by phagocytosis, in addition to fulfilling a range of other homeostatic maintenance functions (Sofroniew and Vinters, 2010). Astrocytes undergo a dramatic transformation called "reactive astrocytosis" after brain injury and disease. Liddelow and colleagues have shown that activated microglia is able to induce pro-inflammatory astrocytes, designated as A1-astrocytes, *via* secretion of IL-1α, TNFα, and C1q both *in vitro* and *in vivo*. This subset of astrocytes changes their expression profile and phenotype to form neurotoxic reactive astrocytes. Indeed, A1s lose the ability to promote neuronal survival, outgrowth, synaptogenesis and phagocytosis, and induce death of neurons

and oligodendrocytes (Liddelow et al., 2017). The authors also show that A1s are highly present in human neurodegenerative diseases including AD and PD. Silencing by either knockout gene or antibody drugs for IL-1α, TNFα, and C1q inhibit A1 reactive astrocyte formation, therefore, this pathway has a therapeutic value in neurodegenerative diseases (Liddelow et al., 2017). A prolonged dysfunction of astrocytes and microglia activation reportedly accelerate the degeneration of SNpc dopaminergic neurons during early dysfunction induced by 6-OHDA lesion in rats (Kuter et al., 2018). Upon activation to the M1 phenotype, microglia secrete pro-inflammatory cytokines and neurotoxic molecules leading to the inflammation and cytotoxic responses. In contrast, the M2 polarized microglia secrete anti-inflammatory cytokines such as IL-4 and IL-10, neurotrophic factors (e.g., BDNF and IGF-1), and extracellular matrix proteins such as fibronectin (Subramaniam and Federoff, 2017).

With age, the failure of the astrocytic Nrf2-antioxidant axis response upon inflammation and oxidative stress significantly influences VM astrocyte-microglia-neuron interactions (Chinta et al., 2013; L'Episcopo et al., 2013; Silva-Palacios et al., 2018; Serapide et al., 2020). At the SNpc level, aging-induced decline of astrocytic Nrf2 gene expression promotes an up-regulation of major microglial proinflammatory gene expressions, such as *TNF-α, IL1β, IL-6* and *Nos2* both at striatal (Okamoto et al., 2011; L'Episcopo et al., 2013) and SNpc (L'Episcopo et al., 2011, 2018) levels, further accelerates oxidative stress and inflammation.

In a very recent study, NRF2 knockout and wild-type mice that overexpress human α-Syn (hα-Syn^{+}/Nrf2$^{-/-}$ and hα-Syn^{+}/Nrf2$^{+/+}$ respectively) were developed and an increased phosphorylation and oligomerization of α-Syn was observed in hα-Syn^{+}/Nrf2$^{-/-}$ mice. Further analysis showed a loss of tyrosine hydroxylase expressing dopaminergic neurons in the substantia nigra with amplified oxidative stress, higher inflammatory markers including COX-2 and iNOS-2 levels and an increased autophagic burden, especially in the midbrain, striatum and cortical brain regions (Anandhan et al., 2021).

POTENTIAL NRF2 ACTIVATORS TOWARD NEUROINFLAMMATION CLINICAL TRIALS

So far, we discussed different aspects of Nrf2 signaling pathway in oxidative stress and inflammation in neurodegenerative diseases, therefore, it is also worthwhile to discuss compounds and natural products which could modulate Nrf2-dependent treatment of neuroinflammation. Extensive research has been focused till date on identifying the agents/factors that regulate the association between Nrf2 and Keap1 and there are many chemical compounds, and natural products that have been identified as Nrf2 activators in neuroinflammation (Cuadrado et al., 2019). In this context, dimethyl fumarate (DMF), is the only drug so far approved by US Food and Drug Administration and marketed by Biogen, as an anti-inflammatory therapeutic agent in multiple sclerosis with the ability to inhibit inflammation *via* Nrf2 antioxidant pathway (Linker et al., 2011; Gold et al., 2012). More importantly, in a pre-clinical study performed in an animal model of PD, it was observed that the oral administration of DMF protected nigral dopaminergic neurons against α-synuclein toxicity and reduced astrocytosis and microgliosis from stereotaxic delivery to the ventral midbrain of recombinant adeno-associated viral vector expressing human α-synuclein (Lastres-Becker et al., 2016). Furthermore, *in vitro* studies showed that the neuroprotective effect of DMF was associated with the altered regulation of autophagy markers SQTSM1/p62 and LC3 in MN9D, BV2 and IMA 2.1 and a switch in microglial phenotype toward a less pro-inflammatory type (Lastres-Becker et al., 2016). DMF and its bioactive metabolite monomethylfumarate (MMF) activate *in vitro* the Nrf2 pathway by promoting S-alkylation of Keap1 and by determining nuclear exit of the Nrf2 repressor Bach1 (Ahuja et al., 2016). Nrf2 activation by DMF was associated with glutathione depletion, decreased cell viability, and inhibition of mitochondrial oxygen consumption and glycolysis rates, whereas MMF determined an increase of these activities. However, despite these differences, both DMF and MMF showed neuroprotective effects and blocked neurotoxicity in a mouse model of PD. Interestingly, this effect was not observed in Nrf2 null mice (Ahuja et al., 2016). Mechanistically, Linker and colleagues demonstrated that in an animal model of chronic multiple sclerosis DMF treatment improved preservation of myelin, axons and neurons (Linker et al., 2011). In the same study, *in vitro* experiments demonstrated that fumarates were able to increase murine neuronal survival and to protect human or rodent astrocytes against oxidative stress. Moreover, it was observed that MMF was able to promote Nrf2 activation by determining a direct modification of Keap1 at cysteine residue 151 (Linker et al., 2011). More recently, a study performed in human astrocytes demonstrated that cytoprotective activity of MMF is mediated by the upregulation of the oxidative stress induced growth inhibitor 1 (OSGIN1)-61 kDa isoform (Brennan et al., 2017). MMF-induced OSGIN1 expression is NRF2-dependent and modulates inflammatory markers thus contributing to cell protection against oxidative challenge (Brennan et al., 2017).

More recently, Bach1 inhibitor by vTv Therapeutics (High Point NC, USA) proved to be effective against MPTP-induced dopinergic neurodegeneration *via* Nrf2 activation (Ahuja et al., 2016). Another compound has been identified to bind Keap1 in the *in vitro* assay in the low micromolar range, by Biogen Idec, Merrimack Pharmaceuticals, Celgene Corporation (USA), Evotec AG (Germany), and NoValix (France) (Marcotte et al., 2013). Another compound within the isothiocyanate group of organosulfur compounds, Sulforaphane (SFN), activates Nrf2 in the basal ganglia leading to the upregulation of phase II antioxidant enzymes HO-1 and NQO1 (Jazwa et al., 2011). Importantly, SFN treatment activates Nrf2-dependent pathway to restore glutathione and MTS metabolism in PD hONS cultures (Cook et al., 2011). In wild-type mice, SFN protected against parkinsonian toxin methyl-4-phenyl-1,2,3,6-tetrahydropyridine (MPTP)-induced death of nigral dopaminergic neurons by reducing astrogliosis, microgliosis, and release of pro-inflammatory cytokines (Jazwa et al., 2011). Similar effects have also been shown by SFN treatment in other animal models of PD (Trinh et al., 2008; Morroni et al., 2013; Advedissian et al., 2016). Sulforaphane, originally

isolated from Brassicaceae plants, has been enrolled in clinical trials (NCT04213391) for the treatment of AD based on Nrf2 activation. However, sulforaphane is relatively unstable at room temperature. In this context, its synthetic analogs such as SFX-01 (Evgen Pharma developed drug) are attracting considerable attention for AD drug development.

The expression of HO-1 in microglial cells was observed to be responsible for the anti-inflammatory effect of compounds such as schizandrin C (Park et al., 2013) and several other compounds (Foresti et al., 2013). Moreover, in tauopathy, NRF2- and fractalkine receptor-knock out mice did not express HO-1 in microglia, suggesting their crucial role in the mitigation of neuroinflammation (Lastres-Becker et al., 2014). Cryptotanshinone, a monomer compound, can attenuate LPS-induced neuroinflammation *via* Nrf2/ HO-1 signaling pathway in BV-2 microglial cells (Zhou et al., 2019).

Quercetin, a natural flavonoid, significantly attenuated the LPS-induced synaptic loss in the cortex and hippocampus of the adult mouse brain (Khan et al., 2018). Quercetin protects against mitochondria dysfunction and progressive dopaminergic degeneration of neurons in experimental models of PD (Ay et al., 2017). Quercetin also shows an improvement in cognitive impairment in 6-OHDA-induced PD (Korczyn, 2001). In another study, quercetin prevents NO and iNOS over-expression in PC12 cells and down-regulates pro-inflammatory genes expressions (IL-1ß, COX-2 and TNF-α) in zebrafish (Zhang et al., 2011).

Treatment with synthetic triterpenoids such as CDDO-methyl amide (2-cyano-N-methyl-3,12-dioxooleana-1,9(11)-dien-28 amide; CDDO-MA) of neuroblastoma SH-SY5Y cells resulted in Nrf2 activation and translocation from cytosol to nucleus and significant protection against MPTP-induced nigrostriatal dopaminergic neurodegeneration, pathological α-synuclein accumulation and oxidative damage in mice (Yang et al., 2009). CDDO-MA treatment of fibroblasts from wild type, but not from Nrf2 knockout mice, inhibited ROS production induced by t-butylhydroperoxide by promoting the activation of ARE genes (Yang et al., 2009). The two structural analogs of CDDO (TP-319 and TP-500), obtained by the cyclization of squalene, have demonstrated improved blood-brain-barrier permeability, and protected against oxidative stress and inflammation in MPTP-induced dopaminergic neurotoxicity in mice (Kaidery et al., 2013). This activity was Nrf2-dependent as treatment of Nrf2 knockout mice with these CDDO analogs failed to inhibit MPTP neurotoxicity and to induce Nrf2-dependent cytoprotective genes (Kaidery et al., 2013). Another potent Nrf2 activator, KKPA4026 was identified by virtual screening of the Asinex and Chemdiv databases (Kim et al., 2020). KKPA4026 was demonstrated to induce the expression of the Nrf2-dependent antioxidant enzymes heme oxygenase-1, glutamate-cysteine ligase catalytic subunit, glutamate-cysteine ligase regulatory subunit, and NAD(P)H:quinone oxidoreductase 1 in BV-2 cells. Furthermore, in the MPTP-induced mouse model of PD, KKPA4026 was able to reduce behavioral deficits and protected dopaminergic neurons in an Nrf2-dependent manner. Similarly, a recent report showed a novel therapeutic candidate ALGERNON2 (altered generation of neurons 2) reduced the proinflammatory cytokines secretion and stabilized cyclinD1/p21 complex by inhibiting Dyrk1A activity, leading to Nrf2-dependent antioxidant and anti-inflammatory responses in a MPTP-induced PD model (Kobayashi et al., 2016). Interestingly, this compound enhanced neuronal survival also in other neuroinflammatory conditions, particularly in the transplantation of pluripotent stem cell–derived dopaminergic neurons into murine brains, thus confirming the therapeutic potential of ALGERNON2 in neuroinflammation-triggered neurodegeneration conditions (Kobayashi et al., 2016).

CONCLUSIONS

Oxidative damage and neuroinflammation are the key regulators in the pathogenesis of AD and PD. Therefore, one way to prevent these oxidative stress and inflammation is to upregulate the endogenous protection system in the neuronal cells. Nrf2-Keap1 signaling pathway is the hallmark of redox signaling and controlled neuroinflammation. Here, we reviewed ongoing scientific literature about regulation of Nrf2 signaling pathway in different aspects of neuroinflammation and related cognitive impairment. However, there are still some mechanisms such as interactions between Nrf2 and JAK/STAT signaling in neuronal cells that needs to be studied. Although many clinical studies and pharmaceutical companies are currently targeting Keap1, the key regulator of Nrf2, it is still challenging to enhance the targeting of these compounds against neurodegenerative disorders due to the targeted Nrf2 dissociation from Keap1 and its persistence in the nucleus as well as the permeability through the blood brain barrier as well as their proper biotransformation.

Furthermore, new chemical entities which have entered clinical trials for AD and PD therapy should be analyzed for Nrf2 response to determine their advantages in neuroinflammation.

AUTHOR CONTRIBUTIONS

SS, BB, EP, PT, and LS contributed to conception and design of the study. SS wrote the first draft of the manuscript. All authors contributed to manuscript revision, read, and approved the submitted version.

REFERENCES

Advedissian, T., Deshayes, F., Poirier, F., Viguier, M., and Richarme, G. (2016). The Parkinsonism-associated protein DJ-1/Park7 prevents glycation damage in human keratinocyte. *Biochem. Biophys. Res. Commun.* 473, 87–91. doi: 10.1016/j.bbrc.2016.03.056

Ahuja, M., Kaidery, N. A., Yang, L., Calingasan, N., Smirnova, N., Gaisin, A., et al. (2016). Distinct Nrf2 signaling mechanisms of fumaric acid esters and their role in neuroprotection against 1-methyl-4-phenyl-1,2,3,6-tetrahydropyridine-induced experimental Parkinson's-like disease. *J. Neurosci.* 36, 6332–6351. doi: 10.1523/JNEUROSCI.0426-16.2016

Anandhan, A., Nguyen, N., Syal, A., Dreher, L. A., Dodson, M., Zhang, D. D., et al. (2021). NRF2 loss accentuates parkinsonian pathology and behavioral

dysfunction in human α-synuclein overexpressing mice. *Aging Dis.* 12, 964–982.

Ansari, M. A., and Scheff, S. W. (2010). Oxidative stress in the progression of Alzheimer disease in the frontal cortex. *J. Neuropathol. Exp. Neurol.* 69, 155–167. doi: 10.1097/NEN.0b013e3181cb5af4

Arlt, S., Beisiegel, U., and Kontush, A. (2002). Lipid peroxidation in neurodegeneration: new insights into Alzheimer's disease. *Curr. Opin. Lipidol.* 13, 289–294. doi: 10.1097/00041433-200206000-00009

Ay, M., Luo, J., Langley, M., Jin, H., Anantharam, V., Kanthasamy, A., et al. (2017). Molecular mechanisms underlying protective effects of quercetin against mitochondrial dysfunction and progressive dopaminergic neurodegeneration in cell culture and MitoPark transgenic mouse models of Parkinson's Disease. *J. Neurochem.* 141, 766–782 doi: 10.1111/jnc.14033

Bahn, G., and Jo, D. G. (2019). Therapeutic approaches to Alzheimer's disease through modulation of NRF2. *Neuromol. Med.* 21, 1–11. doi: 10.1007/s12017-018-08523-5

Bahn, G., Park, J. S., Yun, U. J., Lee, Y. J., Choi, Y., Park, J. S., et al. (2019). NRF2/ARE pathway negatively regulates BACE1 expression and ameliorates cognitive deficits in mouse Alzheimer's models. *Proc. Natl. Acad. Sci. U S A* 116, 12516–12523. doi: 10.1073/pnas.1819541116

Barone, M. C., Sykiotis, G. P., and Bohmann, D. (2011). Genetic activation of Nrf2 signaling is sufficient to ameliorate neurodegenerative phenotypes in a Drosophila model of Parkinson's disease. *Dis. Model. Mech.* 4, 701–707. doi: 10.1242/dmm.007575

Bloom, D. A., and Jaiswal, A. K. (2003). Phosphorylation of Nrf2 at Ser40 by protein kinase C in response to antioxidants leads to the release of Nrf2 from INrf2, but is not required for Nrf2 stabilization/accumulation in the nucleus and transcriptional activation of antioxidant response element-mediated NAD(P)H:quinone oxidoreductase-1 gene expression. *J. Biol. Chem.* 278, 44675–44682. doi: 10.1074/jbc.M307633200

Blum-Degen, D., Müller, T., Kuhn, W., Gerlach, M., Przuntek, H., and Riederer, P. (1995). Interleukin-1 beta and interleukin-6 are elevated in the cerebrospinal fluid of Alzheimer's and de novo Parkinson's disease patients. *Neurosci. Lett.* 202, 17–20. doi: 10.1016/0304-3940(95)12192-7

Branca, C., Ferreira, E., Nguyen, T.-V., Doyle, K., Caccamo, A., and Oddo, S. (2017). Genetic reduction of Nrf2 exacerbates cognitive deficits in a mouse model of Alzheimer's disease. *Hum. Mol. Genet.* 26, 4823–4835. doi: 10.1093/hmg/ddx361

Brennan, M. S., Matos, M. F., Richter, K. E., Li, B., and Scannevin, R. H. (2017). The NRF2 transcriptional target, OSGIN1, contributes to monomethyl fumarate mediated cytoprotection in human astrocytes. *Sci. Rep.* 7:42054. doi: 10.1038/srep42054

Buendia, I., Michalska, P., Navarro, E., Gameiro, I., Egea, J., and León, R. (2016). Nrf2–ARE pathway: An emerging target against oxidative stress and neuroinflammation in neurodegenerative diseases. *Pharmacol. Ther.* 157, 84–104. doi: 10.1016/j.pharmthera.2015.11.003

Canning, P., Sorrell, F. J., and Bullock, A. N. (2015). Structural basis of Keap1 interactions with Nrf2. *Free Radic. Biol. Med.* 88, 101–107. doi: 10.1016/j.freeradbiomed.2015.05.034

Chambel, S. S., Santos-Goncalves, A., and Duarte, T. L. (2015). The dual of Nrf2 in nonalcoholic fatty liver disease: regulation of antioxidant defences and hepatic lipid metabolism. *Biomed. Res. Int.* 15:597134. doi: 10.1155/2015/597134

Chen, C. M., Liu, J. L., Wu, Y. R., Chen, Y. C., Cheng, H. S., Cheng, M. L., et al. (2009). Increased oxidative damage in peripheral blood correlates with severity of Parkinson's disease. *Neurobiol. Dis.* 33, 429–435. doi: 10.1016/j.nbd.2008.11.011

Chhetri, J., King, A. E., and Gueven, N. (2018). Alzheimer's Disease and NQO1: Is there a Link? *Curr. Alzheimer Res.*15, 56–66. doi: 10.2174/1567205014666170203095802

Chinta, S. J., Lieu, C. A., Demaria, M., Laberge, R. M., Campisi, J., and Andersen, J. K. (2013). Environmental stress, ageing and glial cell senescence: a novel mechanistic link to Parkinson's disease? *J. Int. Med.* 273, 429–436. doi: 10.1111/joim.12029

Chinta, S. J., Mallajosyula, J. K., Rane, A., and Andersen, J. K. (2010). Mitochondrial alpha-synuclein accumulation impairs complex I function in dopaminergic neurons and results in increased mitophagy *in vivo*. *Neurosci. Lett.* 486, 235–239. doi: 10.1016/j.neulet.2010.09.061

Chowdhry, S., Zhang, Y., McMahon, M., Sutherland, C., Cuadrado, A., and Hayes, J. D. (2013). Nrf2 is controlled by two distinct beta-TrCP recognition motifs in its Neh6 domain, one of which can be modulated by GSK-3 activity. *Oncog.* 32, 3765–3781. doi: 10.1038/onc.2012.388

Cicchetti, F., Brownell, A. L., Williams, K., Chen, Y. I., Livni, E., and Isacson, O. (2002). Neuroinflammation of the nigrostriatal pathway during progressive 6-OHDA dopamine degeneration in rats monitored by immunohistochemistry and PET imaging. *Eur. J. Neurosci.* 15, 991–998. doi: 10.1046/j.1460-9568.2002.01938.x

Ciechanover, A., and Kwon, Y. T. (2015). Degradation of misfolded proteins in neurodegenerative diseases: therapeutic targets and strategies. *Exp. Mol. Med.* 47:e147doi: 10.1038/emm.2014.117

Clements, C. M., McNally, R. S., Conti, B. J., Mak, T. W., and Ting, J. P. (2006). DJ-1, a cancer- and Parkinson's disease-associated protein, stabilizes the antioxidant transcriptional master regulator Nrf2. *Proc. Natl. Acad. Sci. USA* 103, 15091–15096. doi: 10.1073/pnas.0607260103

Cook, A. L., Vitale, A. M., Ravishankar, S., Matigian, N., Sutherland, G. T., Shan, J., et al. (2011). NRF2 activation restores disease related metabolic deficiencies in olfactory neurosphere-derived cells from patients with sporadic Parkinson's disease. *PLoS ONE* 6:e21907. doi: 10.1371/journal.pone.0021907

Cookson, M. R. (2010). DJ-1, PINK1, and their effects on mitochondrial pathways. *Mov. Disord.* 25, S44–48. doi: 10.1002/mds.22713

Cuadrado, A., Moreno-Murciano, P., and Pedraza-Chaverri, J. (2009). The transcription factor Nrf2 as a new therapeutic target in Parkinson's disease. *Expert Opin. Ther. Targets* 13, 319–329. doi: 10.1517/13543780802716501

Cuadrado, A., Rojo, A. I., Wells, G., Hayes, J. D., Cousin, S. P., Rumsey, W. L., et al. (2019). Therapeutic targeting of the NRF2 and KEAP1 partnership in chronic diseases. *Nat. Rev. Drug Discov.* 18, 295–317 doi: 10.1038/s41573-018-0008-x

Dexter, D. T., Carter, C. J., Wells, F. R., Javoy-Agid, F., Agid, Y., Lees, A., et al. (1989). Basal lipid peroxidation in substantia nigra is increased in Parkinson's disease. *J. Neurochem.* 52, 381–389. doi: 10.1111/j.1471-4159.1989.tb09133.x

Di Filippo, M., Chiasserini, D., Tozzi, A., Picconi, B., and Calabresi, P. (2010). Mitochondria and the link between neuroinflammation and neurodegeneration. *J. Alz. Dis.* 20 (Suppl 2), S369–S379.

Dias, V., Junn, E., and Mouradian, M. M. (2013). The role of oxidative stress in Parkinson's disease. *J. Parkinsons. Dis.* 3, 461–491. doi: 10.3233/JPD-130230

Erejuwa, O. O., Sulaiman, S. A., and Ab Wahab, M. S. (2013). Evidence in support of potential applications of lipid peroxidation products in cancer treatment. *Oxid. Med. Cell Longev.* 2013:931251; doi: 10.1155/2013/931251

Foresti, R., Bains, S. K., Pitchumony, T. S., de Castro Brás, L. E., Drago, F., Dubois-Randé, J. L., et al. (2013). Small molecule activators of the Nrf2-HO-1 antioxidant axis modulate heme metabolism and inflammation in BV2 microglia cells. *Pharmacol. Res.* 76, 132–148. doi: 10.1016/j.phrs.2013.07.010

Fragoulis, A., Laufs, J., Müller, S., Soppa, U., Siegl, S., Reiss, L. K., et al. (2012). Sulforaphane has opposing effects on TNF-alpha stimulated and unstimulated synoviocytes. *Arth. Res. Ther.* 14:R220. doi: 10.1186/ar4059

Fulop, G. A., Kiss, T., Tarantini, S., Balasubramanian, P., Yabluchanskiy, A., Farkas, E., et al. (2018). Nrf2 deficiency in aged mice exacerbates cellular senescence promoting cerebrovascular inflammation. *Geroscien.* 40, 513–521. doi: 10.1007/s11357-018-0047-6

Gold, R., Linker, R. A., and Stangel, M. (2012). Fumaric acid and its esters: An emerging treatment for multiple sclerosis with antioxidative mechanism of action. *Clin. Immunol.* 142, 44–48. doi: 10.1016/j.clim.2011.02.017

Griffin, W. S., Stanley, L. C., Ling, C., White, L., MacLeod, V., Perrot, L. J., et al. (1989). Brain interleukin 1 and S-100 immunoreactivity are elevated in Down syndrome and Alzheimer disease. *Pro. Nat. Acad. Sci.* 86, 7611–7615. doi: 10.1073/pnas.86.19.7611

Halle, A., Hornung, V., Petzold, G. C., Stewart, C. R., Monks, B. G., Reinheckal, T., et al. (2008). The NALP3 inflammasome is involved in the innate immune response to amyloid-β. *Nature Immunol.* 9, 857–865. doi: 10.1038/ni.1636

Hara, T., Nakamura, K., Matsui, M., Yamamoto, A., Nakahara, Y., Suzuki-Migishima, R., et al. (2006). Suppression of basal autophagy in neural cells causes neurodegenerative disease in mice. *Nature* 441, 885–889 doi: 10.1038/nature04724

Hattingen, E., Magerkurth, J., Pilatus, U., Mozer, A., Seifried, C., et al. (2009). Phosphorus and proton magnetic resonance spectroscopy demonstrates mitochondrial dysfunction in early and advanced Parkinson's disease. *Brain.* 132(Pt 12), 3285–97. doi: 10.1093/brain/awp293

Hayes, J. D., and McMahon, M. (2009). NRF2 and KEAP1 mutations: Permanent activation of an adaptive response in cancer. *Trends Biochem. Sci.* 34, 176–188. doi: 10.1016/j.tibs.2008.12.008

Hayes, J. D., McMahon, M., Chowdhry, S., and Dinkova-Kostova, A. T. (2010). Cancer chemoprevention mechanisms mediated through the Keap1-Nrf2 pathway. *Antioxid. Redox Signal.* 13, 1713–1748. doi: 10.1089/ars.2010.3221

Heiss, E. H., Schachner, D., Zimmermann, K., and Dirsch, V. M. (2013). Glucose availability is a decisive factor for Nrf2-mediated gene expression. *Redox Biol.* 1, 359–365. doi: 10.1016/j.redox.2013.06.001

Heneka, M. T., Golenbock, D. T., and Latz, E. (2015). Innate immunity in Alzheimer's disease. *Nat. Immunol.* 16, 229–236. doi: 10.1038/ni.3102

Hoenen, C., Gustin, A., Birck, C., Kirchmeyer, M., Beaume, N., Felten, P., et al. (2016). Alpha-synuclein proteins promote proinflammatory cascades in microglia: stronger effects of the A53T mutant. *PLoS ONE* 11:e0162717. doi: 10.1371/journal.pone.0162717

Hubbs, A. F., Benkovic, S. A., Miller, D. B., O'Callaghan, J. P., Battelli, L., Schwegler-Berry, D., et al. (2007). Vacuolar leukoencephalopathy with widespread astrogliosis in mice lacking transcription factor Nrf2. *Am. J. Pathol.* 170, 2068–2076. doi: 10.2353/ajpath.2007.060898

Ichimura, Y., Waguri, S., Sou, Y. S., Kageyama, S., Hasegawa, J., Ishimura, R., et al. (2013). Phosphorylation of p62 activates the Keap1-Nrf2 pathway during selective autophagy. *Mol. Cell* 51, 618–631. doi: 10.1016/j.molcel.2013.08.003

Ikeyama, S., Kokkonen, G., Shack, S., Wang, X. T., and Holbrook, N. J. (2002). Loss in oxidative stress tolerance with aging linked to reduced extracellular signal-regulated kinase and Akt kinase activities. *Faseb J.* 16, 114–116. doi: 10.1096/fj.01-0409fje

Im, J. Y., Lee, K. W., Woo, J. M., Junn, E., and Mouradian, M. M. (2012). DJ-1 induces thioredoxin 1 expression through the Nrf2 pathway. *Hum. Mol. Genet.* 21, 3013–3024. doi: 10.1093/hmg/dds131

Inoue, K., Rispoli, J., Kaphzan, H., Klann, E., Chen, E. I., Kim, J., et al. (2012). Macroautophagy deficiency mediates age-dependent neurodegeneration through a phospho-tau pathway. *Mol. Neurodegener.* 7:48. doi: 10.1186/1750-1326-7-48

Itoh, K., Wakabayashi, N., Katoh, Y., Ishii, T., Igarashi, K., Engel, J. D., et al. (1999). Keap1 represses nuclear activation of antioxidant responsive elements by Nrf2 through binding to the amino-terminal Neh2 domain. *Gene Dev.* 13, 76–86. doi: 10.1101/gad.13.1.76

Jain, A. K., and Jaiswal, A. K. (2007). GSK-3beta acts upstream of Fyn kinase in regulation of nuclear export and degradation of NF-E2 related factor 2. *J. Biol. Chem.* 282, 16502–16510. doi: 10.1074/jbc.M611336200

Jarrott, B., and Williams, S. J. (2016). Chronic brain inflammation: the neurochemical basis for drugs to reduce inflammation. *Neurochem. Res.* 41, 523–533. doi: 10.1007/s11064-015-1661-7

Jazwa, A., Rojo, A. I., Innamorato, N. G., Hesse, M., Fernández-Ruiz, J., and Cuadrado, A. (2011). Pharmacological targeting of the transcription factor Nrf2 at the basal ganglia provides disease modifying therapy for experimental Parkinsonism. *Antioxid. Redox Signal.* 14, 2347–2360. doi: 10.1089/ars.2010.3731

Jiang, D., Men, L., Wang, J., Zhang, Y., Chickenyen, S., Wang, Y., et al. (2007). Redox reactions of copper complexes formed with different beta-amyloid peptides and their neuropathological [correction of neuropathalogical] relevance. *Biochem.* 46, 9270–9282. doi: 10.1021/bi700508n

Jo, C., Gundemir, S., Pritchard, S., Jin, Y. N., Rahman, I., and Johnson, G. V. (2014). Nrf2 reduces levels of phosphorylated tau protein by inducing autophagy adaptor protein NDP52. *Nat. Commun.* 5:3496. doi: 10.1038/ncomms4496

Johnson, J. A., Johnson, D. A., Kraft, A. D., Calkins, M. J., Jakel, R. J., Vargas, M. R., et al. (2008). The Nrf2-ARE pathway: an indicator and modulator of oxidative stress in neurodegeneration. *Ann. N Y Acad. Sci.* 1147, 61–69. doi: 10.1196/annals.1427.036

Joshi, G., Gan, K. A., Johnson, D. A., and Johnson, J. A. (2015). Increased Alzheimer's disease-like pathology in the APP/ PS1DeltaE9 mouse model lacking Nrf2 through modulation of autophagy. *Neurobiol. Ag.* 36, 664–679. doi: 10.1016/j.neurobiolaging.2014.09.004

Kaidery, N. A., Banerjee, R., Yang, L., Smirnova, N. A., Hushpulian, D. M., Liby, K. T., et al. (2013). Targeting Nrf2-mediated gene transcription by extremely potent synthetic triterpenoids attenuate dopaminergic neurotoxicity in the MPTP mouse model of Parkinson's disease. *Antioxid. Redox Signal.* 18, 139–157. doi: 10.1089/ars.2011.4491

Kärkkäinen, V., Pomeshchik, Y., Savchenko, E., Dhungana, H., Kurronen, A., Lehtonen, S., et al. (2014). Nrf2 regulates neurogenesis and protects neural progenitor cells against Aβ toxicity. *Stem Cells.* 32, 1904–1916. doi: 10.1002/stem.1666

Kerr, J. S., Adriaanse, B. A., Greig, N. H., Mattson, M. P., Cader, M. Z., et al. (2017). Mitophagy and Alzheimer's Disease: Cellular and Molecular Mechanisms. *Trends Neurosci.* 40, 151–166. doi: 10.1016/j.tins.2017.01.002

Keum, Y. S., and Choi, B. Y. (2014). Molecular and chemical regulation of the Keap1-Nrf2 signaling pathway. *Mol.* 19, 10074–10089. doi: 10.3390/molecules190710074

Keum, Y. S., Yu, S., Chang, P. P., Yuan, X., Kim, J. H., Xu, C., et al. (2006). Mechanism of action of sulforaphane: inhibition of p38 mitogen-activated protein kinase isoforms contributing to the induction of antioxidant response element-mediated heme oxygenase-1 in human hepatoma HepG2 cells. *Cancer Res.* 66, 8804–8813. doi: 10.1158/0008-5472.CAN-05-3513

Khan, A., Ali, T., Rehman, S. U., Khan, M. S., Alam, S. I., Ikram, M., et al. (2018). Neuroprotective Effect of Quercetin Against the Detrimental Effects of LPS in the Adult Mouse Brain. *Front. Pharmacol.* 9, 1383. doi: 10.3389/fphar.2018.01383

Kim, S., Indu Viswanath, A. N., Park, J. H., Lee, H. E., Park, A. Y., Choi, J. W., et al. (2020). Nrf2 activator *via* interference of Nrf2-Keap1 interaction has antioxidant and anti-inflammatory properties in Parkinson's disease animal model. *Neuropharmacology* 1:107989. doi: 10.1016/j.neuropharm.2020.107989

Kim, S. K., Yang, J. W., Kim, M. R., Roh, S. H., Kim, H. G., et al. (2008). Increased expression of Nrf2/ARE-dependent anti-oxidant proteins in tamoxifen-resistant breast cancer cells. *Free Rad. Biol. Med.* 45, 537–546.

Kobayashi, E. H., Suzuki, T., Funayama, R., Nagashima, T., Hayashi, M., Sekine, H., et al. (2016). Nrf2 suppresses macrophage inflammatory response by blocking proinflammatory cytokine transcription. *Nat. Comm.* 7:11624. doi: 10.1038/ncomms11624

Komatsu, M., Kurokawa, H., Waguri, S., Taguchi, K., Kobayashi, A., Ichimura, Y., et al. (2010). The selective autophagy substrate p62 activates the stress responsive transcription factor Nrf2 through inactivation of Keap1. *Nat. Cell Biol.* 12, 213–223. doi: 10.1038/ncb2021

Korczyn, A. D. (2001). Dementia in Parkinson's disease. *J. Neurol.* 248, III1-III4. doi: 10.1007/pl00022916

Kraft, A. D., Johnson, D. A., and Johnson, J. A. (2004). Nuclear factor E2-related factor 2-dependent antioxidant response element activation by tert-butylhydroquinone and sulforaphane occurring preferentially in astrocytes conditions neurons against oxidative insult. *J. Neurosci.* 24, 1101–1112. doi: 10.1523/JNEUROSCI.3817-03.2004

Kuter, K., Olech, L., and Glowacka, U. (2018). Prolonged dysfunction of astrocytes and activation of microglia accelerate degeneration of dopaminergic neurons in the rat substantia nigra and block compensation of early motor dysfunction induced by 6-OHDA. *Mol. Neurobiol.* 55, 3049–3066. doi: 10.1007/s12035-017-0529-z

Kwok, J. B., Hallupp, M., Loy, C. T., Chan, D. K., Woo, J., Mellick, G. D., et al. (2005). GSK3B polymorphisms alter transcription and splicing in Parkinson's disease. *Ann. Neurol.* 58, 829–839. doi: 10.1002/ana.20691

Lastres-Becker, I., García-Yagüe, A. J., Scannevin, R. H., Casarejos, M. J., Kügler, S., Rábano, A., et al. (2016). Repurposing the NRF2 activator dimethyl fumarate as therapy against synucleinopathy in Parkinson's Disease. *Antioxid. Redox Signal.* 25, 61–77. doi: 10.1089/ars.2015.6549

Lastres-Becker, I., Innamorato, N. G., Jaworski, T., Rabano, A., Kugler, S., Van Leuven, F., et al. (2014). Fractalkine activates NRF2/NFE2L2 and heme oxygenase 1 to restrain tauopathy-induced microgliosis. *Brain* 137, 78–91. doi: 10.1093/brain/awt323

Lee, J. M., Calkins, M. J., Chan, K., Kan, Y. W., and Johnson, J. A. (2003). Identification of the NF-E2-related factor-2-dependent genes conferring protection against oxidative stress in primary cortical astrocytes using oligonucleotide microarray analysis. *J. Biol. Chem.* 278, 12029–12038. doi: 10.1074/jbc.M211558200

L'Episcopo, F., Tirolo, C., Peruzzotti-Jametti, L., Serapide, M. F., Testa, N., Caniglia, S., et al. (2018). Neural stem cell grafts promote astroglia-driven

neurorestoration in the aged parkinsonian brain *via* wnt/β-catenin signaling. *Stem Cell*. 36, 1179–1197. doi: 10.1002/stem.2827

L'Episcopo, F., Tirolo, C., Testa, N., Caniglia, S., Morale, M. C., Cossetti, C., et al. (2011). Reactive astrocytes and Wnt/β-catenin signaling link nigrostriatal injury to repair in 1-methyl-4-phenyl-1,2,3,6-tetrahydropyridine model of Parkinson's disease. *Neurobiol. Dis*. 41, 508–527. doi: 10.1016/j.nbd.2010.10.023

L'Episcopo, F., Tirolo, C., Testa, N., Caniglia, S., Morale, M. C., Impagnatiello, F., et al. (2013). Ageing-induced Nrf2-ARE pathway disruption in the subventricular zone drives neurogenic impairment in parkinsonian mice *via* PI3K-Wnt/β-catenin dysregulation. *J. Neurosci*. 33, 1462–1485. doi: 10.1523/JNEUROSCI.3206-12.2013

Lev, N., Barhum, Y., Ben-Zur, T., Aharony, I., Trifonov, L., Regev, N., et al. (2015). A DJ-1 based peptide attenuates dopaminergic degeneration in mice models of Parkinson's disease *via* enhancing Nrf2. *PLoS ONE*. 10:e0127549. doi: 10.1371/journal.pone.0127549

Li, C., and Götz, J. (2017). Tau-based therapies in neurodegeneration: opportunities and challenges. *Nat. Rev. Drug Discov*. 16, 863–883. doi: 10.1038/nrd.2017.155

Licht-Murava, A., Paz, R., Vaks, L., Avrahami, L., Plotkin, B., Eisenstein, M., et al. (2016). A unique type of GSK-3 inhibitor brings new opportunities to the clinic. *Sci. Sig*. 9:454. doi: 10.1126/scisignal.aah7102

Liddell, J. (2017). Are astrocytes the predominant cell type for activation of Nrf 2 in aging and neurodegeneration? *Antiox*. 6:65. doi: 10.3390/antiox6030065

Liddelow, S. A., Guttenplan, K. A., Clarke, L. E., Bennett, F. C., Bohlen, C. J., Schirmer, L., et al. (2017). Neurotoxic reactive astrocytes are induced by activated microglia. *Nature* 541, 481–487. doi: 10.1038/nature21029

Lim, J. H., Kim, K. M., Kim, S. W., Hwang, O., and Choi, H. J. (2008). Bromocriptine activates NQO1 *via* Nrf2-PI3K/Akt signaling: novel cytoprotective mechanism against oxidative damage. *Pharmacol. Res*. 57, 325–331. doi: 10.1016/j.phrs.2008.03.004

Lin, M., Zhai, X., Wang, G., Tian, X., Gao, D., Shi, L., et al. (2015). Salvianolic acid B protects against acetaminophen hepatotoxicity by inducing NrF2 and phase II detoxification gene expression *via* activation of the P13K and PKC signaling pathway. *J. Pharmacol. Sci*. 127, 203–210. doi: 10.1016/j.jphs.2014.12.010

Linker, R. A., Lee, D. H., Ryan, S., van Dam, A. M., Conrad, R., Bista, P., et al. (2011). Fumaric acid esters exert neuroprotective effects in neuroinflammation *via* activation of the Nrf2 antioxidant pathway. *Brain* 134, 678–692. doi: 10.1093/brain/awq386

Liu, G. H., Qu, J., and Shen, X. (2008). NF-kappaB/p65 antagonizes Nrf2- ARE pathway by depriving CBP from Nrf2 and facilitating recruitment of HDAC3 to MafK. *Biochim. Biophys. Acta*. 1783, 713–727. doi: 10.1016/j.bbamcr.2008.01.002

Lok, K., Zhao, H., Shen, H., Wang, Z., Gao, X., Zhao, W., et al. (2013). Characterization of the APP/PS1 mouse model of Alzheimer's disease in senescence accelerated background. *Neurosci. Lett*.17, 84–89. doi: 10.1016/j.neulet.2013.10.051

Lu, M. C., Ji, J. A., Jiang, Z. Y., and You, Q. D. (2016). The Keap1-Nrf2-ARE pathway as a potential preventive and therapeutic target: an update. *Med. Res. Rev*. 36, 924–963. doi: 10.1002/med.21396

Mahul-Mellier, A. -L., Burtscher, J., Maharjan, N., Weerens, L., Croisier, M., and Kuttler, F., et al. (2020). The process of Lewy body formation, rather than simply a-synuclein fibrillization, is one of the major drivers. *Neurodegeneration*. 117, 4971–4982. doi: 10.1073/pnas.1913904117

Mao, L., Wang, H., Qiao, L., and Wang, X. (2010). Disruption of Nrf2 enhances the upregulation of nuclear factor-kappab activity, tumor necrosis factor-alpha, and matrix metalloproteinase-9 after spinal cord injury in mice. *Mediat. Inflamm*. 2010:238321. doi: 10.1155/2010/238321

Marcotte, D., Zeng, W., Hus, J. C., McKenzie, A., Hession, C., Jin, P., et al. (2013). Small molecules inhibit the interaction of Nrf2 and the Keap1 Kelch domain through a non-covalent mechanism. *Bioorg. Med. Chem*. 21, 4011–4019. doi: 10.1016/j.bmc.2013.04.019

Martelli, D., McKinley, M. J., and McAllen, R. M. (2014). The cholinergic anti-inflammatory pathway: a critical review. *Auton. Neurosci*. 182, 65–69. doi: 10.1016/j.autneu.2013.12.007

Martin, D., Rojo, A. I., Salinas, M., Diaz, R., Gallardo, G., Alam, J., et al. (2004). Regulation of heme oxygenase-1 expression through the phosphatidylinositol 3-kinase/Akt pathway and the Nrf2 transcription factor in response to the antioxidant phytochemical carnosol. *J. Biol. Chem*. 279, 8919–8929. doi: 10.1074/jbc.M309660200

Matigian, N., Abrahamsen, G., Sutharsan, R., Cook, A. L., Vitale, A. M., Nouwens, A., et al. (2010). Disease-specific, neurosphere-derived cells as models for brain disorders. *Dis. Model. Mech*. 3, 785–798. doi: 10.1242/dmm.005447

Miller, D. B., and O'Callaghan, J. P. (2015). Biomarkers of Parkinson's disease: Present and future, Metabolism 64. *S*40–S46. doi: 10.1016/j.metabol.2014.10.030

Moehle, M. S., and West, A. B. (2015). M1 and M2 immune activation in Parkinson's Disease: Foe and ally? *Neuroscience*. 302, 59–73. doi: 10.1016/j.neuroscience.2014.11.018

Mogi, M., Harada, M., Riederer, P., Narabayashi, H., Fujita, K., and Nagatsu, T. (1994). Tumor necrosis factor-alpha (TNF-alpha) increases both in the brain and in the cerebrospinal fluid from parkinsonian patients. *Neurosci. Lett*. 165, 208–210. doi: 10.1016/0304-3940(94)90746-3

Mogi, M., Togari, A., Tanaka, K., Ogawa, N., Ichinose, H., and Nagatsu, T. (1999). Increase in level of tumor necrosis factor (TNF)-alpha in 6-hydroxydopamine-lesioned striatum in rats without influence of systemic L-DOPA on the TNF-alpha induction. *Neurosci. Lett*. 268, 101–104. doi: 10.1016/S0304-3940(99)00388-2

Moon, H. E., and Paek, S. H. (2015). Mitochondrial dysfunction in Parkinson's disease. *Exp. Neurobiol*. 24, 103–16.

Morroni, F., Tarozzi, A., Sita, G., Bolondi, C., Zolezzi, M. J. M., et al. (2013). Neuroprotective effect of sulforaphane in 6-hydroxydopamine-lesioned mouse model of Parkinson's disease. *Neurotoxicol*. 36, 63–71. doi: 10.1016/j.neuro.2013.03.004

Mota, S. I., Costa, R. O., Ferreira, I. L., Santana, I., Caldeira, G. L., Padovano, C., et al. (2015). Oxidative stress involving changes in Nrf2 and ER stress in early stages of Alzheimer's disease. *Biochim. Biophys. Acta*. 1852, 1428–1441. doi: 10.1016/j.bbadis.2015.03.015

Muftuoglu, M., Elibol, B., Dalmizrak, O., Ercan, A., Kulaksiz, G., Ogus, H., et al. (2004). Mitochondrial complex I and IV activities in leukocytes from patients with parkin mutations. *Mov Disord* 19, 544–548. doi: 10.1002/mds.10695

Nakabeppu, Y., Tsuchimoto, D., Yamaguchi, H., and Sakumi, K. (2007). Oxidative damage in nucleic acids and Parkinson's disease. *J. Neurosci. Res*. 85, 919–934. doi: 10.1002/jnr.21191

Nakaso, K., Yano, H., Fukuhara, Y., Takeshima, T., Wada-Isoe, K., and Nakashima, K. (2003). PI3K is a key molecule in the Nrf2-mediated regulation of antioxidative proteins by hemin in human neuroblastoma cells. *FEBS Lett*. 546, 181–184. doi: 10.1016/S0014-5793(03)00517-9

Nioi, P., Nguyen, T., Sherratt, P. J., and Pickett, C. B. (2005). The carboxy-terminal Neh3 domain of Nrf2 is required for transcriptional activation. *Mol. Cell Biol*. 25, 10895–10906. doi: 10.1128/MCB.25.24.10895-10906.2005

Numazawa, S., Ishikawa, M., Yoshida, A., Tanaka, S., and Yoshida, T. (2003). Atypical protein kinase C mediates activation of NF-E2-related factor 2 in response to oxidative stress. *Am. J. Physiol. Cell Physiol*. 285, C334–342. doi: 10.1152/ajpcell.00043.2003

Ogura, T., Tong, K. I., Mio, K., Maruyama, Y., Kurokawa, H., Sato, C., et al. (2010). Keap1 is a forked-stem dimer structure with two large spheres enclosing the intervening, double glycine repeat, and C-terminal domains. *Proc. Natl. Acad. Sci. USA* 107, 2842–2847. doi: 10.1073/pnas.0914036107

Okamoto, M., Inoue, K., Iwamura, H., Terashima, K., Soya, H., Asashima, M., et al. (2011). Reduction in paracrine Wnt3 factors during ageing causes impaired adult neurogenesis. *Faseb. J*. 25, 3570–3582. doi: 10.1096/fj.11-184 697

Oksanen, M., Hyötyläinen, I., Trontti, K., Rolova, T., Wojciechowski, S., Koskuvi, M., et al. (2020). NF-E2-related factor 2 activation boosts antioxidant defenses and ameliorates inflammatory and amyloid properties in human Presenilin-1 mutated Alzheimer's disease astrocytes. *Glia*. 68, 589–599. doi: 10.1002/glia.23741

Oksanen, M., Petersen, A. J., Naumenko, N., Puttonen, K., Lehtonen, S., Gubert Olive, M., et al. (2017). PSEN1 mutant iPSC-derived model reveals severe astrocyte pathology in Alzheimer's disease. *Stem Cell Rep*. 9, 1885–1897. doi: 10.1016/j.stemcr.2017.10.016

Pajares, M., I Rojo, A., Manda, G., Boscá, L., and Cuadrado, A. (2020). Inflammation in Parkinson's disease: mechanisms and therapeutic implications. *Cells*. 9:1687.

Pajares, M., Jiménez-Moreno, N., García-Yagüe, Á. J., Escoll, M., de Ceballos, M. L., Van Leuven, F., et al. (2016). Transcription factor NFE2L2/NRF2 is a regulator of macroautophagy genes. *Autop*. 12, 1902–1916. doi: 10.1080/15548627.2016.1208889

Pajares, M., Rojo, A. I., Arias, E., Diaz-Carretero, A., Cuervo, A. M., and Cuadrado, A. (2018). Transcription factor NFE2L2/NRF2 modulates chaperone-mediated autophagy through the regulation of LAMP2A. *Autop*. 14, 1310–1322. doi: 10.1080/15548627.2018.1474992

Pan, H., Wang, H., Zhu, L., Mao, L., Qiao, L., and Su, X. (2011). Depletion of Nrf 2 enhances inflammation induced by oxyhemoglobin in cultured mice astrocytes. *Neurochem. Res*. 36, 2434–2441. doi: 10.1007/s11064-011-0571-6

Pappolla, M. A., Omar, R. A., Kim, K. S., and Robakis, N. K. (1992). Immunohistochemical evidence of oxidative stress in Alzheimer's disease. Am. J. *Pathol*. 140, 621–628.

Parada, E., Buendia, I., Leon, R., Negredo, P., Romero, A., Cuadrado, A., et al. (2014). Neuroprotective effect of melatonin against ischemia is partially mediated by alpha-7 nicotinic receptor modulation and HO-1 overexpression. *J. Pineal Res*. 56, 204–212. doi: 10.1111/jpi.12113

Park, S. Y., Park, S. J., Park, T. G., Rajasekar, S., Lee, S. J., and Choi, Y. W. (2013). Schizandrin C exerts anti-neuroinflammatory effects by upregulating phase II detoxifying/antioxidant enzymes in microglia. *Int. Immunopharmacol*. 17, 415–426. doi: 10.1016/j.intimp.2013.06.032

Pedersen, W. A., Fu, W., Keller, J. N., Markesbery, W. R., Appel, S., Smith, R. G., et al. (1998). Protein modification by the lipid peroxidation product 4-hydroxynonenal in the spinal cords of amyotrophic lateral sclerosis patients. *Ann. Neurol*. 44, 819–824. doi: 10.1002/ana.410440518

Pi, J., Bai, Y., Reece, J. M., Williams, J., Liu, D., Freeman, M. L., et al. (2007). Molecular mechanism of human Nrf2 activation and degradation: role of sequential phosphorylation by protein kinase CK2. *Free Radic. Biol. Med*. 42, 1797–1806. doi: 10.1016/j.freeradbiomed.2007.03.001

Prasad, K. N. (2017). Oxidative stress and pro-inflammatory cytokines may act as one of the signals for regulating microRNAs expression in Alzheimer's disease. *Mech. Ag. Devel*. 162, 63–71. doi: 10.1016/j.mad.2016.12.003

Rachakonda, G., Xiong, Y., Sekhar, K. R., Stamer, S. L., Liebler, D. C., and Freeman, M. L. (2008). Covalent modification at Cys151 dissociates the electrophile sensor Keap1 from the ubiquitin ligase CUL3. *Chem. Res. Toxicol*. 21, 705–710. doi: 10.1021/tx700302s

Rada, P., Rojo, A. I., Chowdhry, S., McMahon, M., Hayes, J. D., et al. (2011). SCF/beta-TrCP promotes glycogen synthase kinase 3-dependent degradation of the Nrf2 transcription factor in a Keap1-independent manner. *Mol. Cell Biol*. 31, 1121–33.

Rada, P., Rojo, A. I., Evrard-Todeschi, N., Innamorato, N. G., Cotte, A., Jaworski, T., et al. (2012). Structural and functional characterization of Nrf2 degradation by the glycogen synthase kinase 3/beta-TrCP axis. *Mol. Cell Biol*. 32, 3486–3499. doi: 10.1128/MCB.00180-12

Ramsey, C. P., Glass, C. A., Montgomery, M. B., Lindl, K. A., Ritson, G. P., Chia, L. A., et al. (2007). Expression of Nrf2 in neurodegenerative diseases. *J. Neuropathol. Exp. Neurol*. 66, 75–85. doi: 10.1097/nen.0b013e31802d6da9

Ren, P., Chen, J., Li, B., Zhang, M., Yang, B., Guo, X., et al. (2020). Nrf2 ablation promotes Alzheimer's disease-like pathology in APP/PS1 transgenic mice: The role of neuroinflammation and oxidative stress. *Oxid. Med. Cell Longev*. 2020:3050971. doi: 10.1155/2020/3050971

Riley, B. E., Kaiser, S. E., and Kopito, R. R. (2014). Autophagy inhibition engages Nrf 2-p 62 Ub-associated signaling. *Autophagy* 7, 338–340. doi: 10.4161/auto.7.3.14780

Rojo, A. I., Innamorato, N. G., Martín-Moreno, A. M., De Ceballos, M. L., Yamamoto, M., and Cuadrado, A. (2010). Nrf2 regulates microglial dynamics and neuroinflammation in experimental Parkinson's disease. *Glia*. 58, 588–598. doi: 10.1002/glia.20947

Rojo, A. I., Pajares, M., García-Yagüe, A. J., Buendia, I., Van Leuven, F., Yamamoto, M., et al. (2018). Deficiency in the transcription factor NRF2 worsens inflammatory parameters in a mouse model with combined tauopathy and amyloidopathy. *Redox Biol*. 18, 173–180. doi: 10.1016/j.redox.2018.07.006

Rojo, A. I., Pajares, M., Rada, P., Nuñez, A., Nevado-Holgado, A. J., Killik, R., et al. (2017). NRF2 deficiency replicates transcriptomic changes in Alzheimer's patients and worsens APP and TAU pathology. *Redox Biol*. 13, 444–451. doi: 10.1016/j.redox.2017.07.006

Rojo, A. I., Sagarra, M. R., and Cuadrado, A. (2008). GSK-3beta down-regulates the transcription factor Nrf2 after oxidant damage: relevance to exposure of neuronal cells to oxidative stress. *J. Neurochem*. 105, 192–202. doi: 10.1111/j.1471-4159.2007.05124.x

Ross, D., and Siegel, D. (2017). Functions of NQO1 in cellular protection and CoQ10 metabolism and its potential role as a redox sensitive molecular switch. *Free. Physiol*. 8:595. doi: 10.3389/fphys.2017.00595

Salazar, M., Rojo, A. I., Velasco, D., de Sagarra, R. M., and Cuadrado, A. (2006). Glycogen synthase kinase-3beta inhibits the xenobiotic and antioxidant cell response by direct phosphorylation and nuclear exclusion of the transcription factor Nrf2. *J. Biol. Chem*. 281, 14841–14851. doi: 10.1074/jbc.M513737200

SantaCruz, K. S., Yazlovitskaya, E., Collins, J., Johnson, J., and DeCarli, C. (2004). Regional NAD(P)H:quinone oxidoreductase activity in Alzheimer's disease. *Neurobiol Aging* 25, 63–69. doi: 10.1016/S0197-4580(03)00117-9

Sarlus, H., and Heneka, M. T. (2017). Microglia in Alzheimer's disease. *J. Clin. Invest*. 127, 3240–3249. doi: 10.1172/JCI90606

Sayre, L. M., Smith, M. A., and Perry, G. (2001). Chemistry and biochemistry of oxidative stress in neurodegenerative disease. *Curr. Med. Chem*. 8, 721–738. doi: 10.2174/0929867013372922

Schapira, A. H. (2008). Mitochondria in the aetiology and pathogenesis of Parkinson's disease. *Lancet Neurol*. 7, 97–109.

Schapira, A. H., Cooper, J. M., Dexter, D., Clark, J. B., Jenner, P., et al. (1990). Mitochondrial complex I deficiency in Parkinson's disease. *J. Neurochem*. 54, 823–7.

Schapira, A. H., Cooper, J. M., Dexter, D., Jenner, P., Clark, J. B., et al. (1989). Mitochondrial complex I deficiency in Parkinson's disease. *Lancet*. 1, 1269.

Selley, M. L., Close, D. R., and Stern, S. E. (2002). The effect of increased concentrations of homocysteine on the concentration of (E)-4-hydroxy-2-nonenal in the plasma and cerebrospinal fluid of patients with Alzheimer's disease. *Neurobiol. Aging* 23, 383–388. doi: 10.1016/S0197-4580(01)00327-X

Serapide, M. F., L'Episcopo, F., Tirolo, C., Testa, N., Caniglia, S., Giachino, C., et al. (2020). Boosting antioxidant self-defenses by grafting astrocytes rejuvenates the aged microenvironment and mitigates nigrostriatal toxicity in parkinsonian brain via an Nrf2-driven Wnt/β-catenin prosurvival axis. *Front. Ag. Neurosci*. 12:24. doi: 10.3389/fnagi.2020.00024

Shi, X., Jin, L., Dang, E., Chang, T., Feng, Z., et al. (2011). IL-17A upregulates keratin 17 expression in keratinocytes through STAT1- and STAT3-dependent mechanisms. *J. Invest. Dermatol*. 131, 2401–2408.

Shi, Y., and Holtzman, D. M. (2018). Interplay between innate immunity and Alzheimer disease: APOE and TREM2 in the spotlight. *Nat. Rev. Immunol*. 18, 759–772. doi: 10.1038/s41577-018-0051-1

Shih, H. C., Shiozawa, T., Miyamoto, T., Uchikawa, J., Feng, Y., Kashima, H., et al. (2003). Nuclear localization of beta-catenin is correlated with the expression of cyclin D1 in endometrial carcinomas. *Anticancer Res*. 23, 3749–3754. doi: 10.1677/ERC-08-0117

Shih, R. H., Wang, C. Y., and Yang, C. M. (2015). NF-kappaB signaling pathways in neurological inflammation: a mini review. *Front. Mol. Neurosci*. 8:77. doi: 10.3389/fnmol.2015.00077

Silva-Palacios, A., Ostolga-Chavarría, M., Zazueta, C., and K?onigsberg, M. (2018). Nrf2: molecular and epigenetic regulation during ageing. *Ageing Res. Rev*. 18, 31–40. doi: 10.1016/j.arr.2018.06.003

Simard, A. R., and Rivest, S. (2006). Neuroprotective properties of the innate immune system and bone marrow stem cells in Alzheimer's disease. *Mol. Psych*. 11, 327–335. doi: 10.1038/sj.mp.4001809

Sofroniew, M. V., and Vinters, H. V. (2010). Astrocytes: biology and pathology. *Acta Neuropathol*. 119, 7–35. doi: 10.1007/s00401-009-0619-8

Starhof, C., Winge, K., Heegaard, N. H. H., Skogstrand, K., Friis, S., and Hejl, A. (2018). Cerebrospinal fluid pro-inflammatory cytokines differentiate parkinsonian syndromes. *J. Neuroinflammation*. 15:305. doi: 10.1186/s12974-018-1339-6

Stephenson, J., Nutma, E., van der Valk, P., and Amor, S. (2018). Inflammation in CNS neurodegenerative diseases. *Immunology* 154, 204–219. doi: 10.1111/imm.12922

Subramaniam, S. R., and Federoff, H. J. (2017). Targeting microglial activation states as a therapeutic avenue in Parkinson's disease. *Front. Ag. Neurosci*. 9:176. doi: 10.3389/fnagi.2017.00176

Sultana, R., Perluigi, M., and Butterfield, D. (2013). Lipid peroxidation triggers neurodegeneration: a redox proteomics view into the Alzheimer disease brain. *Free Radic. Biol. Med*. 62, 157–169 doi: 10.1016/j.freeradbiomed.2012.09.027

Sun, Z., Chin, Y. E., and Zhang, D. D. (2009). Acetylation of Nrf2 by p300/CBP augments promoter-specific DNA binding of Nrf2 during the antioxidant response. *Mol. Cell Biol*. 29, 2658–2672. doi: 10.1128/MCB.01639-08

Suzuki, T., and Yamamoto, M. (2015). Molecular basis of the Keap1-Nrf2 system. *Free Radic. Biol. Med*. 88, 93–100. doi: 10.1016/j.freeradbiomed.2015.06.006

Tang, M., Ji, C., Pallo, S., Rahman, I., and Johnson, G. V. W. (2018). Nrf2 mediates the expression of BAG3 and autophagy cargo adaptor proteins and tau clearance in an age dependent manner. *Neurobiol. Ag*. 63, 128–139. doi: 10.1016/j.neurobiolaging.2017.12.001

Tarantini, S., Valcarcel-Ares, M. N., Yabluchanskiy, A., Tucsek, Z., Hertelendy, P., Kiss, T., et al. (2018). Nrf2 deficiency exacerbates obesity-induced oxidative stress, neurovascular dysfunction, blood-brain barrier disruption, neuroinflammation, amyloidogenic gene expression, and cognitive decline in mice, mimicking the aging phenotype. *J. Gerontol. A Biol. Sci. Med. Sci*. 73, 853–863. doi: 10.1093/gerona/glx177

Theodore, M., Kawai, Y., Yang, J., Kleshchenko, Y., Reddy, S. P., Villalta, F., et al. (2008). Multiple nuclear localization signals function in the nuclear import of the transcription factor Nrf2. *J. Biol. Chem.* 283, 8984–8994. doi: 10.1074/jbc.M709040200

Trimmer, P. A., Swerdlow, R. H., Parks, J. K., Keeney, P., Bennett, J. P. Jr, et al. (2000). Abnormal mitochondrial morphology in sporadic Parkinson's and Alzheimer's disease cybrid cell lines. *Exp Neurol*. 162, 37–50. doi: 10.1006/exnr.2000.7333

Trinh, K., Moore, K., Wes, P. D., Muchowski, P. J., Dey, J., Andrews, L., et al. (2008). Induction of the phase II detoxification pathway suppresses neuron loss in Drosophila models of Parkinson's disease. *J. Neuro*. 28, 465–472. doi: 10.1523/JNEUROSCI.4778-07.2008

Tysnes, O. B., and Storstein, A. (2017). Epidemiology of Parkinson's disease. *J. Neural Transm*. 124, 901–905. doi: 10.1007/s00702-017-1686-y

van Muiswinkel, F. L., de Vos, R. A., Bol, J. G., Andringa, G., Jansen Steur, E. N., Ross, D., et al. (2004). Expression of NAD(P)H:quinone oxidoreductase in the normal and Parkinsonian substantia nigra. *Neurobiol. Ag*. 25, 1253–1262. doi: 10.1016/j.neurobiolaging.2003.12.010

Vranová, H. P., Hényková, E., Kaiserová, M., Menšíková, K., Vaštík, M., Mareš, J., et al. (2014). Tau protein, beta-amyloid 1–42 and clusterin CSF levels in the differential diagnosis of Parkinsonian syndrome with dementia. *J. Neurol. Sci*. 343, 120–124. doi: 10.1016/j.jns.2014.05.052

Wakabayashi, N., Itoh, K., Wakabayashi, J., Motohashi, H., Noda, S., Takahashi, S., et al. (2003). Keap1-null mutation leads to postnatal lethality due to constitutive Nrf2 activation. *Nat. Genet*. 35, 238–245. doi: 10.1038/ng1248

Wang, H., Liu, K., Geng, M., Gao, P., Wu, X., Hai, Y., et al. (2013). RXRalpha inhibits the NRF2-ARE signaling pathway through a direct interaction with the Neh7 domain of NRF2. *Cancer Res*. 73, 3097–3108. doi: 10.1158/0008-5472.CAN-12-3386

Wei, Z., Li, X., Li, X., Liu, Q., and Cheng, Y. (2018). Oxidative stress in Parkinson's disease: A systematic review and metaanalysis. *Front. Mol. Neurosci* 11:236. doi: 10.3389/fnmol.2018.00236

Wu, Q., Zhang, X. S., Wang, H. D., Zhang, X., Yu, Q., et al. (2014). Astaxanthin activates nuclear factor erythroid-related factor 2 and the antioxidant responsive element (Nrf2-ARE) pathway in the brain after subarachnoid hemorrhage in rats and attenuates early brain injury. *Mar. Drugs*. 12, 6125–41.

Wunder, C., and Potter, R. F. (2003). The heme oxygenase system: Its role in liver inflammation. *Curr. Drug Target. Cardiovasc. Haematol. Disord*. 3, 199–208. doi: 10.2174/1568006033481410

Yan, W., Wang, H. D., Hu, Z. G., Wang, Q. F., and Yin, H. X. (2008). Activation of Nrf2-ARE pathway in brain after traumatic brain injury. *Neurosci. Lett*. 431, 150–154. doi: 10.1016/j.neulet.2007.11.060

Yang, L., Calingasan, N. Y., Thomas, B., Chaturvedi, R. K., Kiaei, M., Wille, E. J., et al. (2009). Neuroprotective effects of the triterpenoid, CDDO methyl amide, a potent inducer of Nrf2-mediated transcription. *PLoS ONE* 4, e5757. doi: 10.1371/journal.pone.0005757

Yoo, M. S., Chun, H. S., Son, J. J., DeGiorgio, L. A., Kim, D. J., Peng, C., et al. (2013). Oxidative stress regulated genes in nigral dopaminergic neuronal cells: Correlation with the known pathology in Parkinson's disease. *Brain Res. Mol. Brain Res*. 110, 76–84. doi: 10.1016/S0169-328X(02)00586-7

Youdim, M. B., Stephenson, G., and Shachar, B. D. (2004). Ironing iron out in Parkinson's disease and other neurodegenerative diseases with iron chelators: a lesson from 6-hydroxydopamine and iron chelators, desferal and VK-28. *Ann. NY Acad. Sci*. 1012, 306–325. doi: 10.1196/annals.1306.025

Yu, I. I., Paraiso, H. C., Kuo, P., Scofield, B. A., Sweazey, R. D., Chang, F., et al. (2019). Functional Nrf2 restrains inflammatory and transcriptional phenotypes in microglia and its deficiency recapitulates the aging phenotype. *J. Immunol*. 202, 185–117. doi: 10.1002/jcp.27185

Zhang, H., Davies, K. J. A., and Forman, H. J. (2015). Oxidative stress response and Nrf2 signaling in aging. *Free Rad. Biol. Med*. 88, 314–336. doi: 10.1016/j.freeradbiomed.2015.05.036

Zhang, J., Zhu, Y., Zhou, D., Wang, Z., and Chen, G. (2010). Recombinant human erythropoietin (rhEPO) alleviates early brain injury following subarachnoid hemorrhage in rats: possible involvement of Nrf2- ARE pathway. *Cytokine* 52, 252–257. doi: 10.1016/j.cyto.2010.08.011

Zhang, M., Teng, C. H., Wu, F. F., Ge, L. Y., Xiao, J., Zhang, H. Y., et al. (2019). Edaravone attenuates traumatic brain injury through anti-inflammatory and anti-oxidative modulation. *Exp. Therap. Med*. 18, 467–474. doi: 10.3892/etm.2019.7632

Zhang, X. X., Tian, Y., Wang, Z. T., Ma, Y. H., Tan, L., and Yu, J. T. (2021). The epidemiology of Alzheimer's disease modifiable risk factors and prevention. *J. Prev. Alz. Dis*. 8, 313–321. doi: 10.14283/jpad.2021.15

Zhang, Z. J., Cheang, L. C. V., Wang, M. W., and Lee, S. M. Y. (2011). Quercetin exerts a neuroprotective effect through inhibition of the iNOS/NO system and pro-inflammation gene expression in PC12 cells and in zebrafish. *Int. J. Mol. Med*. 27, 195–203. doi: 10.3892/ijmm.2010.571

Zhou, W., and Freed, C. R. (2005). DJ-1 up-regulates glutathione synthesis during oxidative stress and inhibits A53T alpha-synuclein toxicity. *J. Biol. Chem*. 280, 43150–43158. doi: 10.1074/jbc.M507124200

Zhou, Y., Wang, X., Ying, W., Wu, D., and Zhong, P. (2019). Cryptotanshinone Attenuates Inflammatory Response of Microglial Cells *via* the Nrf2/HO-1 Pathway. *Front. Neurosci*. 13, 852. doi: 10.3389/fnins.2019.00852

Zipper, L. M., and Mulcahy, R. T. (2002). The Keap1 BTB/POZ dimerization function is required to sequester Nrf2 in cytoplasm. *J. Biol. Chem*. 277, 36544–36552. doi: 10.1074/jbc.M206530200

Conflict of Interest: The authors declare that the research was conducted in the absence of any commercial or financial relationships that could be construed as a potential conflict of interest.

Publisher's Note: All claims expressed in this article are solely those of the authors and do not necessarily represent those of their affiliated organizations, or those of the publisher, the editors and the reviewers. Any product that may be evaluated in this article, or claim that may be made by its manufacturer, is not guaranteed or endorsed by the publisher.

frontiers | Frontiers in Cellular Neuroscience

ORIGINAL RESEARCH
published: 13 April 2022
doi: 10.3389/fncel.2022.783346

Heme Oxygenase-1 Protects Hair Cells From Gentamicin-Induced Death

Yang Yang[1], Xin Chen[1], Keyong Tian[1], Chaoyong Tian[1], Liyang Chen[2], Wenjuan Mi[1], Qiong Li[1], Jianhua Qiu[1], Ying Lin[1] and Dingjun Zha[1]**

[1] Department of Otolaryngology-Head and Neck Surgery, Xijing Hospital, Air Force Military Medical University, Xi'an, China, [2] Smartgenomics Technology Institute, Tianjin, China

Gentamicin ototoxicity can generate free radicals within the inner ear, leading to permanent damage to sensory hair cells (HCs) and eventually hearing loss. The following study examined the alterations of oxidative damage-related genes in the cochlea and important molecules responsible for oxidation following gentamicin injury *in vitro*. The RT^2 Profiler polymerase chain reaction (PCR) array was used to screen candidate targets for treatment to prevent hearing loss caused by gentamicin. We found that during gentamicin-induced death in HCs, Heme oxygenase-1 (HO-1) had a high fold change in the HCs of the cochlea. Moreover, the use of CoPPIX to induce HO-1 inhibited gentamicin-induced HC death, while HO-1 inhibitors ZnPPIX after CoPPIX reversed this process. Furthermore, the inhibitors of NF-E2-related factor-2 (Nrf2) reduced the expression of HO-1 and inhibited the protective effect of HO-1 after gentamicin, thus suggesting that the Nrf2/HO-1 axis might regulate gentamicin-associated ototoxicity. We further demonstrated that induction of HO-1 up-regulated the expression of Nrf2 in both cochlear and HEI-OC1 cells. In summary, these findings indicated that HO-1 protects HCs from gentamicin by up-regulating its expression in HCs and interacting with Nrf2 to inhibit reactive oxygen species (ROS).

Keywords: gentamicin, ototoxicity, differential gene expression, HO-1, hair cells, Nrf2

OPEN ACCESS

Edited by:
Arturo Ortega, Centro de Investigación y de Estudios Avanzados del Instituto Politécnico Nacional, Mexico

Reviewed by:
Mika Takarada-Iemata, Kanazawa University, Japan
Hongzhe Li, VA Loma Linda Healthcare System, United States

***Correspondence:**
Ying Lin
lytemple@fmmu.edu.cn
Dingjun Zha
zhadjun@fmmu.edu.cn

Specialty section:
This article was submitted to Non-Neuronal Cells, a section of the journal Frontiers in Cellular Neuroscience

Received: *26 September 2021*
Accepted: *28 February 2022*
Published: *13 April 2022*

Citation:
Yang Y, Chen X, Tian K, Tian C, Chen L, Mi W, Li Q, Qiu J, Lin Y and Zha D (2022) Heme Oxygenase-1 Protects Hair Cells From Gentamicin-Induced Death. Front. Cell. Neurosci. 16:783346. doi: 10.3389/fncel.2022.783346

INTRODUCTION

Hearing loss is the most common sensory impairment worldwide. According to the WHO statistics,[1] approximately 700 million hearing loss cases were recorded worldwide in 2018, and this number is expected to increase over 900 million by 2050 (Guo et al., 2019). Hearing loss usually results from the death of hair cells (HCs) in the inner ear. HCs constitute auditory and balance sensory cells that convert mechanical stimuli into neural signals (WenWei et al., 2018). These cells are susceptible to various stressors, such as aging, noise trauma, gene mutations, and treatment with ototoxic drugs, e.g., aminoglycosides and cisplatin (Fettiplace, 2017; Pang et al., 2019; Han et al., 2020). HC death resulting from ototoxic drugs represents an important health challenge. Aminoglycoside antibiotics remain one of the most commonly used antibiotic groups worldwide. Approximately 20% of individuals using these agents have shown serious hearing loss and/or balance damage, especially those using gentamicin (Kirst and Marinelli, 2014). Apparently, gentamicin generates free radicals within the inner ear, which leads to subsequent permanent damage to sensory cells (Zhou et al., 2018; Fujimoto and Yamasoba, 2019).

[1] https://www.who.int/health-topics/hearing-loss#tab=tab_1

Reactive oxygen species (ROS) has a crucial role in the promotion of apoptosis by interfering mitochondrial permeability, release of cytochrome c and caspases (Pyun et al., 2011). Quan et al. (2015) demonstrated that up-regulation of Sirt3, a member of the Sirtuin family, may inhibit the production of ROS in apoptotic cells induced by gentamicin.

Moreover, preliminary experiments revealed that heme oxygenase-1 (Hmox-1/HO-1) was up-regulated in gentamicin-induced HC death. HO constitutes the rate-limiting enzymes in the process of heme degradation, causing the production of biliverdin, free iron, and CO (Medina et al., 2019). As an important protein in cell response to stress, HO-1 is triggered by numerous oxidative substances or conditions such as heme (Maines, 1988), hyperoxia (Chan Kwon et al., 2020), hypoxia (Tian et al., 2020), and electrophiles via AP-1, STAT, and Nrf2 up-regulation at the mRNA level (Alam et al., 2020; Lee et al., 2020). HO-1 is widely present in the kidneys, liver, lungs, and other organs, including the inner ear (He et al., 2019; Yi et al., 2020). Previous studies have suggested that pharmacological HO-1 activation exerts protective effect on a variety of stresses in the retina and liver following ischemia-reperfusion injury (Cheng and Rong, 2017; Hirao et al., 2020). Some reports also suggested that HO-1 has cochlear localization and is induced upon heat shock (Fairfield et al., 2004). Meanwhile, HO-1 inducers exert protective effects on cisplatin-associated HEI-OC1 cell death (Lee et al., 2019; Sun et al., 2019). Another study demonstrated that inducing HO-1 protects the organs of Corti explants from cisplatin-related HC death in newborn rats (Kim et al., 2015). The functional effect of HO-1 induction has been studied by assessing the ability of cell to resist multiple stress injuries with under- or over-expressed HO-1. These reports mainly focused on the critical cell defense effect of HO-1 on oxidative stress (Fontecha-Barriuso et al., 2020; Tian et al., 2020).

The current study focused on the alterations of oxidative damage-related genes in the cochlea following gentamicin treatment. We further aimed to quantify and characterize the differential expression of the important molecule responsible for oxidation and to clarify the protective effect of HO-1 in the process of gentamicin injury. The current study provides insight into molecular targets to prevent gentamicin ototoxicity.

MATERIALS AND METHODS

Animals

Neonatal (P2) Sprague-Dawley (SD) rats were provided by the Laboratory Animal Center of the Air Force Medical University. All the animals were housed in an environment with a temperature of 22 ± 1°C, relative humidity of 50 ± 1%, and a light/dark cycle of 12/12 h (lights on at 8 a.m. and off at 5 p.m.). All animal studies, including the mice euthanasia procedure, were done in compliance with Air Force Medical University institutional animal care regulations and guidelines and conducted according to the AAALAC and the IACUC guidelines.

Tissues Culture

At P2, the organs of Corti dissection from the rat's cochlear tissue were performed. The specimens were placed in Hank's balanced salt solution (H1045, Solabio, Beijing, China). The entire organs of Corti were cultured in Hanging Cell Culture Inserts (MCSP24H48, EMD Millipore Corp, Billerica, MA, United States). The culture medium consisted of Minimum Essential Medium supplemented with Earle's salt and L-glutamine (11095080, Gibco, Grand Island, NY, United States), 3 mg/mL glucose, and 0.3 mg/mL penicillin (P3032, Sigma-Aldrich, St. Louis, MO, United States). The organs of Corti were cultured at 37°C in a humid environment with 5% CO_2. The final concentrations of gentamicin (E003632-1G, Sigma-Aldrich, St. Louis, MO, United States) were 0.3 mM, 0.6 mM, and 1 mM. The HO-1 activator Co (III) protoporphyrin IX chloride (CoPPIX) (Co654, Frontier Scientific, Logan, UT, United States) was used at 5 μM in the CoPPIX group with a 12 h incubation. Tissues undergoing both CoPPIX and gentamicin treatments were first cultured with CoPPIX for 12 h, after which the medium was replaced by gentamicin-loaded medium for 24 h incubation. Meanwhile, the HO-1 suppressor Zn (II) protoporphyrin IX (ZnPPIX) (Zn625, Frontier Scientific, Logan, UT, United States) was prepared based on a previous report (Francis et al., 2011). ZnPPIX was then diluted to 20μM in culture medium for 12 h, as described in a previous study (Kim et al., 2006). Nrf2 inhibitor ML385 (846557-71-9, Selleck Chemicals, Houston, TX, United States) was used at 15 μM in the medium for 24 h. The gentamicin + ML385 group received both gentamicin (0.6 mM) and ML385 (15 μM) for 24 h.

RT^2 Profiler Polymerase Chain Reaction Array

Approximately 20 organs of Corti were dissected from postnatal (P2) SD rats and cultured in medium with or without 0.6 mM gentamicin for 24 h. Total RNA extraction from the collected tissues was performed with the RNeasy Micro Kit (74004, QIAGEN, Hilden, Germany). The RT^2 First Strand Kit (330401, QIAGEN, Hilden, Germany) was utilized for cDNA preparation from 1 μg of total RNA. The expression of 84 oxidative damage-related genes was assessed with the Oxidative Stress RT^2 Profiler^{TM} PCR Array kit (PARN-065ZC, QIAGEN, Hilden, Germany). The RT^2 SYBR Green/ROX qPCR Mastermix (330522, QIAGEN, Hilden, Germany) was employed for quantitative real-time PCR (qPCR), as directed by the manufacturer, on an ABI ViiTM7 Real-Time PCR System in 25 μL reactions. The following protocol was used for amplification: 95°C, 10 min; 40 cycles of 95°C (15 s) and 60°C (60 s). The experiments were carried out in triplicate. The results of qPCR were uploaded on the RT^2 Profiler^{TM} PCR Array Data

Abbreviations: HC, hair cell; SC, supporting cell; HO-1, heme oxygenase-1; CoPPIX, Co (III) protoporphyrin IX chloride; ZnPPIX, Zn (II) protoporphyrin IX; Nrf2, nuclear factor erythroid 2 (NF-E2)-related factor 2; ROS, reactive oxygen species; P2, postnatal day 2; SD, sprague-dawley; PBS, phosphate buffered saline; DAPI, 4′, 6′-diamidino-2-phenylindole; GAPDH, glyceraldehyde-3-phosphate dehydrogenase; GO, gene ontology; NADPH, nicotinamide adenine dinucleotide phosphate; NMDA, *N*-methyl-*D*-aspartate; PCR: polymerase chain reaction; qPCR: quantitative real-time polymerase chain reaction.

Analysis website.[2] According to the instructions of the software, Ct cut-off value was set at 35. $2^{-\Delta Ct}$ was used to calculate the fold-change of mRNA expression. Student *t*-tests were used for the assessment of statistical significance. A *P*-value < 0.05 was considered statistically significant. The genes with $P < 0.05$ and more than 2-fold difference in expression were considered to be differentially expressed genes with biological significance.

Gene Ontology Enrichment Analysis and Protein Interaction Network Construction

DAVID 6.8[3] online analysis platform was used to annotate the screened differential genes in the GO and to classify processes or functions the differential genes mainly affect. R language was used to convert the data into a visual bubble chart. The protein interaction relationship of differentially expressed genes was analyzed through the STRING protein interaction database V11.0.[4]

Quantitative Real-Time PCR

PCR was performed on the selected genes in order to verify the results of RT^2 Profiler PCR Array. The entire organs of Corti were treated with 0 mM, 0.3 mM, 0.6 mM, and 1 mM gentamicin, after which they were collected. The total RNA was extracted with the RNeasy Micro Kit (74004, QIAGEN, Hilden, Germany). The RT^2 First Strand Kit (330401, QIAGEN, Hilden, Germany) was utilized for cDNA preparation from 1 μg of total RNA. The following primers were employed: HO-1, sense 5′-TTTCACCTTCCCGAGCATC-3′ and antisense 5′-TCTTAGC CTCTTCTGTCACCCT-3′; β-actin, sense 5′-GAAGAGCTATG AGCTGCCTGA-3′ and antisense 5′-TGATCCACATCTGCTGG AAGG-3′; Nrf2, sense 5′-TTCCTCTGCTGCCATTAGTCAGTC-3′ and antisense 5′-GCTCTTCCATTTCCGAGTCACTG-3′; NQO1, sense 5′- GCGAGAAGAGCCCTGATTGTACTG -3′ and antisense 5′- TCTCAAACCAGCCTTTCAGAATGG -3′; GCLC, sense 5′- ACATCTACCACGCAGTCAAGGACC -3′ and antisense 5′- CTCAAGAACATCGCCTCCATTCAG -3′. β-actin was utilized for normalization. Data were obtained in triplicate and presented as mean.

Cells Culture

Supporting cells were separated from the organs of Corti and cultured *in vitro*. The organs of Corti of three newborn rats (P2) were minced into small pieces and digested with PBS containing 0.5 mg/mL collagenase IV (17104-019, Gibco, Grand Island, NY, United States) for 20 min. DMEM/F-12 medium (11330032, Gibco, Grand Island, NY, United States) with 10% fetal bovine serum (FBS; 10091148, Gibco, Grand Island, NY, United States) and 1% antibiotic cocktail (penicillin and streptomycin; 15140-12, Gibco, Grand Island, NY, United States) were used to culture the cells in suspension for 24 h. Adherent-sphere cells were cultured in culture medium including factor DMEM/F-12, B-27^{TM} Supplement (1:50, 17504044, Gibco, Grand Island, NY, United States), human EGF (5 ng/mL, AF100-15, PeproTech, Rocky Hill, NJ, United States), human FGF-basic (2.5 ng/mL, 100-18B, PeproTech, Rocky Hill, NJ, United States) and 1% antibiotic cocktail, in a humid environment containing 5% CO_2 at 37°C for 24 h. Adherent cells were then transferred to DMEM/F-12 medium with 10% FBS and 1% antibiotic cocktail and cultured for additional 2 days.

HEI-OC-1 cells were cultured at 37°C with 5% CO_2 in DMEM (C11995500BT, Gibco, Grand Island, NY, United States) containing 10% FBS (10099141, Gibco, Grand Island, NY, United States) and 1% penicillin (SV30010, HyClone, South Logan, UT, United States). The cells were subcultured at 80% confluence using 0.25% trypsin/EDTA (25200056, Gibco, Grand Island, NY, United States). When cells were cultured to a suitable density, the serum was removed, and cells were washed with PBS three times. CoPPIX (5 μM) and ZnPPIX (20 μM) were then added in the medium for 12 h.

Immunofluorescence Staining

The entire organs of Corti underwent fixation with 4% paraformaldehyde for 8 h at 4°C. Supporting cells and HEI-OC1 cells underwent fixation with 4% paraformaldehyde for 20 min at room temperature. Blocking was carried out in phosphate-buffered saline (PBS) with 1% Triton X-100 (V900502, Sigma-Aldrich, St. Louis, MO, United States) and 5% bovine serum solution for 1 h. The tissue specimens underwent overnight incubation with rabbit anti-HO-1 (1:100, GTX101147, Gene Tex, Alton Pkwy Irvine, CA, United States), mouse anti-Nrf2 (1:200, ab89443, Abcam, Cambridge, MA, United States), goat anti-Sox2 (1:100, AF2018-SP, R&D Systems, Minneapolis, MN, United States), mouse anti-$p27^{Kip1}$ (1:100, sc-1641, Santa Cruz, Santa Cruz, CA, United States), and rabbit anti-Myosin VII-a (1:800, 25-6790, Proteus Bioscience, Ramona, CA, United States) primary antibodies, respectively, at 4°C. Following four PBS washes, Alexa Fluor 488-linked donkey anti-mouse (AP192F, Millipore, Billerica, MA, United States), Alexa Fluor 594-linked donkey anti-rabbit (AP182C, Millipore, Billerica, MA, United States), and Alexa Fluor Plus 647 Donkey anti-Goat (H + L; A32849, Invitrogen, Carlsbad, CA, United States) secondary antibodies (1:200) were added to the specimens, respectively, for 12 h at 25°C. Rhodamine Phalloidin (1:200, PHDR1, Cytoskeleton, Denver, CO, United States) was used to mark HCs for 20min. Counterstaining was performed using 4′, 6′-diamidino-2-phenylindole (DAPI; 1:1000, D9542, Sigma-Aldrich, St. Louis, MO, United States). The entire specimen was evaluated in different turns under a confocal microscope (Nikon, Tokyo, Japan). 3D reconstructions were made by using Imaris (×64) software (Version: 9.0, Bitplane).

Cell Counting

The cultured organs of Corti were placed under a confocal microscope. HCs of each turn were separately enumerated from micrographs acquired.

MitoSOX Red Assay

Mitochondrial ROS amounts were assessed by MitoSOX Red staining (M36008, Invitrogen, Carlsbad, CA, United States).

[2]https://geneglobe.qiagen.com/cn/analyze/

[3]https://david.ncifcrf.gov/

[4]https://string-db.org/

MitoSOX Red was used for the detection of mitochondrial reactive oxygen species by live-cell imaging. After organs of Corti were cultured with gentamicin (0.6 mM), CoPPIX (10 μM) or ZnPPIX (100 μM) for 48 h, the specimens underwent PBS washing and incubation with MitoSOX Red (5 μM) at 37°C in the presence of 5% CO_2 for 10 min. Next, 4% paraformaldehyde was used for cell fixation at room temperature for 30 min before immunofluorescent staining.

Western Blotting

The entire organs of Corti were treated in different groups. Total protein from cochlear specimens was obtained with the RIPA buffer that contained 1% PMSF. Nuclear–cytoplasmic fractionation was conducted using the NE-PER Nuclear and Cytoplasmic Extraction Reagents kit (Pierce, Thermo Fisher Scientific, Waltham, MA, United States) according to the manufacturer's protocol. After clearing the lysate by centrifugation, the proteins were resolved by 8% SDS-PAGE and electro-transferred onto PVDF membranes. Upon blocking with 5% non-fat milk (1h at ambient), the membranes underwent overnight incubation with anti-HO-1 (1:100, GTX101147, Gene Tex, Alton Pkwy Irvine, CA, United States), anti-Nrf2 (1:100, ab89443, Abcam, Cambridge, MA, United States), and anti-GAPDH (1:1000, 10494-1-AP, Proteintech) and β-actin (1:1000, sc-47778, Santa Cruz, Santa Cruz, CA, United States) primary antibodies, respectively, at 4°C. This was followed by incubation with HRP-linked secondary antibodies (1:2000, SA00001-2, Proteintech) for 1h at ambient. The ECL kit (Pierce, Thermo Fisher Scientific, Waltham, MA, United States) was used for visualization.

Statistical Analysis

SPSS 26 (SPSS Software, Chicago, IL, United States) and GraphPad 5.01 (GraphPad Software, San Diego, CA, United States) were used for data analysis. Data were compared by one-way analysis of variance (ANOVA). A P-value < 0.05 indicated statistically significant differences.

RESULTS

Gentamicin Induced Gene Differential Expression

The organs of Corti of the inner ear from 24 P2 rats were cultured in a medium with or without 0.6 mM gentamicin. After 24 h of culture, the RT^{2}Profiler^{TM} PCR Array Rat Oxidative Stress kit was used to investigate the expression of 84 known oxidative-related genes. Re-collect the organs of Corti and conduct three individual experiments. Gene expression assessment of triplicate assays was carried out as described on the RT^2 Profiler^{TM} PCR Array Data Analysis website (see text footnote 2), based on cycle threshold (Ct). Hierarchical clustering was used to evaluate the transcriptional levels of 84 oxidative stress-related genes in the cochlea (**Figure 1A**); volcano plots were used to compare gene expression between the control and gentamicin groups (**Figure 1B**). **Figure 1C** shows a scatter plot highlighting several notable genes based on large differences in expression fold between the control and gentamicin groups (**Figure 1C**). Of the 84 genes, 18 were up-regulated by more than 2-fold (**Supplementary Table 1**), and three genes were down-regulated by ≥2-fold (**Supplementary Table 2**). HO-1 was the gene with a relatively high up-regulation multiple which ranked the 3rd among these 21 genes, while with the smallest p-value in the whole group.

Gene Ontology and Networks of the Differentially Expressed Genes

To classify the processes and functions among genes with differential expression between the control and gentamicin groups, gene ontology (GO) analysis was carried out to categorize the 21 differentially expressed genes for their molecular functions (**Figure 2A**). Based on biological processes, these genes were involved in response to oxygen-containing compounds, cellular response to chemical stimulus, response to oxidative stress, response to the drug, and response to chemicals. Genes with altered expression in the gentamicin group were highly enriched in functional categories such as oxidoreductase activity, organic cyclic compound binding, ion binding, heme binding, and cofactor binding. The molecular components of the genes were highly enriched in the plasma membrane, cell part, NADPH oxidase complex, cytoplasm, and cytosol. In addition, a STRING protein-protein interaction network was constructed to visualize the possible connections between differentially expressed genes (**Figure 2B**). Among them, HO-1 showed an interaction with eight genes; PTGS2 interacted with six genes, and APOE and NOS2 interacted with five genes.

Immunofluorescence Staining, QPCR, and Immunoblot Confirmed Heme Oxygenase-1 Expression

The organs of Corti were cultured in a medium with or without 0.6 mM gentamicin. After 24 h of culture, immunofluorescence staining showed that HO-1 highly expressed in SCs, and only slightly expressed in HCs in the control group. Treatment with 0.6 mM gentamicin increased the expression of HO-1 in HCs and decreased its expression in SCs (**Figure 3A**). SCs were separated from control group rats for *in vitro* culture. SOX2 and p27^{Kip1} are known markers of SCs. *In vitro* assays also confirmed that HO-1 was expressed in SCs in the control group (**Figure 3B**). In order to verify the expression of HO-1 up-regulated by gentamicin, the organs of Corti were treated with varying concentrations (0, 0.3, 0.6, and 1 mM) of gentamicin. The quantitative RT-PCR (qPCR) (**Figure 3C**) and immunoblot (**Figures 3D,E**) data indicated that gentamicin up-regulated HO-1 in a concentration-dependent manner ($^{***}P < 0.001$, $^{*}P < 0.05$, $n = 3$), which suggested that HO-1 participates in the process of gentamicin injury.

Heme Oxygenase-1 Induction Inhibited Gentamicin-Related Hair Cell Death

To explore the role of HO-1 in the process of gentamicin injury, the HO-1 inducer CoPPIX (Ferrandiz and Devesa, 2008) was utilized to determine whether activating HO-1 protects HCs from

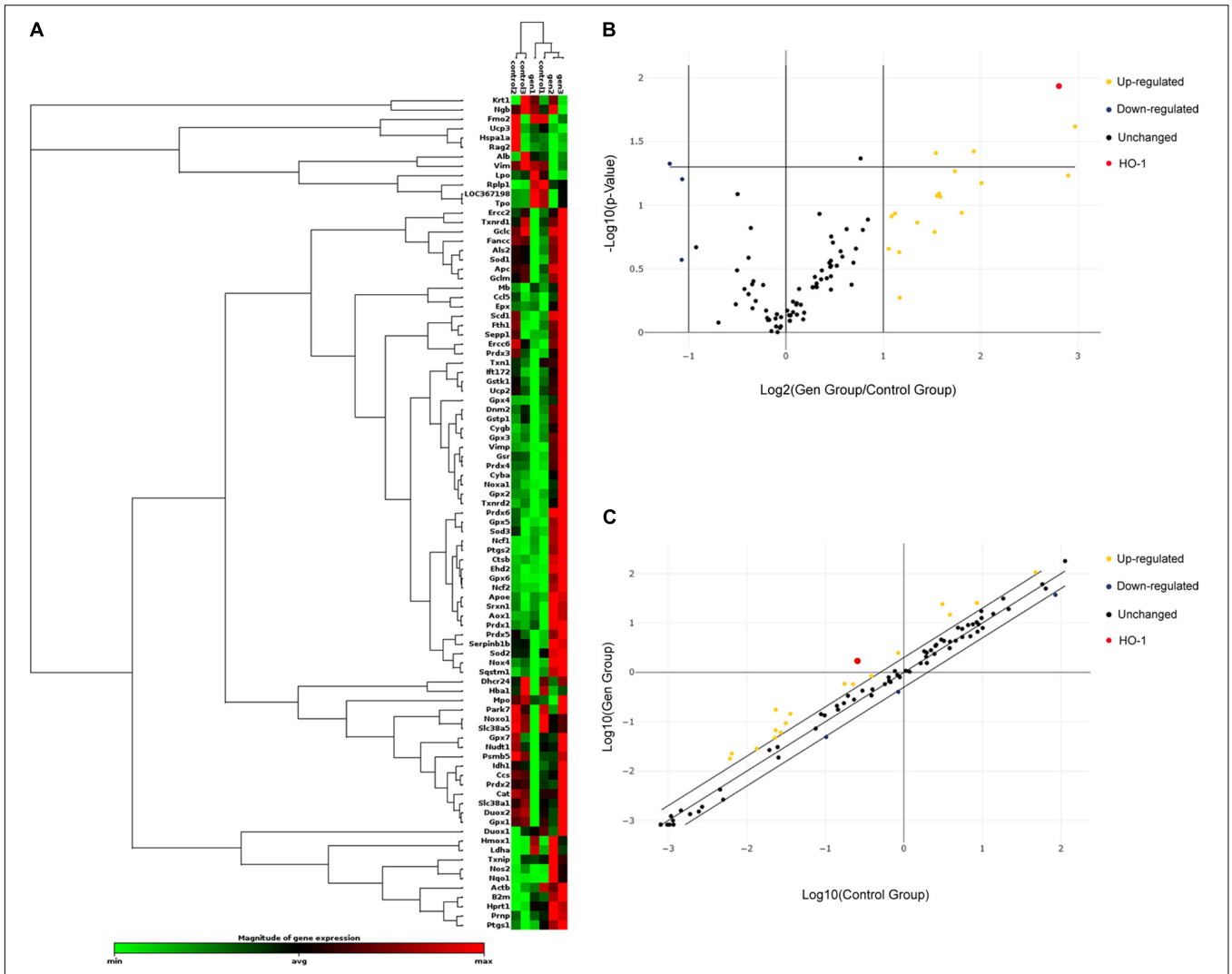

FIGURE 1 | Relative expression of 84 oxidative stress-related genes in the control and gentamicin (0.6 mM) groups. **(A)** Hierarchical clustering of the 84 detected genes involved in oxidative stress in the cochlea, with expression levels ranging from low (green) to high (red). **(B)** The volcano plot shows notable gene expression changes between the control and gentamicin groups by plotting the log2 fold change in mRNA amounts on the x-axis and their statistical significance on the y-axis. **(C)** The scatter plot illustrates log-transformed relative expression levels for various genes ($2^{-\Delta Ct}$) between the control group (x-axis) and the gentamicin group (y-axis).

gentamicin damage. The immunostaining showed that HO-1 induced in both HCs and SCs by CoPPIX (**Figure 4A**).The organs of Corti were pretreated with CoPPIX (5 μM) in the presence or absence of the HO-1 inhibitor ZnPPIX (20 μM) for 12 h and then further incubated with 0.6 mM gentamicin for 24 h. Myosin VII-a was used as a marker of inner and outer HCs. In control cells, the four HC rows were neatly arranged. Gentamicin administration for 24 h resulted in elevated HC loss in basal turns versus apical turns, forming a gradient from apex to base (**Figure 4B**); compared to the control group, the number of HCs in the apical turns was reduced by 68.20%, 83.01% in middle turns and approximately 87% in basal turn in the gentamicin group (***$P < 0.001$, $n = 5$) (**Figures 4C–E**, Formula for calculating ratio was (X-Y)/X. X means the number of HCs in each turn of control group, 56.6, 62.4, and 60, respectively. Y means the number of HCs in each turn of gentamicin group, 18, 10.6 and 7.8, respectively). Meanwhile, compared to the gentamicin group, the number of HCs in the apical, middle, and basal turns respectively increased by 185.56, 447.17, and 369.239% in the gentamicin + CoPPIX group (**Figures 4C–E**, Formula for calculating ratio was (Z-Y)/Z. Z means the average number of HCs in each turn of gentamicin + CoPPIX group, 51.4, 58, and 36.6, respectively). To further confirm that the protective effects involved HO-1 activation, the HO-1 inhibitor ZnPPIX (Wong et al., 2011) was applied. The gentamicin + CoPPIX + ZnPPIX group showed no protection by CoPPIX in the apical, middle, and basal turns (**Figures 4B–E**). We confirmed that HO-1 was required for the protection against gentamicin-induced HC death. No loss of HCs was observed in the CoPPIX and ZnPPIX groups. Furthermore, HC counts showed the same trend in cell

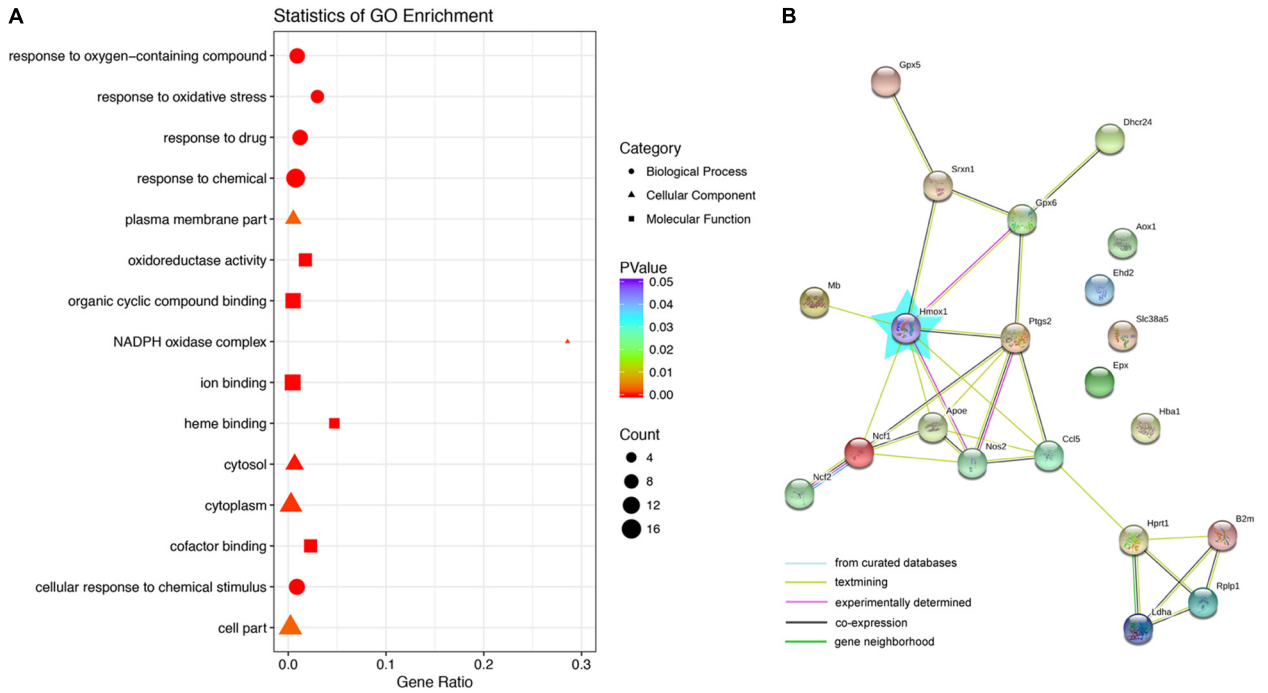

FIGURE 2 | Gene ontology (GO) and network analysis of genes with differential expression between the control and gentamicin groups. **(A)** GO analysis of genes with differential expression between the control and gentamicin groups. **(B)** STRING protein-protein interaction analysis of genes. The blue star represents Hmox1 (HO-1).

density changes from apical to basal turns in various groups (**Figures 4C–E**).

Heme Oxygenase-1 Induction Decreased Intracellular Reactive Oxygen Species Levels

MitoSOX Red, a redox fluorophore specifically measuring superoxide amounts in the mitochondria, was utilized to investigate the effects of HO-1 on ROS production after gentamicin treatment. Immunofluorescence staining revealed that the amount of ROS in cochlear HCs treated with gentamicin increased to 34.73-times of that in the control group. In the gentamicin +CoPPIX group, the amounts of ROS-positive HCs decreased by 73.55% compared to gentamicin group. The gentamicin + CoPPIX + ZnPPIX group exhibited more ROS-positive HCs than the gentamicin + CoPPIX group. ROS were seldom found in the control, CoPPIX and ZnPPIX groups ($^{**}P < 0.01$ and $^{*}P < 0.05$, $n = 3$) (**Figures 5A,B**).

Gentamicin Induced Heme Oxygenase-1 Activation via Nrf2 Signaling

To further investigate the pathway, through which gentamicin up-regulated HO-1, Nrf2 inhibitor ML385 was used. In the experiment, the organs of Corti were randomly divided into four groups: the control group, the gentamicin group, the ML385 group only received ML385 (15 μM), and the gentamicin + ML385 group. Immunoblot showed a significant increase in Nrf2 and HO-1 levels after 0.6 mM gentamicin. Nrf2 and HO-1 levels were not suppressed significantly in the organs of Corti following treatment with Nrf2 inhibitors ML385. However, compared with the gentamicin group, ML385 inhibited both Nrf2 and HO-1 induced by gentamicin ($^{***}P < 0.001$ and $^{*}P < 0.05$, $n = 4$) (**Figures 6A,B**). Immunofluorescence staining revealed that the ML385 + gentamicin group exhibited more ROS-positive HCs than the gentamicin group. ROS were seldom found in the control and ML385 groups ($^{***}P < 0.001$, $n = 3$) (**Figures 6C,D**). These suggested that disrupting Nrf2 activity prevents the upregulation of HO-1 and the protection after gentamicin treatment.

Heme Oxygenase-1 Induction Increased the Expression of Nrf2

Nrf2 transcriptionally activates several antioxidant genes, including NAD(P)H: quinone oxidoreductase 1 (NQO1) and gamma- glutamate cysteine ligase catalytic subunit (GCLC). mRNA levels of HO-1, Nrf2, and Nrf2 target genes were analyzed by qPCR. CoPPIX treatment of the organs of Corti remarkably up-regulated HO-1 mRNA expression. Further, mRNA levels of Nrf2, NQO1 and GCLC increased in response to CoPPIX treatment ($^{***}P < 0.001$, $^{*}P < 0.05$, $n = 3$) (**Figure 7A**). CoPPIX and ZnPPIX treatment of the organs of Corti for 12 h were analyzed for HO-1 and Nrf2 proteins by Western blot. In the nucleus, two HO-1 immunoreactive bands were observed upon Western analysis, with one band migrating at 28 kDa and the other migrating at 32 kDa. In the nucleus CoPPIX treatment of the organs of Corti, 32 kDa HO-1 and 28 kDa HO-1 were up-regulated at the same time. ZnPPIX treatment inhibited 28 kDa

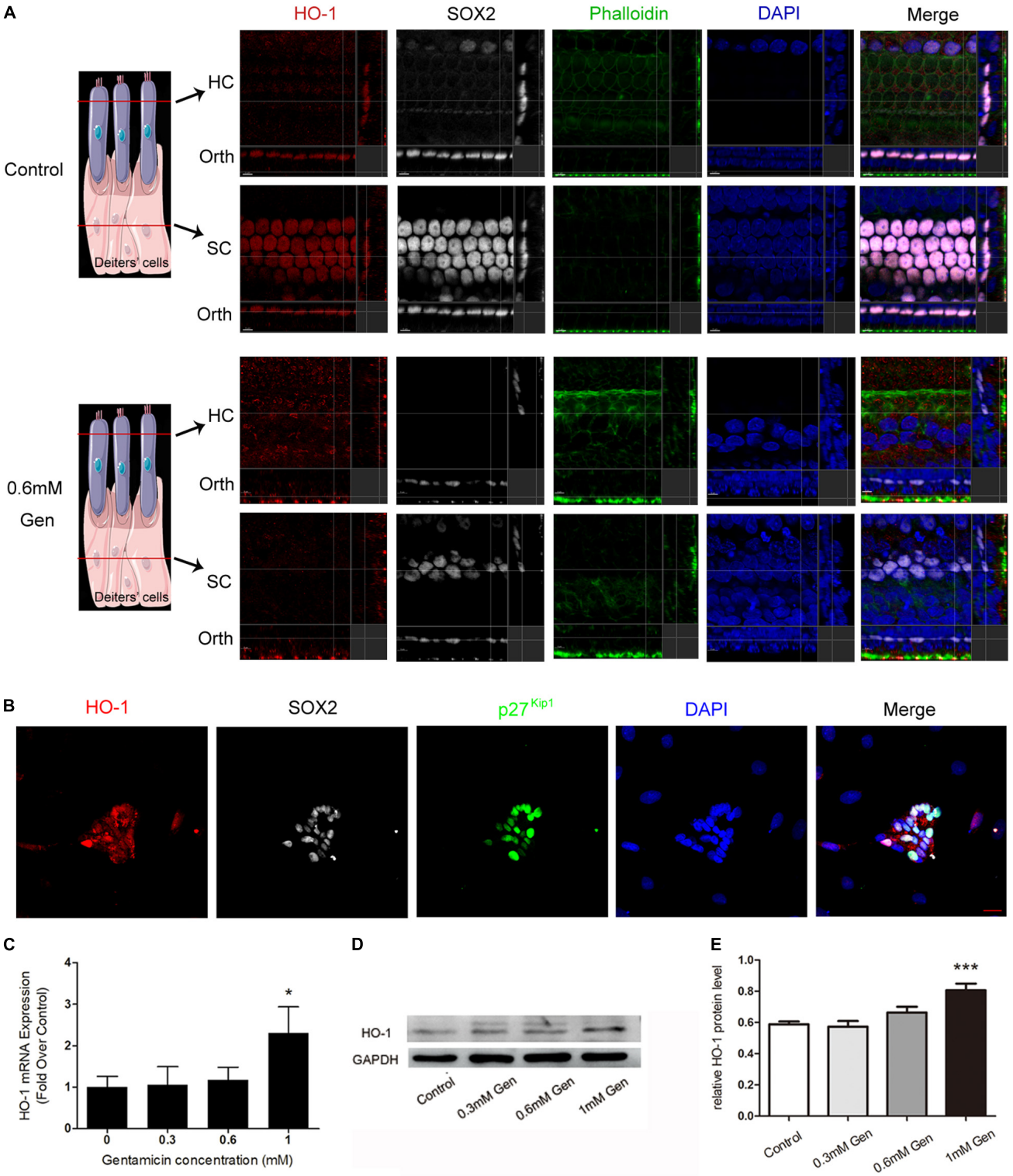

FIGURE 3 | Verification of heme oxygenase-1 (HO-1) expression. **(A)** The localization of HO-1 (red), phalloidin (green), SOX2 (white), and DAPI (blue) before and after gentamicin (0.6 mM) treatment. The schematic showed the location of each panel. The upper panels show confocal images taken at the level of the hair cell cuticular plates; the lower panels show confocal images from the same field taken at the level of the supporting cell plates. Scale bar = 7 μm. Orth, orthogonal. **(B)** Micrographs depicting immunostaining for HO-1 in SCs without gentamicin *in vitro*. Scale bar = 20 μm. **(C)** The mRNA levels of HO-1 in the organs of Corti cultured separately in media containing different concentrations of gentamicin (*$P < 0.05$, $n = 3$). **(D)** Immunoblot detection of HO-1 in the organs of Corti at different gentamicin concentrations. **(E)** The signal of HO-1 (from D) quantitated after normalization to GAPDH and represented in bar diagrams (***$P < 0.001$, $n = 3$).

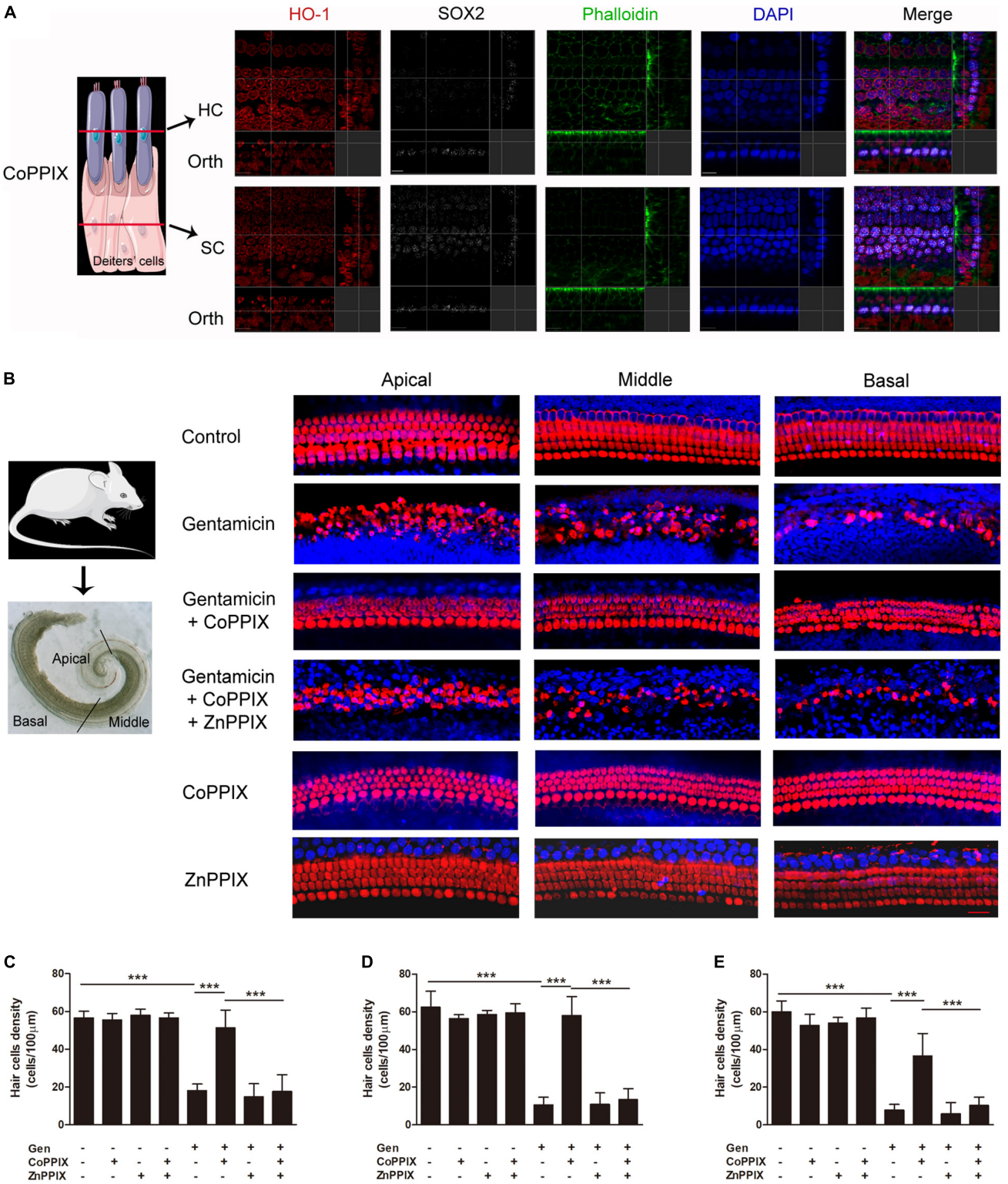

FIGURE 4 | Heme oxygenase-1 (HO-1) activation inhibited gentamicin-associated hair cell death. **(A)** The localization of HO-1 (red), phalloidin (green), SOX2 (white), and DAPI (blue) after CoPPIX treatment. The schematic showed the location of each panel. The upper panels show confocal images taken at the level of the hair cell cuticular plates; the lower panels show confocal images from the same field taken at the level of the supporting cell plates. Scale bar = 7 μm. Orth, orthogonal. **(B)** Representative micrographs of immunofluorescent staining. Myosin VII-a was the marker of inner and outer HCs (red). Scale bar = 20 μm. **(C–E)** Amounts of surviving HCs in various groups upon gentamicin-induced damage in the apical, middle, and basal turns (***$P < 0.001$, $n = 5$).

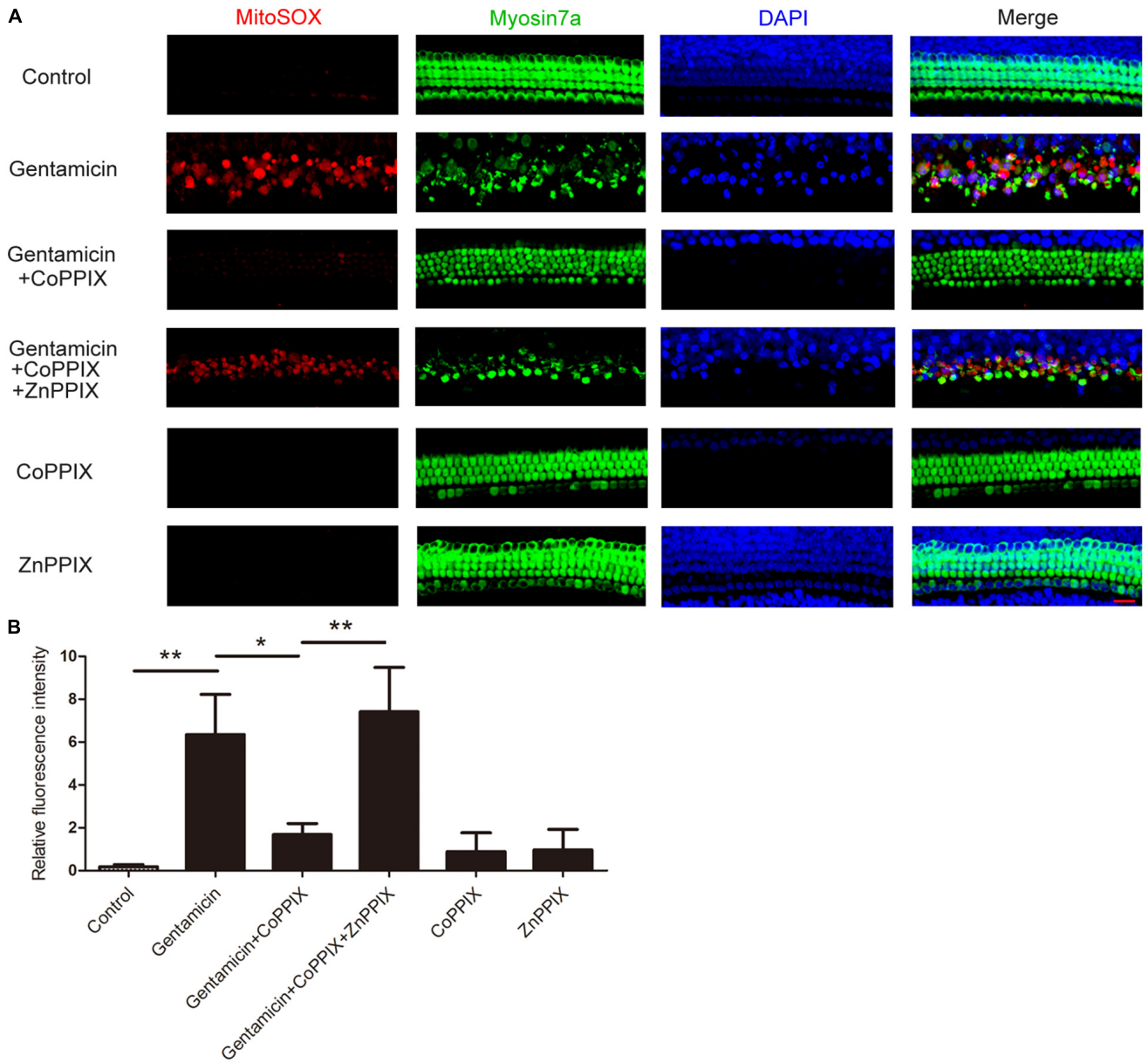

FIGURE 5 | Induction of heme oxygenase-1 (HO-1) by CoPPIX reduces intracellular reactive oxygen species (ROS) levels, and ZnPPIX increases intracellular ROS levels. **(A)** Representative micrographs showing MitoSOX Red immunostaining. The organs of Corti were pretreated with CoPPIX (5 μM) in the presence or absence of ZnPPIX (20 μM) for 12 h and then further incubated with 0.6mM gentamicin for 24 h. Scale bar = 20 μm. **(B)** Quantification of relative fluorescence intensities of ROS in each group (*$P < 0.05$ and **$P < 0.01$, $n = 3$).

HO-1 but not 32 kDa HO-1 compared with the control group. There were no significant changes in nuclear Nrf2 whether CoPPIX or ZnPPIX treatment. After CoPPIX treatment, HO-1 in the cytoplasm appeared a band at 32 kDa and a faint band at 28 kDa, which was accompanied with a simultaneous increase of Nrf2. ZnPPIX treatment inhibited 32 kDa HO-1 in the cytoplasm significantly. However, neither 28 kDa HO-1 nor Nrf2 has changed significantly after ZnPPIX treatment (*$P < 0.05$, **$P < 0.01$, $n = 3$) (**Figures 7B,C**). Immunofluorescence staining of HEI-OC1 cells verified that the expression of Nrf2 was induced by the HO-1 induction. In addition, Nrf2 was mainly accumulated in the cytoplasm (**Figure 7D**). These data suggested that HO-1 may modulate the accumulation of Nrf2.

DISCUSSION

Reactive oxygen species formation is one of the key mediators of aminoglycoside-induced HC death (He et al., 2017, 2020). Gentamicin generates free radicals within the inner ear, including

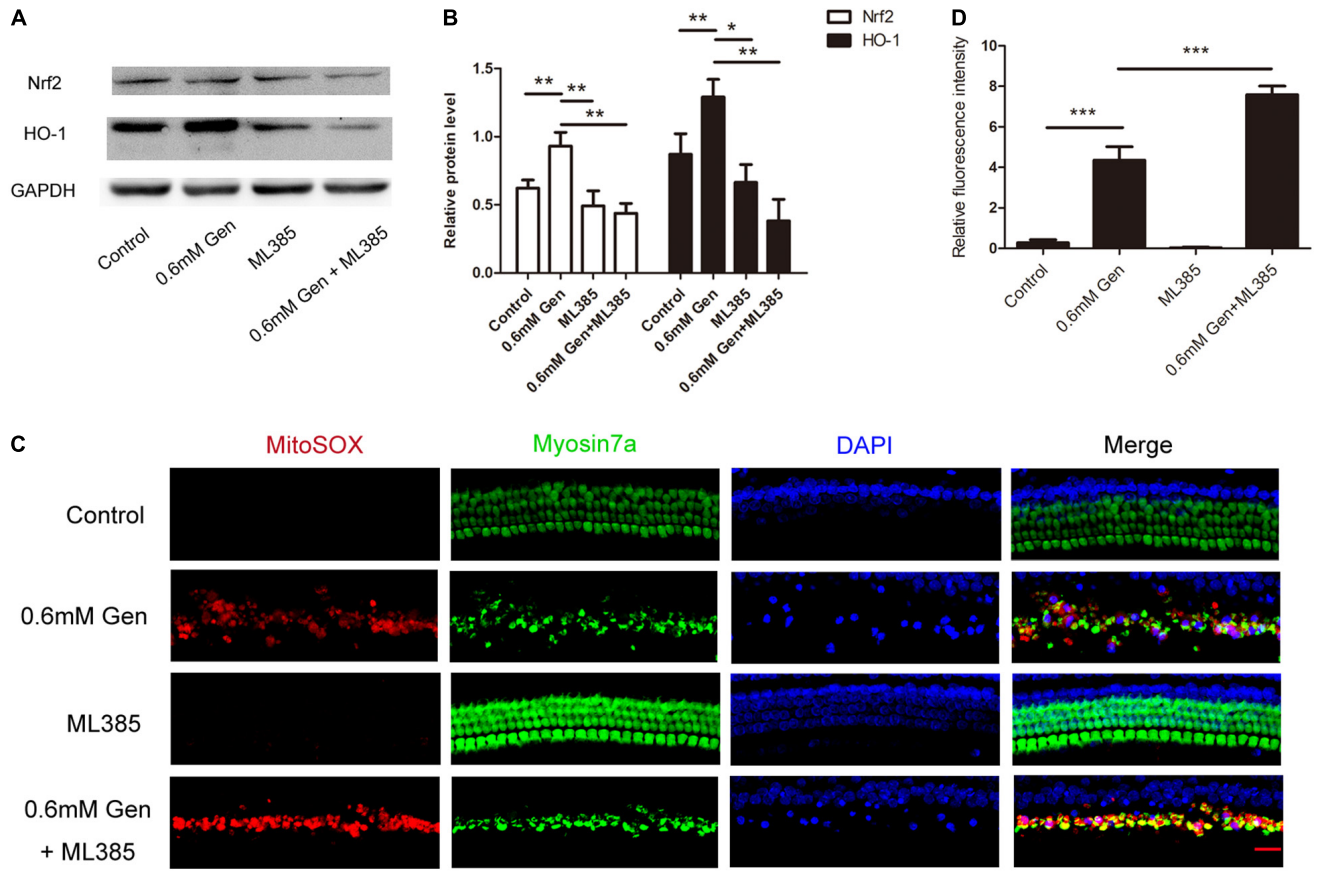

FIGURE 6 | Gentamicin induced heme oxygenase-1 (HO-1) activation via Nrf2 signaling. **(A)** The level of Nrf2 and HO-1 expression was determined by Western blot in different groups at 24 h after culture. **(B)** The signal of Nrf2 and HO-1 [from **(A)**] quantitated after normalization to β- actin and represented in bar diagrams (*$P < 0.05$, **$P < 0.01$, ***$P < 0.001$, $n = 4$). **(C)** Representative micrographs showing MitoSOX Red immunostaining in different groups. **(D)** Quantification of relative fluorescence intensities of reactive oxygen species (ROS) in each group (***$P < 0.001$, $n = 3$).

the highly reactive hydroxyl radical and lipid peroxidation products (Sha and Schacht, 1999). Previous reports have also revealed that antioxidants may prevent gentamicin-induced cochlear damage involving ROS (Niwa et al., 2016). The present study assessed the expression of oxidative damage-related genes as well as the mechanism of drug ototoxicity. We examined oxidative damage-related genes after gentamicin treatment for 24 h, the late stage of redox reactions. Our results revealed that HO-1 levels on the organs of Corti after gentamicin treatment increased 6.99 times ($p < 0.05$) compared to control values. In addition, we also found that HO-1 interacted with the other eight genes (Mb, Ncf1, Apoe, Nos2, Pstgs2, Gpx6, Srxn1, Ccl5). Based on this, we speculated that HO-1 played a role in gentamicin injury.

Our study showed that HO-1 slightly expressed in the inner and outer HCs and SCs in normal rat cochlea. After gentamicin treatment, HO-1 significantly decreased in SCs, while it increased in the inner and outer HCs. Compared with the control group, CoPPIX induced an increase in the expression of HO-1 mainly in HCs. Fairfield et al. (2004) found a constitutive but limited production of HO-1 in the outer HCs of normal rat cochlea. Furthermore, the expression of HO-1 significantly increased after hyperthermia, being selectively localized in all three rows of outer HCs in the organ of Corti as well as in marginal and intermediate cells of stria vascularis (Fairfield et al., 2004). Previous studies have reported on supporting cells as critical determinants of whether a hair cell under stress ultimately lives or dies (May et al., 2013). Yet, the mechanisms through which hair cells send stress signals and supporting cells sense and respond to these signals remain unclear.

In this study, we found that the induction of HO-1 by CoPPIX inhibited ROS production and reduced the damage of gentamicin to HCs. These findings suggested that HO-1 induction by CoPPIX might contribute to HC protection against gentamicin-induced damage. Recent evidence also suggested that HO-1 was essential in modulating antioxidant effects in other tissues (Shalaby et al., 2019; Niu et al., 2020). Park et al. (2017) found that in the cochlear tissue, a peroxisome proliferator-activated receptor (PPAR) inducer protected HCs from gentamicin-induced toxicity by increasing the expression of HO-1. Based on previous studies, herein, we focused on the location of the up-regulated expression of HO-1 after gentamicin and the signal

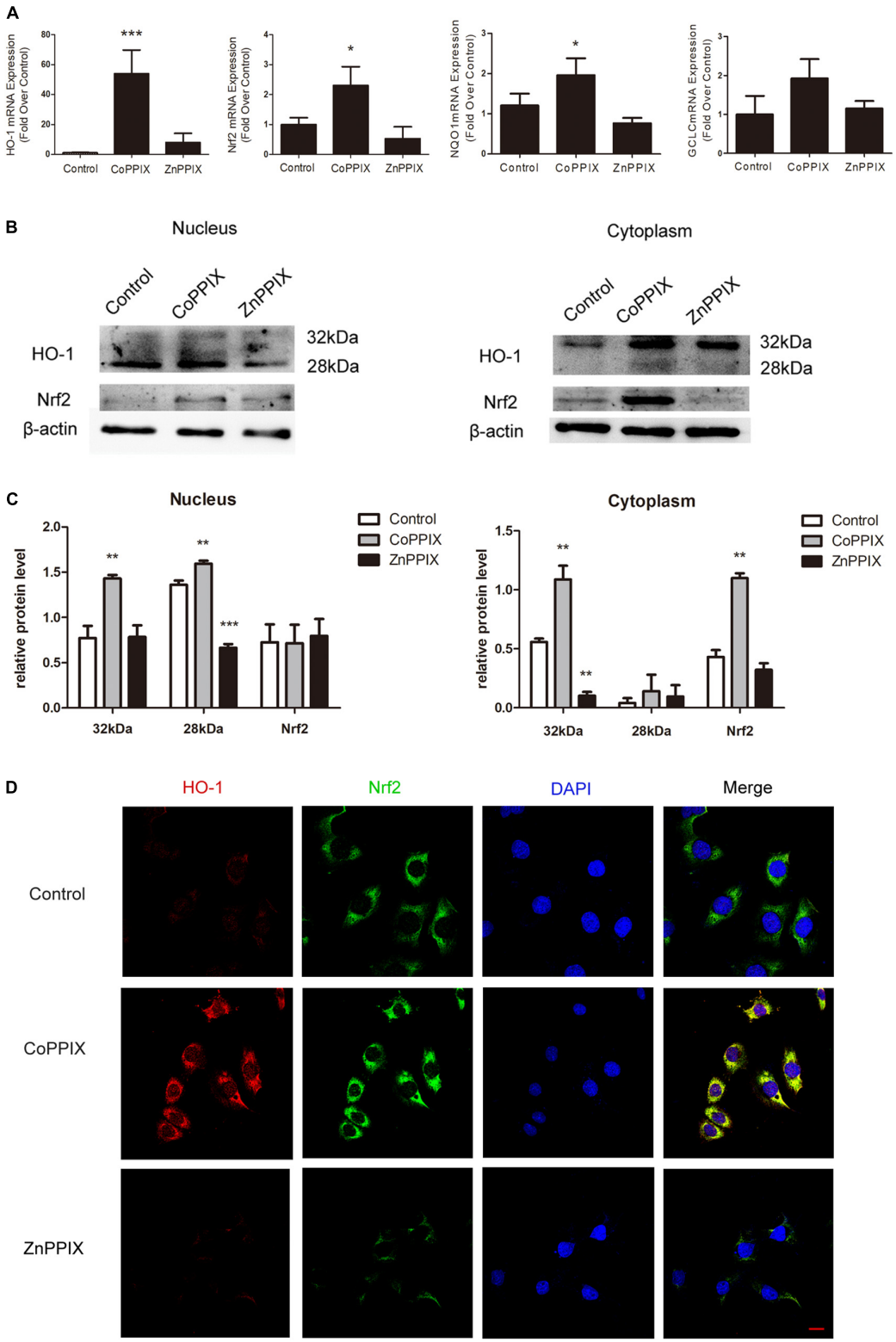

FIGURE 7 | Heme oxygenase-1 (HO-1) induction increased the expression of Nrf2. **(A)** The mRNA levels of HO-1, Nrf2, NQO1, and GCLC in the organs of Corti incubated with CoPPIX or ZnPPIX for 12 h (*$P < 0.05$, ***$P < 0.001$, $n = 3$). **(B)** The level of HO-1 and Nrf2 expression were determined by Western blot in the nuclear and cytoplasmic fractions of the organs of Corti incubated with CoPPIX or ZnPPIX for 12 h. **(C)** The signal of HO-1 and Nrf2 [from **(B)**] quantitated after normalization to β- actin and represented in bar diagrams (*$P < 0.05$, **$P < 0.01$, n = 3). **(D)** Immunofluorescence staining of HEI-OC1 in different groups. Scale bar = 20 μm.

pathway of HO-1. Therefore, specifically activating HO-1 gene expression by pharmacological regulation might constitute a new treatment target for gentamicin-related cochlear ototoxicity.

Our results revealed that while HO-1 was regulated by Nrf2, it could also promote the accumulation of Nrf2. HO-1 can prevent the damage of gentamicin by mutually regulating Nrf2. Nrf2/HO-1 is a classic signaling pathway in antioxidant reactions. Under oxidative stress conditions, the transcription factor Nrf2 undergoes nuclear translocation and regulates the expression of corresponding downstream genes, thus reducing oxidative stress (Fetoni et al., 2015; Ni et al., 2017). Up-regulation of Nrf2/HO-1 signaling alleviates gentamicin-induced nephrotoxicity (Subramanian et al., 2014; He et al., 2015). Celastrol activates the Nrf2-transcription factor and induces HO-1, which inhibits pro-apoptotic JNK activation and HC death, possibly through the action of CO (Francis et al., 2011). Although it is well known that Nrf2 induces HO-1 leading to mitigation of oxidant stress, evidence proves that nuclear isoform of HO-1 could also regulate Nrf2 activation by using hyperoxia exposure in mouse embryonic fibroblasts (MEFs) (Biswas et al., 2014). Our study found that there were two HO-1 immunoreactive bands in whole cell lysates upon Western analysis. Same as 32 kDa HO-1, the expression of 28 kDa HO-1 increases with the increase of gentamicin dose. Our study suggested that the 32 kDa isoform constitutively was predominant in the cytoplasm, whereas, the 28 kDa HO-1 was primarily localized to the nucleus. Different from the results of Biswas, we found that the Nrf2 up-regulated by 32 kDa HO-1 in the cytoplasm, not in the nucleus. Participation of various signaling pathways has been implicated in Nrf2 transcription. Accumulation and nucleocytoplasmic trafficking of Nrf2 may be affected by phosphorylation. GSK3β, a kinase that sensitizes cells for cell death, can phosphorylate and activate Fyn kinase, leading to phosphorylation, nuclear exclusion and accumulation in the cytoplasm of Nrf2 protein (Salazar et al., 2006). In addition, CoPPIX is a potent inducer of HO-1. Many data indicated that CoPPIX had a significant induction of HO-1 and the induction of HO-1 played a protective role in other system diseases (Chora et al., 2007; Song et al., 2018). However, it is not clear whether COPPIX only upregulates HO-1, but not other proteins, which causes the upregulation of Nrf2. The fact that HO-1 regulates the accumulation of Nrf2 in the cytoplasm still needs further verification.

CONCLUSION

Gentamicin-associated HC death represents a complex process involving the changes in protein expression of different cell types as well as the signaling pathways in HCs. In this study, we found that HO-1 protects HCs from gentamicin by up-regulating its expression in HCs and interacting with Nrf2 to inhibit ROS. Our results also suggest that HO-1 could be considered as a candidate target for designing regimens to efficiently prevent gentamicin-associated hearing loss. In the next step, we plan to use new technologies such as hydrogels and nanoparticles to deliver CoPPIX to the inner ear so as to study the protective effect of HO-1 on gentamicin-induced hearing loss *in vivo*.

DATA AVAILABILITY STATEMENT

The original contributions presented in the study are included in the article/**Supplementary Material**, further inquiries can be directed to the corresponding author/s.

ETHICS STATEMENT

The animal study was reviewed and approved by Air Force Military Medical University.

AUTHOR CONTRIBUTIONS

YY: conceptualization, investigation, methodology, validation, data curation, and writing—original draft. XC: methodology and writing—original draft. KYT: methodology and software. CYT: methodology and picture processing. LYC: data curation. WJM: picture processing and software. QL: writing—reviewing and editing. JHQ: conceptualization and writing—reviewing and editing. YL: methodology, project administration, and funding acquisition. DJZ: conceptualization, writing—reviewing and editing, and funding acquisition. All authors contributed to the article and approved the submitted version.

FUNDING

This work was supported by the National Key R&D Program (grant number 2020YFC200520); National Natural Science Foundation of China (grant numbers 81870732, 81670924, 82171161, and 82000978); Key Science and Technique Programs in Shaanxi Province (grant number 2018PT-01); National Key R&D Program (grant number 2019YFB1311605); Major Clinical Technology Innovation Project of Xijing Hospital (grant number XJZT19Z21); and Xijing Boost-Advanced Discipline Construction Project (grant numbers XJZT14X07, XJZT18X23, and XJZT19X27).

ACKNOWLEDGMENTS

We would like to thank all of our subjects for their dedicated and diligent participation. Thanks to the State Key Laboratory of Military Stomatology of the Fourth Military Medical University for providing the experimental equipment. Our deepest gratitude goes to the editor and reviewers for their careful work and thoughtful suggestions that have helped improve this manuscript substantially.

SUPPLEMENTARY MATERIAL

The Supplementary Material for this article can be found online at: https://www.frontiersin.org/articles/10.3389/fncel.2022.783346/full#supplementary-material

REFERENCES

Alam, M. B., Chowdhury, N. S., Sohrab, M. H., Rana, M. S., Hasan, C. M., and Lee, S.-H. (2020). Cerevisterol Alleviates Inflammation via Suppression of MAPK/NF-κB/AP-1 and Activation of the Nrf2/HO-1 Signaling Cascade. *Biomolecules* 10:199. doi: 10.3390/biom10020199

Biswas, C., Shah, N., Muthu, M., La, P., Fernando, A. P., Sengupta, S., et al. (2014). Nuclear Heme Oxygenase-1 (HO-1) Modulates Subcellular Distribution and Activation of Nrf2, Impacting Metabolic and Anti-oxidant Defenses. *J. Biol. Chem.* 289:26882. doi: 10.1074/jbc.M114.567685

Chan Kwon, Y., Sik Kim, H., and Lee, B.-M. (2020). Detoxifying effects of optimal hyperoxia (40% oxygenation) exposure on benzo[a]pyrene-induced toxicity in human keratinocytes. *J. Toxicol. Environ. Health A* 83, 82–94. doi: 10.1080/15287394.2020.1730083

Cheng, Y., and Rong, J. (2017). Therapeutic Potential of Heme Oxygenase-1/carbon Monoxide System Against Ischemia-Reperfusion Injury. *Curr. Pharm. Des.* 23, 3884–3898. doi: 10.2174/1381612823666170413122439

Chora, A. A., Fontoura, P., and Cunha, A. (2007). Heme oxygenase–1 and carbon monoxide suppress autoimmune neuroinflammation. *J. Clin. Invest.* 117:438. doi: 10.1172/JCI28844

Fairfield, D. A., Kanicki, A. C., Lomax, M. I., and Altschuler, R. A. (2004). Induction of heat shock protein 32 (Hsp32) in the rat cochlea following hyperthermia. *Hear. Res.* 188, 1–11. doi: 10.1016/S0378-5955(03)00369-1

Ferrandiz, M., and Devesa, I. (2008). Inducers of Heme Oxygenase-1. *Curr. Pharm. Des.* 14, 473–86. doi: 10.2174/138161208783597399

Fetoni, A. R., Paciello, F., Rolesi, R., Eramo, S. L. M., Mancuso, C., Troiani, D., et al. (2015). Rosmarinic acid up-regulates the noise-activated Nrf2/HO-1 pathway and protects against noise-induced injury in rat cochlea. *Free Radic. Biol. Med.* 85, 269–281. doi: 10.1016/j.freeradbiomed.2015.04.021

Fettiplace, R. (2017). Hair Cell Transduction, Tuning, and Synaptic Transmission in the Mammalian Cochlea. *Compr. Physiol.* 7, 1197–1227. doi: 10.1002/cphy.c160049

Fontecha-Barriuso, M., Martín-Sanchez, D., Martinez-Moreno, J. M., Cardenas-Villacres, D., Carrasco, S., Sanchez-Niño, M. D., et al. (2020). Molecular pathways driving omeprazole nephrotoxicity. *Redox Biol.* 32:101464. doi: 10.1016/j.redox.2020.101464

Francis, S. P., Kramarenko, I. I., Brandon, C. S., Lee, F. S., Baker, T. G., and Cunningham, L. L. (2011). Celastrol inhibits aminoglycoside-induced ototoxicity via heat shock protein 32. *Cell Death Dis.* 2:e195. doi: 10.1038/cddis.2011.76

Fujimoto, C., and Yamasoba, T. (2019). Mitochondria-Targeted Antioxidants for Treatment of Hearing Loss: a Systematic Review. *Antioxidants* 8:109. doi: 10.3390/antiox8040109

Guo, J., Chai, R., Li, H., and Sun, S. (2019). Protection of Hair Cells from Ototoxic Drug-Induced Hearing Loss. *Adv. Exp. Med. Biol.* 5:115. doi: 10.1007/978-981-13-6123-4_2

Han, S., Du, Z., Liu, K., and Gong, S. (2020). Nicotinamide riboside protects noise-induced hearing loss by recovering the hair cell ribbon synapses. *Neuroence. Lett.* 725:134910. doi: 10.1016/j.neulet.2020.134910

He, L., Peng, X., Zhu, J., Liu, G., Chen, X., Tang, C., et al. (2015). Protective effects of curcumin on acute gentamicin-induced nephrotoxicity in rats. *Can. J. Phys. Pharmacol.* 93, 275–282. doi: 10.1139/cjpp-2014-0459

He, Y., Li, W., Zheng, Z., Zhao, L., and Li, H. (2020). Inhibition of Protein arginine methyltransferase 6 reduces reactive oxygen species production and attenuates aminoglycoside- and cisplatin-induced hair cell death. *Theranostics* 10, 133–150. doi: 10.7150/thno.37362

He, Z., Guo, L., Shu, Y., Fang, Q., Zhou, H., Liu, Y., et al. (2017). Autophagy protects auditory hair cells against neomycin-induced damage. *Autophagy* 13, 1884–1904. doi: 10.1080/15548627.2017.1359449

He, Z., Zhang, S., Ma, D., Fang, Q., and Wang, J. (2019). HO-1 promotes resistance to an EZH2 inhibitor through the pRB-E2F pathway: correlation with the progression of myelodysplastic syndrome into acute myeloid leukemia. *J. Trans. Med.* 17:366. doi: 10.1186/s12967-019-2115-9

Hirao, H., Dery, K. J., Kageyama, S., Nakamura, K., and Kupiec-Weglinski, J. W. (2020). Heme Oxygenase-1 in liver transplant ischemia-reperfusion injury: from bench-to-bedside. *Free Radic. Biol. Med.* 157, 75–82. doi: 10.1016/j.freeradbiomed.2020.02.012

Kim, H. J., So, H. S., Lee, J. H., Lee, J. H., Park, C., Park, S. Y., et al. (2006). Heme oxygenase-1 attenuates the cisplatin-induced apoptosis of auditory cells via down-regulation of reactive oxygen species generation. *Free Radic. Biol. Med.* 40, 1810–1819. doi: 10.1016/j.freeradbiomed.2006.01.018

Kim, S. J., Ho Hur, J., Park, C., Kim, H. J., Oh, G. S., Lee, J. N., et al. (2015). Bucillamine prevents cisplatin-induced ototoxicity through induction of glutathione and antioxidant genes. *Exp. Mol. Med.* 47:e142. doi: 10.1038/emm.2014.112

Kirst, H. A., and Marinelli, F. (2014). "Aminoglycoside Antibiotics" In *Antimicrobials*. Eds F. Marinelli., O. Genilloud. (Heidelberg: Springer).

Lee, J., Jung, S. Y., Yang, K. J., Kim, Y., Lee, D., Lee, M. H., et al. (2019). α-Lipoic acid prevents against cisplatin cytotoxicity via activation of the NRF2/HO-1 antioxidant pathway. *PLoS One* 14:e0226769. doi: 10.1371/journal.pone.0226769

Lee, W., Kim, J., Park, E. K., and Bae, J.-S. (2020). Maslinic Acid Ameliorates Inflammation via the Downregulation of NF-κB and STAT-1. *Antioxidants* 9:106. doi: 10.3390/antiox9020106

Maines, M. D. (1988). Heme oxygenase: function, multiplicity, regulatory mechanisms, and clinical applications. *Faseb J.* 2, 2557–2568. doi: 10.1096/fasebj.2.10.3290025

May, L. A., Kramarenko, I. I., Brandon, C. S., Voelkel-Johnson, C., Roy, S., Truong, K., et al. (2013). Inner ear supporting cells protect hair cells by secreting HSP70. *J. Clin. Invest.* 123, 3577–3587. doi: 10.1172/JCI68480

Medina, M. V., Sapochnik, D., Sola, M. E. G., and Coso, O. A. (2019). Regulation of the Expression of Heme Oxygenase-1. Signal Transduction, Gene Promoter Activation and Beyond. *Antioxidants Redox Signal.* 32, 1033–1044. doi: 10.1089/ars.2019.7991

Ni, Y. H., Huo, L. J., and Li, T. T. (2017). Antioxidant axis Nrf2-keap1-ARE in inhibition of alcoholic liver fibrosis by IL-22. *World J. Gastroenterol.* 23, 2002–2011. doi: 10.3748/wjg.v23.i11.2002

Niu, T., Fu, G., Zhou, J., Han, H., Chen, J., Wu, W., et al. (2020). Floridoside Exhibits Antioxidant Properties by Activating HO-1 Expression via p38/ERK MAPK Pathway. *Mar. Drugs* 18:105. doi: 10.3390/md18020105

Niwa, K., Matsunobu, T., Kurioka, T., Kamide, D., Tamura, A., Tadokoro, S., et al. (2016). The beneficial effect of Hangesha-shin-to (TJ-014) in gentamicin-induced hair cell loss in the rat cochlea. *Auris. Nasus. Larynx.* 43, 507–513. doi: 10.1016/j.anl.2015.12.012

Pang, J., Xiong, H., Ou, Y., Yang, H., Xu, Y., Chen, S., et al. (2019). SIRT1 protects cochlear hair cell and delays age-related hearing loss via autophagy. *Neurobiol. Aging* 80, 127–137. doi: 10.1016/j.neurobiolaging.2019.04.003

Park, C., Ji, H. M., Kim, S. J., Kil, S. H., Lee, J. N., Kwak, S., et al. (2017). Fenofibrate exerts protective effects against gentamicin-induced toxicity in cochlear hair cells by activating antioxidant enzymes. *Int. J. Mol. Med.* 39, 960–968. doi: 10.3892/ijmm.2017.2916

Pyun, J. H., Kang, S. U., and Hwang, H. S. (2011). Epicatechin inhibits radiation-induced auditory cell death by suppression of reactive oxygen species generation. *Neuroscience* 199, 410–420. doi: 10.1016/j.neuroscience.2011.09.012

Quan, Y., Xia, L., Shao, J., Yin, S., Cheng, C. Y., Xia, W., et al. (2015). Adjudin protects rodent cochlear hair cells against gentamicin ototoxicity via the SIRT3-ROS pathway. *Sci. Rep.* 5, 8181. doi: 10.1038/srep08181

Salazar, M., Rojo, A. I., Velasco, D., de Sagarra, R. M., and Cuadrado, A. (2006). Glycogen Synthase Kinase-3β Inhibits the Xenobiotic and Antioxidant Cell Response by Direct Phosphorylation and Nuclear Exclusion of the Transcription Factor Nrf2. *J. Biol. Chem.* 281, 14841–14851. doi: 10.1074/jbc.M513737200

Sha, S. H., and Schacht, J. (1999). Formation of reactive oxygen species following bioactivation of gentamicin. *Free Radic. Biol. Med.* 26, 341–347. doi: 10.1016/s0891-5849(98)00207-x

Shalaby, Y. M., Menze, E. T., Azab, S. S., and Awad, A. S. (2019). Involvement of Nrf2/HO-1 antioxidant signaling and NF-κB inflammatory response in the potential protective effects of vincamine against methotrexate-induced

nephrotoxicity in rats: cross talk between nephrotoxicity and neurotoxicity. *Arch. Toxicol.* 93, 1417–1431. doi: 10.1007/s00204-019-02429-2

Song, Y. J., Dai, C. X., Li, M., Cui, M. M., Ding, X., Zhao, X. F., et al. (2018). The potential role of HO-1 in regulating the MLK3-MKK7-JNK3 module scaffolded by JIP1 during cerebral ischemia/reperfusion in rats. *Behav. Brain Res.* 359, 528–535. doi: 10.1016/j.bbr.2018.11.003

Subramanian, P., Anandan, R., Jayapalan, J. J., and Hashim, O. H. (2014). Hesperidin protects gentamicin-induced nephrotoxicity via Nrf2/HO-1 signaling and inhibits inflammation mediated by NF-κB in rats. *J. Funct. Foods* 13, 89–99. doi: 10.1016/j.jff.2014.12.035

Sun, C., Yao, Y., Zhang, C., Tong, D., and Xie, B. (2019). EPO Attenuates Cisplatin-Induced Ototoxicity in HEI-OC1 Auditory Cell Via the Nrf2-ARE Signaling Pathway. *Otol. Neurotol.* 40, 965–971. doi: 10.1097/MAO.0000000000002288

Tian, Y., Song, H., Jin, D., Hu, N., and Sun, L. (2020). MST1-Hippo pathway regulates inflammation response following myocardial infarction through inhibiting HO-1 signaling pathway. *J. Recept. Signal. Transduct. Res.* 40, 231–236. doi: 10.1080/10799893.2020.1726954

WenWei, L., XinWei, W., Rui, M., FangLu, C., Ping, C., Ning, C., et al. (2018). Junctional E-cadherin/p120-catenin Is Correlated with the Absence of Supporting Cells to Hair Cells Conversion in Postnatal Mice Cochleae. *Front. Mol. Neurosci.* 11:20. doi: 10.3389/fnmol.2018.00020

Wong, R. J., Vreman, H. J., Schulz, S., Kalish, F. S., Pierce, N. W., and Stevenson, D. K. (2011). In vitro inhibition of heme oxygenase isoenzymes by metalloporphyrins. *J. Perinatol.* 31:S35. doi: 10.1038/jp.2010.173

Yi, Z. W., Xia, Y. J., Liu, X. F., Wang, G. Q., Xiong, Z. Q., and Ai, L. Z. (2020). Antrodin A from mycelium of Antrodia camphorata alleviates acute alcoholic liver injury and modulates intestinal flora dysbiosis in mice. *J. Ethnopharmacol.* 254:112681. doi: 10.1016/j.jep.2020.112681

Zhou, M., Sun, G., Zhang, L., Zhang, G., Yang, Q., Yin, H., et al. (2018). STK33 alleviates gentamicin-induced ototoxicity in cochlear hair cells and House Ear Institute-Organ of Corti 1 cells. *J. Cell Mol. Med.* 22, 5286–5299. doi: 10.1111/jcmm.13792

Conflict of Interest: LC was employed by Smartgenomics Technology Institute.

The remaining authors declare that the research was conducted in the absence of any commercial or financial relationships that could be construed as a potential conflict of interest.

Publisher's Note: All claims expressed in this article are solely those of the authors and do not necessarily represent those of their affiliated organizations, or those of the publisher, the editors and the reviewers. Any product that may be evaluated in this article, or claim that may be made by its manufacturer, is not guaranteed or endorsed by the publisher.

frontiers | Frontiers in Cellular Neuroscience

REVIEW
published: 15 June 2022
doi: 10.3389/fncel.2022.900725

UPR Responsive Genes *Manf* and *Xbp1* in Stroke

Helike Lõhelaid[1], Jenni E. Anttila[2,3], Hock-Kean Liew[4], Kuan-Yin Tseng[5], Jaakko Teppo[6], Vassilis Stratoulias[1] and Mikko Airavaara[1,2]**

[1] HiLIFE – Neuroscience Center, University of Helsinki, Helsinki, Finland, [2] Drug Research Program, Division of Pharmacology and Pharmacotherapy, Faculty of Pharmacy, University of Helsinki, Helsinki, Finland, [3] Individualized Drug Therapy Research Program, Faculty of Medicine, University of Helsinki, Helsinki, Finland, [4] Department of Medical Research, Hualien Tzu Chi Hospital, Buddhist Tzu Chi Medical Foundation, Hualien City, Taiwan, [5] Department of Neurological Surgery, Tri-Service General Hospital, National Defense Medical Center, Taipei, Taiwan, [6] Drug Research Program, Division of Pharmaceutical Chemistry and Technology, Faculty of Pharmacy, University of Helsinki, Helsinki, Finland

Stroke is a devastating medical condition with no treatment to hasten recovery. Its abrupt nature results in cataclysmic changes in the affected tissues. Resident cells fail to cope with the cellular stress resulting in massive cell death, which cannot be endogenously repaired. A potential strategy to improve stroke outcomes is to boost endogenous pro-survival pathways. The unfolded protein response (UPR), an evolutionarily conserved stress response, provides a promising opportunity to ameliorate the survival of stressed cells. Recent studies from us and others have pointed toward mesencephalic astrocyte-derived neurotrophic factor (MANF) being a UPR responsive gene with an active role in maintaining proteostasis. Its pro-survival effects have been demonstrated in several disease models such as diabetes, neurodegeneration, and stroke. MANF has an ER-signal peptide and an ER-retention signal; it is secreted by ER calcium depletion and exits cells upon cell death. Although its functions remain elusive, conducted experiments suggest that the endogenous MANF in the ER lumen and exogenously administered MANF protein have different mechanisms of action. Here, we will revisit recent and older bodies of literature aiming to delineate the expression profile of MANF. We will focus on its neuroprotective roles in regulating neurogenesis and inflammation upon post-stroke administration. At the same time, we will investigate commonalities and differences with another UPR responsive gene, X-box binding protein 1 (XBP1), which has recently been associated with MANF's function. This will be the first systematic comparison of these two UPR responsive genes aiming at revealing previously uncovered associations between them. Overall, understanding the mode of action of these UPR responsive genes could provide novel approaches to promote cell survival.

Keywords: ARMET, CDNF, ER stress, IRE1, mesencephalic astrocyte-derived neurotrophic factor, unfolded protein response, XBP1

OPEN ACCESS

Edited by:
Wei Yang,
Duke University Medical Center, United States

Reviewed by:
Miguel Angel Burguillos, University of Seville, Spain
Yuntian Shen, Nantong University, China

****Correspondence:***
Helike Lõhelaid
helike.lohelaid@helsinki.fi
Mikko Airavaara
mikko.airavaara@helsinki.fi

Specialty section:
This article was submitted to Cellular Neuropathology, a section of the journal Frontiers in Cellular Neuroscience

Received: *21 March 2022*
Accepted: *02 May 2022*
Published: *15 June 2022*

Citation:
Lõhelaid H, Anttila JE, Liew H-K, Tseng K-Y, Teppo J, Stratoulias V and Airavaara M (2022) UPR Responsive Genes Manf and Xbp1 in Stroke. Front. Cell. Neurosci. 16:900725. doi: 10.3389/fncel.2022.900725

INTRODUCTION: STROKE, MANF, AND UPR

Stroke is the second leading cause of death worldwide and the third leading cause of death and disability combined (Collaborators, 2021). Cerebral ischemic stroke is caused by local thrombosis or embolism leading to a lack of blood supply to a focal area of the brain. Globally, 62% of all new strokes are estimated to be ischemic (Collaborators, 2021). Hemorrhagic stroke encompasses

the rest of stroke cases, caused by either intracerebral or subarachnoid hemorrhage. Risk factors for stroke include age, arterial atherosclerosis, cardiac diseases, hypertension, diabetes, obesity, smoking, low physical activity, and unhealthy diet. Current treatment practice for ischemic stroke includes reperfusion therapies, which involve the usage of thrombolytic tissue plasminogen activator (tPA) or endovascular thrombectomy (Campbell et al., 2019). However, new treatment strategies are needed, as the recovery from stroke is often incomplete, and there is no drug therapy that could promote the functional recovery of stroke survivors.

Mesencephalic astrocyte-derived neurotrophic factor (MANF) has been originally described as a neurotrophic factor (Petrova et al., 2003) but has subsequently been found to be an important regulator of endoplasmic reticulum (ER) lumen homeostasis (Lindahl et al., 2014) and to have a protective effect on ischemic stroke outcome (Airavaara et al., 2009). The main function of the ER lumen is to maintain protein homeostasis, e.g., folding and quality control of secretory proteins, extracellular matrix proteins, plasma membrane proteins, and ER luminal proteins. There are many excellent reviews on unfolded protein response (UPR) (Hetz et al., 2011, 2020; Walter and Ron, 2011), which is an essential part of maintaining ER lumen and cell homeostasis. The signaling of UPR occurs through three ER transmembrane receptor pathways, inositol-requiring enzyme 1 (IRE1), protein kinase RNA-like ER kinase (PERK), and activating transcription factor 6 (ATF6). Disturbances in ER homeostasis are followed by functional deficits in the cell. If unfolded proteins accumulate in the ER lumen, the IRE1, PERK, and ATF6 pathways signal to the nucleus to induce the transcription-translation of proteins required to handle and/or reduce a load of misfolded proteins to overcome the stressful event, leading to cell survival. In addition, the modulation of ER-homeostasis *via* the IRE1/X-box binding protein 1 (XBP1) pathway leads to immune regulation (Hetz et al., 2011; Pramanik et al., 2018). In case of continuous and chronic ER stress, cell can undergo necroptosis or mitochondrial apoptosis (Iurlaro and Munoz-Pinedo, 2016). UPR can be activated by different mechanisms interfering with protein folding homeostasis such as changes in ER luminal Ca^{2+} concentration, energy or glucose depletion, lipid accumulation, and viruses (Foufelle and Fromenty, 2016). UPR can be pharmacologically induced, e.g., by thapsigargin, which depletes ER Ca^{2+}, or tunicamycin, which inhibits N-glycosylation of newly synthetized proteins, leading to accumulation of unfolded proteins. However, the physiological relevance of these pharmacological manipulations needs to be considered with caution. Moreover, the quantity of protein secretion is likely the critical factor in how detrimental chronic UPR is. It should be noted that in neurons, protein secretion quantity is rather small, but quality demand together with the structural complexity of cells can lead to detrimental effects of chronic UPR (Sree et al., 2021). An essential player in UPR regulation is GRP78/BiP, an ER resident chaperone importing nascent proteins from cytosol to the ER, which under normal conditions also binds to UPR receptors (Bertolotti et al., 2000; Kopp et al., 2019). GRP78 binding to unfolded proteins is ADP/ATP-dependent, and the activity of GRP78 as a chaperone is controlled by different cofactors (e.g., GRP170 (alias HYOU1) and ORP150) and SIL1 (Behnke et al., 2015). Interestingly, there is evidence that signaling *via* the IRE1/XBP1 and ATF6 pathways is protective in ischemic injury (Glembotski et al., 2019).

The primary focus of this review is to highlight the importance of the UPR and IRE1/XBP1 pathway in brain injuries and the potential of MANF as a therapeutic agent in stroke. We will focus on comparing the role of XBP1 and MANF in stroke and the function of MANF as a regulator of inflammation and neurogenesis.

MESENCEPHALIC ASTROCYTE-DERIVED NEUROTROPHIC FACTOR

MANF and cerebral dopamine neurotrophic factor (CDNF) are proteins with pleiotropic effects on various disease models (Lindahl et al., 2017; Albert and Airavaara, 2019; Jäntti and Harvey, 2020; Lindholm and Saarma, 2021) and form together a family of proteins (amino acid identity is 59%) (Lindholm et al., 2007). MANF was originally discovered and named ARMET (arginine-rich, mutated in early-stage tumor) (Shridhar et al., 1996) but was subsequently renamed MANF when the protein was first successfully isolated from a mesencephalic astrocyte cell line, and its neurotrophic properties were reported using dopaminergic neuronal cultures (Petrova et al., 2003). Since the initial *in vitro* studies that suggested selectivity for protecting dopaminergic neurons (Petrova et al., 2003), follow up studies have found very little activity when the MANF protein is applied into cell culture media (Hellman et al., 2011). Because MANF lacks the plasma membrane receptor – however, notice some binding to neuroplastin (Yagi et al., 2020) – one can argue how accurate the name neurotrophic factor is. Furthermore, MANF's very high mRNA expression levels in adult mouse brain and in various other secretory tissues suggest that it is not acting as a neurotrophic factor and definitely not as a growth factor (Zhang et al., 2014; Danilova et al., 2019b; Karlsson et al., 2021). Moreover, the part in MANF's name referring to mesencephalic astrocytes is not that accurate either, since *Manf* mRNA is expressed at very high levels in all cells (Lindholm et al., 2008; Zhang et al., 2014; Danilova et al., 2019b; Karlsson et al., 2021).

MANF is a small soluble protein (18–20 kDa) with a signal peptide targeting the protein into the ER lumen (Petrova et al., 2003; Mizobuchi et al., 2007). The MANF protein is comprised of two domains: N-terminal Saposin-like (Parkash et al., 2009) and the C-terminal SAP-like domain connected by a flexible linker region (Hellman et al., 2011; **Figure 1**). Other proteins with Saposin-like domain bind lipids and, indeed, the N-terminal domain of MANF have been shown to bind sulfatides (3-O-sulfogalactosylceramide) (Bai et al., 2018) that are enriched in myelin (Grassi et al., 2015). The structure of the C-terminal domain of MANF obtained by NMR was strikingly similar to the Ku70 C-terminal SAP-like domain. Ku70C and other similarly structured proteins bind DNA and

proteins (Hellman et al., 2011); however, the Ku70-related anti-apoptotic effect of MANF has not been detected. MANF has 8 cysteines and contains two CxxC-motifs, one per domain. Proteins with a CxxC-motif are abundant in the ER, e.g., reductases and protein disulfide isomerases (PDIs) that can help to fold proteins (Kersteen and Raines, 2003). Thus, the presence of an CxxC-motif in MANF could indicate a reductase or disulfide isomerase activity. This hypothesis has been tested several times with no evidence of PDI activity in MANF. Importantly, mutation of the C-terminal domain CxxC-motif (**Figure 1**) erases MANF's protective functions regardless of delivery method: the neuroprotective activity induced by gene therapy *in vitro* and with recombinant protein *in vivo* (Matlik et al., 2015). It should be noted that MANF's protective activity by gene therapy *in vitro* was abolished with the deletion of the C-terminal RTDL domain, but the protein was biologically active and showed protective effects on ischemic stroke *in vivo*. Thus, only the C-terminal CxxC is essential for the neuroprotective activity of MANF in ischemic stroke *in vivo* (Matlik et al., 2015) and antagonizes cell death (Božok et al., 2018).

Interestingly, MANF is an UPR activated gene (Tseng et al., 2017; Hartman et al., 2019; Jäntti and Harvey, 2020; Pakarinen et al., 2020, 2022). MANF works under reductive ER stress in the heart as well (Arrieta et al., 2020). Previous studies have shown that MANF interacts with ER-resident proteins: GRP78 (Glembotski et al., 2012), PDI6 (Bell et al., 2018) and CH60, KCRB, and PGAM (Eesmaa et al., 2021). The C-terminal domain of MANF was proposed to bind the N-terminal nucleotide-binding domain of GRP78 and to prolong the interaction of GRP78 with its "client" proteins by nucleotide exchange of GRP78 (Yan et al., 2019), indicating that the biological function of MANF in the ER lumen is to act as an ER lumen chaperone and to maintain ER homeostasis. However, MANF's interaction with GRP78 is not required for neuroprotective activity *in vitro* by gene therapy when microinjected as plasmid to the nucleus of the neuron (Eesmaa et al., 2021). How these results would relate to effects of the recombinant MANF protein without the ER signal sequence and the possibility to enter the ER lumen in animal models *in vivo* remains unclear and requires further studies.

MANF is an evolutionarily highly conserved protein found in many branches of life, from humans to sponges. The amino acid similarity of MANF between human and sponges is ∼50–59%, while the similarity to leech and octopus is ∼41 and 45%, respectively (**Figure 2**). Homology is selectively maintained because of structural or functional constraints, e.g., cysteines present in MANF are important for building disulfide bonds, which in turn is important for the function of the protein.

MANF expression is induced by ATF6 and XBP1 activation (Lee et al., 2003; Shaffer et al., 2004; Tadimalla et al., 2008). *Manf* expression was shown to be upregulated most efficiently by the transcription factor ATF6α and moderately by ATF6β and spliced XBP1 (XPB1s) in Neuro2a cells (Oh-Hashi et al., 2013). The *Manf* promoter sequence contains ERSE binding elements, and *Manf* was suggested to be induced upon ER stress *via* ER stress response element II (ERSE-II) (Mizobuchi et al., 2007). In a later study, XBP1s was found to induce MANF by binding ERSE-I in the *Manf* promoter region (Wang et al., 2018). MANF is involved in protein folding homeostasis in the ER and is able to restrict ER stress *in vivo* (Lindahl et al., 2014; Hartman et al., 2019). Still, the molecular mechanism of how the recombinant MANF protein facilitates neuroprotective effects *in vivo* remains unknown. However, immunomodulation may also play a role in mediating MANF's cytoprotective effects.

Under normal conditions, a major part of expressed MANF has been shown to localize in the ER by co-staining with ER-resident proteins Hrd1, PDI, and GRP78 (Mizobuchi et al., 2007; Apostolou et al., 2008; Tadimalla et al., 2008; Matlik et al., 2015) and only a small amount is secreted (Apostolou et al., 2008; Tadimalla et al., 2008; Henderson et al., 2013; **Figure 3**). However, MANF secretion is significantly enhanced upon ER Ca^{2+} depletion but not upon protein misfolding or alteration of ER redox status (Glembotski et al., 2012; Henderson et al., 2013), indicating ER stress *per se* is not a trigger for MANF secretion but ER Ca^{2+} depletion is needed (**Figure 3**). Extracellular levels of MANF also increase in response to cell death. In addition, the action and secretion of MANF could vary in different cells, as MANF (and CDNF) regulates ER homeostasis in a tissue-specific manner (Pakarinen et al., 2022).

While the exact mechanism for extracellular MANF is not fully resolved, it has become clear that ER-luminal MANF has an active role in maintaining ER lumen proteostasis (**Figure 3**). Therefore, it is not surprising that MANF is expressed widely in different tissues and is particularly highly expressed in metabolic and secretory tissues, such as those of the liver and pancreas, and in tissues related to the immune system, such as those of the bone marrow, and lymphoid tissues (Uhlen et al., 2015; Danilova et al., 2019b; Karlsson et al., 2021). The MANF protein is also found in circulating blood (Galli et al., 2016, 2019a,b; Wei et al., 2020; Wang et al., 2021c). In the brain, the MANF protein is expressed mainly in neurons under normal conditions (Lindholm et al., 2008; Tseng et al., 2018; Danilova et al., 2019b) but *Manf* mRNA is also expressed at high levels in astrocytes, microglia, oligodendrocytes, and endothelial cells (Zhang et al., 2014; Karlsson et al., 2021). MANF has been shown to protect against many types of cerebral injuries in *in vivo* disease models, including ischemic stroke (Airavaara et al., 2009, 2010; Yang et al., 2014; Wang et al., 2016; Matlik et al., 2018), hemorrhagic stroke (Xu et al., 2018; Li et al., 2019), traumatic brain injury (Li et al., 2018), and Parkinson's disease (Voutilainen et al., 2009; Hao et al., 2017). However, MANF has cytoprotective properties not only in the brain but also in the heart (Glembotski et al., 2012), retina (Neves et al., 2016; Gao et al., 2017; Lu et al., 2018), pancreas (Lindahl et al., 2014; Danilova et al., 2019a; Montaser et al., 2021), liver (Sousa-Victor et al., 2019), and kidney cells (Park et al., 2019).

Cerebral MANF expression has been shown to occur already during early embryonic development: mRNA at embryonic day (E) 7.5 and protein at E9.5 in mice (Danilova et al., 2019b). A study on postnatal cerebral MANF expression in rats revealed that MANF protein expression is highest during the early postnatal development on days P3–5 and is significantly decreased when adulthood is reached (Wang et al., 2014).

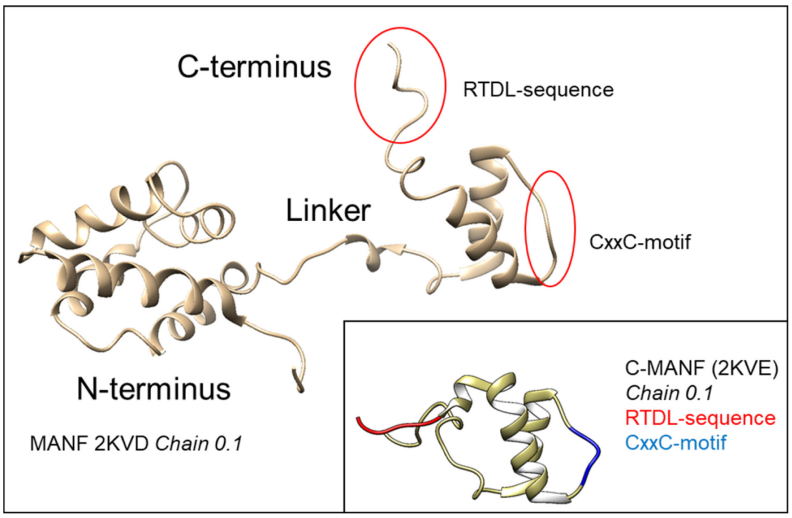

FIGURE 1 | Structure-function relationship of mesencephalic astrocyte-derived neurotrophic factor (MANF). The figure is based on the NMR structures of MANF and C-MANF (Hellman et al., 2011) (PDB codes: 2KVD and 2KVE, respectively. Image created with Chimera 1.16). The C-terminal RTDL-sequence of MANF corresponds to the canonical ER-retrieval signal "KDEL".

Notably, the expression of the MANF protein has been shown to further decrease with aging. A recent study found significantly reduced MANF protein levels in the brain of 18- to 20-month-old mice compared to 2- to 3-month-old mice (Han et al., 2021) and additional groups of 6- and 9-month-old mice (Liu et al., 2021). MANF protein expression has been also shown to decrease with aging in the fruit fly, in mouse plasma, retinal choroid, white adipose tissue, skin, liver, and muscle tissues, and in human serum and retinal choroid (Sousa-Victor et al., 2019; Neves et al., 2020; Liu et al., 2021). Decreased MANF expression could predispose for many age-related diseases and worsen the outcome of stroke.

MANF is a highly soluble protein (Mizobuchi et al., 2007) and spreads well in the brain parenchyma after intracerebral recombinant protein injection (Voutilainen et al., 2009, 2011). This high volume of distribution and spreading in the brain parenchyma is also evident with CDNF (Mätlik et al., 2017). Compared to glial cell line-derived neurotrophic factor (GDNF), the MANF (and CDNF) protein has significantly better tissue diffusion properties (Voutilainen et al., 2009, 2011; Mätlik et al., 2017).

How the exogenous MANF protein affects/enters cells is not fully understood. MANF is suggested to bind neuroplastin in the plasma membrane (Yagi et al., 2020); however, the binding efficacy is far from that of classical plasma membrane receptors. Furthermore, it should be kept in mind that in previous studies the radiolabeled MANF failed to bind anything (Hellman et al., 2011). Endogenous MANF is retrieved back to the ER lumen *via* KDEL receptors (KDELR) because of its C-terminal RTDL motif. MANF may also be internalized into a cell *via* KDEL-receptors, as they can be found in the plasma membrane fraction, but KDELRs are not classically thought to be transmembrane receptors in the plasma membrane (Henderson et al., 2013). Indeed, after ER stress and ER Ca^{2+} depletion, the level of KDELRs present in the plasma membrane may be increased. Due to the fusion of secretion vesicles in the plasma membrane, this seems quite likely. However, MANF without the RTDL sequence is still protective *in vivo* in ischemic stroke (Matlik et al., 2015), indicating that KDELRs are not necessary for mediating MANF's neuroprotective effects *in vivo*. Also, the fractalkine receptor CX3CR1 expressed by immune cells has been implicated as a mediator of MANF's cytoprotective effects on mouse retina (Neves et al., 2016). In addition, sulfatides have been shown to bind the extracellular MANF protein and to mediate its endocytosis into cells and were, thus, suggested to function as cell surface receptors (Bai et al., 2018). Furthermore, the cytoprotective effect of extracellular MANF was sulfatide-dependent, and the sulfatide-bound MANF was able to reduce ER stress in both *C. elegans* and in mammalian cells. However, it is still not known how MANF would enter the cell after binding to sulfatides. Interestingly, the recombinant CDNF protein, when delivered into the brain parenchyma, enters neurons very efficiently *via* unspecific endocytosis, and most CDNF was found in multivesicular bodies (Mätlik et al., 2017). Likely, a similar phenomenon also occurs with MANF (**Figure 3**); but so far, there is no evidence that neither protein would end up in the ER lumen after endocytosis (Mätlik et al., 2017), and how the transport would be possible without the ER signal peptide is not known. A recent study indicates that the recombinant MANF protein, when added to cell culture media, was protective only on stressed dopamine neurons treated with thapsigargin, a SERCA pump inhibitor (Eesmaa et al., 2021). In the future, studies should be conducted with radiolabeled MANF to determine the affinity together with competitive binding and deletion of KDELRs and/or neuroplastin. In summary, there has been tremendous progress in determining the actions of ER luminal MANF during the past 10 years. However, it is rather likely that the pleiotropic protective effects of the extracellular recombinant MANF protein

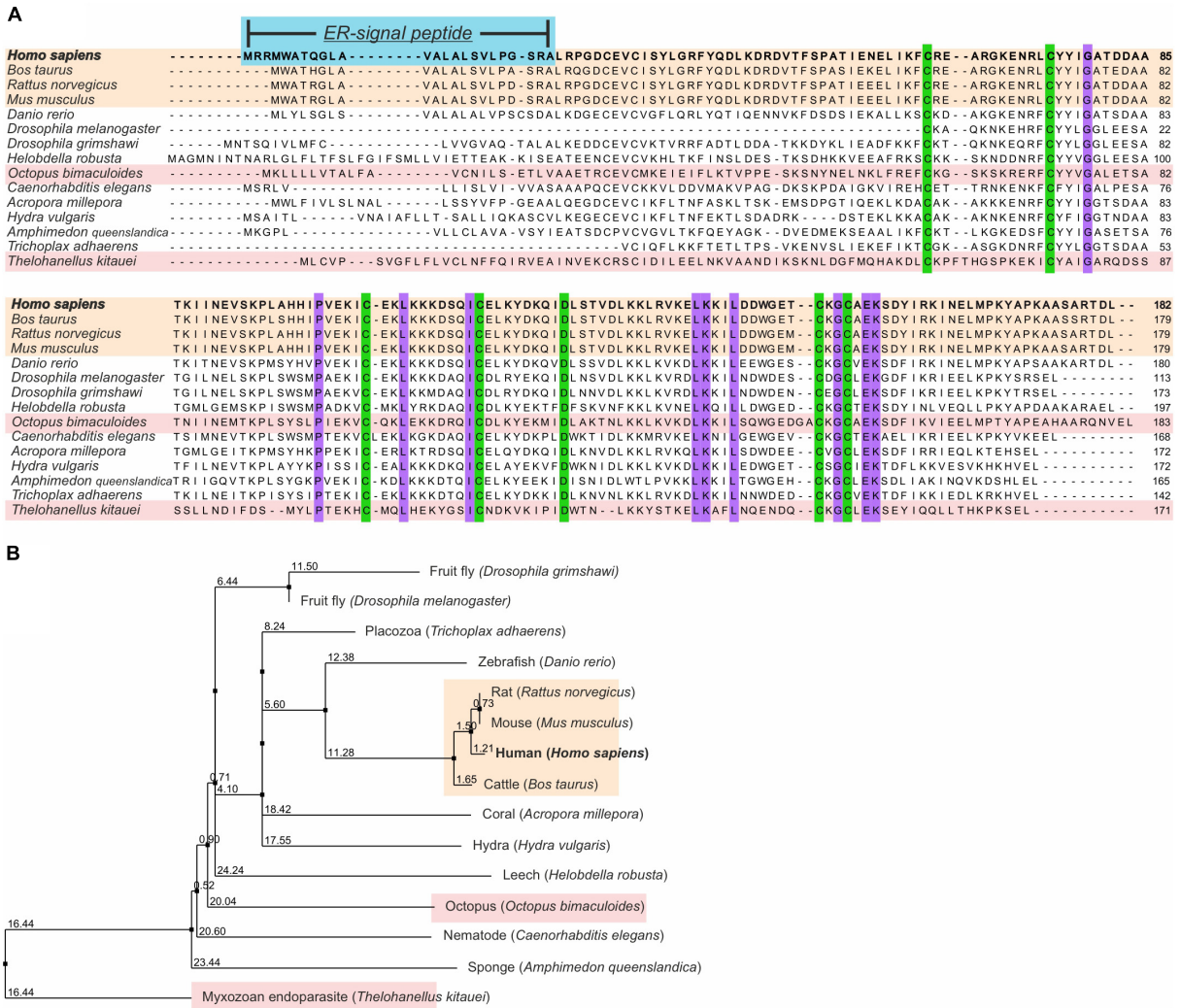

FIGURE 2 | Phylogenetic analysis of MANF. **(A)** Vertebrate MANF orthologs (cream boxes) were obtained by NCBI, as calculated by NCBI's Eukaryotic Genome Annotation pipeline for the NCBI Gene dataset. Non-vertebrate MANF orthologs were obtained with the NCBI "similar gene" pipeline. For two of the metazoans presented (pink boxes), human protein sequence was blasted in the EnsemblMetazoan database (metazoa.ensembl.org). Protein sequences were aligned using ClustaOWS in Jalview v. 2.10.5 (Clamp et al., 2004). Conserved amino acids in all organisms are highlighted in purple or green for cysteines. Numbers denote the amino acid number. **(B)** Phylogenetic tree of MANF is based on protein sequence similarity. It was calculated from distance matrices determined from % identity using the neighbor joining algorithm. Each number is a score, and each branch is an additive allowing for comparison of distances in the tree branches. Used sequence IDs: *Homo sapiens* (T1FAB3), *Bos Taurus* (Q9N3B0), *Rattus norvegicus* (A0A0C2MNP5), *Mus musculus* (A0A0L8FVI8), *Danio rerio* (B3RIB4), *Drosophila grimshawi* (B4JT39), *Drosophila melanogaster* (Q9XZ63), *Helobdella robusta* (Q3TMX5), *Octopus bimaculoides* (P55145), *Caenorhabditis elegans* (P80513), *Acropora millepora* (F1QDQ5), *Hydra vulgaris* (B2RZ09), *Amphimedon queenslandica* (T2MFG7), *Trichoplax adhaerens* (A0A1 × 7TYG8), and *Thelohanellus kitauei* (LOC114953444).

(without the ER signal peptide) are mediated differently, and more studies are needed to discover the mechanism of MANF's cellular uptake and possible cell surface receptors.

SUMMARY OF MANF NEUROPROTECTION STUDIES

MANF is an ER stress-inducible protein (Apostolou et al., 2008) that conveys neuroprotective and neurorestorative properties. Microinjection of recombinant MANF or MANF overexpression by plasmid microinjection into the nucleus inhibits apoptosis in primary neuronal cultures treated with the UPR inducers thapsigargin and tunicamycin, topoisomerase II inhibitor etoposide, and protein kinase inhibitor staurosporine, or nerve growth factor (NGF) deprivation in culture media (Hellman et al., 2011; Matlik et al., 2015; Eesmaa et al., 2021). Extracellularly applied MANF was shown to reduce apoptosis and downregulate the ATF6 and IRE1 UPR pathways in thapsigargin-treated dopaminergic primary cultures (Eesmaa et al., 2021). The protective effect of both intracellularly and extracellularly applied MANF in primary neuronal cells was inhibited by IRE1 and

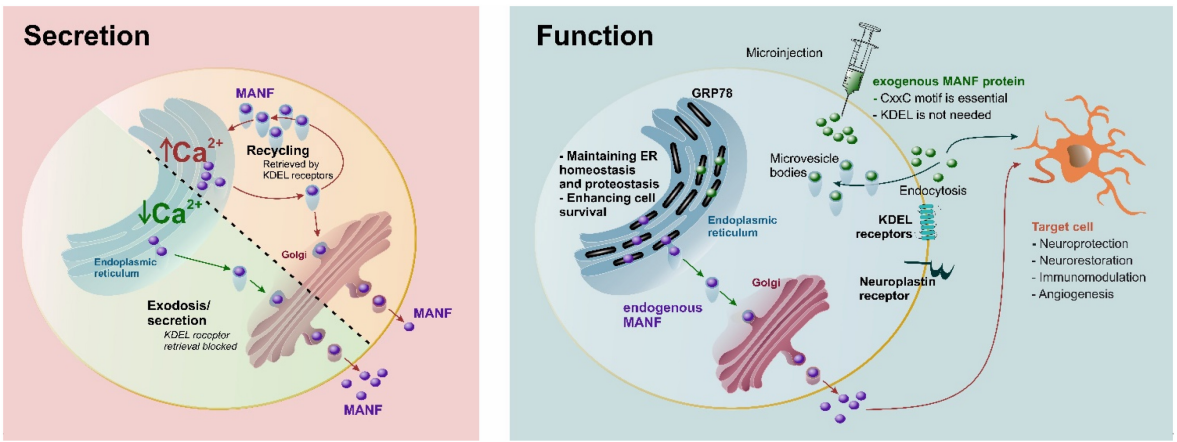

FIGURE 3 | Secretion and proposed function of MANF. Under normal conditions, MANF is maintained in the endoplasmic reticulum (ER) by KDEL receptor-mediated retrieval and secreted in response to Ca^{2+} depletion. MANF maintains ER homeostasis and proteostasis, as well as enhances cell survival. A CxxC-motif is essential for neuroprotection for both endogenous and exogenous MANF, while the C-terminal RTDL sequence of MANF (corresponding to the canonical KDEL ER-retrieval signal) is not needed for the neuroprotective effect of exogenous MANF (Matlik et al., 2015). It is possible that KDEL and neuroplastin receptors may participate in internalization of extracellular MANF, and interaction with sulfatides may be important for internalization. It should be emphasized the majority of KDEL receptors are in the Golgi, and only a fraction of them can be at the plasma membrane at any given time point. Purple circles, endogenous MANF; green circles, recombinant exogenous MANF.

PERK inhibitors (Eesmaa et al., 2021), indicating that MANF's cytoprotective effect is mediated by UPR regulation. However, in 6-OHDA treated SH-SY5Y cells, UPR downregulation was observed only after MANF overexpression and not after applying the recombinant protein extracellularly into media (Hao et al., 2017). In the *in vivo* 6-OHDA toxin model of Parkinson's disease, the recombinant MANF protects the dopaminergic cell bodies of the substantia nigra (Voutilainen et al., 2009; Hao et al., 2017). MANF not only prevents the degeneration of dopaminergic neurons but also potentiates stimulus-evoked dopaminergic neurotransmission, thereby enhancing dopamine turnover in the brain of freely moving rats without lesion (Renko et al., 2018). Also, *in vitro*, recombinant MANF protects the SH-SY5Y neuroblastoma cell line from 6-OHDA-induced apoptosis (Huang et al., 2016; Hao et al., 2017; Sun et al., 2017; Zhang et al., 2017). In *D. melanogaster,* the *Manf* homolog *DmManf* is required for the maturation and maintenance of dopaminergic neurites during the embryonic stage, implying the importance of MANF in Parkinson's disease, where dopaminergic neuronal loss is the major factor (Palgi et al., 2009). Furthermore, neuronal MANF knockdown sporadically affects dopaminergic neuron development, suggesting a cell autonomous function in these cells (Stratoulias and Heino, 2015a). Similarly in zebrafish, embryonic *Manf* knockdown results in dopaminergic neuron impairment, a phenotype which is rescued by exogenous *Manf* mRNA (Chen et al., 2012). In *C. elegans,* mutation of the *Manf* homolog *manf-1* showed increased α-synuclein accumulation in the body wall muscle cells together with increased ER stress (Richman et al., 2018). Inability to cope with the UPR machinery might, in turn, lead to degeneration of dopaminergic neurons, as dopaminergic degeneration was found to occur with age in the *manf-1* mutant *C. elegans.* Also, deletion of MANF in *C. elegans* abrogated tunicamycin-induced toxicity, and even high concentrations did not decrease survival (Hartman et al., 2019). MANF overexpression or the recombinant MANF protein has been shown to protect against Aβ toxicity in N2a cells and SH-SY5Y cells possibly by inhibiting Aβ-induced ER stress, whereas knockdown of the *Manf* gene was shown to aggravate Aβ accumulation and ER stress (Xu et al., 2019). Additionally, recombinant MANF has been shown to be neuroprotective in a rat model of traumatic brain injury, where the protective effect was attributed to increased BBB integrity and decreased activation of the NF-κβ signaling pathway (Li et al., 2018). MANF was speculated to inhibit the apoptosis of endothelial cells constituting the BBB by downregulating ER stress and/or inflammation. MANF has also shown protective effects on a mouse model of multiple sclerosis, where recombinant MANF-treated mice showed less motor deficits compared to vehicle-treated mice in an early time-point after experimental autoimmune encephalomyelitis induction (Nam et al., 2021).

MANF AND XBP1 IN STROKE

MANF

MANF expression is upregulated by ischemia (**Table 1**). A short 10-min global forebrain ischemia in rat transiently increased neuronal *Manf* mRNA levels at 24 h in the hippocampus and the levels returned to baseline by 1-week post-ischemia (Lindholm et al., 2008). The protein expression of neuronal MANF was found elevated 2–48 h post-stroke after transient middle cerebral artery occlusion (MCAo) in rats, and most prominently in the peri-infarct region (Apostolou et al., 2008; Yu et al., 2010). Interestingly, Shen et al. reported that the MANF protein was upregulated not only in neurons of the ischemic cortex but also in CD68-positive microglia/macrophages and in oligodendrocytes

TABLE 1 | Effect of MANF in stroke.

Model	Treatment	Effect	References
In vivo Studies			
1 h MCAo in aged mice	rhMANF 2 h post-stroke	Functional recovery ↑ Infarct volume ↓ IL-6, IL-1β, TNF-α ↓, BBB integrity ↑	Han et al., 2021
2 h MCAo in rat	DHA *i.v.* 3 h post-stroke	MANF in neurons and astrocytes ↑ Neurobehavioral recovery ↑ TREM2 in microglia ↓ Infarct size ↓	Belayev et al., 2020
Permanent MCAo in rat	rhMANF 24 h post-stroke	Neurobehavioral recovery ↑ CD34 ↑ Regional cerebral blood flow ↑ Vessel surface area ↑ Microvessel branch points ↑ VEGF pathway activation	Gao et al., 2020
1 h dMCAo in rat	AAV1-MANF 2 days post-stroke	Some immune response-related transcripts ↑ S100A8; S100A9 ↓	Teppo et al., 2020
2 h MCAo in rat	MANF-knockdown BMSC transplant 1-day pre-stroke	M1 markers ↑ M2 markers ↓ BMSC-induced functional recovery ↓ MANF-mediated MANF upregulation ↓	Yang et al., 2020
1.5 h dMCAo in rat	rhMANF 7 days post-stroke	Functional recovery ↑	Anttila et al., 2019
Subarachnoid hemorrhage in rat	rhMANF at stroke	p-Akt, p-MDM2, Bcl-2 ↑ BBB integrity ↑ P53, Bax, CC3, MMP9 ↓ Neurological deficit ↓ Effects reversed by MK2206	Li et al., 2019
1 h dMCAo in rat	AAV7-MANF 2 days post-stroke	Functional recovery ↑ Phagocytic macrophages ↑ *Complement 3* and *Emr1* ↑	Matlik et al., 2018
1.5 h dMCAo in rat	chronic rhMANF 3–16 days post-stroke	Functional recovery ↑	Matlik et al., 2018
Permanent dMCAo in mouse	$Nestin^{Cre/+}$:$Manf^{fl/fl}$ MANF KO	Infarction volume ↑ *Manf* mRNA ↑ in $Manf^{fl/fl}$ control mouse cortex	Matlik et al., 2018
1.5 h dMCAo in rat	rhMANF 3-, 7-, and 10-days post-stroke or continuously on days 3–16 post-stroke	Migration of DCX^{+} cells toward corpus callosum and infarct boundary ↑	Tseng et al., 2018
Intracerebral hemorrhage in rat	rhMANF 1-day post-stroke	p-Akt, p-MDM2, Bcl/Bax ratio ↑ Neurological function ↑ P53, caspase-3, neuronal death ↓ Effects reversed by MK2206	Xu et al., 2018
1.5 h MCAo in rat	rhMANF 3 h post-stroke	Neurological function ↑ Mortality ↓ Infarct volume and brain tissue injury ↓	Wang et al., 2016
1 h dMCAo in rat	rhMANF C-terminal mutations 20 min pre-stroke	CKGC sequence required for neuroprotective activity, RTDL not	Matlik et al., 2015
2 h MCAo in rat	rhMANF 20 min pre-stroke	Neuronal loss ↓ Caspase-3 cleavage, apoptosis ↓ BIP/GRP78, p-IRE1, and XBP1 ↓	Yang et al., 2014
2 h or 4 h MCAo in rat		MANF is primarily expressed in neurons MANF expression in neurons, microglia/macrophages, and oligodendrocytes. Only mild MANF upregulation in astrocytes	Shen et al., 2012
1 h dMCAo in rat	AAV7-MANF 1 week pre-stroke	Behavioral recovery ↑ Infarction volume ↓ MCAo causes redistribution of MANF immunoreactivity after overexpression	Airavaara et al., 2010
2 h or 4 h MCAo in rat		MANF expression in neurons and glial cells ↑ 2–48 h post-MCAo	Yu et al., 2010

(Continued)

TABLE 1 | (Continued)

Model	Treatment	Effect	References
In vivo studies			
1 h dMCAo in rat	rhMANF 20 min pre-stroke	Behavioral recovery ↑ Infarction volume ↓ Apoptosis ↓	Airavaara et al., 2009
10 min oCCA *(Global forebrain ischemia)* in rat		MANF mRNA ↑ at 24 h, expression mostly neuronal	Lindholm et al., 2008
In vitro studies			
Thapsigargin or OGD on SH-SY5Y cell culture	Various compounds for 16 h pretreatment	Compounds that stabilize the ER-resident proteome reverse MANF secretion	Henderson et al., 2021
OGD on senescent bEnd.3 cells	rhMANF 24 h pretreatment	IL-6, IL-1β, TNF-α ↓ TLR4, MyD88, nuclear NF-κB p65 ↓ ZO-1, occludin ↑	Han et al., 2021
LPS-stimulated primary microglia or HAPI cell culture	Microglia: BMSC-co-culture 1-day post-LPS; HAPI: PDGF-AA 1-day post-LPS	Microglia: MANF ↑, reversed if BMSCs are MANF-knockdown HAPI: MANF ↑, miR-30a ↓	Yang et al., 2020
OGD on NSC culture, SVZ explants	NSC: rhMANF 15 min pre-OGD; SVZ: LV-hMANF	NSC: neuronal and glial differentiation ↑, STAT3 activation SVZ: Cell migration ↑, STAT3 and ERK1/2 activation	Tseng et al., 2018
Etoposide or thapsigargin on sympathetic or sensory neuron culture	Plasmid DNA of MANF C-terminal mutants at treatment	CKGC sequence required for neuroprotective activity RTDL sequence required for ER retention and neuroprotection in sympathetic but not sensory neurons	Matlik et al., 2015
OGD in primary rat astrocytes	rhMANF	IL-1β, IL-6, TNF-α ↓ GRP78, NF-κB p65 ↓	Zhao et al., 2013
Primary glial cell culture	Starvation, MG132, or tunicamycin	MANF expression ↑	Shen et al., 2012
Hypoxia on primary cortical neuron culture	AAV7-MANF pre-hypoxia	Hypoxia causes redistribution of MANF immunoreactivity after overexpression	Airavaara et al., 2010
Serum deprivation or tunicamycin on SH-SY5Y culture, tunicamycin on primary neuron culture	rhMANF for 2 weeks pretreatment	MANF expression after tunicamycin ↑ rhMANF: neuronal survival ↑	Yu et al., 2010

AAV, adeno-associated virus; Bax, Bcl-2-associated X protein; BBB, blood-brain barrier; Bcl-2, B-cell lymphoma 2; BIP/GRP78, binding immunoglobulin protein/glucose-regulated protein 78; BMSC, bone marrow mesenchymal stem cell; CC3, cleaved caspase 3; oCCA, occlusion of common carotid artery; DCX^+, double cortin-positive neurons; DHA, docosahexaenoic acid; dMCAo, distal middle cerebral artery occlusion; Emr1, EGF-like module-containing mucin-like hormone receptor-like 1; ER, endoplasmic reticulum; ERK1/2, Extracellular signal-regulated protein kinase 1/2; HAPI, highly aggressively proliferating immortalized rat microglia; IL, interleukin; i.v., intravenous; KO, knockout; LPS, lipopolysaccharide; LV, lentivirus; M1, classically activated microglia/macrophages; M2, alternatively activated microglia/macrophages; MANF, mesencephalic astrocyte-derived neurotrophic factor; MCAo, middle cerebral artery occlusion; MMP9, matrix metallopeptidase 9; MyD88, myeloid differentiation factor 88; NF-κB, nuclear factor kappa-light-chain-enhancer of activated B cells; NSC, neural stem cell; OGD, oxygen-glucose deprivation; P53, tumor suppressor p53; p-Akt, phosphorylated protein kinase B; PDGF-AA, platelet-derived growth factor-AA; p-IRE1, phosphorylated IRE1; p-MDM2, phosphorylated murine double minute 2; rhMANF, recombinant human MANF; S100A8/9, calgranulin A/B; STAT3, signal transducer and activator of transcription 3; SVZ, subventricular zone; TLR4, toll-like receptor 4; TREM2, triggering receptor expressed on myeloid cell 2; VEGF, vascular endothelial growth factor; XBP1, X-box binding protein; ZO-1, zonula occludens-1; TNF-a, tumor necrosis factor a.

24 h after transient MCAo in rat (Shen et al., 2012). MANF expression colocalized with GRP78 in CD68-positive cells, indicating UPR activation in microglia/macrophages after ischemic stroke. Minor MANF expression was also found in astrocytes of the ischemic cortex but not in the normal healthy brain (Shen et al., 2012). In a more recent study, Belayev et al. found that docosahexaenoic acid increased MANF protein expression in neurons and astrocytes of the peri-ischemic region 24 h after transient MCAo in rats (Belayev et al., 2020). Yang et al. showed increased MANF expression in microglia/macrophages at the same time point after transient MCAo, and a further increase in MANF positive microglia/macrophages was seen when animals with stroke were pretreated with bone marrow mesenchymal stem cells (Yang et al., 2020). When we overexpressed the MANF transgene in the rat cortex before cortical stroke induction by distal MCAo (dMCAo), the expression pattern of transduced MANF was changed 6 h after ischemia, causing redistribution of MANF from the cell soma to the processes of neurons and glia (Airavaara et al., 2010). Furthermore, we observed a punctate pattern of transduced MANF after ischemia, suggestive that the MANF protein is released from cells after ischemia or locally translated in axonal/dendritic processes. The observed phenomena may be related to "ER exodosis," the exit of ER luminal proteins upon ER stress (Henderson et al., 2021), as MANF is known to be secreted from cells upon ER Ca^{2+} depletion (Glembotski et al., 2012; Henderson et al., 2013).

Like cerebral ischemia, myocardial ischemia was shown to upregulate MANF protein levels (Tadimalla et al., 2008). Increased MANF protein levels were found in the peri-infarct area 4–14 days after permanent myocardial infarction in mice (Tadimalla et al., 2008). Additionally, hypoxia in rat primary retinal ganglion cells increased *Manf* mRNA and protein levels 24–48 h after hypoxia (Gao et al., 2016). Furthermore, hemorrhagic stroke has been shown to increase MANF protein expression, mainly in neurons (Xu et al., 2018; Li et al., 2019). In both intracerebral hemorrhage and subarachnoid hemorrhage rat models, MANF protein expression increased 3 h after hemorrhage, peaked at 24 h, and remained elevated up to 72 h post-hemorrhage in the peri-hematoma area.

Collectively, stroke robustly increases the expression of MANF in animal models. Many studies have focused on analyzing neuronal MANF expression, but prominent upregulation in glia has also been reported. However, studies on post-ischemic MANF expression have focused on acute time-points, and a thorough long-term study on MANF expression after ischemic stroke in animal models and in ischemic stroke post-mortem patient samples is further warranted.

When exogenous MANF is administered into the brain *via* a viral vector or as a recombinant protein before or a few hours after stroke, it has neuroprotective effects on ischemic stroke models (Airavaara et al., 2009, 2010; Yang et al., 2014; Matlik et al., 2015; Wang et al., 2016; Han et al., 2021). Neuroprotection can be observed both at the tissue level as reduced infarction volume and at the behavioral level as improved functional recovery. MANF can inhibit apoptosis/necrosis in the ischemic brain (Airavaara et al., 2009; Yang et al., 2014), and the CxxC-motif is indispensable for the neuroprotective effect of MANF in ischemic stroke, possibly because of its importance in maintaining MANF's structural conformation (Matlik et al., 2015). However, in the rat dMCAo model, the RTDL sequence is not needed for neuroprotection, implying that KDEL receptors do not have a significant role in mediating MANF's neuroprotective effect on cerebral ischemia (Matlik et al., 2015). Taking a different approach, Belayev et al. used docosahexaenoic acid (DHA) to increase endogenous MANF protein expression after transient MCAo and observed neuroprotection and enhanced neurogenesis associated with DHA therapy (Belayev et al., 2020). An important study on 18- to 20-month-old mice was conducted recently by Han et al. and showed that the recombinant MANF protein given 2 h post-MCAo is also neuroprotective in the aging brain (Han et al., 2021). MANF treatment also increased the BBB integrity of aged mice. Moreover, endogenous neuronal *Manf* is protective against ischemic stroke, as we have shown that $Nestin^{Cre/+}$:$Manf^{flox/flox(fl/fl)}$ mice with conditional deletion of *Manf* from the neural lineage cells have larger infarcts than $Manf^{fl/fl}$ control mice (Matlik et al., 2018). In *Manf* knockout (KO) mouse primary neuronal stem cell culture, extracellularly applied recombinant MANF protein protected the KO cells from apoptosis after oxygen-glucose deprivation (Tseng et al., 2018). The cytoprotective effect of MANF against ischemia is not limited to neuronal cells, but the recombinant MANF protein reduced the myocardial infarct size in a mouse model of transient myocardial ischemia (Glembotski et al., 2012) as well as reduced hypoxia-induced apoptosis in rat retinal ganglion cells *in vivo* and *in vitro* (Gao et al., 2017). Furthermore, MANF is neuroprotective in hemorrhagic stroke (Xu et al., 2018; Li et al., 2019). Intracerebroventricular injection of the recombinant MANF protein 1 h after intracerebral hemorrhage induction in rats improved neurological function, decreased apoptosis, and activated Akt in the peri-hematoma area (Xu et al., 2018). Comparable results were found in a rat model of subarachnoid hemorrhage, and an additional finding of MMP-9 downregulation suggested MANF may protect the integrity of the BBB (Li et al., 2019).

Notably, post-stroke MANF administration promotes functional recovery (Matlik et al., 2018; Anttila et al., 2019). We overexpressed the MANF protein in the peri-infarct area 2 days after dMCAo by intracerebral AAV7-MANF injection and found improved neurological function already on day 4 and up to day 14 post-stroke (Matlik et al., 2018). Similarly, chronic infusion of the recombinant MANF protein into the peri-infarct area starting 3 days post-dMCAo and continuing for 14 days promoted neurological recovery (Matlik et al., 2018). Even a single intracranial MANF recombinant protein injection 7 days post-stroke was able to alleviate neurological deficits a week later (Anttila et al., 2019).

The mechanisms by which MANF promotes recovery after the acute phase of stroke remain poorly understood. MANF represents an emerging regulator of tissue clearance after stroke (Matlik et al., 2018), and at the cellular level, post-stroke MANF delivery supports many endogenous beneficial cellular repair processes that occur after ischemic stroke (Matlik et al., 2018; Tseng et al., 2018; Gao et al., 2020). Post-stroke MANF administration facilitates neurogenesis (Tseng et al., 2018), promotes innate immunity responses (Matlik et al., 2018), and enhances angiogenesis (Gao et al., 2020). Indeed, all our unbiased approaches with RNA sequencing, metabolomics, and proteomics indicated that MANF mediates innate immunity, and additional studies are needed to clarify the role of both endogenous and exogenous MANF effects. In the rat transient dMCAo model, intracerebral infusion of the recombinant MANF protein starting 3 days post-stroke increased the migration of neural progenitor cells into the infarct region (Tseng et al., 2018). One and 2 weeks after permanent MCAo in rats, Gao et al. found increased angiogenesis and subsequent improvement in cerebral blood flow after recombinant MANF protein administration 1-day post-stroke, possibly due to activation of the vascular endothelial growth factor (VEGF) pathway (Gao et al., 2020). However, we did not find a difference in laminin-positive blood vessel density in the peri-infarct area 2 weeks after transient dMCAo and AAV7-MANF treatment (Matlik et al., 2018). The diverse findings regarding MANF's angiogenetic properties may be related to differences in the ischemic model used (permanent MCAo vs. transient dMCAo) and the method of MANF delivery (recombinant protein vs. AAV).

To sum up, MANF has both neuroprotective and neurorestorative effects on stroke. The acute mechanisms involve anti-apoptotic effects and, possibly, protection of BBB integrity. The restorative mechanisms may involve neurogenesis, angiogenesis, and immunomodulation. MANF's effects on

immunomodulation and neurogenesis will be further discussed below.

XBP1 and Modulators of XBP1

Spliced X-box binding protein (XBP1s) is a highly active transcription factor controlling protein translation and UPR; thus it is involved in multiple cellular processes (e.g., maintaining ER homeostasis, immunomodulation, required for autophagy, cell death, and involved in glucose and lipid metabolism) (Hetz et al., 2011, 2020; Walter and Ron, 2011). Xbp1 mRNA expression is induced by ATF6 and spliced by IRE1a in response to ER stress (Yoshida et al., 2001). Xbp1 mRNA is the only splicing target of IRE1a, and removal of 26 nucleotide intron creates functionally active XBP1s (Calfon et al., 2002). The unspliced version of X-box binding protein (XBP1u) is expressed constitutively and acts as a negative feedback regulator during the recovery phase of ER stress; it also maintains cell size (Shaffer et al., 2004). XBP1s upregulates UPR-related genes involved in protein folding, entry to the ER and ERAD, and phospholipid biosynthesis (required for increasing the volume of ER and Golgi). The targets of XBP1s can vary in different tissues or under variable ER stress conditions, as XBP1 can interact and heterodimerize with other transcription factors (Hetz et al., 2011). B-lymphocyte differentiation to plasma cells is dependent on XBP1 (Reimold et al., 2001). Intriguingly, MANF is also widely expressed in secretory cells that require highly developed ER (Lindholm et al., 2008), and MANF is one of the XBP1s target genes (Shaffer et al., 2004; Oh-Hashi et al., 2013; Wang et al., 2018). XBP1 deletion diminishes the mRNA expression of MANF in B-cells (Shaffer et al., 2004). Furthermore, our MANF KO studies have shown a clear link between MANF and XBP1. MANF ablation causes prolonged UPR activation, and sXBP1 is highly upregulated in MANF KO tissues (Pakarinen et al., 2020, 2022). In comparison, neuron-specific MANF expression *in vivo* improved the outcome in the 6-OHDA toxin model of Parkinson's disease by reducing the levels of p-eIF2a, ATF4, CHOP, XBP1s, GRP78, and ATF6α (Hao et al., 2017). Interestingly, *in vitro*, the positive effect of endogenous MANF overexpression in neurons was achieved by reducing UPR, while the positive effect of extracellularly applied MANF protein was mediated *via* Akt and mTOR (Hao et al., 2017).

The role of XBP1 and UPR in ischemic stroke has been studied for almost 3 decades. As transient ischemic stroke and ER stress cause similar defects, Paschen proposed that the acute detrimental effects of ischemia are caused by disturbed calcium homeostasis causing ER stress and UPR activation in affected cells (Paschen, 1996). Since then, many studies have confirmed the increase in ER stress markers after stroke (**Table 2**). Initial experiments *in vivo* detected a rapid increase in Xbp1 mRNA and XBP1s levels among other UPR markers after transient forebrain ischemia, indicating disturbance of the ER during damage (Paschen et al., 2003). Following studies with XBP1 transgenic mice confirmed the results and indicated long-term upregulation of XBP1s (signal peaking at 24 h and still present after 3 days). XBP1 expression was detected in glial cells on days 1 and 3 by GFAP co-staining (Morimoto et al., 2007). A similar XBP1 expression pattern was accompanied by the activation of other UPR pathways (Nakka et al., 2010), collectively showing that stroke induces ER stress at the lesion site and penumbra. Clinical relevance was found in genetic studies. The polymorphism of the XBP1 (−116C/G) promoter was investigated in relation to ischemic stroke, atherosclerosis, and hyperhomocysteinemia in human patients, and the XBP1 (−116 G/G) genotype was found to be a risk factor for pediatric ischemic stroke (Yilmaz et al., 2010).

Over the years, different treatments aiming to reduce or modify ER stress during stroke have been tested. For example, a selective inhibitor of eIF2α dephosphorylation, salubrinal, reduced lesion size (Nakka et al., 2010). A week of pretreatment with 2-deoxyglucose improved neurological score within hours and decreased lesion size after 24 h while increasing GRP78 (max at 12 h) and XBP1 protein levels (Wu et al., 2014). Injection of rhMANF 2 h post-stroke reduced the levels of XBP1s, GRP78, and p-IRE1, and enhanced neuron numbers and behavioral recovery while inhibiting caspase 3 (Yang et al., 2014). The protective effect of *Ligusticum chuanxiong*, *Radix Paeoniae Rubra*, and their combination was tested in rats. A significant decrease in the protein levels of UPR-related factors (XBP1, PERK, ATF6, and CHOP) was detected, accompanied by increased expression of GRP78 and microvessel density (Gu et al., 2016).

Stroke activates O-linked beta-N-acetylglucosamine (O-GlcNAc) modification in the penumbra in neurons of young mice, and XBP1-dependent O-GlcNAc modification was neuroprotective (Jiang et al., 2017). However, the regulation of glucose homeostasis *via* XBP1 is independent of ER stress and acts through XBP1s interaction with FoxO1 (Zhou et al., 2011). Thiamet-G, the activator of O-GlcNAc, improved the outcome in Xbp1 KO mice and induced long-term functional recovery in both young and aged mice. In addition, Xbp1s overexpression by AAVs in neurons induced O-GlcNAcylation, and it improved the outcome after stroke (Wang et al., 2021b).

In adult tissues of mice, XBP1 can regulate the proliferation of endothelial cells and angiogenesis after stroke *via* the VEGF signaling pathway (Zeng et al., 2013). Pretreatment with anti-VEGF antibody reduced edema, infarct volume, and improved neurological scores while decreasing IRE1 pathway and ER stress-mediated apoptosis in mice stroke models (Feng et al., 2019). In contrast, MANF enhanced stroke recovery and angiogenesis by stimulating the VEGF pathway (Gao et al., 2020), depicting quite opposite outcomes while modulating the same pathway.

Taurine is an inhibitory neurotransmitter that can protect from ER-stress in primary cell culture and reduce lesion size in ischemic stroke after 4 days by decreasing GRP78, p-IRE1, CHOP, and caspase-12 levels (Gharibani et al., 2013). Delivery of S-methyl-N, N-diethyldithiocarbamate sulfoxide (DETC-MeSO, partial NMDA antagonist) for 4–8 days reduced cell death and infarct size. After the treatment, a decrease in protein levels of ER stress markers, XBP1, ATF4, JNK, p-PERK, p-eIF2α, GADD34, and CHOP, were detected (Mohammad-Gharibani et al., 2014). Granulocyte colony-stimulating factor (G-CSF) is an anti-apoptotic and immunomodulatory protein that mediates angiogenesis and neurogenesis. Daily dose for 4 days improved the behavior in corner and locomotor tests, and induced the expression of GRP78 while reducing the expression of XBP1, ATF4,

TABLE 2 | Modulation of XBP1 in stroke.

Model	Treatment	Effect	References
Clinical studies			
Pediatric stroke		XBP1 (-116 C/G) gene polymorphism is a risk factor for pediatric ischemic stroke	Yilmaz et al., 2010
In vivo studies			
30 or 45 min MCAo, photothrombotic stroke, and 15 min forebrain ischemia in mouse, 60 min MCAo in rat	XBP1 over-expression and knockout, Thiamet-G, glucosamine	Overexpression: UDP-GlcNAc, neurological function ↑ Infarct volume ↓ Knockout: UDP-GlcNAc ↓ Thiamet-G: neurological function in knockout and old and young wt ↑ Glucosamine: neurological function ↑ Infarct volume ↓	Wang et al., 2021b
30 min BCAo in mouse	G-CSF	Neurological and behavioral recovery ↑ p-Akt ↑ ER stress (XBP1 and other markers) ↓ Autophagy, mitochondrial stress, apoptosis ↓	Modi et al., 2020
2 h MCAo in mouse	anti-VEGF antibody	Infarct size, edema, degenerated neurons, apoptosis, IRE1α ↓ Neurological function, intact neurons ↑	Feng et al., 2019
30 or 45 min MCAo and pMCAo in mouse	Neuronal XBP1 LoF and GoF, Thiamet-G	LoF: stroke outcome, O-GlcNAcylation ↓ GoF: O-GlcNAcylation ↑ Thiamet-G: O-GlcNAcylation, stroke outcome ↑	Jiang et al., 2017
2 h MCAo in rat	Taurine, DETC-MeSO	GRP78, cleaved ATF6/ATF6 ratio, ATF4, p-IRE1, CHOP ↓ Infarct size, neurological deficit ↓	Prentice et al., 2017a
pMCAo in rat	*Ligusticum chuanxiong*, *Radix Paeoniae*	Combination: neurological deficit, infarction volume, ER stress (incl. XBP1) ↓ Antioxidant enzyme activity ↑	Gu et al., 2016
2 h MCAo in rat	Taurine, DETC-MeSO	Taurine: p-IRE1, infarct volume ↓ Combination: p-IRE1, infarct volume, neurological deficit, gliosis ↓	Gharibani et al., 2015
2 h MCAo	DETC-MeSO	Cell death, infarction volume, neurological deficit ↓ XBP1 but not p-IRE1 ↓	Mohammad-Gharibani et al., 2014
2 h MCAo in rat	2-deoxyglucose	Neurological function, XBP1 ↑ Infarction volume ↓	Wu et al., 2014
2 h MCAo in rat	rhMANF 20 min pre-stroke	Neuronal loss ↓ Caspase-3 cleavage, apoptosis ↓ BIP/GRP78, p-IRE1, and XBP1 ↓	Yang et al., 2014
2 h MCAo in rat	Taurine	Cleaved ATF6 and its ratio to ATF6, p-IRE1 ↓ Infarct size ↓	Gharibani et al., 2013
2 h MCAo in rat	Salubrinal	Characterization of ER stress gene expression after stroke, including increased Xbp1 mRNA processing Salubrinal: eIF2α phosphorylation ↑ Infarction volume ↓	Nakka et al., 2010
pMCAo in mouse		Characterization of ER stress gene expression after stroke Xbp1 mRNA splicing and XBP expression increased at 6 h to 3 days post-stroke, localized to the neuron cytosol and dendrites, and glial cells	Morimoto et al., 2007
30 min MCAo in mouse		Xbp1 mRNA increased at 1 and 3 h, protein at 6 h in mouse	Paschen et al., 2003
In vitro studies			
OGD/R in primary rat microglia and cortical neuron cultures	Icariin, IRE1 overexpression	Microglia: secreted IL-1 β, IL-6, TNF-α ↓ Neurons: XBP1u, XBP1s, cleaved caspase-3, p-IRE1α/IRE1α ratio, apoptosis ↓ Cell viability ↑ IRE1 overexpression impaired icariin effect	Mo et al., 2020
LPS-stimulated primary microglia or HAPI cell culture	Microglia: BMSC-co-culture 1-day post-LPS; HAPI: PDGF-AA 1-day post-LPS	Microglia: MANF ↑, reversed if BMSCs are MANF-knockdown HAPI: MANF ↑, miR-30a ↓ XBP1 ↑	Yang et al., 2020

(Continued)

TABLE 2 | (Continued)

Model	Treatment	Effect	References
OGD in primary rat brain microvascular endothelial cell culture	DANCR overexpression and knockdown, XBP1 knockdown	DANCR overexpression: proliferation, migration, angiogenesis, XBP1s ↑ Apoptosis ↓ DANCR knockdown: proliferation, migration, angiogenesis, XBP1s ↓ Apoptosis ↑ XBP1 knockdown: proliferation, migration, angiogenesis ↓ Apoptosis ↑ miR-33a-5p directly binds to DANCR and XBP1 and reverses DANCR effects XBP1 overexpression reverses miR-33a-5p effects DANCR/miR-33a-5p/XBP1s activates WNT/β-catenin signaling	Zhang et al., 2020
OGD/R in mouse brain microvascular endothelial bEnd.3 cell culture	VEGF siRNA	Cell viability, proliferation ↑ Apoptosis, ROS, XBP1, GRP78 ↓	Feng et al., 2019
OGD in rat brain microvascular endothelial cell culture	XBP1 overexpression and knockdown	XBP1s and XBP1u upregulated after OGD Overexpression: cell survival, proliferation, migration, angiogenesis, cyclin D1, MMP-2, MMP-9, and PI3K/AKT, ERK, and HIF-1α/VEGF signaling ↑ Apoptosis, cleaved Caspase-3, cleaved Caspase-9 ↓ Knockdown: opposite effects	Shi et al., 2018
Hypoxia/reoxygenation in primary rat cortical neuron and PC12 cell culture	Taurine, sulindac	Taurine: cleaved ATF6/ATF6 ratio, p-IRE1 ↓ Taurine + sulindac: cell viability ↑	Prentice et al., 2017b
Hypoxia/reoxygenation in primary rat neuronal cell culture	DETC-MeSO	Cell viability ↑	Mohammad-Gharibani et al., 2014
Hypoxia/reoxygenation in primary rat cortical neuron culture	Taurine	Cleaved ATF6 and its ratio to ATF6, p-IRE1 ↓ Cell viability ↑	Gharibani et al., 2013
OGD and other *in vitro* ischemia and hypoxia models in rat oligodendrocyte precursor cell line and primary cell culture	XBP1 knockdown	Validation of ischemia models XBP1 knockdown does not affect cell viability in ischemia or hypoxia models	Kraskiewicz and FitzGerald, 2011
Human embryonic kidney and mouse embryonic fibroblast cell culture	XBP1 overexpression and knockout	UPR target genes ERdj4 and $p58^{IPK}$ are XBP1-dependent Identification of other target genes (e.g., MANF)	Lee et al., 2003

BCAO, bilateral carotid artery occlusion; BIP/GRP78, binding immunoglobulin protein/glucose-regulated protein 78; BMSC, bone marrow mesenchymal stem cells; CHOP, C/EBP homologous protein; DANCR, differentiation antagonizing non-protein coding RNA; DETC-MeSO, S-methyl-N, N-diethyldithiocarbamate sulfoxide; ERK1/2-extracellular signal-regulated protein kinase 1/2; G-CSF, granulocyte colony-stimulating factor; GoF, gain of function; HAPI, highly aggressively proliferating immortalized rat microglia; HIF-1a, hypoxia-inducible factor 1-alpha; IL, interleukin; LoF, loss of function; LPS, lipopolysaccharide; MANF, mesencephalic astrocyte-derived neurotrophic factor; MCAo, middle cerebral artery occlusion; MMP, matrix metallopeptidase; OGD, oxygen-glucose deprivation; p-Akt, phosphorylated protein kinase B; PDGF-AA, platelet-derived growth factor-AA; p-IRE1, phosphorylated IRE1; pMCAo, permanent middle cerebral artery occlusion; rhMANF, recombinant human MANF; ROS, reactive oxygen species; TNF-α, tumor necrosis factor α; UDP-GlcNAc, uridine diphosphate N-acetylglucosamine; VEGF, vascular endothelial growth factor; XBP1, X-box binding protein; wt, wild type; ER, endoplasmic reticulum; OGD/R, oxygen-glucose deprivation and reoxygenation; UPR, unfolded protein response.

ATF6, eIF2α, Caspase 12, and CHOP close to the baseline level after 30 min of bilateral carotid artery occlusion (BCAO) (Modi et al., 2020).

XBP1 mRNA and protein expression is induced by oxygen and glucose deprivation (OGD) in rat oligodendrocyte precursor cells (OPCs) (Kraskiewicz and FitzGerald, 2011), brain microvascular endothelial cells (BMEC) (Shi et al., 2018; Zhang et al., 2020), and primary cortical neurons (Mo et al., 2020) *in vitro*. Surprisingly, XBP1 knockdown had no effect on viability following OGD (Kraskiewicz and FitzGerald, 2011). In a co-culture of microglia and neurons, OGD increased the production of inflammatory cytokines in microglia and apoptosis of primary neurons. Increased mRNA and protein levels of XBP1u and XBPs, as well as phosphorylation of IRE1a, were detected, while icariin, an anti-atherosclerotic drug, reversed the effect by decreasing cytokine production (Mo et al., 2020). In comparison, MANF protects neural stem cells against OGD (Tseng et al., 2018) while reducing the levels of IL-1β, IL-6, TNF-α, and GRP78 in astrocytes (Zhao et al., 2013).

Collectively, the research conducted thus far indicates activation of UPR and cell death pathways after ischemic stroke. In some cases, enhancing XBP1 is beneficial (e.g., 2-deoxyglucose and XBP1 dependent O-GlcNAc); in others, the beneficial effect was accompanied by reduction of XBP1. However, most of the tested compounds affected/modulated cell survival pathways and

were not specific for XBP1. Thus, more studies targeting the effect of XBP1s in stroke are needed.

In summary, the expression of MANF and XBP1 after stroke has been detected in several time points (**Figure 4**). As quantification of the data between publications is difficult, we used the number of publications reporting the expression of MANF or XBP1 at each time point as an indication of gene expression after stroke resulting in an "overexpression confidence" (**Figure 4**). MANF and XBP1 are both detected right after ischemic stroke, and their expression is still elevated even 2 weeks after the injury.

IMMUNOMODULATORY EFFECTS OF MANF

There is very strong evidence that MANF modulates inflammation both *in vitro* and *in vivo* in different disease models and in different model organisms (**Table 3**). Interestingly, the MANF protein is highly expressed in bone marrow and lymphoid tissues, and *Manf* mRNA is expressed in immune cells including microglia, monocytes, T-cells, B-cells, granulocytes, and dendritic cells to name a few, and the expression is especially high in plasma cells (Karlsson et al., 2021), which could implicate a role in immune cell function. Immune cell activation after ischemic stroke or systemic LPS has been shown to upregulate MANF in microglia (Shen et al., 2012; Sousa et al., 2018).

The main immunomodulatory effects by MANF recognized so far are: (1) downregulation of pro-inflammatory cytokine production *via* the NF-κB pathway, (2) alteration of phagocytic activity after ischemic stroke, and (3) induction of alternative activation of microglia/macrophages.

Mesencephalic astrocyte-derived neurotrophic factor has been shown to downregulate the NF-κB pathway and decrease pro-inflammatory cytokine production in several *in vitro* studies (Zhao et al., 2013; Chen et al., 2015; Zhu et al., 2016; Cunha et al., 2017; Hakonen et al., 2018; Liu et al., 2020; Han et al., 2021). There is a link between inflammation and ER stress, and activation of the IRE1α UPR pathway, and possibly other UPR pathways, can activate NF-κB (Chaudhari et al., 2014). It is, thus, plausible that endogenous MANF could downregulate NF-κB and downstream cytokine production indirectly by downregulating IRE1α and other UPR pathways in the ER. However, in some studies, MANF was suggested to be the link between ER stress and NF-κB pathway regulation, as direct interaction in the nucleus between endogenous MANF and the transcription factor NF-κB has been implicated (Chen et al., 2015; Liu et al., 2020). MANF is typically localized in the ER lumen, but based on studies with kidney and hepatic cell lines, it was suggested that the membrane protein SUMO1 (small ubiquitin-related modifier 1) would mediate MANF translocation to the nucleus upon ER stress/inflammation, and that the MANF C-terminal domain would inhibit the binding of NF-κB subunit p65 to the DNA (Chen et al., 2015; Liu et al., 2020). Nuclear colocalization of MANF and p65 was also found in liver tissue sections of patients with hepatocellular carcinoma (Liu et al., 2020). MANF was suggested to reduce NF-κB signaling and suppress cancer in hepatocytes (Liu et al., 2020). Yang et al. reported a colocalization of MANF and nuclear marker DAPI in the ischemic brain after transient MCAo in rats (Yang et al., 2020). However, the prevalence of MANF's nuclear localization is unknown, as it is reported only in few studies. Furthermore, MANF does not have a nuclear targeting sequence, and there is no evidence that exogenous MANF would translocate to the nucleus or that it would be taken up to the ER lumen from the extracellular space. Consequently, MANF has been proposed to bind neuroplastin in the plasma membrane and to block the NF-κB activating effect of neuroplastin (Yagi et al., 2020). It is noteworthy to mention that MANF occupied only about 5–6% of the receptor, and that shRNA for neuroplastin decreased this to 2–3%. This is not very typical receptor binding for proteins with a plasma membrane receptor, e.g., GDNF (Allen et al., 2013).

In an ischemic MCAo stroke model in aged mice of 18–20 months, intracerebroventricular injection of the recombinant MANF protein 2 h after MCAo decreased the production of pro-inflammatory cytokines in the infarct area, reduced neutrophil infiltration into the brain parenchyma, and decreased BBB damage 72 h post-stroke (Han et al., 2021). Using a mouse endothelial cell line, downregulation of the TLR/MyD88/NF-κB signaling pathway was suggested to be behind MANF's beneficial effect on BBB integrity (Han et al., 2021). In a rat model of traumatic brain injury, MANF treatment decreased the levels of pro-inflammatory cytokines around the contusion (Li et al., 2018). The recombinant MANF protein has been shown to decrease pro-inflammatory cytokines in the liver of old wild-type (WT) mice (Sousa-Victor et al., 2019), and there is evidence

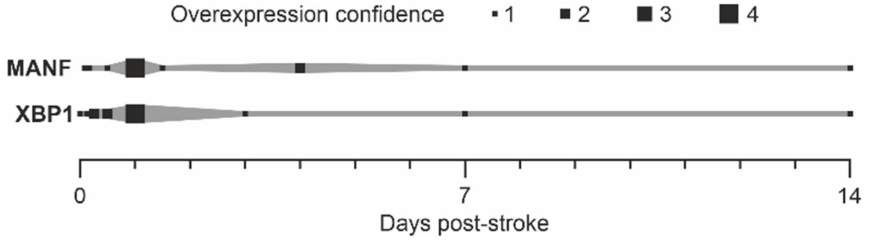

FIGURE 4 | Upregulation of MANF and XBP1 after stroke. "Overexpression confidence" = number of publications showing the upregulation of MANF or XBP1 after stroke (references: **Tables 1**, **2**).

TABLE 3 | Immunomodulatory effects of MANF.

Model	MANF therapy	Effect	References
Ischemia			
1 h MCAo in aged mice	rhMANF	IL-6, IL-1β, TNF-α ↓	Han et al., 2021
OGD on senescent bEnd.3 cells	rhMANF	IL-6, IL-1β, TNF-α ↓ TLR4, MyD88, nuclear NF-κB p65 ↓	Han et al., 2021
1 h dMCAo in rat	AAV1-MANF	S100A8; S100A9 ↓	Teppo et al., 2020
2 h MCAo in rat	MANF-knockdown BMSC transplant	M1 markers ↑ M2 markers ↓	Yang et al., 2020
1 h dMCAo in rat	AAV7-MANF	Number of CD68 + and Arg1 + cells ↑ *Emr1*; *C3* ↑	Matlik et al., 2018
OGD in primary rat astrocytes	rhMANF	IL-1β, IL-6, TNF-α ↓ GRP78, NF-κB p65 ↓	Zhao et al., 2013
MCAo in rat	–	MANF ↑ in microglia/macrophages	Shen et al., 2012
Other tissue damage			
Elective knee arthroplasty in patients	–	Negative correlation between MANF and cytokine levels in the serum after knee operation	Liu et al., 2021
Laparotomy in mouse	rhMANF	IL-1β, IL-6, TNF-α in serum and cortex ↓ Number of Iba1 + and iNOS + cells in cortex ↓	Liu et al., 2021
Light-induced retinal damage in an aging mouse	rhMANF	CD68 + cells in retina ↓	Neves et al., 2020
Alcohol-induced liver injury	–	MANF expression ↑	Chhetri et al., 2020
Liver cancer in humans	–	Colocalization with NF-κB subunit p65 Low MANF levels associated with poor survival	Liu et al., 2020
Old WT mouse	rhMANF or plasmid	Liver inflammation and damage ↓	Sousa-Victor et al., 2019
TBI in rat	rhMANF	IL-1β; TNF-α; NF-κB ↓	Li et al., 2018
Light-induced retinal damage in *D. melanogaster* and mouse	rhMANF	Alternative activation of innate immune cells ↑	Neves et al., 2016
Inflammation			
LPS-induced kidney injury in mouse		CD68 + cells in MANF ko ↑	Hou et al., 2021
LPS-induced myocarditis in mouse	rhMANF	Pro-inflammatory markers in myocardium tissue ↓ CD68 + and CCL2 + cells in myocardium tissue ↓	Wang et al., 2021a
LPS-induced C6, MEF, and INS-1E cells	rhMANF	MANF downregulated NF-κB activation via neuroplastin	Yagi et al., 2020
Cytokine-induced damage in human β cells	rhMANF	Apoptosis ↓ NF-κB pathway ↓ UPR ↓	Cunha et al., 2017; Hakonen et al., 2018
LPS-injected mice	–	*Manf* ↑ in microglia	Sousa et al., 2018
TNF-α-induced 293T cells LPS-induced rat primary FLS	plasmid rhMANF –	NF-κB ↓ IL-1β, TNF-α ↓ Interaction between MANF and p65 in nucleus	Chen et al., 2015
Manf removal			
Monocyte-macrophage-specific MANF KO mouse	LPS-induced kidney injury	CD68 + and CCL2 + cells in kidney ↑ Pro-inflammatory markers in kidney, serum, and peritoneal macrophages ↑ NF-κB activation in kidney ↑	Hou et al., 2021
Monocyte-macrophage-specific MANF KO mouse	LPS-induced myocarditis	Pro-inflammatory markers in serum and myocardium tissue ↑ CD68 + and CCL2 + cells in myocardium tissue ↑ NF-κB activation in myocardium tissue ↑	Wang et al., 2021a

(Continued)

TABLE 3 | (Continued)

Model	MANF therapy	Effect	References
MANF heterozygous mouse	–	CD68 + cells in retinal choroid ↑	Neves et al., 2020
MANF knockdown in C6 cells	–	NF-κB activation ↑	Yagi et al., 2020
Hepatocyte-specific MANF KO mouse	Alcohol-induced liver injury	Liver injury and inflammation ↑ ER stress ↑ Oxidative stress ↑	Chhetri et al., 2020
MANF knockdown in *C. elegans*	–	Changes in innate immunity-related gene expression Altered growth in the presence of bacteria	Hartman et al., 2019
Monocyte-macrophage-specific MANF KO mouse	–	Healthy: Number of M1 macrophages in the spleen ↑ Hepatic fibrosis: Number of M2 macrophages in the spleen ↑	Hou et al., 2019
MANF heterozygous mouse	-	Liver inflammation and damage ↑	Sousa-Victor et al., 2019
Hepatocyte-specific MANF KO mouse	–	Liver IL-1α, TNF-α ↑	Liu et al., 2020
MANF knockdown in 293T cells	–	IL-1β, TNF-α ↑ NF-κB ↑	Chen et al., 2015
Glial DmMANF knockdown in *D. melanogaster*	–	Appearance of new DmMANF + microglia-like cell type	Stratoulias and Heino, 2015b
MANF-deficient *D. melanogaster*	–	Immune and defense response-related genes ↑	Palgi et al., 2012
Other			
S. domuncula	–	SDMANF colocalization with Toll-like receptor	Sereno et al., 2017

AAV, adeno-associated virus; Arg1, arginase 1; C3, complement component 3; CCL2, C-C motif chemokine ligand 2; CD68, cluster of differentiation 68, dMCAo, distal middle cerebral artery occlusion; Emr1, EGF module-containing mucin-like receptor; FLS, fibroblast-like synoviocytes; GRP78, 78-kDa glucose-regulated protein; Iba1, ionized calcium-binding adaptor molecule 1; IL, interleukin; iNOS, inducible nitric oxide synthase; KO, knockout; LPS, lipopolysaccharide; M1, classically activated microglia/macrophages; M2, alternatively activated microglia/macrophages; MAPK, mitogen-activated protein kinase; MCAo, middle cerebral artery occlusion; MEF, mouse embryonic fibroblast; MyD88, myeloid differentiation factor 88; NF-κB, nuclear factor kappa-light-chain-enhancer of activated B cells; NSC, neural stem cell; OGD, oxygen-glucose deprivation; S100A8, calgranulin A; S100A9, calgranulin B; TBI, traumatic brain injury; TLR4, toll-like receptor 4; TNF-α, tumor necrosis factor α; UPR, unfolded protein response; WT, wild type; BMSC, bone marrow mesenchymal stem cells; Dm, Drosophila melanogaster; ER, endoplasmic reticulum; MANF, mesencephalic astrocyte-derived neurotrophic factor; rhMANF, recombinant human MANF; SD, Suberites domuncula.

from MANF KO mice that the inflammation is increased in the liver upon removal (Chhetri et al., 2020) or downregulation of *Manf* (Sousa-Victor et al., 2019). Removal of MANF from macrophages was shown to increase pro-inflammatory macrophages in the healthy spleen (Hou et al., 2019), and upon LPS treatment in the kidney (Hou et al., 2021) and myocardium tissue (Wang et al., 2021a). Recombinant MANF was able to downregulate inflammation in KO mice after myocarditis (Wang et al., 2021a). Furthermore, intraperitoneal injection of the recombinant MANF protein was shown to downregulate pro-inflammatory cytokines in the serum and prefrontal cortex after abdominal operation in WT mice (Liu et al., 2021). The finding in the brain is interesting, since the brain was not manipulated in any way, and indicates inflammatory crosstalk between the periphery and the CNS, which is a contributing factor in stroke pathogenesis as well. In patients, the same study found implications of a negative correlation between endogenous MANF protein levels and cytokine levels in the serum after knee operation, indicating that low MANF serum levels may contribute to postoperative systemic inflammation (Liu et al., 2021). Another patient study found elevated *Manf* mRNA levels in leukocytes in inflammatory diseases such as rheumatoid arthritis and systemic lupus erythematosus (Chen et al., 2015).

We have shown that Arg1-positive (arginase 1) and phagocytic CD68-positive cells are increased after viral vector-mediated MANF gene delivery in a rat dMCAo cortical ischemic stroke model (Matlik et al., 2018), coinciding with elevated brain repair processes after stroke. Increased number of these innate immune cells was observed in the external capsule and dorsal striatum on post-stroke day 4 after peri-infarct area-targeted MANF gene delivery. The effect was transient, as on day 14 post-stroke there were no differences in the amount of Arg1- or CD68-positive cells in the peri-infarct region. By double immunofluorescence on day 4 post-stroke, the amount of MBP (myelin basic protein) and CD68 double-positive cells was increased in the external capsule of AAV7-MANF-treated rats compared to the AAV7-GFP control group, indicating enhanced phagocytosis of myelin debris after AAV7-MANF treatment. The mRNA levels of innate immunity-related genes *EGF module-containing mucin-like receptor 1 (Emr1)* and *complement component 3 (C3)* were upregulated in the lateral peri-infarct cortex of AAV7-MANF-treated rats at the same time point. However, the mRNA levels of myeloid cell "alternative activation" marker genes *Tgfb1* and *mannose receptor C-type 1 (Mrc1* a.k.a. *CD206)* were unchanged.

Using the same approach of expressing the MANF transgene in the peri-infarct region in the rat dMCAo model (Matlik

et al., 2018), we conducted multiomics to study the effects of peri-infarct-targeted AAV1-MANF administration 2 days post-stroke (Teppo et al., 2020). The peri-infarct region was sampled 4 days post-stroke and subjected to untargeted transcriptomics, proteomics, and metabolomics analyses. The most notable effect of MANF was upregulation of transcripts related to immune response, especially toward virus, that could be detected despite the massive inflammation caused by the stroke itself. Interestingly, this effect was not observed with AAV7-MANF, suggesting that it is serotype-specific. The cause for this remains unknown but can be due to the serotypes' differences in transduction efficiency, time frame, or tissue/cell type specificity. In addition, MANF reversed the stroke-induced upregulation of the innate immunity proteins S100A8 and S100A9, which are highly expressed in phagocytic cells, involved in phagocyte recruitment and released from phagocytes upon activation. By double immunofluorescence, S100A9 was localized to cells resembling neutrophils, but the number of S100A9-positive cells in the peri-infarct region was unchanged between the MANF and eGFP (enhanced green fluorescent protein) control groups. The observed changes can be due to altered RNA and protein dynamics or, more likely, altered proportions of cell populations in the peri-infarct region. Although the mechanisms require further study, both results provide further evidence of the immunomodulatory effects of MANF.

MANF has been found to induce alternative activation of microglia/macrophages, which is considered beneficial in the repair processes of tissue injury. In retinal damage in mice and *D. melanogaster*, the recombinant MANF protein increased the number of alternatively activated pro-regenerative/anti-inflammatory innate immune cells, protected from retinal degeneration, and promoted integration of transplanted photoreceptors (Neves et al., 2016). Importantly, MANF was also shown to modulate inflammation in the retina of aging mice by downregulating the number of CD68-positive cells and similarly protect the retina from degeneration and promote the integration after retinal transplantation in aged mice (Neves et al., 2020). Interestingly, Neves et al. suggested that CX3CR1 is needed for MANF-induced cytoprotection and immunomodulation, as the protective effect was abolished in CX3CR1 KO mouse retina and MANF failed to induce alternative activation in primary macrophage cultures from these mice (Neves et al., 2016). Similarly, in *D. melanogaster*, hemocyte-specific knockdown of the KDEL receptor abolished endogenous MANF's protective and immunomodulatory effect. Thus, this is another evidence that KDELRs are needed to keep the endogenous MANF in the ER lumen where it acts. Furthermore, MANF was found to be the key regulator in bone marrow mesenchymal stem cell (BMSC)-mediated alternative activation ("M2" polarization) of microglia/macrophages (Yang et al., 2020). In a rat transient MCAo model, treatment with WT BMSCs enhanced behavioral recovery, decreased infarct volume, and increased "M2" polarization, while knockdown of MANF from BMSCs abolished the beneficial effects. Additionally, the BMSC-treated animals had higher number of MANF-positive and Arg1-positive "M2" microglia/macrophages and lower number of iNOS-positive pro-inflammatory "M1" microglia/macrophages than the vehicle-treated or BMSC-MANF knockdown ones 24 h post-MCAo, indicating that the exogenous MANF secreted by BMSCs could act in a paracrine manner and enhance endogenous MANF protein expression in myeloid cells and polarize these immune cells toward the anti-inflammatory "M2" state. However, conflicting results were found in macrophage-specific MANF KO mice with hepatic fibrosis, where the number of alternatively activated spleen macrophages was increased in the MANF KO compared to WT mice (Hou et al., 2019).

Collectively, MANF has immunomodulatory effects, which may be important for the therapeutic function of MANF under different disease conditions. Our results with unbiased methods also clearly demonstrate toward this direction. Mostly, MANF has been shown to downregulate inflammation and removal of *Manf* to increase inflammation in different tissues and cell lines. However, in ischemic stroke, we have reported that MANF induced a transient increase in CD68-positive innate immune cells, which is likely beneficial for tissue repair (Matlik et al., 2018). Therefore, MANF may have a general function aiming to restore tissue homeostasis under pathological conditions. Notably, it has been proposed that MANF affects immune cells in an autocrine/paracrine manner, thus inducing a phenotypic shift toward reparative functions (Neves et al., 2016; Yang et al., 2020). We hypothesize that when MANF is released from injured cells upon ER Ca^{2+} depletion, the released MANF could modulate the immune cell phenotype and, in ischemic stroke, the recruitment of phagocytic cells to the area of injury.

NEUROGENESIS

Previously, neurogenesis was thought to occur only during embryonic and perinatal development. However, research findings in the past decade have made it clear that neurogenesis is a process that occurs throughout adulthood, ensuring lost neurons are being replaced by new ones in distinct parts of the brain (Ming and Song, 2011). There are two neurogenic regions in the brain: the subventricular zone (SVZ) and the subgranular layer (SGL) of the hippocampus. In the central nervous system, the SVZ and the SGL regions maintain a distinct population of neural stem cells (NSCs) that show multipotency and higher plasticity. NSCs located in the SVZ give rise to neural progenitor cells (NPCs), giving rise to neuroblasts. From there, these neuroblasts migrate through the rostral migratory system into the olfactory bulb, where they become periglomerular neurons or granules throughout the whole period of adulthood. Newly formed neurons in the process of neurogenesis have diverse and multifaceted functions ensuring olfaction and hippocampal-mediated learning and memory (Aimone et al., 2014). Various factors influence this neurogenesis process, including aging, Alzheimer's disease, Parkinson's disease, and stroke. Therapeutic interventions to ensure neurogenesis under different conditions have been a significant area of focus in the field of biomedical research.

In the past, the MANF protein was shown to be predominantly expressed in neuronal lineage cells of the mammalian cortex (Lindholm et al., 2008). Meanwhile, under ischemic or hypoxic

conditions, MANF is inducible in glial cells, which are essential for maintaining homeostatic condition and neuronal activity (Shen et al., 2012). Although deletion of *Manf* does not affect the generation of cortical neurons in the developing cortex, it causes a deficit in neurite outgrowth, especially neurofilament-expressed axonal extension (Tseng et al., 2017). In addition, delayed subtype neuron specification and abnormal neuronal density accompanied by 10% reduction of *Manf* KO cortical thickness were found during corticogenesis, suggesting that loss of MANF leads to aberrant neuronal migration and differentiation (Tseng et al., 2017). Showing clinical relevance, the symptoms of a patient with type 2 diabetes mellitus, hypothyroidism, primary hypogonadism, short stature, mild intellectual disability, obesity, deafness, high myopia, microcephaly, and partial alopecia were likely caused by a mutation in MANF (Yavarna et al., 2015). Similar symptoms of deafness, developmental delay, microcephaly, and short stature were found in two patients with childhood-onset diabetes lacking MANF because of mutation in the *Manf* gene (Montaser et al., 2021). In short, endogenous MANF is involved in neuronal migration and neurite outgrowth and may play a crucial role in cortical development. However, it does not seem to affect neurogenesis by modulating the proliferation of neuronal stem cells. To further elucidate the mechanistic action of MANF in neuronal migration, the level of MANF in SVZ explants was manipulated by deleting *Manf*. SVZ cells lacking MANF showed a shorter distance of migration compared with WT cells. Also, we found that administration of MANF could induce neural/glial differentiation accompanied by morphological change in bipolar shape as well as promotion of cell migration in our SVZ explants (Tseng et al., 2018). Furthermore, deletion of *Manf* in NPC cultures was shown to activate UPR signals during neuronal differentiation. These data were among the first to show that UPR can regulate neurogenesis and brain development. This study again suggests a critical role of MANF in ER homeostasis, which is implicated in differentiation of NPCs, development of neurite-like processes, and, subsequently, migration of neuronal cells. It should be noted that the ER extends all the way to the tip of the processes in a neuron (Sree et al., 2021), and that migration of cells and extension of the ER during neuronal development result in enhanced need for ER homeostasis. Although many studies assume that MANF mediates trophic effects in neuronal cells, further studies will be required to address a more mechanistic understanding of MANF's effect on neurogenesis during brain development.

In previous studies, MANF protein expression was shown to be robustly increased after MCAo (Belayev et al., 2020), and increasing MANF abundance could improve neurobehavioral recovery by means of promoting neuronal survival and modulation of innate immune cells (Matlik et al., 2018). Also, application of the exogenous MANF protein can promote NPC differentiation *in vitro* as well as migration toward the infarct boundary *in vivo* (Tseng et al., 2018). Furthermore, MANF has been shown to have immunomodulatory properties to improve the success of cell-replacement regenerative therapies in a mouse model of degenerative retina (Neves et al., 2016). This neuroregenerative capacity of MANF might be attributed to faster clearance of dead cells and improve the microenvironment. Further studies should be conducted to explore the molecular mechanisms involved in MANF's regulation of these processes, which may lead to the development of more efficient therapeutic approaches for patients with stroke.

FUTURE PERSPECTIVES

Although studies have proven MANF's pleiotropic therapeutic effect in several disease models and tissues, the molecular mechanism of action of MANF remains a conundrum. MANF is a neuro-restorative, immunomodulatory protein, and it facilitates behavioral recovery after stroke. As an ER lumen resident protein and a factor needed for maintaining the homeostasis of the ER, the ER is probably the main site of action, but the secretion of MANF and exogenous activity indicate that the mechanism of action is more complicated. The initial hypothesis was that MANF works in the ER to enhance survival/prevent apoptosis. Indeed, the main target of MANF in the ER seems to be UPR modulation *via* the IRE1 pathway in collaboration with other ER proteins (e.g., GRP78 and PDI6), but MANF could also mediate protein transport to/into mitochondria (interaction with CH60) and/or the cytoplasm (KCRB and PGAM). The localization of MANF has been determined based on co-staining with ER resident proteins (e.g., Hrd1, PDI, and GRP78, not always ideally superimposing); thus the interaction of MANF with proteins located in the cytoplasm and mitochondria in other cell types requires further studies, and particularly we should show localization of endogenous MANF by electron microscopy.

MANF interacts with GRP78, PDI6, and ATP, all modulating UPR activation in a specific manner; thus, MANF functions as a negative feedback regulator fine-tuning ER homeostasis. However, in the brain, *Manf* mRNA is expressed in many cells at high level, but the MANF protein is expressed only in neurons. This is reversed in the case of an injury, indicating cellular differences that may be originating from the complexity of the ER and may provide a protective mechanism in case of a disturbance at tissue level. It should be studied further, are high mRNA levels of *Manf* present in a cell as a resource to translate it promptly when needed? Also, it is not known why or how the elevated levels of *Manf* mRNA are maintained in glial cells. In addition, we should investigate whether the phenomenon observed in our model systems also exists in human cells, as even for conserved proteins this is not always the case. Since the mechanism of action for MANF seems to be broad, we should be careful and accurate when discussing ER luminal effects or extracellular effects of MANF. As it is well-known that proteins can interact with many partners after overexpression, it is important to perform studies at physiologically relevant concentrations when we investigate and determine the mechanism of action of MANF. In the ER lumen, MANF has been shown to act as an ER chaperone, and other mechanisms of action have been postulated. We should further clarify what the primary functions of the native protein are, e.g., is it so that the majority of proteins is fulfilling some function in homeostasis and the minority is doing something else, and how the function/action changes during increased folding

load demand in the ER lumen. Furthermore, when clarifying the mechanisms of action, we should implement pharmacological inhibitors, activators, siRNA and overexpression, and CRISPR deletion experiments to show robustly that the downstream effect is mediated *via* proposed way. Instead of conducting more correlative studies, it would be more beneficial to actually show the mechanism of action with tools that are already available.

Comparative studies on MANF in combination with XBP1 would shed more light on whether and how the pathways are connected and what the mechanism is, and how the modulation of UPR and inflammatory pathways improves recovery. Also, more studies would be needed where the IRE1 pathway is inhibited, deleted, increased, or overexpressed together with MANF administration to reveal whether XBP1 is mediating MANF's beneficial effects. As stroke is more prevalent in the elderly and aging causes reduced protein folding capacity, it would be of interest to discover how the regulation of XBP1 and MANF (and/or interactions) remains the same in aged animals. Innovative technologies for single-cell analysis are emerging, and they could provide more information on functional similarities and differences in cellular level *in vivo*. Alternatively, isolation of the nucleus and snRNA-seq could be conducted. Cell isolation and separation are lengthy processes, thus, one option would be to use primary cell cultures (e.g., microglia, astrocytes) or iPSC of neurons (as isolation of intact neurons is difficult) to study the underlying molecular mechanisms. Still, all new genomic tools will enhance data load but may not be specific enough to detect genes of interest. We would need to develop specific antibodies for all UPR arm proteins that could be used to study how UPR is regulated in a time-dependent manner after stroke in the peri-infarct area and in which cells. Furthermore, it would be important to clarify which UPR arms are activated in dendrites, axons, and presynaptic and postsynaptic terminals after ischemic injury. Lastly, we should determine the role of UPR in a cell-specific manner and take into account whether chronic increase in ER folding quantity or quality can lead to degeneration of a cell.

AUTHOR CONTRIBUTIONS

HL and MA conceived the review. HL, JA, H-KL, K-YT, JT, VS, and MA wrote the manuscript. All authors revised and approved the final version of the manuscript for submission.

FUNDING

HL was funded by the Academy of Finland (Grant No: 322757), JA was funded under the Academy of Finland PROFI6 project UHBRAIN, and JT was funded by the Academy of Finland (Grant No: 321472). MA was funded by Academy of Finland, 324177, PROFI 5 project FinPharma, Neuroscience Center, HiLIFE, University of Helsinki and Sigrid Juselius Foundation.

REFERENCES

Aimone, J. B., Li, Y., Lee, S. W., Clemenson, G. D., Deng, W., and Gage, F. H. (2014). Regulation and function of adult neurogenesis: from genes to cognition. *Physiol. Rev.* 94, 991–1026. doi: 10.1152/physrev.00004.2014

Airavaara, M., Chiocco, M. J., Howard, D. B., Zuchowski, K. L., Peranen, J., Liu, C., et al. (2010). Widespread cortical expression of MANF by AAV serotype 7: localization and protection against ischemic brain injury. *Exp. Neurol.* 225, 104–113. doi: 10.1016/j.expneurol.2010.05.020

Airavaara, M., Shen, H., Kuo, C. C., Peranen, J., Saarma, M., Hoffer, B., et al. (2009). Mesencephalic astrocyte-derived neurotrophic factor reduces ischemic brain injury and promotes behavioral recovery in rats. *J. Comp. Neurol.* 515, 116–124. doi: 10.1002/cne.22039

Albert, K., and Airavaara, M. (2019). Neuroprotective and reparative effects of endoplasmic reticulum luminal proteins – mesencephalic astrocyte-derived neurotrophic factor and cerebral dopamine neurotrophic factor. *Croatian Med. J.* 60, 99–109. doi: 10.3325/cmj.2019.60.99

Allen, S. J., Watson, J. J., Shoemark, D. K., Barua, N. U., and Patel, N. K. (2013). GDNF, NGF and BDNF as therapeutic options for neurodegeneration. *Pharmacol. Therapeutics* 138, 155–175. doi: 10.1016/j.pharmthera.2013.01.004

Anttila, J. E., Poyhonen, S., and Airavaara, M. (2019). Secondary Pathology of the Thalamus after Focal Cortical Stroke in Rats is not Associated with Thermal or Mechanical Hypersensitivity and is Not Alleviated by Intra-Thalamic Post-Stroke Delivery of Recombinant CDNF or MANF. *Cell Trans.* 28, 425–438. doi: 10.1177/0963689719837915

Apostolou, A., Shen, Y., Liang, Y., Luo, J., and Fang, S. (2008). Armet, a UPR-upregulated protein, inhibits cell proliferation and ER stress-induced cell death. *Exp. Cell Res.* 314, 2454–2467. doi: 10.1016/j.yexcr.2008.05.001

Arrieta, A., Blackwood, E. A., Stauffer, W. T., Santo Domingo, M., Bilal, A. S., Thuerauf, D. J., et al. (2020). Mesencephalic astrocyte-derived neurotrophic factor is an ER-resident chaperone that protects against reductive stress in the heart. *J. Biol. Chem.* 295, 7566–7583. doi: 10.1074/jbc.RA120.013345

Bai, M., Vozdek, R., Hnízda, A., Jiang, C., Wang, B., Kuchar, L., et al. (2018). Conserved roles of C. elegans and human MANFs in sulfatide binding and cytoprotection. *Nat. Commun* 9:897 doi: 10.1038/s41467-018-03355-0

Behnke, J., Feige, M. J., and Hendershot, L. M. (2015). BiP and its nucleotide exchange factors Grp170 and Sil1: mechanisms of action and biological functions. *J. Mol. Biol.* 427, 1589–1608. doi: 10.1016/j.jmb.2015.02.011

Belayev, L., Hong, S. H., Freitas, R. S., Menghani, H., Marcell, S. J., Khoutorova, L., et al. (2020). DHA modulates MANF and TREM2 abundance, enhances neurogenesis, reduces infarct size, and improves neurological function after experimental ischemic stroke. *CNS Neurosci. Ther.* 26, 1155–1167. doi: 10.1111/cns.13444

Bell, P. A., Dennis, E. P., Hartley, C. L., Jackson, R. M., Porter, A., Boot-Handford, R. P., et al. (2018). Mesencephalic astrocyte-derived neurotropic factor is an important factor in chondrocyte ER homeostasis. *Cell Stress Chaper.* 24, 159–173. doi: 10.1007/s12192-018-0953-7

Bertolotti, A., Zhang, Y., Hendershot, L. M., Harding, H. P., and Ron, D. (2000). Dynamic interaction of BiP and ER stress transducers in the unfolded-protein response. *Nat. Cell Biol.* 2, 326–332. doi: 10.1038/35014014

Božok, V., Yu, L.-Y., Palgi, J., and Arumäe, U. (2018). Antioxidative CXXC Peptide Motif From Mesencephalic Astrocyte-Derived Neurotrophic Factor Antagonizes Programmed Cell Death. *Front. Cell Dev. Biol.* 6:106. doi: 10.3389/fcell.2018.00106

Calfon, M., Zeng, H., Urano, F., Till, J. H., Hubbard, S. R., Harding, H. P., et al. (2002). IRE1 couples endoplasmic reticulum load to secretory capacity by processing the XBP-1 mRNA. *Nature* 415, 92–96. doi: 10.1038/415092a

Campbell, B. C. V., De Silva, D. A., Macleod, M. R., Coutts, S. B., Schwamm, L. H., Davis, S. M., et al. (2019). Ischaemic stroke. *Nat. Rev. Dis. Primers* 5:70.

Chaudhari, N., Talwar, P., Parimisetty, A., Lefebvre d'Hellencourt, C., and Ravanan, P. (2014). A molecular web: endoplasmic reticulum stress, inflammation, and oxidative stress. *Front. Cell Neurosci.* 8:213. doi: 10.3389/fncel.2014.00213

Chen, L., Feng, L., Wang, X., Du, J., Chen, Y., Yang, W., et al. (2015). Mesencephalic astrocyte-derived neurotrophic factor is involved in inflammation by negatively regulating the NF-kappaB pathway. *Sci. Rep.* 5:8133. doi: 10.1038/srep08133

Chen, Y. C., Sundvik, M., Rozov, S., Priyadarshini, M., and Panula, P. (2012). MANF regulates dopaminergic neuron development in larval zebrafish. *Dev. Biol.* 370, 237–249. doi: 10.1016/j.ydbio.2012.07.030

Chhetri, G., Liang, Y., Shao, J., Han, D., Yang, Y., Hou, C., et al. (2020). Role of Mesencephalic Astrocyte-Derived Neurotrophic Factor in Alcohol-Induced Liver Injury. *Oxid Med. Cell Longev.* 2020:9034864. doi: 10.1155/2020/9034864

Clamp, M., Cuff, J., Searle, S. M., and Barton, G. J. (2004). The Jalview Java alignment editor. *Bioinformatics* 20, 426–427. doi: 10.1093/bioinformatics/btg430

Collaborators, G. B. D. S. (2021). Global, regional, and national burden of stroke and its risk factors, 1990-2019: a systematic analysis for the Global Burden of Disease Study 2019. *Lancet Neurol.* 20, 795–820. doi: 10.1016/S1474-4422(21)00252-0

Cunha, D. A., Cito, M., Grieco, F. A., Cosentino, C., Danilova, T., Ladriere, L., et al. (2017). Pancreatic beta-cell protection from inflammatory stress by the endoplasmic reticulum proteins thrombospondin 1 and mesencephalic astrocyte-derived neutrotrophic factor (MANF). *J. Biol. Chem.* 292, 14977–14988. doi: 10.1074/jbc.M116.769877

Danilova, T., Galli, E., Pakarinen, E., Palm, E., Lindholm, P., Saarma, M., et al. (2019b). Mesencephalic Astrocyte-Derived Neurotrophic Factor (MANF) Is Highly Expressed in Mouse Tissues With Metabolic Function. *Front. Endocrinol.* 10:765. doi: 10.3389/fendo.2019.00765

Danilova, T., Belevich, I., Li, H., Palm, E., Jokitalo, E., Otonkoski, T., et al. (2019a). MANF Is Required for the Postnatal Expansion and Maintenance of Pancreatic β-Cell Mass in Mice. *Diabetes* 68, 66–80.

Eesmaa, A., Yu, L. Y., Goos, H., Noges, K., Kovaleva, V., Hellman, M., et al. (2021). The cytoprotective protein MANF promotes neuronal survival independently from its role as a GRP78 cofactor. *J. Biol. Chem.* 296:100295. doi: 10.1016/j.jbc.2021.100295

Feng, S.-Q., Zong, S.-Y., Liu, J.-X., Chen, Y., Xu, R., Yin, X., et al. (2019). VEGF Antagonism Attenuates Cerebral Ischemia/Reperfusion-Induced Injury *via* Inhibiting Endoplasmic Reticulum Stress-Mediated Apoptosis. *Biol. Pharmaceutical Bull.* 42, 692–702.
0

Foufelle, F., and Fromenty, B. (2016). Role of endoplasmic reticulum stress in drug-induced toxicity. *Pharmacol. Res. Perspect.* 4:e00211. doi: 10.1002/prp2.211

Galli, E., Harkonen, T., Sainio, M. T., Ustav, M., Toots, U., Urtti, A., et al. (2016). Increased circulating concentrations of mesencephalic astrocyte-derived neurotrophic factor in children with type 1 diabetes. *Sci. Rep.* 6:29058. doi: 10.1038/srep29058

Galli, E., Planken, A., Kadastik-Eerme, L., Saarma, M., Taba, P., and Lindholm, P. (2019a). Increased Serum Levels of Mesencephalic Astrocyte-Derived Neurotrophic Factor in Subjects With Parkinson's Disease. *Front. Neurosci.* 13:929. doi: 10.3389/fnins.2019.00929

Galli, E., Rossi, J., Neumann, T., Andressoo, J. O., Drinda, S., and Lindholm, P. (2019b). Mesencephalic Astrocyte-Derived Neurotrophic Factor Is Upregulated with Therapeutic Fasting in Humans and Diet Fat Withdrawal in Obese Mice. *Sci. Rep.* 9:14318. doi: 10.1038/s41598-019-50841-6

Gao, B., Deng, J., Zhang, X., Sun, H., Jia, G., Li, J., et al. (2020). Effects of mesencephalic astrocyte-derived neurotrophic factor on cerebral angiogenesis in a rat model of cerebral ischemia. *Neurosci. Lett.* 715:134657. doi: 10.1016/j.neulet.2019.134657

Gao, F. J., Wu, J. H., Li, T. T., Du, S. S., and Wu, Q. (2017). Identification of Mesencephalic Astrocyte-Derived Neurotrophic Factor as a Novel Neuroprotective Factor for Retinal Ganglion Cells. *Front. Mol. Neurosci.* 10:76. doi: 10.3389/fnmol.2017.00076

Gao, F. J., Zhang, S. H., Li, T. T., Wu, J. H., and Wu, Q. (2016). Expression and Distribution of Mesencephalic Astrocyte-Derived Neurotrophic Factor in the Retina and Optic Nerve. *Front. Hum. Neurosci.* 10:686. doi: 10.3389/fnhum.2016.00686

Gharibani, P., Modi, J., Menzie, J., Alexandrescu, A., Ma, Z., Tao, R., et al. (2015). Comparison between single and combined post-treatment with S-Methyl-N,N-diethylthiolcarbamate sulfoxide and taurine following transient focal cerebral ischemia in rat brain. *Neuroscience* 300, 460–473. doi: 10.1016/j.neuroscience.2015.05.042

Gharibani, P. M., Modi, J., Pan, C., Menzie, J., Ma, Z., Chen, P. C., et al. (2013). The mechanism of taurine protection against endoplasmic reticulum stress in an animal stroke model of cerebral artery occlusion and stroke-related conditions in primary neuronal cell culture. *Adv. Exp. Med. Biol.* 776, 241–258. doi: 10.1007/978-1-4614-6093-0_23

Glembotski, C. C., Rosarda, J. D., and Wiseman, R. L. (2019). Proteostasis and Beyond: ATF6 in Ischemic Disease. *Trends Mol. Med.* 25, 538–550. doi: 10.1016/j.molmed.2019.03.005

Glembotski, C. C., Thuerauf, D. J., Huang, C., Vekich, J. A., Gottlieb, R. A., and Doroudgar, S. (2012). Mesencephalic astrocyte-derived neurotrophic factor protects the heart from ischemic damage and is selectively secreted upon sarco/endoplasmic reticulum calcium depletion. *J. Biol. Chem.* 287, 25893–25904. doi: 10.1074/jbc.M112.356345

Grassi, S., Prioni, S., Cabitta, L., Aureli, M., Sonnino, S., and Prinetti, A. (2015). The Role of 3-O-Sulfogalactosylceramide, Sulfatide, in the Lateral Organization of Myelin Membrane. *Neurochem. Res.* 41, 130–143. doi: 10.1007/s11064-015-1747-2

Gu, J., Chen, J., Yang, N., Hou, X., Wang, J., Tan, X., et al. (2016). Combination of Ligusticum chuanxiong and Radix Paeoniae ameliorate focal cerebral ischemic in MCAO rats via endoplasmic reticulum stress-dependent apoptotic signaling pathway. *J. Ethnopharmacol.* 187, 313–324. doi: 10.1016/j.jep.2016.04.024

Hakonen, E., Chandra, V., Fogarty, C. L., Yu, N. Y., Ustinov, J., Katayama, S., et al. (2018). MANF protects human pancreatic beta cells against stress-induced cell death. *Diabetologia* 61, 2202–2214. doi: 10.1007/s00125-018-4687-y

Han, D., Li, F., Zhang, H., Ji, C., Shu, Q., Wang, C., et al. (2021). Mesencephalic astrocyte-derived neurotrophic factor restores blood–brain barrier integrity of aged mice after ischaemic stroke/reperfusion through anti-inflammation via TLR4/MyD88/NF-κB pathway. *J. Drug Target.* 30:430–441. doi: 10.1080/1061186X.2021.2003803

Hao, F., Yang, C., Chen, S. S., Wang, Y. Y., Zhou, W., Hao, Q., et al. (2017). Long-term protective effects of AAV9-mesencephalic astrocyte-derived neurotrophic factor gene transfer in parkinsonian rats. *Exp. Neurol.* 291, 120–133. doi: 10.1016/j.expneurol.2017.01.008

Hartman, J. H., Richie, C. T., Gordon, K. L., Mello, D. F., Castillo, P., Zhu, A., et al. (2019). MANF deletion abrogates early larval Caenorhabditis elegans stress response to tunicamycin and *Pseudomonas aeruginosa*. *Eur. J. Cell Biol.* 98:151043 doi: 10.1016/j.ejcb.2019.05.002

Hellman, M., Arumae, U., Yu, L. Y., Lindholm, P., Peranen, J., Saarma, M., et al. (2011). Mesencephalic astrocyte-derived neurotrophic factor (MANF) has a unique mechanism to rescue apoptotic neurons. *J. Biol. Chem.* 286, 2675–2680. doi: 10.1074/jbc.M110.146738

Henderson, M. J., Richie, C. T., Airavaara, M., Wang, Y., and Harvey, B. K. (2013). Mesencephalic astrocyte-derived neurotrophic factor (MANF) secretion and cell surface binding are modulated by KDEL receptors. *J. Biol. Chem.* 288, 4209–4225. doi: 10.1074/jbc.M112.400648

Henderson, M. J., Trychta, K. A., Yang, S. M., Back, S., Yasgar, A., and Wires, E. S. (2021). A target-agnostic screen identifies approved drugs to stabilize the endoplasmic reticulum-resident proteome. *Cell Rep.* 35:109040. doi: 10.1016/j.celrep.2021.109040

Hetz, C., Martinon, F., Rodriguez, D., and Glimcher, L. H. (2011). The Unfolded Protein Response: Integrating Stress Signals Through the Stress Sensor IRE1α. *Physiol. Rev.* 91, 1219–1243. doi: 10.1152/physrev.00001.2011

Hetz, C., Zhang, K., and Kaufman, R. J. (2020). Mechanisms, regulation and functions of the unfolded protein response. *Nat. Rev. Mol. Cell Biol.* 21, 421–438. doi: 10.1038/s41580-020-0250-z

Hou, C., Mei, Q., Song, X., Bao, Q., Li, X., Wang, D., et al. (2021). Monocyte-macrophage-Derived MANF Protects Against Lipopolysaccharide-Induced Acute Kidney Injury via Inhibiting Inflammation and Renal M1 Macrophages. *Inflammation* 44, 693–703. doi: 10.1007/s10753-020-01368-w

Hou, C., Wang, D., Li, X., He, Y., Wei, C., Jiang, R., et al. (2019). MANF regulates splenic macrophage differentiation in mice. *Immunol. Lett.* 212, 37–45. doi: 10.1016/j.imlet.2019.06.007

Huang, J., Chen, C., Gu, H., Li, C., Fu, X., Jiang, M., et al. (2016). Mesencephalic astrocyte-derived neurotrophic factor reduces cell apoptosis via upregulating GRP78 in SH-SY5Y cells. *Cell Biol. Int.* 40, 803–811. doi: 10.1002/cbin.10621

Iurlaro, R., and Munoz-Pinedo, C. (2016). Cell death induced by endoplasmic reticulum stress. *FEBS J.* 283, 2640–2652.

Jiang, M., Yu, S., Yu, Z., Sheng, H., Li, Y., Liu, S., et al. (2017). XBP1 (X-Box–Binding Protein-1)–Dependent O-GlcNAcylation Is Neuroprotective in

Ischemic Stroke in Young Mice and Its Impairment in Aged Mice Is Rescued by Thiamet-G. *Stroke* 48, 1646–1654. doi: 10.1161/STROKEAHA.117.016579

Jäntti, M., and Harvey, B. K. (2020). Trophic activities of endoplasmic reticulum proteins CDNF and MANF. *Cell Tissue Res.* 382, 83–100. doi: 10.1007/s00441-020-03263-0

Karlsson, M., Zhang, C., Mear, L., Zhong, W., Digre, A., and Katona, B. (2021). A single-cell type transcriptomics map of human tissues. *Sci. Adv.* 7:eabh2169

Kersteen, E. A., and Raines, R. T. (2003). Catalysis of Protein Folding by Protein Disulfide Isomerase and Small-Molecule Mimics. *Antioxidants Redox Signal.* 5, 413–424. doi: 10.1089/152308603768295159

Kopp, M. C., Larburu, N., Durairaj, V., Adams, C. J., and Ali, M. M. U. (2019). UPR proteins IRE1 and PERK switch BiP from chaperone to ER stress sensor. *Nat. Struct. Mol. Biol.* 26, 1053–1062. doi: 10.1038/s41594-019-0324-9

Kraskiewicz, H., and FitzGerald, U. (2011). Partial XBP1 knockdown does not affect viability of oligodendrocyte precursor cells exposed to new models of hypoxia and ischemia in vitro. *J. Neurosci. Res.* 89, 661–673. doi: 10.1002/jnr.22583

Lee, A. H., Iwakoshi, N. N., and Glimcher, L. H. (2003). XBP-1 regulates a subset of endoplasmic reticulum resident chaperone genes in the unfolded protein response. *Mol. Cell Biol.* 23, 7448–7459. doi: 10.1128/MCB.23.21.7448-7459.2003

Li, Q. X., Shen, Y. X., Ahmad, A., Shen, Y. J., Zhang, Y. Q., Xu, P. K., et al. (2018). Mesencephalic Astrocyte-Derived Neurotrophic Factor Prevents Traumatic Brain Injury in Rats by Inhibiting Inflammatory Activation and Protecting the Blood-Brain Barrier. *World Neurosurg.* 117, e117–e129. doi: 10.1016/j.wneu.2018.05.202

Li, T., Xu, W., Gao, L., Guan, G., Zhang, Z., He, P., et al. (2019). Mesencephalic astrocyte-derived neurotrophic factor affords neuroprotection to early brain injury induced by subarachnoid hemorrhage via activating Akt-dependent prosurvival pathway and defending blood-brain barrier integrity. *FASEB J.* 33, 1727–1741. doi: 10.1096/fj.201800227RR

Lindahl, M., Danilova, T., Palm, E., Lindholm, P., Voikar, V., Hakonen, E., et al. (2014). MANF is indispensable for the proliferation and survival of pancreatic beta cells. *Cell Rep.* 7, 366–375. doi: 10.1016/j.celrep.2014.03.023

Lindahl, M., Saarma, M., and Lindholm, P. (2017). Unconventional neurotrophic factors CDNF and MANF: Structure, physiological functions and therapeutic potential. *Neurobiol.Dis.* 97, 90–102. doi: 10.1016/j.nbd.2016.07.009

Lindholm, P., Peranen, J., Andressoo, J. O., Kalkkinen, N., Kokaia, Z., Lindvall, O., et al. (2008). MANF is widely expressed in mammalian tissues and differently regulated after ischemic and epileptic insults in rodent brain. *Mol. Cell Neurosci.* 39, 356–371.

Lindholm, P., and Saarma, M. (2021). Cerebral dopamine neurotrophic factor protects and repairs dopamine neurons by novel mechanism. *Mol. Psychiat.* 27, 1310–1321. doi: 10.1038/s41380-021-01394-6

Lindholm, P., Voutilainen, M. H., Lauren, J., Peranen, J., Leppanen, V. M., Andressoo, J. O., et al. (2007). Novel neurotrophic factor CDNF protects and rescues midbrain dopamine neurons in vivo. *Nature* 448, 73–77. doi: 10.1038/nature05957

Liu, J., Shen, Q., Zhang, H., Xiao, X., Lv, C., Chu, Y., et al. (2021). The Potential Protective Effect of Mesencephalic Astrocyte-Derived Neurotrophic Factor on Post-Operative Delirium via Inhibiting Inflammation and Microglia Activation. *J. Inflamm. Res.* 14, 2781–2791. doi: 10.2147/JIR.S316560

Liu, J., Wu, Z., Han, D., Wei, C., Liang, Y., Jiang, T., et al. (2020). Mesencephalic Astrocyte-Derived Neurotrophic Factor Inhibits Liver Cancer Through Small Ubiquitin-Related Modifier (SUMO)ylation-Related Suppression of NF-kappaB/Snail Signaling Pathway and Epithelial-Mesenchymal Transition. *Hepatology* 71, 1262–1278. doi: 10.1002/hep.30917

Lu, J., Luo, L., Huang, D., Liu, X., Xia, X., Wang, Z., et al. (2018). Photoreceptor Protection by Mesencephalic Astrocyte-Derived Neurotrophic Factor (MANF). *eNeuro* 5, ENEURO.0109–18.2018 doi: 10.1523/ENEURO.0109-18.2018

Matlik, K., Anttila, J. E., Kuan-Yin, T., Smolander, O. P., Pakarinen, E., Lehtonen, L., et al. (2018). Poststroke delivery of MANF promotes functional recovery in rats. *Sci. Adv.* 4:eaa8957. doi: 10.1126/sciadv.aap8957

Mätlik, K., Vihinen, H., Bienemann, A., Palgi, J., Voutilainen, M. H., Booms, S., et al. (2017). Intrastriatally Infused Exogenous CDNF Is Endocytosed and Retrogradely Transported to Substantia Nigra. *eneuro* 4.ENEURO.012816.2017 doi: 10.1523/ENEURO.0128-16.2017

Matlik, K., Yu, L. Y., Eesmaa, A., Hellman, M., Lindholm, P., Peranen, J., et al. (2015). Role of two sequence motifs of mesencephalic astrocyte-derived neurotrophic factor in its survival-promoting activity. *Cell Death Dis.* 6:e2032. doi: 10.1038/cddis.2015.371

Ming, G. L., and Song, H. (2011). Adult neurogenesis in the mammalian brain: significant answers and significant questions. *Neuron* 70, 687–702. doi: 10.1016/j.neuron.2011.05.001

Mizobuchi, N., Hoseki, J., Kubota, H., Toyokuni, S., Nozaki, J., Naitoh, M., et al. (2007). ARMET is a soluble ER protein induced by the unfolded protein response via ERSE-II element. *Cell Struct. Funct.* 32, 41–50. doi: 10.1247/csf.07001

Mo, Z. T., Liao, Y. L., Zheng, J., and Li, W. N. (2020). Icariin protects neurons from endoplasmic reticulum stress-induced apoptosis after OGD/R injury via suppressing IRE1alpha-XBP1 signaling pathway. *Life Sci.* 255:117847. doi: 10.1016/j.lfs.2020.117847

Modi, J., Menzie-Suderam, J., Xu, H., Trujillo, P., Medley, K., Marshall, M. L., et al. (2020). Mode of action of granulocyte-colony stimulating factor (G-CSF) as a novel therapy for stroke in a mouse model. *J. Biomed. Sci.* 27:19 doi: 10.1186/s12929-019-0597-7

Mohammad-Gharibani, P., Modi, J., Menzie, J., Genova, R., Ma, Z., Tao, R., et al. (2014). Mode of Action of S-Methyl-N, N-Diethylthiocarbamate Sulfoxide (DETC-MeSO) as a Novel Therapy for Stroke in a Rat Model. *Mol. Neurobiol.* 50, 655–672. doi: 10.1007/s12035-014-8658-0

Montaser, H., Patel, K. A., Balboa, D., Ibrahim, H., Lithovius, V., Näätänen, A., et al. (2021). Loss of MANF Causes Childhood-Onset Syndromic Diabetes Due to Increased Endoplasmic Reticulum Stress. *Diabetes* 70, 1006–1018. doi: 10.2337/db20-1174

Morimoto, N., Oida, Y., Shimazawa, M., Miura, M., Kudo, T., Imaizumi, K., et al. (2007). Involvement of endoplasmic reticulum stress after middle cerebral artery occlusion in mice. *Neuroscience* 147, 957–967. doi: 10.1016/j.neuroscience.2007.04.017

Nakka, V. P., Gusain, A., and Raghubir, R. (2010). Endoplasmic Reticulum Stress Plays Critical Role in Brain Damage After Cerebral Ischemia/Reperfusion in Rats. *Neurotox. Res.* 17, 189–202. doi: 10.1007/s12640-009-9110-5

Nam, J., Koppinen, T. K., and Voutilainen, M. H. (2021). MANF Is Neuroprotective in Early Stages of EAE, and Elevated in Spinal White Matter by Treatment With Dexamethasone. *Front. Cell Neurosci.* 15:640084. doi: 10.3389/fncel.2021.640084

Neves, J., Chirco, K. R., Cedron-Craft, W., Chew, S., Zhu, J., Jasper, H., et al. (2020). MANF delivery improves retinal homeostasis and cell replacement therapies in ageing mice. *Exp. Gerontol.* 134:110893. doi: 10.1016/j.exger.2020.110893

Neves, J., Zhu, J., Sousa-Victor, P., Konjikusic, M., Riley, R., Chew, S., et al. (2016). Immune modulation by MANF promotes tissue repair and regenerative success in the retina. *Science* 353:aaf3646. doi: 10.1126/science.aaf3646

Oh-Hashi, K., Hirata, Y., and Kiuchi, K. (2013). Transcriptional regulation of mouse mesencephalic astrocyte-derived neurotrophic factor in Neuro2a cells. *Cell Mol. Biol. Lett,* 18, 398–415. doi: 10.2478/s11658-013-0096-x

Pakarinen, E., Danilova, T., Võikar, V., Chmielarz, P., Piepponen, P., Airavaara, M., et al. (2020). MANF Ablation Causes Prolonged Activation of the UPR without Neurodegeneration in the Mouse Midbrain Dopamine System. *eneuro* 7, ENEURO.0477–19.2019 doi: 10.1523/ENEURO.0477-19.2019

Pakarinen, E., Lindholm, P., Saarma, M., and Lindahl, M. (2022). CDNF and MANF regulate ER stress in a tissue-specific manner. *Cell. Mol. Life Sci.* 79:124 doi: 10.1007/s00018-022-04157-w

Palgi, M., Greco, D., Lindstrom, R., Auvinen, P., and Heino, T. I. (2012). Gene expression analysis of Drosophilaa Manf mutants reveals perturbations in membrane traffic and major metabolic changes. *BMC Genomics* 13:134. doi: 10.1186/1471-2164-13-134

Palgi, M., Lindstrom, R., Peranen, J., Piepponen, T. P., Saarma, M., and Heino, T. I. (2009). Evidence that DmMANF is an invertebrate neurotrophic factor supporting dopaminergic neurons. *Proc. Natl. Acad. Sci. U.S.A.* 106, 2429–2434. doi: 10.1073/pnas.0810996106

Park, S. J., Kim, Y., Yang, S. M., Henderson, M. J., Yang, W., Lindahl, M., et al. (2019). Discovery of endoplasmic reticulum calcium stabilizers to rescue ER-stressed podocytes in nephrotic syndrome. *Proc. Natl. Acad. Sci. U.S.A.* 116, 14154–14163. doi: 10.1073/pnas.1813580116

Parkash, V., Lindholm, P., Peranen, J., Kalkkinen, N., Oksanen, E., Saarma, M., et al. (2009). The structure of the conserved neurotrophic factors MANF and

CDNF explains why they are bifunctional. *Protein Eng. Des. Sel.* 22, 233–241. doi: 10.1093/protein/gzn080

Paschen, W. (1996). Disturbances of calcium homeostasis within the endoplasmic reticulum may contribute to the development of ischemic-cell damage. *Med. Hypotheses* 47, 283–288. doi: 10.1016/s0306-9877(96)90068-7

Paschen, W., Aufenberg, C., Hotop, S., and Mengesdorf, T. (2003). Transient Cerebral Ischemia Activates Processing of xbp1 Messenger RNA Indicative of Endoplasmic Reticulum Stress. *J. Cerebral Blood Flow Metab.* 23, 449–461. doi: 10.1097/01.WCB.0000054216.21675.AC

Petrova, P., Raibekas, A., Pevsner, J., Vigo, N., Anafi, M., Moore, M. K., et al. (2003). MANF: a new mesencephalic, astrocyte-derived neurotrophic factor with selectivity for dopaminergic neurons. *J. Mol. Neurosci.* 20, 173–188. doi: 10.1385/jmn:20:2:173

Pramanik, J., Chen, X., Kar, G., Henriksson, J., Gomes, T., Park, J. E., et al. (2018). Genome-wide analyses reveal the IRE1a-XBP1 pathway promotes T helper cell differentiation by resolving secretory stress and accelerating proliferation. *Genome Med.* 10:76. doi: 10.1186/s13073-018-0589-3

Prentice, H., Gharibani, P. M., Ma, Z., Alexandrescu, A., Genova, R., Chen, P.-C., et al. (2017a). Neuroprotective Functions Through Inhibition of ER Stress by Taurine or Taurine Combination Treatments in a Rat Stroke Model. *Taurine* 10, 193–205. doi: 10.1007/978-94-024-1079-2_17

Prentice, H., Pan, C., Gharibani, P. M., Ma, Z., Price, A. L., Giraldo, G. S., et al. (2017b). Analysis of Neuroprotection by Taurine and Taurine Combinations in Primary Neuronal Cultures and in Neuronal Cell Lines Exposed to Glutamate Excitotoxicity and to Hypoxia/Re-oxygenation. *Adv. Exp. Med. Biol.* 975(Pt 1), 207–216. doi: 10.1007/978-94-024-1079-2_18

Reimold, A. M., Iwakoshi, N. N., Manis, J., Vallabhajosyula, P., Szomolanyi-Tsuda, E., Gravallese, E. M., et al. (2001). Plasma cell differentiation requires the transcription factor XBP-1. *Nature* 412, 300–307. doi: 10.1038/35085509

Renko, J. M., Back, S., Voutilainen, M. H., Piepponen, T. P., Reenila, I., Saarma, M., et al. (2018). Mesencephalic Astrocyte-Derived Neurotrophic Factor (MANF) Elevates Stimulus-Evoked Release of Dopamine in Freely-Moving Rats. *Mol. Neurobiol.* 55, 6755–6768. doi: 10.1007/s12035-018-0872-8

Richman, C., Rashid, S., Prashar, S., Mishra, R., Selvaganapathy, P. R., and Gupta, B. P. (2018). C. elegans MANF Homolog Is Necessary for the Protection of Dopaminergic Neurons and ER Unfolded Protein Response. *Front. Neurosci.* 12:544. doi: 10.3389/fnins.2018.00544

Sereno, D., Muller, W. E. G., Bausen, M., Elkhooly, T. A., Markl, J. S., and Wiens, M. (2017). An evolutionary perspective on the role of mesencephalic astrocyte-derived neurotrophic factor (MANF): At the crossroads of poriferan innate immune and apoptotic pathways. *Biochem. Biophys. Rep.* 11, 161–173. doi: 10.1016/j.bbrep.2017.02.009

Shaffer, A. L., Shapiro-Shelef, M., Iwakoshi, N. N., Lee, A.-H., Qian, S.-B., Zhao, H., et al. (2004). XBP1, Downstream of Blimp-1, Expands the Secretory Apparatus and Other Organelles, and Increases Protein Synthesis in Plasma Cell Differentiation. *Immunity* 21, 81–93. doi: 10.1016/j.immuni.2004.06.010

Shen, Y., Sun, A., Wang, Y., Cha, D., Wang, H., Wang, F., et al. (2012). Upregulation of mesencephalic astrocyte-derived neurotrophic factor in glial cells is associated with ischemia-induced glial activation. *J. Neuroinflam.* 9:254. doi: 10.1186/1742-2094-9-254

Shi, S., Tang, M., Li, H., Ding, H., Lu, Y., Gao, L., et al. (2018). X-box binding protein l splicing attenuates brain microvascular endothelial cell damage induced by oxygen-glucose deprivation through the activation of phosphoinositide 3-kinase/protein kinase B, extracellular signal-regulated kinases, and hypoxia-inducible factor-1α/vascular endothelial growth factor signaling pathways. *J. Cell. Physiol.* 234, 9316–9327.

Shridhar, V., Rivard, S., Shridhar, R., Mullins, C., Bostick, L., Sakr, W., et al. (1996). A gene from human chromosomal band 3p21.1 encodes a highly conserved arginine-rich protein and is mutated in renal cell carcinomas. *Oncogene* 12, 1931–1939.

Sousa, C., Golebiewska, A., Poovathingal, S. K., Kaoma, T., Pires-Afonso, Y., Martina, S., et al. (2018). Single-cell transcriptomics reveals distinct inflammation-induced microglia signatures. *EMBO Rep.* 19:e46171 doi: 10.15252/embr.201846171

Sousa-Victor, P., Neves, J., Cedron-Craft, W., Ventura, P. B., Liao, C.-Y., Riley, R. R., et al. (2019). MANF regulates metabolic and immune homeostasis in ageing and protects against liver damage. *Nat. Metab.* 1, 276–290. doi: 10.1038/s42255-018-0023-6

Sree, S., Parkkinen, I., Their, A., Airavaara, M., and Jokitalo, E. (2021). Morphological Heterogeneity of the Endoplasmic Reticulum within Neurons and Its Implications in Neurodegeneration. *Cells* 10:970 doi: 10.3390/cells10050970

Stratoulias, V., and Heino, T. I. (2015a). Analysis of the conserved neurotrophic factor MANF in the Drosophila adult brain. *Gene. Expr. Patterns* 18, 8–15. doi: 10.1016/j.gep.2015.04.002

Stratoulias, V., and Heino, T. I. (2015b). MANF silencing, immunity induction or autophagy trigger an unusual cell type in metamorphosing Drosophila brain. *Cell Mol. Life Sci.* 72, 1989–2004. doi: 10.1007/s00018-014-1789-7

Sun, H., Jiang, M., Fu, X., Cai, Q., Zhang, J., Yin, Y., et al. (2017). Mesencephalic astrocyte-derived neurotrophic factor reduces cell apoptosis via upregulating HSP70 in SHSY-5Y cells. *Transl. Neurodegener.* 6:12. doi: 10.1186/s40035-017-0082-8

Tadimalla, A., Belmont, P. J., Thuerauf, D. J., Glassy, M. S., Martindale, J. J., Gude, N., et al. (2008). Mesencephalic astrocyte-derived neurotrophic factor is an ischemia-inducible secreted endoplasmic reticulum stress response protein in the heart. *Circ. Res.* 103, 1249–1258. doi: 10.1161/CIRCRESAHA.108.180679

Teppo, J., Vaikkinen, A., Stratoulias, V., Matlik, K., Anttila, J. E., Smolander, O. P., et al. (2020). Molecular profile of the rat peri-infarct region four days after stroke: Study with MANF. *Exp. Neurol.* 329:113288. doi: 10.1016/j.expneurol.2020.113288

Tseng, K. Y., Anttila, J. E., Khodosevich, K., Tuominen, R. K., Lindahl, M., Domanskyi, A., et al. (2018). MANF Promotes Differentiation and Migration of Neural Progenitor Cells with Potential Neural Regenerative Effects in Stroke. *Mol. Ther.* 26, 238–255. doi: 10.1016/j.ymthe.2017.09.019

Tseng, K. Y., Danilova, T., Domanskyi, A., Saarma, M., Lindahl, M., and Airavaara, M. (2017). MANF Is Essential for Neurite Extension and Neuronal Migration in the Developing Cortex. *eNeuro* 4, ENEURO.0214–17.2017 doi: 10.1523/ENEURO.0214-17.2017

Uhlen, M., Fagerberg, L., Hallstrom, B. M., Lindskog, C., Oksvold, P., and Mardinoglu, A. (2015). Proteomics. Tissue-based map of the human proteome. *Science* 347:1260419. doi: 10.1126/science.1260419

Voutilainen, M. H., Back, S., Peranen, J., Lindholm, P., Raasmaja, A., Mannisto, P. T., et al. (2011). Chronic infusion of CDNF prevents 6-OHDA-induced deficits in a rat model of Parkinson's disease. *Exp. Neurol.* 228, 99–108.

Voutilainen, M. H., Back, S., Porsti, E., Toppinen, L., Lindgren, L., Lindholm, P., et al. (2009). Mesencephalic astrocyte-derived neurotrophic factor is neurorestorative in rat model of Parkinson's disease. *J. Neurosci.* 29, 9651–9659. doi: 10.1523/JNEUROSCI.0833-09.2009

Walter, P., and Ron, D. (2011). The unfolded protein response: from stress pathway to homeostatic regulation. *Science* 334, 1081–1086. doi: 10.1126/science.1209038

Wang, C., Bao, Q., Hou, C., Sun, M., Song, X., Cao, S., et al. (2021a). Mono-macrophage-Derived MANF Alleviates Bacterial Myocarditis by Inhibiting NF-kappaB Activation and Myocardial Inflammation. *Inflammation* 44, 1916–1926. doi: 10.1007/s10753-021-01469-0

Wang, C., Peng, J. J., Miao, H., Liu, D. F., and Zhang, L. L. (2021c). Decreased Plasma MANF Levels are Associated with Type 2 Diabetes. *Biomed. Environ. Sci.* 34, 236–240. doi: 10.3967/bes2021.030

Wang, D., Hou, C., Cao, Y., Cheng, Q., Zhang, L., Li, H., et al. (2018). XBP1 activation enhances MANF expression via binding to endoplasmic reticulum stress response elements within MANF promoter region in hepatitis B. *Int. J. Biochem. Cell Biol.* 99, 140–146. doi: 10.1016/j.biocel.2018.04.007

Wang, H., Ke, Z., Alimov, A., Xu, M., Frank, J. A., Fang, S., et al. (2014). Spatiotemporal expression of MANF in the developing rat brain. *PLoS One* 9:e90433. doi: 10.1371/journal.pone.0090433

Wang, X. Y., Song, M. M., Bi, S. X., Shen, Y. J., Shen, Y. X., and Yu, Y. Q. (2016). MRI Dynamically Evaluates the Therapeutic Effect of Recombinant Human MANF on Ischemia/Reperfusion Injury in Rats. *Int. J. Mol. Sci.* 17:1476 doi: 10.3390/ijms17091476

Wang, Z., Li, X., Spasojevic, I., Lu, L., Shen, Y., Qu, X., et al. (2021b). Increasing O-GlcNAcylation is neuroprotective in young and aged brains after ischemic stroke. *Experimental Neurology* 339:113646

Wei, J., Wang, C., Yang, G., Jia, Y., Li, Y., Deng, W., et al. (2020). Decreased Circulating MANF in Women with PCOS is Elevated by Metformin Therapy

and is Inversely Correlated with Insulin Resistance and Hyperandrogenism. *Horm. Metab. Res.* 52, 109–116. doi: 10.1055/a-1082-1080

Wu, X., Zhao, H., Min, L., Zhang, C., Liu, P., and Luo, Y. (2014). Effects of 2-Deoxyglucose on ischemic brain injuries in rats. *Int. J. Neurosci.* 124, 666–672. doi: 10.3109/00207454.2013.868807

Xu, S., Di, Z., He, Y., Wang, R., Ma, Y., Sun, R., et al. (2019). Mesencephalic astrocyte-derived neurotrophic factor (MANF) protects against Abeta toxicity via attenuating Abeta-induced endoplasmic reticulum stress. *J. Neuroinflamm.* 16:35. doi: 10.1186/s12974-019-1429-0

Xu, W., Gao, L., Li, T., Zheng, J., Shao, A., and Zhang, J. (2018). Mesencephalic Astrocyte-Derived Neurotrophic Factor (MANF) Protects Against Neuronal Apoptosis via Activation of Akt/MDM2/p53 Signaling Pathway in a Rat Model of Intracerebral Hemorrhage. *Front. Mol. Neurosci.* 11:176. doi: 10.3389/fnmol.2018.00176

Yagi, T., Asada, R., Kanekura, K., Eesmaa, A., Lindahl, M., Saarma, M., et al. (2020). "Neuroplastin Modulates Anti-inflammatory Effects of MANF.". iScience 23:101810. doi: 10.1016/j.isci.2020.101810

Yan, Y., Rato, C., Rohland, L., Preissler, S., and Ron, D. (2019). MANF antagonizes nucleotide exchange by the endoplasmic reticulum chaperone BiP. *Nat. Commun.* 10:541 doi: 10.1038/s41467-019-08450-4

Yang, F., Li, W. B., Qu, Y. W., Gao, J. X., Tang, Y. S., Wang, D. J., et al. (2020). Bone marrow mesenchymal stem cells induce M2 microglia polarization through PDGF-AA/MANF signaling. *World J. Stem Cells* 12, 633–658. doi: 10.4252/wjsc.v12.i7.633

Yang, W., Shen, Y., Chen, Y., Chen, L., Wang, L., Wang, H., et al. (2014). Mesencephalic astrocyte-derived neurotrophic factor prevents neuron loss via inhibiting ischemia-induced apoptosis. *J. Neurol. Sci.* 344, 129–138. doi: 10.1016/j.jns.2014.06.042

Yavarna, T., Al-Dewik, N., Al-Mureikhi, M., Ali, R., Al-Mesaifri, F., Mahmoud, L., et al. (2015). High diagnostic yield of clinical exome sequencing in Middle Eastern patients with Mendelian disorders. *Hum. Gene.* 134, 967–980. doi: 10.1007/s00439-015-1575-0

Yilmaz, E., Akar, R., Eker, S. T., Deda, G., Adiguzel, Y., and Akar, N. (2010). Relationship between functional promoter polymorphism in the XBP1 gene (-116C/G) and atherosclerosis, ischemic stroke and hyperhomocysteinemia. *Mol. Biol. Rep.* 37, 269–272. doi: 10.1007/s11033-009-9674-4

Yoshida, H., Matsui, T., Yamamoto, A., Okada, T., and Mori, K. (2001). XBP1 mRNA Is Induced by ATF6 and Spliced by IRE1 in Response to ER Stress to Produce a Highly Active Transcription Factor. *Cell* 107, 881–891. doi: 10.1016/s0092-8674(01)00611-0

Yu, Y. Q., Liu, L. C., Wang, F. C., Liang, Y., Cha, D. Q., Zhang, J. J., et al. (2010). Induction profile of MANF/ARMET by cerebral ischemia and its implication for neuron protection. *J. Cereb. Blood Flow Metab.* 30, 79–91. doi: 10.1038/jcbfm.2009.181

Zeng, L., Xiao, Q., Chen, M., Margariti, A., Martin, D., Ivetic, A., et al. (2013). Vascular endothelial cell growth-activated XBP1 splicing in endothelial cells is crucial for angiogenesis. *Circulation* 127, 1712–1722. doi: 10.1161/CIRCULATIONAHA.112.001337

Zhang, J., Cai, Q., Jiang, M., Liu, Y., Gu, H., Guo, J., et al. (2017). Mesencephalic astrocyte-derived neurotrophic factor alleviated 6-OHDA-induced cell damage via ROS-AMPK/mTOR mediated autophagic inhibition. *Exp. Gerontol.* 89, 45–56. doi: 10.1016/j.exger.2017.01.010

Zhang, M., Tang, M., Wu, Q., Wang, Z., Chen, Z., Ding, H., et al. (2020). LncRNA DANCR attenuates brain microvascular endothelial cell damage induced by oxygen-glucose deprivation through regulating of miR-33a-5p/XBP1s. *Aging* 12, 1778–1791. doi: 10.18632/aging.102712

Zhang, Y., Chen, K., Sloan, S. A., Bennett, M. L., Scholze, A. R., O'Keeffe, S., et al. (2014). An RNA-sequencing transcriptome and splicing database of glia, neurons, and vascular cells of the cerebral cortex. *J. Neurosci.* 34, 11929–11947. doi: 10.1523/JNEUROSCI.1860-14.2014

Zhao, H., Liu, Y., Cheng, L., Liu, B., Zhang, W., Guo, Y. J., et al. (2013). Mesencephalic astrocyte-derived neurotrophic factor inhibits oxygen-glucose deprivation-induced cell damage and inflammation by suppressing endoplasmic reticulum stress in rat primary astrocytes. *J. Mol. Neurosci.* 51, 671–678. doi: 10.1007/s12031-013-0042-4

Zhou, Y., Lee, J., Reno, C. M., Sun, C., Park, S. W., Chung, J., et al. (2011). Regulation of glucose homeostasis through a XBP-1–FoxO1 interaction. *Nat. Med.* 17, 356–365. doi: 10.1038/nm.2293

Zhu, W., Li, J., Liu, Y., Xie, K., Wang, L., and Fang, J. (2016). Mesencephalic astrocyte-derived neurotrophic factor attenuates inflammatory responses in lipopolysaccharide-induced neural stem cells by regulating NF-kappaB and phosphorylation of p38-MAPKs pathways. *Immunopharmacol. Immunotoxicol.* 38, 205–213. doi: 10.3109/08923973.2016.1168433

Conflict of Interest: The authors declare that the research was conducted in the absence of any commercial or financial relationships that could be construed as a potential conflict of interest.

Publisher's Note: All claims expressed in this article are solely those of the authors and do not necessarily represent those of their affiliated organizations, or those of the publisher, the editors and the reviewers. Any product that may be evaluated in this article, or claim that may be made by its manufacturer, is not guaranteed or endorsed by the publisher.

frontiers | Frontiers in Cellular Neuroscience

ORIGINAL RESEARCH
published: 08 July 2022
doi: 10.3389/fncel.2022.874258

Progranulin Preserves Autophagy Flux and Mitochondrial Function in Rat Cortical Neurons Under High Glucose Stress

*Cass Dedert[1,2], Vandana Mishra[1], Geetika Aggarwal[2,3,4], Andrew D. Nguyen[2,3,4] and Fenglian Xu[1,2,3]**

[1] Department of Biology, College of Arts and Sciences, Saint Louis University, St. Louis, MO, United States, [2] Henry and Amelia Nasrallah Center for Neuroscience, Saint Louis University, St. Louis, MO, United States, [3] Department of Pharmacology and Physiology, School of Medicine, Saint Louis University, St. Louis, MO, United States, [4] Department of Internal Medicine, Division of Geriatric Medicine, School of Medicine, Saint Louis University, St. Louis, MO, United States

Chronic hyperglycemia in type II diabetes results in impaired autophagy function, accumulation of protein aggregates, and neurodegeneration. However, little is known about how to preserve autophagy function under hyperglycemic conditions. In this study, we tested whether progranulin (PGRN), a neurotrophic factor required for proper lysosome function, can restore autophagy function in neurons under high-glucose stress. We cultured primary cortical neurons derived from E18 Sprague-Dawley rat pups to maturity at 10 days *in vitro* (DIV) before incubation in high glucose medium and PGRN for 24-72 h before testing for autophagy flux, protein turnover, and mitochondrial function. We found that although PGRN by itself did not upregulate autophagy, it attenuated impairments in autophagy seen under high-glucose conditions. Additionally, buildup of the autophagosome marker light chain 3B (LC3B) and lysosome marker lysosome-associated membrane protein 2A (LAMP2A) changed in both neurons and astrocytes, indicating a possible role for glia in autophagy flux. Protein turnover, assessed by remaining advanced glycation end-product levels after a 6-h incubation, was preserved with PGRN treatment. Mitochondrial activity differed by complex, although PGRN appeared to increase overall activity in high glucose. We also found that activation of extracellular signal-regulated kinase 1/2 (ERK1/2) and glycogen synthase kinase 3β (GSK3β), kinases implicated in autophagy function, increased with PGRN treatment under stress. Together, our data suggest that PGRN prevents hyperglycemia-induced decreases in autophagy by increasing autophagy flux via increased ERK1/2 kinase activity in primary rat cortical neurons.

Keywords: autophagy, neurodegeneration, progranulin, hyperglycemia, diabetes, cortical neurons

OPEN ACCESS

Edited by:
Renato Xavier Coelho dos Santos, University of Aberdeen, United Kingdom

Reviewed by:
Cristina Carvalho, University of Coimbra, Portugal
Andrew Arrant, University of Alabama at Birmingham, United States
Selvakumar Govindhasamy Pushpavathi, The University of Iowa, United States

***Correspondence:**
Fenglian Xu
Fenglian.xu@slu.edu

Specialty section:
This article was submitted to Cellular Neuropathology, a section of the journal Frontiers in Cellular Neuroscience

Received: *11 February 2022*
Accepted: *17 June 2022*
Published: *08 July 2022*

Citation:
Dedert C, Mishra V, Aggarwal G, Nguyen AD and Xu F (2022) Progranulin Preserves Autophagy Flux and Mitochondrial Function in Rat Cortical Neurons Under High Glucose Stress. Front. Cell. Neurosci. 16:874258. doi: 10.3389/fncel.2022.874258

INTRODUCTION

Type II diabetes (T2D) is a metabolic disease characterized by chronic hyperglycemia, or elevated blood glucose. Hyperglycemia specifically contributes to pathology through several mechanisms, including pro-inflammatory signaling (Chang and Yang, 2016), accumulation of glycated proteins (Singh et al., 2014), and impairment of autophagy (Moruno et al., 2012; Mir et al., 2015). Additionally, hyperglycemia is a known risk

factor for several neurodegenerative diseases such as Alzheimer's and Parkinson's (Sergi et al., 2019; Madhusudhanan et al., 2020). The prevalence of Parkinson's is higher in those with diabetes compared to non-diabetics, and those with diabetes experience more severe Parkinsonian symptoms (Pagano et al., 2018). Despite the breadth of these conditions, all of them share a common underlying pathology: protein aggregates that are normally removed instead accumulate in the cells due to downregulation of autophagy (Ross and Poirier, 2004).

Autophagy is a cellular self-degradation process that is upregulated in response to a number of cell stressors, including starvation (Mizushima and Klionsky, 2007), endoplasmic reticulum stress (Ogata et al., 2006), and excessive buildup of proteins and organelles (Liu and Li, 2019). Targeted substrates are enclosed in a double-membrane vesicle called an autophagosome, which fuses with a lysosome to facilitate controlled degradation of its contents (Khandia et al., 2019). Despite its known pro-survival properties, uncontrolled autophagy leads to cell death (Denton and Kumar, 2019); because of this, the activity of this process is low under basal conditions, and the signaling pathways leading to its upregulation are tightly controlled. Nonetheless, it remains a powerful tool for maintaining cellular well-being. The importance of proper autophagy function is elevated in the nervous system due to the limited regenerative capacity and post-mitotic nature of neurons (Stavoe and Holzbaur, 2019). However, evidence indicates that the surrounding glia also contribute to neuronal health through regulation of autophagy and protein clearance (Ortiz-Rodriguez and Arevalo, 2020). Likewise, lysosomal dysfunction in astrocytes has been shown to contribute to neurodegeneration (Di Malta et al., 2012).

Progranulin (PGRN) is an endogenous neurotrophic factor expressed in high amounts in brain tissue (Nguyen et al., 2013b) that is implicated in anti-inflammatory activity in microglia (Martens et al., 2012). Furthermore, mutations in the *GRN* gene have been linked to Alzheimer's and frontotemporal lobar dementia (FTLD), indicating a protective role against neurodegenerative disease (Baker et al., 2006; Cruts et al., 2006; Gass et al., 2006; Perry et al., 2013). FTLD is similar to other neurodegenerative diseases in that it is also characterized by buildup of protein aggregates, namely TAR DNA-binding protein 43 (TDP-43) (Cairns et al., 2007). Interestingly, PGRN is important to lysosome function, as it is trafficked to the lysosome and cleaved into granulin subunits that facilitate lysosomal function (Smith et al., 2012; Almeida et al., 2016). Accordingly, overexpression of PGRN in Alzheimer's disease mouse models has been linked to decreased amyloid-β plaques (Minami et al., 2014; Van Kampen and Kay, 2017). These findings suggest a model in which PGRN may prevent the development of neurodegenerative pathology arising from impaired degradation of protein aggregates.

In this study, we examined the role and mechanism that high glucose plays in development of neuropathology with regards to autophagy inhibition, and the potentially protective role of PGRN. We found that autophagic activity and protein turnover were reduced in neurons incubated in high glucose conditions, with PGRN pre-treatment attenuating its harmful effects. PGRN treatment prevented pathology and reduced function due to high glucose in both cases. Mitochondrial function was affected by PGRN in cells cultured in high glucose, although the net effect varied by complex. We also observed changes in extracellular signal-regulated kinase (ERK) and glycogen synthase kinase 3-beta (GSK3β) phosphorylation in response to PGRN under high-glucose conditions.

The data we present suggest a potential role for PGRN in restoring autophagy in neurons affected by high glucose conditions, and further connect hyperglycemia and neurodegeneration through downregulation of autophagy.

MATERIALS AND METHODS

Animals and Cell Culture

All experiments were performed on cortical neurons from the brains of E18 Sprague-Dawley rat pups, which were removed under sterile conditions according to the standard protocol approved by the Institutional Animal Care and Use Committee (IACUC), Saint Louis University, St. Louis, MO guidelines. The dissected cortices were cut into small pieces and incubated in an enzymatic solution containing 40 units of papain (Worthington Biochemical, Cat# LS003126), 2 mM $CaCl_2$ (Sigma, Cat# C4901-100G), 1 mM EDTA (Sigma, Cat# E9884-100G), and 1.5 mM L-cysteine (Sigma, Cat# 168149-25G) in Neurobasal medium (Gibco, Cat# 21103-049). Tissues in solution were incubated for 30 min at 37°C, mixing every few minutes to ensure even dissolution. Tissues were then triturated through fire-polished glass pipettes, then plated on dishes coated with 2 μg/ml laminin (Sigma, Cat# 11243217001) and 100 μg/ml poly-D lysine (Sigma, Cat# P6407-5MG), and cultured in Neurobasal medium supplemented with 1X GlutaMAX (Gibco, Cat# 35050-061), 1% pen/strep (Gibco, Cat# 15140122), 2% B-27 supplement (Gibco, Cat# 17504-044), and 4% fetal bovine serum (Avantor, Cat# 97068-086). One half of the medium was changed every 3 to 4 days, and cells were grown for 10 days *in vitro* (DIV) before experimentation.

For qPCR and western blot studies in microglia, HMC3 human microglial cells (ATCC, Cat# CRL-3304) were cultured at a density of 120,000 cells/dish in 6-well plates in EMEM (Eagle's Minimum Essential Medium) (Corning, Cat# MT10009CV) supplemented with 10% fetal bovine serum (Gibco, Cat# 26140-095), 10 U/ml penicillin, and 10 μg/ml streptomycin. Cells were cultured for 24 h, then treated with filtered glucose dissolved in autoclaved water to get a final concentration of 30 mM. An equal volume of autoclaved water was used for the control. Cells were incubated for 72 h, then checked for mRNA and protein levels.

Treatment in Hyperglycemic Conditions and With Progranulin

For primary cortical neurons, medium was changed at DIV 10 for equivalent medium supplemented (Sigma, Cat# G6152) to reach a final glucose concentration of 100 mM (with control medium containing 25 mM glucose), similar to other *in vitro* studies exploring hyperglycemia in neuronal cultures (Chen et al., 2016; Li et al., 2017). PGRN (R&D Systems, Cat# 2557-PG050) was added to the medium at this time to achieve a final concentration of 200 ng/ml, a concentration that is similar to plasma concentrations in patients and used in previous cell

culture studies (Youn et al., 2009; Zhou et al., 2019a). Cells were treated under their respective conditions for 24 or 72 h before assay testing or harvest. Status of cells was observed using a phase-contrast microscope (IX73, Olympus) and images were taken with a Retiga R1 camera (QImaging).

For protein harvest, primary neurons were washed thrice in PBS (Gibco, Cat# 10010-031), then lysed using ice-cold N-PER lysis buffer (ThermoFisher, Cat# 87792) containing Halt protease inhibitor (ThermoFisher, Cat# 1860932) and phosphatase inhibitor (ThermoFisher, Cat#78420), then scraped from plates using a cell scraper. For PGRN measurements, HMC3 cells were rinsed with PBS, then lysed in RIPA buffer containing protease inhibitors (cOmplete^{TM}, Mini, EDTA-free, Protease Inhibitor Cocktail, Roche, Cat#11836170001). In both cell types, lysates were centrifuged at 14,000 rpm for 10 min and the supernatant was collected. Protein concentration was ascertained using a BCA Protein Assay kit (ThermoFisher, Cat# 23225).

Cell Viability Determination

Cell viability was determined using a fluorescence-based reporter dye kit (LIVE-DEAD^{TM} Cell Imaging Kit, ThermoFisher, R37601). After treatment, cells were washed thrice with PBS, then incubated in HBSS containing 1 μM Calcein AM and 2 μM ethidium homodimer for 45 min. Images were taken using a phase-contrast microscope (IX73, Olympus) with fluorescence light source (Lambda XL, Sutter Instrument) and Retiga R1 camera (QImaging). Viability was determined by counting the number of Calcein AM-stained cells through visual observation and calculating as a ratio to total cells in each image.

Quantitative PCR Analysis

Total RNA was isolated from cultured HMC3 cells using a RNeasy Mini kit (Qiagen, Cat#74106) with on-column DNase digestion (Qiagen, Cat#79256). RNA was reverse-transcribed to obtain cDNA using the iScript cDNA synthesis kit (Bio-Rad, Cat#1708891), and qPCR was performed using PowerUp SYBR Green Master Mix (ThermoFisher, Cat#A25777) with a Bio-Rad CFX384 Real-Time System. The primer sequences were as follows (with F for forward and R for reverse primers): human CYCLO-F, GGAGATGGCACAGGAGGAAA; human CYCLO-R, CCGTAGTGCTTCAGTTTGAAGTTCT; human GRN-F, AGGAGAACGCTACCACGGA; and human GRN-R, GGCAGCAGGTATAGCCATCTG. Results for qPCR were normalized to the housekeeping gene CYCLO and evaluated by the comparative C_T method.

Immunoblotting

Samples were treated with Laemmli sample buffer (Bio-Rad, Cat# 1610611) containing 350 mM DTT (Bio-Rad, Cat# 1610747) and run on a pre-cast MES-SDS gel (NuPage, Cat# NP0323BOX) in a Novex Mini-Cell device (Invitrogen, Cat# EI0001). Transfer to a 0.45 μm nitrocellulose membrane (Bio-Rad, Cat# 1620115) was performed in a Mini Protean Tetra System (Bio-Rad, Cat# 1658004). For PGRN measurement, proteins were separated on SDS-PAGE Bio-Rad TGX gels and transferred onto nitrocellulose membranes using the Bio-Rad Turbo-Blot transfer system.

Membranes were blocked in TBST containing 5% milk (Bio-Rad, Cat#1706404), then blotted using primary antibodies for light chain 3B (LC3B) (E7 × 45 XP(R), CST, Cat# 43566S), lysosome-associated membrane protein 2A (LAMP2A) (Abcam, Cat# ab18528), p-ERK1/2 (CST, Cat# 4370S), ERK1/2 (CST, Cat# 4695S), phosphorylated GSK3β (CST, Cat# 9336S), GSK3β (CST, Cat# 9315S), glyceraldehyde 3-phosphate dehydrogenase (GAPDH) (CST, Cat# 2118S), PGRN (R&D Systems, Cat# AF2557), hPGRN (an anti-human PGRN linker 5 polyclonal antibody #614 that recognizes an epitope between residues 497 and 515 (Nguyen et al., 2013a)), and β-actin (CST, Cat# 3700S). All antibodies were used at a 1:1000 dilution, except for hPGRN, which was at a 1:3000 dilution. A goat anti-rabbit (Invitrogen, Cat# 31460) or donkey anti-sheep (ThermoFisher, Cat#A16041) at a 1:5000 dilution or HRP-conjugated AffiniPure goat anti-rabbit and anti-mouse antibodies (Jackson Immuno Research Labs) at a 1:10000 dilution were used for secondary antibody incubation. Western blot data were captured using an imager (ThermoFisher, iBright FL1000) after incubating the membranes in Pierce substrate (ThermoFisher, Cat#32106). hPGRN western blots were visualized using a Chemi-Doc system (Bio-Rad). Densitometric analysis was performed using ImageJ (NIH).

Immunofluorescence of Primary Cortical Cells

Unless specified, primary cell cultures were fixed with 4% paraformaldehyde (ThermoFisher, Cat# J19943-K2) for 20 min, permeabilized with 0.3% Triton X-100 (VWR, Cat# 0694-1L) for 5 min, and blocked in PBS containing 5% goat serum (Gibco, Cat# 16210-064) for 1 h at room temperature. To visualize autophagosome and lysosome expression, antibodies for LC3B (E7 × 45 XP(R), CST, Cat# 43566S), LAMP2A (Abcam, Cat# ab18528), microtubule-associated protein 2 (MAP2) (Invitrogen, Cat# 13-1500), and glial fibrillary acidic protein (GFAP) (EMD Millipore, Cat# AB5541) were used at a 1:200 dilution in 5% goat serum. To visualize PGRN expression in microglia, a 1:100 dilution of PGRN antibody (R&D Systems, Cat# AF2557) and 1:3000 dilution of allograft inflammatory factor 1 (Iba1) antibody (Wako, Cat# 019-19741) in 5% donkey serum were used. For secondary incubation, the following antibodies were used at a 1:500 dilution in 5% goat serum: goat anti-rabbit conjugated with Alexa Fluor 568 (Invitrogen, Cat# A11036), anti-mouse conjugated with Alexa Fluor 488 (Invitrogen, Cat# A11029), and anti-chick conjugated with Alexa Fluor 488 (Abcam, Cat# ab150169). The following antibodies were used at a 1:500 dilution in 5% donkey serum: donkey anti-rabbit conjugated with Alexa Fluor 546 (Invitrogen, Cat# A10040) and donkey anti-sheep conjugated with Alexa Fluor 647 (Invitrogen, Cat# A21448). Slides were stained with DAPI (1 μg/ml) included in the mounting media (Fluoroshield, Sigma, Cat# F6507), and images were taken using a confocal microscope (Leica, TCS SP8).

Fluorescence intensity analysis was performed by selecting regions of interest (ROIs) of cell bodies, identified by staining with the neuronal marker MAP2 or astrocytic marker GFAP. The mean fluorescence intensity of each ROI was measured, and values were normalized with control equal to 1. To prevent differences in intensity due to user error, slides were viewed under the same acquisition parameters for fluorescence images.

Advanced Glycation End-Product Degradation Assays

Cortical cells were incubated with 50 μg BSA-AGE (Cayman Chemical, Cat# 22968) for 6 h at the end of the 72-h treatment period. Protein samples were harvested and AGE detection was performed using a fluorometric assay kit (Biovision, Cat# K929-100), measuring emission at 460 nm in response to excitation at 360 nm and using BSA control as the baseline. Levels of AGEs were validated by western blot with anti-AGE antibody (Bioss, Cat# bs-1158R) at a 1:1000 dilution, normalized to GAPDH expression.

Mitochondrial Complex Enzyme Activity Assay

Activity of ubiquinone oxidoreductase (UO), succinate dehydrogenase (SDH), and cytochrome C oxidase (COX) were tested to represent mitochondrial complexes I, II, and IV, respectively. Protein samples were harvested after 72 h of treatment at DIV 10 and tested in a 96-well microplate format using a plate reader (Synergy H1, BioTek). Activity was calculated as mΔOD per min, accounting for differences in protein concentration between samples. All reagents listed were obtained from Sigma unless otherwise noted.

UO activity was measured as documented previously (Ma et al., 2011). Samples were added to a reagent containing 25 mM potassium phosphate (pH 7.2) (Cat# P5655), 5 mM $MgCl_2$ (Cat# M4880), 1 mM KCN (Cat# 60178), 0.13 mM NADH (Cat# N8129), 65 μM coenzyme Q10 (Cat# C9538), 2.5 mg/ml BSA (Cat# A9418), and 2 μg/ml antimycin A (Cat# A8764). The reagent was heated to 30°C for 10 min before adding 2 ug/ml rotenone (Cat# R8875), followed by adding samples. Activity was tied to reduction of NADH, measured as a decrease in absorbance at 340 nm over a 20-min period.

SDH activity was measured as documented previously (Cimen et al., 2010). Samples were added to a reagent containing 10 mM KCl (Cat# P5405), 5 mM $MgCl_2$, 50 mM sodium succinate (Cat# S2378), 40 mM NaN_3 (Cat# S2002), 300 mM mannitol (Cat# M4125), and 20 mM potassium phosphate (pH 7.2) (all reagents from Sigma). Activity was tied to the reduction of the electron acceptor DPIP (Fisher Chemical, Cat# S286-5) (50 μM), which manifests as a decrease in absorbance at 600 nm over a 30-min period.

COX activity was measured as documented previously (Ma et al., 2011). Samples were added to a reagent containing 20 mM potassium phosphate, pH 7.2, and 0.45 mM n-dodecyl-β-D-maltoside (Sigma, Cat# D4641). Reagent was heated to 30°C for 10 min before adding 15 μM reduced cytochrome C (Sigma, Cat# C2506), followed by adding samples. Activity was tied to oxidation of cytochrome C, measured as a decrease in absorbance at 550 nm over a 30-min period.

Statistical Analysis

Data were analyzed using Graphpad 8.4.3 software, with the threshold for significance at $p < 0.05$. Values provided are mean ± S.E.M. Student's *t*-test was used to assess significance between two groups; for other experiments involving high glucose and PGRN, one-way ANOVA was used. *Post hoc* testing was performed using Fisher's Least Significant Difference (LSD). The *N* and *p* values for experiments are provided in the figure legend or text.

RESULTS

Neuronal Morphology Is Promoted Due to Progranulin and Maintained Under High-Glucose Stress

To start, we examined neurons to determine if there were any readily noticeable phenotypic differences due to high glucose (HG) or PGRN. Since PGRN is a known neurotrophic and neuroprotective factor (Van Damme et al., 2008), we considered whether this property would be maintained under high-glucose conditions. At DIV 10, cells were treated with 100 mM glucose and 200 ng/ml PGRN for 72 h before testing. This concentration was used in other studies (Chen et al., 2016; Li et al., 2017) and in our case because we saw a significant decrease in cell viability under 100 mM, but not 50 mM, glucose (**Supplementary Figure 1**). Using a fluorescence-based reporter assay, we found that cell viability decreased significantly ($F = 5.307$, $p = 0.005$) (**Figure 1A**). Under high-glucose conditions, viability decreased from 89.55 ± 1.27% to 74.61 ± 4.80% (p = 0.001). Despite no difference compared to control (from 89.55 ± 1.27% to 87.94 ± 1.98%, $p = 0.699$), PGRN treatment led to increased viability under high glucose, from 74.61 ± 4.80% to 84.35 ± 2.29% ($p = 0.025$).

Cells viewed under phase-contrast microscopy showed extensive growth of neuritic processes, while cells in high glucose showed less growth of non-primary (i.e., secondary and tertiary) neurites (**Figure 1C**). Neurite growth appeared to be exceptionally robust with 200 ng/ml PGRN treatment, which was maintained even under high-glucose treatment. While we were unable to perform neurite tracing on matured neurons in culture (>DIV 10) due to the density of cell growth, we were able to assess the effect of PGRN on neurite outgrowth in early developmental (DIV 4) neurons after treatment for 72 h. High glucose incubation resulted in a lower average number of neurites, although this did not reach the threshold of significance (from 9.067 ± 1.181 to 7.325 ± 0.784 neurites, $p = 0.197$) (**Figure 1B**). PGRN positively influenced neurite outgrowth under high-glucose conditions (from 7.325 ± 0.784 to 10.353 ± 1.019 neurites, $p = 0.030$); when viewed in detail, there was a trend toward an increase in primary neurites (4.471 ± 0.438 to 5.471 ± 0.444 primary neurites, $p = 0.080$), and a significant increase in non-primary neurites (2.765 ± 0.481 to 4.882 ± 0.857 non-primary neurites, $p = 0.039$). This indicates that PGRN treatment promotes neuronal outgrowth and viability, even when cultured in high glucose.

Primary and HMC3 Cells Show No Change in Progranulin Expression Under High Glucose

Prior studies have shown that microglia express high levels of PGRN and may be important in neurodegeneration (Mendsaikhan et al., 2019; Choi et al., 2020), so we explored

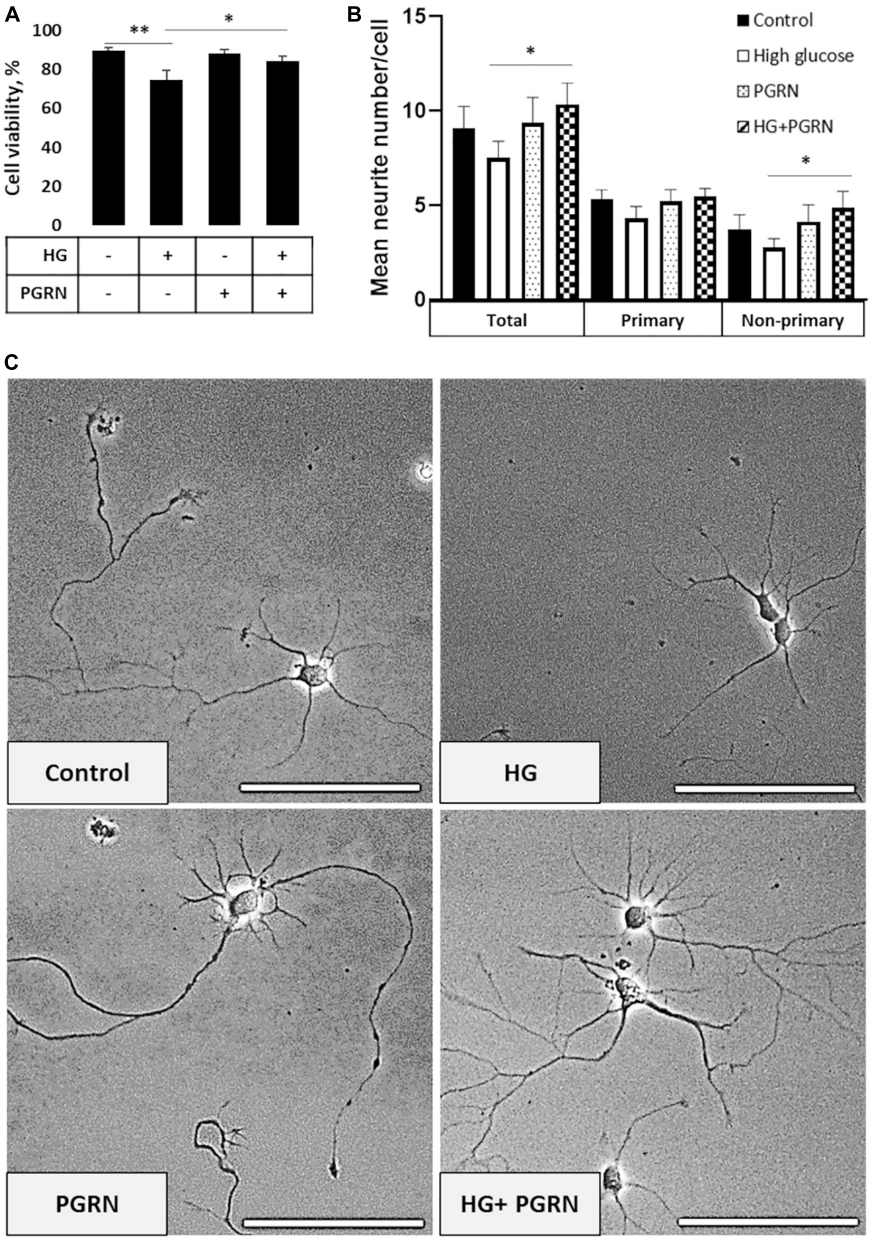

FIGURE 1 | Neuronal viability and neurite outgrowth in neurons treated with high glucose and PGRN. **(A)** Viability of DIV 10 cortical neurons cultured in high-glucose medium (HG) decreased after 72 h from 89.55 ± 1.27% to 74.61 ± 4.80%. PGRN treatment significantly preserved viability under high glucose, with a viability of 84.35 ± 2.29% compared to 74.61 ± 4.80% for HG alone. *N* = 8 fields of view (FoV). **(B)** Number of neurites per cell was counted at DIV 4 after 72 h of treatment using NeuronJ. High glucose lowered mean neurite count from 9.067 ± 1.181 to 7.325 ± 0.784 neurites, while PGRN increased mean neurite count from 7.325 ± 0.784 to 10.353 ± 1.019 neurites. Specifically, this increase was significant in non-primary neurites (2.765 ± 0.481 neurites to 4.882 ± 0.857 neurites) and trending toward significance in primary neurites (4.471 ± 0.438 neurites to 5.471 ± 0.444 neurites). *N* = 13-17 neurons. **(C)** Representative phase-contrast images of primary neurons cultured under high glucose and PGRN after 72 h of treatment. Scale bar, 10 μm. $^{*}p < 0.05$; $^{**}p < 0.01$.

if high glucose affected the degree of PGRN expression in this cell type. We performed qPCR and western blot analyses on HMC3 cells treated with high glucose (in this case, 25 mM, in medium with a basal glucose level of 5.5 mM), and found that mRNA and protein expression of PGRN were similar among control and high glucose-treated cells (**Figures 2A,B**). The mRNA level changed from 1.000 ± 0.139 Arbitrary Units, AU, to 1.022 ± 0.099 AU, and the protein level from 1.000 ± 0.212 AU to 1.069 ± 0.232 AU. This finding was confirmed in primary cortical cultures, which showed abundant PGRN expression in microglia (**Figure 2C**) but no difference due to glucose concentration (from 1.000 ± 0.315 AU to 0.714 ± 0.163 AU (**Figure 2D**). In summary, PGRN expression does not appear to be significantly altered under high glucose, signifying that

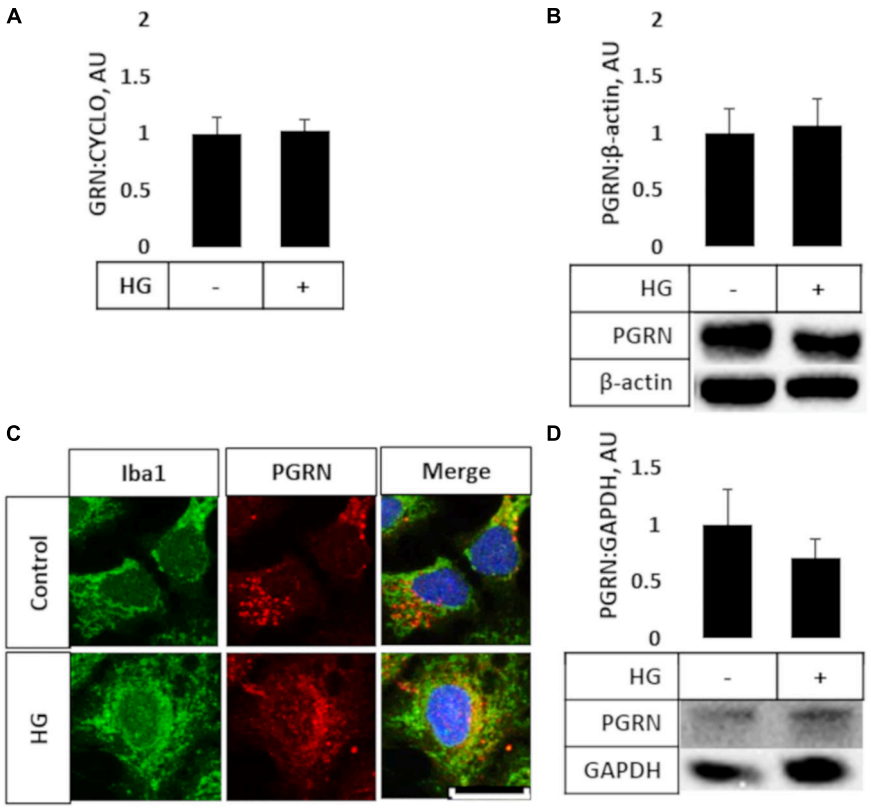

FIGURE 2 | PGRN expression in microglial cells treated with high glucose. HMC3 microglial cells were grown to confluence and treated with high glucose for 72 h before harvest and testing for mRNA **(A)** and protein **(B)** levels of PGRN. A, PGRN mRNA levels were unaffected by high glucose, changing from 1.000 ± 0.139 AU to 1.022 ± 0.099 AU. *N* = 10 samples. **(B)** PGRN protein levels were unaffected by high glucose, changing from 1.000 ± 0.212 AU to 1.069 ± 0.232 AU. *N* = 8 samples. **(C)** Representative immunofluorescence images of primary microglia after 72 h of treatment, with blue as DAPI, green as Iba1, and red as PGRN. Scale bar, 10 μm. **(D)** Western blot analysis of primary cortical cells revealed that PGRN levels were unaffected by glucose concentration, changing from 1.000 ± 0.315 AU to 0.714 ± 0.163 AU. N = 6 samples.

hyperglycemia-induced neurodegeneration is unlikely due to differential PGRN levels *per se*.

Progranulin Preserves Light Chain 3B Flux Under High Glucose Conditions

Impairment of autophagy is seen in diabetes and neurodegenerative conditions, so we tested how high glucose affected autophagy flux using LC3B as an autophagosome marker. Conjugation of LC3 with phosphatidylethanolamine (PE) is an essential step in maturation of the autophagosome, and the rate of autophagy flux can be estimated by measuring the ratio of conjugated to unconjugated protein (i.e., LC3-II:I ratio) via western blot (Mizushima and Yoshimori, 2007). While the overall ANOVA did not reach the threshold of significance (F = 2.195, p = 0.108), there appears to be a trend toward a decrease in the LC3-II:I ratio due to high glucose compared to control, from 1.000 ± 0.208 AU to 0.464 ± 0.092 AU (**Figure 3A**). PGRN treatment did not appear to alter LC3B levels in either control (from 1.000 ± 0.208 AU to 0.931 ± 0.309 AU) or high-glucose conditions (to 0.474 ± 0.076 AU). Treatment with the lysosomal inhibitor chloroquine (CQ) led to an increased LC3-II:I ratio (F = 5.643, p = 0.000), indicative of impaired lysosomal clearance (**Supplementary Figure 2A**). The change in LC3B was significant in all treatment groups except for PGRN alone (0.940 ± 0.426 AU to 2.147 ± 0.595 AU, p = 0.056). Treatment with the autophagy inducer rapamycin also increased LC3B lipidation (F = 2.378, p = 0.042), although this was significant only in cells treated with PGRN (0.940 ± 0.426 AU to 7.012 ± 3.711 AU, p = 0.006) (**Supplementary Figure 2B**).

Light chain 3B can also be used to measure autophagosome formation by immunofluorescence, with an increase in punctate formation indicating increased autophagosome formation or decreased autophagosome clearance. We performed immunofluorescence in cortical cells, with LC3B as red and co-stained with either MAP2 as a neuronal marker or GFAP as a glial cell marker (both in green). We found significant changes in LC3B expression in neurons (F = 10.45, p = 0.001), with a lower (but not significantly so) level of LC3B fluorescence seen when cultured under high-glucose conditions, from 1.000 ± 0.069 AU to 0.916 ± 0.045 AU (p = 0.331) (**Figure 3B**). On the other hand, under high-glucose conditions, PGRN increased puncta levels to 1.190 ± 0.097 AU (p = 0.003). It is worth noting that cells labeled with the neuronal marker MAP2 exhibited substantial

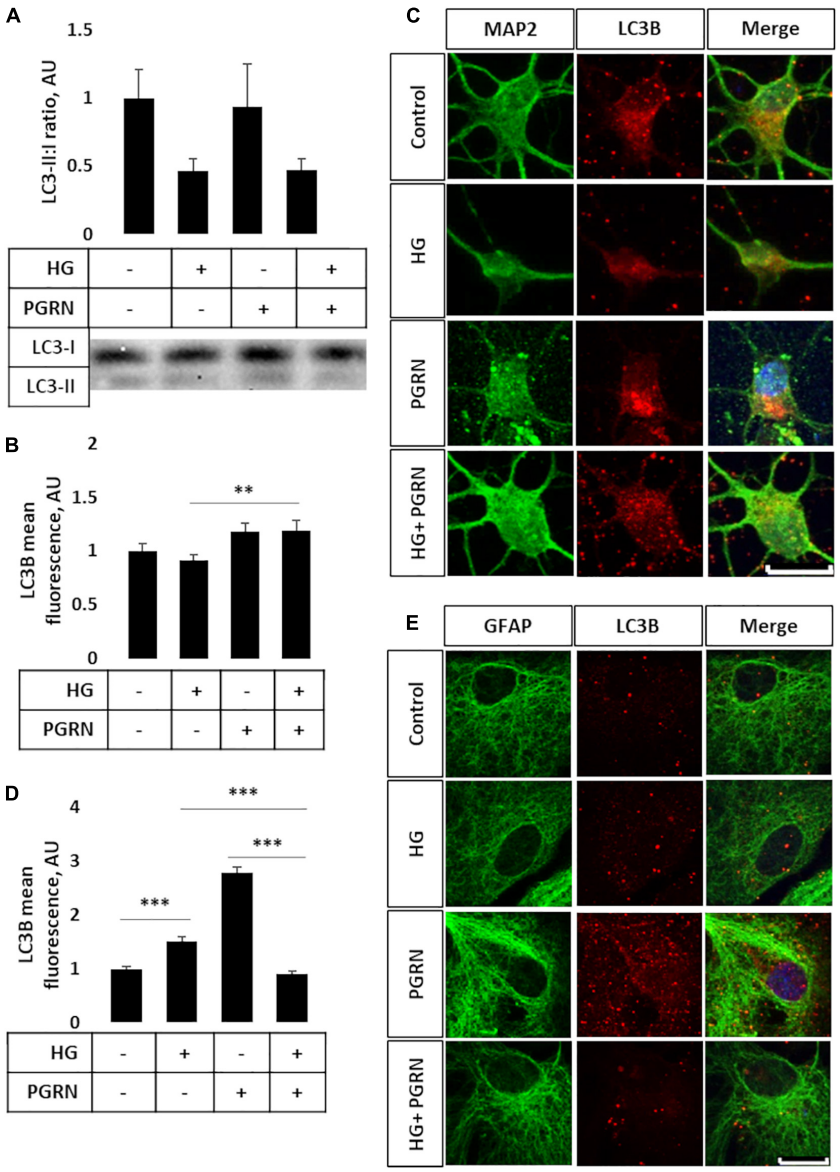

FIGURE 3 | LC3B lipidation and punctate formation in cortical neurons due to high glucose and PGRN. **(A)** Western blot analysis of LC3 lipidation (i.e., LC3-II:I ratio) in primary cortical neurons after 72 h of treatment. The LC3-II:I ratio decreased from control to high glucose (1.000 ± 0.208 AU to 0.464 ± 0.092 AU), an effect that appeared unaffected when treated with PGRN alongside high glucose (0.474 ± 0.076 AU). No difference was observed between control and PGRN-treated samples (0.938 ± 0.309 AU). *N* = 9 samples. **(B)** Immunofluorescence analysis of LC3B puncta expression in neurons after 72 h of treatment. The amount of punctate expression trended toward an increase due to PGRN (from 1.000 ± 0.069 AU, to 1.183 ± 0.077 AU). This difference was significant under high-glucose conditions (from 0.916 ± 0.045 AU, to 1.190 ± 0.097 AU). *N* = 11-29 cells. **(C)** Representative immunofluorescence images of primary neurons after 72 h of treatment, with blue as DAPI, green as MAP2, and red as LC3B. Scale bar, 10 μm. **(D)** Immunofluorescence of LC3B puncta expression in astrocytes after 72 h of treatment increased significantly due to high glucose as well as PGRN treatment (from 1.000 ± 0.0374 AU to 1.512 ± 0.087 AU and 2.792 ± 0.099 AU, respectively). This decreased to control levels under HG + PGRN treatment, to 0.899 ± 0.049 AU. *N* = 12-29 cells. **(E)** Representative immunofluorescence images of primary astrocytes after 72 h of treatment, with blue as DAPI, green as GFAP, and red as LC3B. Scale bar, 10 μm. $^{**}p < 0.01$; $^{***}p < 0.001$.

neurite growth in control conditions, while neurons incubated in high glucose appear to have fewer major primary neurites (**Figure 3C**), similar to our phase-contrast images (**Figure 1C**). Differences in LC3B puncta were also pronounced in astrocytes (F = 104.6, p = 0.000), albeit in the opposite direction, with high glucose significantly increasing LC3B fluorescence in these cells from 1.000 ± 0.037 AU to 1.512 ± 0.087 AU (p = 0.001). PGRN increased LC3B intensity even more so, to 2.792 ± 0.099 (p = 0.000), but decreasing under high-glucose conditions from 1.512 ± 0.087 AU to 0.899 ± 0.049 AU (p = 0.000) (**Figures 3D,E**). These data on LC3B expression collectively suggest that autophagy flux is decreased under high-glucose

conditions and that PGRN alleviates this impairment, with neurons and astrocytes being affected in different ways.

Lysosomal Turnover Is Promoted by Progranulin Under High-Glucose Conditions Despite Unchanged Lysosome-Associated Membrane Protein 2A Levels

Later steps of autophagy consist of autophagosome fusion with lysosomal vesicles, which has been shown to be impaired in diabetes (Ma et al., 2017). To see if this step was affected by PGRN, we performed western blot and immunofluorescence studies for LAMP2A, a lysosome membrane protein that localizes in the perinuclear region upon autophagy activation. By western blot, we observed no change in total LAMP2A levels in cells (F = 3.271, p = 0.621) (**Figure 4A**) and an increase when cells were treated with the lysosomal inhibitor CQ (F = 5.75, p = 0.002) and autophagy inducer rapamycin (F = 3.763, p = 0.004) (**Supplementary Figures 3A,B**). LAMP2A protein levels increased in all groups due to rapamycin and due to CQ except control, which trended toward an increase (1.000 ± 0.074 AU to 2.453 ± 0.497 AU, p = 0.094).

However, we observed differential LAMP2A punctate formation in the perinuclear region of cells treated with PGRN. By immunofluorescence, we observed an increase in LAMP2A puncta in neurons (F = 4.423, p = 0.007), with high glucose increasing punctate levels from 1.000 ± 0.137 AU to 1.463 ± 0.108 AU (p = 0.005) (**Figures 4B,C**). PGRN co-treatment alongside high glucose reduced punctate formation to 1.246 ± 0.096 AU, which was no longer significantly different from control (from 1.000 ± 0.137 AU, p = 0.160) or PGRN treatment alone (from 1.031 ± 0.083 AU, p = 0.152). In astrocytes, we saw a non-significant trend toward an increase in LAMP2A expression in cells treated with PGRN (F = 1.825, p = 0.151) (**Figures 4D,E**). Combined with our data on LC3B, this indicates that lysosome levels are affected by PGRN in cells under high-glucose stress, and that this effect is also different in neurons and astrocytes.

Turnover of AGEs Is Promoted by Progranulin Under High-Glucose Stress

AGEs build up under hyperglycemic conditions as excess glucose spontaneously glycosylates proteins (Singh et al., 2014). Under conditions of impaired autophagy, these modified proteins build up due to a lack of clearance (Takahashi et al., 2017). As a more direct metric of protein turnover, we incubated cortical cells at the end of a 72-h treatment period with 50 μg of AGE-BSA and continued treatment for 6 h at 37°C before harvest. We observed a significant change in AGE levels (F = 3.271, p = 0.047); in particular, AGE levels were higher in cells under high glucose compared to the control, increasing from 5.067 ± 0.385 μg/mg protein to 8.004 ± 0.852 μg/mg protein (p = 0.007) (**Figure 5A**). While AGE levels were slightly higher in samples treated with 200 ng/ml PGRN than in control at 6.158 ± 0.734 μg/mg protein, this was not significant (p = 0.266), and high glucose did not increase concentration further (up to 6.033 ± 0.575 μg/mg protein; p = 0.812 between PGRN and HG + PGRN), suggesting that PGRN treatment aided in clearance of AGE from cells. We also found similar results via western blot (F = 3.231, p = 0.047), with an overall increase due to high glucose from 1.000 ± 0.196 AU to 1.726 ± 0.150 AU (p = 0.009 between control and high glucose). There was no significant increase due to PGRN (to 1.195 ± 0.078 AU) compared to control (p = 0.438 between control and PGRN) and high-glucose treatment did not increase this further (to 1.377 ± 0.260; p = 0.472 between PGRN and HG + PGRN) (**Figure 5B**). These data indicate that PGRN may aid in clearance of protein substrates that accumulate due to high-glucose stress.

Progranulin Modulates Mitochondrial Activity Under High-Glucose Stress in a Complex-Specific Manner

Mitochondrial activity is dysregulated in diabetes and neurodegenerative diseases like Parkinson's. Mitochondrial damage is a major contributor of reactive oxygen species (ROS) leakage and cellular dysfunction, and is also seen in hyperglycemic conditions (Rolo and Palmeira, 2006). Because proper maintenance of mitochondrial function through regular turnover is important to neuronal metabolic health (Rugarli and Langer, 2012), we aimed to see if preserving autophagy also improved mitochondrial function. We therefore monitored mitochondrial enzymatic activity as a metric of mitochondrial function, measuring the function of complex I (ubiquinone oxidoreductase, UO), complex II (succinate dehydrogenase, SDH), and complex IV (cytochrome C oxidase, COX). Our results were mixed, with results varying by complex. UO activity, measured in terms of ΔmOD_{340}, did not change under any treatment condition (F = 1.373, p = 0.283) (**Figure 6A**). SDH activity trended toward significance (F = 2.209, p = 0.119), with a trend toward a decrease under high-glucose conditions, observed as a decrease in ΔmOD_{600} from 1.138 ± 0.069 to 0.817 ± 0.172 (p = 0.060). PGRN treatment attenuated the decrease due to high glucose from 1.203 ± 0.026 to 1.069 ± 0.129 ΔmOD_{600} (p = 0.414 between PGRN and HG + PGRN) (**Figure 6B**). COX activity was significantly altered by high glucose and PGRN (F = 20.89, p = 0.000), with ΔmOD_{550} increasing under high-glucose conditions from 1.596 ± 0.100 to 2.167 ± 0.122 (p = 0.028). PGRN treatment amplified this increase from 1.948 ± 0.183 to 3.482 ± 0.274 (p = 0.000 between PGRN and HG + PGRN) despite no change when comparing control to PGRN treatment alone (ΔmOD_{550} from 1.596 ± 0.100 to 1.948 ± 0.183, p = 0.156) (**Figure 6C**). This indicates that the impact of hyperglycemia and PGRN on the mitochondria is complex-specific.

Extracellular Signal-Regulated Kinase 1/2 and GSK3β Phosphorylation Are Affected by Progranulin Under High-Glucose Conditions

Several signaling pathways are implicated in diabetes, including those involved in cell stress such as GSK3β and ERK1/2. The former is implicated in autophagy activation through

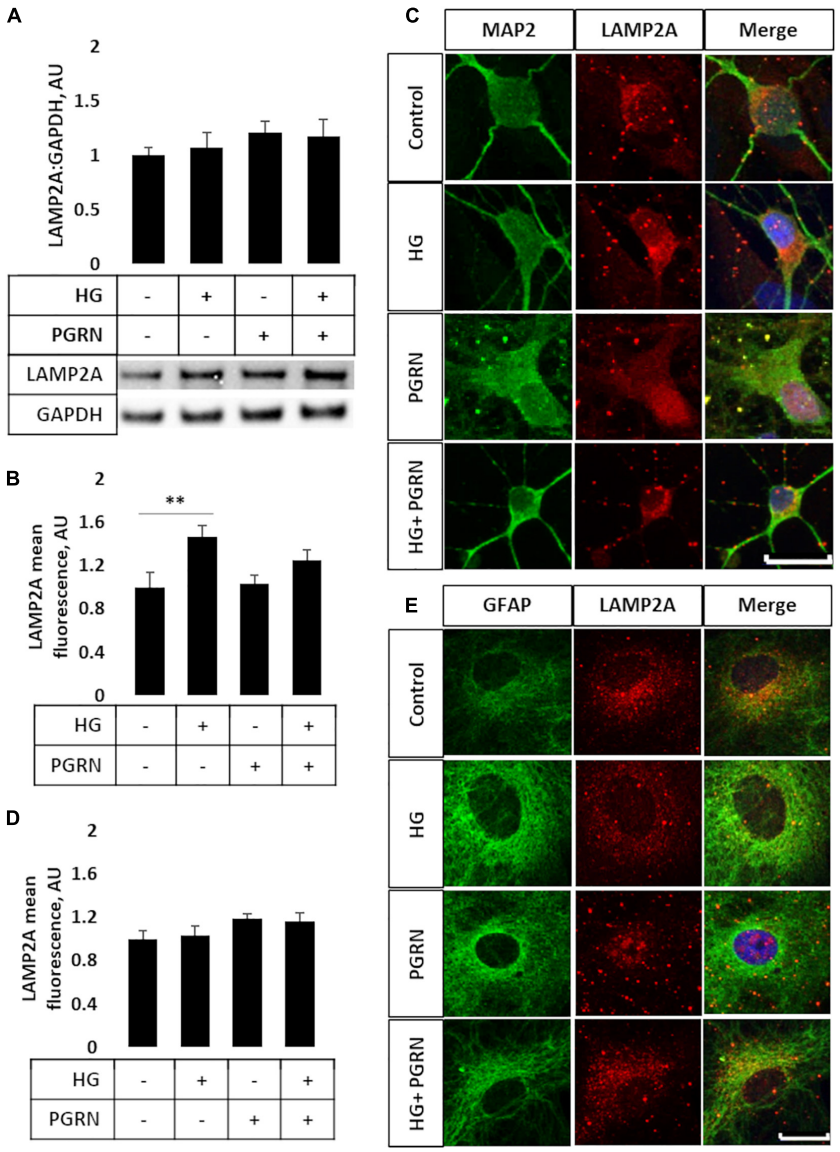

FIGURE 4 | LAMP2A protein levels and punctate localization in cortical neurons and astrocytes due to high glucose and PGRN treatment. **(A)** Total protein LAMP2A levels are unchanged among treatment groups in primary cortical neurons treated for 24 h. $N = 6$ samples. **(B)** Perinuclear LAMP2A punctate formation increased in neurons under HG (from 1.000 ± 0.137 AU to 1.463 ± 0.108 AU), an effect that was attenuated with PGRN (from 1.031 ± 0.083 AU to 1.246 ± 0.096 AU). $N = 12$-27 cells. **(C)** Representative immunofluorescence images of primary neurons after 72 h of treatment, with blue as DAPI, green as MAP2, and red as LAMP2A. Scale bar, 10 μm. **(D)** Perinuclear LAMP2A punctate formation appeared to show a trend toward an increase due to PGRN but was not statistically significant ($F = 1.825$, $p = 0.151$). $N = 16$-22 cells. **(E)** Representative immunofluorescence images of primary astrocytes after 72 h of treatment, with blue as DAPI, green as GFAP, and red as LAMP2A. Scale bar, 10 μm. $^{**}p < 0.01$.

downstream ULK1 activation (Lin et al., 2012), and the latter has been shown to promote autophagy induction under stressful conditions (Cagnol and Chambard, 2010). We found that PGRN influences the phosphorylation of these kinases in high-glucose conditions, albeit with different timings. Inhibitory GSK3β phosphorylation at serine 9 was not significantly affected after 24 h of treatment ($F = 0.809$, $p = 0.504$) (**Figure 7A**). After 72 h of treatment, phosphorylation increased significantly ($F = 7.606$, $p = 0.002$), with high glucose increasing phosphorylation from 1.000 ± 0.078 AU to 2.044 ± 0.445 AU ($p = 0.009$) (**Figure 7B**). PGRN treatment reduced phosphorylation from 1.000 ± 0.078 AU to 0.551 ± 0.112 AU ($p = 0.221$), although a statistically significant decrease was only observed under high-glucose conditions (2.044 ± 0.445 AU to 0.628 ± 0.178 AU, $p = 0.001$). On the other hand, we found that activatory threonine 202 and tyrosine 204 phosphorylation of ERK1/2 significantly increased after 24 h of treatment ($F = 7.750$, $p = 0.009$) (**Figure 7C**) and returned to baseline within 72 h ($F = 0.759$, $p = 0.530$) (**Figure 7D**). At 24 h of treatment, it increased under simultaneous high-glucose and PGRN

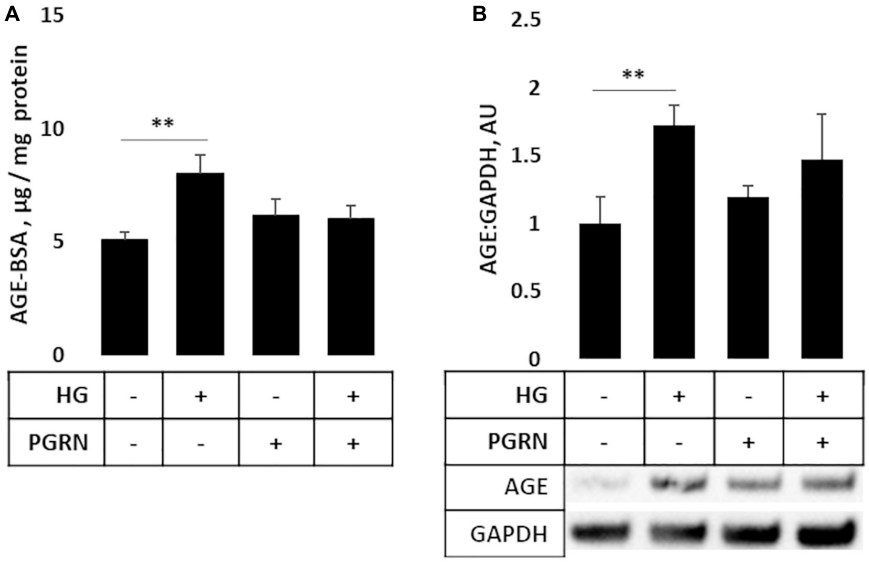

FIGURE 5 | Protein turnover in cortical neurons treated with high glucose and PGRN. **(A)** Cells incubated with high-glucose medium and progranulin for 72 h were treated with 50 μg of AGE-BSA during the remaining 6 h before harvest. Remaining AGE-BSA was measured by fluorescence (360 nm excitation, 460 nm emission) and calculated using a standard curve. High glucose increased AGE-BSA levels from 0.025 ± 0.002 μg/mg protein to 0.040 ± 0.004 μg/mg protein. PGRN was not significantly higher than control (0.031 ± 0.004 μg/mg protein), and no difference was observed due to high glucose alongside PGRN treatment (0.032 ± 0.003 μg/mg protein). *N* = 5-6 samples. **(B)** Western blot analysis of samples in **(A)**. Increased AGE-BSA in high glucose from 1.000 ± 0.197 to 1.726 ± 0.144, indicative of reduced protein turnover, was seen. PGRN prevented the change due to glucose concentration (from 1.198 ± 0.081 to 1.473 ± 0.746) without significantly increasing from control samples ($p = 0.792$). *N* = 5-6 samples. $^{**}p < 0.01$.

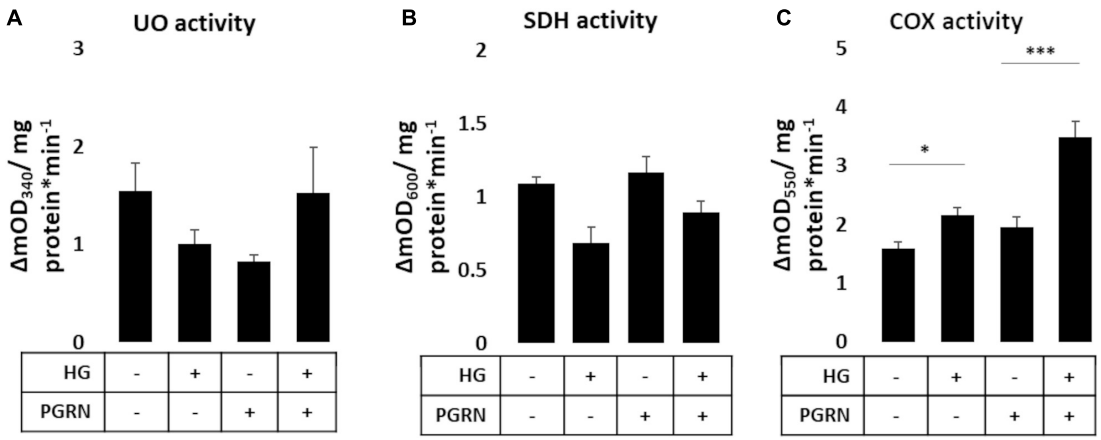

FIGURE 6 | Mitochondrial complex activity in primary cortical neurons in response to high glucose and PGRN. Cells were treated with high glucose and PGRN for 72 h before harvest and enzymatic testing via microplate assay. **(A)** Ubiquinone oxidoreductase (UO) activity was unchanged among treatment conditions. **(B)** Succinate dehydrogenase (SDH) activity decreased under high glucose from 1.138 ± 0.069 ΔmOD_{600} to 0.817 ± 0.172 ΔmOD_{600}. While PGRN alone did not alter activity (1.203 ± 0.026 ΔmOD_{600}), it attenuated the decrease in activity due to high glucose (1.069 ± 0.129 ΔmOD_{600}). N = 6 samples. **(C)** Cytochrome C oxidase (COX) activity was increased by high glucose from 1.596 ± 0.100 ΔmOD_{550} to 2.167 ± 0.122 ΔmOD_{550}. With PGRN, high glucose amplified this increase from 1.948 ± 0.183 ΔmOD_{550} to 3.482 ± 0.274 ΔmOD_{550}. *N* = 5-6 samples. $^{*}p < 0.05$; $^{***}p < 0.001$.

treatment from 1.000 ± 0.145 AU to 2.403 ± 0.381 AU ($p = 0.004$ between control and HG + PGRN). However, high glucose and PGRN treatments alone did not elicit any change, only changing ERK1/2 phosphorylation to 1.342 ± 0.398 and 0.932 ± 0.241 AU, respectively ($p = 0.352$ and 0.848, respectively). This effect appears to affect ERK2 ($F = 8.436$, $p = 0.007$) as well as ERK1 phosphorylation despite a non-significant change in the latter ($F = 1.206$, $p = 0.368$). The lack of significance at 72 h was also present when looking at ERK1 ($F = 1.784$, $p = 0.183$) and ERK2 ($F = 1.115$, $p = 0.366$) in particular. These findings suggest that GSK3β and ERK1/2 activation may play a role in PGRN's autophagy-modulating response in neurons cultured in high glucose in a time-dependent manner.

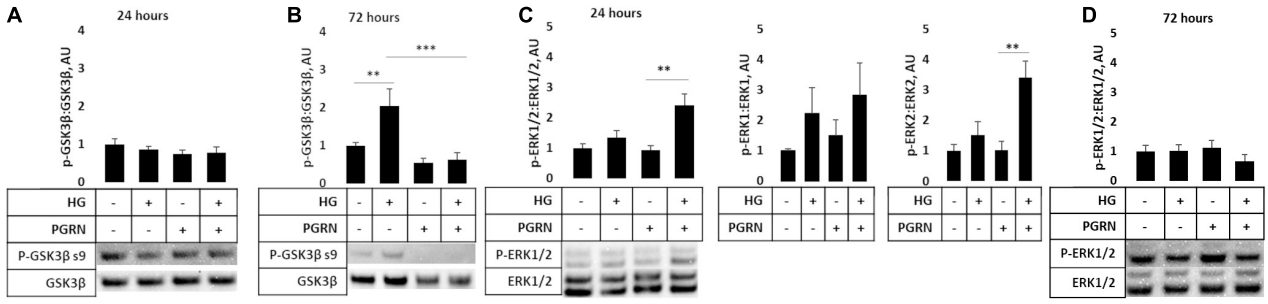

FIGURE 7 | GSK3β and ERK phosphorylation in cortical neurons due to high glucose and PGRN treatment. Cells were treated with high glucose and PGRN for 24 or 72 h before harvest and western blot analysis. **(A,B)** GSK3β phosphorylation at serine nine was unaltered by high glucose or PGRN at 24 h **(A)** but showed significant change at 72 h **(B)**. At 72 h, high glucose increased phosphorylation from 1.000 ± 0.078 AU to 2.044 ± 0.445 AU, while PGRN treatment lowered phosphorylation in both control (1.000 ± 0.078 AU to 0.550 ± 0.112 AU) and high-glucose conditions (2.044 ± 0.445 AU to 0.628 ± 0.178 AU). *N* = 5-6 samples. **(C)** ERK1/2 phosphorylation at threonine 202/tyrosine 204 increased with simultaneous PGRN and high-glucose conditions from 1.000 ± 0.145 AU to 2.403 ± 0.381 AU at 24 h of treatment. Upon closer analysis, ERK2, but not ERK1, phosphorylation was significantly affected, with ERK2 phosphorylation increasing from 1.000 ± 0.197 AU to 3.401 ± 0.544 AU. *N* = 3 samples. **(D)** ERK1/2 phosphorylation at threonine 202/tyrosine 204 was not significantly altered by high glucose or PGRN after 72 h. *N* = 6 samples. $^{**}p < 0.01$; $^{***}p < 0.001$.

DISCUSSION

In this study, we posit that PGRN may have neuroprotective roles against high glucose-induced reductions in neuronal health and autophagy function. Previous work has connected PGRN to neurodegeneration due to FTLD (Paushter et al., 2018), Alzheimer's (Minami et al., 2014), and Parkinson's (Kampen et al., 2014). Research in T2D is mixed, with brain and renal tissues showing a protective effect (Kampen et al., 2014; Zhou et al., 2019b), while in adipose tissue, higher PGRN is deleterious (Zhou et al., 2015). However, no published work to our knowledge has looked at PGRN in the context of hyperglycemia-impaired neuronal autophagy flux and protein turnover. In line with evidence of PGRN's neuroprotective and growth factor properties, we observed preserved cellular viability (**Figure 1A**) and neurite outgrowth in cultured neurons (**Figures 1B,C**) under high-glucose stress.

Microglia express high levels of PGRN (Mendsaikhan et al., 2019), and while studies have explored PGRN levels in brain tissue, those that studied PGRN in the context of T2D examined serum (Youn et al., 2009; Qu et al., 2013) and non-neuronal cell levels (Zhou et al., 2019b). We found that while microglia expressed high levels of PGRN, treatment with high glucose for 72 h did not significantly affect PGRN mRNA or protein expression (**Figure 2**). This suggests that short-term hyperglycemia does not regulate PGRN levels in brain tissue.

Progranulin has been demonstrated to protect against neurodegeneration through autophagy activation (Paushter et al., 2018; Zhou et al., 2019a), but this has not been explored in the context of hyperglycemia; for that reason, we looked into autophagy flux in response to high glucose. The process of autophagy can be broken down into initiation, nucleation, fusion, and degradation steps, with blockage of each having a distinct signature (Khandia et al., 2019). During nucleation, the light chain protein LC3 is conjugated with PE and attached to both membranes of the developing phagophore, serving as a useful metric of autophagy flux via western blot (Mizushima and Yoshimori, 2007). We observed a decrease in the LC3-II:I ratio in neurons under high glucose, with a minor attenuation due to PGRN (**Figure 3A**). Treatment of cells with the lysosomal inhibitor CQ resulted in the expected increase in LC3-II:I due to autophagosome buildup, although this increase did not reach the level of significance when treated with PGRN (**Supplementary Figure 2A**). Rapamycin treatment also increased this ratio, reflective of increased autophagy activation due to mTORC1 inhibition (Li et al., 2014), but this was only significant in cells treated with PGRN (**Supplementary Figure 2B**). Studies of hyperglycemia in other cell types have shown increased LC3 puncta (Lenoir et al., 2015; Ma et al., 2017; Sakai et al., 2019), so we performed immunofluorescence studies as well. We observed greater LC3 accumulation in PGRN-treated neurons and decreased accumulation in astrocytes under high glucose (**Figure 3**). Despite no significant change in the LC3-II:I ratio with PGRN under high-glucose conditions, it is possible that the increased LC3 puncta formation is indicative of greater autophagosome maturation due to PGRN.

While total protein levels of the lysosomal membrane protein LAMP2A were unchanged (**Figure 4A**), we observed increased perinuclear punctate expression of neurons treated with high glucose that was attenuated with PGRN (**Figures 4B,C**). This, coupled with the increase in LAMP2A protein due to CQ (**Supplementary Figure 3A**) and seemingly inverse relationship between LAMP2A puncta and autophagy flux (**Figure 3A**), suggests a buildup of lysosomes in addition to impaired autophagy in neurons under high glucose. PGRN may also play a role in attenuating this, given the reduced buildup of LC3-II when treated alongside CQ (**Supplementary Figure 2A**). Transfecting cells with dual fluorescence-tagged LC3 (Kimura et al., 2007) could determine if the increased LAMP2A observed represents lysosomes or autolysosomes (the fusion of autophagosome and lysosome).

An unexpected finding in our observations is that LC3B and LAMP2A puncta expression differed in astrocytes and in neurons (**Figures 3**, **4**). Specifically, we observed a marked decrease in

LC3B puncta in astrocytes due to PGRN under high glucose (**Figure 4D**). Glia, particularly astrocytes, play important roles in maintaining neuronal health, including mediating immune responses and regulating glucose metabolism (García-Cáceres et al., 2016; Ortiz-Rodriguez and Arevalo, 2020). While there is less research focusing on their role in autophagy, recent work supports a model in which glia, and astrocytes specifically, contribute to autophagy in neurons (Di Malta et al., 2012; Ortiz-Rodriguez and Arevalo, 2020), possibly through secretion and clearance by surrounding microglia (Choi et al., 2020). Future studies in isolated astrocytic and neuronal fractions are needed to verify if high glucose differentially affects autophagy in these cell types.

While LC3B and LAMP2A are commonly-used markers, there are caveats to consider when interpreting (Mizushima and Yoshimori, 2007; Kaushik and Cuervo, 2009). We therefore sought a more direct metric of protein turnover using AGE-BSA as a substrate. Other studies have monitored protein turnover as a measure of autophagy function using radioisotope and fluorescent reporters (Lui et al., 2016; Orhon and Reggiori, 2017), and our interest in AGE specifically is due to its accumulation under hyperglycemic conditions (Nowotny et al., 2015). Through western blot and microplate assay, we observed increased AGE levels under high-glucose conditions, with PGRN preventing this increase (**Figure 5**). Alongside our images of LAMP2A punctate formation (**Figure 4B**), this further supports a model in which proteins targeted for autophagy accumulate under high-glucose conditions, and that PGRN promotes in their breakdown.

Dysfunctional glucose metabolism from hyperglycemia leads to impaired mitochondrial well-being (Sears and Perry, 2015). Defective mitochondria are normally degraded via autophagy as a quality control mechanism (Um and Yun, 2017), which has been shown to be dysregulated under hyperglycemic conditions (Rovira-Llopis et al., 2017). Because prior research has implicated PGRN mutations to impaired mitophagy signaling (Gaweda-Walerych et al., 2021), we investigated if PGRN would aid in preserving mitochondrial function as a downstream consequence of improved mitophagy regulation. Enzymatic studies of mitochondrial function focus on complexes I, II, and IV, so we examined each to obtain a more granular understanding of how high glucose and PGRN affect activity. Our data showed that PGRN and hyperglycemia affect mitochondrial enzyme activity in a complex-specific manner (**Figure 6**), which may be due to the difference in reaction dynamics involved between enzymes. Interestingly, we found that the decrease in SDH activity due to high glucose was prevented by PGRN (**Figure 6B**), and that the increase in COX activity due to high glucose was potentiated by PGRN despite no change due to PGRN alone (**Figure 6C**). Hyperglycemic cell stress increases intracellular Ca^{2+} levels in the cytosol of neurons (Pereira et al., 2010), an effect that has been shown to contribute to de-phosphorylation of an inhibitory site on COX (Ramzan et al., 2021). Since uncontrolled mitochondrial activity leads to excess ROS generation and subsequent cell death, it is possible that PGRN's neuroprotective effects enable cells under high-glucose conditions to sustain increased COX activity with less deleterious outcomes.

Hyperglycemia activates pathways that both upregulate and downregulate autophagy, and it is the balance between them that determines the overall trajectory of the cell. For instance, cell stressors like high glucose can activate autophagy through ERK activation (Cagnol and Chambard, 2010), although hyperglycemia also inhibits it through mTORC1 activation and subsequent GSK3β inhibition (Kim et al., 2011; Muriach et al., 2014). Because of this, we investigated the role of ERK1/2 and GSK3β. We found that activatory ERK1/2 phosphorylation increased in neurons treated with high glucose and PGRN simultaneously after 24 h (**Figure 7C**). Similar time-course results were also observed in the hypothalamus of diabetic mouse models treated with Fibroblast Growth Factor 1 (Brown et al., 2021). This activation of ERK1/2 may also contribute to increased mitochondrial activity, as its activation is implicated in proper mitophagy function (Lei et al., 2018; Liu et al., 2021). Interestingly, GSK3β phosphorylation was unchanged at 24 h, but decreased significantly with simultaneous high glucose and PGRN treatment after 72 h (**Figure 7B**). This could suggest some interplay between the two kinases, as GSK3β has been demonstrated to prevent nuclear localization of ERK1/2, a downstream effect of the latter's activation (Ma et al., 2008). GSK3β has also been implicated in autophagy activation through the GSK3β-TIP60-ULK1 pathway, so this reduced phosphorylation may also reflect autophagy induction (Nie et al., 2016).

Diabetes is a widespread disease that results in impaired autophagy, protein buildup, and neurodegeneration. Hyperglycemia specifically contributes to pathology in the nervous system, and in the search for a mechanistic cause, multiple pathways have been implicated. Dysfunction in the final steps of autophagy, fusion, and degradation via lysosomes, has been postulated as the cause behind hyperglycemic impairment of autophagy (Nixon et al., 2008; Ma et al., 2017). While PGRN has been a candidate of interest in neurodegeneration and diabetes (Nicoletto and Canani, 2015; Paushter et al., 2018), there has been a lack of research tying PGRN, diabetes-induced neurodegeneration, and autophagy together. We found that PGRN may alleviate high-glucose pathology through upregulation of autophagy, and that it also seems to preserve mitochondrial function under high-glucose conditions. Furthermore, our studies indicate that ERK signaling may also play a role in PGRN's mechanism of action. However, further research in diabetic cell and animal models needs to be performed to verify PGRN's neuroprotective role against diabetic stress.

DATA AVAILABILITY STATEMENT

The raw data supporting the conclusions of this article will be made available by the authors, without undue reservation.

ETHICS STATEMENT

The animal study was reviewed and approved by the Saint Louis University Animal Care and Use Committee.

AUTHOR CONTRIBUTIONS

CD, AN, and FX conceptualized and planned the experimental study. CD, VM, and GA performed experiments and performed data analysis. CD, VM, GA, AN, and FX prepared and edited the manuscript.

FUNDING

This work was supported with funding from the Saint Louis University start-up fund to FX, the Saint Louis University Henry and Amelia Nasrallah Center for Neuroscience seed fund to FX and AN, and the Saint Louis University Graduate-Undergraduate Research Collaboration Fund to Cass Dedert and Vandana Mishra.

SUPPLEMENTARY MATERIAL

The Supplementary Material for this article can be found online at: https://www.frontiersin.org/articles/10.3389/fncel.2022.874258/full#supplementary-material

REFERENCES

Almeida, M. R., Macário, M. C., Ramos, L., Baldeiras, I., Ribeiro, M. H., and Santana, I. (2016). Portuguese family with the co-occurrence of frontotemporal lobar degeneration and neuronal ceroid lipofuscinosis phenotypes due to progranulin gene mutation. *Neurobiol. Aging* 41, .e1–.e200. doi: 10.1016/j.neurobiolaging.2016.02.019

Baker, M., Mackenzie, I. R., Pickering-Brown, S. M., Gass, J., Rademakers, R., Lindholm, C., et al. (2006). Mutations in progranulin cause tau-negative frontotemporal dementia linked to chromosome 17. *Nature* 442, 916–919. doi: 10.1038/nature05016

Brown, J. M., Bentsen, M. A., Rausch, D. M., Phan, B. A., Wieck, D., Wasanwala, H., et al. (2021). Role of hypothalamic MAPK/ERK signaling and central action of FGF1 in diabetes remission. *IScience* 24:102944. doi: 10.1016/j.isci.2021.102944

Cagnol, S., and Chambard, J.-C. (2010). ERK and cell death: mechanisms of ERK-induced cell death - apoptosis, autophagy and senescence: ERK and cell death. *FEBS J.* 277, 2–21. doi: 10.1111/j.1742-4658.2009.07366.x

Cairns, N. J., Neumann, M., Bigio, E. H., Holm, I. E., Troost, D., Hatanpaa, K. J., et al. (2007). TDP-43 in Familial and Sporadic Frontotemporal Lobar Degeneration with Ubiquitin Inclusions. *Am. J. Pathol.* 171, 227–240. doi: 10.2353/ajpath.2007.070182

Chang, S.-C., and Yang, W.-C. V. (2016). Hyperglycemia, tumorigenesis, and chronic inflammation. *Crit. Rev. Oncol. Hematol.* 108, 146–153. doi: 10.1016/j.critrevonc.2016.11.003

Chen, M., Zheng, H., Wei, T., Wang, D., Xia, H., Zhao, L., et al. (2016). High Glucose-Induced PC12 Cell Death by Increasing Glutamate Production and Decreasing Methyl Group Metabolism. *BioMed. Res. Internat.* 2016:4125731. doi: 10.1155/2016/4125731

Choi, I., Zhang, Y., Seegobin, S. P., Pruvost, M., Wang, Q., Purtell, K., et al. (2020). Microglia clear neuron-released α-synuclein via selective autophagy and prevent neurodegeneration. *Nat. Comm.* 11:1386. doi: 10.1038/s41467-020-15119-w

Cimen, H., Han, M.-J., Yang, Y., Tong, Q., Koc, H., and Koc, E. C. (2010). Regulation of Succinate Dehydrogenase Activity by SIRT3 in Mammalian Mitochondria. *Biochemistry* 49, 304–311. doi: 10.1021/bi901627u

Cruts, M., Gijselinck, I., van der Zee, J., Engelborghs, S., Wils, H., Pirici, D., et al. (2006). Null mutations in progranulin cause ubiquitin-positive frontotemporal dementia linked to chromosome 17q21. *Nature* 442, 920–924. doi: 10.1038/nature05017

Denton, D., and Kumar, S. (2019). Autophagy-dependent cell death. *Cell Death Diff.* 26, 605–616. doi: 10.1038/s41418-018-0252-y

Di Malta, C., Fryer, J. D., Settembre, C., and Ballabio, A. (2012). Astrocyte dysfunction triggers neurodegeneration in a lysosomal storage disorder. *Proc. Natl. Acad. Sci.* 109, E2334–E2342. doi: 10.1073/pnas.1209577109

García-Cáceres, C., Quarta, C., Varela, L., Gao, Y., Gruber, T., Legutko, B., et al. (2016). Astrocytic Insulin Signaling Couples Brain Glucose Uptake with Nutrient Availability. *Cell* 166, 867–880. doi: 10.1016/j.cell.2016.07.028

Gass, J., Cannon, A., Mackenzie, I. R., Boeve, B., Baker, M., Adamson, J., et al. (2006). Mutations in progranulin are a major cause of ubiquitin-positive frontotemporal lobar degeneration. *Hum. Mol. Genet.* 15, 2988–3001. doi: 10.1093/hmg/ddl241

Gaweda-Walerych, K., Walerych, D., Berdyñski, M., Buratti, E., and Zekanowski, C. (2021). Parkin Levels Decrease in Fibroblasts With Progranulin (PGRN) Pathogenic Variants and in a Cellular Model of PGRN Deficiency. *Front. Mol. Neurosci.* 14:676478. doi: 10.3389/fnmol.2021.676478

Kampen, J. M. V., Baranowski, D., and Kay, D. G. (2014). Progranulin Gene Delivery Protects Dopaminergic Neurons in a Mouse Model of Parkinson's Disease. *PLoS One* 9:e97032. doi: 10.1371/journal.pone.0097032

Kaushik, S., and Cuervo, A. M. (2009). Methods to Monitor Chaperone-Mediated Autophagy. *Methods Enzymol.* 452, 297–324. doi: 10.1016/S0076-6879(08)03619-7

Khandia, R., Dadar, M., Munjal, A., Dhama, K., Karthik, K., Tiwari, R., et al. (2019). A Comprehensive Review of Autophagy and Its Various Roles in Infectious, Non-Infectious, and Lifestyle Diseases: current Knowledge and Prospects for Disease Prevention, Novel Drug Design, and Therapy. *Cells* 8:674. doi: 10.3390/cells8070674

Kim, J., Kundu, M., Viollet, B., and Guan, K.-L. (2011). AMPK and mTOR regulate autophagy through direct phosphorylation of Ulk1. *Nat. Cell Biol.* 13, 132–141. doi: 10.1038/ncb2152

Kimura, S., Noda, T., and Yoshimori, T. (2007). Dissection of the Autophagosome Maturation Process by a Novel Reporter Protein, Tandem Fluorescent-Tagged LC3. *Autophagy* 3, 452–460. doi: 10.4161/auto.4451

Lei, Q., Tan, J., Yi, S., Wu, N., Wang, Y., and Wu, H. (2018). Mitochonic acid 5 activates the MAPK-ERK-yap signaling pathways to protect mouse microglial BV-2 cells against TNFα-induced apoptosis via increased Bnip3-related mitophagy. *Cell. Mol. Biol. Lett.* 23:14. doi: 10.1186/s11658-018-0081-5

Lenoir, O., Jasiek, M., Hénique, C., Guyonnet, L., Hartleben, B., Bork, T., et al. (2015). Endothelial cell and podocyte autophagy synergistically protect from diabetes-induced glomerulosclerosis. *Autophagy* 11, 1130–1145. doi: 10.1080/15548627.2015.1049799

Li, J., Kim, S. G., and Blenis, J. (2014). Rapamycin: One Drug, Many Effects. *Cell Metab.* 19, 373–379. doi: 10.1016/j.cmet.2014.01.001

Li, Y., Zhang, Y., Wang, L., Wang, P., Xue, Y., Li, X., et al. (2017). Autophagy impairment mediated by S-nitrosation of ATG4B leads to neurotoxicity in response to hyperglycemia. *Autophagy* 13, 1145–1160. doi: 10.1080/15548627.2017.1320467

Lin, S.-Y., Li, T. Y., Liu, Q., Zhang, C., Li, X., Chen, Y., et al. (2012). GSK3-TIP60-ULK1 Signaling Pathway Links Growth Factor Deprivation to Autophagy. *Science* 336, 477–481. doi: 10.1126/science.1217032

Liu, H., Ho, P. W.-L., Leung, C.-T., Pang, S. Y.-Y., Chang, E. E. S., Choi, Z. Y.-K., et al. (2021). Aberrant mitochondrial morphology and function associated with impaired mitophagy and DNM1L-MAPK/ERK signaling are found in aged mutant Parkinsonian LRRK2R1441G mice. *Autophagy* 17, 3196–3220. doi: 10.1080/15548627.2020.1850008

Liu, J., and Li, L. (2019). Targeting Autophagy for the Treatment of Alzheimer's Disease: challenges and Opportunities. *Front. Mol. Neurosci.* 12:203. doi: 10.3389/fnmol.2019.00203

Lui, H., Zhang, J., Makinson, S. R., Cahill, M. K., Kelley, K. W., Huang, H.-Y., et al. (2016). Progranulin Deficiency Promotes Circuit-Specific Synaptic Pruning by

Microglia via Complement Activation. *Cell* 165, 921–935. doi: 10.1016/j.cell.2016.04.001

Ma, C., Bower, K. A., Chen, G., Shi, X., Ke, Z. J., and Luo, J. (2008). Interaction between ERK and GSK3beta mediates basic fibroblast growth factor-induced apoptosis in SK-N-MC neuroblastoma cells. *J. Biol. Chem.* 283, 9248–9256. doi: 10.1074/jbc.M707316200

Ma, L.-Y., Lv, Y.-L., Huo, K., Liu, J., Shang, S.-H., Fei, Y.-L., et al. (2017). Autophagy-lysosome dysfunction is involved in Aβ deposition in STZ-induced diabetic rats. *Behav. Brain Res.* 320, 484–493. doi: 10.1016/j.bbr.2016.10.031

Ma, Y.-Y., Zhang, X.-L., Wu, T.-F., Liu, Y.-P., Wang, Q., Zhang, Y., et al. (2011). Analysis of the Mitochondrial Complex I-V Enzyme Activities of Peripheral Leukocytes in Oxidative Phosphorylation Disorders. *J. Child Neurol.* 26, 974–979. doi: 10.1177/0883073811399905

Madhusudhanan, J., Suresh, G., and Devanathan, V. (2020). Neurodegeneration in type 2 diabetes: alzheimer's as a case study. *Brain Behav.* 10:5. doi: 10.1002/brb3.1577

Martens, L. H., Zhang, J., Barmada, S. J., Zhou, P., Kamiya, S., Sun, B., et al. (2012). Progranulin deficiency promotes neuroinflammation and neuron loss following toxin-induced injury. *J. Clin. Invest.* 2012:163113. doi: 10.1172/JCI63113

Mendsaikhan, A., Tooyama, I., and Walker, D. G. (2019). Microglial Progranulin: Involvement in Alzheimer's Disease and Neurodegenerative Diseases. *Cells* 8:230. doi: 10.3390/cells8030230

Minami, S. S., Min, S.-W., Krabbe, G., Wang, C., Zhou, Y., Asgarov, R., et al. (2014). Progranulin protects against amyloid β deposition and toxicity in Alzheimer's disease mouse models. *Nat. Med.* 20, 1157–1164. doi: 10.1038/nm.3672

Mir, S. U. R., George, N. M., Zahoor, L., Harms, R., Guinn, Z., and Sarvetnick, N. E. (2015). Inhibition of Autophagic Turnover in β-Cells by Fatty Acids and Glucose Leads to Apoptotic Cell Death. *J. Biolog. Chem.* 290, 6071–6085. doi: 10.1074/jbc.M114.605345

Mizushima, N., and Klionsky, D. J. (2007). Protein Turnover Via Autophagy: implications for Metabolism. *Annu. Rev. Nutrit.* 27, 19–40. doi: 10.1146/annurev.nutr.27.061406.093749

Mizushima, N., and Yoshimori, T. (2007). How to Interpret LC3 Immunoblotting. *Autophagy* 3, 542–545. doi: 10.4161/auto.4600

Moruno, F., Pérez-Jiménez, E., and Knecht, E. (2012). Regulation of Autophagy by Glucose in Mammalian Cells. *Cells* 1, 372–395. doi: 10.3390/cells1030372

Muriach, M., Flores-Bellver, M., Romero, F. J., and Barcia, J. M. (2014). Diabetes and the Brain: oxidative Stress, Inflammation, and Autophagy. *Oxid. Med. Cell. Long.* 2014, 1–9. doi: 10.1155/2014/102158

Nguyen, A. D., Nguyen, T. A., Martens, L. H., Mitic, L. L., and Farese, R. V. (2013b). Progranulin: at the interface of neurodegenerative and metabolic diseases. *Trends Endocrinol. Metab.* 24, 597–606. doi: 10.1016/j.tem.2013.08.003

Nguyen, A. D., Nguyen, T. A., Cenik, B., Yu, G., Herz, J., Walther, T. C., et al. (2013a). Secreted progranulin is a homodimer and is not a component of high density lipoproteins (HDL). *J. Biol. Chem.* 288, 8627–8635. doi: 10.1074/jbc.m112.441949

Nicoletto, B. B., and Canani, L. H. (2015). The role of progranulin in diabetes and kidney disease. *Diabet. Metab. Syndr.* 7:117. doi: 10.1186/s13098-015-0112-6

Nie, T., Yang, S., Ma, H., Zhang, L., Lu, F., Tao, K., et al. (2016). Regulation of ER stress-induced autophagy by GSK3β-TIP60-ULK1 pathway. *Cell Death Dis.* 7, e2563–e2563. doi: 10.1038/cddis.2016.423

Nixon, R. A., Yang, D.-S., and Lee, J.-H. (2008). Neurodegenerative lysosomal disorders: a continuum from development to late age. *Autophagy* 4, 590–599. doi: 10.4161/auto.6259

Nowotny, K., Jung, T., Höhn, A., Weber, D., and Grune, T. (2015). Advanced Glycation End Products and Oxidative Stress in Type 2 Diabetes Mellitus. *Biomolecules* 5, 194–222. doi: 10.3390/biom5010194

Ogata, M., Hino, S.-I., Saito, A., Morikawa, K., Kondo, S., Kanemoto, S., et al. (2006). Autophagy Is Activated for Cell Survival after Endoplasmic Reticulum Stress. *Mol. Cell. Biol.* 26, 9220–9231. doi: 10.1128/MCB.01453-06

Orhon, I., and Reggiori, F. (2017). Assays to Monitor Autophagy Progression in Cell Cultures. *Cells* 6:20. doi: 10.3390/cells6030020

Ortiz-Rodriguez, A., and Arevalo, M.-A. (2020). The Contribution of Astrocyte Autophagy to Systemic Metabolism. *Internat. J. Mol. Sci.* 21:2479. doi: 10.3390/ijms21072479

Pagano, G., Polychronis, S., Wilson, H., Giordano, B., Ferrara, N., Niccolini, F., et al. (2018). Diabetes mellitus and Parkinson disease. *Neurology* 90, e1654–e1662. doi: 10.1212/WNL.0000000000005475

Paushter, D. H., Du, H., Feng, T., and Hu, F. (2018). The lysosomal function of progranulin, a guardian against neurodegeneration. *Acta Neuropathologica* 136, 1–17. doi: 10.1007/s00401-018-1861-8

Pereira, T., de, O. S., da Costa, G. N. F., Santiago, A. R. S., Ambrósio, A. F., and dos Santos, P. F. M. (2010). High glucose enhances intracellular Ca2+ responses triggered by purinergic stimulation in retinal neurons and microglia. *Brain Res.* 1316, 129–138. doi: 10.1016/j.brainres.2009.12.034

Perry, D. C., Lehmann, M., and Yokoyama, J. S. (2013). Progranulin Mutations as Risk Factors for Alzheimer Disease. *JAMA Neurol.* 70, 774–778. doi: 10.1001/2013.jamaneurol.393

Qu, H., Deng, H., and Hu, Z. (2013). Plasma Progranulin Concentrations Are Increased in Patients with Type 2 Diabetes and Obesity and Correlated with Insulin Resistance. *Mediat. Inflamm.* 2013:360190. doi: 10.1155/2013/360190

Ramzan, R., Kadenbach, B., and Vogt, S. (2021). Multiple Mechanisms Regulate Eukaryotic Cytochrome C Oxidase. *Cells* 10:514. doi: 10.3390/cells10030514

Rolo, A. P., and Palmeira, C. M. (2006). Diabetes and mitochondrial function: role of hyperglycemia and oxidative stress. *Toxicol. Appl. Pharm.* 212, 167–178. doi: 10.1016/j.taap.2006.01.003

Ross, C. A., and Poirier, M. A. (2004). Protein aggregation and neurodegenerative disease. *Nat. Med.* 10, S10–S17. doi: 10.1038/nm1066

Rovira-Llopis, S., Bañuls, C., Diaz-Morales, N., Hernandez-Mijares, A., Rocha, M., and Victor, V. M. (2017). Mitochondrial dynamics in type 2 diabetes: pathophysiological implications. *Redox Biol.* 11, 637–645. doi: 10.1016/j.redox.2017.01.013

Rugarli, E. I., and Langer, T. (2012). Mitochondrial quality control: a matter of life and death for neurons: mitochondrial quality control and neurodegeneration. *EMBO J.* 31, 1336–1349. doi: 10.1038/emboj.2012.38

Sakai, S., Yamamoto, T., Takabatake, Y., Takahashi, A., Namba-Hamano, T., Minami, S., et al. (2019). Proximal Tubule Autophagy Differs in Type 1 and 2 Diabetes. *J. Am. Soc. Nephrol.* 30, 929–945. doi: 10.1681/ASN.2018100983

Sears, B., and Perry, M. (2015). The role of fatty acids in insulin resistance. *Lipids Health Dis.* 14:121. doi: 10.1186/s12944-015-0123-1

Sergi, D., Renaud, J., Simola, N., and Martinoli, M.-G. (2019). Diabetes, a Contemporary Risk for Parkinson's Disease: epidemiological and Cellular Evidences. *Front. Aging Neurosci.* 11:302. doi: 10.3389/fnagi.2019.00302

Singh, V. P., Bali, A., Singh, N., and Jaggi, A. S. (2014). Advanced Glycation End Products and Diabetic Complications. *Korean J. Physiol. Pharm.* 18, 1–14. doi: 10.4196/kjpp.2014.18.1.1

Smith, K. R., Damiano, J., Franceschetti, S., Carpenter, S., Canafoglia, L., Morbin, M., et al. (2012). Strikingly different clinicopathological phenotypes determined by progranulin-mutation dosage. *Am. J. Hum. Genet.* 90, 1102–1107. doi: 10.1016/j.ajhg.2012.04.021

Stavoe, A. K. H., and Holzbaur, E. L. F. (2019). Autophagy in Neurons. *Annu. Rev. Cell Dev. Biol.* 35, 477–500. doi: 10.1146/annurev-cellbio-100818-125242

Takahashi, A., Takabatake, Y., Kimura, T., Maejima, I., Namba, T., Yamamoto, T., et al. (2017). Autophagy Inhibits the Accumulation of Advanced Glycation End Products by Promoting Lysosomal Biogenesis and Function in the Kidney Proximal Tubules. *Diabetes* 66, 1359–1372. doi: 10.2337/db16-0397

Um, J.-H., and Yun, J. (2017). Emerging role of mitophagy in human diseases and physiology. *BMB Rep.* 50, 299–307. doi: 10.5483/BMBRep.2017.50.6.056

Van Damme, P., Van Hoecke, A., Lambrechts, D., Vanacker, P., Bogaert, E., van Swieten, J., et al. (2008). Progranulin functions as a neurotrophic factor to regulate neurite outgrowth and enhance neuronal survival. *J. Cell Biol.* 181, 37–41. doi: 10.1083/jcb.200712039

Van Kampen, J. M., and Kay, D. G. (2017). Progranulin gene delivery reduces plaque burden and synaptic atrophy in a mouse model of Alzheimer's disease. *PLoS One* 12:e0182896. doi: 10.1371/journal.pone.0182896

Youn, B.-S., Bang, S.-I., Kloting, N., Park, J. W., Lee, N., Oh, J.-E., et al. (2009). Serum Progranulin Concentrations May Be Associated With Macrophage Infiltration Into Omental Adipose Tissue. *Diabetes* 58, 627–636. doi: 10.2337/db08-1147

Zhou, B., Li, H., Liu, J., Xu, L., Guo, Q., Sun, H., et al. (2015). Progranulin induces adipose insulin resistance and autophagic imbalance via TNFR1 in mice. *J. Mol. Endocrinol.* 55, 231–243. doi: 10.1530/JME-15-0075

Zhou, D., Zhou, M., Wang, Z., Fu, Y., Jia, M., Wang, X., et al. (2019a). Progranulin alleviates podocyte injury via regulating CAMKK/AMPK-mediated autophagy under diabetic conditions. *J. Mol. Med.* 97, 1507–1520. doi: 10.1007/s00109-019-01828-3

Zhou, D., Zhou, M., Wang, Z., Fu, Y., Jia, M., Wang, X., et al. (2019b). PGRN acts as a novel regulator of mitochondrial homeostasis by facilitating mitophagy and mitochondrial biogenesis to prevent podocyte injury in diabetic nephropathy. *Cell Death Dis.* 10:524. doi: 10.1038/s41419-019-1754-3

Conflict of Interest: The authors declare that the research was conducted in the absence of any commercial or financial relationships that could be construed as a potential conflict of interest.

Publisher's Note: All claims expressed in this article are solely those of the authors and do not necessarily represent those of their affiliated organizations, or those of the publisher, the editors and the reviewers. Any product that may be evaluated in this article, or claim that may be made by its manufacturer, is not guaranteed or endorsed by the publisher.

frontiers | Frontiers in Cellular Neuroscience

ORIGINAL RESEARCH
published: 27 July 2022
doi: 10.3389/fncel.2022.937060

Reduced Expression of TMEM16A Impairs Nitric Oxide-Dependent Cl^- Transport in Retinal Amacrine Cells

*Tyler Christopher Rodriguez, Li Zhong, Hailey Simpson and Evanna Gleason**

Department of Biological Sciences, Louisiana State University, Baton Rouge, LA, United States

Postsynaptic cytosolic Cl^- concentration determines whether GABAergic and glycinergic synapses are inhibitory or excitatory. We have shown that nitric oxide (NO) initiates the release of Cl^- from acidic internal stores into the cytosol of retinal amacrine cells (ACs) thereby elevating cytosolic Cl^-. In addition, we found that cystic fibrosis transmembrane conductance regulator (CFTR) expression and Ca^{2+} elevations are necessary for the transient effects of NO on cytosolic Cl^- levels, but the mechanism remains to be elucidated. Here, we investigated the involvement of TMEM16A as a possible link between Ca^{2+} elevations and cytosolic Cl^- release. TMEM16A is a Ca^{2+}-activated Cl^- channel that is functionally coupled with CFTR in epithelia. Both proteins are also expressed in neurons. Based on this and its Ca^{2+} dependence, we test the hypothesis that TMEM16A participates in the NO-dependent elevation in cytosolic Cl^- in ACs. Chick retina ACs express TMEM16A as shown by Western blot analysis, single-cell PCR, and immunocytochemistry. Electrophysiology experiments demonstrate that TMEM16A functions in amacrine cells. Pharmacological inhibition of TMEM16A with T16inh-AO1 reduces the NO-dependent Cl^- release as indicated by the diminished shift in the reversal potential of $GABA_A$ receptor-mediated currents. We confirmed the involvement of TMEM16A in the NO-dependent Cl^- release using CRISPR/Cas9 knockdown of TMEM16A. Two different modalities targeting the gene for TMEM16A (*ANO1*) were tested in retinal amacrine cells: an all-in-one plasmid vector and crRNA/tracrRNA/Cas9 ribonucleoprotein. The all-in-one CRISPR/Cas9 modality did not change the expression of TMEM16A protein and produced no change in the response to NO. However, TMEM16A-specific crRNA/tracrRNA/Cas9 ribonucleoprotein effectively reduces both TMEM16A protein levels and the NO-dependent shift in the reversal potential of GABA-gated currents. These results show that TMEM16A plays a role in the NO-dependent Cl^- release from retinal ACs.

Keywords: retina, nitric oxide (NO), amacrine cell, TMEM16/anoctamin, CRISPR/Cas9, intracellular Cl^-

OPEN ACCESS

Edited by:
Wallace B. Thoreson, University of Nebraska Medical Center, United States

Reviewed by:
Jozsef Vigh, Colorado State University, United States
In-Beom Kim, Catholic University of Korea, South Korea

****Correspondence:***
Evanna Gleason
egleaso@lsu.edu

Specialty section:
This article was submitted to Cellular Neurophysiology, a section of the journal Frontiers in Cellular Neuroscience

Received: *05 May 2022*
Accepted: *21 June 2022*
Published: *27 July 2022*

Citation:
Rodriguez TC, Zhong L, Simpson H and Gleason E (2022) Reduced Expression of TMEM16A Impairs Nitric Oxide-Dependent Cl^- Transport in Retinal Amacrine Cells. Front. Cell. Neurosci. 16:937060. doi: 10.3389/fncel.2022.937060

INTRODUCTION

The flexibility of synaptic signaling determines the ability of a neural circuit to alter its performance under different demands. Over 40 subtypes of retinal ACs were identified in mouse (Helmstaedter et al., 2013) with more than 60 subtypes discovered by transcriptome analysis (Yan et al., 2020). ACs subserve diverse functions, such as generating cholinergic waves during retinal development

(Feller et al., 1996), regulating activity-dependent maturation of ganglion cell projections (Xu et al., 2016), shaping receptive fields of ganglion cells (Jacoby et al., 1996; de Vries et al., 2011; Kim et al., 2015; Jia et al., 2020), and light and dark adaptation of retinal circuitry (Hampson et al., 1992; Zhang et al., 2008; Ortuno-Lizaran et al., 2020). AC's extreme morphological and functional diversity increases circuit capabilities in the IPL.

Nitric oxide (NO) is a signaling molecule produced by multiple cell types in the chicken retina including four nitric oxide synthase expressing (NOS) AC subtypes (Fischer and Stell, 1999). Two different isoforms of nitric oxide synthase (nNOS and eNOS) were shown to be expressed in avian ACs as well (Tekmen-Clark and Gleason, 2013). Three AC types with nNOS immunoreactivity were found in turtle (Eldred and Blute, 2005), and single-cell RNA sequencing showed three AC types with nNOS expression in mouse (Yan et al., 2020). NO regulates multiple aspects of retinal physiology including phototransduction (Goldstein et al., 1996), retinal blood flow (Izumi et al., 2008), temporal response tuning (Vielma et al., 2014), gap junction coupling (Hampson et al., 1992; Mills and Massey, 1995; Jacoby et al., 2018), and light adaptation (Shi et al., 2020).

In previous work, we showed that postsynaptic cytosolic Cl^- concentration can be elevated by NO thus making GABA-mediated synaptic responses less inhibitory, or even depolarizing (Hoffpauir et al., 2006). We have also shown that this response requires the cystic fibrosis transmembrane conductance regulator (CFTR) (Krishnan et al., 2017). In separate studies, we showed that NO (Zhong and Gleason, 2021) and NO donors (Maddox and Gleason, 2017) produce Ca^{2+} elevations that are required for the effects of NO on cytosolic Cl^-, raising the possibility that internal Ca^{2+}-activated Cl^- channels also contribute to the NO-dependent release of Cl^-.

The TMEM16 family of transmembrane proteins is exclusive to eukaryotes with vertebrates expressing 10 paralogues: TMEM16A, TMEM16B, TMEM16C, TMEM16D, TMEM16E, TMEM16F, TMEM16G, TMEM16H, TMEM16J, and TMEM16K (Milenkovic et al., 2010). Most are activated by Ca^{2+} and function as ion channels, lipid scramblases, or sometimes both (Charlesworth et al., 2012; Yang et al., 2012; Huang et al., 2013; Suzuki et al., 2013; Kim et al., 2018; Bushell et al., 2019; Feng et al., 2019; Reichhart et al., 2019; Kalienkova et al., 2021; Stabilini et al., 2021). TMEM16 proteins are expressed in many tissues and are involved in a range of physiological processes including nociception (Cho et al., 2012; Takayama et al., 2015), mucous secretion (Benedetto et al., 2019), olfactory transduction (Pifferi et al., 2012; Neureither et al., 2017; Zak et al., 2018), bone remodeling (Kim et al., 2019), muscle repair (Whitlock et al., 2018), and macrophage immune defense (Ousingsawat et al., 2015; Wanitchakool et al., 2017). TMEM16A was first identified as the native Ca^{2+} activated Cl^- channel in *Xenopus* oocytes (Yang et al., 2008). Later, it was found in both the outer and inner plexiform layers of the mammalian retina and in GABAergic amacrine cell processes (Jeon et al., 2013). TMEM16A function was demonstrated in photoreceptor synaptic terminals (Caputo et al., 2015) and bipolar cell synapses (Paik et al., 2020) but not in amacrine cells.

TMEM16A is reported to function as a heat sensor in rat nociceptive dorsal root ganglion neurons that is synergistically activated by heat, Ca^{2+}, and depolarizing potentials (Cho et al., 2012). Intracellular sources of Ca^{2+}, in particular the endoplasmic reticulum, were found to be preferred over voltage-gated Ca^{2+} channel-mediated Ca^{2+} influx in rat DRG neurons. The preference for intracellular Ca^{2+} stores likely coincides with close membrane juxtaposition of TMEM16A and molecular components of Ca^{2+} signaling in localized microdomains (Jin et al., 2013). It was shown that TMEM16A, TRPV1, and IP_3Rs were organized in nanodomains that couple ER Ca^{2+} release to TMEM16A activation (Shah et al., 2020).

Functional interactions between TMEM16A and CFTR have been demonstrated in several epithelia. Studies performed in mouse airway epithelia showed a pronounced interdependence between TMEM16A and CFTR in terms of membrane expression and Cl^- conductance (Ruffin et al., 2013; Benedetto et al., 2017). To date, this functional interdependence has not been explored in neurons. CFTR is a protein kinase A-regulated Cl^- and HCO_3^- channel localized to the apical membrane of epithelial cells that functions to passively secrete Cl^- thereby regulating sodium transport, transepithelial water flow, and luminal pH (Hull, 2012; Saint-Criq and Gray, 2017). Although CFTR is widely expressed at the plasma membrane of epithelial cells, it is also found in non-epithelial tissues (Yoshimura et al., 1991; Xue et al., 2016; Reznikov, 2017) with subcellular localization differing among cell types (Bradbury, 1999). When expressed intracellularly, it regulates processes such as plasma membrane recycling (Bradbury et al., 1992), endosomal pH homeostasis (Lukacs et al., 1992), and Cl^- dependent endosome fusion (Biwersi et al., 1996). Mutations in the *CFTR* gene are responsible for cystic fibrosis leading to sticky and viscous mucous. TMEM16A may also contribute to mucous secretion; however, this is disputed (Simoes et al., 2019; Danahay et al., 2020; Cabrita et al., 2021). Because functional interactions between CFTR and TMEM16A are established in epithelia, we hypothesize that in ACs, TMEM16A provides a link between NO-induced Ca^{2+} elevations and Cl^- release in tandem with CFTR.

Here, we test for the involvement of TMEM16A in the NO-dependent cytosolic Cl^- release. The transcript for TMEM16A was identified in mixed retinal cultures and in single ACs. Protein expression was confirmed using Western blots and immunocytochemistry. With electrophysiological experiments designed to monitor cytosolic Cl^-, we look at the effects of pharmacological inhibition of TMEM16A and genetic disruption of TMEM16A with CRISPR/Cas9. We find that inhibition or reduced expression of TMEM16A suppresses the cytosolic Cl^- elevation produced by NO. This is the first report of TMEM16A participating in Cl^- regulation in ACs.

METHODS

Cell Culture

To obtain cultures of retinal cells for use in electrophysiology, immunocytochemistry, and RT-PCR experiments, retinae were extracted from E9 White Leghorn chick embryos in Hanks Balanced Salt Solution (HBSS), Ca^{2+}, and Mg^{2+} free (Corning,

21-021-CV). Retinae were digested with 0.125% trypsin (Thermo Fisher, 25200-056), treated with DNase (Sigma, DN25-1G), and gently triturated to generate a single-cell suspension. The cells were resuspended in Dulbecco's Modified Eagle Medium (DMEM) (Corning, 15-017-CV) containing 5% fetal bovine serum (FBS) and plated at a density of 260cells/mm^2 onto 35mm dishes coated with poly-L-ornithine (Alamanda Polymers, PLO_{100} average MW 20,000Da). Half of the media was replaced every 2–3d with Neurobasal (Thermo Fisher, 21103-049) containing 1% B27 (Thermo Fisher, 17504-044) and 2mM GlutaMAX (Thermo Fisher, 35050-061). ACs were identified in culture as previously described (Gleason et al., 1993).

Mixed Population RT-PCR

Total RNA was extracted using the acid phenol/guanidinium isothiocyanate method (Chomczynski and Sacchi, 2006). The RNA was then digested by DNase I, and acid phenol/guanidinium isothiocyanate was extracted again before final resuspension in RNA storage buffer (1mM citrate pH 6.5). Reverse transcription of RNA was carried out as follows: primers were annealed at 75°C for 5min before the addition of WarmStart RTX (except for no RT control) and cDNA synthesized by incubating at 25°C for 5min, 55°C 10min, 80°C for 10min, and then holding at 4°C. PCR amplification of cDNA was performed with Q5 Hot Start High-Fidelity DNA polymerase. Cycling parameters are as follows: 98°C for 30s for initial denaturation, then 11 cycles of 98°C for 5s, 65°C for 20s (−1°C/cycle), and 72°C for 45s, followed by 26 cycles of 98°C for 5s, 55°C for 20s, and 72°C for 45s, with a final extension at 72°C for 5 min.

Single-Cell RT-PCR

Retinal cultures were washed three times with Tris-buffered saline (Fisher Bioreagents, BP24711). Individual ACs (1cell/rxn) were aspirated with a siliconized borosilicate glass pipette pulled to a tip diameter of ∼5 μm filled with Tris-buffered saline. The collection was performed on an Olympus IX-70 inverted microscope with a micromanipulator (Sutter instrument, MPC-385). The glass pipette tip, containing the AC, was broken into a 1.5ml tube on ice containing 4 μl of dsDNase mix with 0.2 μl dsDNase per reaction (Thermo Fisher, EN0771). DNA was digested at 37°C for 2min. Reverse transcription components (NEB, B0537S, M0314S, and N0446S) were added to a final volume of 15μl, and RNA was denatured at 75°C for 5min. The RecA protein from *Thermus thermophilus* (MCLAB, RPTT-100) was included during RNA denaturation to improve primer hybridization and subsequent cDNA synthesis (Kirkpatrick and Radding, 1992). WarmStart RTX (NEB, M0380S) was added to each sample, except no-reverse transcription controls, and cDNA synthesis was performed as before. The cDNA (2μl/rxn) was then amplified with Q5 Hot Start High-Fidelity DNA polymerase (NEB, M0493S). Touchdown cycling parameters were as follows: 98°C for 30 s for initial denaturation, then 11 cycles of 98°C for 5 s, 65°C for 20 s (−1°C/cycle), and 72°C for 45 s, followed by 41 cycles of 98°C for 5 s, 55°C for 20 s, and 72°C for 45 s, with a final extension at 72°C for 5 min. Reactions were analyzed on a 2% lithium borate agarose gel poststained with ethidium bromide, and sequence identity was verified by Sanger sequencing.

Single-Cell Genomic PCR

Genomic PCR was performed using similar methods for single-cell RT-PCR with the following modifications. Ice-cold HBSS (minus Ca^{2+} and Mg^{2+}) was used to fill the siliconized pipette and collect the cells. The pipette, containing a single AC, was broken into a PCR strip tube on ice containing 5 μl of freshly prepared lysis buffer which comprised of 1mM tris pH 9.0 (Millipore, 9295-OP), 0.1 mg/ml proteinase K (Thermo Fisher, 17916), and 0.01 mM EDTA (Sigma, 03677). The strip was incubated in a thermocycler preheated to 65°C for 2hr and 80°C for 20 min before proceeding to PCR amplification.

Immunocytochemistry

To determine the cellular localization pattern of TMEM16A protein, we performed immunocytochemistry on cultured retinal cells. Mixed retinal cultures plated on coverslips were fixed after 9 days in culture with 4% paraformaldehyde (Thermo Fisher, AA433689L) in Dulbecco's PBS minus Ca^{2+} and Mg^{2+} (Corning, 20-031-CV) for 15 min at room temperature. Cells were washed three times with DPBS and then permeabilized 15 min with DPBS containing 0.1% Tween 80 (VWR, 97063-806) and 30mM glycine. The cells were blocked with 5% NGS before incubating for 24 h in primary anti-TMEM16A rabbit monoclonal antibody (Abcam, ab190803). Cells were incubated for 1 h with secondary antibody and mounted onto slides using ProLong Glass Antifade Mountant (Thermo Fisher, P36984). The cells were washed once, briefly, with permeabilization buffer followed by three times for 5 min each with DPBS after antibody incubation steps.

Western Blot Analysis

To assess the target specificity of the rabbit anti-TMEM16A monoclonal antibody, we performed Western blots to compare the molecular weight of the detected protein with its predicted size. In addition, we compared the immunodetection of TMEM16A and CFTR from membrane extracts of two methods to assess the possibility they interact and to verify that the anti-TMEM16A antibody recognizes a transmembrane protein as expected. Retinal tissue was dissected from chicks on embryonic day 18. Ultracentrifuged samples were lysed with a syringe plunger (Norm-Ject, 4010.200V0) in a microcentrifuge tube. Samples were spun at 700x*g* for 5 min in a fixed-angle centrifuge. Supernatants were spun at 100,000x*g* for 1 h at 4°C in a swinging bucket rotor to pellet the microsomal fraction. The pellet was resuspended in HEPES buffer with 0.5% CHAPS (VWR, 97061-720) and both fractions (supernatant and pellet) were then methanol-precipitated to concentrate and delipidate proteins. Triton X-114 cloud point extraction was performed in a separate experiment to partition hydrophobic proteins from soluble proteins. E18 retinal tissue was lysed in a buffer containing 2% proteomics grade Triton X-114 (VWR, 97063-868) and protease inhibitors (Thermo Fisher, A32955). The tissue was shaken for 1 h at 4°C to break up tissue, triturated with progressively finer needles (21G, 23G, and 27G) to generate a single-cell suspension, and then sonicated to disrupt membranes. After removal of nuclei and cell debris by centrifugation, the lysate was then cloud point extracted (see Bordier, 1981; Taguchi and Schatzl, 2014) followed by methanol precipitation.

TABLE 1 | Antibodies.

Antibody	Supplier Cat# (RRID #)
Rabbit anti-TMEM16A monoclonal	Abcam ab190803 (AB_2892592)
Rabbit anti-CFTR Polyclonal	Abcam ab131553 (AB_2893490)
Goat anti-Rabbit Alexa 488	ThermoFisher A-11034 (AB_2576217)
Goat anti-Rabbit Alexa 555	ThermoFisher A-21429 (AB_2535850)
Goat anti-Rabbit HRP	ThermoFisher A-16110 (AB_2534782)

Protein samples were resuspended in 2x Laemmli buffer containing 6M urea. Samples were diluted to 1x Laemmli buffer, and protein concentration was determined using the Pierce 660 assay (Thermo Fisher, 22662 and 22663). In total, 20–30μg of protein was loaded onto a 7.5% SDS-PAGE stain-free gel (Bio-Rad, 4568023). Separated proteins were transferred to an Immobilon-FL PVDF (Millipore, IPFL00010) membrane using a BioRad transblot semi-dry apparatus at 24V for 1 h with a buffer consisting of 48mM Tris pH 9.2, 39mM glycine, and 10% methanol. The blot was washed briefly with DPBS before blocking for 1 h with 1% casein in DPBS. After a brief wash, the blot was incubated overnight in primary antibody (**Table 1**) (1:1,000 Rb anti-ANO1 or 1:1,000 Rb anti-CFTR, 1% BSA, 0.01% thimerosal). It was washed with DPBS with 0.05% Tween 80, incubated for 1 h with goat anti-rabbit HRP secondary (1:100,000), and developed with Pierce SuperSignal West Pico PLUS (Thermo Fisher, 34580). The images were acquired on a BioRad ChemiDoc XRS+.

Preparation of Custom sgRNA and *in vitro* Validation

To identify candidate guide RNAs capable of targeting TMEM16A, we used the CRISPR 10K track in the UCSC Genome Browser and the Integrated DNA Technologies gRNA checker tool. The selected candidate gRNAs (**Table 2**) were then tested *in vitro* prior to the transfection of retinal neurons to ensure their on-target functionality. Transcription template oligos specific to *TMEM16A* were ordered from IDT, and transcription was performed according to the EnGen sgRNA Synthesis Kit (NEB, E3322V). Target DNA was PCR-amplified from E18 chick retina genomic DNA. We then assessed each guide RNA for on-target efficiency in parallel *in vitro* reactions. RNPs were formed separately with AltR S.p. HiFi Cas9 V3 (Integrated DNA Technologies, 1081060) for each transcribed sgRNA. Reactions were assembled using 500fmol of pre-assembled RNP and 25fmol of target DNA in a total reaction volume of 10 μl.

Ribonucleoprotein and Nucleofection

To genetically disrupt TMEM16A expression, tracrRNA, tagged with ATTO 550, and *in vitro* validated crRNAs (Integrated DNA Technologies) were annealed in a preheated thermocycler at 95°C for 5 min followed by cooling to 25°C at rate of −0.2°C/s. RNP complexes (120pmol gRNA, 104pmol Cas9, and 5 μl total) were formed in the Cas9 dilution buffer. RNPs, electroporation enhancer (Integrated DNA Technologies, 1075915), and Nucleofector solution (Lonza, VPG-1002) were combined with 4–6 × 10^6 primary retinal neurons and electroporated using the Nucleofector IIb device (Lonza, AAB-1001). Control reactions were performed in parallel by transfecting 10 μl of Cas9/tracrRNA only. For plasmid transfections, 1 μg of P222 or control vector was electroporated as described above.

TABLE 2 | Oligonucleotide sequences from the work in this paper.

Oligo	Nucleotide sequence (5′-3′)	Product size (bp)
TMEM16A F	TCCCAGACATTCCCAAGGAC	286
TMEM16A R	CCTGCCCTTTACATGATGGC	
TMEM16B F	TTGGCCGACCTGGTCATTAT	327
TMEM16B R	GTGTGACAAAGCCGAACTGG	
TMEM16C F	TTGCCTGGTTGGGATGGTAT	301
TMEM16C R	ACAGCTCTCCGTCTTTTCCA	
TMEM16D F	ATCAGGTGCTCATGACCCAA	384
TMEM16D R	TTTTGCACAGTGATCCTGCC	
TMEM16E F	CACCAAGCCCTTACCCTGTA	354
TMEM16E R	GAGCAAACTCTACTGCAGGC	
TMEM16F F	CATTTTCCCCCTGGTTTGGG	468
TMEM16F R	GTGACAGCTGCAAGAAACCA	
TMEM16H F	CAAAGCCTGGATGAAGACGG	510
TMEM16H R	GACTTCATCAGCCGCTTGAG	
TMEM16J F	GGTTCACCATCAAGAAAATTGAGGA	415
TMEM16J R	GCGAATCCCAGCAAGTAGGT	
TMEM16K F	CCCTACGTATGCCAGTTTGC	530
TMEM16K R	GTTCAAGGCCCAAGGAAGTG	
TMEM16A gDNA 434 F	GCCCATTTGACTGTGCACTAA	
TMEM16A gDNA 434 R	CACCAGCCATCGTCCTTATCAT	
TMEM16A gDNA 606 F	CCAGCTATCAGGAAAATTGC	
TMEM16A gDNA 606 R	TGTGATCTCCCCAAATCTAC	
TMEM16A gRNA 192	GAGGAAAGTGGATTACATCC	
TMEM16A gRNA 222	ACTACAAGAAGTCTTCAGCA	
TMEM16A gRNA 424	CCTGGAACTGGAACATGATG	
HiFiCas9_SDM_r691a_F	CTTCGCCAACGCGAACTTCATGCAGC	Vakulskas et al. (2018)
HiFiCas9_SDM_r691a_R	CCGTCGGACTTCAGGAAA	

Electrophysiology

Retinal cultures maintained for 6–11 days (E15-E20) were used for electrophysiological recordings to assess functional consequences of TMEM16A pharmacological inhibition or genetic disruption. Dishes were mounted on the stage of an Olympus IX70 inverted microscope, and a 3M KCl agarose bridge connected the reference Ag/AgCl pellet electrode to the dish. Patch electrodes were pulled from thick-walled borosilicate glass (Sutter Instruments, BF150-86-10) by a P-97 micropipette puller (Sutter Instruments, P-97) with a 2.5 mm square box filament (Sutter Instruments, FB255B). Electrode tips were pulled to produce a short taper with resistance between 5 and 8 MΩ. For the T16Ainh-A01 (50 μM) experiment, the inhibitor was added to the internal solution before recordings from a 50mM stock in DMSO. During the experiment, a continuous supply

of external solution was delivered through a pressurized eight-channel perfusion system (Automate Scientific, 01-18). In total, 50 μl of bubbled NO solution was injected into the perfusion line using a gas-tight syringe attached to a repeating dispenser (Hamilton, 81220 and 83700). Whole-cell patch recordings were performed using an Axopatch 1D amplifier with pClamp 10.0 for inhibitor experiments. Recordings from transfected cells were performed with an Axopatch 200B amplifier and pClamp 11.2 software (Molecular Devices, Axopatch 200B-2). The voltage was held at −70 mV for 150 ms and stepped to −90 mV for 50ms, then changed from −90 to 50 mV over 200 ms, and returned to −70 mV. The first ramp recording was used to measure leak currents, and the second ramp was measured in the presence of GABA (20 μM). Series resistance was recorded for each cell, and junction potential was estimated in the pClamp 10.0 calculator to be −13 mV. The reversal potential of GABA-gated current ($E_{revGABA}$) was calculated by correcting for series resistance and junction potential and then subtracting the current from the first ramp from the current from the second ramp. The external solution comprised 116.7 mM NaCl, 5.3 mM KCl, 20 mM tetraethylammonium (TEA)-Cl, 3 mM $CaCl_2$, 0.41 mM $MgCl_2$, 10 mM HEPES, 5.6mM glucose, 300 nM TTX, and 50 μM $LaCl_3$. The internal solution comprised 100 mM Cs-acetate, 10 mM CsCl, 0.1 mM $CaCl_2$, 2 mM $MgCl_2$, 10 mM HEPES, and 1.1 mM EGTA, supplemented with an ATP regeneration system which comprised 1mM ATP disodium, 3 mM ATP dipotassium, 2 mM GTP disodium, 20 mM creatine phosphate, and 50U/ml creatine phosphokinase. All recordings were conducted at room temperature.

Imaging Analysis and Statistics

For knockdown analysis, the images were collected with an Olympus IX-70 with 100x 1.35NA oil immersion objective using Slidebook software. Cells expressing the fluorescent reporter were considered transfected and were subsequently quantified for immunofluorescence of TMEM16A. Transfection with the all-in-one plasmid results in co-expression of tdTomato reporter with sgRNA/Cas9. Transfection of the pre-formed ribonucleoprotein with separate GFP plasmid means reporter expression does not guarantee successful RNP delivery. Cells were selected for tdTomato or GFP expression without prior knowledge of TMEM16A labeling to reduce bias. Analysis was done in Image J using auto local thresholding (Bernsen) to segment the image and create a binary mask for quantification of imaging data. Cells not expressing the fluorescent marker and all cell bodies were manually removed from the binary image so that only processes of transfected cells were analyzed. The D'Agostino–Pearson normality test was performed on samples, and any non-normal data were log-transformed prior to parametric statistical testing. Differences between groups were assessed using two-tailed Welch's *t-tests*. All statistics were performed with GraphPad Prism software, and figures were assembled in Adobe Illustrator.

RESULTS

Nitric oxide induces a cytosolic Cl^- elevation in ACs by the release of Cl^- from an internal acidic store. In addition, Ca^{2+} elevations were demonstrated (Maddox and Gleason, 2017; Zhong and Gleason, 2021) to activate adenylate cyclase 1, cAMP production, and stimulation of PKA which activates CFTR (Zhong and Gleason, 2021). Nonetheless, the full role of these Ca^{2+} elevations is not known. To investigate the possibility that a Ca^{2+}-activated Cl^- channel is involved, we tested for expression of TMEM16 paralogs by RT-PCR in chick retinal cultures. Embryonic day 15-16 mixed chick retinal cultures expressed the transcripts TMEM16A, TMEM16B, TMEM16C, TMEM16D, TMEM16E, TMEM16F, TMEM16H, TMEM16J, and TMEM16K (**Figure 1A**). All products were sequence-verified. To determine whether TMEM16A is expressed in ACs specifically, single ACs were aspirated from the culture dish and tested *via* RT-PCR for TMEM16A transcript (**Figure 1B**). Because not all transcripts are translated into protein, Western blots were performed on extracts from E18 chicken retina to test for TMEM16A protein. Immunoblotting yielded a single band for TMEM16A at the expected molecular weight of ∼117KDa (**Figure 1C**).

To assess the possibility of TMEM16A and CFTR interactions, cytosolic proteins were separated from membrane proteins and immunoblots of each fraction were performed for TMEM16A and CFTR. The membrane fraction generated by ultracentrifugation (**Figure 1Ci**) contained a heterogeneous mixture of membranes from the plasma membrane, mitochondria, endoplasmic reticulum, Golgi proteins, and other subcellular organelles. This assay showed both TMEM16A and CFTR in the membrane fraction while excluding both from the cytosolic fraction, as expected. However, Triton X-114 cloud point extraction unexpectedly enriched both proteins in the aqueous phase and excluded them from the detergent phase (**Figure 1Cii**). Hydrophobic transmembrane proteins are expected to partition to the detergent phase owing to their favorable interaction with non-ionic detergents. Such anomalous partitioning by Triton X-114 was reported for channel-forming membrane proteins possessing multiple transmembrane domains (Maher and Singer, 1985). Importantly, both proteins were found in the same fraction/phase by either method. The same TMEM16A antibody used for Western blots of mixed retinal cells also labeled ACs, specifically (**Figure 1D**). The representative fluorescent image uses a magenta-hot look-up table that displays puncta of increasing fluorescent intensity from magenta to white, respectively. Labeling appeared as distinct puncta in the soma and processes of ACs in culture (**Figure 1D**). It was commonly observed that amacrine cells have one–two processes with higher density labeling compared to other processes of the same cell.

To investigate whether TMEM16A contributes to the NO-dependent elevation of cytosolic Cl^-, we monitored the reversal potential of the Cl^- current through open $GABA_A$ receptors ($E_{revGABA}$) before and after NO (**Figure 2A**). Pairs of voltage ramps were delivered to ACs recorded in the voltage-clamp configuration. The first ramp was delivered without GABA, and the second ramp was delivered in the presence of 20 μM GABA to establish $E_{revGABA}$ without NO. A subsequent double-ramp recording was made on the same cell after exposure to NO. The difference in $E_{revGABA}$ measured from the recordings before and after NO constitutes the shift in $E_{revGABA}$ due to the NO-dependent Cl^- release. To test the involvement of TMEM16A

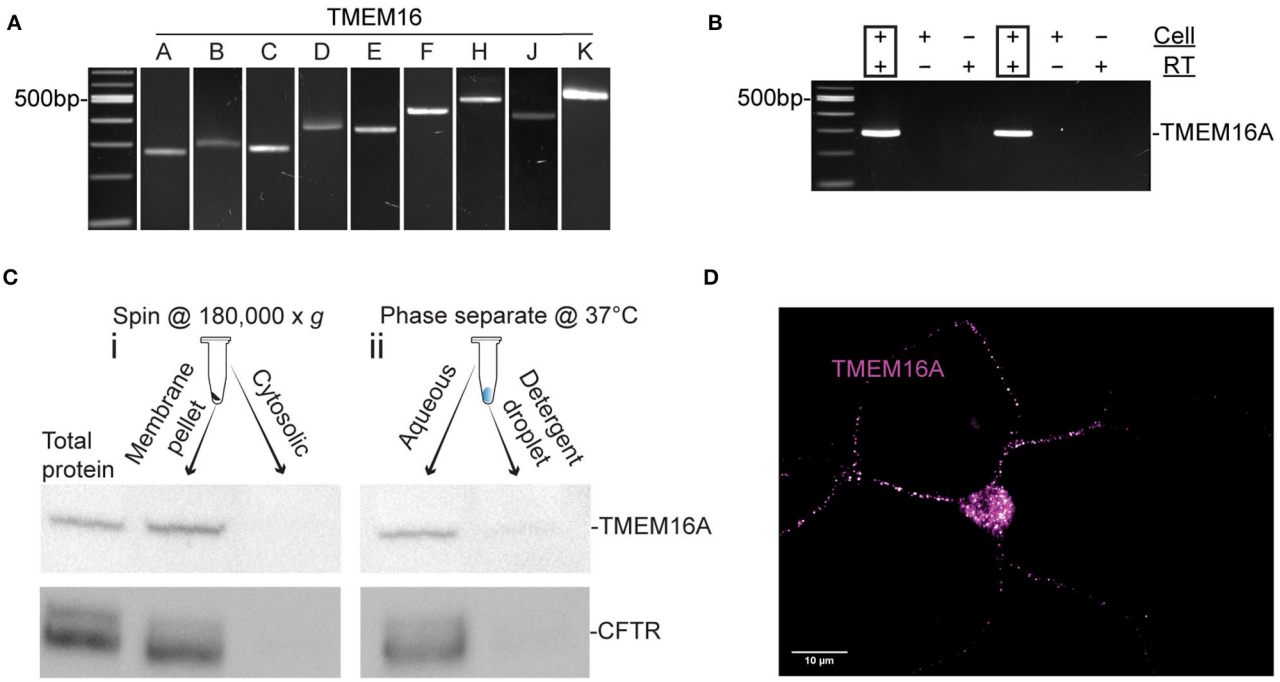

FIGURE 1 | TMEM16A transcript and protein are expressed in retinal amacrine cells. **(A)** RT-PCR of RNA extracted from E16 retinal tissue for TMEM16 paralogues. **(B)** Single-cell PCR amplifying TMEM16A from individual AC. Each cell was DNase-treated prior to reverse transcription. RT (–) and template (–) controls showed no amplification. **(C)** Western blot of subcellular fractionated protein samples (i) and Triton x-114 cloud point extraction samples (ii) show immunodetection of TMEM16A (Abcam ab190803) and CFTR (Abcam ab131553) in the same fraction with both types of membrane preparation. **(D)** Immunocytochemistry for TMEM16A reveals a punctate labeling along with the soma. The image is displayed with a magenta-hot look-up table that shows puncta with high-fluorescence intensity as white.

in the NO-dependent Cl^- release, we examined the effect of including the TMEM16A/TMEM16B inhibitor $T16_{inh}$-A01 in the recording pipette. Under control conditions in the absence of an inhibitor, the NO-induced shift in $E_{revGABA}$ (28.7 ± 2.8 mV, $n = 12$) was significantly higher than the shift from ACs recorded with $T16_{inh}$-A01 in the pipette (14.5 ± 3.1 mV, $n = 11$, Welch's t-test $p < 0.005$, **Figure 2B**). These results suggest that TMEM16A/B is involved in the NO-dependent Cl^- release of retinal ACs.

Pharmacological inhibitors for Cl^- channels are notoriously promiscuous (Sepela and Sack, 2018). Therefore, we sought to evaluate the involvement of TMEM16A more specifically by employing CRISPR/Cas9. CRISPR/Cas9 produces double-stranded breaks in the targeted genetic locus that are erroneously repaired by non-homologous end-joining to yield insertions and deletions (indels). ACs do not divide in culture to produce clones meaning these indels are heterogeneous among different ACs in culture.

The editing tool was delivered on the day neurons are plated (embryonic day 9). TMEM16A protein may be present at the time of transfection; therefore, loss of TMEM16A function will only be evident once pre-existing TMEM16A protein is turned over. We designed three guide RNAs against exon 3 of the TMEM16A gene (*ANO1*) and tested them by *in vitro* Cas9 digestion to confirm effectiveness. The target region of the TMEM16A gene (exon 3 of *ANO1*) was amplified by PCR and incubated with each respective Cas9/sgRNA ribonucleoprotein. Gel electrophoresis of the digests confirmed the on-target efficacy of each sgRNA on the purified TMEM16A target (**Figure 3A**). Guide RNA 222 was chosen for further testing in mixed retinal cell cultures for its greater out-of-frame indel formation score (Bae et al., 2014) compared to the other two guide RNAs. Cells were transfected with a plasmid expressing HiFi Cas9 (Vakulskas et al., 2018), tdTomato, sgRNA 222 (p222), and control cells that were transfected with the same vector minus sgRNA 222 (**Figure 3B**). To assess editing events, individual ACs expressing tdTomato were collected and subjected to genomic amplification (**Figure 3C**). The target region of the TMEM16A gene (*ANO1*) was amplified using a set of primers to give a 434 bp product. The identity of the PCR product and the presence of indels were evaluated by Sanger sequencing. We detected a range of insertions and deletions with the most common being a 1 bp insertion (**Figure 3D**). Single ACs were tested for indels by genomic PCR at 4 days post-transfection and 9–11 days post-transfection which resulted in 20% (1/5) and 67% (10/15) cells with indel mutations per cell amplified, respectively (**Figure 3E**). **Figure 3F** shows a representative sequencing chromatogram for a wild-type cell and a cell heterozygous for a +1 insertion mutation. The adjacent TIDE analysis (**Figure 3G**) shows a high aberrant sequence after the edit, owing to a mixture of a +1 insertion and wild-type sequence. Altogether, these results

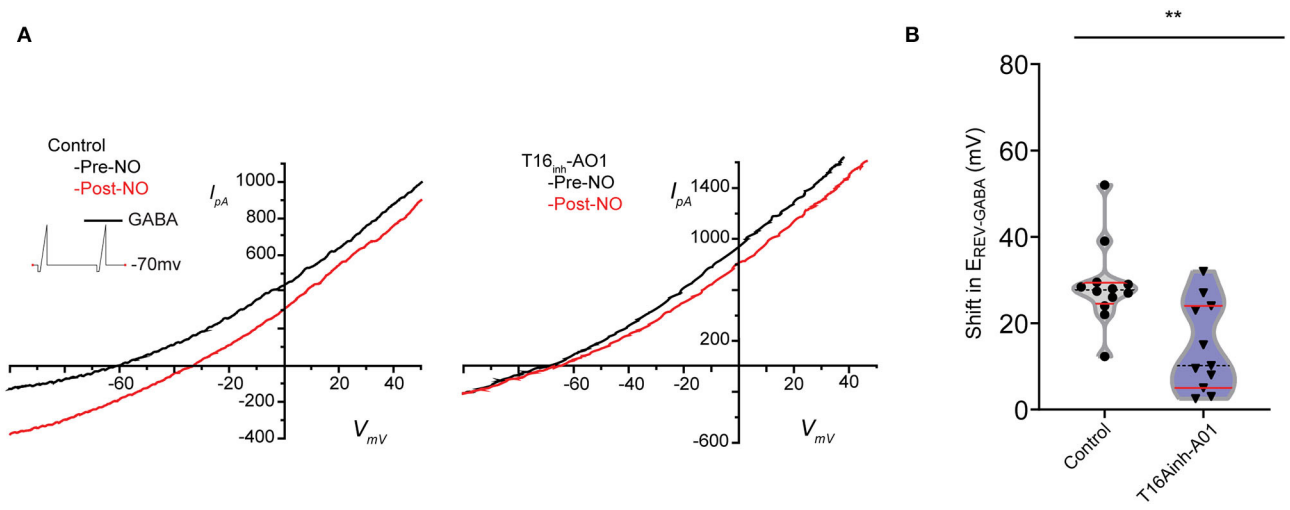

FIGURE 2 | Pharmacological inhibition of TMEM16A reduces the transient shift in $E_{revGABA}$. **(A)** Current–voltage relationship for leak subtracted GABA-gated currents recorded before and after NO injection in control and TMEM16A inhibitor (T16$_{inh}$-AO1) conditions. **(B)** Truncated violin plots for the mean shift in the reversal potential of GABA-gated currents ($E_{revGABA}$). The shape of the violin shows frequency distribution of the data, top and bottom of the violin are data extrema, red lines are quartiles, and the dashed line is the median of the data. The mean shift in $E_{revGABA}$ was reduced, and frequency distribution becomes bimodal when TMEM16A inhibitor ($n = 11$) was in the external solution compared to control conditions ($n = 12$). Recordings were from E16 cultures (Welch's *t*-test, ** denotes $p < 0.005$).

confirm the efficacy of vector p222 to generate indel mutations in ACs.

To detect loss of TMEM16A protein, immunocytochemistry was performed using the anti-TMEM16A antibody on transfected cells. Representative cells from the analysis are shown in **Figures 4A–D**. There was no significant difference in mean integrated density (sum of raw pixel intensities in the fluorescent object) (control = 11.24 ± 1.19, p222 = 9.75 ± 1.06, **Figure 4E**), mean fluorescent intensity (control =222.40 ± 77.31, p222= 202.73 ± 76.09, **Figure 4F**), or the mean size of fluorescent objects immunoreactive for anti-TMEM16A antibody (control = $4.61 \times 10^{-2} \pm 1.56 \times 10^{-3}$ μm^2, p222 = $4.59 \times 10^{-2} \pm 1.17 \times 10^{-3}$ μm^2, **Figure 4G**). We compared the expression of tdTomato and TMEM16A to determine whether higher expression of the construct was associated with reduced TMEM16A. The log-transformed integrated density (**Figure 4H**) for tdTomato is not different between groups ($p = 0.96$) (control $n = 14$, p222 $n = 12$). Pearson's correlation coefficients were determined between tdTomato and TMEM16A to control for reporter expression effects on TMEM16A immunolabeling and showed minimal correlation (control $r = 0.36$ with $p > 0.21$, p222 $r = 0.28$ with $p > 0.38$) (control $n = 14$, p222 $n = 12$). From the data, we concluded that the knockdown was ineffective given the lack of difference in TMEM16A expression between groups.

Whole-cell recordings in the voltage-clamp mode were performed on cells transfected by vector p222 to evaluate the effect of indel mutations on the NO-dependent shift in $E_{revGABA}$ (**Figure 5**). A pair of voltage ramps were delivered with GABA applied during the second ramp of the pair. A subsequent recording was made on the same cell with a bolus of NO injected during the recording to initiate the shift (**Figures 5C,D**). No significant difference in the NO-dependent shift in $E_{revGABA}$ was observed between cells targeted for TMEM16A (*ANO1*) by p222 and cells expressing the construct without the guide RNA (**Figure 5E**, control, 43.28 ± 2.012 mV vs. p222, 44.20 ± 2.096 mV, Welch's *t*-test) consistent with the immunocytochemistry.

Since the plasmid delivery system takes >4 days for efficient indel mutagenesis in ACs (see **Figure 3E**) and the predicted turnover rate of TMEM16A could be days to weeks, (Bill et al., 2014), the pre-formed RNA/Cas9 ribonucleoprotein was used to target TMEM16A (*ANO1*). This method is expected to produce edits within 1–3 days before being degraded by the cell, thus shortening the timeframe to a detectable loss in protein. To increase the likelihood of editing events affecting TMEM16A protein expression in our experimental window (7–11 days post-transfection), we simultaneously delivered Cas9 RNPs formed separately with two guide RNAs (gRNAs 222 and 424) targeting exon 3 of TMEM16A (**Figure 6A**). Single-cell genomic PCR revealed an inversion mutant and deletion mutant for the portion of exon 3 between the two guide RNAs (**Figures 6B,C**). Genomic PCR from pooled lysates also showed a deletion within exon 3 of TMEM16A (*ANO1*) detectable 72 h after transfection of cultured mixed retinal cells (**Figure 6D**).

TMEM16A protein expression of RNP targeted cells was examined by immunofluorescence (**Figures 7A–D**). Quantitative analysis was done only for cells co-expressing GFP to reduce selection bias. The mean integrated density for all objects identified within the TMEM16A mask is reduced in the dual-guide condition (control = 21.8 ± 1.64, dual gRNA = 15.5 ± 0.76, $p = 0.0014$) (**Figure 7E**). The mean fluorescent intensity of the objects (control = 382.8 ± 17.26, dual gRNA = 244.5

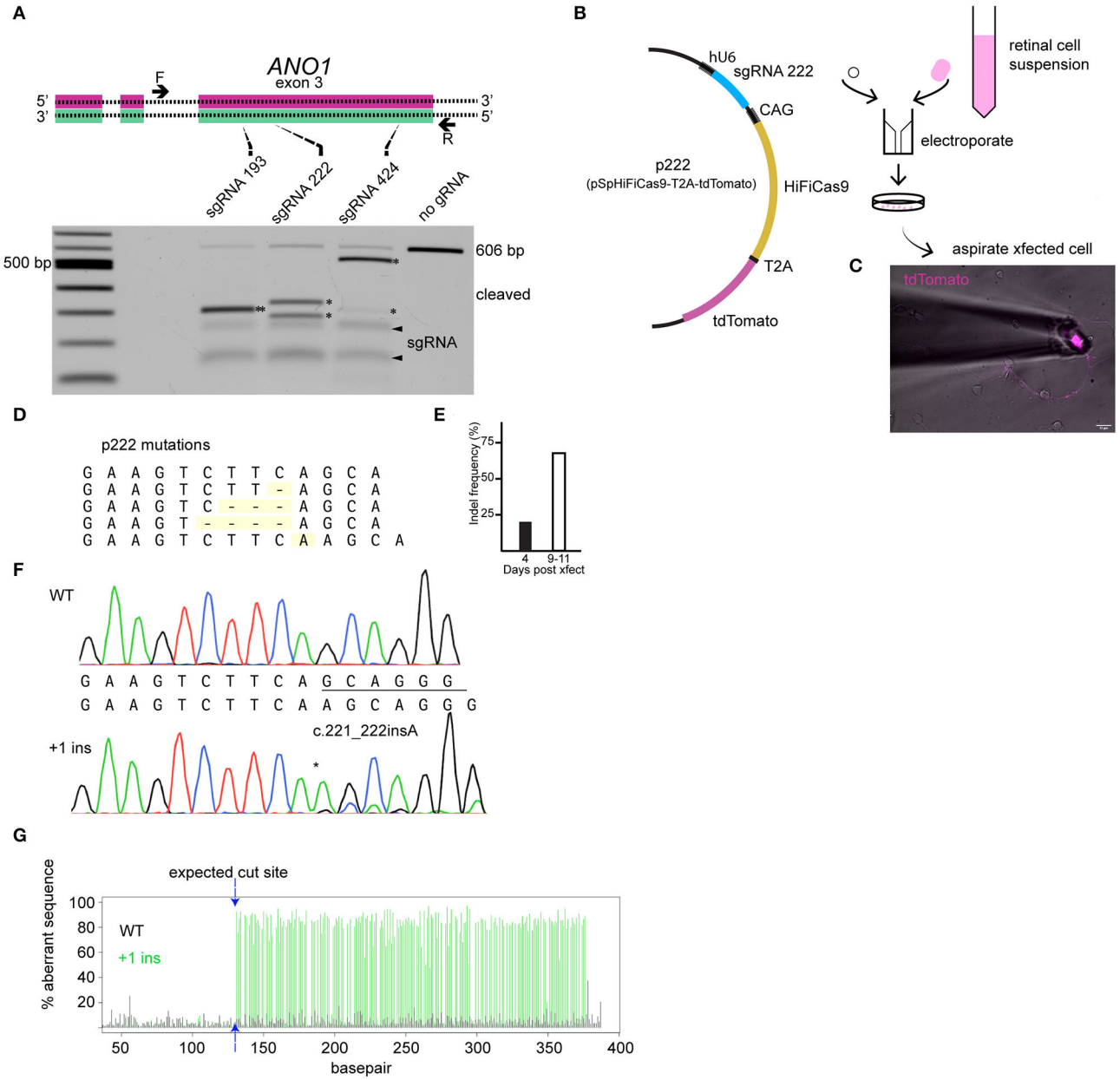

FIGURE 3 | CRISPR/Cas9 edits *TMEM16A* of retinal amacrine cells when delivered by an all-in-one plasmid. **(A)** (top) Graphical representation of target genetic loci showing the cut site for each sgRNA. Primers are denoted by the arrows, and sgRNA target regions are indicated by the dashed lines. (Bottom) Agarose gel electrophoresis of *in vitro* Cas9 cleaved DNA (asterisks) for each sgRNA of a 606 bp PCR product containing exon 3 of *TMEM16A*. The pair of faint bands below the digestion fragments correspond to sgRNA secondary structures (arrowheads). **(B)** Simplified plasmid map of pSpHiFiCas9-T2A-tdTomato which was electroporated into dissociated chick retinal cells. **(C)** AC in culture expressing tdTomato is aspirated into a glass pipette for single-cell genomic PCR. **(D)** List of observed mutations detected in p222 transfected cells. **(E)** Percent indels detected from 4 days and 9–11 days post-transfection. **(F)** Representative sequence traces from genomic PCR of a wild-type cell (wt/wt) and an edited cell with ~30% WT and 70% +1 insertion alleles (wt/c221_222insA) according to TIDE. **(G)** TIDE output from cell in **(F)** shows substantial aberrant sequence starting at the expected cut site due to a mixture of WT and +1 amplicons in the edited cells PCR. * indicates cleavage products.

$\pm$ 11.96, $p = 4.37 \times 10^{-8}$) (**Figure 7F**) and the mean object size (control $= 6.58 \times 10^{-2} \pm 1.74 \times 10^{-3}$ μm^2, dual gRNA $= 6.10 \times 10^{-2} \pm 7.28 \times 10^{-4}$ μm^2, $p = 0.017$) (**Figure 7G**) are significantly reduced as well. These results suggest a loss of TMEM16A protein when transfected with the dual-guide RNP. The log-transformed integrated density for GFP expression is lower in the dual gRNA group (control $= 1.81 \pm 0.19$, dual gRNA $= 1.36 \pm 0.11$, $p = 0.042$) (**Figure 7H**); however, there is no significant correlation between GFP expression and TMEM16A immunolabeling for control ($r = 0.074$ with $p > 0.71$) or dual

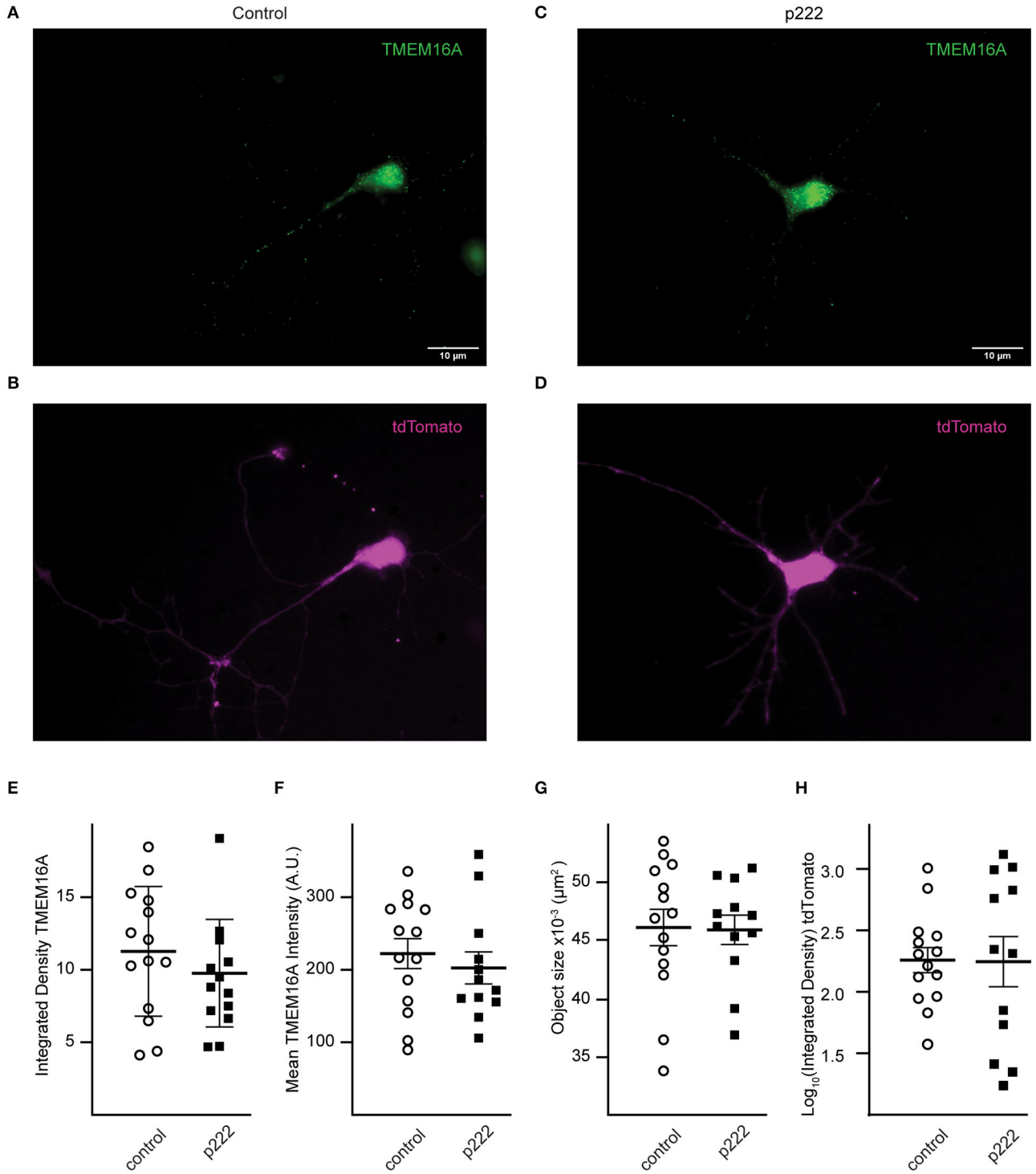

FIGURE 4 | Transfection with P222 has no effect on TMEM16A protein expression **(A–D)**. Representative images of TMEM16A antibody immunofluorescence and tdTomato fluorescence from e18 cells transfected with control plasmid **(A,B)** or p222 plasmid **(C,D)** targeting TMEM16A. **(E)** The mean integrated density for all objects identified within the TMEM16A mask; **(F)** the mean fluorescent intensity of the objects; **(G)** the mean objects size; **(H)** the log-transformed integrated density for tdTomato. There is no statistical difference between groups in **(E–H)** (two-tailed Welch's *t-tests*).

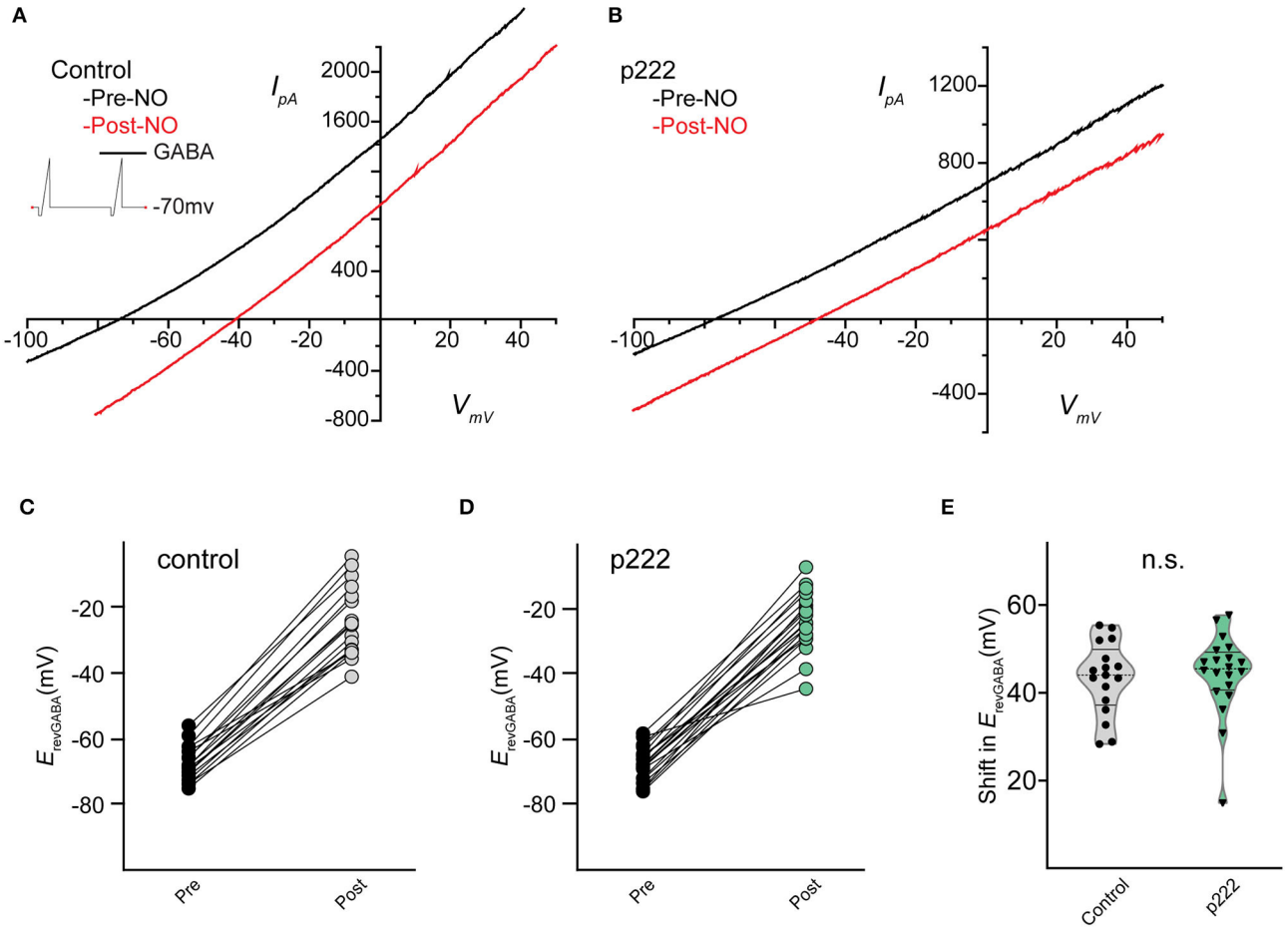

FIGURE 5 | Mean shift in the reversal potential of $GABA_A$Rs for control and cells targeted with p222 do not significantly differ. Current–voltage relationship for leak subtracted GABA-gated currents in a representative control AC **(A)** and in a representative p222 transfected cell **(B)**. Paired data points for $E_{revGABA}$ before and after NO injection shift positively for all cells tested in control **(C)** and p222 transfected **(D)** groups. Violin plots of the mean shift in $E_{revGABA}$ **(E)** show no difference and similar frequency distribution between control and p222 transfected groups (control $n = 17$, p222 $n = 20$, $p = 0.75$ two-tailed Welch's *t-tests*).

gRNA/RNP transfection ($r = 0.19$ with $p > 0.34$) (**Figures 7E,F**) (control n = 26, dual gRNA/RNP $n = 26$), which suggests that GFP expression is independent of TMEM16A detection in the immunocytochemistry analysis.

Recording from GFP expressing cells, we assessed the NO-dependent release of Cl^- in RNP-transfected cells and saw a significant reduction in the NO response (**Figures 8A,B**). Under control conditions, NO induced a mean shift in $E_{revGABA}$ of 39.6 ± 2.4 mV ($n = 23$) (**Figure 8C**), but in the RNP group targeting TMEM16A, the mean NO-induced shift in $E_{revGABA}$ was 23.8 ± 3.7 mV (**Figure 8D**) ($n = 25$, p = 0.001 unpaired *t*-test). Notably, there were a group of three cells (**Figure 8E**, pink) with a shift of <1 mV which may correspond to the ACs lacking any TMEM16A expression. In addition, the lower quartile (**Figures 8D,E**, braces) may represent a subset of ACs that require full TMEM16A expression for Cl^- transport in response to nitric oxide signaling, whereas other subsets do not.

DISCUSSION

Here, we show that chick retinal ACs express the TMEM16A transcript and protein. Pharmacological inhibition of TMEM16A leads to inhibition of the NO-dependent release of internal Cl^- and the shift in $E_{revGABA}$. This suggests that TMEM16A plays a role in the modulation of intracellular Cl^- in retinal ACs. To confirm the results with T16inh-AO1 inhibition, we utilized CRISPR/Cas9 in chick retinal ACs to specifically knock down TMEM16A. Since we use non-dividing cell cultures, mutations are heterogeneous and TMEM16A protein may be present before genetic disruption by CRISPR/Cas9. While an all-in-one plasmid encoding the sgRNA and HiFi Cas9 led to indel formation, it neither resulted in a significant loss of TMEM16A protein nor a detectable change in the NO-dependent Cl^- release over the time frame of culture viability. The plasmid takes days for its components to be transcribed and translated, and for Cas9

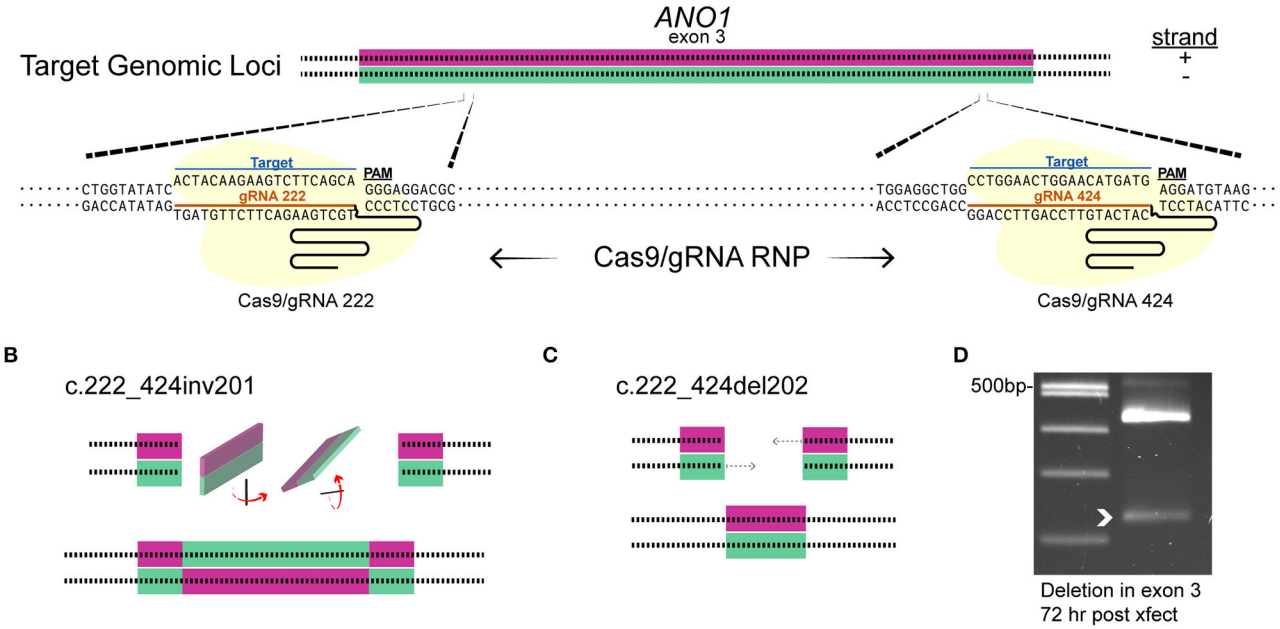

FIGURE 6 | Targeting *TMEM16A* exon 3 with dual gRNA Cas9 ribonucleoprotein produces deletions within 3 days. **(A)** The target loci in *TMEM16A* showing cleavage sites. **(B,C)** Graphical depictions of observed mutations from single amacrine cells that were dual gRNA-transfected showing an inversion c.222_424inv201 **(B)** and deletion c.222_424del202 **(C)** between the two target sites. **(D)** Edits were present as a smaller PCR amplicon from a separate amplification of mixed cultures 3 days post-transfection (white arrowhead).

to combine with the guide RNA in the nucleus for targeted cleavage and erroneous repair (Callif et al., 2017). After an indel is formed, TMEM16A knockdown depends on its rate of degradation which may differ among cell types. Vascular tissue with lower expression of TMEM16A was unaffected by a constitutively expressed *Tmem16a*-siRNA compared to tissue with higher expression in a previous murine study (Jensen et al., 2018). TMEM16A was shown to contribute significantly toward Ca^{2+}-dependent Cl^- secretion even when expressed at low levels in murine airway epithelia (Scudieri et al., 2012). In a separate study, inducible knockout of TMEM16A (*ANO1*) in mouse interstitial cells of Cajal resulted in protein loss that was patchy and incomplete even 2 months after induction (Malysz et al., 2017). In Te11 and FaDu cells, the half-life of TMEM16A was >24 h as determined by cycloheximide inhibition of new protein synthesis (Bill et al., 2014). This suggests that TMEM16A can have a relatively long half-life, especially when expressed at low levels yet still contributes significant Ca^{2+-}dependent Cl^- conductance. The time it takes for the plasmid to form indels may have exceeded our experimental window (7–11 days post-transfection) when considering TMEM16A protein stability. This contrasts with our previous work with CFTR that utilized an all-in-one plasmid encoding the CFTR, targeting sgRNA and wtCas9. This method did show a loss of protein and loss of the NO-dependent Cl^- release. Importantly, CFTR is subjected to rapid degradation immediately following protein synthesis. Intracellular precursor forms of CFTR are reported to have a half-life of ∼33min (Ward and Kopito, 1994).

When the CRISPR/Cas9 RNP was used, there was a significant change in protein expression and a reduction in NO-dependent Cl^- release 7–10 days post-delivery. Since the GFP-encoding plasmid is co-transfected with the dual gRNA/RNP, GFP expression does not guarantee successful RNP delivery. Thus, we likely underestimated the effect of knockdown and knockout because some unknown proportion of cells in the test group expressed GFP yet did not receive the RNP. Still, a few cells appeared to have TMEM16A knocked out entirely after RNP transfection. These cells had no appreciable immunoreactivity for the anti-TMEM16A antibody as determined by immunocytochemistry. Such complete absence of TMEM16A immunoreactivity was never observed in control or plasmid transfected conditions. Also, the frequency of complete knockout corresponds to a similar proportion of cells that have a loss of NO-dependent Cl^- release. Because the knockout of TMEM16A in intestinal epithelia expressing wild-type CFTR eliminated cAMP-activated Cl^- currents (Benedetto et al., 2017), it seems plausible that CFTR is responsible for the NO-dependent Cl^- release but requires expression of the TMEM16A to function in at least a subset of AC cell types. TMEM16A may also work in parallel to provide a direct link between Ca^{2+} and Cl^- conductance on a faster time scale than AdC1/cAMP-mediated Cl^- release *via* CFTR (Zhong and Gleason, 2021).

We identify the expression of TMEM16A transcript and protein in chick retinal ACs, in line with what has been observed in mouse retina (Jeon et al., 2013). Ca^{2+}-activated Cl^- currents

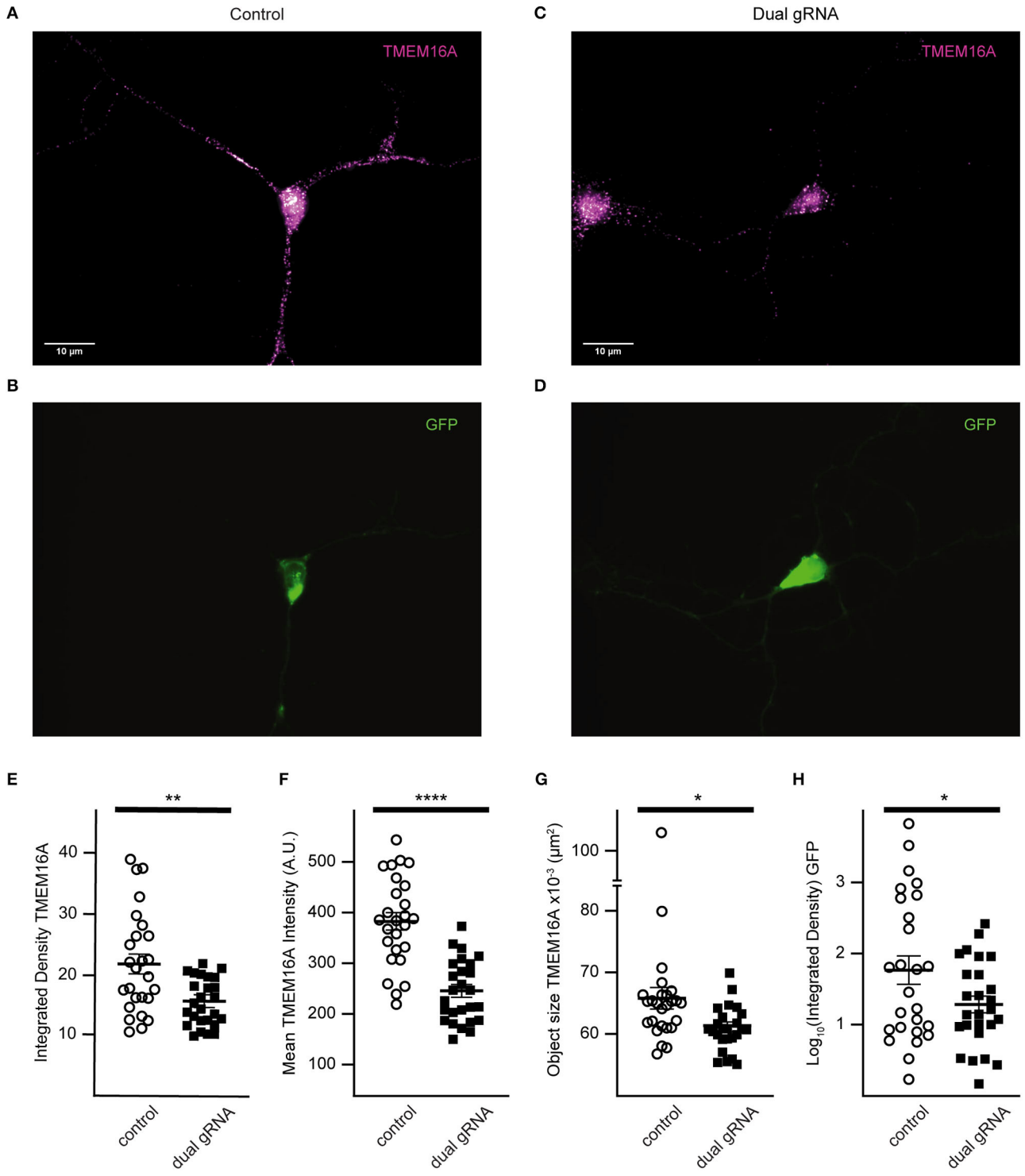

FIGURE 7 | Dual gRNA Cas9 ribonucleoprotein reduces *TMEM16A* expression **(A–D)**. Representative immunofluorescence images of GFP expressing amacrine cells labeled with TMEM16A antibodies in control-transfected **(A,B)** and dual-guide RNA-transfected **(C,D)** conditions. **(E)** The mean integrated density for all objects identified within the TMEM16A mask is reduced in the dual-guide condition. **(F)** The mean fluorescent intensity of TMEM16A objects and the mean TMEM16A object size **(G)** are significantly reduced in dual-guide RNA-transfected cells. **(H)** Log-transformed integrated density of the GFP signal is lower in dual gRNA group. * denotes $p < 0.05$, ** denotes $p < 0.005$, **** denotes $p < 0.00005$.

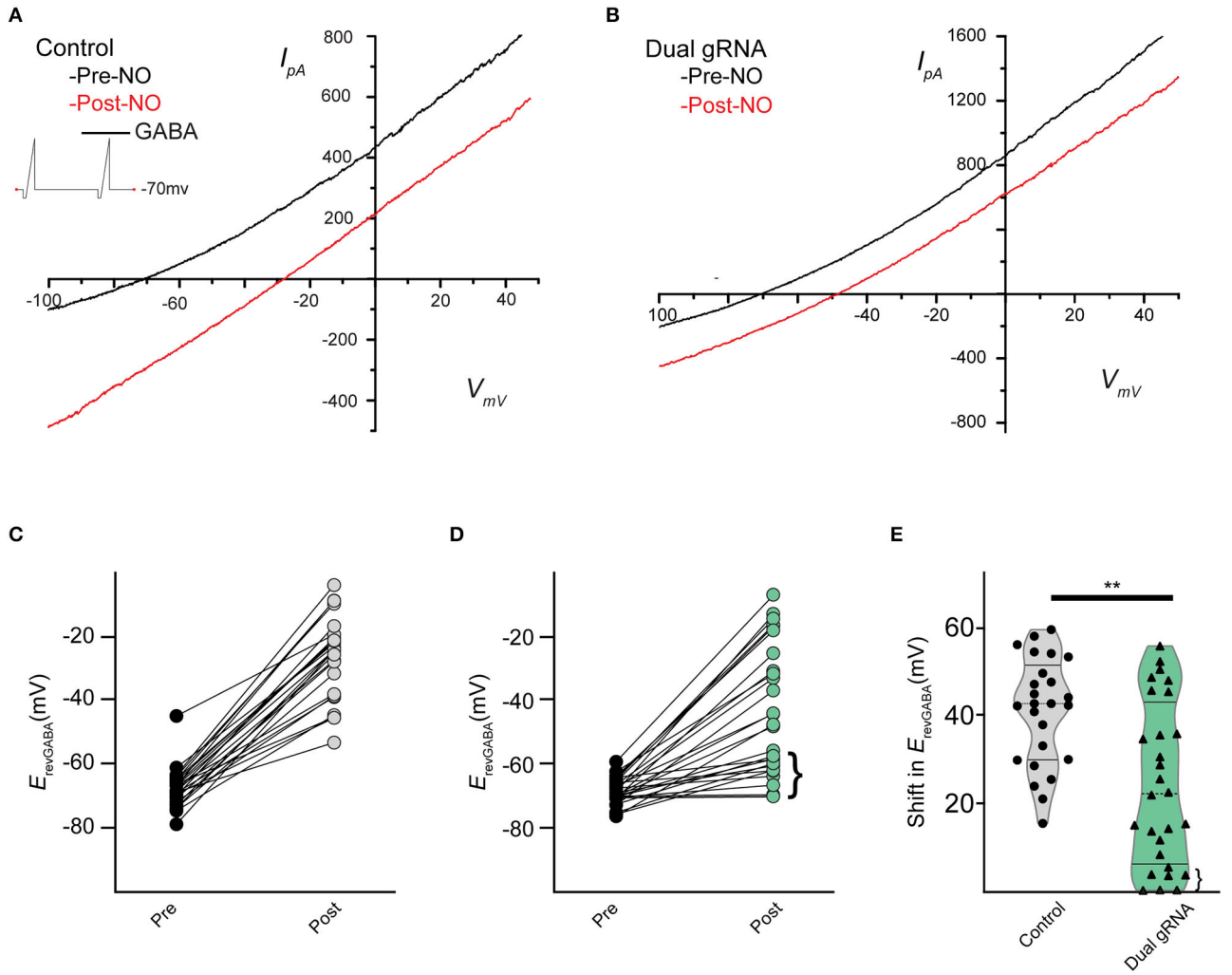

FIGURE 8 | Dual gRNA Cas9 ribonucleoproteins targeting *TMEM16A* reduce the NO-dependent shift in $E_{revGABA}$. Recording traces from GABA-gated currents before and after injecting NO from control-transfected **(A)** ($n = 23$) and dual gRNA/RNP-transfected cells **(B)** ($n = 25$). Paired data showing before and after NO injection for control **(C)** and dual-guide RNA targeting TMEM16A **(D)**. Delivery of the Cas9 ribonucleoprotein led to a population of cells exhibiting significantly reduced NO-dependent shift [**(D)**, brace] **(E)** Violin plots for the mean shift in $E_{revGABA}$ show a reduction under dual gRNA/RNP condition and a lower quartile [**(E)**, brace] that is far lower than control (control $n = 25$, dual gRNA/RNP $n = 28$, $p = 0.003$, ** denotes $p < 0.005$).

(CaCCs) mediated by TMEM16A are found in mouse rod bipolar cells (Jeon et al., 2013; Paik et al., 2020) and probably mediate the CaCCs identified in goldfish bipolar cells (Okada et al., 1995). However, no CaCC was found in chick ACs (Gleason et al., 1994), suggesting an intracellular localization for TMEM16A. Schreiber et al. show that TMEM16A localization may be cell- and tissue-specific depending on the expression of other TMEM16 paralogues that affect trafficking and function (Schreiber et al., 2010, 2015). In our study, we found mRNA transcripts for TMEM16 paralogues B, C, D, E, F, H, J, and K in embryonic chick retinal tissue. TMEM16G is absent from the *Gallus gallus* reference genome assembly (GRCg6a). The medley of TMEM16 paralogues expressed by individual ACs is not yet known, and AC subtypes may differ in TMEM16 expression profiles. Defining the compliment of TMEM16 paralogue expression in single cells could facilitate AC subtype identification in culture.

In our original paper on the NO-dependent release of internal Cl^- (Hoffpauir et al., 2006), we proposed a simple scenario where, in the presence of NO, ACs receiving input from bipolar cells and other amacrine cells would experience a shift in the balance of inputs such that ACs would be more depolarized and thus release more GABA or glycine onto postsynaptic cells and alter the retinal output. AC subset-specific co-expression of specific compliments of TMEM16 with CFTR could adjust the sensitivity of ACs to NO and fine-tune the NO response. Neuromodulation by the NO-dependent release

of internal Cl^- further enhances AC flexibility by allowing a single neurotransmitter to provide both inhibitory and excitatory signals. In this way, circuit flexibility is maximized while metabolic, genetic, and spatial costs are minimized (Grimes et al., 2010) in agreement with the laws of the economy of space, time, and matter (y Cajal, 1999; Chklovskii, 2004).

DATA AVAILABILITY STATEMENT

The raw data supporting the conclusions to this article will be made available by the authors upon request.

ETHICS STATEMENT

The animal study was reviewed and approved by LSU Institutional Animal Care and Use Committee.

AUTHOR CONTRIBUTIONS

TR and EG conceived and designed experiments, interpreted results, and prepared figures and drafted manuscript. TR, LZ, and HS performed experiments. All authors contributed to the article and approved the submitted version.

REFERENCES

Bae, S., Kweon, J., Kim, H. S., and Kim, J. S. (2014). Microhomology-based choice of Cas9 nuclease target sites. *Nat. Methods* 11, 705–706. doi: 10.1038/nmeth.3015

Benedetto, R., Cabrita, I., Schreiber, R., and Kunzelmann, K. (2019). TMEM16A is indispensable for basal mucus secretion in airways and intestine. *FASEB J.* 33, 4502–4512. doi: 10.1096/fj.201801333RRR

Benedetto, R., Ousingsawat, J., Wanitchakool, P., Zhang, Y., Holtzman, M. J., Amaral, M., et al. (2017). Epithelial chloride transport by CFTR requires TMEM16A. *Sci. Rep.* 7, 12397. doi: 10.1038/s41598-017-10910-0

Bill, A., Hall, M. L., Borawski, J., Hodgson, C., Jenkins, J., Piechon, P., et al. (2014). Small molecule-facilitated degradation of ANO1 protein: a new targeting approach for anticancer therapeutics. *J. Biol. Chem.* 289, 11029–11041. doi: 10.1074/jbc.M114.549188

Biwersi, J., Emans, N., and Verkman, A. S. (1996). Cystic fibrosis transmembrane conductance regulator activation stimulates endosome fusion *in vivo*. *Proc. Natl. Acad. Sci. U. S. A.* 93, 12484–12489. doi: 10.26508/lsa.201900462

Bordier, C. (1981). Phase separation of integral membrane proteins in Triton X-114 solution. *J. Biol. Chem.* 256, 1604–1607.

Bradbury, N. A. (1999). Intracellular CFTR: localization and function. *Physiol. Rev.* 79, S175–191. doi: 10.1152/physrev.1999.79.1.S175

Bradbury, N. A., Jilling, T., Berta, G., Sorscher, E. J., Bridges, R. J., Kirk, K. L., et al. (1992). Regulation of plasma membrane recycling by CFTR. *Science* 256, 530–532. doi: 10.1126/science.1373908

Bushell, S. R., Pike, A. C. W., Falzone, M. E., Rorsman, N. J. G., Ta, C. M., Corey, R. A., et al. (2019). The structural basis of lipid scrambling and inactivation in the endoplasmic reticulum scramblase TMEM16K. *Nat. Commun.* 10, 3956. doi: 10.1038/s41467-019-11753-1

Cabrita, I., Benedetto, R., Wanitchakool, P., Lerias, J., Centeio, R., Ousingsawat, J., et al. (2021). TMEM16A mediates mucus production in human airway epithelial cells. *Am. J. Respir. Cell Mol. Biol.* 64, 50–58. doi: 10.1165/rcmb.2019-0442OC

Callif, B. L., Maunze, B., Krueger, N. L., Simpson, M. T., and Blackmore, M. G. (2017). The application of CRISPR technology to high content screening in primary neurons. *Mol. Cell Neurosci.* 80, 170–179. doi: 10.1016/j.mcn.2017.01.003

Caputo, A., Piano, I., Demontis, G. C., Bacchi, N., Casarosa, S., Della Santina, L., et al. (2015). TMEM16A is associated with voltage-gated calcium channels in mouse retina and its function is disrupted upon mutation of the auxiliary alpha2delta4 subunit. *Front. Cell Neurosci.* 9, 422. doi: 10.3389/fncel.2015.00422

Charlesworth, G., Plagnol, V., Hol mstrom, K. M., Bras, J., Sheerin, U. M., Preza, E., et al. (2012). Mutations in ANO3 cause dominant craniocervical dystonia: ion channel implicated in pathogenesis. *Am. J. Hum. Genet.* 91, 1041–1050. doi: 10.1016/j.ajhg.2012.10.024

Chklovskii, D. B. (2004). Synaptic connectivity and neuronal morphology: two sides of the same coin. *Neuron* 43, 609–617. doi: 10.1016/S0896-6273(04)00498-2

Cho, H., Yang, Y. D., Lee, J., Lee, B., Kim, T., Jang, Y., et al. (2012). The calcium-activated chloride channel anoctamin 1 acts as a heat sensor in nociceptive neurons. *Nat. Neurosci.* 15, 1015–1021. doi: 10.1038/nn.3111

Chomczynski, P., and Sacchi, N. (2006). The single-step method of RNA isolation by acid guanidinium thiocyanate-phenol-chloroform extraction: twenty-something years on. *Nat. Protoc.* 1, 581–585. doi: 10.1038/nprot.2006.83

Danahay, H., Fox, R., Lilley, S., Charlton, H., Adley, K., Christie, L., et al. (2020). Potentiating TMEM16A does not stimulate airway mucus secretion or bronchial and pulmonary arterial smooth muscle contraction. *FASEB Bioadv.* 2, 464–477. doi: 10.1096/fba.2020-00035

de Vries, S.E., Baccus, S.A., and Meister, M. (2011). The projective field of a retinal amacrine cell. *J. Neurosci.* 31, 8595–8604. doi: 10.1523/JNEUROSCI.5662-10.2011

Eldred, W. D., and Blute, T. A. (2005). Imaging of nitric oxide in the retina. *Vis. Res.* 45, 3469–3486. doi: 10.1016/j.visres.2005.07.033

Feller, M. B., Wellis, D. P., Stellwagen, D., Werblin, F. S., and Shatz, C. J. (1996). Requirement for cholinergic synaptic transmission in the propagation of spontaneous retinal waves. *Science* 272, 1182–1187.

Feng, S., Dang, S., Han, T. W., Ye, W., Jin, P., Cheng, T., et al. (2019). Cryo-EM studies of TMEM16F calcium-activated ion channel suggest features important for lipid scrambling. *Cell Rep.* 28, 567–579. e564. doi: 10.1016/j.celrep.2019.06.023

Fischer, A. J., and Stell, W. K. (1999). Nitric oxide synthase-containing cells in the retina, pigmented epithelium, choroid, and sclera of the chick eye. *J. Comp. Neurol.* 405, 1–14. doi: 10.1002/(sici)1096-9861(19990301)405:1<1::aid-cne1>3.0.co;2-u

Gleason, E., Borges, S., and Wilson, M. (1993). Synaptic transmission between pairs of retinal amacrine cells in culture. *J. Neurosci.* 13, 2359–2370. doi: 10.1523/JNEUROSCI.13-06-02359.1993

Gleason, E., Borges, S., and Wilson, M. (1994). Control of transmitter release from retinal amacrine cells by Ca^{2+} influx and efflux. *Neuron* 13, 1109–1117. doi: 10.1016/0896-6273(94)90049-3

Goldstein, I. M., Ostwald, P., and Roth, S. (1996). Nitric oxide: a review of its role in retinal function and disease. *Vis. Res.* 36, 2979–2994. doi: 10.1016/0042-6989(96)00017-x

Grimes, W. N., Zhang, J., Graydon, C. W., Kachar, B., and Diamond, J. S. (2010). Retinal parallel processors: more than 100 independent microcircuits operate within a single interneuron. *Neuron* 65, 873–885. doi: 10.1016/j.neuron.2010.02.028

Hampson, E. C., Vaney, D. I., and Weiler, R. (1992). Dopaminergic modulation of gap junction permeability between amacrine cells in mammalian retina. *J. Neurosci.* 12, 4911–4922. doi: 10.1523/JNEUROSCI.12-12-04911.1992

Hel mstaedter, M., Briggman, K. L., Turaga, S. C., Jain, V., Seung, H. S., Denk, W., et al. (2013). Connectomic reconstruction of the inner plexiform layer in the mouse retina. *Nature* 500, 168–174. doi: 10.1038/nature12346

Hoffpauir, B., McMains, E., and Gleason, E. (2006). Nitric oxide transiently converts synaptic inhibition to excitation in retinal amacrine cells. *J. Neurophysiol.* 95, 2866–2877. doi: 10.1152/jn.01317.2005

Huang, F., Wang, X., Ostertag, E. M., Nuwal, T., Huang, B., Jan, Y. N., et al. (2013). TMEM16C facilitates Na(+)-activated K+ currents in rat sensory neurons and regulates pain processing. *Nat. Neurosci.* 16, 1284–1290. doi: 10.1038/nn.3468

Hull, J. (2012). Cystic fibrosis transmembrane conductance regulator dysfunction and its treatment. *J. R. Soc. Med.* 105, S2–8. doi: 10.1258/jrsm.2012.12s001

Izumi, N., Nagaoka, T., Sato, E., Sogawa, K., Kagokawa, H., Takahashi, A., et al. (2008). Role of nitric oxide in regulation of retinal blood flow in

response to hyperoxia in cats. *Invest. Ophthalmol. Vis. Sci.* 49, 4595–4603. doi: 10.1167/iovs.07-1667

Jacoby, J., Nath, A., Jessen, Z. F., and Schwartz, G. W. (2018). A self-regulating gap junction network of amacrine cells controls nitric oxide release in the retina. *Neuron* 100, 1149–1162.e1145. doi: 10.1016/j.neuron.2018.09.047

Jacoby, R., Stafford, D., Kouyama, N., and Marshak, D. (1996). Synaptic inputs to ON parasol ganglion cells in the primate retina. *J. Neurosci.* 16, 8041–8056. doi: 10.1523/JNEUROSCI.16-24-08041.1996

Jensen, A. B., Joergensen, H. B., Dam, V. S., Kamaev, D., Boedtkjer, D., Fuchtbauer, E. M., et al. (2018). Variable contribution of TMEM16A to tone in murine arterial vasculature. *Basic Clin. Pharmacol. Toxicol.* 123, 30–41. doi: 10.1111/bcpt.12984

Jeon, J. H., Paik, S. S., Chun, M. H., Oh, U., and Kim, I. B. (2013). Presynaptic localization and possible function of calcium-activated chloride channel anoctamin 1 in the mammalian retina. *PLoS ONE* 8, e67989. doi: 10.1371/journal.pone.0067989

Jia, Y., Lee, S., Zhuo, Y., and Zhou, Z. J. (2020). A retinal circuit for the suppressed-by-contrast receptive field of a polyaxonal amacrine cell. *Proc. Natl. Acad. Sci. U. S. A.* 117, 9577–9583. doi: 10.1073/pnas.1913417117

Jin, X., Shah, S., Liu, Y., Zhang, H., Lees, M., Fu, Z., et al. (2013). Activation of the Cl-channel ANO1 by localized calcium signals in nociceptive sensory neurons requires coupling with the IP3 receptor. *Sci. Signal* 6, ra73. doi: 10.1126/scisignal.2004184

Kalienkova, V., Clerico Mosina, V., and Paulino, C. (2021). The groovy TMEM16 family: molecular mechanis ms of lipid scrambling and ion conduction. *J. Mol. Biol.* 433, 166941. doi: 10.1016/j.jmb.2021.166941

Kim, H., Kim, H., Lee, J., Lee, B., Kim, H. R., Jung, J., et al. (2018). Anoctamin 9/TMEM16J is a cation channel activated by cAMP/PKA signal. *Cell Calcium* 71, 75–85. doi: 10.1016/j.ceca.2017.12.003

Kim, J. H., Kim, K., Kim, I., Seong, S., Kim, S. W., Kim, N., et al. (2019). Role of anoctamin 5, a gene associated with gnathodiaphyseal dysplasia, in osteoblast and osteoclast differentiation. *Bone* 120, 432–438. doi: 10.1016/j.bone.2018.12.010

Kim, T., Soto, F., and Kerschensteiner, D. (2015). An excitatory amacrine cell detects object motion and provides feature-selective input to ganglion cells in the mouse retina. *Elife* 4, e08025. doi: 10.7554/eLife.08025

Kirkpatrick, D. P., and Radding, C. M. (1992). RecA protein promotes rapid RNA-DNA hybridization in heterogeneous RNA mixtures. *Nucl. Acids Res.* 20, 4347–4353. doi: 10.1093/nar/20.16.4347

Krishnan, V., Maddox, J. W., Rodriguez, T., and Gleason, E. (2017). A role for the cystic fibrosis transmembrane conductance regulator in the nitric oxide-dependent release of Cl(-) from acidic organelles in amacrine cells. *J. Neurophysiol.* 118, 2842–2852. doi: 10.1152/jn.00511.2017

Lukacs, G. L., Chang, X. B., Kartner, N., Rotstein, O. D., Riordan, J. R., Grinstein, S., et al. (1992). The cystic fibrosis transmembrane regulator is present and functional in endosomes. Role as a determinant of endosomal pH. *J. Biol. Chem.* 267, 14568–14572.

Maddox, J. W., and Gleason, E. (2017). Nitric oxide promotes GABA release by activating a voltage-independent Ca(2+) influx pathway in retinal amacrine cells. *J. Neurophysiol.* 117, 1185–1199. doi: 10.1152/jn.00803.2016

Maher, P. A., and Singer, S. J. (1985). Anomalous interaction of the acetylcholine receptor protein with the nonionic detergent Triton X-114. *Proc. Natl. Acad. Sci. U. S. A.* 82, 958–962.

Malysz, J., Gibbons, S. J., Saravanaperumal, S. A., Du, P., Eisenman, S. T., Cao, C., et al. (2017). Conditional genetic deletion of Ano1 in interstitial cells of Cajal impairs Ca(2+) transients and slow waves in adult mouse small intestine. *Am. J. Physiol. Gastrointest. Liver Physiol.* 312, G228–G245. doi: 10.1152/ajpgi.00363.2016

Milenkovic, V. M., Brockmann, M., Stohr, H., Weber, B. H., and Strauss, O. (2010). Evolution and functional divergence of the anoctamin family of membrane proteins. *BMC Evol. Biol.* 10, 319. doi: 10.1186/1471-2148-10-319

Mills, S. L., and Massey, S. C. (1995). Differential properties of two gap junctional pathways made by AII amacrine cells. *Nature* 377, 734–737.

Neureither, F., Stowasser, N., Frings, S., and Mohrlen, F. (2017). Tracking of unfamiliar odors is facilitated by signal amplification through anoctamin 2 chloride channels in mouse olfactory receptor neurons. *Physiol. Rep.* 5, e13373. doi: 10.14814/phy2.13373

Okada, T., Horiguchi, H., and Tachibana, M. (1995). Ca(2+)-dependent Cl-current at the presynaptic terminals of goldfish retinal bipolar cells. *Neurosci. Res.* 23, 297–303.

Ortuno-Lizaran, I., Sanchez-Saez, X., Lax, P., Serrano, G. E., Beach, T. G., Adler, C. H., et al. (2020). Dopaminergic retinal cell loss and visual dysfunction in parkinson disease. *Ann. Neurol.* 88, 893–906. doi: 10.1002/ana.25897

Ousingsawat, J., Wanitchakool, P., Kmit, A., Romao, A. M., Jantarajit, W., Schreiber, R., et al. (2015). Anoctamin 6 mediates effects essential for innate immunity downstream of P2X7 receptors in macrophages. *Nat. Commun.* 6, 6245. doi: 10.1038/ncom ms7245

Paik, S. S., Park, Y. S., and Kim, I. B. (2020). Calcium- and voltage-dependent dual gating ANO1 is an intrinsic determinant of repolarization in rod bipolar cells of the mouse retina. *Cells* 9, 543. doi: 10.3390/cells9030543

Pifferi, S., Cenedese, V., and Menini, A. (2012). Anoctamin 2/TMEM16B: a calcium-activated chloride channel in olfactory transduction. *Exp. Physiol.* 97, 193–199. doi: 10.1113/expphysiol.2011.058230

Reichhart, N., Schoberl, S., Keckeis, S., Alfaar, A. S., Roubeix, C., Cordes, M., et al. (2019). Anoctamin-4 is a bona fide Ca(2+)-dependent non-selective cation channel. *Sci. Rep.* 9, 2257. doi: 10.1038/s41598-018-37287-y

Reznikov, L. R. (2017). Cystic fibrosis and the nervous system. *Chest* 151, 1147–1155. doi: 10.1016/j.chest.2016.11.009

Ruffin, M., Voland, M., Marie, S., Bonora, M., Blanchard, E., Blouquit-Laye, S., et al. (2013). Anoctamin 1 dysregulation alters bronchial epithelial repair in cystic fibrosis. *Biochim. Biophys. Acta* 1832, 2340–2351. doi: 10.1016/j.bbadis.2013.09.012

Saint-Criq, V., and Gray, M. A. (2017). Role of CFTR in epithelial physiology. *Cell Mol. Life Sci.* 74, 93–115. doi: 10.1007/s00018-016-2391-y

Schreiber, R., Faria, D., Skryabin, B. V., Wanitchakool, P., Rock, J. R., Kunzelmann, K., et al. (2015). Anoctamins support calcium-dependent chloride secretion by facilitating calcium signaling in adult mouse intestine. *Pflugers Arch.* 467, 1203–1213. doi: 10.1007/s00424-014-1559-2

Schreiber, R., Uliyakina, I., Kongsuphol, P., Warth, R., Mirza, M., Martins, J. R., et al. (2010). Expression and function of epithelial anoctamins. *J. Biol. Chem.* 285, 7838–7845. doi: 10.1074/jbc.M109.065367

Scudieri, P., Caci, E., Bruno, S., Ferrera, L., Schiavon, M., Sondo, E., et al. (2012). Association of TMEM16A chloride channel overexpression with airway goblet cell metaplasia. *J. Physiol.* 590, 6141–6155. doi: 10.1113/jphysiol.2012.240838

Sepela, R. J., and Sack, J. T. (2018). Taming unruly chloride channel inhibitors with rational design. *Proc. Natl. Acad. Sci. U. S. A.* 115, 5311–5313. doi: 10.1073/pnas.1805589115

Shah, S., Carver, C. M., Mullen, P., Milne, S., Lukacs, V., Shapiro, M. S., et al. (2020). Local Ca(2+) signals couple activation of TRPV1 and ANO1 sensory ion channels. *Sci. Signal* 13, eaaw7963. doi: 10.1126/scisignal.aaw7963

Shi, Q., Teves, M. M., Lillywhite, A., Pagtalunan, E. B., and Stell, W. K. (2020). Light adaptation in the chick retina: dopamine, nitric oxide, and gap-junction coupling modulate spatiotemporal contrast sensitivity. *Exp. Eye Res.* 195, 108026. doi: 10.1016/j.exer.2020.108026

Simoes, F. B., Quaresma, M. C., Clarke, L. A., Silva, I. A., Pankonien, I., Railean, V., et al. (2019). TMEM16A chloride channel does not drive mucus production. *Life Sci. Alliance* 2, e201900462. doi: 10.26508/lsa.201900462

Stabilini, S., Menini, A., and Pifferi, S. (2021). Anion and cation permeability of the mouse TMEM16F calcium-activated channel. *Int. J. Mol. Sci.* 22, 8578. doi: 10.3390/ij ms22168578

Suzuki, J., Fujii, T., Imao, T., Ishihara, K., Kuba, H., Nagata, S., et al. (2013). Calcium-dependent phospholipid scramblase activity of TMEM16 protein family members. *J. Biol. Chem.* 288, 13305–13316. doi: 10.1074/jbc.M113.457937

Taguchi, Y., and Schatzl, H. M. (2014). Small-scale triton X-114 extraction of hydrophobic proteins. *Biol. Protoc.* 4, e1139. doi: 10.21769/BioProtoc.1139

Takayama, Y., Uta, D., Furue, H., and Tominaga, M. (2015). Pain-enhancing mechanism through interaction between TRPV1 and anoctamin 1 in sensory neurons. *Proc. Natl. Acad. Sci. U. S. A.* 112, 5213–5218. doi: 10.1073/pnas.1421507112

Tekmen-Clark, M., and Gleason, E. (2013). Nitric oxide production and the expression of two nitric oxide synthases in the avian retina. *Vis. Neurosci.* 30, 91–103. doi: 10.1017/S0952523813000126

Vakulskas, C. A., Dever, D. P., Rettig, G. R., Turk, R., Jacobi, A. M., Collingwood, M. A., et al. (2018). A high-fidelity Cas9 mutant delivered

as a ribonucleoprotein complex enables efficient gene editing in human hematopoietic stem and progenitor cells. *Nat. Med.* 24, 1216–1224. doi: 10.1038/s41591-018-0137-0

Vielma, A. H., Agurto, A., Valdes, J., Palacios, A. G., and Schmachtenberg, O. (2014). Nitric oxide modulates the temporal properties of the glutamate response in type 4 OFF bipolar cells. *PLoS ONE* 9, e114330. doi: 10.1371/journal.pone.0114330

Wanitchakool, P., Ousingsawat, J., Sirianant, L., Cabrita, I., Faria, D., Schreiber, R., et al. (2017). Cellular defects by deletion of ANO10 are due to deregulated local calcium signaling. *Cell Signal* 30, 41–49. doi: 10.1016/j.cellsig.2016.11.006

Ward, C. L., and Kopito, R. R. (1994). Intracellular turnover of cystic fibrosis transmembrane conductance regulator. Inefficient processing and rapid degradation of wild-type and mutant proteins. *J. Biol. Chem.* 269, 25710–25718.

Whitlock, J. M., Yu, K., Cui, Y. Y., and Hartzell, H. C. (2018). Anoctamin 5/TMEM16E facilitates muscle precursor cell fusion. *J. Gen. Physiol.* 150, 1498–1509. doi: 10.1085/jgp.201812097

Xu, H. P., Burbridge, T. J., Ye, M., Chen, M., Ge, X., Zhou, Z. J., et al. (2016). Retinal wave patterns are governed by mutual excitation among starburst amacrine cells and drive the refinement and maintenance of visual circuits. *J. Neurosci.* 36, 3871–3886. doi: 10.1523/JNEUROSCI.3549-15.2016

Xue, R., Gu, H., Qiu, Y., Guo, Y., Korteweg, C., Huang, J., et al. (2016). Expression of cystic fibrosis transmembrane conductance regulator in ganglia of human gastrointestinal tract. *Sci. Rep.* 6, 30926. doi: 10.1038/srep30926

y Cajal, S.R. (1999). "Physiologic Inferences from the Morphology and Connectivity of Neurons," in *Texture of the Nervous System of Man and the Vertebrates,* ed S.R. y Cajal. (Vienna, Austria: Springer*)*, 85–122.

Yan, W., Laboulaye, M. A., Tran, N. M., Whitney, I. E., Benhar, I., Sanes, J. R., et al. (2020). Mouse retinal cell atlas: molecular identification of over sixty amacrine cell types. *J. Neurosci.* 40, 5177–5195. doi: 10.1523/JNEUROSCI.0471-20.2020

Yang, H., Kim, A., David, T., Palmer, D., Jin, T., Tien, J., et al. (2012). TMEM16F for ms a Ca^{2+}-activated cation channel required for lipid scrambling in platelets during blood coagulation. *Cell* 151, 111–122. doi: 10.1016/j.cell.2012.07.036

Yang, Y. D., Cho, H., Koo, J. Y., Tak, M. H., Cho, Y., Shim, W. S., et al. (2008). TMEM16A confers receptor-activated calcium-dependent chloride conductance. *Nature* 455, 1210–1215. doi: 10.1038/nature07313

Yoshimura, K., Nakamura, H., Trapnell, B. C., Chu, C. S., Dalemans, W., Pavirani, A., et al. (1991). Expression of the cystic fibrosis transmembrane conductance regulator gene in cells of non-epithelial origin. *Nucl. Acids Res.* 19, 5417–5423.

Zak, J. D., Grimaud, J., Li, R. C., Lin, C. C., and Murthy, V. N. (2018). Calcium-activated chloride channels clamp odor-evoked spike activity in olfactory receptor neurons. *Sci. Rep.* 8, 10600. doi: 10.1038/s41598-018-28855-3

Zhang, D. Q., Wong, K. Y., Sollars, P. J., Berson, D. M., Pickard, G. E., McMahon, D. G., et al. (2008). Intraretinal signaling by ganglion cell photoreceptors to dopaminergic amacrine neurons. *Proc. Natl. Acad. Sci. U. S. A.* 105, 14181–14186. doi: 10.1073/pnas.0803893105

Zhong, L., and Gleason, E. L. (2021). Adenylate cyclase 1 links calcium signaling to CFTR-dependent cytosolic chloride elevations in chick amacrine cells. *Front. Cell. Neurosci.* 15, 726605. doi: 10.3389/fncel.2021.726605

Conflict of Interest: The authors declare that the research was conducted in the absence of any commercial or financial relationships that could be construed as a potential conflict of interest.

Publisher's Note: All claims expressed in this article are solely those of the authors and do not necessarily represent those of their affiliated organizations, or those of the publisher, the editors and the reviewers. Any product that may be evaluated in this article, or claim that may be made by its manufacturer, is not guaranteed or endorsed by the publisher.

frontiers | Frontiers in Cellular Neuroscience

TYPE Review
PUBLISHED 23 September 2022
DOI 10.3389/fncel.2022.989637

OPEN ACCESS

EDITED BY
Fengquan Zhou,
Zhejiang University, China

REVIEWED BY
Fang Y. E.,
Sun Yat-sen University, China
Esra Yalcin,
Boston Children's Hospital and Harvard Medical School, United States

*CORRESPONDENCE
Xianhu Zhou
zhouxianhu@nbu.edu.cn
Shiqing Feng
sqfeng@tmu.edu.cn

†These authors have contributed equally to this work

‡These authors have contributed equally to this work and share first authorship

SPECIALTY SECTION
This article was submitted to Cellular Neuropathology, a section of the journal Frontiers in Cellular Neuroscience

RECEIVED 08 July 2022
ACCEPTED 05 September 2022
PUBLISHED 23 September 2022

CITATION
Liu D, Fan B, Li J, Sun T, Ma J, Zhou X and Feng S (2022) N6-methyladenosine modification: A potential regulatory mechanism in spinal cord injury. *Front. Cell. Neurosci.* 16:989637. doi: 10.3389/fncel.2022.989637

N6-methyladenosine modification: A potential regulatory mechanism in spinal cord injury

Derong Liu[1,2‡], Baoyou Fan[1,2‡], Jinze Li[1,2‡], Tao Sun[1,2], Jun Ma[1,2], Xianhu Zhou[3*†] and Shiqing Feng[1,2*†]

[1]Department of Orthopedics, Tianjin Medical University General Hospital, Tianjin, China, [2]Department of Orthopedics, International Science and Technology Cooperation Base of Spinal Cord Injury, Tianjin Key Laboratory of Spine and Spinal Cord Injury, Tianjin Medical University General Hospital, Tianjin, China, [3]The Affiliated Hospital of Medical School, Ningbo University, Ningbo, China

N6-methyladenosine (m6A), an essential post-transcriptional modification in eukaryotes, is closely related to the development of pathological processes in neurological diseases. Notably, spinal cord injury (SCI) is a serious traumatic disease of the central nervous system, with a complex pathological mechanism which is still not completely understood. Recent studies have found that m6A modification levels are changed after SCI, and m6A-related regulators are involved in the changes of the local spinal cord microenvironment after injury. However, research on the role of m6A modification in SCI is still in the early stages. This review discusses the latest progress in the dynamic regulation of m6A modification, including methyltransferases ("writers"), demethylases ("erasers") and m6A -binding proteins ("readers"). And then analyses the pathological mechanism relationship between m6A and the microenvironment after SCI. The biological processes involved included cell death, axon regeneration, and scar formation, which provides new insight for future research on the role of m6A modification in SCI and the clinical transformation of strategies for promoting recovery of spinal cord function.

KEYWORDS

epigenetics, N6-methyladenosine (m6A), post-transcriptional modification, nervous system, spinal cord injury (SCI)

Introduction

N6-methyladenosine (m6A) modification, a type of posttranscriptional modification, has been confirmed to be involved in the post-transcriptional regulation of gene (Roundtree et al., 2017a; Zhao et al., 2017). It was first discovered in mammals in the 1970s (Desrosiers et al., 1974). Notably, m6A is the most common reversible

modification found in higher eukaryotic mRNAs (Desrosiers et al., 1974). The dynamic modification of m6A depends on the action of intracellular methylase and demethylase. The former includes methyltransferase-like (METTL) 3, METTL14, Wilms tumor 1-associating protein (WTAP), etc. And the latter includes Fat mass and obesity-associated protein (FTO) and human AlkB homolog 5 (ALKBH5). In addition, m6A-binding proteins also affect RNA metabolism, such as YT521-B homology domain protein family members (YTHDF1-3/YTHDC1-2), heterogeneous nuclear ribonucleoprotein C (HNRNPC) and insulin-like growth factor 2 mRNA-binding proteins 1/2/3 (IGF2BP1/2/3) (Dominissini et al., 2012; Wang et al., 2014; Liu et al., 2015; Huang et al., 2018; Zaccara and Jaffrey, 2020). Moreover, recent studies have demonstrated that m6A is closely related to biological processes of the nervous system, such as brain and cerebellum development, axonal and synaptic formation, gliogenesis, etc (Walters et al., 2017; Yoon et al., 2017; Ma et al., 2018; Xu et al., 2020; Zhao F. et al., 2021).

Spinal cord injury (SCI), a catastrophic condition resulting from a combination of factors, is associated with high rates of disability and fatality and always reduces patient quality of life and imposes a financial burden on families (National SCI Statistical Center [NSCISC], 2016; Ahuja et al., 2017; Tran et al., 2018). Notably, there are no established strategies for completely alleviating SCI and no ideal methods for completely restoring the function of the spinal cord (Venkatesh et al., 2019). Traumatic spinal cord injury is a common type of SCI in clinic (Ahuja et al., 2017). It has two progressive phases: primary injury and secondary injury (Tator, 1995; McDonald and Sadowsky, 2002). The former describes the damage inflicted by direct impact, and the severity of primary injury is proportional to the magnitude of the force applied and the location of the injury (McDonald and Sadowsky, 2002). Secondary injury occurs shortly after primary injury and is accompanied by a series of microenvironmental changes, such as localized hemorrhage and ischemia, inflammation, ionic and neural factor imbalance, glial scarring, and programmed cell death (PCD) (McDonald and Sadowsky, 2002; Fan et al., 2018). Therefore, reducing secondary injury and enhancing functional recovery are key for treating SCI. Fully elucidating the pathogenic mechanisms of SCI is especially critical. Recent studies have found that after SCI, the overall m6A level in the lesion site is increased, and the content of related regulatory factors, such as METTL3 and METTL14, are increased (Xing et al., 2021; Wang et al., 2021; Gao et al., 2022). Furthermore, it was discovered that the specific knockout of mettl14 helps functional recovery after SCI and reduces neuronal apoptosis (Wang et al., 2021; Gao et al., 2022). However, the function of m6A modification in SCI has yet to be fully elucidated. The pathological changes in nerve-related cells and repair processes after SCI may be related to RNA m6A modification, and determining how m6A modification influences these changes may provide insights into novel therapeutic strategies for SCI.

In this review, we summarize the current state of research on m6A modification and emphasize the regulatory mechanism of this type of modification in various pathological processes associated with dysfunction of the nervous system after injury and subsequent tissue repair after SCI to provide a theoretical basis for future research on SCI.

The regulatory mechanism of N6-methyladenosine modification

Since the discovery of m6A modification, researchers have continued to explore its mechanism and function. With the emergence of various sequencing technologies, such as m6A-seq, MeRIP-seq, m6A-CLIP, and m6A-sensitive HRM analysis, etc., it has been found that m6A modification is ubiquitous in coding and non-coding RNAs (Dominissini et al., 2012; Coker et al., 2019; Wang and Jia, 2020). The deposition of m6A on RNA affects mRNA metabolism, including mRNA nuclear export, splicing, translation, transcription, and degradation (Roundtree et al., 2017b; Huang et al., 2018; Liu J. et al., 2020; Cho et al., 2021; Mendel et al., 2021). Interestingly, numerous studies have confirmed that m6A modification sites are conserved in mRNA and that m6A preferentially binds to regions near stop codons or 3′ and 5′ untranslated regions (Meyer et al., 2012; Meyer et al., 2015). Notably, the conserved mRNA sequence to which m6A binds is generally "RRACH," where R represents adenine or guanine and H can represent adenine, cytosine, or uracil (Harper et al., 1990). Moreover, successful methylation of the sixth N of adenylate is inextricably linked to m6A-regulating factors, including "writers," "erasers," and "readers" (Zaccara et al., 2019).

Writers

Intracellular RNA methylation often requires co-catalysis by various enzymes, which are named "writers" (Oerum et al., 2021). The methyltransferase complex, which consists of a heterodimeric core formed by METTL3-METTL14 and additional enzymes, such as WTAP (Liu et al., 2014; Ping et al., 2014), normally catalyzes m6A modification (Liu et al., 2014). METTL3, which has been widely studied since it was first discovered in 1997, is known to be the catalytic core of the methylase complex (Bokar et al., 1997; Oerum et al., 2021). Another enzyme, METTL14, plays a synergistic role with METTL3, as both are essential components of the methylase complex (Wang et al., 2016). Binding of METTL14 to RNA enhances the methylase activity of METTL3 and stabilizes the complex structure (Wang et al., 2016).

In addition to Mettl3/14, the role of other writers is also worth exploring. First, WTAP plays a regulatory role in the methylase complex, linking the complex to RNA, and

deletion of WTAP results in in aberrant gene expression and alternative splicing (Ping et al., 2014). Recent research on the development and progression of ataxia and neuronal degeneration has revealed that WTAP expression is associated with disease progression and prognosis (Yang et al., 2022). WTAP-deficient mice not only had lower methylation levels in cerebellar Purkinje cells, but they also developed cerebellar atrophy and ataxia over time (Yang et al., 2022). Moreover, METTL16, another member of the METTL family, binds to U6 snRNA, ncRNAs, lncRNAs, and pre-mRNAs to catalyze methyl synthesis and is implicated in RNA splicing and translating (Pendleton et al., 2017; Warda et al., 2017; Satterwhite and Mansfield, 2022). Additionally, METTL16 can promote translation initiation by interacting with eukaryotic initiation factor 3a/b and rRNA in the cytoplasmic matrix, which is dependent on Mtase domain of METTL16 (Su et al., 2022). Furthermore, translation-related rRNAs can be methylated by another methylase, METTL5. METTL5 is essential for cell activity and differentiation potential and is required for effective translation (Ignatova et al., 2020). Mettl5 deficiency reduces overall translation rate, cell pluripotency, and differentiation potential in mouse embryonic stem cells (Ignatova et al., 2020). Additionally, cell translation and proliferation are related to ZCCHC4, a novel m6A writer that can interact with human 28S rRNA and mRNAs *in vitro* and *in vivo* (Ma et al., 2019). A study shows that ZCCHC4 knockout eliminates m6A modification in 28S rRNA, reduces global translation, and inhibits cell proliferation (Ma et al., 2019).

Erasers

Demethylases can remove methyl groups from nucleotides, and the discovery of m6A demethylases, generally known as "erasers," reveals that the m6A modification of RNA may be reversed dynamically (Yu et al., 2018). FTO and ALKBH5, both of which are AlkB proteins, can effectively decreased m6A levels (Jia et al., 2011; Zheng et al., 2013). FTO was the first demethylase to be discovered (Jia et al., 2011). Guifang Jia identified the enzyme "FTO" as m6A demethylase in 2011 and established that m6A is the predominant FTO substrate in the nucleus *in vivo* and *in vitro* (Jia et al., 2011). In addition to fat metabolism, FTO has recently been shown to be involved in nervous system pathologies in different contexts (Fischer et al., 2009; Li et al., 2017; Walters et al., 2017; Zhuang et al., 2019).

AlkB homolog 5, another enzyme capable of reversing m6A modification, has also been implicated in posttranscriptional RNA regulation, including mRNA splicing, stability, export and RNA metabolism (Zheng et al., 2013; Covelo-Molares et al., 2021). Inactivation of ALKBH5 causes an increase in m6A levels on mRNAs, and studies have shown that ALKBH5 is essential for the progression of non-neoplastic and neoplastic diseases of the reproductive, immune, circulatory, and nervous systems (Zheng et al., 2013; Cheng et al., 2021; Dong et al., 2021).

Readers

Eukaryotes produce a variety of proteins that can bind to the m6A modification site and affect RNA translation, splicing, and disintegration and other biological processes (Shi et al., 2017). These proteins are referred to as "readers" and include, most notably, YTH domain family protein 1/2/3(YTHDF1/2/3), YTH domain containing 1/2(YTHDC1/2), HNRNPC, and IGF2BP1/2/3 (Dominissini et al., 2012; Wang et al., 2014; Liu et al., 2015; Huang et al., 2018; Zaccara and Jaffrey, 2020).

YTHDF2 interacts with the m6A modification site on RNA, increasing the likelihood of RNA degradation (Wang et al., 2014). YTHDF2 exerts its effect through several pathways. For instance, YTHDF2 accelerates RNA degradation by recruiting the CCR4/NOT complex (Du et al., 2016). It was also shown that YTHDF2 regulates m6A-mediated RNA decay through the YTHDF2-HRSP12-RNase P/MRP axis (Park et al., 2019). Additionally, after YTHDF1 binds to m6A-tagged mRNAs in the cytoplasm, it stimulates ribosome occupancy of its target mRNA and acts in concert with initiation factors to improve the efficiency of mRNA translation (Wang et al., 2015). YTHDF3, another m6A binder, has been found to have two functions (Shi et al., 2017). It can work with YTHDF1 and YTHDF2 to increase mRNA translation or speed up methylated mRNA degradation, respectively (Shi et al., 2017). Furthermore, YTHDC1, a particular nuclear ribonucleic acid-binding protein, promotes alternative splicing by attracting the RNA splicing factor SRSF3 and preventing SRSF10 from binding to mRNAs in the nucleus (Xiao et al., 2016). It also regulates mRNA export from the nucleus to the cytoplasm (Roundtree et al., 2017b). Another member of this family, YTHDC2, is capable of altering the translation efficiency and mRNA abundance of its targets (Hsu et al., 2017). In addition, HNRNPC is also a common nuclear protein that detects and binds to m6A-modified sequences in mRNAs and lncRNAs, affecting target RNA abundance and splicing (Liu et al., 2015). In contrast to YTHDF2, IGF2BP1/2/3 are novel m6A readers that can protect m6A-modified mRNAs from degradation (Huang et al., 2018). They help thousands of potential mRNA targets remain stable and undergo translation (Huang et al., 2018). Recently, a novel m6A "reader," Prrrc2a, which is strongly associated with oligodendrocyte formation and axonal myelination, was identified by Wu R. et al. (2019). Their study found that Prrc2a can stabilize Oligo2 mRNA after binding to the m6A site (Wu R. et al., 2019). Additionally, when Prrc2a was removed, mice showed developmental abnormalities, such as enlarged lateral ventricles and significantly reduced myelin sheaths (Wu R. et al., 2019).

N6-methyladenosine modification after spinal cord injury

The nervous system is a multicellular network, and the close interactions among numerous nerve cells, such as neurons and glial cells, is essential for the coordination of its functions (Sousa et al., 2017). Direct damage to the spinal cord can disrupt the blood–spinal cord barrier and cause local blood supply insufficiency, directly resulting in cell death (Ahuja et al., 2017). Notably, the subsequent changes in the internal environment of the spinal cord broaden the scope of injury, and local structures undergo corresponding changes, including scar formation and axonal regeneration (Hara et al., 2017; Fan et al., 2018). M6A modifications are at higher levels in the nervous system (Meyer et al., 2012). Changes in M6A content and associated regulatory factors influence nervous system development and function. For instance, METTLl14 deficiency reduced m6A levels in mouse cerebral cortex and prolonged cortical neurogenesis (Yoon et al., 2017). A study has also demonstrated that the deletion of the methylase METTL3 results in ataxia, hypoplastic development of the mouse cerebellum, and an increase in the apoptosis of immature granulosa cells (Wang et al., 2018). Another study found that peripheral nerve damage raised the levels of FTO, G9a protein, and decreased Ehmt2 mRNA m6A methylation level, all of which contributed to the development of neuropathic pain. Additionally, it was shown that reducing FTO expression in the dorsal root ganglion can reduce neuropathic pain caused by injury (Li et al., 2020).

Recent studies have also reported that after SCI, the levels of m6A as well as writers, such as mettl3 and mettl14, in tissues rise dramatically and specific knockout of methylase can alleviate the severity of SCI (Wang et al., 2021; Xing et al., 2021; Gao et al., 2022). This indicates that dynamic m6A modification has a strong potential to regulate the injury mechanism after SCI and influencing functional recovery.

N6-methyladenosine modification and cell death after spinal cord injury

The structural and functional integrity of the spinal cord are the foundations for proper physiological activity (Ahuja et al., 2017). However, SCI is a multistep disorder usually accompanied by massive neuronal cell death, which is one of the reasons why SCI is difficult to treat (Anjum et al., 2020). In addition to the cell destruction induced by direct impact, secondary injury changes the internal environment and structure of the spinal cord and induces PCD of nerve cells (Fan et al., 2018; Shi et al., 2021). Therefore, preserving nerve cells and reducing or even eliminating cell death are critical for the treatment of SCI. To achieve better treatment outcomes, it is essential to explore the mechanism of PCD after SCI.

Programmed cell death is tightly linked to m6A modification (Wang et al., 2020; Lan et al., 2021; Shen et al., 2021; Liu et al., 2022). Apoptosis is a common form of PCD in the nervous system (Fricker et al., 2018). A study showed that knockout of mettl3 results in massive apoptosis of newborn cerebellar granule cells, resulting in dysplasia in the mouse cerebellum (Wang et al., 2018). Similarly, Mettl3 deficiency in the mouse hippocampus increases local apoptosis and alter the cell cycle (Zhao F. et al., 2021). In addition, after ischemic brain injury, overexpression of YTHDC1 reduces neuronal apoptosis (Zhang et al., 2020).

Recently, several studies have shown that methylation regulators can influence cell survival after SCI by regulating m6A levels (**Figure 1**). Haoyu Wang et al. verified that significant neuronal death and cell dysfunction occur at the site of injury in a rat spinal cord contusion model (Wang et al., 2021). Moreover, m6A levels were increased, and the expression of the "writer" mettl14 is increased (Wang et al., 2021). Surprisingly, inhibiting local Mettl14 expression lowers overall m6A levels and the severity of SCI in experimental animals while also promoting motor function recovery after injury (Wang et al., 2021). To explore the changes at the cellular level, the researchers performed HE staining and immunofluorescence (Wang et al., 2021). The results showed the presence of fewer reactive astrocytes in the injury area and more surviving neurons in the mettl14 knockout group compared to the control group (Wang et al., 2021). More importantly, further experiments also showed that overexpression of Mettl14 can induce apoptosis *in vitro*, as Mettl14 can promote the conversion of pri-miR-375 to miR-375, which is related to apoptosis and inhibits neural recovery (Wang et al., 2021). In addition, increased expression of METTL14 during SCI mediates the m6A modification of EEF1A2, which accelerates neuronal degeneration through the apoptotic pathway and impairs recovery after injury (Gao et al., 2022). EEF1A2 expression is reduced after SCI, while silencing of mettl14 increases EEF1A2 levels, decreases inflammatory cytokine production, and reduces neuronal degeneration in the spinal cord (Gao et al., 2022).

The above experiments show that the regulation of cell death after SCI, particularly neuronal apoptosis, is influenced by RNA m6A modification, providing a new direction for reducing cellular dysfunction and promoting functional recovery. However, apoptosis is not the only cause of cell loss after injury, and previous studies have shown that other forms of PCD, such as ferroptosis, autophagy, and necroptosis, also mediate cell death after SCI (Fan et al., 2016; Zhou et al., 2020; Feng et al., 2021; Shi et al., 2021). There have been multiple studies on the effect of m6A modification on PCD in different disorders (Yang et al., 2019; Lan et al., 2021; Shen et al., 2021); however, there has been no research on the relationship between m6A modification and other forms of PCD after SCI. Therefore, to properly elucidate the pathogenic mechanism of

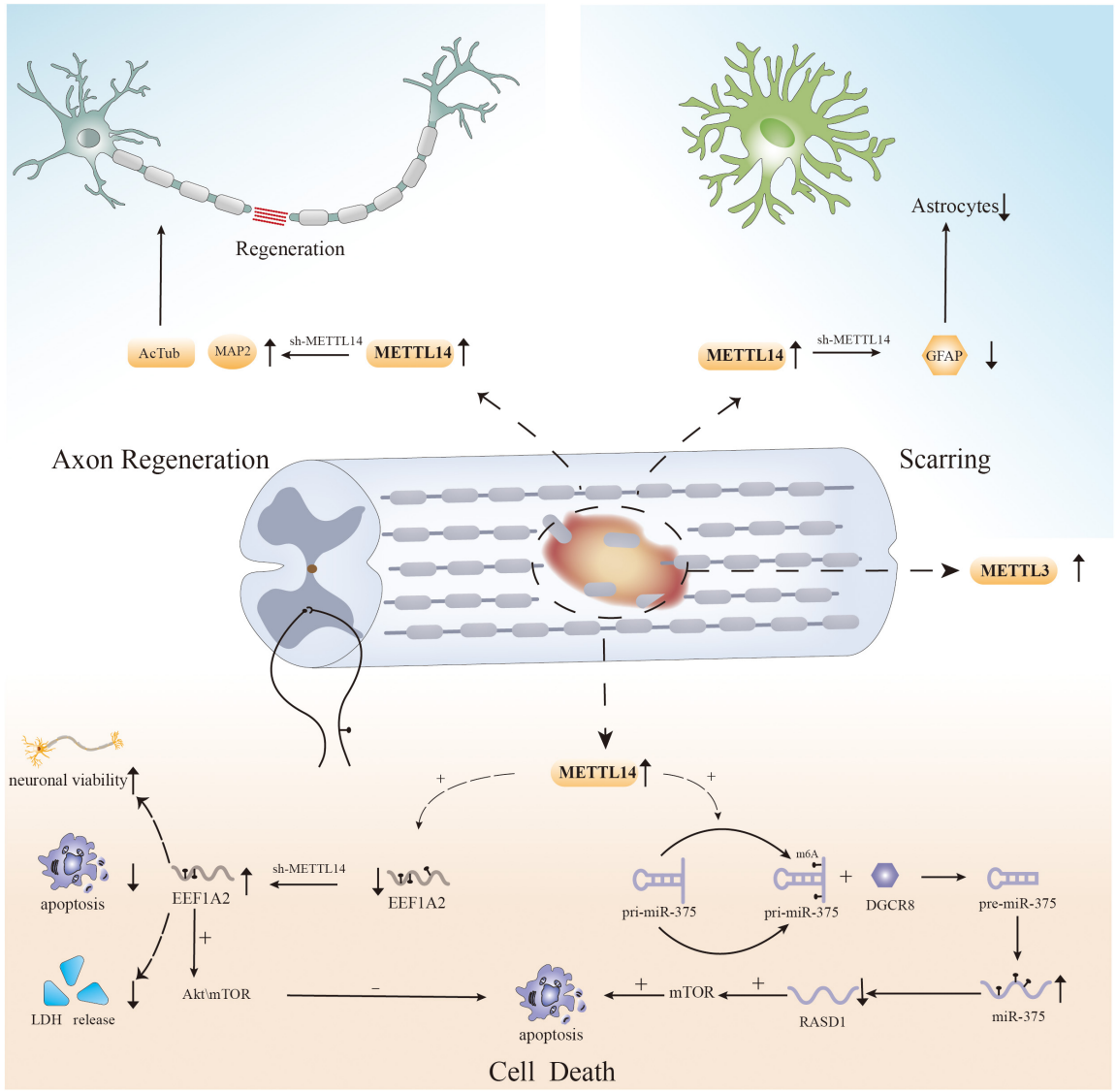

FIGURE 1
The role of m6A in spinal cord injury.

SCI, researchers must examine the role of m6A modification in other types of PCD after SCI.

N6-methyladenosine modification and axonal regeneration after spinal cord injury

Another cause of functional deficiency following SCI is the disruption of spinal nerve continuity (Ramer et al., 2014; Tran et al., 2018; Varadarajan et al., 2022). Unfortunately, compared to that of the peripheral nervous system, the axonal regeneration capacity of the central nervous system is extremely limited (Hutson and Di Giovanni, 2019; Avraham et al., 2021). Failure of regeneration results in permanent loss of neurological function. Although we have conducted in-depth research on the internal and external environment and regeneration mechanisms after axonal injury, complete axonal regeneration is difficult to achieve (Liu et al., 2011; Varadarajan et al., 2022). Studies have shown that changes related to gene expression can effectively regulate axonal regeneration, which involves physiological processes such as translation and transcription (Moore et al., 2009; Song et al., 2015; Mahar and Cavalli, 2018). Recent research on m6A modification also revealed that RNA modification can influence axonal regeneration, providing a solid theoretical basis for our ongoing research on axonal regeneration (Weng et al., 2018; Zhang et al., 2021; Qi et al., 2022).

In the nervous system, regeneration of neuronal axons is likewise affected by m6A modification. Following sciatic nerve damage, the levels of m6A-tagged transcripts associated with axonal regeneration are increased in mouse dorsal root neurons, facilitating axonal regeneration. Primary neurite length is considerably decreased *in vitro* when METTL14 is knocked out, as is the capacity to increase the axon length *in vivo*. In addition to that in the peripheral nervous system, Pten deletion-induced axonal regeneration in CNS neurons is considerably impeded following METTL14 loss. Furthermore, the YTHDF1 reader is required for injury-induced protein translation and axonal regeneration in neurons (Weng et al., 2018). Additionally, another study pointed out that FTO can reduce RNA m6A levels in axons and dynamically regulate local protein translation (Yu et al., 2018). After inhibition of intraneuronal axonal FTO expression by rhein, m6A levels are significantly decreased, and axonal elongation is inhibited (Yu et al., 2018). Interestingly, Mengru Zhuang's team discovered that the m6A-binding protein YTHDF1 recognizes transcripts and regulates the translation of Robo3.1, which is modified by m6A, provides axonal pathfinding guiding signals, and affects the guidance of crossing axons of spinal cord commissure neurons (Zhuang et al., 2019). In addition, YTHDF1 and YTHDF2 are highly expressed in cerebellar granule cell axons *in vitro* and *in vivo*, and knock out of these proteins might enhance axonal development (Yu et al., 2021). To govern neuronal axonal development, YTHDF1 and YTHDF2 synergistically regulate Wnt5a signaling, which is involved in axonal guidance and can influence axonal development (Yu et al., 2021).

Recently, m6A modification was shown to have the potential to regulate axonal regeneration after SCI (**Figure 1**). In an experiment on SCI in zebrafish and mice, MeRIP-seq and RNA-seq analysis of injured tissue after SCI revealed that RNAs that showed obvious differences in m6A levels, such as hsp90ab1, taf1, igf2bp1, and tp53, were associated with axonal growth and neuronal development (Xing et al., 2021). Simultaneously, the expression of METTL3 was found to be upregulated in local tissues in mouse and zebrafish SCI models, as well as in neural stem cell and astrocyte SCI models (Xing et al., 2021). This is the first study on the role of RNA m6A modification in SCI, and the results suggest that dynamic changes in the methylation of associated genes have an effect on axonal regeneration (Xing et al., 2021). In addition, specific knockout of METTL14 can significantly increase the expression of AcTub and MAP2 after SCI, which are two markers associated with axons whose expression is decreased after SCI. These findings indicate that METTL14 is involved in the regulation of axons after SCI (Wang et al., 2021). And another study found that METTL14 catalyzes the m6A methylation of EEF1A2 mRNA (Gao et al., 2022). Knockdown of mettl14 can increase the level of EEF1A2, and the opposite occurs after mettl14 overexpression (Gao et al., 2022). Moreover, the reduction in EEF1A2 expression after SCI inhibits the Akt/mTOR pathway, which previous studies have shown to affect pathway regeneration (Zhao Y. et al., 2021; Gao et al., 2022). Therefore, m6A modification may have an effect on nerve recovery. The results of the abovementioned experiments suggest that m6A modification could be a potential strategy for affecting axonal regeneration after SCI.

N6-methyladenosine modification and scarring after spinal cord injury

One of the secondary characteristics of SCI is the aggregation of a considerable number of reactive astrocytes, which always results in localized scarring (Hara et al., 2017). Spatially, scars can be used to isolate damaged tissue and prevent damage from spreading further (Tran et al., 2018). In addition to exerting a protective effect, scars inhibit nerve regeneration, which is closely related to the recovery of spinal cord function (Silver and Miller, 2004). Recently, research has shown that scar formation after injury does not necessarily hinder axonal regeneration but may actually promote recovery (Anderson et al., 2016). Compared to that of astrocytes, the role of pericytes in scar formation has received less attention. Pericytes are also crucial for the scarring process (Göritz et al., 2011; Dias et al., 2018). Therefore, research on scar formation from the perspective of m6A modification could open up a new field of research related to SCI.

N6-methyladenosine modification can regulate the physiological functions of astrocytes (Huang et al., 2020; Teng et al., 2021). In a study on major depressive disorder, it was verified that circSTAG1 can bind to the demethylase ALKBH5 in the mouse hippocampus, decreasing ALKBH5 levels to alter the m6A level of FAAH mRNA and limit FAAH expression (Huang et al., 2020). Ultimately, astrocyte dysfunction and astrocyte loss are reduced (Huang et al., 2020). Additionally, METTL14 knockdown reduces m6A levels in the substantia nigra, decreases TH expression, and enhances microglial and astrocyte survival (Teng et al., 2021).

Recently, several studies have shown that changes in m6A modification affect the aggregation of astrocytes following SCI (**Figure 1**; Wanner et al., 2013). Lingyan Xing et al. found that the expression of METTL3 in astrocytes increases dramatically after SCI, possibly affecting the activation and proliferation of cells (Xing et al., 2021). Although more research is needed, the results indicate a new direction for the study of astrocytes after SCI. Moreover, another study reported that GFAP expression was decreased and the number of astrocytes produced at the injury site was reduced in an SCI model with selective deletion of Mettl14 compared to the control group (Wang et al., 2021). Surprisingly, *in vitro*, lack of Mettl14 was shown to reduce the apoptosis of C8-D1A murine astrocytes after simulation of SCI-induced apoptosis with H2O2 (Wang et al., 2021). This implies that m6A modification is linked to astrocyte survival after SCI, which can alter scar formation. However, since there are only

few related studies, the relationship between m6A and astrocytes after SCI still needs to be further explored.

While astrocytes are involved in scarring postinjury, the role of pericytes in SCI cannot be ignored (Dias et al., 2018). Pericytes are involved in the establishment of the blood–brain barrier and the blood–spinal cord barrier, as well as the stability of the internal environment of the brain and spinal cord (Cheng et al., 2018; Sweeney et al., 2019). Previous studies have shown that pericytes are closely related to the formation of scars and the recovery of function after SCI (Dias et al., 2018; Hesp et al., 2018; Zhu et al., 2022). Some studies have confirmed that m6A modification in pericytes is involved in the occurrence and development of hypertension and diabetes (Wu Q. et al., 2019; Suo et al., 2022). For instance, Qingbin Wu et al. discovered that in pericytes, mRNAs undergo m6A modification in coding regions under hypertensive conditions. Subsequent GO and KEGG enrichment analyses revealed that the differentially expressed genes are linked to hypertension genes and pathways. This suggests that changes in m6A modification in pericytes play a role in the pathogenesis of vascular diseases such as hypertension (Wu Q. et al., 2019). Moreover, a recent study found that diabetes-induced pericyte dysfunction is associated with changes in RNA m6A levels, which are regulated by m6A-related enzymes and proteins (Suo et al., 2022). Selective METTL3 silencing can reduce YTHDF2-induced degradation of PKC, FAT4, and PDGFRA mRNA, reducing the occurrence of diabetes-induced vascular complications and pericyte dysfunction (Suo et al., 2022).

Future directions related to the role of N6-methyladenosine modification after spinal cord injury

In addition to the pathological processes mentioned above, the effects of local inflammation and myelination dysfunction on prognosis after SCI should not be ignored (Plemel et al., 2014; Zrzavy et al., 2021), and m6A modification is also likely to be involved in these effects. Microglia, which are key factors affecting inflammation after SCI, have two polarization states, the proinflammatory M1 phenotype and the anti-inflammatory M2 phenotype (Lan et al., 2017). After injuries such as stroke, cerebral hemorrhage, SCI, M1 polarization of microglia is often induced (Fan et al., 2018; Liao et al., 2020; Sun et al., 2020). While M1 microglia play a defensive role, they also aggravate neuroinflammation and nerve cell damage, affecting the recovery of nervous system function (Fan et al., 2018). Therefore, reducing the polarization of M1 glial cells or driving their conversion to the anti-inflammatory M2 phenotype can aid nerve recovery and lessen secondary damage (Liu W. et al., 2020). According to recent studies, m6A modification plays a critical role in glial phagocytosis and polarization (**Figure 2**; Li et al., 2021; Zhou et al., 2021; Chen et al., 2022). A study on uveitis found that deletion of the m6A reader YTHDC1 enhances the M1 polarization of microglia and accelerates inflammation (Zhou et al., 2021). Furthermore,

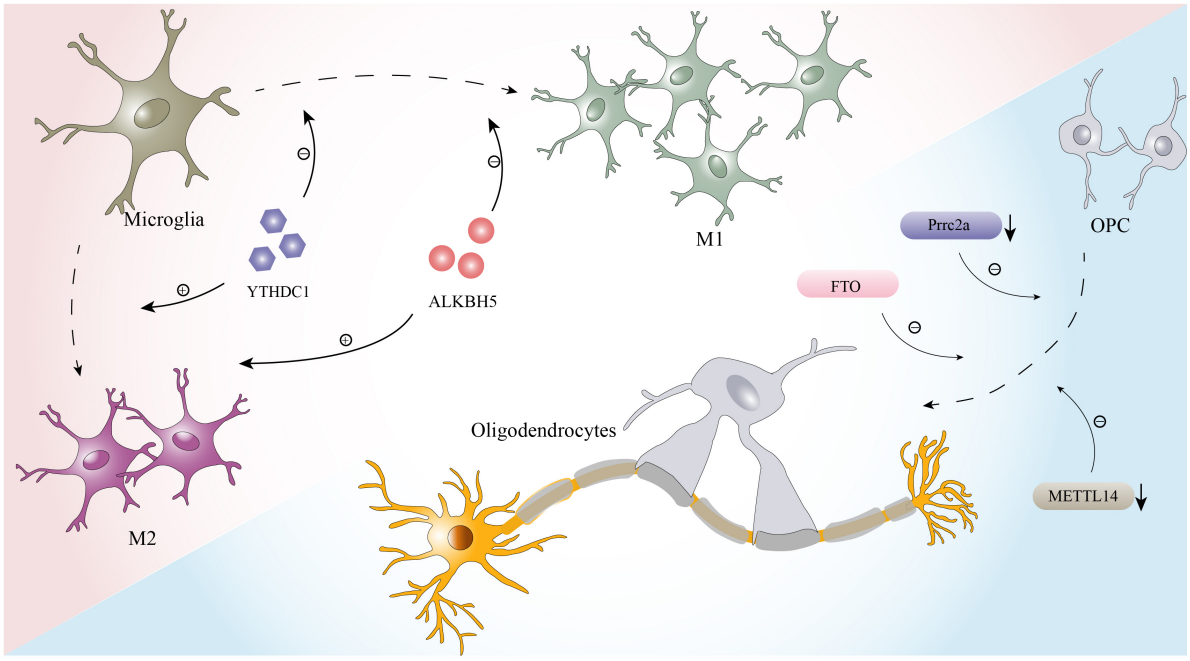

FIGURE 2
The effects of m6A on microglia and oligodendrocytes.

another bioinformatics study showed that m6A has a high potential to modulate the microglia-mediated inflammatory response. A large number of m6A-modified transcripts are among the genes that are differentially expressed between different subtypes of microglia (Li et al., 2021). Researchers have also observed that when microglia are active, m6A levels of the transcripts of many pro- and anti-inflammatory components are altered (Li et al., 2021).

Furthermore, oligodendrocytes, whose primary function is to form the myelin sheath of axons and contribute to the efficient and rapid transmission of information, are inextricably linked to myelin regeneration during the process of nerve repair after SCI (Bradl and Lassmann, 2010; Sankavaram et al., 2019). In recent years, it was proven that m6A modification plays a key role in the development and maturation of oligodendrocytes and maintains the normal function of oligodendrocytes (**Figure 2**; Wu R. et al., 2019; Xu et al., 2020). For example, Prrrc2a, a novel m6A "reader" identified by Wu R. et al. (2019) is strongly associated with oligodendrocyte formation and axonal myelination. When prrc2a is specifically knocked out, the proliferation and differentiation of OPCs are affected, and the number of mature oligodendrocytes is markedly reduced (Wu R. et al., 2019). Moreover, axons in the corpus callosum exhibit hypomyelination (Wu R. et al., 2019). Interestingly, Xu et al. (2020) performed RNA-seq and m6A-seq of OPCs and successfully induced the differentiation of OPCs from neonatal mice into oligodendrocytes. When METTL14 is inactivated by Cre-loxP, the number of mature oligodendrocytes in postnatal mice is significantly reduced, but the formation and proliferation of OPCs are not affected (Xu et al., 2020).

Conclusion

This review discusses in detail the current status of research on m6A modification and the relationship between m6A modification and pathophysiological processes after SCI, including cell death, axonal regeneration, and scarring. Although there has been research on the role of m6A modification in some neurological diseases, such as Alzheimer's disease and stroke, research on the role of this posttranslational modification in SCI is still in its infancy. Research on this topic is limited to bioinformatics analysis of gene expression and differential expression at the tissue and cell levels, and studies on the specific mechanism of m6A modification after SCI are extremely rare. Simultaneously, the only m6A modification-regulating molecules that have been studied after SCI are "writers," and more research on the impact of demethylases and binding proteins after SCI is needed. The importance of m6A modification in neurological diseases cannot be overstated. This dynamic modification could be a possible target for influencing the pathological process of SCI and promoting recovery of spinal cord function. Clearly, the role of m6A modification in SCI needs to be explored further.

Author contributions

DL, BF, and JL contributed the central idea and wrote the manuscript. JM and TS collected the related data. XZ and SF participated in key revisions of the manuscript and finalized the final version. All authors contributed to the revision of the manuscript and approved the submitted version.

Funding

This work was supported by National Natural Science Foundation of China (82102563) and the Tianjin Key Medical Discipline (Specialty) Construct Project (TJYXZDXK-027A).

Conflict of interest

The authors declare that the research was conducted in the absence of any commercial or financial relationships that could be construed as a potential conflict of interest.

Publisher's note

References

Ahuja, C. S., Wilson, J. R., Nori, S., Kotter, M. R. N., Druschel, C., Curt, A., et al. (2017). Traumatic spinal cord injury. *Nat. Rev. Dis. Primers* 3:17018. doi: 10.1038/nrdp.2017.18

Anderson, M. A., Burda, J. E., Ren, Y., Ao, Y., O'Shea, T. M., Kawaguchi, R., et al. (2016). Astrocyte scar formation aids central nervous system axon regeneration. *Nature* 532, 195–200. doi: 10.1038/nature17623

Anjum, A., Yazid, M. D., Fauzi Daud, M., Idris, J., Ng, A. M. H., Selvi Naicker, A., et al. (2020). Spinal cord injury: pathophysiology, multimolecular interactions, and underlying recovery mechanisms. *Int. J. Mol. Sci.* 21:7533. doi: 10.3390/ijms21207533

Avraham, O., Feng, R., Ewan, E. E., Rustenhoven, J., Zhao, G., and Cavalli, V. (2021). Profiling sensory neuron microenvironment after peripheral and central

axon injury reveals key pathways for neural repair. *ELife* 10:e68457. doi: 10.7554/eLife.68457

Bokar, J. A., Shambaugh, M. E., Polayes, D., Matera, A. G., and Rottman, F. M. (1997). Purification and cDNA cloning of the AdoMet-binding subunit of the human mRNA (N6-adenosine)-methyltransferase. *RNA* 3, 1233–1247.

Bradl, M., and Lassmann, H. (2010). Oligodendrocytes: biology and pathology. *Acta Neuropathol.* 119, 37–53.

Chen, T., Zhu, W., Wang, C., Dong, X., Yu, F., Su, Y., et al. (2022). ALKBH5-Mediated mA Modification of A20 Regulates Microglia Polarization in Diabetic Retinopathy. *Front. Immunol.* 13:813979. doi: 10.3389/fimmu.2022.813979

Cheng, J., Korte, N., Nortley, R., Sethi, H., Tang, Y., and Attwell, D. (2018). Targeting pericytes for therapeutic approaches to neurological disorders. *Acta Neuropathol.* 136, 507–523. doi: 10.1007/s00401-018-1893-0

Cheng, P., Han, H., Chen, F., Cheng, L., Ma, C., Huang, H., et al. (2021). Amelioration of acute myocardial infarction injury through targeted ferritin nanocages loaded with an ALKBH5 inhibitor. *Acta Biomater* 140, 481–491. doi: 10.1016/j.actbio.2021.11.041

Cho, S., Lee, G., Pickering, B. F., Jang, C., Park, J. H., He, L., et al. (2021). mTORC1 promotes cell growth via mA-dependent mRNA degradation. *Mol. Cell* 81, 2064–2075. doi: 10.1016/j.molcel.2021.03.010

Coker, H., Wei, G., and Brockdorff, N. (2019). m6A modification of non-coding RNA and the control of mammalian gene expression. *Biochim. Biophys. Acta. Gene Regul. Mech.* 1862, 310–318. doi: 10.1016/j.bbagrm.2018.12.002

Covelo-Molares, H., Obrdlik, A., Poštulková, I., Dohnálková, M., Gregorová, P., Ganji, R., et al. (2021). The comprehensive interactomes of human adenosine RNA methyltransferases and demethylases reveal distinct functional and regulatory features. *Nucleic Acids Res.* 49, 10895–10910. doi: 10.1093/nar/gkab900

Desrosiers, R., Friderici, K., and Rottman, F. (1974). Identification of methylated nucleosides in messenger RNA from Novikoff hepatoma cells. *Proc. Natl. Acad. Sci. U.S.A.* 71, 3971–3975.

Dias, D. O., Kim, H., Holl, D., Werne Solnestam, B., Lundeberg, J., Carlén, M., et al. (2018). Reducing pericyte-derived scarring promotes recovery after spinal cord injury. *Cell* 173, 153–165. doi: 10.1016/j.cell.2018.02.004

Dominissini, D., Moshitch-Moshkovitz, S., Schwartz, S., Salmon-Divon, M., Ungar, L., Osenberg, S., et al. (2012). Topology of the human and mouse m6A RNA methylomes revealed by m6A-seq. *Nature* 485, 201–206. doi: 10.1038/nature11112

Dong, F., Qin, X., Wang, B., Li, Q., Hu, J., Cheng, X., et al. (2021). ALKBH5 Facilitates Hypoxia-Induced Paraspeckle Assembly and IL8 Secretion to Generate an Immunosuppressive Tumor Microenvironment. *Cancer Res.* 81, 5876–5888. doi: 10.1158/0008-5472.Can-21-1456

Du, H., Zhao, Y., He, J., Zhang, Y., Xi, H., Liu, M., et al. (2016). YTHDF2 destabilizes m(6)A-containing RNA through direct recruitment of the CCR4-NOT deadenylase complex. *Nat. Commun.* 7:12626. doi: 10.1038/ncomms12626

Fan, B., Wei, Z., Yao, X., Shi, G., Cheng, X., Zhou, X., et al. (2018). Microenvironment imbalance of spinal cord injury. *Cell Transplant.* 27, 853–866. doi: 10.1177/0963689718755778

Fan, H., Zhang, K., Shan, L., Kuang, F., Chen, K., Zhu, K., et al. (2016). Reactive astrocytes undergo M1 microglia/macrohpages-induced necroptosis in spinal cord injury. *Mol. Neurodegener.* 11:14. doi: 10.1186/s13024-016-0081-8

Feng, Z., Min, L., Chen, H., Deng, W., Tan, M., Liu, H., et al. (2021). Iron overload in the motor cortex induces neuronal ferroptosis following spinal cord injury. *Redox Biol.* 43:101984. doi: 10.1016/j.redox.2021.101984

Fischer, J., Koch, L., Emmerling, C., Vierkotten, J., Peters, T., Brüning, J. C., et al. (2009). Inactivation of the Fto gene protects from obesity. *Nature* 458, 894–898.

Fricker, M., Tolkovsky, A. M., Borutaite, V., Coleman, M., and Brown, G. C. (2018). Neuronal Cell Death. *Physiol. Rev.* 98, 813–880.

Gao, G., Duan, Y., Chang, F., Zhang, T., Huang, X., and Yu, C. (2022). METTL14 promotes apoptosis of spinal cord neurons by inducing EEF1A2 m6A methylation in spinal cord injury. *Cell Death Discov.* 8:15. doi: 10.1038/s41420-021-00808-2

Göritz, C., Dias, D. O., Tomilin, N., Barbacid, M., Shupliakov, O., and Frisén, J. (2011). A pericyte origin of spinal cord scar tissue. *Science* 333, 238–242. doi: 10.1126/science.1203165

Hara, M., Kobayakawa, K., Ohkawa, Y., Kumamaru, H., Yokota, K., Saito, T., et al. (2017). Interaction of reactive astrocytes with type I collagen induces astrocytic scar formation through the integrin-N-cadherin pathway after spinal cord injury. *Nat. Med.* 23, 818–828. doi: 10.1038/nm.4354

Harper, J. E., Miceli, S. M., Roberts, R. J., and Manley, J. L. (1990). Sequence specificity of the human mRNA N6-adenosine methylase in vitro. *Nucl. Acids Res.* 18, 5735–5741.

Hesp, Z. C., Yoseph, R. Y., Suzuki, R., Jukkola, P., Wilson, C., Nishiyama, A., et al. (2018). Proliferating NG2-Cell-dependent angiogenesis and scar formation alter axon growth and functional recovery after spinal cord injury in mice. *J. Neurosci.* 38, 1366–1382. doi: 10.1523/JNEUROSCI.3953-16.2017

Hsu, P. J., Zhu, Y., Ma, H., Guo, Y., Shi, X., Liu, Y., et al. (2017). Ythdc2 is an N(6)-methyladenosine binding protein that regulates mammalian spermatogenesis. *Cell Res.* 27, 1115–1127. doi: 10.1038/cr.2017.99

Huang, H., Weng, H., Sun, W., Qin, X., Shi, H., Wu, H., et al. (2018). Recognition of RNA N-methyladenosine by IGF2BP proteins enhances mRNA stability and translation. *Nat. Cell Biol.* 20, 285–295.

Huang, R., Zhang, Y., Bai, Y., Han, B., Ju, M., Chen, B., et al. (2020). N-Methyladenosine Modification of Fatty Acid Amide Hydrolase Messenger RNA in Circular RNA STAG1-Regulated Astrocyte Dysfunction and Depressive-like Behaviors. *Biol. Psychiatry* 88, 392–404. doi: 10.1016/j.biopsych.2020.02.018

Hutson, T. H., and Di Giovanni, S. (2019). The translational landscape in spinal cord injury: focus on neuroplasticity and regeneration. *Nat. Rev. Neurol.* 15, 732–745. doi: 10.1038/s41582-019-0280-3

Ignatova, V. V., Stolz, P., Kaiser, S., Gustafsson, T. H., Lastres, P. R., Sanz-Moreno, A., et al. (2020). The rRNA m(6)A methyltransferase METTL5 is involved in pluripotency and developmental programs. *Genes Dev.* 34, 715–729. doi: 10.1101/gad.333369.119

Jia, G., Fu, Y., Zhao, X., Dai, Q., Zheng, G., Yang, Y., et al. (2011). N6-methyladenosine in nuclear RNA is a major substrate of the obesity-associated FTO. *Nat. Chem. Biol.* 7, 885–887. doi: 10.1038/nchembio.687

Lan, H., Liu, Y., Liu, J., Wang, X., Guan, Z., Du, J., et al. (2021). Tumor-Associated Macrophages Promote Oxaliplatin Resistance METTL3-Mediated mA of TRAF5 and Necroptosis in Colorectal Cancer. *Mol. Pharm.* 18, 1026–1037. doi: 10.1021/acs.molpharmaceut.0c00961

Lan, X., Han, X., Li, Q., Yang, Q.-W., and Wang, J. (2017). Modulators of microglial activation and polarization after intracerebral haemorrhage. *Nat. Rev. Neurol.* 13, 420–433.

Li, L., Zang, L., Zhang, F., Chen, J., Shen, H., Shu, L., et al. (2017). Fat mass and obesity-associated (FTO) protein regulates adult neurogenesis. *Hum. Mol. Genet.* 26, 2398–2411.

Li, Q., Wen, S., Ye, W., Zhao, S., and Liu, X. (2021). The potential roles of mA modification in regulating the inflammatory response in microglia. *J. Neuroinflamm.* 18:149. doi: 10.1186/s12974-021-02205-z

Li, Y., Guo, X., Sun, L., Xiao, J., Su, S., Du, S., et al. (2020). N-Methyladenosine Demethylase FTO Contributes to Neuropathic Pain by Stabilizing G9a Expression in Primary Sensory Neurons. *Adv. Sci.* 7:1902402. doi: 10.1002/advs.201902402

Liao, S., Wu, J., Liu, R., Wang, S., Luo, J., Yang, Y., et al. (2020). A novel compound DBZ ameliorates neuroinflammation in LPS-stimulated microglia and ischemic stroke rats: Role of Akt(Ser473)/GSK3β(Ser9)-mediated Nrf2 activation. *Redox Biol.* 36:101644. doi: 10.1016/j.redox.2020.101644

Liu, J., Dou, X., Chen, C., Chen, C., Liu, C., Xu, M. M., et al. (2020). -methyladenosine of chromosome-associated regulatory RNA regulates chromatin state and transcription. *Science* 367, 580–586.

Liu, J., Yue, Y., Han, D., Wang, X., Fu, Y., Zhang, L., et al. (2014). A METTL3-METTL14 complex mediates mammalian nuclear RNA N6-adenosine methylation. *Nat. Chem. Biol.* 10, 93–95. doi: 10.1038/nchembio.1432

Liu, K., Tedeschi, A., Park, K. K., and He, Z. (2011). Neuronal intrinsic mechanisms of axon regeneration. *Ann. Rev. Neurosci.* 34, 131–152. doi: 10.1146/annurev-neuro-061010-113723

Liu, L., Li, H., Hu, D., Wang, Y., Shao, W., Zhong, J., et al. (2022). Insights into N6-methyladenosine and programmed cell death in cancer. *Mol. Cancer* 21:32.

Liu, N., Dai, Q., Zheng, G., He, C., Parisien, M., and Pan, T. (2015). N(6)-methyladenosine-dependent RNA structural switches regulate RNA-protein interactions. *Nature* 518, 560–564. doi: 10.1038/nature14234

Liu, W., Rong, Y., Wang, J., Zhou, Z., Ge, X., Ji, C., et al. (2020). Exosome-shuttled miR-216a-5p from hypoxic preconditioned mesenchymal stem cells repair traumatic spinal cord injury by shifting microglial M1/M2 polarization. *J. Neuroinflamm.* 17:47. doi: 10.1186/s12974-020-1726-7

Ma, C., Chang, M., Lv, H., Zhang, Z.-W., Zhang, W., He, X., et al. (2018). RNA mA methylation participates in regulation of postnatal development of the mouse cerebellum. *Genome Biol.* 19:68.

Ma, H., Wang, X., Cai, J., Dai, Q., Natchiar, S. K., Lv, R., et al. (2019). N(6-)Methyladenosine methyltransferase ZCCHC4 mediates ribosomal RNA methylation. *Nat. Chem. Biol.* 15, 88–94.

Mahar, M., and Cavalli, V. (2018). Intrinsic mechanisms of neuronal axon regeneration. *Nat. Rev. Neurosci.* 19, 323–337.

McDonald, J. W., and Sadowsky, C. (2002). Spinal-cord injury. *Lancet* 359, 417–425.

Mendel, M., Delaney, K., Pandey, R. R., Chen, K.-M., Wenda, J. M., Vågbø, C. B., et al. (2021). Splice site mA methylation prevents binding of U2AF35 to inhibit RNA splicing. *Cell* 184, 3125–3142. doi: 10.1016/j.cell.2021.03.062

Meyer, K. D., Patil, D. P., Zhou, J., Zinoviev, A., Skabkin, M. A., Elemento, O., et al. (2015). 5′ UTR m(6)A Promotes Cap-Independent Translation. *Cell* 163, 999–1010. doi: 10.1016/j.cell.2015.10.012

Meyer, K. D., Saletore, Y., Zumbo, P., Elemento, O., Mason, C. E., and Jaffrey, S. R. (2012). Comprehensive analysis of mRNA methylation reveals enrichment in 3′ UTRs and near stop codons. *Cell* 149, 1635–1646. doi: 10.1016/j.cell.2012.05.003

Moore, D. L., Blackmore, M. G., Hu, Y., Kaestner, K. H., Bixby, J. L., Lemmon, V. P., et al. (2009). KLF family members regulate intrinsic axon regeneration ability. *Science* 326, 298–301. doi: 10.1126/science.1175737

National SCI Statistical Center [NSCISC] (2016). Spinal cord injury (SCI) 2016 facts and figures at a glance. *J. Spinal Cord Med.* 39, 493–494. doi: 10.1080/10790268.2016.1210925

Oerum, S., Meynier, V., Catala, M., and Tisné, C. (2021). A comprehensive review of m6A/m6Am RNA methyltransferase structures. *Nucl. Acids Res.* 49, 7239–7255. doi: 10.1093/nar/gkab378

Park, O. H., Ha, H., Lee, Y., Boo, S. H., Kwon, D. H., Song, H. K., et al. (2019). Endoribonucleolytic Cleavage of m(6)A-Containing RNAs by RNase P/MRP Complex. *Mol. Cell* 74, 494–507.

Pendleton, K. E., Chen, B., Liu, K., Hunter, O. V., Xie, Y., Tu, B. P., et al. (2017). The U6 snRNA m(6)A Methyltransferase METTL16 Regulates SAM Synthetase Intron Retention. *Cell* 169, 824–835. doi: 10.1016/j.cell.2017.05.003

Ping, X.-L., Sun, B.-F., Wang, L., Xiao, W., Yang, X., Wang, W.-J., et al. (2014). Mammalian WTAP is a regulatory subunit of the RNA N6-methyladenosine methyltransferase. *Cell Res.* 24, 177–189. doi: 10.1038/cr.2014.3

Plemel, J. R., Keough, M. B., Duncan, G. J., Sparling, J. S., Yong, V. W., Stys, P. K., et al. (2014). Remyelination after spinal cord injury: is it a target for repair? *Prog. Neurobiol.* 117, 54–72.

Qi, Z., Wang, S., Li, J., Wen, Y., Cui, R., Zhang, K., et al. (2022). Protective role of mRNA demethylase FTO on axon guidance molecules of nigro-striatal projection system in manganese-induced parkinsonism. *J. Hazard. Mater.* 426:128099. doi: 10.1016/j.jhazmat.2021.128099

Ramer, L. M., Ramer, M. S., and Bradbury, E. J. (2014). Restoring function after spinal cord injury: towards clinical translation of experimental strategies. *Lancet. Neurol.* 13, 1241–1256. doi: 10.1016/S1474-4422(14)70144-9

Roundtree, I. A., Evans, M. E., Pan, T., and He, C. (2017a). Dynamic RNA modifications in gene expression regulation. *Cell* 169, 1187–1200. doi: 10.1016/j.cell.2017.05.045

Roundtree, I. A., Luo, G.-Z., Zhang, Z., Wang, X., Zhou, T., Cui, Y., et al. (2017b). YTHDC1 mediates nuclear export of N-methyladenosine methylated mRNAs. *ELife* 6:e31311. doi: 10.7554/eLife.31311

Sankavaram, S. R., Hakim, R., Covacu, R., Frostell, A., Neumann, S., Svensson, M., et al. (2019). Adult neural progenitor cells transplanted into spinal cord injury differentiate into oligodendrocytes, enhance myelination, and contribute to recovery. *Stem Cell Rep.* 12, 950–966.

Satterwhite, E. R., and Mansfield, K. D. (2022). RNA methyltransferase METTL16: Targets and function. *Wiley Interdiscip. Rev. RNA* 13:e1681. doi: 10.1002/wrna.1681

Shen, M., Li, Y., Wang, Y., Shao, J., Zhang, F., Yin, G., et al. (2021). N-methyladenosine modification regulates ferroptosis through autophagy signaling pathway in hepatic stellate cells. *Redox Biol.* 47:102151. doi: :10.1016/j.redox.2021.102151

Shi, H., Wang, X., Lu, Z., Zhao, B. S., Ma, H., Hsu, P. J., et al. (2017). YTHDF3 facilitates translation and decay of N-methyladenosine-modified RNA. *Cell Res.* 27, 315–328. doi: 10.1038/cr.2017.15

Shi, Z., Yuan, S., Shi, L., Li, J., Ning, G., Kong, X., et al. (2021). Programmed cell death in spinal cord injury pathogenesis and therapy. *Cell Prolif.* 54:e12992.

Silver, J., and Miller, J. H. (2004). Regeneration beyond the glial scar. *Nat. Rev. Neurosci.* 5, 146–156.

Song, Y., Sretavan, D., Salegio, E. A., Berg, J., Huang, X., Cheng, T., et al. (2015). Regulation of axon regeneration by the RNA repair and splicing pathway. *Nat. Neurosci.* 18, 817–825.

Sousa, A. M. M., Meyer, K. A., Santpere, G., Gulden, F. O., and Sestan, N. (2017). Evolution of the human nervous system function, structure, and development. *Cell* 170, 226–247.

Su, R., Dong, L., Li, Y., Gao, M., He, P. C., Liu, W., et al. (2022). METTL16 exerts an mA-independent function to facilitate translation and tumorigenesis. *Nat. Cell Biol.* 24, 205–216. doi: 10.1038/s41556-021-00835-2

Sun, Z., Wu, K., Gu, L., Huang, L., Zhuge, Q., Yang, S., et al. (2020). IGF-1R stimulation alters microglial polarization via TLR4/NF-κB pathway after cerebral hemorrhage in mice. *Brain Res. Bull.* 164, 221–234. doi: 10.1016/j.brainresbull.2020.08.026

Suo, L., Liu, C., Zhang, Q.-Y., Yao, M.-D., Ma, Y., Yao, J., et al. (2022). METTL3-mediated -methyladenosine modification governs pericyte dysfunction during diabetes-induced retinal vascular complication. *Theranostics* 12, 277–289. doi: 10.7150/thno.63441

Sweeney, M. D., Zhao, Z., Montagne, A., Nelson, A. R., and Zlokovic, B. V. (2019). Blood-Brain barrier: from physiology to disease and back. *Physiol. Rev.* 99, 21–78. doi: 10.1152/physrev.00050.2017

Tator, C. H. (1995). Update on the pathophysiology and pathology of acute spinal cord injury. *Brain Pathol.* 5, 407–413.

Teng, Y., Liu, Z., Chen, X., Liu, Y., Geng, F., Le, W., et al. (2021). Conditional deficiency of m6A methyltransferase Mettl14 in substantia nigra alters dopaminergic neuron function. *J. Cell. Mol. Med.* 25, 8567–8572. doi: 10.1111/jcmm.16740

Tran, A. P., Warren, P. M., and Silver, J. (2018). The biology of regeneration failure and success after spinal cord injury. *Physiol. Rev.* 98, 881–917. doi: 10.1152/physrev.00017.2017

Varadarajan, S. G., Hunyara, J. L., Hamilton, N. R., Kolodkin, A. L., and Huberman, A. D. (2022). Central nervous system regeneration. *Cell* 185, 77–94. doi: 10.1016/j.cell.2021.10.029

Venkatesh, K., Ghosh, S. K., Mullick, M., Manivasagam, G., and Sen, D. (2019). Spinal cord injury: pathophysiology, treatment strategies, associated challenges, and future implications. *Cell Tissue Res.* 377, 125–151. doi: 10.1007/s00441-019-03039-1

Walters, B. J., Mercaldo, V., Gillon, C. J., Yip, M., Neve, R. L., Boyce, F. M., et al. (2017). The Role of The RNA Demethylase FTO (Fat Mass and Obesity-Associated) and mRNA Methylation in Hippocampal Memory Formation. *Neuropsychopharmacology* 42, 1502–1510. doi: 10.1038/npp.2017.31

Wang, C.-X., Cui, G.-S., Liu, X., Xu, K., Wang, M., Zhang, X.-X., et al. (2018). METTL3-mediated m6A modification is required for cerebellar development. *PLoS Biol.* 16:e2004880. doi: 10.1371/journal.pbio.2004880

Wang, H., Yuan, J., Dang, X., Shi, Z., Ban, W., and Ma, D. (2021). Mettl14-mediated m6A modification modulates neuron apoptosis during the repair of spinal cord injury by regulating the transformation from pri-mir-375 to miR-375. *Cell Biosci.* 11:52. doi: 10.1186/s13578-020-00526-9

Wang, X., Feng, J., Xue, Y., Guan, Z., Zhang, D., Liu, Z., et al. (2016). Structural basis of N(6)-adenosine methylation by the METTL3-METTL14 complex. *Nature* 534, 575–578. doi: 10.1038/nature18298

Wang, X., Lu, Z., Gomez, A., Hon, G. C., Yue, Y., Han, D., et al. (2014). N6-methyladenosine-dependent regulation of messenger RNA stability. *Nature* 505, 117–120. doi: 10.1038/nature12730

Wang, X., Wu, R., Liu, Y., Zhao, Y., Bi, Z., Yao, Y., et al. (2020). m 6 A mRNA methylation controls autophagy and adipogenesis by targeting Atg5 and Atg7. *Autophagy* 16, 1221–1235. doi: 10.1080/15548627.2019.1659617

Wang, X., Zhao, B. S., Roundtree, I. A., Lu, Z., Han, D., Ma, H., et al. (2015). N(6)-methyladenosine Modulates Messenger RNA Translation Efficiency. *Cell* 161, 1388–1399. doi: 10.1016/j.cell.2015.05.014

Wang, Y., and Jia, G. (2020). Detection methods of epitranscriptomic mark N6-methyladenosine. *Essays Biochem.* 64, 967–979.

Wanner, I. B., Anderson, M. A., Song, B., Levine, J., Fernandez, A., Gray-Thompson, Z., et al. (2013). Glial scar borders are formed by newly proliferated, elongated astrocytes that interact to corral inflammatory and fibrotic cells via STAT3-dependent mechanisms after spinal cord injury. *J. Neurosci.* 33, 12870–12886. doi: 10.1523/JNEUROSCI.2121-13.2013

Warda, A. S., Kretschmer, J., Hackert, P., Lenz, C., Urlaub, H., Höbartner, C., et al. (2017). Human METTL16 is a N(6)-methyladenosine (m(6)A) methyltransferase that targets pre-mRNAs and various non-coding RNAs. *EMBO Rep.* 18, 2004–2014. doi: 10.15252/embr.201744940

Weng, Y.-L., Wang, X., An, R., Cassin, J., Vissers, C., Liu, Y., et al. (2018). Epitranscriptomic mA regulation of axon regeneration in the adult mammalian nervous system. *Neuron* 97, 313–325. doi: 10.1016/j.neuron.2017.12.036

Wu, Q., Yuan, X., Han, R., Zhang, H., and Xiu, R. (2019). Epitranscriptomic mechanisms of N6-methyladenosine methylation regulating mammalian hypertension development by determined spontaneously hypertensive rats pericytes. *Epigenomics* 11, 1359–1370. doi: 10.2217/epi-2019-0148

Wu, R., Li, A., Sun, B., Sun, J.-G., Zhang, J., Zhang, T., et al. (2019). A novel mA reader Prrc2a controls oligodendroglial specification and myelination. *Cell Res.* 29, 23–41. doi: 10.1038/s41422-018-0113-8

Xiao, W., Adhikari, S., Dahal, U., Chen, Y. S., Hao, Y. J., Sun, B. F., et al. (2016). Nuclear m(6)A Reader YTHDC1 Regulates mRNA Splicing. *Mol. Cell* 61, 507–519. doi: 10.1016/j.molcel.2016.01.012

Xing, L., Cai, Y., Yang, T., Yu, W., Gao, M., Chai, R., et al. (2021). Epitranscriptomic m6A regulation following spinal cord injury. *J. Neurosci. Res.* 99, 843–857. doi: 10.1002/jnr.24763

Xu, H., Dzhashiashvili, Y., Shah, A., Kunjamma, R. B., Weng, Y.-L., Elbaz, B., et al. (2020). mA mRNA methylation is essential for oligodendrocyte maturation and cns myelination. *Neuron* 105, 293–309. doi: 10.1016/j.neuron.2019.12.013

Yang, S., Wei, J., Cui, Y.-H., Park, G., Shah, P., Deng, Y., et al. (2019). mA mRNA demethylase FTO regulates melanoma tumorigenicity and response to anti-PD-1 blockade. *Nat. Commun.* 10:2782. doi: 10.1038/s41467-019-10669-0

Yang, Y., Huang, G., Jiang, X., Li, X., Sun, K., Shi, Y., et al. (2022). Loss of Wtap results in cerebellar ataxia and degeneration of Purkinje cells. *J. Genet. Genomics* *, doi: 10.1016/j.jgg.2022.03.001

Yoon, K.-J., Ringeling, F. R., Vissers, C., Jacob, F., Pokrass, M., Jimenez-Cyrus, D., et al. (2017). Temporal control of mammalian cortical neurogenesis by ma methylation. *Cell* 171, 877–889. doi: 10.1016/j.cell.2017.09.003

Yu, J., Chen, M., Huang, H., Zhu, J., Song, H., Zhu, J., et al. (2018). Dynamic m6A modification regulates local translation of mRNA in axons. *Nucl. Acids Res.* 46, 1412–1423. doi: 10.1093/nar/gkx1182

Yu, J., She, Y., Yang, L., Zhuang, M., Han, P., Liu, J., et al. (2021). The m A Readers YTHDF1 and YTHDF2 Synergistically Control Cerebellar Parallel Fiber Growth by Regulating Local Translation of the Key Wnt5a Signaling Components in Axons. *Adv. Sci.* 8:e2101329. doi: 10.1002/advs.202101329

Zaccara, S., and Jaffrey, S. R. (2020). A Unified Model for the Function of YTHDF Proteins in Regulating mA-Modified mRNA. *Cell* 181, 1582–1595. doi: 10.1016/j.cell.2020.05.012

Zaccara, S., Ries, R. J., and Jaffrey, S. R. (2019). Reading, writing and erasing mRNA methylation. *Nat. Rev. Mol Cell Biol.* 20, 608–624. doi: 10.1038/s41580-019-0168-5

Zhang, L., Hao, D., Ma, P., Ma, B., Qin, J., Tian, G., et al. (2021). Epitranscriptomic Analysis of m6A Methylome After Peripheral Nerve Injury. *Front. Genet.* 12:686000. doi: 10.3389/fgene.2021.686000

Zhang, Z., Wang, Q., Zhao, X., Shao, L., Liu, G., Zheng, X., et al. (2020). YTHDC1 mitigates ischemic stroke by promoting Akt phosphorylation through destabilizing PTEN mRNA. *Cell Death Dis.* 11:977. doi: 10.1038/s41419-020-03186-2

Zhao, B. S., Roundtree, I. A., and He, C. (2017). Post-transcriptional gene regulation by mRNA modifications. Nature Reviews. *Mol. Cell Biol.* 18, 31–42. doi: 10.1038/nrm.2016.132

Zhao, F., Xu, Y., Gao, S., Qin, L., Austria, Q., Siedlak, S. L., et al. (2021). METTL3-dependent RNA mA dysregulation contributes to neurodegeneration in Alzheimer's disease through aberrant cell cycle events. *Mol. Neurodegener.* 16:70. doi: 10.1186/s13024-021-00484-x

Zhao, Y., Wang, Q., Xie, C., Cai, Y., Chen, X., Hou, Y., et al. (2021). Peptide ligands targeting FGF receptors promote recovery from dorsal root crush injury via AKT/mTOR signaling. *Theranostics* 11, 10125–10147. doi: 10.7150/thno.62525

Zheng, G., Dahl, J. A., Niu, Y., Fedorcsak, P., Huang, C.-M., Li, C. J., et al. (2013). ALKBH5 is a mammalian RNA demethylase that impacts RNA metabolism and mouse fertility. *Mol. Cell* 49, 18–29. doi: 10.1016/j.molcel.2012.10.015

Zhou, H., Xu, Z., Liao, X., Tang, S., Li, N., and Hou, S. (2021). Low Expression of YTH Domain-Containing 1 Promotes Microglial M1 Polarization by Reducing the Stability of Sirtuin 1 mRNA. *Front. Cell. Neurosci.* 15:774305. doi: 10.3389/fncel.2021.774305

Zhou, K., Zheng, Z., Li, Y., Han, W., Zhang, J., Mao, Y., et al. (2020). TFE3, a potential therapeutic target for Spinal Cord Injury via augmenting autophagy flux and alleviating ER stress. *Theranostics* 10, 9280–9302. doi: 10.7150/thno.46566

Zhu, S., Chen, M., Ying, Y., Wu, Q., Huang, Z., Ni, W., et al. (2022). Versatile subtypes of pericytes and their roles in spinal cord injury repair, bone development and repair. *Bone Res.* 10:30. doi: 10.1038/s41413-022-00203-2

Zhuang, M., Li, X., Zhu, J., Zhang, J., Niu, F., Liang, F., et al. (2019). The m6A reader YTHDF1 regulates axon guidance through translational control of Robo3.1 expression. *Nucl. Acids Res.* 47, 4765–4777. doi: 10.1093/nar/gkz157

Zrzavy, T., Schwaiger, C., Wimmer, I., Berger, T., Bauer, J., Butovsky, O., et al. (2021). Acute and non-resolving inflammation associate with oxidative injury after human spinal cord injury. *Brain* 144, 144–161. doi: 10.1093/brain/awaa360

frontiers | Frontiers in Cellular Neuroscience

TYPE Original Research
PUBLISHED 10 November 2022
DOI 10.3389/fncel.2022.998512

OPEN ACCESS

EDITED BY
Feng Zhang,
The Third Hospital of Hebei Medical University, China

REVIEWED BY
Hung Wen Lin,
Ochsner LSU Health, United States
Sanaz Nasoohi,
Shahid Beheshti University of Medical Sciences, Iran

*CORRESPONDENCE
Xingliang Liu
liuxingliang2022@163.com

SPECIALTY SECTION
This article was submitted to Cellular Neuropathology, a section of the journal Frontiers in Cellular Neuroscience

RECEIVED 08 August 2022
ACCEPTED 18 October 2022
PUBLISHED 10 November 2022

CITATION
Liu X, Bai M, Fan L and Lou Z (2022) Serum 4-hydroxynonenal associates with the recurrence of patients with primary cerebral infarction. *Front. Cell. Neurosci.* 16:998512. doi: 10.3389/fncel.2022.998512

Serum 4-hydroxynonenal associates with the recurrence of patients with primary cerebral infarction

Xingliang Liu[1]*, Meiling Bai[2], Lei Fan[1] and Zhan Lou[1]

[1]Department of Neurology, The First Affiliated Hospital of Hebei North University, Zhangjiakou, China, [2]Hebei North University, Zhangjiakou, China

Background: 4-Hydroxynonenal (4-HNE), an α, β-unsaturated hydroxyalkenal, has been found to be associated with aspirin resistance, which is a risk factor for recurrent cerebral infarction. However, its effect on recurrent cerebral infarction is less defined. We designed this study to investigate the association between 4-HNE and increased risk of recurrent cerebral infarction.

Methods: We recruited 189 patients with primary cerebral infarction from 2017 to 2019. According to the recurrence of cerebral infarction during the 3-year follow-up period, they were divided into two groups, namely, the non-recurrence group (n = 93) and the recurrence group (n = 96). All patients were analyzed to explore the risk factors for the recurrence of primary cerebral infarction and the predictive value of serum 4-HNE for the recurrence of cerebral infarction.

Results: The levels of serum 4-HNE in patients of the recurrence group were significantly higher than that in patients of the non-recurrence group. There was a positive correlation between serum 4-HNE levels and the serum levels of triglyceride (r = 0.448, p = 0.008) and low-density lipoprotein cholesterol (LDL-C; r = 0.442, p = 0.002) in primary cerebral infarction patients. Cox proportional hazards modeling showed that demographic and certain clinical parameters, such as age, serum triglyceride levels, the National Institutes of Health Stroke Scale (NIHSS) scores, and serum 4-HNE levels, were independent factors for the recurrence in patients. The results of the receiver operating characteristic (ROC) curve showed that the area under the curve (AUC) value of serum 4-HNE in patients with cerebral infarction recurrence was 0.703, and when the cutoff value of serum 4-HNE was set at 42.34 ng/ml, the sensitivity and specificity values of serum 4-HNE in predicting recurrent cerebral infarction were 79.20 and 52.70%, respectively.

Conclusion: Serum 4-HNE is an independent risk factor for the recurrence of patients with primary cerebral infarction, and it may become a new intervention way to prevent the recurrence of patients with cerebral infarction.

KEYWORDS

4-hydroxynonenal, recurrence, cerebral infarction, risk, patients

Introduction

Cerebral infarction, also known as ischemic stroke, is one of the most common cerebrovascular diseases, accounting for about 70% of all acute cerebrovascular diseases (Zhao et al., 2022). In China, cerebral infarction has the characteristics of high morbidity, high recurrence rate, high disability rate, and high mortality rate (Liu et al., 2021). In addition, the recurrence rate of patients with cerebral infarction can be as high as 14–17%, accounting for 30% of new patients with stroke in China every year (Huang et al., 2021; Liu et al., 2021). At present, the specific molecular mechanism of cerebral infarction recurrence has not been revealed, but a large number of studies have analyzed the risk factors, such as age, low-density lipoprotein cholesterol (LDL-C), hypertension, white matter lesions, and heart disease, affecting the recurrence of cerebral infarction (Anniwaer et al., 2019). These risk factors are of great significance to effectively prevent and control the recurrence of cerebral infarction.

The underlying pathology of cerebral infarction is one of oxidative stress (Fan et al., 2019). Exogenous and endogenous oxygen radicals trigger lipid peroxidation by attacking polyunsaturated fatty acids in phospholipids of biological membranes and generate a complex series of products and new free radicals, among which aldehyde products are the main breakdown products and end products of lipid peroxidation reactions (Zheng et al., 2020; Wang et al., 2022). When compared with free radicals, aldehyde-based products are more stable and can diffuse to many cellular components and extracellular with the damaging potential of the original free radicals (Hou et al., 2020; Pozdnyakov et al., 2020). Aldehyde products can also react with some nucleophilic substances, such as thiol compounds, DNA, proteins, and phospholipids, interfering with the normal functional activities of cells, damaging cellular components, and leading to the development of diseases (Hou et al., 2020; Pozdnyakov et al., 2020). In addition, aldehyde-based products can also act as bioactive molecules that are involved in functional activities, such as cell signaling, cell proliferation, and gene expression, at very low non-toxic concentrations (Li et al., 2015). In conclusion, aldehyde-based products play an important role in the occurrence and development of many diseases.

4-Hydroxynonenal (4-HNE) is the most representative substance among the aldehyde products of lipid peroxidation, mainly produced by linoleic acid and arachidonic acid, etc., in lipid peroxidation (Castro et al., 2017; Gallo et al., 2020). Importantly, Guo et al. (2020) found that 4-HNE was closely related to aspirin sensitivity in patients with acute cerebral infarction, with higher levels associated with a greater risk of aspirin resistance in patients. Moreover, aspirin resistance is considered to be a risk factor for the recurrence of cerebral infarction (Yi et al., 2013; Wiśniewski et al., 2020), so 4-HNE may also be associated with the recurrence of cerebral infarction, but there is a lack of direct research evidence. In the present study, we compared the serum 4-HNE levels at the initial diagnosis of cerebral infarction in different patients with cerebral infarction and studied the effect of serum 4-HNE levels on the recurrence of cerebral infarction in patients with primary cerebral infarction.

Patients and methods

Patients

From January 2017 to June 2019, we prospectively recruited 189 patients with primary cerebral infarction. All patients or their guardians were informed about all aspects of this study and signed informed consent. In addition, the research protocol for this study was reviewed and approved by Ethics Committee of our hospital. Inclusion criteria were as follows: (1) age over 18 years old; (2) the first diagnosis of cerebral infarction; (3) CT and/or magnetic resonance imaging (MRI) confirmed evident focal neurological symptoms/signs; (4) complete clinical data and signed informed consent; and (5) all patients are sensitive to aspirin and can be treated with aspirin. Exclusion criteria were as follows: (1) cerebral hemorrhage or non-primary cerebral infarction, such as traumatic cerebral infarction or old cerebral infarction; (2) history of traumatic brain injury and cerebrovascular disease in the past 3 months; (3) history of antiplatelet, anticoagulant, or non-steroidal anti-inflammatory drugs (NSAIDs) medication; (4) malignant tumor, infectious disease, autoimmune disease, or organ dysfunction; (5) liver injury, kidney injury, chronic obstructive pulmonary disease, pneumonia, and other diseases affecting serum 4-hydroxytonic; and (6) glucocorticoid, low molecular weight heparin sodium, erythromycin, Salvia miltiorrhiza injection, Shuxuening injection, montelukast sodium, and other drugs that affect serum 4-hydroxytonic.

Data collection

We collected the clinical data of patients at admission, such as age, gender, admission time, medication history, medical history, hospitalization history, laboratory test data, comorbidities (hypertension, diabetes, and coronary disease), and living habits (smoking). The National Institutes of Health Stroke Scale (NIHSS) was used to assess the severity of stroke in patients with cerebral infarction at the time of admission.

Criteria for recurrence of cerebral infarction were as follows: the symptoms of the patient worsened before or other new symptoms of cerebral infarction occurred and new lesions of cerebral infarction were found through transcranial brain CT or magnetic resonance imaging.

Serological tests

Fasting peripheral blood was collected from all patients the next morning after admission and centrifuged (1,000 × *g*, room temperature, 10 min) to collect serum. We used an automatic biochemical analyzer (BS-280, Mindray) to detect levels of serum LDL-C, high-density lipoprotein cholesterol (HDL-C), triglyceride, and total cholesterol. In addition, we used Human 4-HNE ELISA Kit (CSB-E16214h, Cusabio Biotech) to detect the levels of 4-HNE.

Follow-up protocol

All patients were followed up for 3 years after the first diagnosis of cerebral infarction. During the follow-up period, the patients were interviewed by telephone every 3 months to collect information on the recurrence of cerebral infarction. For the patients with regular review, only the information on the recurrence of cerebral infarction was collected through outpatient information.

Statistical analysis

Data in the present study were analyzed by SPSS 19.0 software (SPSS Inc., Chicago, IL, USA). Qualitative data were presented as counts (%), and *p*-values were calculated using chi-square or Fisher's exact test as appropriate. The Kolmogorov-Smirnov test was used to check whether quantitative data conformed to a normal distribution, data that conformed to a normal distribution were presented as [mean ± standard deviation (SD)], and unpaired Student's *t*-test was used to compare differences and calculate *p*-values. Quantitative data that did not conform to a normal distribution were presented as the median [interquartile range (IQR)], and Mann-Whitney U-test was used to compare differences and calculate *p*-values. Spearman's correlation coefficient was used to analyze the association of serum 4-HNE levels with other clinical features. Receiver operating characteristic (ROC) curves were constructed and the area under the curve (AUC) was calculated to assess the performance of serum 4-HNE levels in distinguishing between primary cerebral infarction patients with and without recurrence at 3 years after cerebral infarction.

Results

Recurrence of cerebral infarction and baseline data

We prospectively enrolled 202 patients with primary cerebral infarction in this study. However, during the 3-year follow-up period, 7 patients were excluded due to missing or incomplete follow-up data and 6 patients died due to other diseases. At last, a total of 189 patients were finally included in this study. During the 3-year follow-up period, 96 of 189 patients with primary cerebral infarction developed recurrent cerebral infarction, namely, 93 patients in the non-recurrence group and 96 in the recurrence group. In comparison of baseline data between these two groups we found that there is no significantly different between the two groups on gender, smoking, coronary disease, serum HDL-C, total cholesterol, and NIHSS scores, while the age, proportion of patients with hypertension and diabetes, the serum level of triglyceride, and LDL-C in the non-recurrence group are all significantly lower than those in the recurrence group (Table 1).

Serum 4-hydroxynonenal in different cerebral infarction patients

The mean value of serum 4-HNE level is 45.78 ng/ml (20.18–72.35 ng/ml) in 189 patients with primary cerebral

TABLE 1 Baseline data of primary cerebral infarction patients.

Variable	No-recurrence ($n = 93$)	Recurrence ($n = 96$)	t/χ^2	*P*
Age (years)	63.25 ± 5.68	68.82 ± 6.39	4.281	0.028
Gender [male, *n* (%)]	52 (55.92%)	56 (58.33%)	0.113	0.737
Smoking [*n* (%)]	38 (40.86%)	40 (41.67%)	0.013	0.910
Hypertension [*n* (%)]	55 (59.14%)	79 (82.29)	12.272	< 0.001
Diabetes [*n* (%)]	18 (19.35%)	42 (43.75%)	12.970	< 0.001
Coronary disease [n (%)]	10 (10.75)	13 (13.54)	0.344	0.558
Triglyceride (mmol/L)	1.49 ± 0.18	1.87 ± 0.30	10.640	< 0.001
LDL-C (mmol/L)	3.01 ± 0.40	3.37 ± 0.49	5.503	< 0.001
HDL-C (mmol/L)	1.01 ± 0.21	1.05 ± 0.23	0.532	0.419
Total cholesterol (mmol/L)	4.28 ± 1.28	4.28 ± 1.17	0.089	0.823
NHISS scores	6.57 ± 1.42	6.82 ± 1.49	0.452	0.627

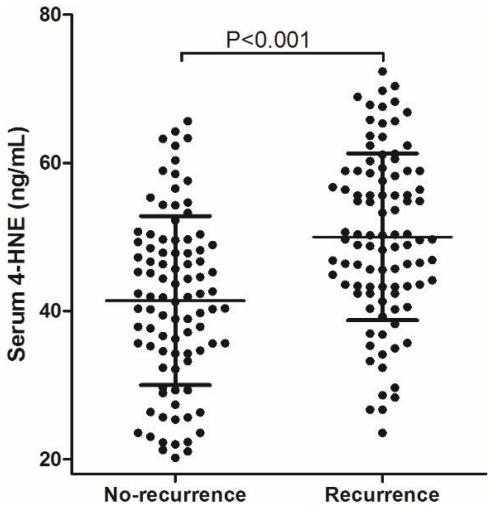

FIGURE 1
Comparison of serum 4-hydroxynonenal (4-HNE) level between non-recurrence group and recurrence group.

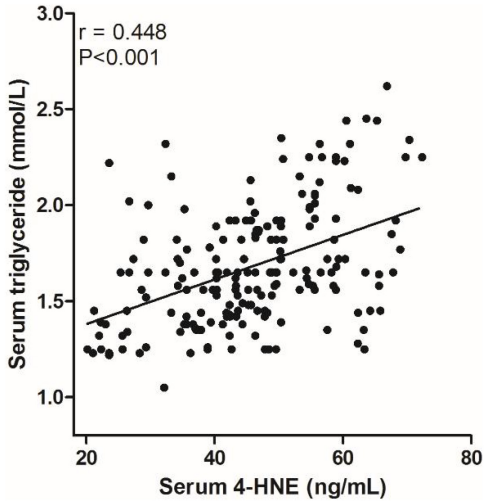

FIGURE 2
Scatter plot suggests a positive correlation between serum 4-hydroxynonenal (4-HNE) and triglyceride in primary cerebral infarction patients.

infarction, 41.42 ng/ml (20.18–65.62 ng/ml) in 93 patients with no-recurrent primary cerebral infarction, and 50.00 ng/ml (23.56–72.35 ng/ml) in 96 patients with recurrent primary cerebral infarction. The mean value of serum 4-HNE was 41.42 ng/ml (20.18–65.62 ng/ml) in the non-recurrence group and 50.00 ng/ml (23.56–72.35 ng/ml) in the recurrence group. Importantly, the levels of serum 4-HNE in the recurrent group were significantly higher than that in the non-recurrence group ($p < 0.05$; **Figure 1**).

Correlation between serum 4-hydroxynonenal and clinical data of cerebral infarction

We analyzed the correlation between serum 4-HNE levels and clinical data of primary cerebral infarction patients and found that there is no significant correlation between serum 4-HNE levels and the age, gender, smoking, hypertension, diabetes, coronary disease, HDL-C, total cholesterol, and NIHSS scores of primary cerebral infarction patients, while there was a positive correlation between serum 4-HNE levels and the serum levels of triglyceride (**Figure 2**) and LDL-C (**Figure 3**) in primary cerebral infarction patients (**Table 2**).

Predictive factors for recurrence of cerebral infarction

Univariate analysis showed that there were statistical differences in age, history of hypertension, triglyceride, low-density lipoprotein, NIHSS score, and 4-HNE level between

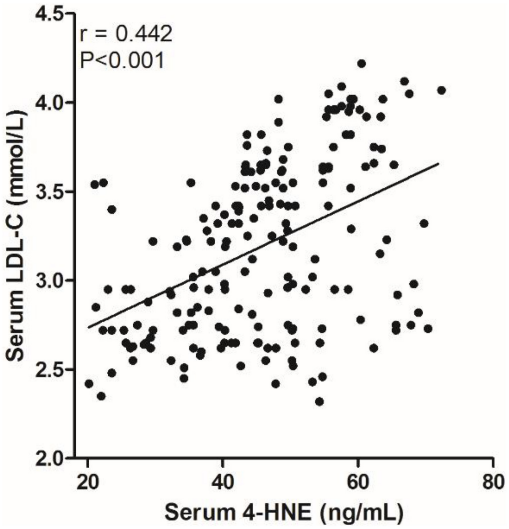

FIGURE 3
Scatter plot suggests a positive correlation between serum 4-hydroxynonenal (4-HNE) and low-density lipoprotein cholesterol (LDL–C) in primary cerebral infarction patients.

the two groups. To further confirm whether 4-HNE was an independent factor, multivariate analysis was further performed, and the results showed that demographic and certain clinical parameters, such as age [hazard ratio (HR) = 1.071, 95% CI: 1.002–1.138, $p < 0.001$], serum triglyceride levels (HR = 1.628, 95% CI: 1.013–2.267, $p = 0.042$), NIHSS scores (HR = 1.421, 95% CI: 1.056–2.934, $p = 0.023$), and serum 4-HNE levels (HR = 2.631, 95% CI: 1.639–4.413, $p < 0.001$), were independent factors for recurrence in patients (**Table 3**).

TABLE 2 Correlation between serum 4-hydroxynonenal (4-HNE) and other variables using spearman correlation coefficient in primary cerebral infarction patients.

Variables	*R*	*P* value
Age	0.042	0.722
Gender	0.092	0.667
Smoking	0.035	0.828
Hypertension	0.209	0.083
Diabetes	0.108	0.304
Coronary disease	0.143	0.195
Triglyceride	0.448	0.008
LDL-C	0.442	0.002
HDL-C	0.095	0.663
Total cholesterol	0.038	0.809
NIHSS scores	0.038	0.811

Predictive value of serum 4-HNE on recurrent cerebral infarction

The receiver operator characteristic curve was used to assess the predictive value of serum 4-HNE on recurrent cerebral infarction. The results showed that the AUC value of serum 4-HNE in patients with cerebral infarction recurrence was 0.703 (95% CI: 0.630–0.777, $p < 0.001$; **Figure 4**). In addition, when the cutoff value of serum 4-HNE was set at 42.34 ng/ml, the sensitivity and specificity values of serum 4-HNE in predicting recurrent cerebral infarction were 79.20 and 52.70%, respectively.

Discussion

4-Hydroxynonenal is a biomarker of oxidative stress and plays an important role in the pathophysiology of diseases, such as ischemic stroke (Lee et al., 2012; Li et al., 2018), metabolic disease (Castro et al., 2017), coronary heart disease (Chapple et al., 2013; Rosen et al., 2018), and cancer (Zhong and Yin, 2015; Gasparovic et al., 2017). In a study on patients with cerebral infarction, the authors found that serum 4-HNEs were significantly higher in patients with cerebral infarction than in healthy subjects and that serum 4-HNE levels were associated with the severity of brain injury in patients, suggesting that serum 4-HNE is a biomarker for assessing the condition of patients with cerebral infarction (Lee et al., 2012). In this study, our main finding was that the level of serum 4-HNE in patients with recurrent cerebral infarction was significantly higher than that in patients with no-recurrent cerebral infarction. In addition, multivariate regression also confirmed that the high level of serum 4-HNE was an independent risk factor for the recurrence of cerebral infarction, and linear analysis confirmed that its level was positively correlated with serum triglyceride and LDL-C levels. These results indicated that serum 4-hydroxynonenal might increase the risk of recurrence in patients with primary cerebral infarction.

The pathological process of cerebral ischemia is extremely complex. After the ischemic injury, brain tissue will undergo changes, such as energy metabolism disorder, central neurotransmitter disorder, oxidative stress injury, and inflammatory response, leading to complex pathophysiological changes and apoptosis of neurons (Chamorro et al., 2016; Orellana-Urzúa et al., 2020). In recent years, the theory of oxidative stress has become a hotspot in ischemic stroke research. Hypoxia can cause tissues to produce large amounts of oxygen free radicals that act on unsaturated fatty acids in the cell membrane, causing peroxidation of membrane lipids, which in turn leads to cellular damage and the formation of lipid peroxides (Nathaniel et al., 2015; Jiang et al., 2020). 4-HNE is an aldehyde substance closely related to oxidative stress and lipid peroxidation, and oxidative stress is one of the main factors causing ischemic injury, suggesting that the increase of serum 4-HNE might be one of the main mechanisms underlying the increased risk of stroke induced by oxidative stress (Poli and Schaur, 2000; Liu et al., 2020). Importantly, a previous study found that serum 4-HNE level was significantly higher in patients with aspirin-resistant cerebral infarction than in patients with aspirin-sensitive cerebral infarction, and the recurrence rate of aspirin-resistant cerebral infarction patients was significantly higher than that of aspirin-sensitive patients with cerebral infarction, indirectly suggesting that serum 4-HNE may be associated with the recurrence of cerebral infarction (Guo et al., 2020).

On the one hand, as a consequence of cerebral ischemia, post-cerebral ischemia causes increased oxidative stress in the brain, ultimately leading to increased 4-HNE levels (McKracken et al., 2001; Guo et al., 2017). On the other hand, increased 4-HNE levels increase brain damage from ischemic stroke (Dou et al., 2012; Shoeb et al., 2014). To elaborate, former studies have revealed that excess 4-HNE may cause severe biotoxicity to cells through various pathways (Geib et al., 2021; Schröter et al., 2021), such as the induction of intramolecular and intermolecular cross-linking of proteins by 4-HNE and inhibition of protein synthesis by modifying the relevant sites of thiol-containing proteins. Moreover, 4-HNE binds to the sulfhydryl group of intracellular glutathione, which reduces the consumption of glutathione, weakens the intracellular antioxidant capacity, and further aggravates intracellular oxidative stress (Balogh and Atkins, 2011). Moreover, as the end product of lipid peroxidation, 4-HNE can induce the aggregation and activation of macrophages, induce the expression of inflammatory factors, promote the occurrence of inflammation, and aggravate cerebral ischemia injury (Liu et al., 2020; Hsu et al., 2022). As the severity of ischemic brain injury is closely related to the recurrence of cerebral infarction, the level of serum 4-HNE may be one of

TABLE 3 Multivariate Cox regression results of influencing factors for recurrent cerebral infarction.

Variables	Univariate analysis			Multivariate analysis		
	HR	95%CI	*P*	HR	95%CI	*P*
Age	1.121	1.032–1.321	<0.001	1.071	1.002–1.138	<0.001
Gender	0.932	0.634–1.567	0.925			
Smoking	0.689	0.441–1.328	0.192			
Hypertension	1.933	1.689–2.651	0.039	1.705	1.068–3.231	0.071
Diabetes	0.966	0.827–1.634	0.272			
Coronary disease	0.905	0.213–3.227	0.728			
Triglyceride	1.742	1.512–1.768	0.008	1.628	1.013–2.267	0.042
LDL-C	1.352	0.923–1.984	0.042	1.065	0.937–2.624	0.089
HDL-C	0.652	0.569–0.986	0.139			
Total cholesterol	0.936	0.892–1.657	0.413			
NIHSS scores	1.321	1.218–2.392	0.011	1.421	1.056–2.934	0.023
4-HNE	2.325	2.025–4.963	<0.001	2.631	1.639–4.413	<0.001

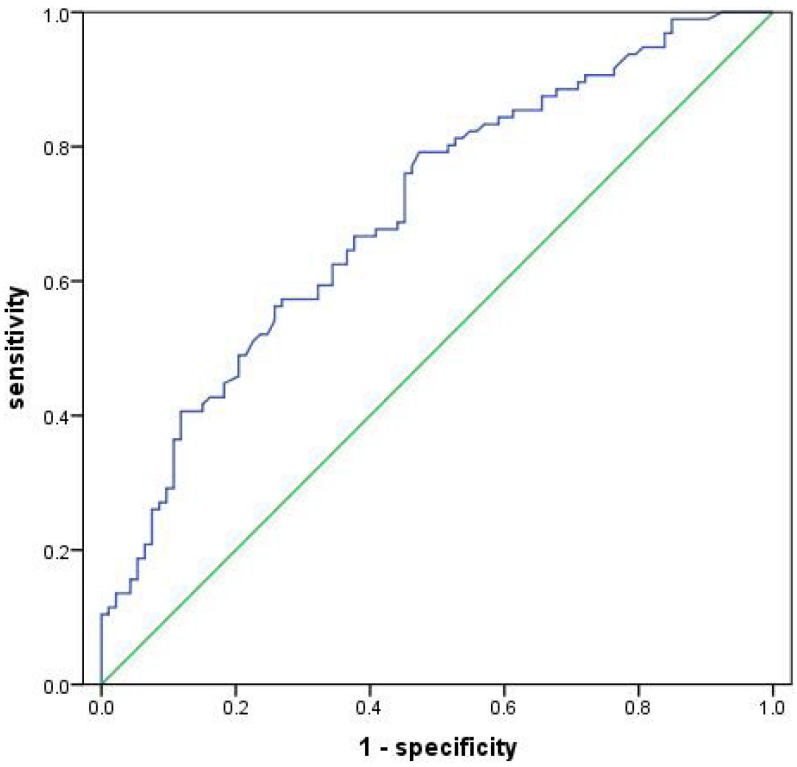

FIGURE 4
Receiver operator characteristic curve demonstrating a predictive value of serum 4-hydroxynonenal (4-HNE) on recurrent cerebral infarction.

the main mechanisms related to the recurrence of cerebral infarction by affecting the progress of ischemic brain injury.

Another possible mechanism by which 4-HNE increases recurrence in patients with cerebral infarction is that 4-HNE affects platelet aggregation. Platelets is associated with the pathophysiology of stroke and their reactivity is not only an important clinical indicator of stroke (Järemo et al., 2013; Järemo et al., 2015), but also significantly correlated with the degree of brain injury and the risk of recurrence in patients with cerebral infarction (Guo et al., 2021; Yuan et al., 2021). Platelet-inhibiting drugs, such as aspirin, are effective in reducing the recurrence rate of cerebral infarction, while aspirin resistance is an independent risk factor for recurrence of cerebral infarction (Guo et al., 2020).

Importantly, previous studies found that 4-HNE could affect platelet aggregation and might act as a negative feedback regulator of platelet function (Chapple et al., 2013; Ravi et al., 2016). In addition, we found that the high level of 4-HNE is more likely to play a negative feedback regulation role in platelet aggregation when LDL level is increased, suggesting that the influence mechanism of 4-HNE on the recurrence risk of patients with cerebral infarction may be similar to aspirin resistance (Malle et al., 1995).

Conclusion

All in all, our results in the present study showed that serum 4-HNE was higher in patients with recurrent cerebral infarction, and serum 4-HNE was an independent risk factor for recurrence in patients with primary cerebral infarction.

Data availability statement

The original contributions presented in the study are included in the article/supplementary material, further inquiries can be directed to the corresponding author.

Ethics statement

This study was approved by the ethics committee of Hebei North University Hospital. The patients/participants provided their written informed consent to participate in this study.

Author contributions

XL and ZL were mainly responsible for the writing and research design of the article. MB and LF were mainly responsible for data analysis. XL was responsible for ensuring that the descriptions are accurate and agreed by all authors. All authors contributed to the article and approved the submitted version.

Funding

This study was supported by the 2021 Hebei Provincial Government Funded Clinical Medicine Talent Training Project (no. 10).

Conflict of interest

The authors declare that the research was conducted in the absence of any commercial or financial relationships that could be construed as a potential conflict of interest.

Publisher's note

References

Anniwaer, J., Liu, M. Z., Xue, K. D., Maimaiti, A., and Xiamixiding, A. (2019). Homocysteine might increase the risk of recurrence in patients presenting with primary cerebral infarction. *Int. J. Neurosci.* 129, 654–659. doi: 10.1080/00207454.2018.1517762

Balogh, L. M., and Atkins, W. M. (2011). Interactions of glutathione transferases with 4-hydroxynonenal. *Drug Metab. Rev.* 43, 165–178.

Castro, J. P., Jung, T., Grune, T., and Siems, W. (2017). 4-Hydroxynonenal (HNE) modified proteins in metabolic diseases. *Free Radic. Biol. Med.* 111, 309–315.

Chamorro, Á, Dirnagl, U., Urra, X., and Planas, A. M. (2016). Neuroprotection in acute stroke: Targeting excitotoxicity, oxidative and nitrosative stress, and inflammation. *Lancet Neurol.* 15, 869–881.

Chapple, S. J., Cheng, X., and Mann, G. E. (2013). Effects of 4-hydroxynonenal on vascular endothelial and smooth muscle cell redox signaling and function in health and disease. *Redox Biol.* 1, 319–331. doi: 10.1016/j.redox.2013.04.001

Dou, X., Li, S., Wang, Z., Gu, D., Shen, C., Yao, T., et al. (2012). Inhibition of NF-κB activation by 4-hydroxynonenal contributes to liver injury in a mouse model of alcoholic liver disease. *Am. J. Pathol.* 181, 1702–1710. doi: 10.1016/j.ajpath.2012.08.004

Fan, Q. Y., Qiu, Z., and Zhang, X. D. (2019). Influences of urinary kallidinogenase on neuronal apoptosis in cerebral infarction rats through Nrf2/ARE oxidative stress pathway. *Eur. Rev. Med. Pharmacol. Sci.* 23, 6665–6671. doi: 10.26355/eurrev_201908_18557

Gallo, G., Sprovieri, P., and Martino, G. (2020). 4-hydroxynonenal and oxidative stress in several organelles and its damaging effects on cell functions. *J. Physiol. Pharmacol.* 71, 15–33.

Gasparovic, A. C., Milkovic, L., Sunjic, S. B., and Zarkovic, N. (2017). Cancer growth regulation by 4-hydroxynonenal. *Free Radic. Biol. Med.* 111, 226–234.

Geib, T., Iacob, C., Jribi, R., Fernandes, J., Benderdour, M., and Sleno, L. (2021). Identification of 4-hydroxynonenal-modified proteins in human osteoarthritic chondrocytes. *J. Proteomics* 232:104024. doi: 10.1016/j.jprot.2020.104024

Guo, C., Wang, S., Duan, J., Jia, N., Zhu, Y., Ding, Y., et al. (2017). Protocatechualdehyde protects against cerebral ischemia-reperfusion-induced oxidative injury via protein kinase Cε/Nrf2/HO-1 pathway. *Mol. Neurobiol.* 54, 833–845. doi: 10.1007/s12035-016-9690-z

Guo, J., Wang, J., Guo, Y., and Feng, J. (2020). Association of aspirin resistance with 4-hydroxynonenal and its impact on recurrent cerebral infarction in patients with acute cerebral infarction. *Brain Behav.* 10:e01562. doi: 10.1002/brb3.1562

Guo, S., Lin, Y., Ma, X., Zhao, Y., Jin, A., Liu, X., et al. (2021). Long-term safety and efficacy of antiplatelet therapy in patients with cerebral infarction with thrombocytopenia. *Clin. Appl. Thromb. Hemost.* 27:1076029620980067.

Hou, J. Y., Zhong, Z. X., Deng, Q. T., Liu, S. D., and Lin, L. F. (2020). Association between the polymorphism of aldehyde dehydrogenase 2 gene and cerebral infarction in a Hakka population in southern China. *Biochem. Genet.* 58, 322–334. doi: 10.1007/s10528-020-09950-5

Hsu, C. G., Chávez, C. L., Zhang, C., Sowden, M., Yan, C., and Berk, B. C. (2022). The lipid peroxidation product 4-hydroxynonenal inhibits NLRP3 inflammasome activation and macrophage pyroptosis. *Cell Death Differ.* 29, 1790–1803. doi: 10.1038/s41418-022-00966-5

Huang, Z. X., Gu, H. Q., Yang, X., Wang, C. J., Wang, Y. J., and Li, Z. X. (2021). Risk factors for in-hospital mortality among acute ischemic stroke patients in China: A nationwide prospective study. *Neurol. Res.* 43, 387–395. doi: 10.1080/01616412.2020.1866356

Järemo, P., Eriksson, M., Lindahl, T. L., Nilsson, S., and Milovanovic, M. (2013). Platelets and acute cerebral infarction. *Platelets* 24, 407–411.

Järemo, P., Eriksson-Franzen, M., and Milovanovic, M. (2015). Platelets, gender and acute cerebral infarction. *J. Transl. Med.* 13:267.

Jiang, Q., Geng, X., Warren, J., Eugene Paul Cosky, E., Kaura, S., Stone, C., et al. (2020). Hypoxia inducible factor-1α (HIF-1α) mediates NLRP3 inflammasome-dependent-pyroptotic and apoptotic cell death Following ischemic stroke. *Neuroscience* 448, 126–139. doi: 10.1016/j.neuroscience.2020.09.036

Lee, W. C., Wong, H. Y., Chai, Y. Y., Shi, C. W., Amino, N., Kikuchi, S., et al. (2012). Lipid peroxidation dysregulation in ischemic stroke: Plasma 4-HNE as a potential biomarker? *Biochem. Biophys. Res. Commun.* 425, 842–847. doi: 10.1016/j.bbrc.2012.08.002

Li, Q. Y., Zhao, N. M., Ma, J. J., Duan, H. F., Ma, Y. C., Zhang, W., et al. (2015). ALDH2*2 allele is a negative risk factor for cerebral infarction in Chinese women. *Biochem. Genet.* 53, 260–267. doi: 10.1007/s10528-015-9686-9

Li, Y., Liu, S. L., and Qi, S. H. (2018). ALDH2 protects against ischemic stroke in rats by facilitating 4-HNE clearance and AQP4 down-regulation. *Neurochem. Res.* 43, 1339–1347. doi: 10.1007/s11064-018-2549-0

Liu, H., Gambino, F. Jr., Algenio, C. S., Wu, C., Gao, Y., Bouchard, C. S., et al. (2020). Inflammation and oxidative stress induced by lipid peroxidation metabolite 4-hydroxynonenal in human corneal epithelial cells. *Graefes Arch. Clin. Exp. Ophthalmol.* 258, 1717–1725. doi: 10.1007/s00417-020-04647-2

Liu, L., Wang, Y., Xie, X., Liu, D., Wang, A., Wang, P., et al. (2021). China antihypertensive trial in acute ischemic stroke II (CATIS-2): Rationale and design. *Stroke Vasc. Neurol.* 6, 286–290. doi: 10.1136/svn-2020-000828

Malle, E., Ibovnik, A., Leis, H. J., Kostner, G. M., Verhallen, P. F., and Sattler, W. (1995). Lysine modification of LDL or lipoprotein(a) by 4-hydroxynonenal or malondialdehyde decreases platelet serotonin secretion without affecting platelet aggregability and eicosanoid formation. *Arterioscler. Thromb. Vasc. Biol.* 15, 377–384.

McKracken, E., Graham, D. I., Nilsen, M., Stewart, J., Nicoll, J. A., and Horsburgh, K. (2001). 4-Hydroxynonenal immunoreactivity is increased in human hippocampus after global ischemia. *Brain Pathol.* 11, 414–421. doi: 10.1111/j.1750-3639.2001.tb00409.x

Nathaniel, T. I., Williams-Hernandez, A., Hunter, A. L., Liddy, C., Peffley, D. M., Umesiri, F. E., et al. (2015). Tissue hypoxia during ischemic stroke: Adaptive clues from hypoxia-tolerant animal models. *Brain Res. Bull.* 114, 1–12. doi: 10.1016/j.brainresbull.2015.02.006

Orellana-Urzúa, S., Rojas, I., Líbano, L., and Rodrigo, R. (2020). Pathophysiology of ischemic stroke: Role of oxidative stress. *Curr. Pharm. Des.* 26, 4246–4260.

Poli, G., and Schaur, R. J. (2000). 4-Hydroxynonenal in the pathomechanisms of oxidative stress. *IUBMB Life* 50, 315–321.

Pozdnyakov, D. I., Voronkov, A. V., and Rukovitsyna, V. M. (2020). Chromon-3-aldehyde derivatives restore mitochondrial function in rat cerebral ischemia. *Iran J. Basic Med. Sci.* 23, 1172–1183. doi: 10.22038/ijbms.2020.46369.10710

Ravi, S., Johnson, M. S., Chacko, B. K., Kramer, P. A., Sawada, H., Locy, M. L., et al. (2016). Modification of platelet proteins by 4-hydroxynonenal: Potential mechanisms for inhibition of aggregation and metabolism. *Free Radic. Biol. Med.* 91, 143–153. doi: 10.1016/j.freeradbiomed.2015.10.408

Rosen, M., Chan, P., Saleem, M., Herrmann, N., Adibfar, A., Andreazza, A., et al. (2018). Longitudinal associations between 4-hydroxynonenal and depression in coronary artery disease patients. *Psychiatry Res.* 270, 219–224. doi: 10.1016/j.psychres.2018.09.046

Schröter, A., Mahler, H. C., Sayed, N. B., Koulov, A. V., Huwyler, J., and Jahn, M. (2021). 4-Hydroxynonenal - a toxic leachable from clinically used administration materials. *J. Pharm Sci.* 110, 3268–3275. doi: 10.1016/j.xphs.2021.05.014

Shoeb, M., Ansari, N. H., Srivastava, S. K., and Ramana, K. V. (2014). 4-Hydroxynonenal in the pathogenesis and progression of human diseases. *Curr. Med. Chem.* 21, 230–237.

Wang, G., Zeng, X., Gong, S., Wang, S., Ge, A., Liu, W., et al. (2022). Exploring the mechanism of edaravone for oxidative stress in rats with cerebral infarction based on quantitative proteomics technology. *Evid. Based Complement Alternat. Med.* 2022:8653697. doi: 10.1155/2022/8653697

Wiśniewski, A., Filipska, K., Sikora, J., and Kozera, G. (2020). Aspirin resistance affects medium-term recurrent vascular events after cerebrovascular incidents: A three-year follow-up study. *Brain Sci.* 10:179. doi: 10.3390/brainsci10030179

Yi, X., Zhou, Q., Lin, J., and Chi, L. (2013). Aspirin resistance in Chinese stroke patients increased the rate of recurrent stroke and other vascular events. *Int. J. Stroke* 8, 535–539. doi: 10.1111/j.1747-4949.2012.00929.x

Yuan, Q., Yu, L., and Wang, F. (2021). Efficacy of using thromboelastography to detect coagulation function and platelet function in patients with acute cerebral infarction. *Acta Neurol. Belg.* 121, 1661–1667.

Zhao, Y., Zhang, X., Chen, X., and Wei, Y. (2022). Neuronal injuries in cerebral infarction and ischemic stroke: From mechanisms to treatment (Review). *Int. J. Mol. Med.* 49:15.

Zheng, M., Wang, X., Yang, J., Ma, S., Wei, Y., and Liu, S. (2020). Changes of complement and oxidative stress parameters in patients with acute cerebral infarction or cerebral hemorrhage and the clinical significance. *Exp. Ther. Med.* 19, 703–709.

Zhong, H., and Yin, H. (2015). Role of lipid peroxidation derived 4-hydroxynonenal (4-HNE) in cancer: Focusing on mitochondria. *Redox Biol.* 4, 193–199. doi: 10.1016/j.redox.2014.12.011

frontiers | Frontiers in Cellular Neuroscience

TYPE Brief Research Report
PUBLISHED 13 January 2023
DOI 10.3389/fncel.2022.1106593

OPEN ACCESS

EDITED BY
C. Andrew Frank,
The University of Iowa, United States

REVIEWED BY
Quan Yuan,
National Institute of Neurological Disorders and Stroke (NIH), United States
Kate O'Connor-Giles,
Brown University, United States
Kimberly Rose Madhwani,
Brown University, United States, in collaboration with reviewer KO'C-G
Robert J. Kittel,
Leipzig University, Germany

*CORRESPONDENCE
Matthias Landgraf
✉ ml10006@cam.cam.uk
Daniel Sobrido-Cameán
✉ ds918@cam.ac.uk

†These authors have contributed equally to this work

SPECIALTY SECTION
This article was submitted to Cellular Neurophysiology, a section of the journal Frontiers in Cellular Neuroscience

RECEIVED 23 November 2022
ACCEPTED 27 December 2022
PUBLISHED 13 January 2023

CITATION
Sobrido-Cameán D, Oswald MCW, Bailey DMD, Mukherjee A and Landgraf M (2023) Activity-regulated growth of motoneurons at the neuromuscular junction is mediated by NADPH oxidases.
Front. Cell. Neurosci. 16:1106593.
doi: 10.3389/fncel.2022.1106593

Activity-regulated growth of motoneurons at the neuromuscular junction is mediated by NADPH oxidases

Daniel Sobrido-Cameán*†, Matthew C. W. Oswald†, David M. D. Bailey, Amrita Mukherjee and Matthias Landgraf*

Department of Zoology, University of Cambridge, Cambridge, United Kingdom

Neurons respond to changes in the levels of activity they experience in a variety of ways, including structural changes at pre- and postsynaptic terminals. An essential plasticity signal required for such activity-regulated structural adjustments are reactive oxygen species (ROS). To identify sources of activity-regulated ROS required for structural plasticity *in vivo* we used the Drosophila larval neuromuscular junction as a highly tractable experimental model system. For adjustments of presynaptic motor terminals, we found a requirement for both NADPH oxidases, Nox and dual oxidase (Duox), that are encoded in the Drosophila genome. This contrasts with the postsynaptic dendrites from which Nox is excluded. NADPH oxidases generate ROS to the extracellular space. Here, we show that two aquaporins, Bib and Drip, are necessary ROS conduits in the presynaptic motoneuron for activity regulated, NADPH oxidase dependent changes in presynaptic motoneuron terminal growth. Our data further suggest that different aspects of neuronal activity-regulated structural changes might be regulated by different ROS sources: changes in bouton number require both NADPH oxidases, while activity-regulated changes in the number of active zones might be modulated by other sources of ROS. Overall, our results show NADPH oxidases as important enzymes for mediating activity-regulated plasticity adjustments in neurons.

KEYWORDS

motoneuron, plasticity, Drosophila, reactive oxygen species, NADPH oxidase, dual oxidase, Nox, aquaporin genes

1. Introduction

Reactive oxygen species (ROS) have commonly been associated with detrimental processes such as oxidative stress, toxicity, aging, neurodegeneration, and cell death because increases in ROS levels seen with aging and neurodegenerative disorders, including Parkinson's (Spina and Cohen, 1989) and Alzheimer's disease (Martins et al., 1986). However, it is appreciated that ROS are not simply cytotoxic agents, but more generally function as signaling molecules in a multitude of processes, (Rhee, 1999; Sauer et al., 2001) including growth

factor signaling (Suzukawa et al., 2000; Goldsmit et al., 2001; Kamata et al., 2005; Nitti et al., 2010), wound healing (Razzell et al., 2013), and in development (Milton et al., 2011; Oswald M. C. et al., 2018; Oswald M. et al., 2018; Dhawan et al., 2021 for a reviews see Owusu-Ansah and Banerjee, 2009; Massaad and Klann, 2011; Wilson and González-Billault, 2015; Terzi and Suter, 2020).

During nervous system development, ROS signaling is involved at all stages, from neurogenesis to pathfinding to synaptic transmission (Knapp and Klann, 2002; Kishida and Klann, 2007; Massaad and Klann, 2011; Wilson and González-Billault, 2015; Wilson et al., 2018; Terzi and Suter, 2020). When studying ROS signaling *in vivo,* challenges include the ability to disentangle cell autonomous from indirect or systemic effects; or to determine sources and types of ROS. Using the fruit fly, *Drosophila melanogaster*, as a highly tractable experimental model system, genetic manipulations targeted to single motoneurons were able to identify hydrogen peroxide as a synaptic plasticity signal, generated as a consequence of neuronal overactivation and both necessary and sufficient for activity-regulated adaptive changes of synaptic terminal structure and transmission (Oswald M. C. et al., 2018; Dhawan et al., 2021). We found mitochondria to be a major source of activity-regulated hydrogen peroxide with opposing effects on the growth of pre- vs. postsynaptic terminals: at the presynaptic terminal of the neuromuscular junction (NMJ) overactivation and hydrogen peroxide cause increases in terminals (Milton et al., 2011; Oswald M. C. et al., 2018). This change in presynaptic terminal growth is mediated by activation of the JNK signaling pathway (Milton et al., 2011), and it utilizes the conserved Parkinson's disease-linked protein, DJ-1β, as a redox sensor, which regulates the PTEN-PI3 Kinase growth pathway (Oswald M. C. et al., 2018). In contrast, the size of postsynaptic dendritic arbors is negatively regulated by over-activation and activity-regulated hydrogen peroxide (Tripodi et al., 2008; Oswald M. C. et al., 2018; Dhawan et al., 2021). These studies using the Drosophila larval neuromuscular model system contrast with findings from cultured hippocampal neurons, which posit mitochondrially generated superoxide as the principal ROS signal downstream of over-activation (Hongpaisan et al., 2003, 2004). The extent to which both types of ROS operate as neuronal plasticity signals downstream of over-activation remains to be resolved, though it is possible that apparent discrepancies might be due to the use of different cellular models and/or a reflection of the degree of overactivation.

Another principal source of ROS are NADPH oxidases, whose location in the plasma membrane could facilitate sub-cellular signaling discrete from mitochondrial ROS production. NADPH oxidases are integral membrane proteins that mediate a single electron transfer from NADPH to oxygen, thereby converting it to superoxide (Lambeth, 2002). These enzymes are prevalent throughout the evolutionary ladder from Amoebozoa and fungi to higher plants and mammals. NADPH oxidases are involved in growth and plasticity during nervous system development (Serrano et al., 2003; Tejada-Simon et al., 2005; Kishida et al., 2006; Munnamalai and Suter, 2009; Munnamalai et al., 2014; Olguín-Albuerne and Morán, 2015; Wilson et al., 2015, 2016; Terzi and Suter, 2020). In contrast to mammalian genomes, which encode seven Nox isoforms (Nox 1–5 and Duox 1 and 2; Lambeth, 2002; Kawahara et al., 2007), *Drosophila melanogaster* encodes just two NADPH oxidases: dual oxidase (Duox) and a Nox-5 homolog (Nox). Enzymatic activity of both is calcium-regulated, *via* their N-terminal calcium binding EF-hands (Ha et al., 2005a,b, 2009; Moreira et al., 2010; Razzell et al., 2013). Curiously, the mouse genome does not encode a calcium-regulated Nox-5 homolog, which has therefore not been studied extensively *in vivo* (Kawahara et al., 2007). Recently, we identified the NADPH oxidase Duox as necessary in motoneurons to reduce their dendritic arbors in response to neuronal over-activation, an adaptive response to reduce the numbers of presynaptic inputs and thus synaptic drive (Zwart et al., 2013; Dhawan et al., 2021). We further found that these activity-regulated ROS, generated by Duox at the extracellular face of the plasma membrane, required the aquaporins, Bib and Drip; presumably for efficient entry into the cytoplasm to regulate dendritic growth and/or stability (Dhawan et al., 2021).

Here, we investigated the role of NADPH oxidases at the presynaptic terminal of the NMJ, whose growth response to neuronal over-activation is distinct to that of the dendritic compartment of the motoneuron. We show that the NADPH oxidases Duox and Nox are sources of activity-regulated ROS that mediate activity-regulated growth of NMJ terminals. In contrast to motoneuron dendrites, both NADPH oxidases function at the presynaptic NMJ, necessary and sufficient to elicit changes in growth. At the NMJ too, we find the aquaporins, Bib and Drip, are necessary for ROS signaling at the NMJ. This arrangement at the presynaptic NMJ terminal contrasts with their dendritic function within these motoneurons, where only Duox, but not Nox, is required. This differential requirement of Nox mirrors its sub-cellular localization, with Nox largely excluded from dendrites. Furthermore, at the postsynaptic compartment extracellular ROS, including from other neurons in the vicinity, act as local plasticity signals that cause reductions in dendritic arbor size (Dhawan et al., 2021).

2. Results

2.1. NADPH oxidases, Duox and Nox, are both required for activity-regulated growth at the neuromuscular junction

Mitochondria are a major source of activity-generated ROS, notably within the cytoplasm. Here, we sought to investigate the role of membrane localized ROS generators,

the NADPH oxidases Nox and Duox, during activity-regulated adjustment of presynaptic terminals. As a highly tractable experimental model we used the well-characterized neuromuscular junction (NMJ) of the Drosophila larva (Frank et al., 2013). Specifically, we focused on the NMJ of the so called "anterior Corner Cell" (aCC), which innervates the most dorsal body wall muscle, known as muscle 1 (Crossley, 1978) or dorsal acute muscle 1 (DA1; Sink and Whitington, 1991; Bate, 1993; Landgraf et al., 1997; Baines et al., 1999, 2001; Hoang and Chiba, 2001; Choi et al., 2004). For cell-specific over-activation of aCC motoneurons, we used the established paradigm of targeted mis-expression of the warmth-gated cation channel, dTRPA1 Gain-of-Function (GoF; Hamada et al., 2008; Oswald M. C. et al., 2018; Dhawan et al., 2021). This allows aCC motoneurons to be selectively overactivated simply by placing larvae at >24°C, the temperature threshold for dTRPA1 ion channel opening (Pulver et al., 2009).

First, we re-confirmed that at 25°C *dTrpA1[GoF]* in aCC motoneurons leads to significant increases in bouton number at the aCC-DA1 NMJ relative to non-manipulated controls, as previously shown (Oswald M. C. et al., 2018; Figure 1). An advantage of using cell-specific dTRPA1-mediated activity manipulations in this system is that these can be carried out at 25°C, a temperature considered optimal for *Drosophila melanogaster* development (Lachaise et al., 1988; Pool et al., 2012) and therefore generally considered neutral, while sufficient to mildly activate neurons that mis-express dTRPA1 (Pulver et al., 2009; Tsai et al., 2012).

Next, we tested the requirement for the two NADPH oxidases encoded in the Drosophila genome, Duox and Nox, in mediating these activity-regulated structural changes at the NMJ. To this end, we expressed RNAi transgenes for knocking down endogenous Duox or Nox in aCC motoneurons. By themselves, expression of *Duox[RNAi]* or *Nox[RNAi]* transgenes in aCC motoneurons have no measurable effect on NMJ morphology. However, in motoneurons that have been overactivated by *dTrpA1[GoF]*, the characteristic activity-induced bouton overgrowth phenotype is suppressed by co-expression of *Duox[RNAi]* or *Nox[RNAi]* transgenes, individually or combined (Figures 1A, B). Neuronal overactivation by *dTrpA1[GoF]* also causes a reduction in active zone numbers (Oswald M. C. et al., 2018). We find that simultaneous knockdown of NADPH oxidases seems to ameliorate active zone reductions, though differences were subtle and not statistically significant (Figure 1C). These results show that the membrane localized ROS generators, Nox and Duox, are required primarily for activity-regulated changes in presynaptic terminal growth, while the impact on presynaptic release sites was less clear.

2.2. Duox and Nox activity is sufficient for mediating structural changes at the NMJ

We next asked if the activity of these NADPH oxidases might also be sufficient for regulating presynaptic terminal growth. To test this, we induced a NADPH oxidase gain-of-function by overexpression of *Duox[GoF]* or *Nox[GoF]* transgenes in aCC motoneurons. Quantification showed comparable increases in bouton number at the NMJ as a consequence of overexpression of either *Duox[GoF]* or *Nox[GoF]*. No enhancement of this phenotype occurs when both are co-expressed (Figure 2). In contrast, active zone numbers are not significantly impacted by overexpression of either NADPH oxidase (Figure 1).

For the postsynaptic compartment, namely the dendritic arbor of motoneurons, we had previously shown that only Duox, but not Nox, has a role in activity-regulated plasticity (Dhawan et al., 2021). To further explore this difference in NADPH oxidase requirement between pre- vs. postsynaptic compartments, we generated tagged transgenes of both NADPH oxidases, UAS-Duox::mRuby2::HA and UAS-Nox::YPet. When expressed in aCC motoneurons to reveal subcellular localization, we see exclusion of Nox::YPet from the postsynaptic dendrites, while Duox::mRuby2::HA is fairly homogeneously distributed within the plasma membrane (Figure 2C). These patterns of distinct subcellular distributions, notably exclusion of Nox::YPet from dendrites, are compatible with the genetic manipulations phenotypes. They point to selective sorting of Nox to soma and presynaptic compartments, based on the fluorescently tagged transgene.

2.3. Aquaporin channel proteins Bib and Drip are necessary for NADPH oxidase-regulated structural changes at the NMJ

The NADPH oxidases Duox and Nox are transmembrane proteins that generate ROS at the extracellular face of the plasma membrane (Lambeth, 2002; Panday et al., 2015). We reasoned that if NADPH oxidase-generated ROS are indeed instrumental in activity-regulated adjustment of synaptic terminals, then neutralization of extracellular ROS should rescue NMJ phenotypes associated with NADPH oxidase overexpression. To test this, we mis-expressed in aCC motoneurons two different forms of catalases that are secreted to the extracellular space; a human version and the Drosophila immune-regulated catalase (IRC; Ha et al., 2005a,b; Fogarty et al., 2016). These catalases neutralize extracellular hydrogen peroxide by conversion to water. On their own, their mis-expression in aCC motoneurons has no significant impact on NMJ structure or size. To test

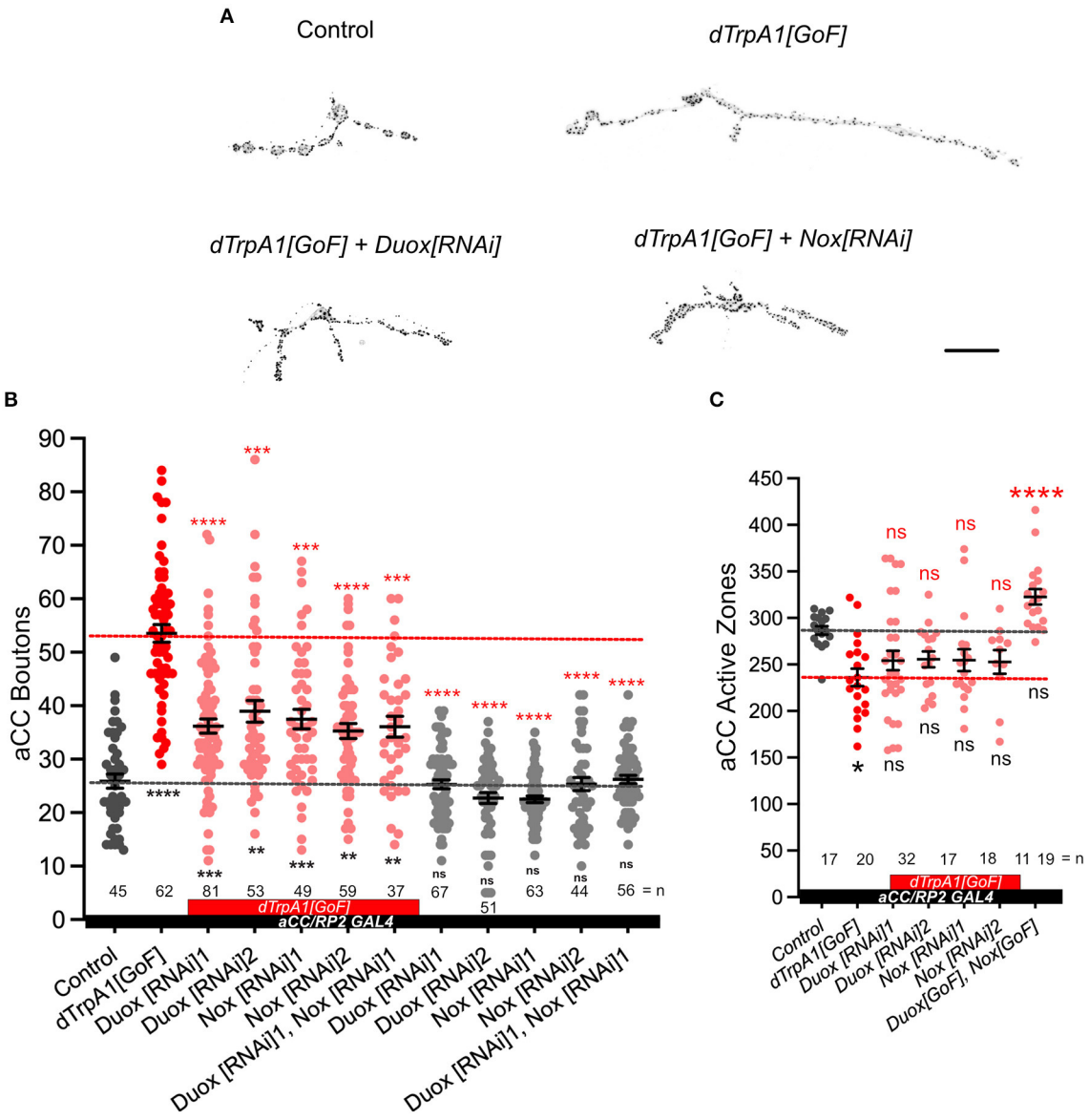

FIGURE 1
NADPH oxidases, dDuox and dNox, are both required for activity-regulated growth of the neuromuscular junction. **(A)** Representative images of aCC motoneuron terminals on their target muscle, DA1 (muscle 1, according to Crossley, 1978) in third instar larvae [100 h after larva hatching (ALH)] labeled with a *20xUAS-6xmCherry* reporter expressed by *aCC/RP2-Gal4* (see Section 4) and active zones (black spots): control (*aCC/RP2-Gal4/+*); dTrpA1 overactivated; dTrpA1 overactivated while either Duox or Nox is concomitantly knocked down *via* targeted RNAi ["*dTrpA1[GoF] + Duox[RNAi]*" and "*dTrpA1[GoF] + Nox[RNAi]*"]. **(B)** Dot-plot quantification shows NMJ bouton number increases in response to cell-specific activity increases. This phenotype is rescued by simultaneous NADPH oxidase knockdown. **(C)** Dot-plot quantification shows active zone number decreases following overactivation [*dTrpA1[GoF]*], but there are not significant differences when manipulating NADPH oxidases. Mean ± SEM, ANOVA, *$p < 0.05$, **$p < 0.01$, ***$p < 0.001$, and ****$p < 0.0001$. ns = not significant. Red asterisks indicate comparisons with the *dTrpA1[GoF]* group, while black indicate comparison with the un-manipulated wild type control. Scale bar = 20 μm.

the model of neuronal activity leading to NADPH oxidase activation, leading to extracellular ROS production, we co-expressed secreted catalase in aCC motoneurons while over-activating these with *dTrpA1[GoF]*. The presence of a secreted catalase suppresses the NMJ growth that would otherwise ensue with neuronal overactivation (Figure 3A). Similarly, NMJ over-growth stimulated by over-expression of Duox (*Duox[GoF]*) is also neutralized by co-expression of secreted catalase in the same neuron (Figure 3B). These experiments demonstrate that it is the presence of extracellular ROS, notably hydrogen peroxide generated by NADPH oxidases, which leads to activity-induced changes in NMJ growth.

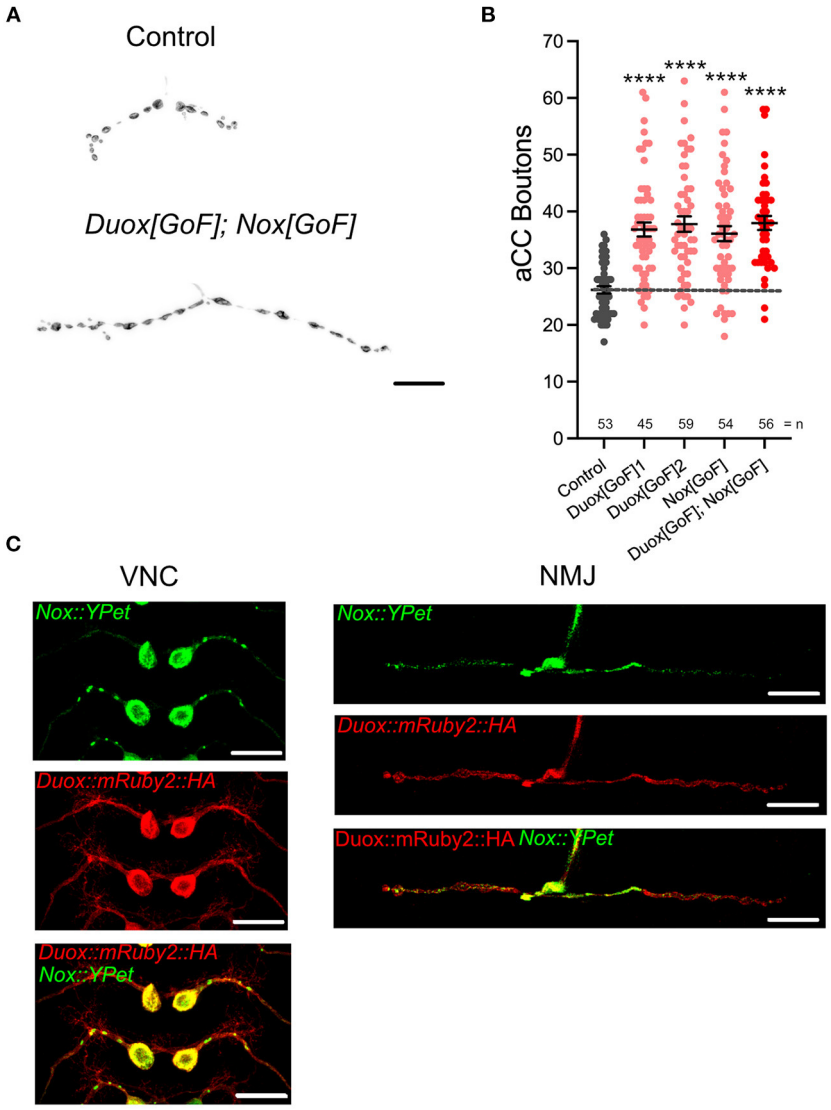

FIGURE 2
dDuox or dNox activity is sufficient for mediating structural changes at the NMJ. **(A)** Representative images of aCC presynaptic terminals on muscle DA1 from third instar larvae (100 h ALH) of control (*aCC/RP2-Gal4/+*) and those overexpressing *Duox[GoF]* and *Nox[GoF]*. **(B)** Dot-plot quantification shows NMJ bouton number increases in response to cell-specific over-expression of NADPH oxidases. **(C)** Localization of tagged Duox and Nox transgenes in neurons: representative confocal micrograph images of aCC somata and dendrites in the ventral nerve cord (VNC) and aCC presynaptic terminals at the DA1 muscle in third instar larvae (72 h ALH), showing subcellular localization of tagged over-expressed Duox::mRuby2::HA (in red) and Nox::YPet (in green). Mean ± SEM, ANOVA, ****$p < 0.0001$. Comparisons are made with the control group. Scale bar = 20 μm.

Because NAPDH oxidases generate ROS extracellularly, we wanted to explore how extracellular ROS might enter the cell so as to act on intracellular signaling pathways that would regulate NMJ growth. Several studies, including one from this lab, have postulated a role for aquaporin channels, specifically those encoded by the genes Bib and Drip (Albertini and Bianchi, 2010; Dhawan et al., 2021; Dutta and Das, 2022). Indeed, for the presynaptic NMJ, we found that co-expression of *UAS-RNAi* constructs designed to knock down Bib or Drip, but not those for Prip, rescue NMJ growth phenotypes caused by dTRPA1-mediated overactivation. Expression of the *UAS-RNAi* constructs alone had no significant effect (Figure 3A). To further test the model that extracellular ROS generated by NADPH oxidases cause structural change at the NMJ, we overexpressed *Duox[GoF]* in aCC motoneurons and at the same time co-expressed *UAS-RNAi* constructs designed to knock down the aquaporin channel proteins *Bib[RNAi]* or *Drip[RNAi]*. In those neurons

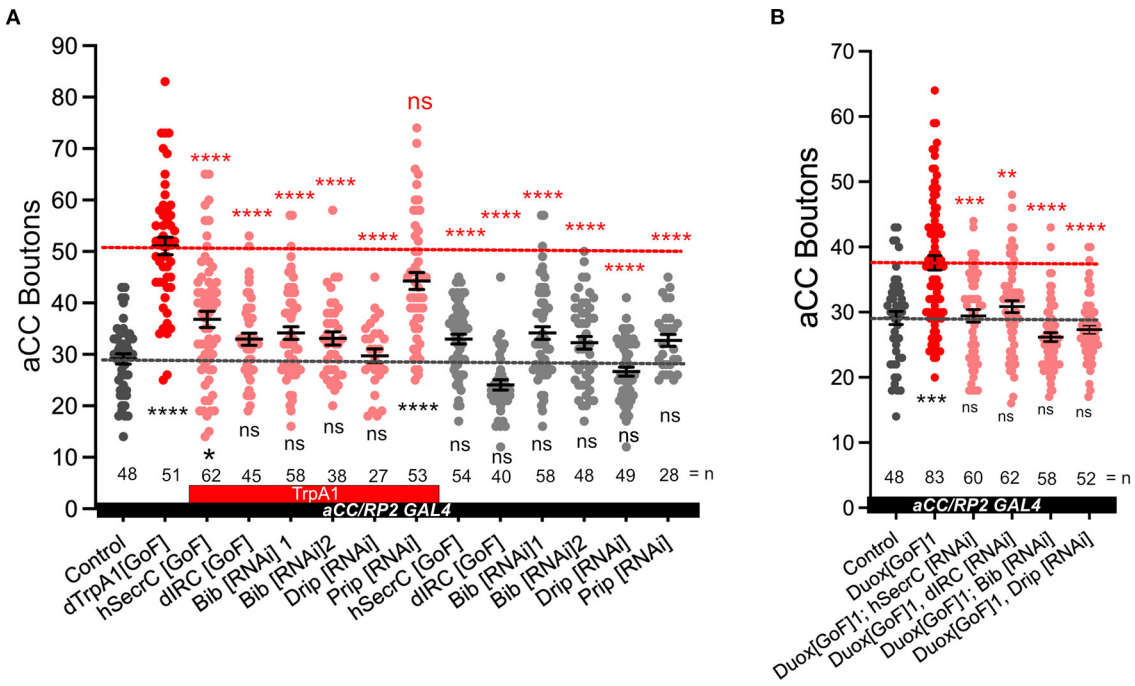

FIGURE 3
Aquaporins Bib and Drip are required for activity-regulated plasticity at the neuromuscular junction. **(A)** Dot-plot quantification shows NMJ bouton number increases in response to cell-specific activity and the rescue of the phenotype when secreted catalases are expressed *[GoF]* or aquaporins Bib or Drip are knocked down; control (*aCC/RP2-Gal4/+*). **(B)** Dot-plot quantification shows NMJ bouton number increases in response *Duox[GoF]* and the rescue of the phenotype when secreted catalases are expressed or aquaporins Bib or Drip are knocked down; control (*aCC/RP2-Gal4/+*). Mean ± SEM, Kruskal-Wallis test, $*p < 0.05$, $**p < 0.01$, $***p < 0.001$, and $****p < 0.0001$. ns = not significant. Red asterisks indicate statistical comparisons with the *dTrpA1 [GoF]* group, while black asterisks comparison with the un-manipulated wild type control.

the *Duox[GoF]* NMJ growth phenotype is fully rescued (Figure 3B).

In summary, our observations suggest that at the presynaptic NMJ, neuronal overactivation leads to activation of both NADPH oxidases, Duox and Nox, at the plasma membrane. These enzymes generate ROS at the extracellular face, which are then brought into the cytoplasm by aquaporin channels comprising Bib and Drip. Inside the cell, the ROS act on intracellular membrane-localized signaling pathways that regulate synaptic terminal structure and size, including the phosphatase PTEN and DJ-1ß, as previously shown (Oswald M. C. et al., 2018; Figure 4).

3. Discussion

ROS have increasingly been recognized as signaling molecules required for nervous system development and function, from regulating the dynamics of the growth cone cytoskeleton to synaptic transmission and learning (see Terzi and Suter, 2020). At the Drosophila NMJ, ROS have been shown necessary for activity-induced synaptic terminal growth (Oswald M. C. et al., 2018). ROS have also been shown causative and sufficient to induce changes at synaptic terminals; when accumulating as a result of physiological dysfunction, leading to oxidative stress (Milton et al., 2011), or following manipulations that increase ROS levels (Milton et al., 2011; Hussain et al., 2018; Peng et al., 2019). While mitochondria are a major source of cellular ROS (Murphy, 2009; Zorov et al., 2014; Sanz, 2016), it has remained unclear to what extent mitochondrial or indeed other sources of ROS, as explored in this study, directly impact effectors that regulate synaptic terminal growth. At the larval NMJ, different signaling pathways feed into growth regulation, notably Wnt (Budnik and Salinas, 2011; Koles and Budnik, 2012), BMP (Bayat et al., 2011; Berke et al., 2013; Sulkowski et al., 2014; Osses and Henríquez, 2015), PKA, CREB, and the transcription factor AP-1 (Davis et al., 1996; Davis et al., 1998; Sanyal et al., 2002, 2003; Davis, 2006; Walker et al., 2013; Cho et al., 2015; Davis and Müller, 2015). ROS might serve a general role in amplifying signaling pathway activity by disinhibition of pathway-associated protein kinases. For example, at the Drosophila NMJ, we previously showed that activity-regulated ROS inhibit the phosphatase PTEN, and thus disinhibit PI3Kinase, whose activity promotes synaptic terminal growth (Martín-Peña et al., 2006; Acebes and Morales, 2012; Jordán-Álvarez et al., 2012; Oswald M. C. et al., 2018). ROS have

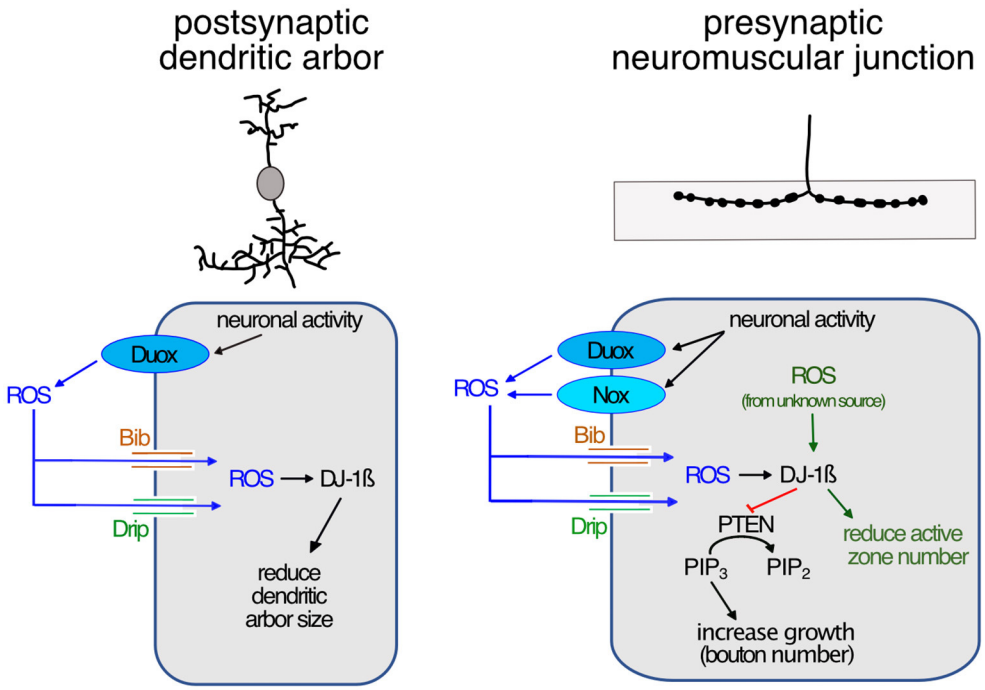

FIGURE 4
Model of activity-regulated plasticity at the postsynaptic dendritic arbor and the presynaptic neuromuscular junction mediated by ROS signaling. Neuronal activity leads to activation of calcium-regulated NADPH oxidases in synaptic terminals; of Duox only in postsynaptic dendrites, while at the presynaptic neuromuscular junction both Duox and Nox are activated. Extracellularly generated ROS reintroduced into the cytoplasm *via* aquaporin channels, including Bib and Drip. This leads to reduced dendritic growth, while at the presynaptic neuromuscular junction ROS promotes growth by modulating PI3Kinase signaling at the plasma membrane *via* oxidation of DJ-1ß. Oxidized DJ-1ß increases binding and inhibition of the PTEN phosphatase, thus causing increased PI3Kinase signaling activity, stimulating growth and addition of synaptic release sites. ROS from unknown sources regulate the active zone number.

further been shown to modulate BMP signaling in sympathetic neurons (Chandrasekaran et al., 2015; Sánchez-de-Diego et al., 2019) and Wnt pathways in non-neuronal cells (Funato et al., 2006; Love et al., 2013; Rharass et al., 2014). The link between PKA and ROS is not well-understood though ROS can activate PKA in Amygdala neurons, increasing their excitability (Li et al., 2011). Changes in neuronal excitability can also be directly modulated by oxidation of any number of ion channels, for example of the K-channel auxiliary subunit, Hyperkinetic (Fogle et al., 2015; Kempf et al., 2019). We therefore hypothesize that ROS may provide neuronal activity-regulated modulation of multiple canonical synaptic plasticity pathways. In such a scenario, one might expect that the necessary spatial precision is achieved through distinct sources of ROS generation.

3.1. Differential requirements for NADPH oxidases in pre- vs. postsynaptic compartments

In this study, we focused on NADPH oxidases as generators of ROS that are ideally positioned to influence signaling at the plasma membrane. Working with the NMJ in the Drosophila larva as an experimental *in vivo* model system, we demonstrated that both NADPH oxidases, Nox and Duox, are required for activity-induced growth (Figure 1). Both enzymes are endowed with N-terminal calcium binding EF-hand motifs, linking their activity to intracellular calcium levels, as shown for Drosophila Duox (Ha et al., 2009; Rigutto et al., 2009; Razzell et al., 2013) and the vertebrate homolog, Nox5 (Bánfi et al., 2004; Millana Fañanás et al., 2020). Conversely, overexpression of either enzyme is sufficient to phenocopy such presynaptic terminal growth (Figure 2). Curiously, the requirement for NADPH oxidases in regulating dendritic growth is different, with only Duox, but not Nox, mediating activity-induced reduction of dendritic arbor size (Dhawan et al., 2021). This difference in pre- vs. postsynaptic compartment regulation is mirrored by their differential sub-cellular localization, with tagged Nox protein being effectively excluded from the postsynaptic dendritic arbors, unlike Duox (Figure 2C). Apart from this differential pre- vs. postsynaptic requirement, it is unclear to what extent Nox and Duox might perform different functions during activity-regulated growth. At the NMJ, where both are present and required, we found no difference in phenotypes

following RNAi knockdown or mis-expression. Curiously, phenotypes were also comparable regardless of whether the expression of both enzymes was manipulated simultaneously or individually, suggesting either a saturation of phenotype or, speculatively, that Nox and Duox might operate in the same signaling pathway with their activation contingent on one another.

3.2. NADPH oxidases generate extracellular ROS and can mediate autocrine signaling

Because Nox and Duox generate ROS at the extracellular face they have the potential for inter-cellular signaling, as during wound healing (Niethammer et al., 2009; Razzell et al., 2013; Niethammer, 2016). Indeed, within the dense meshwork of neuronal processes and synapses of the CNS, we recently found that reduction of extracellular hydrogen peroxide in the vicinity of dendritic processes (by mis-expression of a secreted catalase) or attenuation of ROS entry into those dendrites (by knock-down of aquaporins), both cause significant dendritic over-growth (Dhawan et al., 2021). This suggests that within the densely innervated central neuropile, extracellular ROS generated, including by activity-regulated NADPH oxidases, might function as local signals to which neurons respond with adjustments of their synaptic terminals. This contrasts with the peripheral Drosophila larval NMJ, where we did not see any significant changes in synaptic terminal morphology following manipulations that would either reduce entry of ROS into the presynaptic terminal or reductions of extracellular ROS (Figure 3). These observations suggest that at the presynaptic NMJ, NADPH oxidases might be required primarily under conditions of elevated neuronal activity. While this suggests that at the presynaptic NMJ, NADPH oxidase-generated ROS might be engaged in autocrine signaling, there is potential for inter-cellular signaling with adjacent muscles and glia.

Extracellular ROS signaling at both pre- and postsynaptic compartments is underlined by the requirement for the aquaporin channel proteins, Bib and Drip (Figure 3; Dhawan et al., 2021). Some studies have questioned the extent to which Bib might function as an aquaporin, as unable to form effective water channels in a heterologous expression system (Tatsumi et al., 2009; Kourghi et al., 2018). However, in this and in a previous study (Dhawan et al., 2021), *Bib[RNAi]* knockdown produces synaptic terminal phenotypes indistinguishable from knockdown of *Drip[RNAi]*, or from mis-expression *[GoF]* of secreted forms of catalase (Dhawan et al., 2021). This suggests that Bib functions in the same pathway as the aquaporin Drip, potentially forming part of a heteromeric channel with permeability for hydrogen peroxide.

3.3. Independent, local regulation of pre- and postsynaptic terminal growth

Overactivation of neurons results in changes to both pre- and postsynaptic terminals, though it has been unclear in how far such changes in growth of input and output compartments might be co-ordinately regulated. Working with this experimental system we identified two sets of manipulations that suggest the growth of pre- and postsynaptic terminals can be regulated independently. First, in motoneurons that have been over-activated by mis-expression of *dTrpA1[GoF]*, RNAi knockdown of Nox has no effect on the activity-induced reduction of the postsynaptic dendrites, which receive all synaptic input from pre-motor interneurons (Nox protein appears to be excluded from dendrites); while at the presynaptic NMJ of those same neurons, activity-linked overgrowth is significantly suppressed by knockdown of *Nox[RNAi]*. This contrasts with the ability of *Duox[RNAi]* knockdown to suppresses *dTrpA1[GoF]* over-activation phenotypes at both pre- and postsynaptic terminals.

Second, RNAi knockdown alone of the genes coding for aquaporin channel proteins Bib or Drip cause significant dendritic overgrowth, without affecting the presynaptic NMJ. These manipulations suggest that, at least in Drosophila larval motoneurons, synaptic terminal growth can be regulated locally through ROS signaling, such that pre- and postsynaptic compartments can adjust independently from each other. This makes sense when viewing extracellular ROS as local signals for over-activation, to which cells respond by adjusting their synaptic terminals. It remains to be seen to what extent extracellular ROS might impact on the regulation of synaptic transmission.

In summary, it is increasingly appreciated that ROS are important signals, whose signaling capability is proportional to the spatiotemporal precision attained. Sub-cellular specificity of ROS generators, such as the NAPDH oxidases studied here, is an important facet.

4. Materials and methods

4.1. Fly genetics

Drosophila melanogaster strains were maintained on standard apple juice-based agar medium at 25°C. Fly strains used were: *OregonR* (#2376 Bloomington Drosophila Stock Center), *dTrpA1* in attP16 (Hamada et al., 2008; FBtp0089791), *Duox[RNAi]*1 (#32903 BDSC; FBtp0064955), *Duox[RNAi]*2 (#38916 BDSC; FBgn0283531), *Nox[RNAi]*1 (Ha et al., 2005a,b; FBal0191562), *Nox[RNAi]*2 (#32433 BDSC; FBgn0085428), *bib[RNAi]*1 (#57493 BDSC; FBtp0096443), *bib[RNAi]*2 (#27691 BDSC; FBtp0052515), *Drip[RNAi]*1 (#44661 BDSC; FBtp0090566), *Drip[RNAi]*2 (#106911 Vienna Drosophila

Resource Center; FBtp0045814; Bergland et al., 2012), *Prip[RNAi]2* (#44464 BDSC; FBtp0090258), *Duox[GoF]*1 (Ha et al., 2005a,b), *Duox::mRuby2::HA* (*Duox[GoF]2*; this paper), *Nox::YPet* (*Nox[GoF]*; this paper), *hSecrC[GoF] (human secreted catalase*; FBal0190351; Ha et al., 2005a,b; Fogarty et al., 2016), *dIRC[GoF] (Drosophila extracellular immune-regulated catalase*; FBal0191070, Ha et al., 2005a,b).

Transgene expression was carried out at 25°C targeted to RP2 and aCC motoneurons using the Gal4 expression line "*aCC/RP2-Gal4*": *RN2-O-Gal4, UAS-FLP, tubulin84b-FRT-CD2-FRT-Gal4; RRFa-Gal4, 20xUAS-6XmCherry::HA* (Pignoni et al., 1997; Fujioka et al., 2003; Shearin et al., 2014). *RN2-GAL4* expression in RP2 and aCC motoneurons is restricted to the embryo, subsequently maintained by FLPase-gated *tubulin84B-FRT-CD2-FRT-GAL4* (Ou et al., 2008). We studied the mCherry expression to confirm that Gal4 expression is restricted to aCC and RP2 (Supplementary Figure 1). To study the localization of tagged *Nox::YPet* and *Duox::mRuby2::HA,* transgene expression was targeted to aCC motoneurons using *GMR94G06-Gal4* (#40701 BDSC; FBgn0053512; Pérez-Moreno and O'Kane, 2019). *pJFRC12-10XUAS-IVS-Nox-YPet* (GenBank OP716753) in VK00040 [cytogenetic 87B10] was generated by Klenow assembly cloning (tinyurl.com/4r99uv8m). Briefly, from pJFRC12-10XUAS-IVS-myr-GFP plasmid DNA we removed the coding sequence for *myr::GFP* using XhoI and XbaI, and replaced it with *Nox* cDNA from DGRC clone FI15205 (kindly provided by Kenneth H. Wan, DGRC Stock 1661239; https://dgrc.bio.indiana.edu//stock/1661239; RRID:DGRC_1661239), its 3' stop codon replaced by a flexible glycine-serine linker, followed by YPet (Nguyen and Daugherty, 2005). Similarly, we created *pJFRC12-10XUAS-IVS-Duox-mRuby2-HA* (GenBank OP716752) in landing site VK00022 [cytogenetic 57A5] using *Duox* cDNA kindly provided by Won-Jae Lee, its 3' stop codon replaced by a flexible glycine-serine linker, followed by mRuby2 (Lam et al., 2012), followed by another glycine-serine flexible linker and four tandem repeats of the hemagglutinin (HA) epitope. Transgenics were generated *via* phiC31 integrase-mediated recombination (Bischof et al., 2007) into defined landing sites by the FlyORF Injection Service (Zürich, Switzerland).

4.2. Dissections and immunocytochemistry

Flies were allowed to lay eggs on apple-juice agar based medium overnight at 25°C. Larvae were reared at 25°C on yeast paste, avoiding over-crowding. Precise staging of the late wandering third instar stage was achieved by: (a) checking that a proportion of animals from the same time-restricted egg lay had initiated pupariation; (b) larvae had reached a certain size and (c) showed gut-clearance of food [yeast paste supplemented with Bromophenol Blue Sodium Salt (Sigma-Aldrich)]. Larvae were dissected in Sorensen's saline, fixed for 5 min at room temperature in Bouins fixative or 10 min 4% paraformaldehyde (Agar Scientific) when staining for GFP/YPet epitopes, as detailed (Oswald M. C. et al., 2018). Wash solution was Sorensen's saline containing 0.3% Triton X-100 (Sigma-Aldrich) and 0.25% BSA (Sigma-Aldrich). Primary antibodies, incubated overnight at 10°C, were: Goat-anti-HRP Alexa Fluor 488 (1:1000; Jackson ImmunoResearch Cat. No. 123-545-021), Rabbit-anti-dsRed (1:1000; ClonTech Cat. No. 632496), Mouse nc82 (Bruchpilot; Developmental Studies Hybridoma Bank Cat No nc82), Chicken anti-GFP (1:5000; abcam Cat No ab13970); secondary antibodies, 2 h at room temperature: Donkey anti-mouse Alexa Fluor 647; Donkey-anti-Rabbit CF568 (1:1200; Biotium Cat. No. 20098), Donkey anti-Chicken CF488 (1:1000; Cambridge Bioscience Cat No 20166), and goat anti-Rabbit Atto594 (1:1000; Sigma-Aldrich Cat No 77671-1ML-F). Specimens were cleared in 70% glycerol, overnight at 4°C, then mounted in Mowiol.

Each experiment was performed at least two independent times. The "control" genotype is *aCC/RP2-Gal4/+* generated by crossing wild type Oregon R flies to the *aCC/RP2-Gal4* line.

4.3. Image acquisition and analysis

Specimens were imaged using a Leica SP5 point-scanning confocal, and a 63x/1.3 N.A. (Leica) glycerol immersion objective lens and Leica Application Suite Advanced Fluorescence software. Confocal images were processed using ImageJ (to quantify active zones) and Affinity Photo (Adobe; to prepare figures). Bouton number of the NMJ on muscle DA1 from segments A3-A5 was determined by counting every distinct spherical varicosity along the NMJ branch.

To study if genetic manipulations targeted to aCC and RP2 motoneurons change muscle size we measured surface area of DA1 muscles, imaged with DIC optics using a Zeiss Axiophot microscope and a Plan-Neofluar 10x/0.3 N.A. objective lens. Images were taken with an Orca CCD camera (Hamamatsu) and muscle surface area was determined using ImageJ by multiplying muscle length by width. Differences in animal or muscle growth would lead to clear correlations between muscle surface area and bouton number. No changes in animal growth were observed, irrespective of aCC manipulation. In line with this, quantification of key representative experiments, covering most transgenic lines and conditions where genetic manipulation of aCC motoneurons cause significant changes in bouton number, shows no statistically significant differences in average muscle size. Correlating individual muscle size with bouton number shows that the biggest differences in muscle surface area are

due to dissection artifact, e.g., extent of stretching larval filets (see Supplementary Figure 2). Taking account of this, bouton numbers are shown as raw counts, not normalized to average muscle surface area.

Representative schematics, drawings and plates of photomicrographs were generated with Affinity Photo (Serif Ltd., United Kingdom).

4.4. Statistical analysis

All data handling was performed using Prism software (GraphPad). NMJ bouton number data were tested for normal/Gaussian distribution using the D'Agostino-Pearson omnibus normality test. For normally distributed data one-way analysis of variance (ANOVA), with Tukey's multiple comparisons test was applied, while for non-normal distributions Kruskal-Wallis test was applied.

Data availability statement

The datasets presented in this study can be found in online repositories. The names of the repository/repositories and accession number(s) can be found at: https://www.ncbi.nlm.nih.gov/genbank/, OP716752 and OP716753.

Author contributions

DS-C, MO, AM, and ML conceived of the study and wrote the manuscript. DB cloned Duox and Nox transgenes. ML generated transgenic stocks. DS-C and MO carried out all experiments and analyzed data. All authors contributed to the article and approved the submitted version.

Funding

This work was made possible through support by the Biotechnology and Biological Sciences Research Council (BBSRC) to ML (BB/R016666/1 and BB/V014943/1). DS-C was supported by the European Molecular Biology Organization (EMBO) with a long-term EMBO fellowship (ALTF 62-2021) and a John Stanley Gardiner studentship to AM. The work benefited from the Imaging Facility, Department of Zoology, supported by Matt Wayland and funds from a Wellcome Trust Equipment Grant (WT079204) with contributions by the Sir Isaac Newton Trust in Cambridge, including Research Grant [18.07ii(c)].

Acknowledgments

The authors would like to thank Niklas Krick for feedback on the manuscript. The authors are grateful to Andreas Bergmann, Paul Garrity, Won-Jae Lee, Paul Martin, Sean Sweeney, Helen Weavers, and Will Wood, as well as the Bloomington Drosophila Stock Center and Vienna Drosophila Resource Center for generously providing fly stocks; and to Won-Jae Lee for providing DNA containing Duox cDNA, and the Drosophila Genomics Resource Center (DGRC), supported by NIH grant 2P40OD010949, for clone FI15205 containing Nox cDNA.

Conflict of interest

The authors declare that the research was conducted in the absence of any commercial or financial relationships that could be construed as a potential conflict of interest.

Publisher's note

Supplementary material

The Supplementary Material for this article can be found online at: https://www.frontiersin.org/articles/10.3389/fncel.2022.1106593/full#supplementary-material

SUPPLEMENTARY FIGURE 1
aCC/RP2 Gal4. **(A)** Schematic representation of internal muscles of a 3rd instar larva with muscle DA1 shown in magenta. The highlighted area was imaged, shown in **(B)**; **(B)** Peripheral projections of Gal4-expressing aCC and RP2 motoneurons were visualized by UAS-6xmCherry. HRP staining reveals all neurons, the composite with mCherry shows specificity of Gal4 restricted to aCC and RP2 motoneurons. Scale bar: 100 μm.

SUPPLEMENTARY FIGURE 2
Muscles size. **(A)** Dot-plot quantification shows no statistically significant differences in average muscle surface area (MSA) between genotypes, including with mis-expression of UAS-dTrpA1 (red). Mean ± SEM, Kruskal-Wallis test. **(B)** Linear regression using the control data shows not correlation between aCC NMJ terminal bouton numbers and muscle size, p-value = 0.7866.

References

Acebes, A., and Morales, M. (2012). At a PI3K crossroads: Lessons from flies and rodents. *Rev. Neurosci.* 23, 29–37. doi: 10.1515/rns.2011.057

Albertini, R., and Bianchi, R. (2010). Aquaporins and glia. *Curr. Neuropharmacol.* 8, 84–91. doi: 10.2174/157015910791233178

Baines, R. A., Robinson, S. G., Fujioka, M., Jaynes, J. B., and Bate, M. (1999). Postsynaptic expression of tetanus toxin light chain blocks synaptogenesis in Drosophila. *Curr. Biol.*. 9, 1267–1270. doi: 10.1016/S0960-9822(99)80510-7

Baines, R. A., Uhler, J. P., Thompson, A., Sweeney, S. T., and Bate, M. (2001). Altered electrical properties in Drosophila neurons developing without synaptic transmission. *J. Neurosci.* 21, 1523–1531. doi: 10.1523/JNEUROSCI.21-05-01523.2001

Bánfi, B., Tirone, F., Durussel, I., Knisz, J., Moskwa, P., Molnár, G. Z., et al. (2004). Mechanism of Ca^{2+} activation of the NADPH oxidase 5 (NOX5). *J. Biol. Chem.* 279, 18583–18591. doi: 10.1074/jbc.M310268200

Bate, M. (1993). "The mesoderm and its derivatives," in *The Development of Drosophila Melanogaster Vol. II*, eds C. M. Bate and A. Martinez-Arias (Cold Spring Harbor, NY: The development of Drosophila melanogaster), 1013–1090.

Bayat, V., Jaiswal, M., and Bellen, H. J. (2011). The BMP signaling pathway at the Drosophila neuromuscular junction and its links to neurodegenerative diseases. *Curr. Opin. Neurobiol.* 21, 182–188. doi: 10.1016/j.conb.2010.08.014

Bergland, A. O., Chae, H. S., Kim, Y. J., and Tatar, M. (2012). Fine-scale mapping of natural variation in fly fecundity identifies neuronal domain of expression and function of an aquaporin. *PLoS Genet.* 8, e1002631. doi: 10.1371/journal.pgen.1002631

Berke, B., Wittnam, J., McNeill, E., Van Vactor, D. L., and Keshishian, H. (2013). Retrograde BMP signaling at the synapse: A permissive signal for synapse maturation and activity-dependent plasticity. *J. Neurosci.* 33, 17937–17950. doi: 10.1523/JNEUROSCI.6075-11.2013

Bischof, J., Maeda, R. K., Hediger, M., Karch, F., and Basler, K. (2007). An optimized transgenesis system for Drosophila using germ-line-specific phiC31 integrases. *Proc. Natl. Acad. Sci. U. S. A.* 104, 3312–3317. doi: 10.1073/pnas.0611511104

Budnik, V., and Salinas, P. C. (2011). Wnt signaling during synaptic development and plasticity. *Curr. Opin. Neurobiol.* 21, 151–159. doi: 10.1016/j.conb.2010.12.002

Chandrasekaran, V., Lea, C., Sosa, J. C., Higgins, D., and Lein, P. J. (2015). Reactive oxygen species are involved in BMP-induced dendritic growth in cultured rat sympathetic neurons. *Mol. Cell. Neurosci.* 67, 116–125. doi: 10.1016/j.mcn.2015.06.007

Cho, R. W., Buhl, L. K., Volfson, D., Tran, A., Li, F., Akbergenova, Y., et al. (2015). Phosphorylation of complexin by PKA regulates activity-dependent spontaneous neurotransmitter release and structural synaptic plasticity. *Neuron* 88, 749–761. doi: 10.1016/j.neuron.2015.10.011

Choi, J. C., Park, D., and Griffith, L. C. (2004). Electrophysiological and morphological characterization of identified motor neurons in the Drosophila third instar larva central nervous system. *J. Neurophysiol.* 91, 2353–2365. doi: 10.1152/jn.01115.2003

Crossley, A. C. (1978). "The morphology and development of the Drosophila muscular system," in *The Genetics and Biology of Drosophila, Vol. 2b*, eds M. Ashburner and T. Wright (New York, NY: Academic), 499–560.

Davis, G. W. (2006). Homeostatic control of neural activity: From phenomenology to molecular design. *Ann. Rev. Neurosci.* 29, 307–323. doi: 10.1146/annurev.neuro.28.061604.135751

Davis, G. W., DiAntonio, A., Petersen, S. A., and Goodman, C. S. (1998). Postsynaptic PKA controls quantal size and reveals a retrograde signal that regulates presynaptic transmitter release in Drosophila. *Neuron* 20, 305–315. doi: 10.1016/S0896-6273(00)80458-4

Davis, G. W., and Müller, M. (2015). Homeostatic control of presynaptic neurotransmitter release. *Ann. Rev. Physiol.* 77, 251–270. doi: 10.1146/annurev-physiol-021014-071740

Davis, G. W., Schuster, C. M., and Goodman, C. S. (1996). Genetic dissection of structural and functional components of synaptic plasticity. III. CREB is necessary for presynaptic functional plasticity. *Neuron.* 17, 669–679. doi: 10.1016/s0896-6273(00)80199-3

Dhawan, S., Myers, P., Bailey, D., Ostrovsky, A. D., Evers, J. F., and Landgraf, M. (2021). Reactive oxygen species mediate activity-regulated dendritic plasticity through NADPH oxidase and aquaporin regulation. *Front. Cell. Neurosci.* 15, 641802. doi: 10.3389/fncel.2021.641802

Dutta, A., and Das, M. (2022). Deciphering the role of aquaporins in metabolic diseases: A mini review. *Am. J. Med. Sci.* 364, 148–162. doi: 10.1016/j.amjms.2021.10.029

Fogarty, C. E., Diwanji, N., Lindblad, J. L., Tare, M., Amcheslavsky, A., Makhijani, K., et al. (2016). Extracellular reactive oxygen species drive apoptosis-induced proliferation *via* Drosophila macrophages. *Curr. Biol.* 26, 575–584. doi: 10.1016/j.cub.2015.12.064

Fogle, K. J., Baik, L. S., Houl, J. H., Tran, T. T., Roberts, L., Dahm, N. A., et al. (2015). CRYPTOCHROME-mediated phototransduction by modulation of the potassium ion channel β-subunit redox sensor. *Proc. Natl. Acad. Sci. U. S. A.* 112, 2245–2250. doi: 10.1073/pnas.1416586112

Frank, C. A., Wang, X., Collins, C. A., Rodal, A. A., Yuan, Q., Verstreken, P., et al. (2013). New approaches for studying synaptic development, function, and plasticity using Drosophila as a model system. *J. Neurosci.* 33, 17560–17568. doi: 10.1523/JNEUROSCI.3261-13.2013

Fujioka, M., Lear, B. C., Landgraf, M., Yusibova, G. L., Zhou, J., Riley, K. M., et al. (2003). Even-skipped, acting as a repressor, regulates axonal projections in Drosophila. *Development* 130, 5385–5400. doi: 10.1242/dev.00770

Funato, Y., Michiue, T., Asashima, M., and Miki, H. (2006). The thioredoxin-related redox-regulating protein nucleoredoxin inhibits Wnt-beta-catenin signalling through dishevelled. *Nat. Cell Biol.* 8, 501–508. doi: 10.1038/ncb1405

Goldsmit, Y., Erlich, S., and Pinkas-Kramarski, R. (2001). Neuregulin induces sustained reactive oxygen species generation to mediate neuronal differentiation. *Cell. Mol. Neurobiol.* 21, 753–769. doi: 10.1023/A:1015108306171

Ha, E. M., Lee, K. A., Park, S. H., Kim, S. H., Nam, H. J., Lee, H. Y., et al. (2009). Regulation of DUOX by the G alpha q-phospholipase Cbeta-Ca^{2+} pathway in Drosophila gut immunity. *Develop. Cell* 16, 386–397. doi: 10.1016/j.devcel.2008.12.015

Ha, E. M., Oh, C. T., Bae, Y. S., and Lee, W. J. (2005a). A direct role for dual oxidase in Drosophila gut immunity. *Science* 310, 847–850. doi: 10.1126/science.1117311

Ha, E. M., Oh, C. T., Ryu, J. H., Bae, Y. S., Kang, S. W., Jang, I. H., et al. (2005b). An antioxidant system required for host protection against gut infection in Drosophila. *Develop. Cell* 8, 125–132. doi: 10.1016/j.devcel.2004.11.007

Hamada, F. N., Rosenzweig, M., Kang, K., Pulver, S. R., Ghezzi, A., Jegla, T. J., et al. (2008). An internal thermal sensor controlling temperature preference in Drosophila. *Nature* 454, 217–220. doi: 10.1038/nature07001

Hoang, B., and Chiba, A. (2001). Single-cell analysis of Drosophila larval neuromuscular synapses. *Develop. Biol.* 229, 55–70. doi: 10.1006/dbio.2000.9983

Hongpaisan, J., Winters, C. A., and Andrews, S. B. (2003). Calcium-dependent mitochondrial superoxide modulates nuclear CREB phosphorylation in hippocampal neurons. *Mol. Cell. Neurosci.* 24, 1103–1115. doi: 10.1016/j.mcn.2003.09.003

Hongpaisan, J., Winters, C. A., and Andrews, S. B. (2004). Strong calcium entry activates mitochondrial superoxide generation, upregulating kinase signaling in hippocampal neurons. *J. Neurosci.* 24, 10878–10887. doi: 10.1523/JNEUROSCI.3278-04.2004

Hussain, A., Pooryasin, A., Zhang, M., Loschek, L. F., La Fortezza, M., Friedrich, A. B., et al. (2018). Inhibition of oxidative stress in cholinergic projection neurons fully rescues aging-associated olfactory circuit degeneration in Drosophila. *eLife* 7, e32018. doi: 10.7554/eLife.32018

Jordán-Álvarez, S., Fouquet, W., Sigrist, S. J., and Acebes, A. (2012). Presynaptic PI3K activity triggers the formation of glutamate receptors at neuromuscular terminals of Drosophila. *J. Cell Sci.* 125, 3621–3629. doi: 10.1242/jcs.102806

Kamata, H., Oka, S., Shibukawa, Y., Kakuta, J., and Hirata, H. (2005). Redox regulation of nerve growth factor-induced neuronal differentiation of PC12 cells through modulation of the nerve growth factor receptor, TrkA. *Archiv. Biochem. Biophys.* 434, 16–25. doi: 10.1016/j.abb.2004.07.036

Kawahara, T., Quinn, M. T., and Lambeth, J. D. (2007). Molecular evolution of the reactive oxygen-generating NADPH oxidase (Nox/Duox) family of enzymes. *BMC Evolution. Biol.* 7, 109. doi: 10.1186/1471-2148-7-109

Kempf, A., Song, S. M., Talbot, C. B., and Miesenböck, G. (2019). A potassium channel β-subunit couples mitochondrial electron transport to sleep. *Nature* 568, 230–234. doi: 10.1038/s41586-019-1034-5

Kishida, K. T., Hoeffer, C. A., Hu, D., Pao, M., Holland, S. M., and Klann, E. (2006). Synaptic plasticity deficits and mild memory impairments in mouse

models of chronic granulomatous disease. *Mol. Cell. Biol.* 26, 5908–5920. doi: 10.1128/MCB.00269-06

Kishida, K. T., and Klann, E. (2007). Sources and targets of reactive oxygen species in synaptic plasticity and memory. *Antioxid. Redox Signal.* 9, 233–244. doi: 10.1089/ars.2007.9.233

Knapp, L. T., and Klann, E. (2002). Role of reactive oxygen species in hippocampal long-term potentiation: Contributory or inhibitory? *J. Neurosci. Res.* 70, 1–7. doi: 10.1002/jnr.10371

Koles, K., and Budnik, V. (2012). Wnt signaling in neuromuscular junction development. *Cold Spring Harbor Perspect. Biol.* 4, a008045. doi: 10.1101/cshperspect.a008045

Kourghi, M., Pei, J. V., De Ieso, M. L., Nourmohammadi, S., Chow, P. H., and Yool, A. J. (2018). Fundamental structural and functional properties of Aquaporin ion channels found across the kingdoms of life. *Clin. Exper. Pharmacol. Physiol.* 45, 401–409. doi: 10.1111/1440-1681.12900

Lachaise, D., Cariou, M. L., David, J. R., Lemeunier, F., Tsacas, L., and Ashburner, M. (1988). "Historical biogeography of the *Drosophila melanogaster* species subgroup," in *Evolutionary Biology* (Boston, MA: Springer), 159–225. doi: 10.1007/978-1-4613-0931-4_4

Lam, A. J., St-Pierre, F., Gong, Y., Marshall, J. D., Cranfill, P. J., Baird, M. A., et al. (2012). Improving FRET dynamic range with bright green and red fluorescent proteins. *Nat. Methods* 9, 1005–1012. doi: 10.1038/nmeth.2171

Lambeth, J. D. (2002). Nox/Duox family of nicotinamide adenine dinucleotide (phosphate) oxidases. *Curr. Opin. Hematol.* 9, 11–17. doi: 10.1097/00062752-200201000-00003

Landgraf, M., Bossing, T., Technau, G. M., and Bate, M. (1997). The origin, location, and projections of the embryonic abdominal motorneurons of Drosophila. *J. Neurosci.* 17, 9642–9655. doi: 10.1523/JNEUROSCI.17-24-09642.1997

Li, Z., Ji, G., and Neugebauer, V. (2011). Mitochondrial reactive oxygen species are activated by mGluR5 through IP3 and activate ERK and PKA to increase excitability of amygdala neurons and pain behavior. *J. Neurosci.* 31, 1114–1127. doi: 10.1523/JNEUROSCI.5387-10.2011

Love, N. R., Chen, Y., Ishibashi, S., Kritsiligkou, P., Lea, R., Koh, Y., et al. (2013). Amputation-induced reactive oxygen species are required for successful Xenopus tadpole tail regeneration. *Nat. Cell Biol.* 15, 222–228. doi: 10.1038/ncb2659

Martín-Peña, A., Acebes, A., Rodríguez, J. R., Sorribes, A., de Polavieja, G. G., Fernández-Fúnez, P., et al. (2006). Age-independent synaptogenesis by phosphoinositide 3 kinase. *J. Neurosci.* 26, 10199–10208. doi: 10.1523/JNEUROSCI.1223-06.2006

Martins, R. N., Harper, C. G., Stokes, G. B., and Masters, C. L. (1986). Increased cerebral glucose-6-phosphate dehydrogenase activity in Alzheimer's disease may reflect oxidative stress. *J. Neurochem.* 46, 1042–1045. doi: 10.1111/j.1471-4159.1986.tb00615.x

Massaad, C. A., and Klann, E. (2011). Reactive oxygen species in the regulation of synaptic plasticity and memory. *Antioxid. Redox Signal.* 14, 2013–2054. doi: 10.1089/ars.2010.3208

Millana Fañanás, E., Todesca, S., Sicorello, A., Masino, L., Pompach, P., Magnani, F., et al. (2020). On the mechanism of calcium-dependent activation of NADPH oxidase 5 (NOX5). *FEBS J.* 287, 2486–2503. doi: 10.1111/febs.15160

Milton, V. J., Jarrett, H. E., Gowers, K., Chalak, S., Briggs, L., Robinson, I. M., et al. (2011). Oxidative stress induces overgrowth of the Drosophila neuromuscular junction. *Proc. Natl. Acad. Sci. U. S. A.* 108, 17521–17526. doi: 10.1073/pnas.1014511108

Moreira, S., Stramer, B., Evans, I., Wood, W., and Martin, P. (2010). Prioritization of competing damage and developmental signals by migrating macrophages in the Drosophila embryo. *Curr. Biol.* 20, 464–470. doi: 10.1016/j.cub.2010.01.047

Munnamalai, V., and Suter, D. M. (2009). Reactive oxygen species regulate F-actin dynamics in neuronal growth cones and neurite outgrowth. *J. Neurochem.* 108, 644–661. doi: 10.1111/j.1471-4159.2008.05787.x

Munnamalai, V., Weaver, C. J., Weisheit, C. E., Venkatraman, P., Agim, Z. S., Quinn, M. T., et al. (2014). Bidirectional interactions between NOX2-type NADPH oxidase and the F-actin cytoskeleton in neuronal growth cones. *J. Neurochem.* 130, 526–540. doi: 10.1111/jnc.12734

Murphy, M. P. (2009). How mitochondria produce reactive oxygen species. *Biochem. J.* 417, 1–13. doi: 10.1042/BJ20081386

Nguyen, A. W., and Daugherty, P. S. (2005). Evolutionary optimization of fluorescent proteins for intracellular FRET. *Nat. Biotechnol.* 23, 355–360. doi: 10.1038/nbt1066

Niethammer, P. (2016). The early wound signals. *Curr. Opin. Genet. Develop.* 40, 17–22. doi: 10.1016/j.gde.2016.05.001

Niethammer, P., Grabher, C., Look, A. T., and Mitchison, T. J. (2009). A tissue-scale gradient of hydrogen peroxide mediates rapid wound detection in zebrafish. *Nature* 459, 996–999. doi: 10.1038/nature08119

Nitti, M., Furfaro, A. L., Cevasco, C., Traverso, N., Marinari, U. M., Pronzato, M. A., et al. (2010). PKC delta and NADPH oxidase in retinoic acid-induced neuroblastoma cell differentiation. *Cell. Signal.* 22, 828–835. doi: 10.1016/j.cellsig.2010.01.007

Olguín-Albuerne, M., and Morán, J. (2015). ROS produced by NOX2 control *in vitro* development of cerebellar granule neurons development. *ASN Neuro* 7, 1759091415578712. doi: 10.1177/1759091415578712

Osses, N., and Henríquez, J. P. (2015). Bone morphogenetic protein signaling in vertebrate motor neurons and neuromuscular communication. *Front. Cell. Neurosci.* 8, 453. doi: 10.3389/fncel.2014.00453

Oswald, M., Garnham, N., Sweeney, S. T., and Landgraf, M. (2018). Regulation of neuronal development and function by ROS. *FEBS Lett.* 592, 679–691. doi: 10.1002/1873-3468.12972

Oswald, M. C., Brooks, P. S., Zwart, M. F., Mukherjee, A., West, R. J., Giachello, C. N., et al. (2018). Reactive oxygen species regulate activity-dependent neuronal plasticity in Drosophila. *eLife* 7, e39393. doi: 10.7554/eLife.39393

Ou, Y., Chwalla, B., Landgraf, M., and van Meyel, D. J. (2008). Identification of genes influencing dendrite morphogenesis in developing peripheral sensory and central motor neurons. *Neural Develop.* 3, 16. doi: 10.1186/1749-8104-3-16

Owusu-Ansah, E., and Banerjee, U. (2009). Reactive oxygen species prime Drosophila haematopoietic progenitors for differentiation. *Nature* 461, 537–541. doi: 10.1038/nature08313

Panday, A., Sahoo, M. K., Osorio, D., and Batra, S. (2015). NADPH oxidases: An overview from structure to innate immunity-associated pathologies. *Cell. Mol. Immunol.* 12, 5–23. doi: 10.1038/cmi.2014.89

Peng, J. J., Lin, S. H., Liu, Y. T., Lin, H. C., Li, T. N., and Yao, C. K. (2019). A circuit-dependent ROS feedback loop mediates glutamate excitotoxicity to sculpt the Drosophila motor system. *eLife* 8, e47372. doi: 10.7554/eLife.47372

Pérez-Moreno, J. J., and O'Kane, C. J. (2019). GAL4 drivers specific for Type Ib and Type Is motor neurons in Drosophila. *G3* 9, 453–462. doi: 10.1534/g3.118.200809

Pignoni, F., Hu, B., and Zipursky, S. L. (1997). Identification of genes required for Drosophila eye development using a phenotypic enhancer-trap. *Proc. Nat. Acad. Sci. USA.* 94, 9220–9225. doi: 10.1073/pnas.94.17.9220

Pool, J. E., Corbett-Detig, R. B., Sugino, R. P., Stevens, K. A., Cardeno, C. M., Crepeau, M. W., et al. (2012). Population genomics of sub-saharan *Drosophila melanogaster*: African diversity and non-African admixture. *PLoS Genet.* 8, e1003080. doi: 10.1371/journal.pgen.1003080

Pulver, S. R., Pashkovski, S. L., Hornstein, N. J., Garrity, P. A., and Griffith, L. C. (2009). Temporal dynamics of neuronal activation by Channelrhodopsin-2 and TRPA1 determine behavioral output in Drosophila larvae. *J. Neurophysiol.* 101, 3075–3088. doi: 10.1152/jn.00071.2009

Razzell, W., Evans, I. R., Martin, P., and Wood, W. (2013). Calcium flashes orchestrate the wound inflammatory response through DUOX activation and hydrogen peroxide release. *Curr. Biol.* 23, 424–429. doi: 10.1016/j.cub.2013.01.058

Rharass, T., Lemcke, H., Lantow, M., Kuznetsov, S. A., Weiss, D. G., and Panáková, D. (2014). Ca^{2+}-mediated mitochondrial reactive oxygen species metabolism augments Wnt/β-catenin pathway activation to facilitate cell differentiation. *J. Biol. Chem.* 289, 27937–27951. doi: 10.1074/jbc.M114.573519

Rhee, S. G. (1999). Redox signaling: hydrogen peroxide as intracellular messenger. *Exp. Mol. Med.* 31, 53–59. doi: 10.1038/emm.1999.9

Rigutto, S., Hoste, C., Grasberger, H., Milenkovic, M., Communi, D., Dumont, J. E., et al. (2009). Activation of dual oxidases Duox1 and Duox2: differential regulation mediated by camp-dependent protein kinase and protein kinase C-dependent phosphorylation. *J. Biol. Chem.* 284, 6725–6734. doi: 10.1074/jbc.M806893200

Sánchez-de-Diego, C., Valer, J. A., Pimenta-Lopes, C., Rosa, J. L., and Ventura, F. (2019). Interplay between BMPs and reactive oxygen species in cell signaling and pathology. *Biomolecules* 9, 534. doi: 10.3390/biom9100534

Sanyal, S., Narayanan, R., Consoulas, C., and Ramaswami, M. (2003). Evidence for cell autonomous AP1 function in regulation of Drosophila motor-neuron plasticity. *BMC Neurosci.* 4, 20. doi: 10.1186/1471-2202-4-20

Sanyal, S., Sandstrom, D. J., Hoeffer, C. A., and Ramaswami, M. (2002). AP-1 functions upstream of CREB to control synaptic plasticity in Drosophila. *Nature* 416, 870–874. doi: 10.1038/416870a

Sanz, A. (2016). Mitochondrial reactive oxygen species: Do they extend or shorten animal lifespan? *Biochim. Biophys. Acta* 1857, 1116–1126. doi: 10.1016/j.bbabio.2016.03.018

Sauer, H., Wartenberg, M., and Hescheler, J. (2001). Reactive oxygen species as intracellular messengers during cell growth and differentiation. *Cell. Physiol. Biochem.* 11, 173–186. doi: 10.1159/000047804

Serrano, F., Kolluri, N. S., Wientjes, F. B., Card, J. P., and Klann, E. (2003). NADPH oxidase immunoreactivity in the mouse brain. *Brain Res.* 988, 193–198. doi: 10.1016/S0006-8993(03)03364-X

Shearin, H. K., Macdonald, I. S., Spector, L. P., and Stowers, R. S. (2014). Hexameric GFP and mCherry reporters for the Drosophila GAL4, Q, and LexA transcription systems. *Genetics* 196, 951–960. doi: 10.1534/genetics.113.161141

Sink, H., and Whitington, P. M. (1991). Location and connectivity of abdominal motoneurons in the embryo and larva of *Drosophila melanogaster*. *J. Neurobiol.* 22, 298–311. doi: 10.1002/neu.480220309

Spina, M. B., and Cohen, G. (1989). Dopamine turnover and glutathione oxidation: Implications for Parkinson disease. *Proc. Natl. Acad. Sci. U. S. A.* 86, 1398–1400. doi: 10.1073/pnas.86.4.1398

Sulkowski, M., Kim, Y. J., and Serpe, M. (2014). Postsynaptic glutamate receptors regulate local BMP signaling at the Drosophila neuromuscular junction. *Development* 141, 436–447. doi: 10.1242/dev.097758

Suzukawa, K., Miura, K., Mitsushita, J., Resau, J., Hirose, K., Crystal, R., et al. (2000). Nerve growth factor-induced neuronal differentiation requires generation of Rac1-regulated reactive oxygen species. *J. Biol. Chem.* 275, 13175–13178. doi: 10.1074/jbc.275.18.13175

Tatsumi, K., Tsuji, S., Miwa, H., Morisaku, T., Nuriya, M., Orihara, M., et al. (2009). Drosophila big brain does not act as a water channel, but mediates cell adhesion. *FEBS Lett.* 583, 2077–2082. doi: 10.1016/j.febslet.2009.05.035

Tejada-Simon, M. V., Serrano, F., Villasana, L. E., Kanterewicz, B. I., Wu, G. Y., Quinn, M. T., et al. (2005). Synaptic localization of a functional NADPH oxidase in the mouse hippocampus. *Mol. Cell. Neurosci.* 29, 97–106. doi: 10.1016/j.mcn.2005.01.007

Terzi, A., and Suter, D. M. (2020). The role of NADPH oxidases in neuronal development. *Free Rad. Biol. Med.* 154, 33–47. doi: 10.1016/j.freeradbiomed.2020.04.027

Tripodi, M., Evers, J. F., Mauss, A., Bate, M., and Landgraf, M. (2008). Structural homeostasis: compensatory adjustments of dendritic arbor geometry in response to variations of synaptic input. *PLoS Biol.* 6:e260. doi: 10.1371/journal.pbio.0060260

Tsai, P. I., Wang, M., Kao, H. H., Cheng, Y. J., Lin, Y. J., Chen, R. H., et al. (2012). Activity-dependent retrograde laminin A signaling regulates synapse growth at Drosophila neuromuscular junctions. *Proc. Natl. Acad. Sci. U. S. A.* 109, 17699–17704. doi: 10.1073/pnas.1206416109

Walker, J. A., Gouzi, J. Y., Long, J. B., Huang, S., Maher, R. C., Xia, H., et al. (2013). Genetic and functional studies implicate synaptic overgrowth and ring gland cAMP/PKA signaling defects in the *Drosophila melanogaster* neurofibromatosis-1 growth deficiency. *PLoS Genet.* 9, e1003958. doi: 10.1371/journal.pgen.1003958

Wilson, C., and González-Billault, C. (2015). Regulation of cytoskeletal dynamics by redox signaling and oxidative stress: Implications for neuronal development and trafficking. *Fronti. Cell. Neurosci.* 9, 381. doi: 10.3389/fncel.2015.00381

Wilson, C., Muñoz-Palma, E., and González-Billault, C. (2018). From birth to death: A role for reactive oxygen species in neuronal development. *Semin. Cell Dev. Biol.* 80, 43–49. doi: 10.1016/j.semcdb.2017.09.012

Wilson, C., Muñoz-Palma, E., Henríquez, D. R., Palmisano, I., Núñez, M. T., Di Giovanni, S., et al. (2016). A feed-forward mechanism involving the NOX complex and RyR-mediated Ca^{2+} release during axonal specification. *J. Neurosci.* 36, 11107–11119. doi: 10.1523/JNEUROSCI.1455-16.2016

Wilson, C., Núñez, M. T., and González-Billault, C. (2015). Contribution of NADPH oxidase to the establishment of hippocampal neuronal polarity in culture. *J. Cell Sci.* 128, 2989–2995. doi: 10.1242/jcs.168567

Zorov, D. B., Juhaszova, M., and Sollott, S. J. (2014). Mitochondrial reactive oxygen species (ROS) and ROS-induced ROS release. *Physiol. Rev.* 94, 909–950. doi: 10.1152/physrev.00026.2013

Zwart, M. F., Randlett, O., Evers, J. F., and Landgraf, M. (2013). Dendritic growth gated by a steroid hormone receptor underlies increases in activity in the developing Drosophila locomotor system. *Proc. Natl. Acad. Sci. U. S. A.* 110, E3878–E3887. doi: 10.1073/pnas.1311711110

Frontiers in
Cellular Neuroscience

Leading research in cellular mechanisms underlying brain function and development

Part of the world's most cited neuroscience journal series that advances our understanding of the cellular mechanisms underlying cell function in the nervous system across all species.

Discover the latest Research Topics

See more →

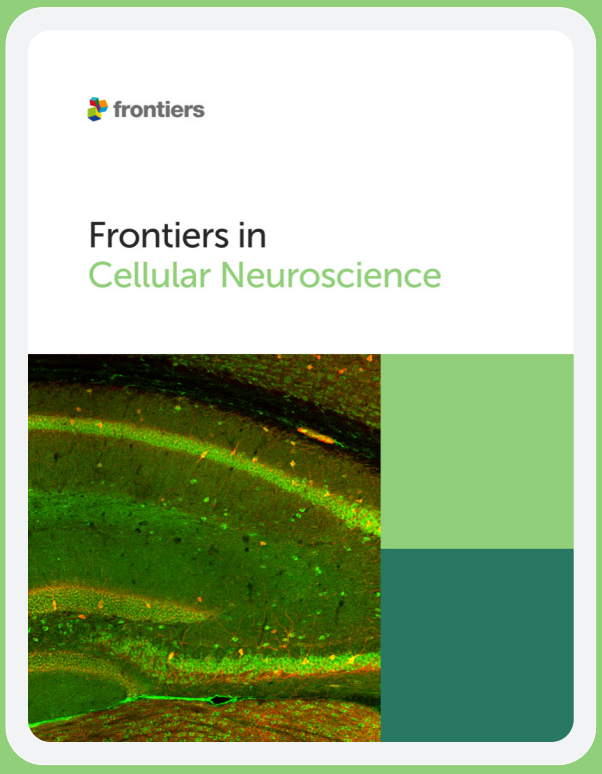

Frontiers

Avenue du Tribunal-Fédéral 34
1005 Lausanne, Switzerland
frontiersin.org

Contact us

+41 (0)21 510 17 00
frontiersin.org/about/contact